

Editorial

The *Journal of Biosciences* is entering its twelfth year of publication. It gives us a sense of pride to note that the journal has achieved the highest impact factor among the Indian journals published in the area of life sciences. However, this distinction is a small achievement, considering the huge gap in impact factor between international and Indian journals. More than considerations of impact factor and other such incomplete parameters to assess the quality of our journal, it is the failure of the journal to reflect the renaissance that is taking place in research in the area of life sciences in the country that should be bothering scientists in the country. Every one realises that the quality of research in life sciences in the country has improved considerably as evidenced by the increasing number of good contributions from the country appearing in standard international journals published abroad. While science is international, it is a national pride to have a journal published in our country to be rated as first class. The emergence of such a journal will also make the international community to look into the scientific contributions coming from the country with more interest and respect. The egg and chicken story is often stated to explain the problems of building an Indian journal of international repute. If the journal is good, it will attract good papers. If good papers are published, the journal becomes good.

We have made a start. The following decisions of the Editorial Board towards achieving the objectives of building a sound journal may be highlighted:

1. The journal invites papers dealing with the cellular and molecular aspects of biological phenomena interpreted in a broad sense. However, papers that are more suited for publication in Medical, Agricultural and other professional journals will be returned based on the judgement of the Editor/Editorial Board.
2. The journal invites original contributions in research. It will publish full papers as well as short communications. Mini reviews (not exceeding 5 printed pages) are invited from those, who have made original research contributions to the field.
3. All papers can be sent to the Editor. In addition, depending on the area of expertise, papers can also be sent to any member of the Editorial Board, who will assume responsibility for processing such papers.
4. The list of referees has been updated to include several young active research scientists and mechanisms for a quicker review process have been evolved.
5. Manuscripts should be accompanied by a potential list of referees. Please suggest atleast 3 names.
6. Suggestions to improve the quality of the journal from the readership are welcome.

G. Padmanaban

Journal of Biosciences

Vol. 15, March–December 1990

CONTENTS

Affinity chromatography of estrogen- and progesterone-binding proteins of human uterus	
<i>M. Thapar, P. Sujata, G. L. Kumari, T. G. Shrivastava and S. K. Sachdeva</i>	1
Cholecystokinin antagonist, proglumide, stimulates growth hormone release in the rat	
<i>E. Vijayan and S. M. McCann</i>	17
Non-enzymatic glycosylation induced changes <i>in vitro</i> in some molecular parameters of collagen	
<i>A. N. Rathi and G. Chandrakasan</i>	23
Effect of doxorubicin on the intestinal membranes in rats—Influence of α -tocopherol administration	
<i>A. Geetha, R. Sankar, Thankamani Marar and C. S. Shyamala Devi</i>	31
Analysis, characterization and diagnostic use of circulating filarial antigen in bancroftian filariasis	
<i>K. A. Parkhe, M. V. R. Reddy, K. Cheiramaraj, P. Ramaprasad and B. C. Harinath</i>	37
5-Methylcytosine content and methylation status in six millet DNAs	
<i>Lalitha S. Kumar, R. R. Hendre and P. K. Ranjekar</i>	47
Predicted secondary structure of maltodextrin phosphorylase from <i>Escherichia coli</i> as deduced using Chou-Fasman model	
<i>Anil Kumar</i>	53
Effect of king cobra venom on α_2 -macroglobulin and proteases in human blood plasma	
<i>Maya Roche and T. N. Pattabiraman</i>	59
Optimization of sodium orthovanadate to treat streptozotocin-induced diabetic rats	
<i>N. Sekar, S. William, N. Balasubramaniam, P. Kamarajan and S. Govindasamy</i>	67
Enzyme activities associated with developing wheat (<i>Triticum aestivum</i> L.) grain amyloplasts	
<i>R. Mahajan and Randhir Singh</i>	77
Control of ornithine decarboxylase activity in jute seeds by antizyme	
<i>Malabika Pandit and Bharati Ghosh</i>	83
Lamellar dispersion and phase separation of chloroplast membrane lipids by negative staining electron microscopy	
<i>R. C. YashRoy</i>	93
<i>In situ</i> study of chorion gene amplification in ovarian follicle cells of <i>Drosophila nasuta</i>	
<i>P. K. Tiwari and S. C. Lakhotia</i>	99
Developmental regulation of cytochrome P-450(b + e) and glutathione transferase (Ya + Yc) gene expression in rat liver	
<i>V. J. Dwarki, V. S. N. K. Francis and G. Padmanaban</i>	107

Nuclear magnetic resonance and thermal studies of drug doped dipalmitoyl phosphatidyl choline-H₂O systems	
..... <i>K. Usha Deniz, P. S. Parvathanathan, Geeta Datta, C. L. Khetrapal, K. V. Ramanathan, N. Suryaprakash and S. Raghotama</i>	117
Magnetic resonance methods for studying intact spermatozoa	
..... <i>Ratna S. Phadke, Sudha Srivastava and Girjesh Govil</i>	125
Erythrocyte stability under imposed fields	<i>V. Sitaramam</i> 135
Depth profiling in membranes by fluorescence quenching	
..... <i>Amitabha Chattopadhyay</i>	143
Role of nicotinic acid as modulator of liposomal microviscosity	
..... <i>M. Chatterjee, R. Basu and P. Nandy</i>	145
Fluidity of detergent micelles plays an important role in muscarinic receptor solubilization	<i>Anu Kõiv, Ago Rinken and Jaak Järv</i> 149
Peptide induced polymorphism in model membranes	
..... <i>Ratna S. Phadke, Sudha Srivastava and Girjesh Govil</i>	153
Kinetic mechanism of mitochondrial carriers catalysing exchange reactions ..	
..... <i>F. E. Sluse, A. Evens, C. Duyckaerts and C. M. Sluse-Goffart</i>	159
Identification and isolation of ATP transport protein in mycobacillin sensitive <i>Aspergillus niger</i>	<i>Bhabadeb Chowdhury and S. K. Bose</i> 163
pH-Dependent membrane interactions of diphtheria toxin: A genetic approach	<i>R. John Collier</i> 169
Iron-regulated membrane proteins and bacterial virulence	<i>E. Griffiths</i> 173
Inhibition of anion transport in the red blood cell membrane by anionic and non-anionic arginine-specific reagents	<i>Laila Zaki</i> 179
Functional and pathological significance of phospholipid asymmetry in erythrocyte membranes	
..... <i>Robert A. Schlegel, Susan Kemper and Patrick Williamson</i>	187
Calcium and magnesium induced changes in the relative fluidity of phosphatidylethanolamine liposomes	<i>R. K. Mishra and Gauri S. Singhal</i> 193
Expression of 5-amino levulinic acid induced photodynamic damage to the thylakoid membranes in dark sensitized by brief pre-illumination	
..... <i>N. Chakraborty and B. C. Tripathy</i>	199
Polyvanadate acts at the level of plasma membranes through α-adrenergic receptor and affects cellular calcium distribution and some oxidation activities	
..... <i>T. Ramasarma, Sharada Gullapalli, Vidya Shivaswamy and C. K. Ramakrishna Kurup</i>	205
Membrane lipid peroxidation by ultrasound: Mechanism and implications ...	
..... <i>A. K. Jana, S. Agarwal and S. N. Chatterjee</i>	211
Dephosphorylation of cell-surface phosphoproteins of goat spermatozoa	
..... <i>M. Barua and G. C. Majumder</i>	217

Activities of myelin bound cytidine 5'-diphosphate-choline 1,2 diacyl-glycerol choline phosphotransferase and uridine 5'-diphosphate-galactose-ceramide galactosyltransferase under restricted food intake	<i>S. Padmini and P. Srinivasarao</i>	223
Desmosome and intermediate filament assembly during differentiation and stratification of epithelial cells	<i>Asima Lahiri Majumder and Charles F. Shuler</i>	227
Coupling of proteins to liposomes and their role in understanding delayed type of hypersensitivity in human and mice.....	<i>...U. Sengupta, Sudhir Sinha, V. Chaturvedi, R. B. Narayanan, Sreevatsa and C. M. Gupta</i>	235
Organization and chromosomal localization of β -tubulin genes in <i>Leishmania donovani</i>	<i>Saumitra Das and Samit Adhya</i>	239
Transcription and processing of β -tubulin messenger RNA in <i>Leishmania donovani</i> promastigotes	<i>Samith Adhya, Saumitra Das and Mantu Bhaumik</i>	249
Molecular cloning and restriction enzyme analysis of a long repetitive DNA sequence in rice	<i>V. S. Gupta, M. S. Dhar, B. G. Patil, G. S. Narvekar, S. R. Rawat and P. K. Ranjekar</i>	261
Porphyrin metabolism in lead and mercury treated bajra (<i>Pennisetum typhoideum</i>) seedlings	<i>D. D. K. Prasad and A. R. K. Prasad</i>	271
Magnetic resonance studies of dynamic organisation of lipids in chloroplast membranes	<i>R. C. YashRoy</i>	281
Mechanism of impaired skin collagen maturity in riboflavin or pyridoxine deficiency	<i>R. Lakshmi, A. V. Lakshmi and M. S. Bamji</i>	289
Hypoglycemic action of the pectin present in the juice of the inflorescence stalk of plantain (<i>Musa sapientum</i>)—Mechanism of action	<i>R. Gomathy, N. R. Vijayalekshmi and P. A. Kurup</i>	297
Antiatherogenic effect of a low lysine:arginine ratio of protein involves alteration in the aortic glycosaminoglycans and glycoproteins.....	<i>T. Rajamohan and P. A. Kurup</i>	305
Uptake of volatile <i>n</i> -alkanes by <i>Pseudomonas</i> PG-I	<i>S. S. Cameotra and H. D. Singh</i>	313
Lactate dehydrogenase isozyme patterns in the denervated quail (<i>Coturnix coturnix japonica</i>) muscles.....	<i>Abdul Quaium, T. K. Virupaksha, R. V. Krishnamoorthy and L. Sudharshana</i>	323
Role of heme in mitochondrial biogenesis: Transcriptional and post-transcriptional regulation of the expression of Iso-1-cytochrome C gene during glucose repression-derepression in cells of <i>Saccharomyces cerevisiae</i>	<i>K. S. K. Balaji, G. Gopalan and C. Rajamanickam</i>	329

genicity of the tryptic fragments Usha Natraj, K. S. N. Iyer,
Vijaya Raghavan, Smita Mahale and Jacintha Pereira

Translocation of plasminogen activator inhibitor-1 during serum stimulated
growth of mouse embryo fibroblasts
.....S. Srinivas, T. Nagashunmugam and G. Shanmugam

Isolation, characterization and effect of acidic pH on the unfolding-refolding
mechanism of serum albumin domains ... M. Yahiya Khan and A. Salahuddin

Two forms of trehalase in rabbit enterocyte: Purification and chemical
modificationS. Sanker and S. Sivakami

Adenosine and ATP: mutually exclusive modifiers of the kinetics of ADP-
induced aggregation of calf-platelets M. Jamaluddin and L. K. Krishnan

Purification and characterization of cathepsin B from goat brain
..... Ramesh C. Kamboj, Suresh Pal and Hari Singh

Role of Ca^{2+} in induction and secretion of dengue virus-induced cytokines
.....Ritu Dhawan, Madhu Khanna, U. C. Chaturvedi and Asha Mathur

Biological activity of an antibiotic puromycin—A theoretical study.....
..... R. P. Ojha and N. K. Sanyal

Human placental calcium activated neutral proteinase: Separation and
functional characterization of subunits
..... Radhika Shastri, G. Jagadeesh and M. P. J. S. Anandaraj

Endogenous inhibitor of calcium activated neutral proteinase from human
placenta: Purification and possible mechanism of proteinase regulation
..... Radhika Shastri, B. Shailaja and M. P. J. S. Anandaraj

Affinity chromatography of estrogen- and progesterone-binding proteins of human uterus

M. THAPAR, P. SUJATA, G. L. KUMARI†, T. G. SHRIVASTAVA and S. K. SACHDEVA*

Department of Reproductive Biomedicine, National Institute of Health and Family Welfare, Munirka, New Delhi 110 067, India

*Department of Obstetrics and Gynaecology, Safdarjung Hospital, New Delhi 110 016, India

MS received 7 August 1989; revised 26 December 1989

Abstract. The purification of estrogen- and progesterone-binding proteins of human uterus by employing affinity resins coupled with steroid-bovine serum albumin conjugates, led to the isolation of preparations with estrogen- and progesterone-binding sites having K_d values in the range of 0.96 to 1.20×10^{-9} M. These were different from the K_d values of 10^{-10} M and 10^{-8} M obtained for two types of binding sites present in the crude cytosolic and nuclear fractions. The purified proteins sedimented on sucrose gradient with S values in the range of 3.6–4.4.

The cytosolic and nuclear estrogen- and progesterone-binding proteins, thus purified, showed differences in specificity of binding to the hormone. While the cytoplasmic proteins were more specific in their binding to estradiol or progesterone, the nuclear proteins bound cortisol with equal or moderate affinity. These results demonstrate the presence of distinct physiological forms of estrogen- and progesterone-binding proteins in the cytoplasm and nucleus, thus pointing to the importance of both these compartments in hormone action.

Keywords. Human uterus; estrogen-binding protein; progesterone-binding protein; affinity chromatography.

Introduction

The concept that steroid hormones manifest their biological actions by binding to specific intracellular proteins is well accepted. Many of the processes involved in the uptake and binding of steroids to specific receptors, the activation and degradation of receptors, and the events concerned with gene expression are still not completely understood. Intracellular localization of unoccupied receptor and the structure and biological relevance of cytosolic receptors have become controversial, with recent immunocytochemical (Gasc *et al.*, 1984; King and Green, 1984; McClennan *et al.*, 1984; Perrot–Applanat *et al.*, 1985) and biochemical (Welshons *et al.*, 1985) evidences pointing to the predominant presence of unliganded free receptor within the nucleus. The extranuclear receptor appeared to be a consequence of loosely bound nuclear receptor released during the homogenization process. Steroid

†To whom all correspondence should be addressed.

Abbreviations used: BSA, Bovine serum albumin; CNBr-Sepharose, cyanogen bromide activated Sepharose-4B; E₂-6-CMO, estradiol-6-one-6-O-carboxymethyl oxime; DOC-21-HS, deoxycortisosterone-

hormone action apparently results in a tighter association of the steroid receptor complex with the nuclear components. The extranuclear form mostly exists as 8'S' form. The biological significance of the activation of cytosolic receptor to a form that will interact with nuclei or DNA is still to be established. In this context, both these proteins need to be evaluated for their biological relevance and physicochemical properties.

Affinity resins complexed with steroid-protein conjugates have been used as tools for the purification as well as histochemical localization of estradiol and progesterone-binding proteins of mammalian uterus (Parikh *et al.*, 1974; Nerei *et al.*, 1976; Chalmness *et al.*, 1980; Greene *et al.*, 1980; Pertschuk *et al.*, 1980; Rataczak and Hahnel, 1980; Panko *et al.*, 1981; Smith *et al.*, 1981; Manz *et al.*, 1982; Westphal, 1983; Katzenellenbogen and Katzenellenbogen, 1984). As several types of hormone binding sites can be distinguished in the target cells (Clark *et al.*, 1978; Eriksson *et al.*, 1978; Markaverich and Clark, 1979), direct evidence of steroid-protein conjugates binding to high affinity proteins is lacking. The coupling position in the steroid, stability and steroid: protein ratios of the conjugates may influence the specific binding of uterine proteins (De Goeij *et al.*, 1986). Therefore, steroid-affinity matrices, prepared by linking bovine serum albumin (BSA) with a limited number of steroid residues at different positions on the molecule and then attaching to cyanogen bromide activated Sepharose-4B (CNBr-Sepharose), have been utilized for purifying the estrogen- and progesterone-binding proteins of the nuclear and cytosolic fractions of the human uterus. This paper describes the practical aspects in the use of affinity matrices and the differential outcome on the purification of both types of proteins from cytoplasmic and nuclear components.

Materials and methods

Radioactive steroids, [2,4,6,7-³H]estradiol (93.2 Ci/mmol) and [1,2,6,7-³H]progesterone (112 Ci/mmol) were procured from New England Nuclear Corp (USA). Cold hormones such as estradiol, progesterone, cortisol, 1,3,5 (10)-estratriene-3, 17 β -diol-6-one-6-O-carboxymethyl oxime (E₂-6-CMO), deoxycortisosterone-11-hemisuccinate (DOC-21-HS), 11-hydroxy-4-pregnene-3, 20-dione-11-hemisuccinate (11-OH-P-HS), CNBr-Sepharose, dimethylformamide, 1-ethyl-3-(3-dimethylaminopropyl)-carbodiimide hydrochloride, γ -globulin and BSA (RIA grade) were obtained from Sigma Chemical Co., St. Louis, Missouri, USA. Estradiol-3-O-carboxymethyl ether (E₂-3-CME) was a kind gift from Dr. P. N. Rao, Southwest Foundation for Biomedical Research, San Antonio, Texas, USA. Sephacryl S-300, Sephadex G-75, molecular weight (*M_r*) markers were purchased from Pharmacia Fine Chemicals, Uppsala, Sweden. All other chemicals used were of analytical reagent grade.

The following buffers were used in the experiments: Buffer A (pH 7.4) consisted of 10 mM Tris-HCl, 1.5 mM ethylene diamine tetraacetic acid disodium salt, 1 mM dithiothreitol, 5 mM magnesium chloride, and 10% (w/v) glycerol. Buffer B was made of buffer A plus 0.4 mM KCl, and buffer C contained 10 mM Tris HCl, 5 mM magnesium chloride and 1 mM dithiothreitol (pH 7.4). Buffer D was prepared from C after addition of 0.5 M sodium chloride. In addition, phosphate buffered saline (PBS) of pH 7 was also used.

Human uterine tissues

Human uteri were obtained from women undergoing hysterectomy for third degree

utero-vaginal prolapse. The uteri were collected over ice and flash frozen immediately in liquid nitrogen. These were stored at -80°C for not more than 2 months before processing.

Preparation of cytosolic and nuclear fractions

All procedures were performed at 4°C unless otherwise stated. After removing the perimetrium, the thawed uteri were washed several times with buffer A. The tissue was finely minced and homogenized in buffer A (1:4 w/v) using a Polytron PT-20 homogenizer (Brinkmann Instruments). The homogenate was centrifuged at 800 g to obtain the nuclear pellet and the supernatant was centrifuged at $105,000\text{ g}$ for 90 min to furnish cytosol. The nuclear pellet was washed 3 times with buffer A and then gently rehomogenized in buffer B and incubated for 2 h. It was centrifuged at 800 g and the supernatant containing nuclear fraction was further processed.

Protein concentration of the cytosol was estimated following the method of Kalcker (1947) and that of DNA in nuclear fraction by the procedure described by Groft and Lubran (1965).

Assay of hormone-binding proteins

The estrogen- and progesterone-binding proteins in the cytosol were estimated by displacement analysis in which the cytosol was incubated with fixed concentration of labelled hormone (10,000 cpm) in the absence or presence of increasing concentrations of either estradiol or progesterone (0.1–100 nM). The bound proteins were separated by the addition of $500\text{ }\mu\text{l}$ of dextran-coated charcoal (DCC, 0.5% activated Norit A and 0.05% dextran T-70 in buffer A) and counted for radioactivity (Korenman, 1975).

The nuclear receptors were measured by exchange assay as described by Anderson *et al.* (1972). The receptor proteins were quantitated by Scatchard (1949) analysis.

Ammonium sulphate fractionation

A saturated solution of ammonium sulphate in buffer A was added to cytosol and nuclear fractions over 30–40 min with gentle stirring until a final concentration of 30% was achieved. It was then centrifuged at $10,000\text{ g}$ for 15 min. The pellet was redissolved in buffer A in a volume equivalent to one tenth of the total volume of original fraction and centrifuged at $100,000\text{ g}$ for 15 min to remove any undissolved material.

Affinity chromatography

Preparation of steroid-BSA conjugates: Steroid-BSA conjugates were prepared following the method of Mattox *et al.* (1979) with minor modifications. Steroid (8–9 μmol) was dissolved in 100 μmol of dimethyl formamide to which 50 μmol of 1-ethyl-3-(3'-diaminopropyl)-carbodiimide was added and the mixture was agitated for 30–60 min at room temperature. The activated steroid was added to 10 mg (0.15 μM) of BSA and gently agitated for another 14–16 h at 4°C . It was then

chromatographed on Sephadex G-75 column (10 × 200 mm), equilibrated with 0.1 M PBS and 0.5 ml fractions were collected. The absorbance was measured at 280 nm to estimate the number of steroid molecules attached per molecule of BSA following the method described by Erlanger *et al.* (1957). The material was then dialysed against distilled water and lyophilized.

Coupling of steroid-BSA conjugates to CNBr-Sepharose: Commercial preparation of CNBr-Sepharose (3 g), was washed with 1 mM HCl, to which 10 ml of steroid-BSA conjugate (4 mg) in 0.2 M NaHCO₃ with 8 M urea (pH 9) was added and stirred overnight at 4°C. This was filtered and washed with 200 ml of 1 M NaCl followed by 200 ml distilled water. The remaining sites on the CNBr-Sepharose were inactivated by incubating the gel cake with 1 M ethanolamine in 0.2 M NaHCO₃ (pH 9) for 2 h. The resultant gel cake was thoroughly washed with 500 ml dioxane followed by 500 ml distilled water and 500 ml of 80% methanol for 24 h at room temperature.

The amount of estradiol bound to the resin was determined by hydrolyzing an aliquot with 1 M NaOH for 24 h followed by ether extraction (3 × 10 ml) and subsequently estimating the amount by radioimmunoassay (RIA) (Abraham, 1974). Deoxycorticosterone or 11-hydroxy progesterone hemisuccinate coupled to CNBr-Sepharose were measured by radioreceptor assay following the method of Smith *et al.* (1981).

Purification of cytosolic and nuclear hormone-binding proteins

Affinity matrices consisting of BSA conjugates of different hormone derivatives such as E₂-17-HS, E₂-6-CMO and E₂-3-CME for estrogen-binding proteins and DOC-21-HS and 11-OH-P-HS for progesterone-binding components coupled to CNBr-Sepharose were respectively used. Packed affinity matrix equivalent to 2 ml was incubated with ammonium sulphate precipitated cytosol or nuclear fraction for 14–16 h at 4°C. It was gently agitated and then centrifuged. The gel cake was washed with buffer B to remove the loosely associated proteins. This was continued until the optical density at 280 nm of the effluent was same as that of the buffer.

The adsorbed estrogen-binding proteins were eluted from the affinity gel by incubating with 3 ml of [³H]E₂ (110 nmol) in buffer A for 30 min at 30°C. The supernatant was removed and the gel was again incubated with 2 ml of [³H]E₂ (73 nmol) in buffer A for another 15 min at 30°C. The two supernatants were combined and chromatographed on Sephadex G-75 column (10 × 150 mm) which was equilibrated with buffer A. Fractions of 0.5 ml were collected and an aliquot of each fraction (10 µl) was counted for radioactivity.

Similarly, the adsorbed progesterone-binding proteins were eluted from the affinity gel by incubating it with buffer A containing [³H] P (159 nmol/5 ml) at 22°C. The supernatants were fractionated on Sephadex G-75 as described for estrogen-binding protein.

The peak protein fractions eluted in the void volume contained the radioactive hormone-protein complex, while the free radioactive hormone was eluted later. These were pooled together separately for each matrix and checked for affinity, specificity, sedimentation value and *M_r* as described below. The protein content of the affinity eluate was estimated after lyophilization following the method of Peterson (1984).

Affinity, specificity of hormone-protein complexes

The purified protein was tested by competition studies at 4°C by incubating the eluted [³H]estradiol-protein complex (ER) or [³H]progesterone-protein complex (PR) with 1000-fold excess of either of cold estradiol or progesterone, testosterone, or cortisol for 16 h at 4°C. At the end of the incubation, the free steroid was removed using DCC as described earlier and the supernatant counted for radioactivity. The binding sites were quantitated by exchange assay using increasing concentrations of either estradiol or progesterone. Scatchard analysis of the data provided the dissociation constants (K_d).

Sedimentation analysis

Linear 5–10% sucrose gradient (4.2 ml) in buffer A was prepared and left undisturbed overnight at 4°C. The purified hormone-protein complex was layered as such on sucrose gradient, while the crude cytosol or nuclear fraction was incubated with 10 pM of either [³H]E₂ or [³H]P for 2 h and the free steroid was removed by DCC method before layering on the sucrose gradient tubes. These tubes were centrifuged at 219,000 *g* (TV-875, vertical rotor, Sorvall OTD-75B ultracentrifuge) for 4 h. At the end of centrifugation, the tubes were punctured at the bottom and the fractions were collected (30–35 tubes). Radioactivity was counted in each fraction. BSA and γ -globulin were run as reference standards. Sedimentation coefficient was determined according to the method of Martin and Ames (1962).

Sodium dodecyl sulphate-polyacrylamide gel electrophoresis

Sodium dodecyl sulphate (SDS)-polyacrylamide gel electrophoresis (PAGE) was performed according to the method of Laemmli (1970) using a discontinuous buffer system (LKB-200 vertical slab gel electrophoresis unit coupled to LKB 2209 multitemp and LKB 2197 power supply). Gels with 10% T were cast and after polymerisation, the stacking gel was poured. Test samples (15–30 μ g) were dissolved in sample buffer containing SDS and mercaptoethanol. Sucrose (30%) was added and the samples were heated for 2 min in boiling water bath. Standard proteins were treated in a similar manner. The test samples and standard proteins were applied and electrophoresis was carried out at 20 mA. After completion of the run, the gel was removed and stained with 0.1% Coomassie brilliant blue (R-250) dissolved in 50% ethanol and 5% acetic acid.

Gel permeation chromatography on Sephacryl S-300

A calibration curve for standard proteins was prepared by chromatographing 2–3 mg of each protein on Sephacryl S-300 column (16 \times 350 mm), equilibrated and eluted with buffer A. The optical density was monitored for all the fractions and retention time for different proteins was noted. Void volume (V_o) and total volume (V_t) were determined by running blue dextran and dinitrophenyl-glycine separately.

K_{av} values of the binding proteins were used to assess the molecular weights

Evaluation of different affinity matrices for purification of estrogen- and progesterone-binding proteins of human uterus

Steroid (mol) attached per mol of BSA were restricted to not more than 4 number. This caused less steric hindrance on BSA molecule, so that it could be easily conjugated to CNBr-Sephrose. The steroid coupled to the activated Sepharose-4B was estimated either by RIA or radioreceptor assay after extracting the steroid from the affinity gel. Approximately 12–19 nmol of steroid were attached per ml of packed gel.

Chromatographic patterns of the affinity eluates of cytosolic estradiol and progesterone-protein complexes on Sephadex G-75 columns using different matrices are presented in figures 1 and 2. The hormone-protein complexes, [^3H]E $_2$ and [^3H]PR were eluted in the void volume, with the free radioactive hormones recovered in later fractions. Using equal volume of the same ammonium sulfate precipitated cytosol, maximum retention of estradiol-binding protein was observed with E $_2$ -17-HS-Sepharose, followed by E $_2$ -6-CMO-Sepharose. The degree of purification achieved with E $_2$ -17-HS-Sepharose was 3-fold greater than with E $_2$ -6-CMO-Sepharose, while E $_2$ -3-CME-Sepharose was ineffective (figure 1). Both E $_2$ -21-HS-Sepharose and 11-OH-P-HS-Sepharose were equally effective in retaining the progesterone-binding protein of the cytosol (figure 2).

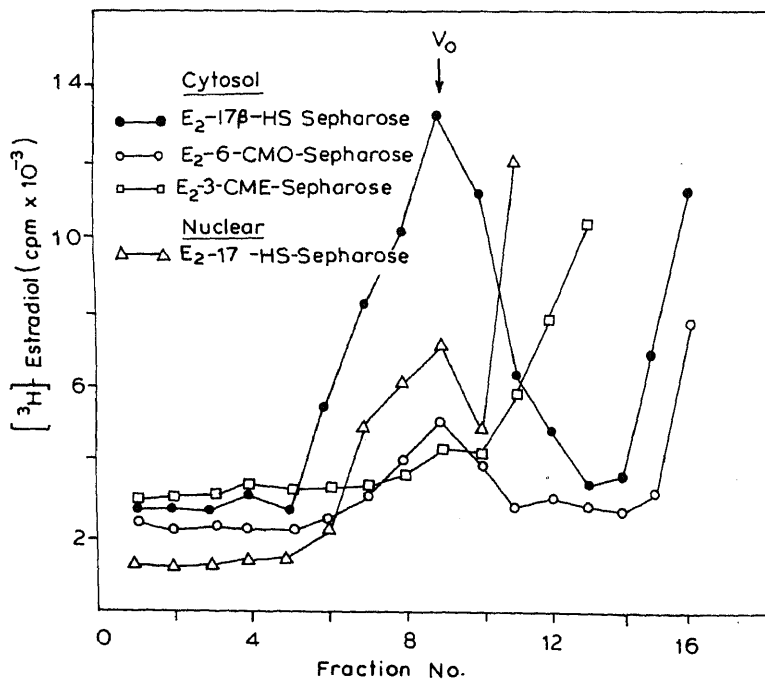


Figure 1. Chromatography of eluates obtained from different estradiol affinity matrices on Sephadex G-75 column. Increase in radioactivity in a second peak corresponds to [^3H]estradiol.

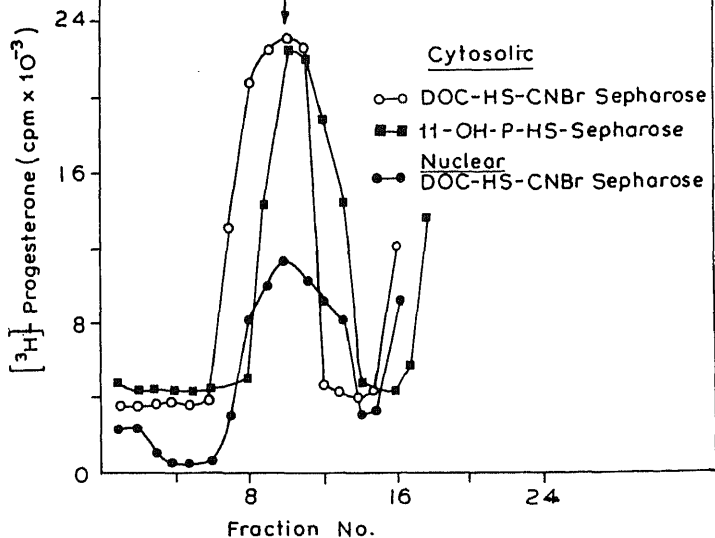


Figure 2. Chromatography of eluates obtained from different progestin-affinity matrices on Sephadex G-75 column. The secondary rise in radioactivity corresponded to [³H]progesterone (15 tube onwards).

Purification of estrogen- and progesterone-binding proteins from human uterus by affinity chromatography

Starting from a total protein of 4750 mg, 180 μ g of [³H]ER and 76 μ g [³H]PR were isolated (tables 1 and 2). Around 150–180 nmol of radioactive estradiol or progesterone of low specific activity was used to dissociate the binding proteins attached to 2 ml of packed affinity gel containing 24–38 nmol of steroid residues. After the protein was adsorbed to the affinity matrix, the loosely associated proteins were removed by washing it several times with the buffer and then the adsorbed or covalently-linked proteins were dissociated with buffer containing radioactive hormone. Purification factor was calculated on the basis of radioactivity incorporated into the hormone-protein complex. The cytosolic and nuclear [³H]ER components were purified approximately 30,000- and 5700-fold, respectively (table 1). From a total nuclear protein of 4120 mg, 80 μ g of ER was isolated. Similarly, the cytosolic and nuclear [³H]PR components were purified 68,000- and 22,000-fold, respectively (table 2). The nuclear ER and PR were comparatively less purified than cytosolic components.

Sucrose density gradient sedimentation analysis

Crude cytosolic and nuclear fractions along with the affinity eluates were subjected to sucrose density gradient analysis. Crude uterine cytosol showed two types of binding proteins for [³H]E₂ and [³H]P with sedimentation coefficients (*S* value) in the range of 7.1–7.2 and 4.0–4.4 (figures 3 and 4).

Table 1. Purification of estrogen-binding proteins on E₂-17-HS-Sepharose.

Preparation	Total protein	cpm/mg protein	Purification fold ^a	Sedimentation value S	M _r	Specificity	K _d (nM)
1. Cytosol (crude)	4750 mg	18,418 ^b	—	7.2, 4.0	260,000 63,000	P > E > F	4.46 × 10 ⁻⁸ 1.81 × 10 ⁻⁸
Ammonium sulphate precipitated cytosol	473 mg	37,621 ^b	2.2	—	— (290,000) ^d	—	—
Affinity eluate	180 µg	5,677,333 ^c	30,824	4.5	64,000	E	1.0 × 10 ⁻⁸
2. Nuclear extract	4122 mg	7,029 ^b	—	4.9	54,000	P > E > F	1.0 × 10 ⁻⁸ 2.06 × 10 ⁻⁸
Ammonium sulphate precipitated nuclear extract	871 mg	13,724 ^b	1.91	—	— (180,000) ^d	—	—
Affinity eluate	80 µg	405,625 ^c	5,700	4.4	54,000	E > F	1.25 × 10 ⁻⁸

^aCalculated on the basis of specific activity of radioactive steroid incorporated; ^bspecific activity of [³H]E₂ = 53 Ci/mmol; ^cspecific activity of [³H]E₂ = 0.54 Ci/mmol; ^dM_r calculated with reference to K_{av} values on Sephacryl S-300 chromatography.
P, Progesterone; E, estradiol-17β; F, cortisol.

Table 2. Purification of progesterone-binding proteins on DOC-21-HS-Sepharose.

Preparation	Total protein	cpm/mg protein	Purification fold ^a	Sedimentation value S	M _r	Specificity	K _d (nM)
1. Cytosol (crude)	4750 mg	12,526 ^b	—	7.1, 4.4	240,000 45,000	P > E > F	0.79 × 10 ⁻⁸ 3.00 × 10 ⁻⁸
Ammonium sulphate precipitated cytosol	473 mg	50,300 ^b	4	—	— (270,000) ^d	—	—
Affinity eluate	76 µg	3,604,210 ^c	68,540	3.6	44,000	P > F	0.96 × 10 ⁻⁸
2. Nuclear extract	4122 mg	10,718 ^b	—	4.8	54,000	P > E > F	1.06 × 10 ⁻⁸ 2.63 × 10 ⁻⁸
Ammonium sulphate precipitated nuclear extract	871 mg	22,526 ^b	2.2	—	— (195,000) ^d	—	—
Affinity eluate	42 µg	999,404 ^c	22,192	4.4	45,000	P > F > E	1.20 × 10 ⁻⁸

^aCalculated in terms of specific activity of the radioactive steroid incorporated; ^bspecific activity of [³H]P = 112 Ci/mmol; ^cspecific activity of [³H]P = 0.47 Ci/mmol; ^dM_r calculated with reference to K_{av} values obtained on Sephacryl S-300 chromatography.
P, Progesterone; E, estradiol-17β; F, cortisol.

The affinity eluate of cytosolic [³H]ER sedimented at 4.5 S, while the nuclear at 4.4 S. In case of PR, the cytosolic and nuclear affinity eluates had S values of 3.6 and 4.4, respectively (tables 1 and 2).

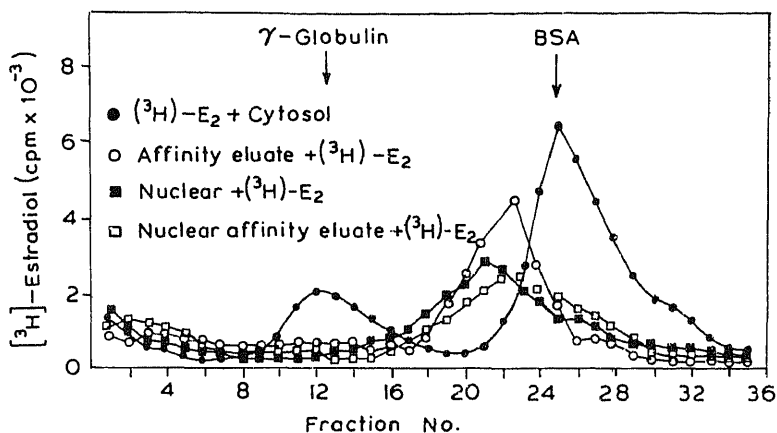


Figure 3. Sucrose density gradient analysis of crude cytosolic and nuclear fractions and final purified affinity eluates of $[^3\text{H}]$ estradiol-protein complexes.

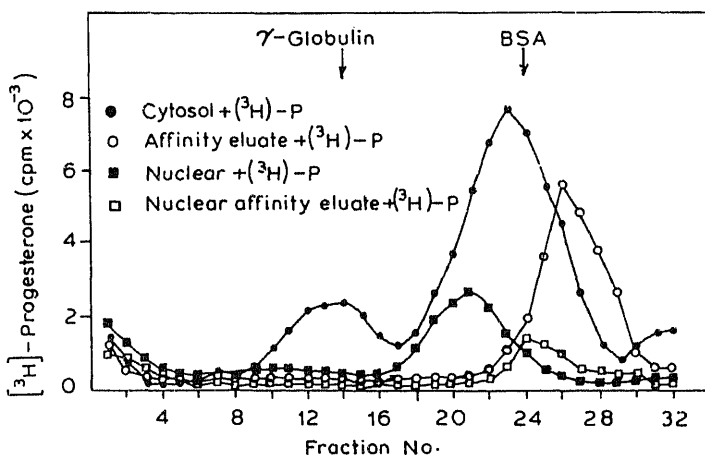
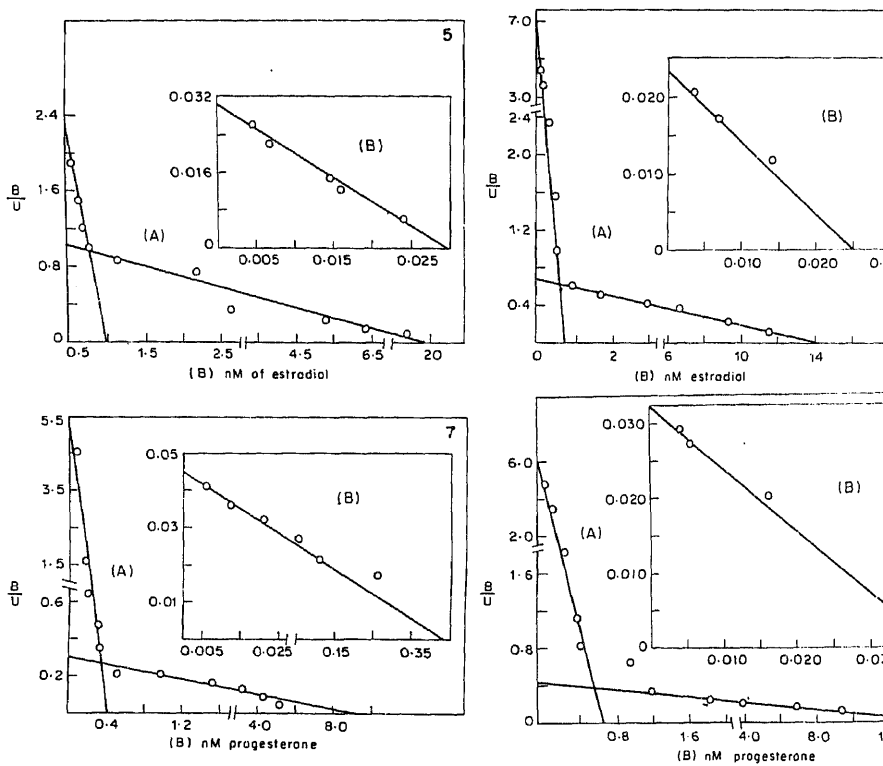


Figure 4. Sucrose density gradient analysis of the labelled crude uterine cytosol and nuclear PR and affinity purified $[^3\text{H}]$ PR.

Specificity

The cytosolic $[^3\text{H}]$ ER was displaced by cold estradiol, but not by progesterone or testosterone or cortisol, while the crude fraction showed relatively more binding to progesterone. This was due to the use of uteri from women suffering for prolapse of uterus. The nuclear $[^3\text{H}]$ ER still had some affinity to cortisol, which was comparatively less than with estradiol. Progesterone in the protein complex could be displaced more by the cold hormone, followed by cortisol. In the nuclear binding protein, progesterone and cortisol could equally displace the radioactive progesterone (tables 1 and 2). DOC-21-HS-Sepharose proved to be more specific

Scatchard analysis of crude cytosolic and nuclear proteins demonstrated K_d corresponding to type I and II binding proteins (10^{-10} and 10^{-8} M). However, the purified affinity eluates showed K_d values for the presence of a protein of moderate affinity (10^{-9} M) (figures 5–8).



Figures 5–8. Scatchard plots of (A) crude and (B) purified (5) cytosolic $[^3H]$ ER complexes, (6) nuclear $[^3H]$ ER complexes, (7) cytosolic $[^3H]$ PR complexes, (8) nuclear $[^3H]$ PR complexes.

Gel permeation chromatography

The hormone-protein complexes were subjected to Sephacryl S-300 chromatography (figure 9) after partial concentration on Amicon UM-20 filter. Simultaneously, cytosolic and nuclear fractions and standard marker proteins were also processed. The cytosolic and nuclear $[^3H]$ ER were found to have M_r of 64 and 52 kDa, respectively. Whereas the affinity eluates of both cytosolic and nuclear PR had M_r in the range of 44–45 kDa (tables 1 and 2). In addition, the purified proteins showed aggregated molecules of the protein complexes in the range of 180–290 kDa.

SDS-PAGE

The cytosolic hormone-protein complexes of ER and PR were checked on

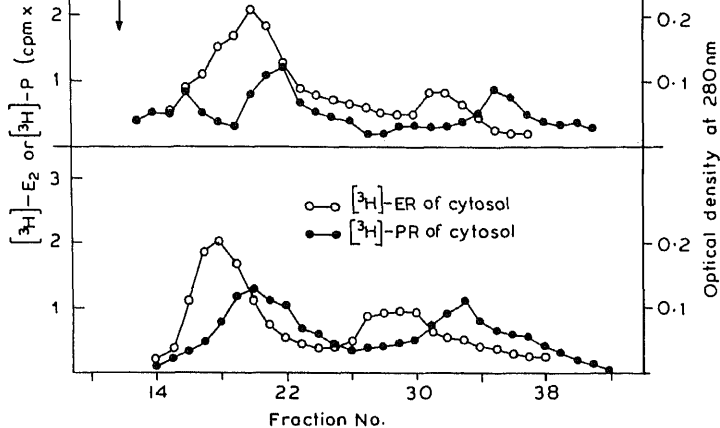


Figure 9. Chromatography of crude and purified cytosolic and nuclear $[^3\text{H}]$ ER and $[^3\text{H}]$ PR complexes on Sepharacryl S-300 column.

PAGE for assessing their purity and M_r . The affinity eluate of ER (25 μg) showed a very intense band corresponding to BSA and had a M_r of 66 kDa. Additional traces of other components could be seen between 45 and 66 kDa. The affinity eluate of $[^3\text{H}]$ PR (15 μg) showed one spot that mainly corresponded to ovalbumin, which had a M_r of 45 kDa (figure 10).

Discussion

The use of steroid-protein conjugates for the purification of hormone-binding proteins or receptors has been known (Parikh *et al.*, 1974; De Goeij *et al.*, 1986). Sica *et al.* (1973) clearly demonstrated that agarose covalently linked to estradiol at 17-position, but not at 3- or 6-positions proved to be effective in achieving 10,000–100,000-fold purification of estrogen receptor. Following the same procedures, (1977) purified a peptide having a M_r of 30 kDa from human myometrial cytosol with a purification factor of 24,000. In another affinity column in which Sepharose-6B was linked through a di-n-propyl thioether bridge at the 17 α -position of estradiol, Greene *et al.* (1980) isolated ER of 65 kDa (3.5 S) from MCF-7 human breast cancer cells.

In all these attempts at purification of ER, affinity matrices were prepared following the procedure of Sica *et al.* (1973), Puca *et al.* (1979) and Sica and Bresciani (1979), in which denatured albumin-Sepharose was conjugated with the steroid derivative and the number of steroid molecules attached to albumin-Sepharose was not controlled. In the present experiments, the steroid molecules were first attached to BSA following the method of Mattox *et al.* (1979). The number of steroid residues conjugated to BSA was also restricted to 4–6. It was then linked to CNBr-Sepharose in such a manner that only 12–20 nmol of steroid per ml of packed gel were attached. This ensured that approximately 25–40 nmol of



Figure 10. SDS-PAGE of purified estradiol and progesterone-binding proteins (A), Marker proteins (1, albumin; 2, ovalbumin; 3, trypsinogen; 4, lactogen; 5, lysozyme); (B) and (C), purified cytosolic [^3H]ER and [^3H]PR.

steroid molecules are available for the hormone specific proteins to bind and expected to be displaced with 150–180 nmol of radioactive estradiol or progesterone. The affinity matrix after adsorption with the receptor protein was repeatedly washed until no protein was detectable in the washings to make sure that only high affinity proteins were retained.

E_2 -17-HS-Sepharose was found to be more effective in retaining estrogen-binding protein (ER) compared to the matrices prepared through covalent linkage of Sepharose-BSA to estradiol at 6- or 3-positions. The integrity of phenolic group seemed to be essential for the binding of specific proteins. Although E_2 -6-HS-Sepharose could bind protein, it was comparatively less than with E_2 -17-HS-Sepharose, thus implying that close proximity of 6-position to the phenolic group probably resulted in some steric hindrance. Other affinity labelling methods at positions in ring-C provide better matrices.

For progesterone-binding proteins, the method was similar to that described by Smith *et al.* (1981), except an additional steroid matrix, 11-OH-P-HS-Sepharose was also attempted. Both DOC-21-HS and 11-OH-P-HS behaved similarly in binding progesterone-specific proteins and comparable results were obtained with both the affinity matrices. Adopting DOC-21-HS-Sepharose matrix, both cytosolic and nuclear [³H]PR having M_r of 44 and 45 kDa, respectively were obtained. As with nuclear estrogen-binding proteins, the nuclear PR was less purified and bound equally well with progesterone and cortisol. Other affinity matrices such as that used by Manz *et al.* (1982) gave two peptides of M_r of 43 and 108 kDa.

Preparation of cytosol, ammonium sulphate precipitation, followed by affinity chromatography produced specific cytosolic [³H]ER of 64 kDa M_r , which appeared as a major component on SDS-PAGE system. However, nuclear [³H]ER showed non-specificity and had an M_r of 54 kDa. Both these after concentration on UM-20 Amicon filter followed by gel permeation chromatography aggregated to large size molecules.

Several reports point to the presence of a single molecule of ER (a 4 S monomer) having an M_r of 65 kDa (King, 1986; Greene and Press, 1986). Green *et al.* (1986) were able to clone and select MCF-7 breast cancer cell mRNA, which could be translated *in vitro* to a protein of 65 kDa. The cytosolic [³H]ER purified in the present studies apparently corresponded to this native form. However, the nuclear [³H]ER differed from the cytosolic protein in its molecular size and specificity.

Structural data on PR from chick oviduct (Schrader *et al.*, 1981) and human breast cancer (Horwitz and Alexander, 1983) suggested that PR was composed of two subunits A and B, both having hormone and DNA binding properties. Holmes *et al.* (1981) using photoaffinity labelling showed a single protein in human uterus. In a majority of studies related to PR isolation, molybdate was used to stabilize the proteins. Therefore, the possibility of progesterone-binding protein, isolated in the present study without the addition of molybdate, being a fragment of PR can not be excluded.

In general, 3 classes of hormone-binding sites in cells can be distinguished. Of these, type I binder has high affinity and a K_d value in the range of 10^{-10} to 10^{-9} M, while type II described by Clark *et al.* (1978), Eriksson *et al.* (1978) and Markaverich and Clark (1979) have lower affinity in the range of 10^{-9} to 10^{-7} M. Type III sites apparently correspond to soluble molecules like albumin and other low affinity proteins (Westphal, 1983). Scatchard analysis of the purified estrogen- and progesterone-binding proteins, obtained in the present investigation, however, demonstrated K_d values in the range of 10^{-9} M for both cytosolic and nuclear proteins. The crude fractions, before affinity chromatography, showed two types of binding sites corresponding to those reported by Clark *et al.* (1978) for type I and II proteins.

The hormones, similar to those used in affinity columns, on conjugation with fluorescein, seemed to recognise all estrogen-binding proteins within the target cells (Chalmers and McGuire, 1982). Raam (1986) and Raam and Vrabel (1986), demonstrated that monoclonal antibodies to estrogen receptors coated on solid phase recognised only the secondary estrogen binding sites having low or moderate affinity for estradiol. They argued that affinity purified proteins used for developing monoclonal antibodies probably recognised only the low affinity binding proteins. The affinity constants for these purified proteins were never reported. In the present

investigation, the K_d values obtained for the purified proteins differ even from the K_d values of the two types of binding proteins. Whether these are related to the secondary binding sites as suggested by Raam and Vrabel (1986) or to the fragments of the binding proteins is still not clear.

It is difficult to explain the displacement of radioactive estradiol or progesterone by cortisol from purified nuclear proteins, while cytosolic estrogen and progesterone-binding proteins are more specific for the respective hormones. The ability of dexamethasone to decrease the levels of nuclear type II sites was described (Clark *et al.*, 1980). The distinct role of the type II proteins of nuclear origin in uterine growth was also emphasized by these investigators. The present findings definitely suggest specific differences between cytoplasmic and nuclear hormone-binding proteins.

Acknowledgements

This work was supported by a financial grant from the Indian Council of Medical Research, New Delhi. Our grateful thanks are due to Prof. S. Duraiswami, University of Delhi for his keen interest in the study. We are also indebted to Prof. Somnath Roy, who evinced interest and encouragement throughout the study.

References

- Abraham, G. E. (1974) *Acta Endocrinol. (Copenhagen) Suppl.*, **183**, 1.
- Anderson, J., Clark, J. H. and Peck, E. J. Jr. (1972) *Biochem. J.*, **126**, 561.
- Chalmness, G. C., Mercer, W. D. and McGuire, W. L. (1980) *J. Histochem. Cytochem.*, **28**, 792.
- Chalmness, G. C. and McGuire, W. L. (1982) in *XI Int. Congress of Clin. Chem.*, (eds E. Kaiser, M. M. Muller and M. Bayer) (Berlin: Walter de Gruyter and Co.) p. 467.
- Clark, J. H., Hardin, J. W. and Upchurch, S. (1978) *J. Biol. Chem.*, **253**, 7630.
- Clark, J. H., Markaverich, B., Upchurch, S., Eriksson, H., Hardin, J. W. and Peck, E. J. Jr. (1980) *Rec. Prog. Horm. Res.*, **36**, 89.
- Coffer, A. I., Milton, P. J. D., Pryse-Davies, J. and King, R. J. B. (1977) *Mol. Cell. Endocrinol.*, **6**, 231.
- De Goeij, A. F. P. M., Van Zeeland, J. K., Beck, C. J. L. and Bosman, F. T. (1986) *J. Steroid Biochem.*, **24**, 1017.
- Eriksson, H., Upchurch, S., Hardin, J. W., Peck, E. J. Jr. and Clark, J. H. (1978) *Biochem. Biophys. Res. Commun.*, **81**, 1.
- Erlanger, B. F., Bork, F., Beiser, S. M. and Lieberman, S. (1957) *J. Biol. Chem.*, **228**, 713.
- Gasc, J. M., Radanyi, C., Joab, I., Tuohimaa, P. and Baulieu, E. E. (1984) *J. Cell Biol.*, **99**, 1193.
- Greene, G. L., Nolan, C., Engler, J. P. and Jensen, E. V. (1980) *Proc. Natl. Acad. Sci. USA*, **77**, 5151.
- Greene, G. L. and Press, M. F. (1986) *J. Steroid Biochem.*, **24**, 1.
- Green, S., Walter, P., Greene, G., Krust, A., Goffin, C., Jensen, E., Scrace, G., Waterfield, M. and Chambon, P. (1986) *J. Steroid Biochem.*, **24**, 77.
- Groft, D. M. and Lubran, M. (1965) *Biochem. J.*, **95**, 612.
- Holmes, S. D., Van, N. T., Stevens, S. and Smith, R. G. (1981) *Endocrinology*, **109**, 670.
- Horwitz, K. B. and Alexander, P. S. (1983) *Endocrinology*, **113**, 2195.
- Kalckar, H. M. (1947) *J. Biol. chem.*, **167**, 461.
- Katzenellenbogen, J. A. and Katzenellenbogen, B. S. (1984) *Vitam. Horm. NY*, **41**, 213.
- King, W. J. and Green, G. L. (1984) *Nature (London)*, **307**, 745.
- King, R. J. B. (1986) *J. Steroid Biochem.*, **25**, 451.
- Korenman, S. (1975) *Methods Enzymol.*, **36**, 49.
- Laemmli, U. K. (1970) *Nature (London)*, **227**, 680.
- Manz, B., Grill, H. J., Kohler, I., Heubner, A. and Pollow, K. (1982) *Eur. J. Biochem.*, **125**, 249.
- Markaverich, B. M. and Clark, J. H. (1979) *Endocrinology*, **105**, 1458.

- Martin, R. G. and Ames, B. N. (1962) *J. Biol. Chem.*, **8**, 1392.
- Mattox, V. R., Litwiller, R. D. and Nelson, A. N. (1979) *J. Steroid Biochem.*, **10**, 167.
- McClennan, M. C., West, N. B., Tacha, D. B., Greene, G. L. and Brenner, R. M. (1984) *Endocrinology*, **114**, 2002.
- Nerei, I., Baccati, M. D., Piffanelli, A. and Lanza, G. (1976) *J. Steroid Biochem.*, **7**, 505.
- Panko, W. B., Watson, C. S. and Clark, J. H. (1981) *J. Steroid Biochem.*, **14**, 1311.
- Parikh, I., Sica, V., Nola, E., Puca, G. A. and Cuatrecasas, P. (1974) *Methods Enzymol.*, **34**, 670.
- Perrot-Applanat, M., Logeat, F., Groyer-Picard, M. T. and Milgrom, E. (1985) *Endocrinology*, **116**, 1473.
- Pertschuk, L. P., Tobin, E. H., Tanapat, P., Gaetjens, E., Carter, A. C., Bloom, N. D., Macchia, R. J. and Eisenberg, K. (1980) *J. Histochem. Cytochem.*, **28**, 799.
- Peterson, G. L. (1984) *Methods Enzymol.*, **91**, 95.
- Puca, G. A., Sica, V., Nola, V. and Bresciani, F. (1979) *J. Steroid Biochem.*, **11**, 301.
- Raam, S. (1986) *Steroids*, **47**, 337.
- Raam, S. and Vrabel, D. M. (1986) *Clin. Chem.*, **32**, 1496.
- Raam, S. and Vrabel, D. M. (1988) *Clin. Chem.*, **34**, 2053.
- Rataczak, T. and Hahnel, R. (1980) *J. Steroid Biochem.*, **13**, 439.
- Scatchard, G. (1949) *Ann. N. Y. Acad. Sci. USA*, **51**, 660.
- Schrader, W. T., Birnbaumer, M., Hughes, M. R., Wiegel, N., Grody, W. and O'Malley, B. (1981) *Rec. Prog. Horm. Res.*, **37**, 583.
- Sica, V., Parikh, I., Nola, E., Puca, G. A. and Cuatrecasas, P. (1973) *J. Biol. Chem.*, **248**, 6543.
- Sica, V. and Bresciani, F. (1979) *Biochemistry*, **18**, 2369.
- Siegel, L. M. and Monty, K. G. (1966) *Biochim. Biophys. Acta*, **112**, 346.
- Smith, R. G., D'Istria, M. and Van, N. T. (1981) *Biochemistry*, **20**, 5557.
- Welshons, W. V., Krummel, B. M. and Gorski, J. (1985) *Endocrinology*, **117**, 2140.
- Westphal, U. (1983) *J. Steroid Biochem.*, **19**, 1.

Cholecystokinin antagonist, proglumide, stimulates growth hormone release in the rat

E. VIJAYAN*† and S. M. McCANN

Department of Physiology, UTHSC Southwestern Medical Center, Dallas, Texas 75235, USA

*J. C. Bose School of Life Sciences, Pondicherry University, Pondicherry 605 104, India

MS received 18 September 1989; revised 9 April 1990

Abstract. Previous studies have revealed a stimulatory action of cholecystokinin on growth hormone release in the rat. To evaluate the physiologic significance of these effects we employed the cholecystokinin antagonist, proglumide and injected it intravenously and intraventricularly (third cerebral ventricle, 3V) to determine its actions on growth hormone. The experiments were performed in conscious, freely moving rats with indwelling cannulae in the 3V and/or external jugular vein. Intraventricular injection of 2 or 10 µg of proglumide significantly elevated plasma growth hormone concentrations in intact and castrated male rats and in ovariectomized females. Intravenous injections of 10 or 100 µg of proglumide were also effective in elevating growth hormone in a dose-related manner. Surprisingly, the response to the lower dose given intraventricularly was somewhat greater than that of the higher dose. We speculate that these stimulatory effects of proglumide given intraventricularly are due to the agonist action of proglumide at these doses since action of cholecystokinin itself is to increase plasma growth hormone following its intraventricular injection. The studies therefore do not establish a physiologically significant growth hormone-releasing action of brain cholecystokinin but provide more evidence that activation of cholecystokinin receptors in the brain can induce a stimulation of growth hormone release either by activation of the release of growth hormone-releasing hormone or by inhibition of the release of somatostatin or by a combination of these two actions.

Keywords. Plasma growth hormone; third ventricle cannulae; hypothalamus; cholecystokinin-antagonist; cholecystokinin-receptors.

Introduction

The release of growth hormone (GH) from the anterior pituitary is regulated mainly by two hypothalamic peptides, GH-release inhibiting hormone (SRIH, somatostatin) (Reichlin, 1983) and GH-releasing hormone (Guillemin *et al.*, 1982; Rivier *et al.*, 1982). Lesion and stimulation studies have revealed that the ventromedial nucleus (VMH) and the arcuate nucleus (ARC) of the hypothalamus are important structures in regulating GH release (Reichlin, 1985) and immunoreactive cholecystokinin (CCK) neuronal cell bodies were demonstrated in the VMH, the ARC and the medial perifornical region of the lateral hypothalamus in the rat (Straus *et al.*, 1978) which suggested a possible functional role for CCK in the hypothalamus (Dockray, 1983). To test this possibility, CCK-8 was injected into the 3V of ovariectomized, conscious rats. It produced significant elevations in plasma GH levels (Vijayan *et al.*, 1979). Since there was no effect on release of GH by

†To whom all correspondence should be addressed.

Abbreviations used: GH, Growth hormone; VMH, ventromedial nucleus; ARC, arcuate nucleus; CCK, cholecystokinin; LH, luteinizing hormone.

pituitaries incubated *in vitro*, we concluded that this effect was mediated hypothalamic action.

Proglumide, a derivative of glutamic acid, is a selective antagonist for receptors (Hahne *et al.*, 1981; Chiodo and Bunney 1983; Hsiao *et al.*, 1984; Wa *et al.*, 1984). The availability of such specific antagonists provides a powerful tool to further delineate the physiological role of CCK in the control of GH secretion. Consequently, we investigated the effect of intraventricular or intravenous injection of proglumide on the release of GH in unanesthetized rats.

Materials and methods

Virgin, female and male Sprague-Dawley rats (Sasco Laboratories, St. Louis, Missouri, USA), weighing 200–240 g, were housed under controlled conditions of light (on 0500–1900 h) and temperature ($24 \pm 1^\circ\text{C}$) with free access to rat chow and water. One week after arrival the rats were gonadectomized under ether anesthesia. Groups of intact males and rats 3 weeks after gonadectomy were used for the experiments.

One week prior to experimentation a 23 gauge stainless steel cannula was implanted in the 3V and one day prior to experiment an indwelling catheter was placed in the external jugular vein as described previously (Vijayan and McCann 1978). On the day of the experiment an extension of polyethylene tubing (PVC, 12" long) filled with heparin in 0.9% NaCl was attached to the distal end of the intravenous cannula and the animals were left undisturbed in individual cages for 60–120 min. During this time, a preinjection blood sample (0.8 ml) was withdrawn over a period of 60 s just prior to injection of proglumide or the saline diluent.

Proglumide (DL-4-benzamido-N, N-dipropyl-glutamic acid) was microinjected into the 3V in a volume of $2 \mu\text{l}$ of saline using a $10 \mu\text{l}$ Hamilton microsyringe as previously described (Vijayan *et al.*, 1979). The pH of the proglumide solution was similar to that of the physiologic saline. Control rats received an equal volume of saline by the appropriate route of injection. In all cases the injection was around 60 s and all experiments were performed in the morning between 0830–1100 h.

Blood samples (0.8 ml) were collected in heparinized syringes from the external jugular vein at varying intervals (see Results) while the animal was freely moving in the cage. The volume of each blood sample was replaced immediately after bleeding by an equivalent volume of saline. Plasma was separated by centrifugation at 3000 rpm at 4°C and stored frozen until the day of assay.

Radioimmunoassay

Plasma GH concentrations were measured by radioimmunoassay using the method provided by NIDDK and expressed in terms of the RP-1-NIH-GH standard. To eliminate inter assay variation, all samples from each experiment were run in the same assay in duplicate. The quality of assays was controlled according to

Intraventricular injection of 2 or 10 μg proglumide produced a significant elevation of plasma GH levels in intact male rats (figure 1A). The lower dose of 2 μg produced a sharp increase, reaching the peak at 30 min. The hormone levels decreased by 60 min but rose sharply again to peak values at 120 min after injection. Plasma GH levels rose gradually and remained significantly elevated for the 120 min duration of the experiment following the higher 10 μg dose.

Systemic intravenous injection of proglumide at this dose (10 μg) produced a delayed rise in plasma GH levels which became significant at 120 min, whereas the 100 μg dose was already effective at 60 min after the injection and values remained elevated at 120 min (figure 1B).

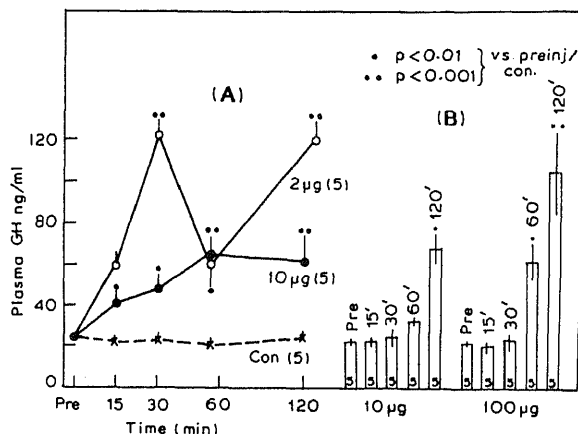


Figure 1. Effects of various doses of proglumide on plasma GH in male rats. (A) Third ventricular injection; (B) intravenous injection. Mean values of plasma GH are shown as symbols in A and by the height of the bars in this and subsequent figures. Vertical lines = SEM.

Intraventricular proglumide produced a dose-related increase in plasma GH in castrated male rats (figure 2A). The magnitude of the increase in GH levels were similar to those observed in intact males. Intravenous injection of proglumide in castrated males produced similar increases in hormone levels at 60 and 120 min as seen in the intact rats (figure 2B).

Ovairectomized rats

Intraventricular injection of 2 μg proglumide had no effect on plasma GH at 15 and 30 min but it increased significantly at 60 and 120 min after injection. The 10 μg dose, however, caused a significant increase only at 30 min following injection (figure 3A). Interestingly, the lower dose of 2 μg produced a greater stimulatory effect than the higher dose as was seen in intact male rats.

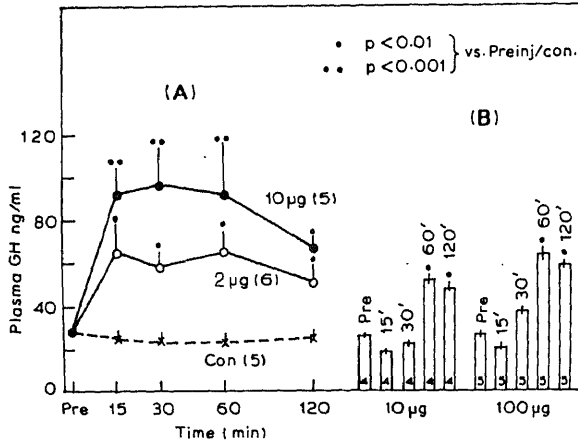


Figure 2. Effect of various doses of proglumide on plasma GH in castrated males.

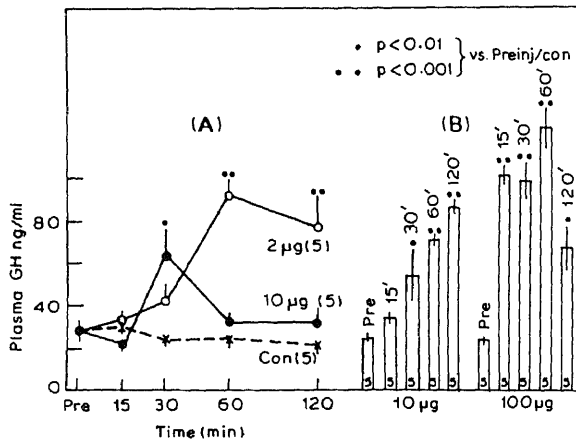


Figure 3. Effect of various doses of proglumide on plasma GH in ovariectomized rats.

Systemic injection, on the other hand, produced a dose-related increase in plasma hormone levels. The lower dose of 10 µg was effective at 30 min while the 100 µg dose was effective at 15 min following injection (figure 3B).

Discussion

The present results indicate that proglumide is a potent GH secretagogue *in vivo* in the rat. Interestingly the effect of proglumide on GH release appears to be identical to that of CCK. The dose of proglumide used, however, is much higher than the effective doses of CCK which stimulated GH release after third ventricular injections (Vijayan *et al.*, 1979). Since proglumide is a specific CCK antagonist one would expect a reversal of the CCK effects on hormone release. This was true in the case of luteinizing hormone (LH) and prolactin since proglumide had opposite

effects to those of CCK on plasma levels of LH and prolactin (Vijayan and McCann, 1986, 1987). In contrast, both doses of 3V and intravenous proglumide produced significant increases in GH release. This is very puzzling in view of the stimulatory effect of intraventricular CCK on GH release (Vijayan *et al.*, 1979). Intravenous injection of 10 μ g dose produced, time-related, progressive increase whereas 100 μ g dose caused significantly higher elevation in plasma GH levels. The responsiveness to intraventricular proglumide was nearly equal in intact males, castrated and ovariectomized rats. However, ovariectomized rats appear to be more sensitive to proglumide after intravenous dose as the hormone levels were significantly higher than in those of intact or castrated animals. Non-specific peripheral effects or the absence of ovarian steroids cannot be ruled out in the case of intravenous doses.

In the cases of both LH and prolactin, as the dose of proglumide was increased it no longer had opposite effects to those of CCK, which suggests that high doses of proglumide had an agonist action instead of an antagonist effect. We speculate that the ability of proglumide to elevate plasma GH may reflect a CCK agonist action. Further experiments with a more specific antagonist or with CCK-antiserum will be needed to establish this hypothesis. Proglumide may inhibit the release of somatostatin from neurons near the third ventricle. Alternatively, it may stimulate the release of growth hormone releasing hormone, or both action may occur. Since CCK coexists within and excites midbrain dopamine neurons (Chiodo and Bunny, 1983) and there is an involvement of central dopaminergic systems in pituitary hormone release (Vijayan and McCann, 1978), it would be of interest to ascertain if the actions of CCK and proglumide on GH release may be mediated by the dopaminergic system. Peripheral effects cannot be ruled out in the case of intravenous injections of proglumide.

Acknowledgement

This research was supported by NIH grant DK 10073.

References

- Chiodo, L. A. and Bunny, B. S. (1983) *Science*, **219**, 1449.
- Dockray, C. J. (1983) in *Brain peptides* (eds D. T. Krieger, M. J. Brownstein and J. B. Martin) (New York: John Wiley) p. 851.
- Guillemin, R., Brazeau, P., Bohlen, P., Esch, F. and Ling, N. (1982) *Science*, **218**, 585.
- Hahne, W. F., Jensen, R. J., Lemp, G. F. and Gardine, J. D. (1981) *Proc. Natl. Acad. Sci. USA*, **78**, 6304.
- Hsiao, S., Katsuura, G. and Itoh, S. (1984) *Life Sci.*, **34**, 2165.
- Reichlin, S. (1983) in *Brain peptides* (eds D. T. Krieger and J. B. Martin) (New York: John Wiley) p. 171.
- Reichlin, S. (1985) in *Textbook of endocrinology* (eds J. E. Wilson and D. W. Foster) (Philadelphia: W. B. Saunders) p. 492.
- Rivier, J., Spiess, J., Thorner, M. and Vale, W. (1982) *Nature (London)*, **300**, 276.
- Rodbrad, D., Rayford, P. L., Cooper and Ross, G. T. (1961) *J. Clin. Endocrinol.*, **28**, 1412.
- Straus, E., Muller, J. E., Chol, H., Paronetto, F. and Yalow, R. S. (1978) *Proc. Natl. Acad. Sci. USA*, **75**, 486.
- Vijayan, E., Samson, W. K. and McCann, S. M. (1979) *Brain Res.*, **172**, 295.
- Vijayan, E. and McCann, S. M. (1978) *Neuroendocrinology*, **25**, 150.
- Vijayan, E. and McCann, S. M. (1986) *Brain Res. Bull.*, **16**, 533.
- Vijayan, E. and McCann, S. M. (1987) *Life Sci.*, **40**, 629.
- Watkins, L. R., Kinschek, I. B. and Mayer, D. J. (1984) *Science*, **224**, 395.

Non-enzymatic glycosylation induced changes *in vitro* in some molecular parameters of collagen

A. N. RATHI and G. CHANDRAKASAN*

Biological Sciences Division, Central Leather Research Institute, Madras 600 020, India

MS received 15 May 1989; revised 2 April 1990

Abstract. Non-enzymatic glycosylation of rat tail tendon collagen was examined by incubation with D-glucose *in vitro*. The changes in molecular parameters such as viscosity, thermal stability, electrophoretic mobility and solubility were determined on non-enzymatically glycosylated collagen *in vitro*. Tendons incubated with 8 and 24 mg glucose/ml showed an increase in dissolution temperature and a 1.6–3-fold increase in thermal isometric tension respectively when compared to tendons incubated in the absence of glucose, indicating the formation of new intermolecular bonds. This conclusion was further supported by the decreased solubility of glycosylated collagen in 0.5 N acetic acid and the change in sub-unit composition as measured from the sodium dodecyl sulphate polyacrylamide gel electrophoresis pattern. Glycosylated collagen gave a characteristic absorption spectra (λ_{max} 248 nm) as distinct from that of control (λ_{max} 242 nm). Denaturation temperature of glycosylated collagen, as determined from temperature dependent viscosity measurements, was reduced. These studies indicate that glycosylation affects the molecular interactions as well as the crosslinking of collagen.

Keywords. Collagen; glycosylation; biophysical changes.

Introduction

Human collagen undergoes progressive browning with aging characterized by yellowing, fluorescence, insolubilization and decreased digestibility by proteolytic enzymes (Hamlin *et al.*, 1975; Schnider and Kohn, 1981). These changes appear to be accelerated in diabetes (Monnier *et al.*, 1984, 1988). Kohn and Schnider (1982) first noted that age-related rate of collagen cross-linking was increased in diabetes. The modifications of diabetic and aging collagen are attributed to the browning reaction which occurs as a consequence of non-enzymatic glycosylation.

Non-enzymatic glycosylation of proteins is initiated by the fixation of glucose on the ϵ -amino group of lysines and hydroxylysines. It depends on the blood glucose level and the duration of exposure (Higgins and Bunn, 1981). Earlier studies (Bailey, 1981; Perejda and Uitto, 1982) have indicated that several proteins become non-enzymatically glycosylated by endogenous free glucose. This phenomenon appears to be involved in at least some physiological alterations in insulin independent tissues e.g., the lens, nerves, basement membrane and connective tissue during diabetes and aging (Stevens *et al.*, 1978).

Studies *in vitro* indicate that glycosylation affects collagen fibrillogenesis (Guitton *et al.*, 1981) and enhances collagen potency to induce normal platelet aggregation (LePape *et al.*, 1983). The available evidence also indicates that non-enzymatic

*To whom all correspondence should be addressed.

Abbreviations used: 5-HMF, 5-Hydroxymethyl-2-furfuraldehyde; SDS, sodium dodecyl sulphate; PAGE, polyacrylamide gel electrophoresis.

glycosylation is able to influence the close packing of collagen fibres (Guitton *et al.*, 1984). Recently, we have reported variations in the extent of glycosylation of the soluble and insoluble fractions of collagen which differ in their degree of crosslinking. We have shown that salt soluble collagen is subject to non-enzymatic glycosylation to a greater extent. In the present paper additional data is given on some of the physico-chemical consequences of glucose fixation *in vitro* on rat tail tendons and on the collagen extracted from these tendons.

Materials and methods

Incubations in vitro

Rat tail tendons (20 mg wet wt.) from 1-year old rats were incubated in 15 ml of phosphate buffered saline in the presence of 3 mM azide at 37°C for 21 days in screw cap bottles. This formed the control. In a second batch, tendons were incubated with glucose solutions (8 and 24 mg/ml, respectively) added to the above medium as reported by Kent *et al.* (1985).

Isometric tension experiments

After incubation *in vitro* tendons were blotted dry and placed between the jaws of a hydrothermal isometric tension apparatus. The length of the tendon between the jaws was measured with vernier callipers and the tendon was immersed in phosphate buffered saline at 30°C. The temperature was raised to 90°C at a rate of 1°C/min. Tension generated was continuously recorded. After the experiment, the tendon was cut close to the jaws with a scalpel, dried and weighed. Tension was measured as kg/mg dry wt. of tendon per cm which in turn is proportional to force/unit cross sectional area. The temperature up to which tension was steady before showing a rise was taken as the shrinkage temperature and the temperature at which the tendon relaxed after reaching a maxima was taken as the dissolution temperature.

Preparation of collagen

Acid soluble collagen from tendons incubated *in vitro* was prepared by the acetic acid solubilisation and sodium chloride precipitation method of Chandrakasan *et al.* (1976).

Viscosity studies

Denaturation temperature was determined by measuring the viscosity (using an Ubbelohde viscometer) of a 0.06% solution of collagen in 0.01 M acetic acid (pH 3.7) by stepwise raise in temperature from 20°–40°C.

Denaturation temperature (T_d) was taken as that temperature at which change in viscosity was half complete.

Extent of glycosylation

Glycosylation of freeze-dried collagen from the above studies was measured after hydrolysis of the samples in 1 N oxalic acid for 3.5 h at 96°C. The quantity of 5-hydroxymethyl-2-furfuraldehyde (5-HMF) was determined colorimetrically at 443 nm using the thiobarbituric acid reaction (Fischer *et al.*, 1980) with some modification as described by Trueb *et al.* (1984).

Sodium dodecyl sulphate polyacrylamide gel electrophoresis

Sodium dodecyl sulphate (SDS) polyacrylamide gel electrophoresis (PAGE) of the different samples was done using a 5% running gel and a 3% stacking gel (Laemmli 1970) using a BioRad vertical slab gel apparatus. Gels were stained with Coomassie brilliant blue R-250, destained and scanned using a scanning densitometer (Hoefer scientific instrument GS 300)

Absorbance

Absorbance spectra of the different collagen samples was recorded after solubilisation in 0.5 N acetic acid at a concentration of 1 mg/ml in a Shimadzu UV-visible spectrophotometer.

Solubility experiments

Solubility of tendons, control and glycosylated *in vitro* was measured as follows: Tendons were blotted dry and cut into small pieces with a scalpel. Acetic acid (0.5 N) was added to give an approximate concentration of 5 mg wet wt. of tendon/ml. After 2 h at room temperature with shaking, the solubilized material was separated by centrifugation. The residue and the supernatant fractions were freeze dried and hydrolysed in 6 N HCl at 110°C for 24 h. HCl was removed and hydroxyproline content was measured (Woessner, 1961).

Results

The physicochemical parameters of control and *in vitro* glycosylated rat tail tendon collagen is given in table 1. The extent of glycosylation estimated as 5-HMF/mg collagen increased significantly upon incubation with 8 and 24 mg glucose/ml by 1.5- and 2.1-fold, respectively. As seen from the table 1 and figure 1, denaturation temperature determined from viscosity measurements of samples submitted to increasing temperature, was reduced from 37°C in control samples to 30.5°C in samples incubated with 24 mg glucose/ml.

Thermal isometric contraction/relaxation is a well known method for the characterization of the stability of collagen. Shrinkage and dissolution temperatures of tendons incubated *in vitro* were recorded from the plot of isometric tension values temperature (figure 2). Shrinkage temperature remained unaltered whereas a significant variation was observed in the dissolution temperature of control (67°C)

Table 1. Physicochemical parameters of control and *in vitro* non enzymatic glycosylated rat tail tendon collagen.

Parameter	Control	Incubated with 8 mg/ml glucose	Incubated with 24 mg/ml glucose
Non enzymatic glycosylation mol/mg collagen	3.2	5.0	6.8
Thermal denaturations temperature (T_d)°C	37.0	35.0	30.5
Shrinkage temperature (°C)	59.0	60.0	60.0
Dissolution temperature (°C)	67.0	72.0	90.0
Subunit composition	35:56:9	26:44:30	15:39:46

Values are mean of 4 experiments.

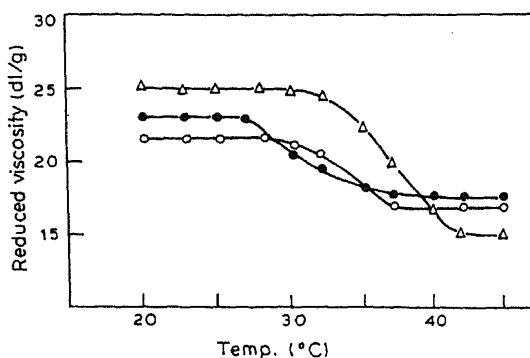


Figure 1. Thermal denaturation curves of control (Δ) and *in vitro* glycosylated collagens with 8 mg glucose/ml (\bullet) and 24 mg glucose/ml (\circ).

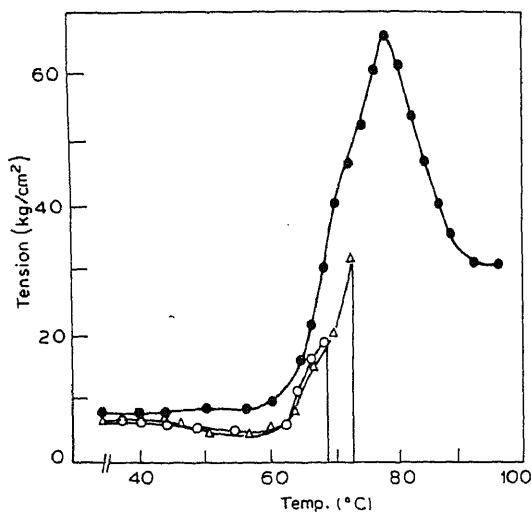


Figure 2. Hydrothermal isometric tension curves from control (\circ) and glycosylated rat tail tendons incubated with 8 mg glucose/ml (Δ) and 24 mg glucose/ml (\bullet). Values are mean of 4 experiments. Tension values are normalised to mg wet wt./cm length and plotted against temperature.

Glycosylated tendons reached a maximum tension of 51 kg/cm² and 36 kg/cm² compared to 19 kg/cm² of control tendons (figure 2). The contraction force of tendons increases with increasing age (Verzar, 1964). This phenomenon has been shown to be associated with a decrease in the density of reducible cross links within the collagen (Allain *et al.*, 1978) and their conversion to multivalent covalent cross links during maturation which are stable under the conditions of thermal contraction. About 2.6 and 1% of tendons glycosylated *in vitro* were solubilised in 0.5 N acetic acid after 2 h at room temperature, whereas 4.4% of non-glycosylated tendon was solubilised under similar experimental conditions.

The absorption spectra of control and glycosylated collagen are shown in figure 3. Collagen incubated with 24 mg of glucose gave a maximum absorption at 248 nm whereas collagen incubated with 8 mg of glucose gave an absorption maxima at 243 nm indicating a change in absorption relative to the extent of glycosylation. Monnier *et al.* (1988) have observed an increase in collagen linked chromophores and fluorophores in experimental hyperglycemia analogous to those of diabetic and aging individuals.

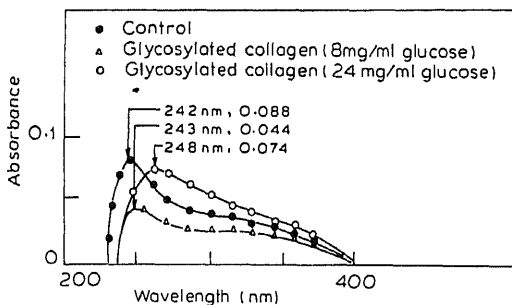


Figure 3. Absorption spectra of tendon collagen from control (●) and glycosylated rat tail tendons incubated with 24 mg glucose/ml (○) or with 8 mg glucose/ml (△). Collagen concentration was adjusted to 1 mg/ml for each sample. Absorbance peak values are indicated at the respective wavelengths.

Variations are also seen in the electrophoretic pattern of collagen from glycosylated and control tendons on SDS-PAGE (table 1). The proportion of α - and β -subunits were decreased together with a concomitant increase of γ and high molecular weight components in glycosylated collagen.

Discussion

During aging, collagen becomes less soluble, less susceptible to proteolytic enzymes and increasingly stronger and more rigid (Light and Bailey, 1979). These changes have always been attributed to the accumulation of covalent cross links between collagen molecules derived from amino acid side chains and appear to be accelerated in diabetes (Trueb *et al.*, 1984). Recent studies by Monnier *et al.* (1988) have shown that diabetes and aging associated collagen linked fluorescence and

crosslinking can be duplicated by incubating collagen with glucose. In the present paper, the denaturation temperature determined from viscometric studies indicates a lowering in intermolecular interactions of glycosylated collagen. Guitton *et al.* (1984) have shown that reduced viscosity of glycosylated collagen is significantly decreased when compared to the control at the same concentration and shear stress, but the molecular structure of acid soluble collagen is unaffected as evaluated by circular dichroism and differential spectrometry. Isometric tension studies have demonstrated that glycosylated tendons show elevated hydrothermal tension and dissolution temperature and that the effect is dependent on the extent of glycosylation. This can be explained only by the presence of covalent, heat stable intermolecular bonds formed as a consequence of glycosylation. Further, this interpretation is supported by the decreased solubility of tendon, glycosylated *in vitro*. Our data is consistent with previous reports on the crosslinking, tensile strength and turnover of newly synthesized less crosslinked collagen, incubated with glucose *in vitro* (Andreassen *et al.*, 1981; Kent *et al.*, 1985; Rathi *et al.*, 1989a).

Glucose and other sugars inhibit collagen fibrillogenesis, a critical step in the crosslinking of collagen *in vitro* (Rathi *et al.*, 1989b). This effect is due to the decrease in the hydrophobic interaction induced by the addition of hydrophilic groups such as the hydroxyl functions from glucose (Guitton *et al.*, 1984).

Cerami *et al.* (1979) have found that prolonged incubation of lens crystallin with glucose was necessary before stable dimers and trimers could be formed. Pognor *et al.* (1984) have postulated that an imidazole compound incorporating two glucose molecules is the possible crosslinking group formed during prolonged incubation *in vitro*. Glucose derived pyrrolic structures have also been identified in a model system in which physiologic conditions of pH and temperature (Njoroge *et al.*, 1987) were used. The shift in the absorption spectra observed in our study supports the concept that a novel compound is formed upon glycosylation, although its actual chemical structure is unknown. These data indicate that incubation *in vitro* can serve as a model system for the study of physicochemical changes in collagen mediated by non-enzymatic glycosylation.

Acknowledgement

The authors thank Dr. R. B. Mitra for permission to publish this work.

References

- Allain, J. C., Le Lous, M., Bazin, S., Bailey, A. J. and Delaunay, A. (1978) *Biochim. Biophys. Acta.*, **533**, 147.
- Andreassen, T. T., Seyer, H. K. and Bailey, A. J. (1981) *Biochem. J.*, **117**, 819.
- Bailey, A. J. (1981) *Horm. Metab. Res. (Suppl.)*, **11**, 90.
- Cerami, A., Stevens, V. J. and Monnier, V. M. (1979) *Metab. Clin. Exp.*, **28**, 431.
- Chandrasekaran, G., Torchia, D. A. and Piez, K. A. (1976) *J. Biol. Chem.*, **251**, 6062.
- Fischer, R. W., DeJong, C., Voight, E., Berger, W. and Winterhalter, K. H. (1980) *Clin. Lab. Haematol.*, **2**, 129.
- Guitton, J. D., LePape, A. and Muh, J. P. (1984) *Collagen Rel. Res.*, **4**, 253.
- Guitton, J. D., LePape, A., Sizarpet, P. Y. and Muh, J. P. (1981) *Biosci. Rep.*, **1**, 945.
- Hamlin, C. R., Kohn, R. R. and Luschin, J. H. (1975) *Diabetes*, **24**, 902.

- Higgins, P. J. and Bunn, H. F. (1981) *J. Biol. Chem.*, **265**, 5204.
- Kohn, R. R. and Schnider, S. L. (1982) *Diabetes (Suppl. 3)*, **31**, 47.
- Kent, M. J. C., Light, N. D. and Bailey, A. J. (1985) *Biochem. J.*, **225**, 745.
- Laemmli, U. K. (1970) *Nature (London)*, **227**, 680.
- LePape, A., Guitton, J. D., Gutman, N., Legard, Y., Fauvel, F. and Muh, J. P. (1983) *Haemostasis*, **13**, 36.
- Light, N. D. and Bailey, A. J. (1979) *FEBS Lett.*, **97**, 183.
- Monnier, V. M., Kohn, R. R., Cerami, A. (1984) *Proc. Natl. Acad. Sci. USA*, **81**, 583.
- Monnier, V. M., Sell, D. R., Abdul-Karim, F. W. and Emancipator, S. N. (1988) *Diabetes*, **37**, 867.
- Njoroge, F. G., Sayre, L. M., Monnier, V. M. (1987) *Carbohydr. Res.*, **167**, 211.
- Pognor, S., Ulrich, P. C., Benssath, F. A. and Cerami, A. (1984) *Proc. Natl. Acad. Sci. USA*, **81**, 2684.
- Perejda, A. J. and Uitto, J. (1982) *Collagen Rel. Res.*, **2**, 81.
- Rathi, A. N., Asokan, R. and Chandrakasan, G. (1989a) *Biochem. Med. Metab. Biol.*, **41**, 70.
- Rathi, A. N., Padmavathi, S. and Chandrakasan, G. (1989b) *Biochem. Med. Metab. Biol.* (in press).
- Schnider, S. L. and Kohn, R. R. (1981) *J. Clin. Invest.*, **67**, 1630.
- Stevens, J. J., Rouzier, C. A., Monnier, V. M. and Cerami, A. (1978) *Proc. Natl. Acad. Sci. USA*, **75**, 2918.
- Trueb, B., Fluckiger, R. and Winterhalter, K. H. (1984) *Collagen Rel. Res.*, **4**, 239.
- Verzar, F. (1964) *Int. Rev. Connect. Tissue Res.*, **2**, 243.
- Voessner, J. F. (1961) *Arch. Biochem. Biophys.*, **93**, 440.

Effect of doxorubicin on the intestinal membranes in rats—Influence of α -tocopherol administration

A. GEETHA, R. SANKAR, THANKAMANI MARAR and
C. S. SHYAMALA DEVI

Department of Biochemistry, University of Madras, Guindy Campus, Madras 600 025, India

MS received 31 October 1989; revised 2 February 1990

Abstract. The effect of α -tocopherol on doxorubicin induced changes in intestinal brush border and basolateral membranes were studied in rats. Rats were treated with doxorubicin (2.5 mg/kg body wt.), intravenously, weekly for 8 weeks. α -Tocopherol (400 mg/kg body wt.) was given orally, daily for 2 months. Intestinal basolateral membrane bound ATPases and brush border membrane bound alkaline phosphatase activities were found to be decreased significantly in doxorubicin treated rats. The lipid peroxide level was found to be elevated with a significant depletion in membrane sulphydryl groups. In α -tocopherol co-administered animals, the enzyme activities were found to be restored with concomitant reduction in lipid peroxide levels and an increase in the membrane sulphydryl groups. The membrane cholesterol and phospholipid levels which were altered in doxorubicin treated animals were found to be maintained significantly. The results are discussed with reference to the effect of α -tocopherol on lipid peroxidation and membrane sulphydryl groups.

Keywords. Doxorubicin; intestine; basolateral membrane; brush border membrane; ATPases; alkaline phosphatase; sulphydryl groups; α -tocopherol; antioxidant.

Introduction

A major cause of morbidity from cancer chemotherapeutic drugs has been suggested to be due to their toxic side effects on the gastro-intestinal tract (Slavin *et al.*, 1978). The drugs that cause such effects on gastro-intestinal tract are mustine, decarbazine cisplatin, lomustine, cyclophosphamide and doxorubicin (George and Holdstock, 1985).

Doxorubicin is an anthracycline antibiotic which is active against a wide range of experimental and human solid tumors (Carter, 1975). The therapeutic usefulness of doxorubicin is seriously limited by the occurrence of cardio toxicity associated with lipid peroxidation (Singal *et al.*, 1983). Generally, biological membranes have been reported to be susceptible for lipid peroxidation because of the presence of polyunsaturated fatty acids in their phospholipids (Tappel, 1973).

The epithelial cells of the mammalian small intestine are polarised in that the plasma membrane is divided into apical brush border and basolateral regions where digestion and absorption of nutrients takes place (Maestracci, 1976).

Since the accumulation of lipid peroxides introduces hydrophilic moieties into the membrane hydrophobic phase, in the present investigation the effect of doxorubicin on intestinal membrane bound enzymes was studied in rats. The sulphydryl groups are important for the functional integrity of membranes and hence the sulphydryl content was determined along with lipid peroxide levels.

Male wistar rats obtained from Central Leather Research Institute, Madras were used for the study. The rats were maintained with food and water *ad libitum*. The rats were divided into 4 groups. Group 1 served as control. Group 2 rats were injected doxorubicin (2.5 mg/kg body wt.), once a week for 8 weeks, intravenously (Richard, 1986). Group 3 rats were administered α -tocopherol orally, daily for a period of 60 days, Group 4 animals received both doxorubicin and α -tocopherol as described for group 2 and 3 rats.

After the experimental period, rats were killed by cervical decapitation. The small intestine was removed and washed with ice-cold water and the mucosa were scrapped using glass slides. Brush border membrane (BBM) was isolated according to the method of Kessler *et al.* (1970). Isolation of basolateral membrane (BSM) was carried out by the method of Mircheff and Wright (1976). Na^+ , K^+ -ATPase (Bonting, 1970) and Ca^{2+} -ATPase (Hjerten and Pan, 1983) activities were determined in the BSM. BBM was used for the assay of alkaline phosphatase (King, 1965). Lipid peroxide levels were assessed by the method of Utley *et al.* (1967). Membrane preparation (0.5 ml) containing 100–150 μg of protein was treated with 2 ml of 20% trichloroacetic acid and 4 ml of 0.67% thiobarbituric acid. The mixture was heated in a boiling water bath for 20–25 min. The colour developed was measured at 533 nm and compared with the standard tetramethoxy propane treated in a similar manner. The values were expressed as nmol malonaldehyde per mg protein. Membrane cholesterol (Parekh and Jung, 1970) and phospholipids (Zilversmit and Davis, 1950) were estimated after extracting the total lipids by using Folsch *et al.* (1957) method.

The protein sulphhydryl contents of the membranes were determined by the method of Ellman (1959). Membrane preparation (0.5 ml) was made up to 2 ml with 0.2 M phosphate buffer pH 8. Five ml of water and 0.02 ml of dithiobisnitro benzoic acid (39.6 mg/10 ml buffer) were added. The colour developed was measured at 412 nm. Values were expressed in terms of glutathione content. Protein was estimated by the method of Lowry *et al.* (1951).

Student's 't' test was conducted for statistical analysis.

Results

Table 1 shows the activities of Na^+ , K^+ -ATPase and Ca^{2+} -ATPase in BSM and alkaline phosphatase in BBM of control and experimental rats. Doxorubicin treatment resulted in a significant decrease in ATPase and alkaline phosphatase activities. The enzyme activities were restored in α -tocopherol co-administered rats (group 4). There was a significant increase in the activities of these enzymes in rats that received only α -tocopherol ($P < 0.05$).

Table 2 presents the levels of lipid peroxides and the sulphhydryl content in intestinal BSM and BBM of control and experimental rats. Statistically significant increase was observed in lipid peroxide levels of both the membranes in

Table 1. Activities of intestinal BSM ATPases and BBM alkaline phosphatase in control and experimental animals.

Group	BSM (μmol of phosphorous liberated/min/mg protein)		BBM (μmol of phenol liberated/min/mg protein)
	Na ⁺ K ⁺ ATPase activity	Ca ²⁺ ATPase activity	Alkaline phosphatase activity
1	8.6 \pm 0.16	2.5 \pm 0.20	6.0 \pm 0.32
2	4.9 \pm 0.21**	1.5 \pm 0.05**	4.2 \pm 0.21**
3	9.0 \pm 0.52 ^{NS}	2.9 \pm 0.32*	6.5 \pm 0.36*
4	7.6 \pm 0.72 ^{NS}	2.2 \pm 0.28 ^{NS}	5.7 \pm 0.42 ^{NS}

The values are expressed as mean \pm SD for 6 animals in each group. Statistically significant variations when compared to control are expressed as * P < 0.05; ** P < 0.001. NS, Not significant.

Table 2. Levels of lipid peroxides and sulphhydryl content in intestinal BBM and BSM of control and experimental animals.

Group	Lipid peroxides (nmol MDA/mg protein)		Sulphydryl content (μg glutathione/mg protein)	
	BBM	BSM	BBM	BSM
1	4.2 \pm 0.21	8.2 \pm 0.31	3.0 \pm 0.35	5.2 \pm 0.21
2	7.2 \pm 0.32**	15.35 \pm 0.81**	1.8 \pm 0.04**	2.6 \pm 0.10**
3	3.0 \pm 0.20**	6.2 \pm 0.29**	3.4 \pm 0.31*	5.6 \pm 0.52 ^{NS}
4	4.8 \pm 0.41*	9.2 \pm 1.40 ^{NS}	2.75 \pm 0.25 ^{NS}	4.87 \pm 0.43 ^{NS}

Values are expressed as mean \pm SD for 6 animals in each group.

Statistically significant variations when compared to control are expressed as * P < 0.05; ** P < 0.001. NS, Not significant.

doxorubicin treatment (group 2). α -Tocopherol + doxorubicin treated rats showed low levels of lipid peroxides when compared to that which received only doxorubicin. In rats that received only α -tocopherol the lipid peroxide levels was very much reduced than that of control rats. There was a drastic depletion of the sulphhydryl content of BSM and BBM in doxorubicin treatment (group 2). α -Tocopherol was found to counteract the effect of doxorubicin in this regard.

Levels of cholesterol and phospholipids in intestinal BSM and BBM are presented in table 3. Cholesterol levels increased significantly but the phospholipid level was decreased in doxorubicin treated rats (group 2). As a result of this, the cholesterol/phospholipid ratio increased. Cholesterol/phospholipid, ratio one of the many factors which maintains membrane fluidity, was restored in doxorubicin + α -tocopherol treated rats to normal levels.

Discussion

The lipid peroxidative nature of doxorubicin might have been responsible for the alterations observed in the small intestinal BSM and BBM bound enzyme activities. This was evidenced by the high lipid peroxide levels in group 2 rats. Lipid peroxidation in biological membrane systems has been postulated to proceed through a complex process *i.e.* it involves a rearrangement and destruction of the double bonds in unsaturated lipids by propagation of lipid free radicals formed

Table 3. Levels of cholesterol and phospholipids in intestinal BBM and BSM of control experimental animals.

	Groups			
	1	2	3	4
BBM				
Cholesterol (C) ($\mu\text{mol}/\text{mg}$ protein)	0.264 ± 0.01	$0.395 \pm 0.015^{***}$	$0.260 \pm 0.01^{\text{NS}}$	0.265 ± 0.009
Phospholipid (P) ($\mu\text{mol}/\text{mg}$ protein)	0.194 ± 0.005	$0.145 \pm 0.003^{**}$	$0.200 \pm 0.007^{\text{NS}}$	0.185 ± 0.01
C/P molar ratio	1.360 ± 0.05	$2.741 \pm 0.04^{**}$	$1.30 \pm 0.1^{\text{NS}}$	$1.432 \pm 0.1^*$
BSM				
Cholesterol (C) ($\mu\text{mol}/\text{mg}$ protein)	0.601 ± 0.031	$0.651 \pm 0.03^{**}$	$0.590 \pm 0.030^{\text{NS}}$	0.615 ± 0.015
Phospholipid (P) ($\mu\text{mol}/\text{mg}$ protein)	0.515 ± 0.025	$0.385 \pm 0.03^{***}$	$0.500 \pm 0.02^{\text{NS}}$	0.510 ± 0.02
C/P molar ratio	1.167 ± 0.04	$1.690 \pm 0.05^{***}$	$1.180 \pm 0.06^{\text{NS}}$	1.205 ± 0.05

Values are expressed as mean \pm SD for 6 animals in each group.

Statistically significant variations when compared to control are expressed as $*P < 0.05$; $**P < 0.01$; $***P < 0.001$.

NS, not significant.

during lipid peroxidation (Svingen *et al.*, 1979). The formation of the hydroperoxides in membrane would result in damage of the membrane structure and inactivation of membrane bound enzymes (Lai and Piette, 1978; Fridovich and Porter, 1981). The accumulation of lipid peroxides introduces hydrophilic moiety into the membrane hydrophobic phase and thus alters membrane permeability and cell functions (Plaa and Witschi, 1976).

Doxorubicin has been shown to be a potential source of free radicals. In *in vitro* studies doxorubicin has been shown to form semiquinone free radical intermediate in the presence of flavin enzymes. This quinone-semiquinone reaction and formation of free radicals and increased peroxidation of polyunsaturated fatty acids have been recognised as one of the possible biochemical mechanisms for the generation of membrane injury (Hess *et al.*, 1982).

Reduced glutathione and other sulphydryl groups protect the cell membrane against free radical attack. In many cases the inhibition of enzymes by a quinone was considered to be due to the attack of the sulphydryl groups essential for the catalytic activity of the enzyme (Ostenhoff-Hoffman, 1963). This was confirmed by a report stating that the inhibition by the quinones was reversed by cysteine or glutathione (Dimonte *et al.*, 1984).

Nicotera *et al.* (1985) has associated the loss of membrane sulphydryl groups with the inactivation of Ca^{2+} -dependent ATPase. Na^+ , K^+ -ATPase which is involved in active transport was reported to contain essential sulphydryl groups (Glynn and Karlsh, 1975). Treatment of the purified enzyme with sulphydryl reagents was reported to result in the inhibition of the activity. So the observed decrease in BSM-ATPases activities could have been due to the sulphydryl group depletion by the nature of doxorubicin through lipid peroxidation. Pascoe and Reed (1982) demonstrated that the prevention of doxorubicin-associated toxicity by α -tocopherol was due to the maintenance of cellular thiols.

Doxorubicin treatment resulted in a drastic change in membrane lipid components such as cholesterol and phospholipids. The membrane cholesterol/phospholipid ratio is one of the many factors which governs the membrane fluidity. Fluidity of the membrane is responsible for the functioning of membrane bound enzymes and various other transport processes (Thilo *et al.*, 1977). Carlson and Bottiger (1972) have demonstrated that Ca^{2+} -ATPase requires phospholipid environment for its activity. The results showed the decrease in the levels of membrane phospholipids as well as Ca^{2+} -ATPase activity.

α -Tocopherol is a major component of vitamin E and is capable of protecting unsaturated lipids from non enzymatic autooxidation processes *in vivo* (Deduve and Hayaishi, 1978). This function of α -tocopherol has been reported to be assisted by a specific interaction with membrane arachidonic acids (Lucy, 1973). Hydrophobic and hydrogen bonding have also been reported (Diplock and Lucy, 1975; Srivastava *et al.*, 1983). The observed protection rendered by α -tocopherol against doxorubicin-induced changes in intestinal membranes could have also been due to its effect on membrane lipids.

Acknowledgement

The financial assistance by the Council of Scientific and Industrial Research, New Delhi to A.G. and R.S. is gratefully acknowledged.

References

- Bonting, S. L. (1970) in *Membrane and ion transport* (ed. E. E. Bilter) (London: Wiley Interscience) Vol. 1, p. 257.
- Carlson, C. A. and Bottiger, L. E. (1972) *Lancet*, **1**, 865.
- Carter, S. K. (1975) *J. Natl. Cancer Inst.*, **55**, 1265.
- Deduve, C. and Hayaishi, O. (1978) *Tocopherol, oxygen and biomembranes* (Amsterdam: Elsevier, North Holland Biochemical Press).
- Dimonte, D., Bellamo, G., Thor, H., Nicotera, P. and Orrhenius, S. (1984) *Arch. Biochem. Biophys.*, **235**, 343.
- Diplock, A. T. and Lucy, J. A. (1973) *FEBS Lett.*, **29**, 205.
- Ellman, G. C. (1959) *Arch. Biochem. Biophys.*, **82**, 70.
- Folsch, J., Lees, M. and Stanley, G. H. (1957) *J. Biol. Chem.*, **226**, 497.
- Fridovich, S. and Porter, N. A. (1981) *J. Biol. Chem.*, **256**, 260.
- George, C. F. and Holdstock, C. E. (1985) *Disorders of the small intestine* (London: Blackwell Scientific Publication).
- Glynn, I. M. and Karlsh, S. J. (1975) *Annu. Rev. Biophys.*, **256**, 167.
- Hess, M. L., Manson, N. H. and Okabe, E. (1982) *Can. J. Physiol. Pharmacol.*, **60**, 1382.
- Hjerten, S. and Pan, H. (1983) *Biochim. Biophys. Acta*, **728**, 281.
- Kessler, M., Austo, O., Storelli, C., Murer, H., Muller, M. and Senenza, G. (1970) *Biochim. Biophys. Acta*, **506**, 136.
- King, J. (1965) *Practical clinical enzymology* (London: D. Von Nostrand Co.).
- Lai, C. S. and Plette, C. H. (1978) *Arch. Biochem. Biophys.*, **190**, 27.
- Lowry, O. H., Rosebrough, N. J., Farr, A. L. and Randall, R. J. (1951) *J. Biol. Chem.*, **193**, 265.
- Lucy, J. A. (1973) *FEBS Lett.*, **29**, 205.
- Maestracci, D. (1978) *Biochim. Biophys. Acta*, **433**, 81.
- Mircheff, A. K. and Wright, E. M. (1976) *J. Membr. Biol.*, **28**, 309.
- Nicotera, P., Moore, M., Mirachelli, F., Bellamo, G. and Orrhenius, S. (1985) *FEBS Lett.*, **163**, 136.
- Ostenhoff-Hoffman, O. (1963) in *Metabolic inhibitors—A comprehensive treatise* (eds R. M. Hochester and J. H. Quastel) (London, New York: Academic Press) Vol. 11, p. 145.

- Pascoe, G. A. and Reed, D. J. (1987a) *Arch. Biochem. Biophys.*, **256**, 150.
- Pascoe, G. A. and Reed, D. J. (1987b) *Arch. Biochem. Biophys.*, **256**, 159.
- Parekh, A. L. and Jung, D. H. (1970) *Anal. Chem.*, **42**, 1423.
- Plaa, G. L. and Witschi, H. (1976) *Annu. Rev. Pharmacol. Toxicol.*, **16**, 125.
- Richard, J. A. (1986) *J. Pharmacol. Exp. Therap.*, **236**, 197.
- Singal, P. K., Beamish, R. E. and Dhalla, N. S. (1983) *Adv. Exp. Med. Biol.*, **161**, 391.
- Slavin, R. E., Dias, M. A. and Saral, R. (1978) *Cancer*, **42**, 1747.
- Srivastava, S., Phadlke, R. S., Govil, G. and Rao, C. N. R. (1983) *Biochim. Biophys. Acta*, **734**, 5892.
- Svingen, B. A., Buege, J. A., O'Neal, F. O. and Aust, S. D. (1979) *J. Biol. Chem.*, **254**, 5892.
- Tappel, A. L. (1973) *Fed. Proc.*, **32**, 1870.
- Thilo, L., Trauble, H. and Ovarath, P. (1977) *Biochemistry*, **16**, 1283.
- Utey, H. G., Berheim, F. and Hochstein, P. (1967) *Arch. Biochem. Biophys.*, **118**, 29.
- Zilversmit, D. E. and Davis, A. K. (1960) *J. Lab. Clin. Med.*, **35**, 155.

Analysis, characterization and diagnostic use of circulating filarial antigen in bancroftian filariasis

K. A. PARKHE, M. V. R. REDDY, K. CHEIRMARAJ,
P. RAMAPRASAD and B. C. HARINATH*

Department of Biochemistry, Mahatma Gandhi Institute of Medical Sciences, Sevagram,
Wardha 442 102, India

MS received 16 August 1989; revised 19 February 1990

Abstract. Sodium dodecyl sulphate-polyacrylamide gel electrophoresis of circulating filarial antigen fraction-2 isolated from plasma of microfilaraemic patients with *Wuchereria bancrofti* infection has shown 21 bands with molecular weights ranging from 12 to ≥ 120 kDa. The gel (12 cm) was sliced at an interval of one cm and the eluates of all the gel slices viz., CFA2-1 to CFA2-12 showed the presence of filarial antigen by sandwich enzyme-linked immunosorbent assay. The low molecular weight circulating filarial antigen fractions were found to share a common epitope with *Wuchereria bancrofti* microfilariae excretory-secretory antigen and urinary filarial antigen. The 3 antigen fractions CFA2-1, CFA2-9 and CFA2-12 showed higher sensitivity in detecting filarial immunoglobulin M antibodies than immunoglobulin G antibodies. However CFA2-9 fraction was found useful in serological differentiation of microfilaraemics from those with disease manifestations when filarial immunoglobulin G antibodies were detected. The antigenic epitope of CFA2-1 appears to be a carbohydrate, whereas CFA2-9 appears to be protein in nature.

Keywords. Enzyme linked immunosorbent assay; filarial serum immunoglobulin G; circulating filarial antigen; sodium dodecyl sulphate; polyacrylamide gel electrophoresis.

Introduction

Antigens released *in vitro* or *in vivo* have been of considerable interest in immunodiagnosis (Harinath, 1986). Analysis and characterization of the filarial antigens may be useful in identifying a suitable antigen for detection of filarial infection. Circulating filarial antigens (CFA) have been detected in humans infected with *Wuchereria bancrofti* (Au *et al.*, 1981; Kaliraj *et al.*, 1981; Dasgupta *et al.*, 1984; Hamilton *et al.*, 1984; Dissanayake *et al.*, 1984; Forsyth *et al.*, 1985; Weil *et al.*, 1986), *Brugia malayi* (Au *et al.*, 1981) and *Onchocerca volvulus* (Ouaisi *et al.*, 1981; Desmoutis *et al.*, 1983) and in animals infected with *Dirofilaria immitis* (Weil *et al.*, 1985), *Brugia pahangi* (Au *et al.*, 1981) and *Litomosoides carinii* (Dasgupta and Bala, 1978). In the previous studies from our laboratory an active CFA fraction-2 (CFA2) was isolated from microfilaraemic plasma and it was shown to be sensitive in detecting filarial immunoglobulin M (IgM) antibodies in patient's sera (Reddy *et al.*, 1986). This paper reports analysis of CFA2 by sodium dodecyl sulphate (SDS)

*To whom all the correspondence should be addressed.

Abbreviations used: CFA, Circulating filarial antigen; IgM, immunoglobulin M; SDS, sodium dodecyl sulphate; PAGE, polyacrylamide gel electrophoresis; Wb mf ES Ag, *Wuchereria bancrofti* excretory-secretory antigen; UFA, urinary filarial antigen; DEC, diethylcarbamazine; IgG, immunoglobulin G; FSIgG, filarial serum IgG, SPB, sodium phosphate buffer; ELISA, enzyme linked immunosorbent assay;

polyacrylamide gel electrophoresis (PAGE), detection of antigen levels in different SDS-PAGE fractions of CFA2, their characterization and diagnostic importance in detection of filariasis.

Materials and methods

Sera

Blood samples were collected from filarial patients (both microfilariae positive individuals and patients with clinical manifestations like elephantiasis, hydrocoele etc.) living in Sevagram and its surrounding villages which are endemic for filariasis. Blood samples were also collected from healthy individuals living in endemic region without any history of filariasis (endemic normal) and from healthy individuals living in regions non-endemic for filariasis (non-endemic normals) such as Punjab and Kashmir. Sera were separated and stored at -20°C with the addition of 0.1% sodium azide as preservative.

Circulating filarial antigen

Circulating filarial antigen was prepared as described by Reddy *et al.* (1986). Microfilariae were removed from citrated blood samples of microfilarial patients by nucleopore membrane (5 μm) filtration. The blood cells were pelleted at 13,000 g for 30 min and the CFA was isolated from the plasma by 36–75% ammonium sulphate precipitation. CFA was fractionated on ultrogel AcA 34 gel column (LKB, France). The pooled fractions of the second protein peak showing filarial antigens were concentrated and designated as CFA2.

W. bancrofti microfilariae excretory-secretory antigen

W. bancrofti microfilariae excretory-secretory antigen (*Wb* mf ES Ag) was obtained by maintenance of microfilariae in medium 199 supplemented with organic acids and sugars of Grace's medium as described by Kharat *et al.* (1982). The culture supernatant was dialysed with a 12,000 molecular weight cut-off membrane and concentrated 200-fold by freeze drying.

Urinary filarial antigen

Urinary filarial antigen (UFA) was isolated from pooled 24 h microfilaraemic urine samples, after diethylcarbamazine (DEC) treatment and concentrated by ultrafiltration. UFA was fractionated on ultrogel AcA 44 gel column (LKB, France). The pooled fractions of second protein peak showing filarial antigen were concentrated and labelled as UFAC2. Albumin in UFAC2 was removed by absorbing with rabbit antihuman albumin immunoglobulin G (IgG) coupled CNBr sepharose 4B beads (Ramaprasad and Harinath, 1987). Albumin absorbed UFAC2 was designated as UFAC2-A.

Filarial serum IgG (FSIgG) was prepared from pooled clinical filarial sera by ammonium sulphate precipitation followed by DEAE cellulose chromatography as previously described (Reddy *et al.*, 1984a)

SDS-PAGE of CFA2

CFA2 (400 μ g protein in 20 μ l) was diluted 10 times with SDS-sample buffer containing 3% SDS, 1% glycerol, 0.1% bromophenol blue and 5% mercaptoethanol (v/v) in 0.5 M Tris-HCl buffer, pH 6.8 heated for 3 min in a boiling waterbath and analysed by SDS-PAGE as described by Laemmli (1970) with slight modifications. Electrophoresis was carried out on vertical 10% acrylamide homogenous slab gels (9 \times 13 cm) with 3.5% stacking gel. The molecular weight marker proteins (Sigma Chemical Co., USA) lysozyme (14.3 kDa), carbonic anhydrase (29 kDa), albumin egg (45 kDa), phosphorylase b (97.4 kDa) were used for calibration of the gel. The samples were stacked at a constant current of 20 mA and separated at 25 mA to a length of 12 cm. Proteins in a strip of the gel were visualized by staining with Coomassie brilliant blue (R-250). The remaining part of the gel was cut into 12 horizontal slices at 1 cm intervals and each slice was subjected to mechanical grinding to facilitate the elution of the protein into 5 ml of 0.05 M sodium phosphate buffer (SPB), pH 7.2 as described by Guellaen *et al.* (1984). The eluates of the 12 fractions were dialysed against 0.05 M SPB, concentrated by ultrafiltration and tested for filarial antigen in sandwich enzyme linked immunosorbent assay (ELISA).

ELISA

For the ELISA, conjugation of *Wb* mf ES Ag, UFAC2-A, FSIgG, antihuman IgG and anti human IgM with penicillinase was achieved by the method of Avrameas (1969) using glutaraldehyde.

The substrate in ELISA consisted of soluble starch (150 mg) in 27.5 ml of 0.25 M SPB (pH 7.2) containing 10.64 mg of penicillin 'V' and 100 μ l of 0.08 M iodine in 3.2 M potassium iodide solution. The substrate was prepared fresh before use.

Sandwich ELISA

Sandwich ELISA was carried out as described by Reddy *et al.* (1984a). FSIgG (25 μ g/ml), SDS-polyacrylamide gel eluates of CFA2 (starting dilution 10 μ g/ml and serially diluted 10-fold) and FSIgG penicillinase conjugate (1:400) were used in the assay.

Inhibition ELISA

Inhibition ELISA was carried out as described by Malhotra and Harinath (1984). FSIgG (25 μ g/ml), SDS-polyacrylamide gel eluates of CFA2 (starting dilution

10 $\mu\text{g/ml}$ and serially diluted 10-fold) and *Wb* mf ES Ag penicillinase conjugate (1:100) or UFAC2-A penicillinase (1:50) were used in the assay.

Indirect ELISA

Stick ELISA for antibody detection was carried out as described by Parkhe *et al.* (1986). Five μl of optimally diluted antigen fractions (0.1 $\mu\text{g/ml}$ each of CFA2-1 and CFA2-9 and 1 $\mu\text{g/ml}$ of CFA2-12) applied on cellulose acetate membrane attached to plastic strip, sera (1:300 diluted and serially diluted 4-fold up to 1:19,200 dilution), antihuman IgG penicillinase conjugate (1:4000) or antihuman IgM penicillinase conjugate (1:1000) were used in the assay.

Characterization of CFA2-1 and CFA2-9 fractions

Four mg of the enzymes chymotrypsin (CSIR, Biochemicals) was coupled to 1 ml CNBr Sepharose 4B beads as described earlier (Ramprasad and Harinath, 1987). The protein in the supernatant was estimated before and after coupling. The binding was 82–85%.

Treatment with enzymes

The antigen fractions CFA2-1 and CFA2-9 (250 μg in 0.5 ml of 0.05 M SPB, pH 7.2) were treated separately with an equal volume of enzyme coupled beads for 24 h at 37°C with gentle shaking (Rolfe and Fingold, 1979). The supernatant was separated by centrifugation (600 *g*, 15 min) at 4°C and diluted (10 $\mu\text{g/ml}$) to use in sandwich ELISA.

Periodate treatment

The 2 antigen fractions (250 μg in 0.5 ml of 0.05 M SPB, pH 7.2) were treated separately with 0.1 M sodium metaperiodate (BDH, England) at 37°C for 24 h with gentle shaking (Mak *et al.*, 1977). The reaction was stopped by dialysis against 0.01 M SPB, pH 7.2 and used in sandwich ELISA.

Heat inactivation

The 2 antigen fractions were heated at 100°C for 45 min in a boiling water bath (Reddy *et al.*, 1984b). The fractions were centrifuged and the supernatants used in sandwich ELISA.

Trichloroacetic acid treatment

The 2 antigen fractions were treated with equal volume of trichloroacetic acid (TCA, 30%) as described by Weil (1987). The fractions were then centrifuged (12,000 *g*, 20 min) and supernatants dialysed against 0.01 M SPB, pH 7.2. The

pernatants were then heated in a boiling water bath for 50 min, again centrifuged (6,000 *g* for 10 min) and used in sandwich ELISA.

Statistical analysis was carried out by Z test.

Results

Analysis of CFA2 by SDS-PAGE showed 21 bands with molecular weights ranging from 12 kDa to ≥ 120 kDa (figure 1). Eluates of all the 12 gel slices were positive for filarial antigen in FSIgG sandwich ELISA (table 1) with the reciprocal of filarial antigen titres ranging from 10 to 100,000, suggesting polydispersed nature of this antigen. Earlier studies from our laboratory have shown the polydispersed nature of antigen activity in *Wb* mf ES Ag (Ramaprasad *et al.*, 1988). However, CFA2-1 and

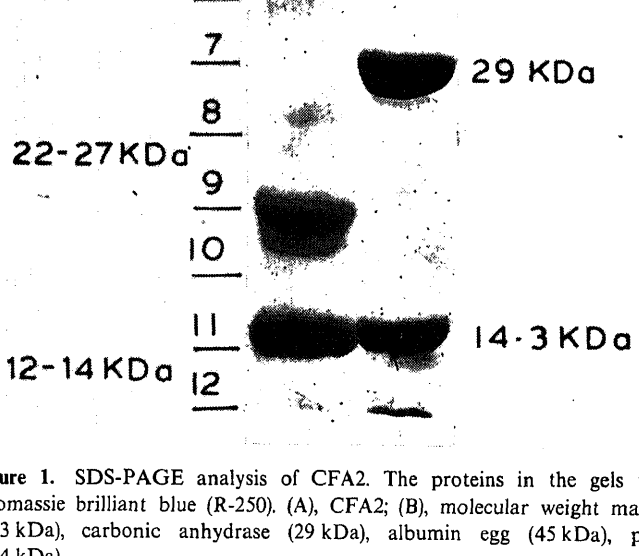


Figure 1. SDS-PAGE analysis of CFA2. The proteins in the gels were stained by Coomassie brilliant blue (R-250). (A), CFA2; (B), molecular weight markers: Lysozyme (14.3 kDa), carbonic anhydrase (29 kDa), albumin egg (45 kDa), phosphorylase b (97.4 kDa).

Table 1. Detection of circulating and excretory-secretory antigens by sandwich and inhibition ELISA.

CFA2 SDS-poly acrylamide gel fractions	Approximate molecular weight ($\times 10^3$)	Reciprocal of filarial antigen titre* by sandwich ELISA using FSIgG	Reciprocal of filarial antigen titre* by inhibition ELISA for detection	
			<i>Wb</i> mf ES Ag	UFAC2-A
CFA2-1	≥ 120	10,000 (76×10^4)	100	—
CFA2-2	100-120	1,000 (6×10^3)	—	—
CFA2-3	80-100	10 (48×10)	100	—
CFA2-4	64-80	Neat (6×10)	—	—
CFA2-5	50-64	10 (48×10)	—	—
CFA2-6	42-50	10 (6×10^2)	—	—
CFA2-7	35-42	Neat (48×1)	—	—
CFA2-8	27-35	1,000 (48×10^3)	—	—
CFA2-9	22-27	100,000 (64×10^5)	10	10,000
CFA2-10	18-22	100 (8×10^2)	10,000	—
CFA2-11	14-18	10 (44×10)	100,000	—
CFA2-12	12-14	10 (44×10)	100,000	10,000

*Starting dilution of polyacrylamide gel fractions 10 μ g protein/ml. Total antigen titre in each fraction is given in parenthesis.

CFA2-9 showed elevated titres of 10,000 and 100,000. In inhibition ELISA, 5 antigen fractions CFA2-1, CFA2-3, CFA2-10, CFA2-11 and CFA2-12 inhibited the binding of *Wb* mf ES Ag to FSIgG and 3 of them CFA2-10, CFA2-11 and CFA2-12 showed very high inhibitory antigen titres ranging from 10,000 to 100,000 (table 1). Two antigen fractions CFA2-9 and CFA2-12 inhibited the binding of UFAC2-A with FSIgG each with inhibitory antigen titres of 10,000. These studies suggest that the low molecular weight SDS-PAGE fractions of CFA2 share common epitope with *Wb* mf ES Ag and UFAC2-A. Indirect ELISA was performed to see the reactivity of these 3 antigenic fractions CFA2-1, CFA2-9 and CFA2-12 with different filarial sera. Ten sera from non endemic normal group and 15 sera from each group (endemic normal, microfilaraemia and clinical filariasis) were screened for filarial IgG and filarial IgM antibodies against these antigens. All 3 antigenic fractions were more sensitive in the detection of IgM antibodies than IgG antibodies (figures 2-4). Thirteen out of 15 microfilaraemics and 14 out of 15 clinical filarial sera were positive for IgM antibodies while 12 out of 15 microfilaraemic and 10 out of 15 clinical filarial sera were positive for IgG antibodies using CFA2-1 antigen (figure 2). The clinical filarial sera showed higher geometric mean of the reciprocal of antibody titre (GMRT 396) than microfilaraemic (GMRT 172, table 2), using CFA2-9 and anti IgG penicillinase conjugate and the difference was statistically significant at 1:1200 dilution ($Z > 2.58$, $P < 0.01$, significant at 1% level). Using CFA2-12 antigen fraction and anti IgM penicillinase conjugate, the microfilaraemic sera showed higher GMRT (3971) than clinical filariasis sera (GMRT 1443). The two active circulating filarial antigen fractions CFA2-1 and CFA2-9 as observed by sandwich ELISA using FSIgG were further characterized and reported in table 3. CFA2-1, the high molecular weight antigen was found to be sensitive to periodate treatment but was not affected by chymotrypsin, heat and TCA treatment. In contrast, CFA2-9 was sensitive to heat, TCA and chymotrypsin treatment but was stable to periodate treatment (table 3).

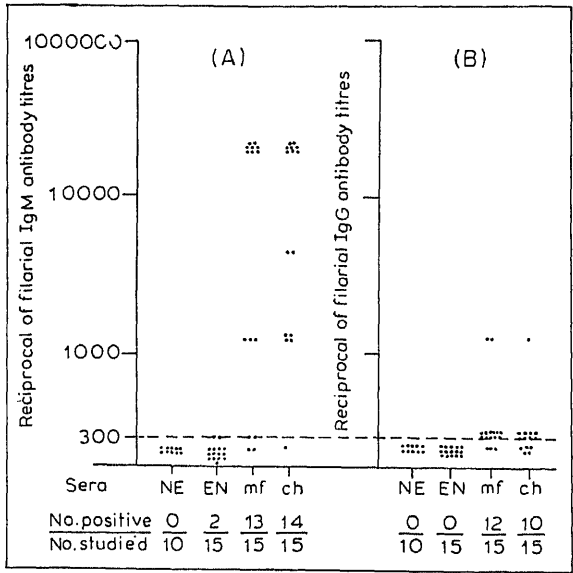


Figure 2. Detection of antibody using CFA2-1 antigen by indirect ELISA. (A), IgM antibody; (B), IgG antibody.

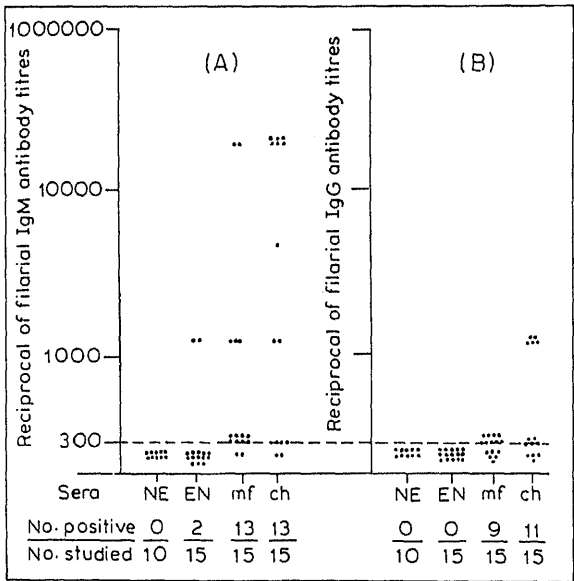


Figure 3. Detection of antibody using CFA2-9 antigen by indirect ELISA. (A), IgM antibody; (B), IgG antibody.

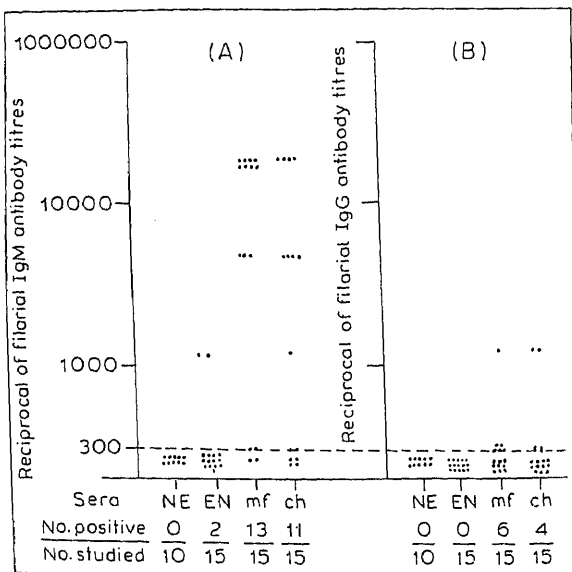


Figure 4. Detection of antibody using CFA2-12 antigen by indirect ELISA. (A), IgM antibody; (B), IgG antibody.

techniques, circulating antigens were detected in humans infected with *W. bancrofti* (Kaliraj *et al.*, 1979), *B. malayi* (Au *et al.*, 1981) and *O. volvulus* (Desmoutis *et al.*, 1983) but relatively little has been reported on the analysis, characterization and diagnostic use of circulating antigens in the human blood.

The low molecular weight SDS-PAGE fractions of CFA-2, CFA2-9 and CFA 2-12, share common epitope with *Wb* mf ES Ag and UFAC2-A. Both *Wb* mf ES Ag and UFAC2A have been shown to be highly sensitive and useful in the diagnosis of filariasis (Ramaprasad and Harinath, 1987; Ramaprasad *et al.*, 1988). Hence their identical fractions in CFA2 and particularly those with high inhibitory antigen titres may be useful as candidate antigens in the diagnosis of filariasis. Moreover, CFA2-1 and CFA2-9 showed very high reciprocal of filarial antigen titre (table 1). Weil and Liftis (1987) and Lal *et al.* (1987) have reported detection of high molecular weight (≈ 200 kDa) circulating antigen in bancroftian filariasis

Table 2. Geometric mean of the reciprocal of filarial IgM and IgG antibody titres in different sera using CFA2 SDS-polyacrylamide gel antigenic fractions (CFA2-1, CFA2-9 and CFA2-12) by indirect ELISA.

Group	GMRT					
	CFA2-1		CFA2-9		CFA2-12	
	IgM	IgG	IgM	IgG	IgM	IgG
Non endemic normal	—	—	—	—	—	—
Endemic normal	90	75	109	75	109	75
Microfilaraemia	3023	273	573	172	3972	143
Clinical filariasis	5264	249	1904	396	1443	131

Table 3. Effect of different biochemical agents on the antigenic activity of CFA2-1 and CFA2-9 fractions as determined by sandwich ELISA.

Biochemical agents	Reciprocal of filarial antigen titres of CFA2 fractions following treatment	
	CFA2-1*	CFA2-9*
Sodium phosphate buffer	10,000	100,000
Heat (100°C)	10,000	0
TCA/heat treatment	10,000	100
Periodate	0	100,000
Chymotrypsin	10,000	100

*Starting dilution of CFA2-1 and CFA2-9 fractions was 10 μ g protein/ml.

using monoclonal antibodies AD 12.1, DH 6.5 and CA 101 respectively which may be equivalent to CFA2-1 based on the size of the molecule. The diagnostic use of 3 circulating filarial antigen fractions was studied by indirect ELISA. The results (figures 2-4) indicate that all the 3 antigen fractions CFA2-1, CFA2-9 and CFA2-12 were found to be more sensitive in the detection of IgM antibodies in filarial sera, confirming earlier reports from this laboratory (Reddy *et al.*, 1986) showing that CFA2 fraction as a whole was more sensitive in detecting IgM antibodies than IgG antibodies in filarial sera. The higher GMRT of clinical filarial sera than GMRT of microfilaraemics using CFA2-9 antigen in detecting IgG antibody is in agreement with the studies of Prasad and Harinath (1988) who showed immune-complex SDS-PAGE fraction-9 (IC-9) to be more useful in differentiating microfilaraemic and clinical filarial cases based on IgG antibody detection. Furthermore, CFA2-12 was shown to be more useful in detection of microfilaraemic carriers than clinical filarial cases by detecting IgM antibodies. Ramaprasad *et al.* (1988) also showed *Wb mf ES Ag* SDS-PAGE fraction-12 (ESA-12) to be useful in detecting elevated IgM antibody in active filarial infection.

Dissanayake *et al.* (1982) reported evidence in favour of circulating glycoprotein antigen in immune-complexes from *W. bancrofti* patients followed by demonstration of immunoblot of parasitic antigens reactive with monoclonal antibody Gib 13 in *W. bancrofti* sera (Dissanayake *et al.*, 1984). Weil *et al.* (1986) showed that the immunoreactivity of circulating antigen was preserved after treatment with heat and TCA but destroyed by metaperiodate. Paranjape *et al.* (1986) reported that the circulating filarial antigen was resistant to heat and TCA treatment but destroyed by pronase and sodium periodate. Our present study shows the high molecular weight antigen (CFA2-1) to be sensitive to periodate treatment but not affected by heat and TCA treatment. In contrast CFA2-9 was found to be sensitive to heat, chymotrypsin, treatment but stable to periodate treatment. Thus antigenic epitope of CFA2-1 appears to be a carbohydrate whereas that of CFA2-9 is protein in nature. The present study reveals that host immune response to the CFA2-9 fraction can be used for serological differentiation of active infection from clinical infection whereas CFA2-1 and CFA2-12 may be used to detect IgM antibodies for diagnosis of filarial infection. Thus, the serum derived circulating antigens from

microfilaraemic patients can be used for the detection of filarial antibodies. This study further reveals that CFA2-9 which is observed in increased levels in microfilaraemic plasma may be target antigen for confirming active infection with a specific polyclonal antibody.

Acknowledgements

This work was supported by the Department of Biotechnology, New Delhi. The authors are grateful to Dr. Sushila Nayar and Dr. K. S. Sachdeva for their interest and encouragement.

References

- Au, A. C., Denham, D. A., Steward, M. W., Draper, C. C., Ismail, M. M., Rao, C. K. and Moore, J. (1981) *Southeast Asian J. Trop. Med. Public Health*, **12**, 492.
- Avrameas, S. (1969) *Immunochemistry*, **6**, 43.
- Dasgupta, A. and Bala, S. (1978) *Indian J. Med. Res.*, **67**, 30.
- Dasgupta, A., Bala, S. and Dutta, S. N. (1984) *Parasite immunol.*, **6**, 341.
- Desmoutis, I., Ouassi, A., Grzych, J. M., Yarzabal, L., Haque, A. and Capron, A. (1983) *Am. J. Med. Hyg.*, **32**, 533.
- Dissanayake, S., Galshitiyawa, S. C. and Ismail, M. M. (1982) *Bull. WHO*, **60**, 919.
- Dissanayake, S., Forsyth, K. P., Ismail, M. M. and Mitchell, G. F. (1984) *Am. J. Trop. Med. Hyg.*, **30**, 1130.
- Forsyth, K. P., Spark, R., Kazura, J., Brown, G. V., Peters, P., Heywood, P., Dissanayake, S., Mitchell, G. F. (1985) *J. Immunol.*, **134**, 1172.
- Franks, M. B. (1946) *J. Parasitol.*, **32**, 400.
- Guellaen, G., Goodhardt, M. and Hanoune, J. (1984) in *Receptor purification procedures* (ed. by J. Drenth and L. C. Harrison) (New York: Alan R. Liss) Vol. 2, p. 109.
- Hamilton, R. G., Hussain, R. and Ottesen, E. A. (1984) *J. Immunol.*, **133**, 2237.
- Harinath, B. C. (1986) *J. Commun. Dis.*, **18**, 261.
- Kaliraj, P., Ghirnikar, S. N. and Harinath, B. C. (1979) *Indian J. Exp. Biol.*, **17**, 1148.
- Kaliraj, P., Kharat, I., Ghirnikar, S. N. and Harinath, B. C. (1981) *J. Helminthol.*, **55**, 133.
- Kharat, I., Ghirnikar, S. N. and Harinath, B. C. (1982) *Indian J. Exp. Biol.*, **20**, 378.
- Laemmli, U. K. (1970) *Nature (London)*, **227**, 680.
- Lal, R. B., Paranjape, R. S., Briles, D. E., Nutman, T. B. and Ottesen, E. A. (1987) *J. Immunol.*, **138**, 1313.
- Mak, W. Y., Buckley, H. R. and Campbell, C. C. (1977) *Infect. Immunol.*, **16**, 461.
- Malhotra, A. and Harinath, B. C. (1984) *Indian J. Med. Res.*, **79**, 194.
- Ouassi, A., Kouemeui, L. E., Haque, A., Ridel, P. R., Sant Andre, P. and Capron, A. (1981) *Am. J. Med. Hyg.*, **30**, 1211.
- Paranjape, R. S., Hussain, R., Nutman, T. B., Hamilton, R. G. and Ottesen, E. A. (1986) *Cell Immunol.*, **63**, 508.
- Parkhe, K. A., Prasad, G. B. K. S., Das, A., Roebber, M., Hamilton, R. G. and Harinath, B. C. (1987) *Indian J. Exp. Biol.*, **24**, 437.
- Prasad, G. B. K. S. and Harinath, B. C. (1988) *Diagn. Clin. Immunol.*, **5**, 269.
- Ramaprasad, P. and Harinath, B. C. (1987) *Asian Pac. J. Allergy Immunol.*, **5**, 173.
- Ramaprasad, P., Reddy, M. V. R., Piessens, W. F. and Harinath, B. C. (1988) *Med. Sci. Res.*, **16**, 105.
- Reddy, M. V. R., Malhotra, A. and Harinath, B. C. (1984a) *J. Helminthol.*, **58**, 259.
- Reddy, M. V. R., Malhotra, A., Prasad, G. B. K. S. and Harinath, B. C. (1984b) *J. Biosci.*, **6**, 161.
- Reddy, M. V. R., Prasad, G. B. K. S. and Harinath, B. C. (1986) *Indian J. Pathol. Microbiol.*, **29**, 105.
- Rolfe, R. D. and Fingold, S. M. (1979) *Infect. Immunol.*, **25**, 191.
- Weil, G. J., Malane, M. S., Powers, K. G. and Blair, L. S. (1985) *J. Immunol.*, **134**, 1185.
- Weil, G. J., Kumar, H., Santharam, S., Sethumadhavan, K. V. P. and Jain, D. C. (1986) *Am. J. Med. Hyg.*, **35**, 565.
- Weil, G. J. (1987) *Exp. Parasitol.*, **64**, 244.
- Weil, G. J. and Lifits, F. (1987) *J. Immunol.*, **138**, 3055.

5-Methylcytosine content and methylation status in six millet DNAs

LALITHA S. KUMAR, R. R. HENDRE and P. K. RANJEKAR*

Division of Biochemical Sciences, National Chemical Laboratory, Pune 411 008, India

MS received 31 August 1989; revised 15 January 1990

Abstract. High performance liquid chromatographic analysis of the total nuclear DNAs of 6 millets plant species indicates that the 5-methylcytosine content ranges from 3% in barn yard millet to 9.6% in great millet while the fraction of cytosines methylated varies between 14% in little millet to 31% in pearl millet. Digestion of millet DNAs with *MspI/HpaII* suggests that CpG methylation is more in great millet DNA while CpC methylation is more in the other 5 millet DNAs. Digestion of millet DNAs with *MboI*, *Sau3AI* and *DpnI* indicates that some of the $5'GATC3'$ sequences are methylated at adenine and/or cytosine residues except in little millet where adenine methylation of the $5'GATC3'$ sequences is insignificant and there is a predominance of cytosine methylation in these sequences.

Keywords. 5-Methylcytosine content; cytosine methylation; adenine methylation; millets.

Introduction

In the DNAs of higher plants, 5-methylcytosine content amounts to almost 30% of the total cytosine residues and is distributed between the sequences m^5CpG and m^5CpXpG where X can be any nucleotide (Shapiro, 1976; Gruenbaum *et al.*, 1981). In addition to 5-methylcytosine, 6-methyladenine has been detected in a few plant DNAs (Vanyushin *et al.*, 1971, 1988; Buryanov *et al.*, 1972; Kovalskaya *et al.*, 1986; Jose Antonio Pintor-Toro, 1987). Though cereals and millets belong to the family Gramineae, cytosine methylation has been studied only in the DNAs of wheat (Gruenbaum *et al.*, 1981; Aleksandrushkina *et al.*, 1988; Flavell *et al.*, 1988; Kirnos *et al.*, 1988), barley (Gerlach *et al.*, 1979) and maize (Antequera and Bird, 1988; Bianchi and Viotti, 1988; Gallardo *et al.*, 1988). Our earlier work focussed on studying the genome structure and organisation in two major millets (great millet and pearl millet) and 4 minor millets (fox tail millet, little millet, finger millet and barn yard millet) (Deshpande and Ranjekar, 1980; Gupta and Ranjekar, 1981, 1982; Sivaraman and Ranjekar, 1984; Sivaraman *et al.*, 1984, 1986). In the present work, we have determined the 5-methylcytosine content of the total nuclear DNAs of these millets by high performance liquid chromatography (HPLC) and have also studied their methylation status using methylation sensitive restriction enzymes.

Materials and methods

All the chemicals used were of analytical reagent grade. The nucleic acid standard bases *i.e.* cytosine, 5-methylcytosine, guanine, adenine and thymine were from

*To whom all correspondence should be addressed.

Abbreviation used: HPLC, High performance liquid chromatography.

Sigma Chemical Co., St. Louis, Missouri, USA. DNA molecular weight markers (λ DNA digested with *Hind*III and ϕ X174 RF DNA digested with *Hae*III) and all the restriction enzymes were obtained from Bethesda Research Laboratories or New England Biolabs, USA.

DNA isolation and criteria of purity

Native, high molecular weight DNA was isolated from 4–5 days old, etiolated shoot tissue by a combination of methods of Ranjekar *et al.* (1976) and Marmur (1961). All the DNA samples were checked for purity using the usual criteria (Bhave *et al.*, 1984).

Restriction enzyme digestion and gel electrophoresis

Two μ g of DNA was digested with 6–8 units of restriction enzyme in a reaction volume of 20 μ l, at 37°C overnight. The assay buffers were prepared according to Maniatis *et al.* (1982). The reaction was stopped by the addition of 10X reaction terminating buffer (50% glycerol, 100 mM EDTA, 0.25% bromophenol blue) to a final concentration of 1X. Control experiments were performed using commercial λ DNA digested with different restriction enzymes to check the reaction conditions. The plant DNAs were checked for any inherent nuclease activity by incubation in the assay buffers (without restriction enzyme) for the same length of time as for digestion with restriction enzymes. The digestion mixtures were analysed on 1% neutral agarose gels as described by Maniatis *et al.* (1982).

HPLC analysis of the total nuclear DNAs

The plant DNAs were hydrolysed with 60–70% perchloric acid for 1 h at 100°C. Following hydrolysis, perchloric acid was neutralised by 10 N potassium hydroxide and the potassium perchlorate precipitate was centrifuged out. Aliquots of the neutralised hydrolysate were applied to the reverse phase RP-18 column (10 μ m, HP No. 79916B, 250 \times 4.6 mm with a micron frit pore). The column was pre-equilibrated in 0.4 M ammonium phosphate buffer (pH 4.3) containing 5% methanol. The chromatography was carried out on Hewlett–Packard HPLC system (Model 1082 B) interfaced with a Hewlett–Packard LC terminal (No. 79850 B) and equipped with an automatic sample injecting system. The UV detector was fixed at 254 nm wavelength. The chromatographic profiles were obtained at a chart speed of 1 cm/min and a flow rate of 0.5 ml/min. The elution was isocratic in the above pre-equilibrium buffer. The instrument was pre-calibrated with authentic bases namely adenine, guanine, thymine, cytosine and 5-methylcytosine prior to injection of DNA hydrolysates. The identification of bases was determined in terms of retention times and in case of 5-methylcytosine, by peak enhancement due to co-injected authentic sample. The amount of 5-methylcytosine was determined from the area of the peak in the profiles.

Results

Content of 5-methylcytosine

Prior to digestion with methylation specific enzymes, the amount of 5-methylcytosine in the total nuclear DNA preparations of the 6 millets was determined by HPLC (table 1). From table 1, it is seen that the 5-methylcytosine content ranges from 3% in barn yard millet to 9.6% in great millet. The fraction of the cytosine residues methylated was also determined and the values vary between 14% in little millet to 31% in pearl millet. These values are higher than the corresponding values in animal cells and thus show a trend complying with those observed in plants (Razin and Riggs, 1980; Shapiro, 1976). As the presence of 5-methylcytosine in the DNA is known to increase its T_m (Dawid *et al.*, 1970; Ehrlich *et al.*, 1975), the relatively high T_m of 89.9°C of pearl millet DNA could be explained by the fact that almost 31% of its cytosine residues are methylated.

Table 1. HPLC analysis of the total nuclear DNAs of the millets.

	Total cytosine (%) (cytosine + 5-methylcytosine) in the DNA	5-Methylcytosine (%) in the DNA	Total cytosines methylated (%)
Great millet	48.68 ± 0.71	9.62 ± 1.05	19.76 ± 0.75
Barn yard millet	19.28 ± 0.95	3.02 ± 0.55	15.66 ± 1.07
Little millet	28.85 ± 0.79	4.19 ± 0.76	14.52 ± 0.63
Fox tail millet	29.47 ± 1.23	7.51 ± 0.82	25.48 ± 0.79
Finger millet	15.13 ± 1.12	3.59 ± 0.87	23.72 ± 1.15
Pearl millet	23.54 ± 1.25	7.28 ± 0.61	30.92 ± 2.12

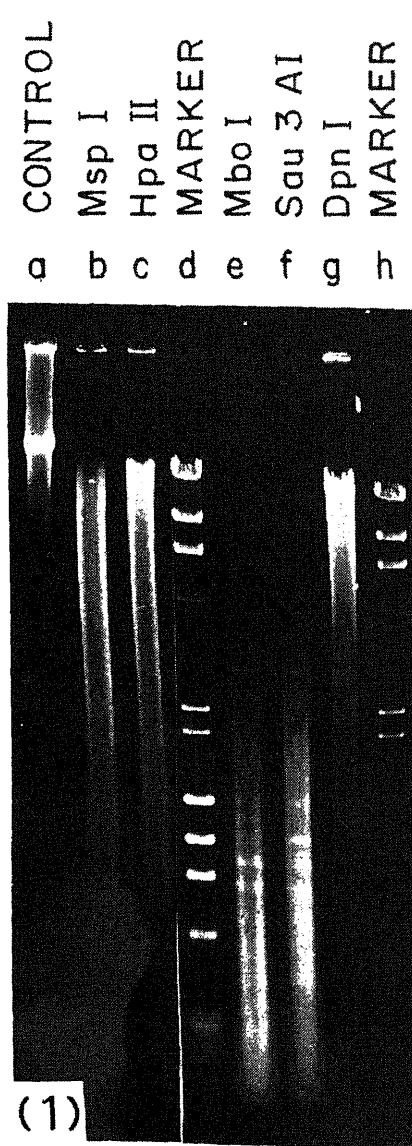
The percentage of cytosine and 5-methylcytosine were determined from the peak height and peak area. The values are an average of 3 DNA samples, each done in duplicate.

Methylation of 5'CCGG^{3'} sequences

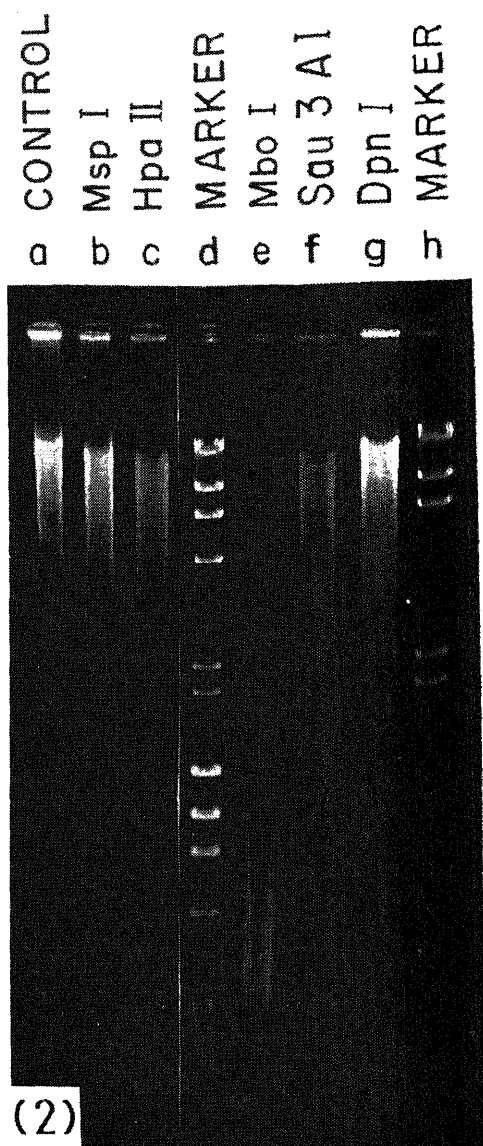
The methylation status of the 5'CCGG^{3'} sequences in the 6 millet DNAs was assessed by using the isoschizomer pair of restriction enzymes namely *Msp*I and *Hpa*II. Both the enzymes recognise the sequence 5'CCGG^{3'} but show a differential sensitivity to cytosine methylation. *Msp*I is insensitive to m⁵CpG while *Hpa*II is insensitive to m⁵CpXpG. When the millet DNAs are restricted with *Msp*I and *Hpa*II, it is seen that great millet DNA is digested to a slightly greater extent with *Msp*I than with *Hpa*II while the reverse is observed in case of the other 5 millet DNAs (figures 1 and 2). These observations indicate that mCpG methylation is more in great millet DNA while mCpC methylation is more in the other 5 millet DNAs.

Methylation of 5'GATC^{3'} sequences

The millet DNAs were next restricted with the restriction enzymes *Mbo*I, *Sau*3AI and *Dpn*I which recognise the sequence 5'GATC^{3'} but show a differential sensitivity



Great millet



Little millet

Figures 1 and 2. Restriction pattern of (1) great millet and (2) little millet DNA digested with methylation sensitive restriction endonucleases namely *Msp*I (lane b), *Hpa*II (lane c), *Mbo*I (lane e), *Sau*3AI (lane f) and *Dpn*I (lane g); control DNA (lane a), *Hind*III digest of λ DNA + *Hae*III digest of ϕ X174 RF DNA (lane d), *Hind*III digest of λ DNA (lane h).

to cytosine and adenine methylation. *Dpn*I cleaves the sequence only if adenine is methylated while *Mbo*I will not cleave the sequence if adenine is methylated and is insensitive to cytosine methylation. *Sau*3AI will not cleave the sequence if the cytosine is methylated and is insensitive to adenine methylation. Based on the

extent of digestions of the millet DNAs with these enzymes, the following conclusions can be arrived (the digestion patterns of only great millet and little millet DNA are shown in figures 1 and 2 respectively).

i) Among the 6 millets, finger millet DNA shows relatively more digestion with *DpnI* indicating the presence of more number of methylated adenine residues as compared to the DNAs of great millet, barn yard millet and fox tail millet. In case of pearl millet and little millet DNA, no significant difference is observed between the *DpnI* digest and the control DNA suggesting that adenine methylation of the 'GATC' sequences is probably absent.

ii) While comparing the digestion of the millet DNAs with *MboI* and *Sau3AI*, it is seen that in each case, except in case of pearl millet and little millet, *MboI* and *Sau3AI* digest the DNA extensively and to a similar extent indicating that many of the 'GATC' sequences are not methylated at cytosine and adenine residues. In case of little millet and pearl millet, *MboI* digests the DNA to a greater extent than *Sau3AI*, suggesting that most of the 'GATC' sequences are methylated only at the cytosine residues. This difference, especially is very significant in little millet. In each plant DNA, several bands of similar molecular weight are shared by the *MboI* and *Sau3AI* digests. These represent repeat families. It is observed that some of these repeat families differ in intensity in the *MboI* and *Sau3AI* digests. This difference is because some members of these repeat families are methylated at adenine or cytosine residues.

iii) A band (greater than 23 kbp) is seen in the *MboI* and *Sau3AI* digests of the DNAs of barn yard millet, fox tail millet and pearl millet. This could be either due to lack of 'GATC' sequences or due to methylation at both cytosine and adenine residues. However, in case of great millet and finger millet DNA, such a band is seen only in the *MboI* digest and is absent or insignificant in the *Sau3AI* digest indicating thereby that this high molecular weight DNA fragment in these two millets contains 'GATC' sequences methylated at adenine residues.

Discussion

The *MspI* and *HpaII* digestion patterns suggest that CpG methylation is more in great millet DNA and CpC methylation is more in the other 5 millet DNAs. The available data on the methylation status of plant DNAs have shown that over 25% of the cytosine residues are methylated in plant cells while only 2–8% of the total cytosines are methylated in animal cells (Shapiro, 1976; Razin and Riggs, 1980). This difference is due to the fact that though in both plants and animals, the primary site of cytosine methylation is the C–G dinucleotide, the dinucleotide is more frequent in plant DNA (3–4%) than in animal DNA (0.5–1%) (Gruenbaum *et al.*, 1981). Moreover in plants, 5-methylcytosine is found in a variety of cytosine containing dinucleotides besides CpG which are a part of the basic trinucleotide C–X–G, which is not the case in animal DNAs. Thus all the methylatable sites of plant DNA are not fully methylated. Approximately 80% of C–G or C–A–G sites are methylated and only 50% of the C–C–G sites are modified at the external cytosine (Gruenbaum *et al.*, 1981). It has been suggested that this incomplete methylation makes these sites potential elements in cellular regulation. Moreover, *HpaII* digestion of the DNAs of the millets under consideration (except great millet)

methylation of closely spaced CpG sites. The search for such closely spaced CpG sites is of interest in view of a recent report in maize where such sites have been shown to be associated with AdhI, aI and ShI genes (Antequera and Bird, 1988).

The restriction enzyme data using *Mbo*I, *Sau*3AI and *Dpn*I indicates that many of the 5'GATC3' sequences are methylated at adenine and/or cytosine residues in the 5 millet DNAs except in little millet DNA where adenine methylation is insignificant. The detection of 6-methyladenine in plants may support the idea of the possible new role of cytokinins (N⁶-substituted adenine derivatives) in cell differentiation as modulators of adenine residue methylation in plant DNA (Vanyushin, 1984; Vanyushin and Kirnos, 1988). Jose Antonio Pintor-Toro (1987) has envisaged a role of 6-methyladenine in DNA repair in plant cells. The presence of 6-methyladenine in the DNA of higher plants relates them in a definite degree to algae which are considered to be predecessors of higher plants. As compared with algae however, the capacity for methylation of adenine in the DNA in higher plants has decreased considerably and the capacity for methylation of cytosine has increased in the course of evolution (Vanyushin et al., 1971).

References

- Antequera, F. and Bird, A. P. (1988) *EMBO J.*, **7**, 2295.
- Aleksandrushkina, N. I., Kirnos, M. D., Rotaenko, E. P. and Vanyushin, B. F. (1988) *Biokhimiya*, **54**, 355.
- Bhave, M., Lagu, M. and Ranjekar, P. K. (1984) *Plant Sci. Lett.*, **33**, 127.
- Bianchi, M. W. and Viotti, A. (1988) *Plant Mol. Biol.*, **11**, 204.
- Buryanov, Ya. I., Erochina, N. V., Vagabova, L. N. and Iliin, A. V. (1972) *Dokl. AN USSR*, **205**, 700.
- Dawid, I. B., Brown, D. D. and Reeder, R. H. (1970) *J. Mol. Biol.*, **51**, 341.
- Deshpande, V. G. and Ranjekar, P. K. (1980) *Hoppe-Seyler's Z. Physiol. Chem.*, **361**, 1223.
- Ehrlich, M., Ehrlich, K. and Mayo, J. A. (1975) *Biochim. Biophys. Acta*, **395**, 109.
- Flavell, R. B., O'Dell, M. and Thompson, W. F. (1988) *J. Mol. Biol.*, **204**, 523.
- Gallardo, D., Reina, M., Rigau, J., Boronat, A. and Palau, J. (1988) *Plant Sci.*, **54**, 211.
- Gerlach, W. L. and Bedbrook, J. R. (1979) *Nucleic Acids Res.*, **7**, 1869.
- Gruenbaum, Y., Naveh-Man, T., Cedar, H. and Razin, A. (1981) *Nature (London)*, **292**, 860.
- Gupta, V. S. and Ranjekar, P. K. (1981) *J. Biosci.*, **3**, 417.
- Gupta, V. S. and Ranjekar, P. K. (1982) *Indian J. Biochem. Biophys.*, **19**, 167.
- Jose Antonio Pintor-Toro (1987) *Biochem. Biophys. Res. Commun.*, **147**, 1082.
- Kirnos, M. D., Aleksandrushkina, N. I., Kutueva, L. I. and Vanyushin, B. F. (1988) *Biokhimiya*, **53**, 1397.
- Kovalskaya, V. S., Kudryashova, I. B. and Vanyushin, B. F. (1986) *Biol. Nauki (Moscow)*, **10**, 19.
- Maniatis, T., Fritsch, E. F. and Sambrook, J. (1982) *Molecular cloning: A laboratory manual* (New York: Cold Spring Harbor Laboratory Press)
- Marmur, J. (1961) *J. Mol. Biol.*, **3**, 208.
- Ranjekar, P. K., Pallota, D. and Lafontaine, J. G. (1976) *Biochim. Biophys. Acta*, **425**, 30.
- Razin, A. and Riggs, A. D. (1980) *Science*, **210**, 604.
- Shapiro, H. S. (1976) *CRC Handb. Biochem. Mol. Biol.*, **2**, 259.
- Sivaraman, L. and Ranjekar, P. K. (1984) *Indian J. Biochem. Biophys.*, **21**, 299.
- Sivaraman, L., Gupta, V. S. and Ranjekar, P. K. (1984) *J. Biosci.*, **6**, 795.
- Sivaraman, L., Gupta, V. S. and Ranjekar, P. K. (1986) *Plant Mol. Biol.*, **6**, 375.
- Vanyushin, B. F. (1984) *Curr. Top. Microbiol. Immunol.*, **108**, 99-114.
- Vanyushin, B. F., Kadyrova, D. C., Karimov, C. C. and Belozerskii, A. N. (1971) *Biochemistry (USSR)*, **36**, 1251.
- Vanyushin, B. F., Aleksandrushkina, N. I. and Kirnos, M. D. (1988) *FEBS Lett.*, **223**, 397.
- Vanyushin, B. F. and Kirnos, M. D. (1988) *Gene*, **74**, 117.

Predicted secondary structure of maltodextrin phosphorylase from *Escherichia coli* as deduced using Chou-Fasman model

ANIL KUMAR

Department of Biochemistry, Devi Ahilya University, Khandwa Road, Indore 452 001, India

MS received 25 September 1989; revised 5 April 1990

Abstract. Secondary structure of maltodextrin phosphorylase from *Escherichia coli* has been predicted using Chou-Fasman model. The enzyme protein contains 28% α -helix, 27% β -pleated sheets and 20% reverse β -turns. The secondary structure predicted 4 regions showing Rossmann-fold super secondary structure. Two regions, one from residue 268–361 and the another from residue 606–684, having 4 consecutive strands of parallel β -pleated sheets and 3 joining α -helix, are predicted. Two regions, one from residue 379–434 and the another from residue 496–573, having 3 consecutive strands of parallel β -pleated sheets and two joining α -helix, are predicted.

Keywords. Maltodextrin phosphorylase; Chou-Fasman analysis; β -pleated sheet; reverse β -turn; α -helix; Rossmann-fold super secondary structure.

Introduction

α -Glucan phosphorylase (EC 2.4.1.1.; α -1,4 glucan: orthophosphate, glucosyl transferase) in the presence of orthophosphate catalyzes the degradation of α -1,4 glucan into glucose 1-phosphate. It is found in animals, plants as well as microorganisms. In *Escherichia coli*, Chen and Segel (1968a,b) reported the presence of two different α -glucan phosphorylases, one called as maltodextrin phosphorylase which is induced by maltose and is specific for low molecular weight maltodextrins, and the another enzyme called as glycogen phosphorylase which prefers high molecular weight glycogen over maltodextrins and is of constitutive type. Two different genes, *mal P* and *glg P* are involved in the coding of maltodextrin phosphorylase and glycogen phosphorylase, respectively. Palm and co-workers (1985, 1987) reported an amino acid sequence of 797 residues (including N-terminal methionine) of maltodextrin phosphorylase, deduced from the nucleotide sequence of the *mal P* gene. Romeo *et al.* (1988), while analyzing *E. coli* glycogen gene cluster, predicted the presence of a gene downstream of *glg A* gene, coding for glycogen phosphorylase. They also reported an incomplete amino acid sequence of 383 residues of the putative protein, as deduced from the nucleotide sequence of the gene. Almost simultaneously although independently, Yu *et al.* (1988) reported the complete 809 residue amino acid sequence of glycogen phosphorylase. This author has determined the secondary structure of *E. coli* glycogen phosphorylase and predicted the presence of a single Rossmann-fold super secondary structure in the region from residue 325–372 which contains a tyrosine residue at position 350 in the area to contain a reverse β -turn (unpublished results). In the present study the secondary structure of maltodextrin phosphorylase, as a part of the studies on the structural and functional relationships of phosphorylases has been elucidated.

The secondary structure of maltodextrin phosphorylase was determined using Chou-Fasman model (Chou-Fasman, 1974). It utilizes empirical rules for predicting the initiation and termination of α -helix and β -sheet regions in proteins. When 4 helix formers out of 6 residues or 3 β -formers out of 5 residues are found clustered together in any native protein segment, the nucleation of these secondary structures begins and propagates in both the directions until terminated by a sequence of tetrapeptides designated as breakers. Chou and Fasman have computed conformational parameters for the β -turns. The reverse β -turn consists of only 4 amino acids enabling a polypeptide chain to reverse itself by nearly 180° with hydrogen bonding between the -CO-group of first residue and the -NH-group of the 4th residue. Rossman-fold super secondary structure (Rao and Rossman, 1973) was predicted by searching for the presence of a segment in the primary structure consisting of at least 3 consecutive strands of parallel β -pleated sheets and two joining α -helix.

Results and discussion

Predicted secondary structure of maltodextrin phosphorylase alongwith the complete amino acid sequence has been shown in figure 1. In general, reverse β -turn involves only 4 residues and it is likely that neighbouring residues before and after the β -turn may be important in stabilizing the conformation. Out of 797 residues, 219 residues showed formation of α -helix (27.5%), 218 residues showed formation of β -pleated sheet (27.3%) and 157 residues showed formation of reverse β -turns (19.7%).

Data on the percentage of α -helix and β -pleated sheet for various α -glucan phosphorylases have been shown in table 1. It seems that the α -helix and β -pleated sheet contents in maltodextrin phosphorylase and glycogen phosphorylase from *E. coli* are quite similar. Here, it is important to state that generally, there are some residues in the sequences which might be uncertain. This would lead to uncertain secondary structure analysis.

Residues 150–260 in rabbit muscle glycogen phosphorylase b contain only β -sheet regions and residues 713–836 contain only α -helix (Johnson *et al.*, 1989). On the contrary, in maltodextrin phosphorylase, residues 46–100 and residues 568–610 contain only β -sheet regions and no region is found containing only α -helix. In *E. coli* glycogen phosphorylase, two regions from residues 96–141 and from residues 465–516 containing only α -helix and two regions from residues 524–633 and from residues 661–688 containing only β -sheets are found (unpublished results).

In the secondary structure, 4 regions showing Rossman-fold super secondary structure have been predicted. Two regions, one from residue 268–361 and another from residue 606–684 have 4 consecutive strands of parallel β -pleated sheets and 3 joining α -helix. Two regions, one from residue 379–434 and another from residue 496–573 have 3 consecutive strands of β -pleated sheets and two joining α -helix.

In Rossman-fold super secondary structure, there is one tyrosine at position 343 in the area of the enzyme predicted to contain a reverse β -turn. Reverse β -turns are not conformationally stable and are regions of least resistance in the folding process

M S Q P I F N $\overline{D K Q F Q E A L}$ $\overline{S R Q W Q^{20}}$
 $\alpha = 1.23$ $rt = 78$

R Y G $\overline{L N S A A E M T P}$ $\overline{R Q W W L A V S^{40}}$
 $rt = 79$ $\alpha = 1.16$ $\alpha = 1.25$

E A L A E $\overline{M L R A Q}$ $\overline{P F A K P V A N Q R^{60}}$
 $\beta = 1.20$

H V N Y $\overline{I S M E}$ $\overline{F L I G R L}$ $\overline{T G N N L L^{80}}$
 $rt = 53$ $\beta = 1.17$ $rt = 78$ $rt = 99$

N $\overline{L G W Y Q D V Q D S L}$ $\overline{K A Y D I N L T^{100}}$
 $\beta = 1.11$ $\beta = 1.10$

D L L E E E I $\overline{D P A L G N G G L}$ $\overline{G R L A^{120}}$
 $\alpha = 1.32$ $rt = 65$ $rt = 84$ $rt = 160$ $rt = 73$

A C F L D $\overline{S M A T V G Q}$ $\overline{S A T G Y G}$ $\overline{L N^{140}}$
 $\alpha = 1.21$ $\beta = 1.26$ $rt = 73$ $rt = 69$

Y Q Y G $\overline{L F R Q S F V}$ $\overline{D G K Q}$ $\overline{V E A P D^{160}}$
 $rt = 151$ $\beta = 1.18$ $rt = 74$ $rt = 54$

$\overline{D W H R S N Y P W F}$ $\overline{R H N E A L D V Q V^{180}}$
 $rt = 92$ $rt = 65$ $rt = 107$ $rt = 59$ $rt = 105$ $\beta = 1.25$

G I G G K $\overline{V T K D G R W}$ $\overline{E P E F T I T G^{200}}$
 $rt = 63$ $rt = 71$ $rt = 84$ $rt = 63$

Q A W D L $\overline{P V V G Y R N G V A Q P L R L^{220}}$
 $\beta = 1.15$ $\beta = 1.26$

W Q A T H A $\overline{H P F D}$ $\overline{L T K F N D G D F L^{240}}$
 $\alpha = 1.13$ $rt = 84$ $rt = 83$

R A E Q Q $\overline{G I N A E K L T K V L Y P N D^{260}}$
 $\alpha = 1.22$ $\beta = 1.21$ $rt = 472$

N H $\overline{T A G K K L R L M Q Q Y F Q C A C S^{280}}$
 $rt = 64$ $\beta = 1.18$

V A D I L R R $\overline{H H L A G R E L H E L A D^{300}}$
 $\alpha = 1.21$

Y E V I Q L N $\overline{D T H P T I A I P E L L R^{320}}$
 $\beta = 1.27$ $rt = 65$

V L I D E H Q M S W D D $\overline{A W A I T S K T^{340}}$
 $\alpha = 1.13$ $\beta = 1.19$

F A Y T N H $\overline{T L M P E A L E R W D V K L^{360}}$
 $rt = 90$ $\alpha = 1.21$ $\beta = 1.21$

V K G L L P R H $\overline{M Q I I N E I N T R F K^{380}}$
 $\beta = 1.35$

T L V E K T $\overline{W P G D E K V W A K L A V V^{400}}$
 $\beta = 1.22$ $rt = 114$ $\alpha = 1.21$

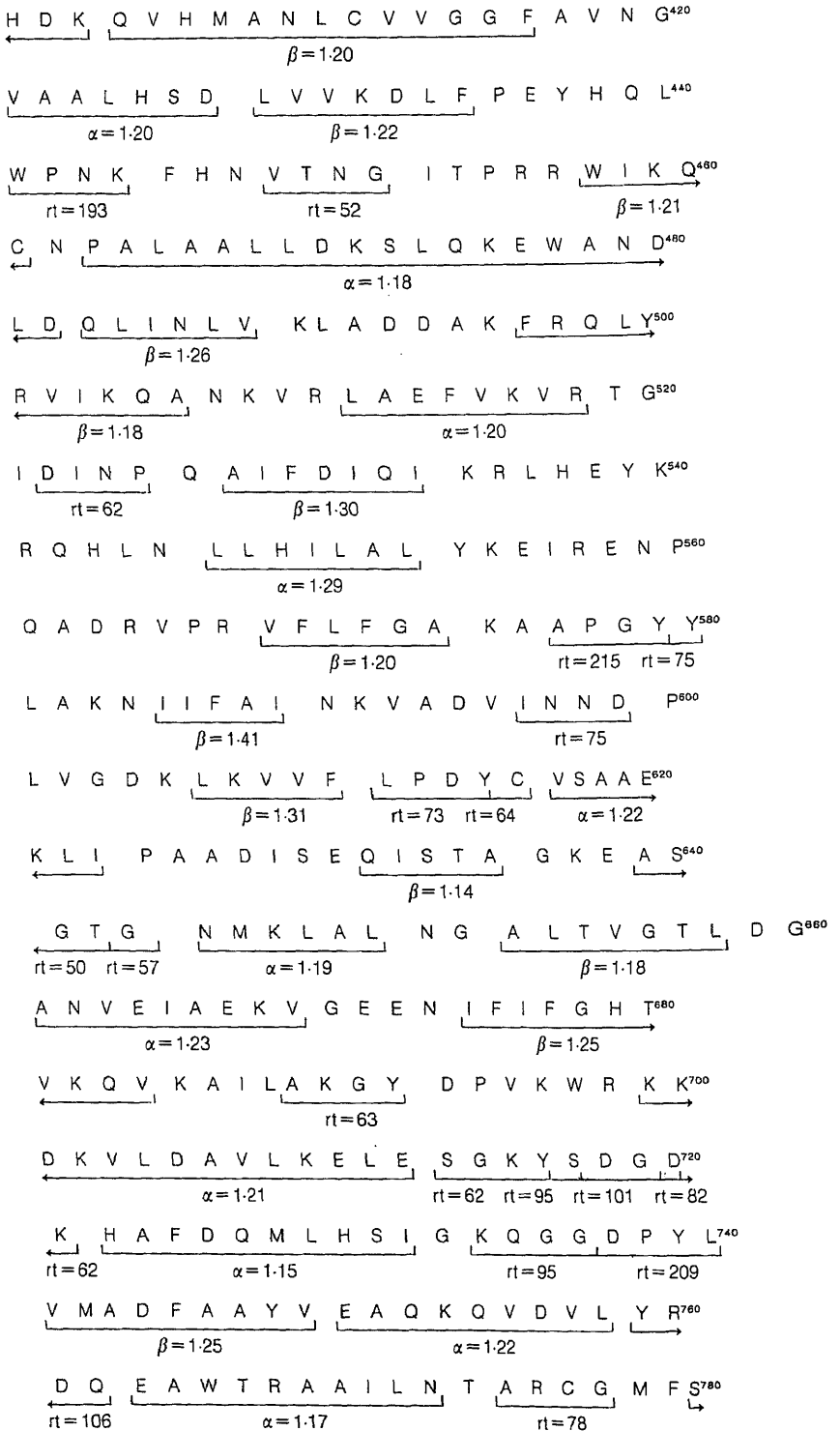


Table 1. Secondary structure of different α -glucan phosphorylases.

Enzyme	α -helix (%)	Pleated sheets (%)	Reference
Potato tuber phosphorylase ^a	16	37	Shimomura <i>et al.</i> (1980)
Rabbit muscle glycogen phosphorylase b ^a	41	21	Shimomura <i>et al.</i> (1980)
Rabbit muscle glycogen phosphorylase b ^b	50	20	Johnson <i>et al.</i> (1989)
Rabbit muscle glycogen phosphorylase a ^c	50	30	Fletterick and Madsen (1980)
<i>E. coli</i> glycogen phosphorylase ^d	30	27	Unpublished data
<i>E. coli</i> maltodextrin phosphorylase ^d	28	27	Present data

From CD measurement; ^bfrom x-ray studies; ^cfrom Kabsch and Sander (1983) prediction; ^dfrom Chou and Fasman (1974) prediction.

of the peptide chains (Schulz and Schirmer, 1979). On alignment of the *E. coli* maltodextrin and glycogen phosphorylases, tyrosine 343 of maltodextrin phosphorylase and tyrosine 350 of glycogen phosphorylase are placed at the same position. The author feels that being at the surface of the molecule, this flexible region of the enzyme is involved in the binding of the effector, adenine nucleotide. GMP has been shown to stimulate maltodextrin phosphorylase (Chen and Segel, 1968a). Tyrosine has been shown to bind adenine nucleotides (Busbis and Taylor, 1987; Larsen *et al.*, 1986). In maltodextrin phosphorylase, there is another tyrosine at position 614 in the area predicted to contain a reverse β -turn in another Rossman-fold super secondary structure. On alignment, this residue, tyrosine 624 of *E. coli* glycogen phosphorylase, tyrosine 648 of rabbit muscle glycogen phosphorylase and tyrosine 730 of potato phosphorylase are placed at the same position. This tyrosine might also be involved in the binding of the nucleotide. Johnson *et al.* (1989) showed that in rabbit muscle glycogen phosphorylase b, region from 562–711 contains 6 consecutive β -pleated sheets and 5 joining α -helix, thus showing the presence of Rossman-fold super secondary structure. They also showed this region is nucleotide binding region.

There are many pairs of amino acids in Rossman-fold super secondary structure regions. Val-val pairs at positions 399–400, 412–413, 608–609; gly-gly pair at position 414–415; leu-leu pair at position 546–547; ala-ala pairs at positions 618–619 and 625–626 have been found. The amino acids pairs might be responsible for the maintenance of proper conformation of the enzyme. In *E. coli* dihydrofolate reductase, there is a gly-gly pair at position 95–96. Changing of gly 95 to ala causes complete inactivation of the enzyme. This has been explained on the basis of disturbed gly-gly cis peptide, thereby affecting the activation of the nicotinamide ring of NADPH (Villafranca *et al.*, 1983). Kumar *et al.* (1989) pointed out the presence of one gly-gly pair at position 336–337 in *E. coli* ADP-glucose synthetase during their studies on mutant enzymes. On changing gly 336 to asp using oligonucleotide site directed mutagenesis, there is formation of a defective enzyme

Figure 1. Predicted secondary structure of *E. coli* maltodextrin phosphorylase using Chou-Fasman conformational analysis. Numerical values given are α -helical or β -pleated

which has been predicted due to alteration in the 3-dimensional structure of the mutant enzyme. Confirmation of the involvement of all these residues in the catalytic mechanism and/or maintenance of the proper conformation, requires further study which can be done using oligonucleotide site directed mutagenesis or to some extent by chemical modification studies. Palm *et al.* (1987) have shown the requirement of C-terminal 7 residues for the enzyme activity.

Acknowledgements

The author is grateful to the Council of Scientific and Industrial Research, New Delhi for financial assistance. The author acknowledges the permission given by Prof. Dieter Palm for using his published amino acid sequence of maltodextrin phosphorylase.

References

- Busbis, J. and Taylor, S. S. (1987) *Biochemistry*, **26**, 5997.
- Chen, G. S. and Segel, I. H. (1968a) *Arch. Biochem. Biophys.*, **127**, 164.
- Chen, G. S. and Segel, I. H. (1968b) *Arch. Biochem. Biophys.*, **127**, 175.
- Chou, P. Y. and Fasman, G. D. (1974) *Biochemistry*, **13**, 222.
- Fletterick, R. J. and Madsen, N. B. (1980) *Annu. Rev. Biochem.*, **49**, 31.
- Johnson, L. N., Hajdu, J., Acharya, K. R., Stuart, D. I., McLaughlin, P. J., Oikonomakos, N. G. and Barford, D. (1989) in *Allosteric enzymes* (ed. G. Herve) (Florida: CRC Press) p. 81.
- Kabsch, W. and Sander, C. (1983) *Biopolymers*, **22**, 2577.
- Kumar, A., Ghosh, P., Lee, Y. M., Hill, M. A. and Preiss, J. (1989) *J. Biol. Chem.*, **264**, 10464.
- Larsen, C. E., Lee, Y. M. and Preiss, J. (1986) *J. Biol. Chem.*, **261**, 15402.
- Palm, D., Goerl, R. and Burger, K. J. (1985) *Nature (London)*, **313**, 500.
- Palm, D., Goerl, R., Weidinger, G., Zeier, R., Fischer, B. and Schinzel, R. (1987) *Z. Naturforsch.*, **42c**, 394.
- Rao, S. T. and Rossman, M. G. (1973) *J. Mol. Biol.*, **76**, 241.
- Romeo, T., Kumar, A. and Preiss, T. (1988) *Gene*, **70**, 363.
- Schulz, G. E. and Schirmer, R. H. (1979) *Principles of protein structure* (New York: Springer-Verlag).
- Shimomura, S., Emman, K. and Fukui, T. (1980) *J. Biochem. (Tokyo)*, **87**, 1043.
- Villafranca, J. F., Howell, E. E., Voet, D. H., Strobel, M. S., Ogden, R. C., Abelson, J. N. and Kraut, J. (1983) *Science*, **222**, 782.
- Yu, P., Jen, Y., Takeuchi, E., Inouye, M., Nakayama, H., Tagaya, M. and Fukui, T. (1988) *J. Biol. Chem.*, **263**, 13706.

Effect of king cobra venom on α_2 -macroglobulin and proteases in human blood plasma

MAYA ROCHE and T. N. PATTABIRAMAN

Department of Biochemistry, Kasturba Medical College, Manipal 576 119, India

MS received 22 January 1990

Abstract. Normal human blood plasma showed hydrolytic activities on several synthetic substrates for proteases, the most effective being H-D-Ile-Pro-Arg-p-nitroanilide, H-D-Pro-Phe-Arg-p-nitroanilide and H-D-Val-Leu-Arg-p-nitroanilide. When plasma was pre-incubated for 12 h at 37°C, there was no significant alteration of the hydrolytic activities. On incubation for 12 h with king cobra venom (2 μ g for 0.1 ml plasma), there was considerable decrease in the activities and complete abolition of the protease binding capacity of α_2 -macroglobulin. On chromatography on Sephadex G-200, α_2 -macroglobulin activity and bulk of the protease activity of normal plasma were eluted in the void volume region. A minor protease peak was eluted with a V_e/V_o value of 2.5. With venom treated plasma, there was no decrease with this peak. The major protease peak and α_2 -macroglobulin activity were drastically reduced. Chromatography on red Sepharose showed that all the α_2 -macroglobulin activity and bulk of the protease activity in normal plasma were bound to the column. In venom treated plasma there was marked reduction in the bound fraction. The data suggest that cobra venom proteases directly or through proteases generated in plasma *in situ* causes limited cleavage of α_2 -macroglobulin as well as α_2 -macroglobulin bound proteases, inactivating them.

Keywords. King cobra venom; plasma α_2 -macroglobulin; venom and plasma proteases.

Introduction

Snake venoms can generate proteolytic activities in blood plasma by activating prothrombin, factor X, factor V and factor XIII (Mähar *et al.*, 1987; Komori *et al.*, 1988). Kallikrein-like and thrombin-like proteases have been identified in several snake venoms (Nikai *et al.*, 1988; Farid *et al.*, 1989). Venom proteases are known to hydrolyze and inactivate plasma protease inhibitors like α -1-protease inhibitor, α -1-antichymotrypsin and inter α -trypsin inhibitor (Catanese and Kress, 1985; Kress, 1986). Evans and Guthrie (1984) showed that cobra venoms inactivate human α_2 -macroglobulin (MG) within 10 min. Earlier studies from this laboratory showed that cobra and viper venoms in catalytic amounts, decreased protease binding capacity of plasma MG in a time-dependent manner without affecting the immunoreactive concentration of the factor (Sujatha *et al.*, 1988). These and other observations led to the suggestion that venoms generate proteases in plasma, which bind to MG. Unlike other protease inhibitors in plasma, MG traps the endopeptidases restricting their interaction with large protein substrates but allowing them to react with small synthetic substrates (Sottrup-Jensen, 1989). Among several venoms tested, king cobra (*Ophiophagus hannah*) venom was found to be most effective in decreasing the biological activity of human plasma MG (Roche

and Pattabiraman, 1989). In this communication, we report the study of the action of *O. hannah* venom on human plasma MG and proteases.

Materials and methods

Lyophilized sample of *O. hannah* venom, anti-human MG, N-acetyl-L-tyrosine ester (ATEE), N-benzoyl-DL-arginine p-nitroanilide (BAPNA) and succinyl-alanyl p-nitroanilide (STANA) were purchased from Sigma Chemical Company, St. Louis, Missouri, USA. Bovine trypsin (twice crystallized) and bovine chymotrypsin (thrice crystallized) were the products of Worthington Biochemical Corporation, Freehold, USA. Sephadex G-200 and red Sepharose CL-6B were procured from Pharmacia Laboratory Separation Division, Uppsala, Sweden. Ile-Pro-Arg-p-nitroanilide (S-2288, substrate for plasminogen activator and plasmin spectrum substrate), H-D-Pro-Phe-Arg-p-nitroanilide (S-2302, substrate for kallikrein), H-D-Val-Leu-Arg-p-nitroanilide (S-2266, substrate for glandular kallikrein), H-D-Phe-Pip-Arg-p-nitroanilide (S-2238, substrate for thrombin), <Glu-C<-p-nitroanilide S-2444, substrate for urokinase), benzoyl-Ile-Glu-Gly-Arg-p-nitroanilide (S-2222, substrate for factor Xa), H-D-Val-Lys-p-nitroanilide (S-2251, substrate for plasmin), methylsuccinyl-Arg-Pro-Tyr-p-nitroanilide (S-2586, substrate for chymotrypsin), acetyl-Ile-Glu-Gly-Arg-p-nitroanilide (S-2423, substrate for elastase), Glu-Pro-Val-p-nitroanilide (S-2484, substrate for granulocyte elastase) and kallikrein were the products of Kabi Vitrum Diagnostica, Mölndal, Sweden. All reagents were analytical grade commercial chemicals. Blood samples from healthy volunteers were collected in heparinized tubes and plasma was separated. Plasma specimens were used immediately or were stored at 4°C for a maximum of 24 h.

Chymotrypsin bound esterase activity of MG was estimated according to the method of Rao *et al.* (1984) using ATEE as substrate. The details of the method were described earlier (Sujatha *et al.*, 1988). Concentration of MG was determined by rocket immunoelectrophoresis as indicated before (Sujatha *et al.* 1988).

For measuring proteolytic activities of plasma or *O. hannah* venom, 10 µmol BAPNA, 10 µmol of STANA or 1.08 mg (1.47–2.43 µmol) of the other substrates was incubated with plasma (or venom) in the presence of 2 mM phosphate buffer pH 7.6 in a volume of 2 ml at 37°C. After definite time intervals the reaction was arrested by the addition of 1 ml of 30% acetic acid. Absorbance was measured at 410 nm.

To study the effect of venom on plasma protease activity and protease binding capacity of MG, aliquots of venom solution (10 µl) in 0.08 M phosphate buffer pH 7.6 was added to 100 µl of plasma and incubated at 37°C. At intervals aliquots were withdrawn and analyzed for the activities as described. Controls without venom were run simultaneously.

Gel filtration of native plasma and plasma treated with venom were performed as follows. The samples (0.5 ml) were diluted to 1 ml with 0.05 M phosphate buffer pH 7.6 and applied to a column of Sephadex G-200 equilibrated with the same phosphate buffer containing 0.15 M NaCl (bed volume 36 ml, 0.9 × 50 cm, 13 ml). One ml fractions were collected at a flow rate of 8 ml/h at 4°C. Aliquots (100 and 200 µl respectively) were used for assay of chymotrypsin binding to MG and proteolytic activities on synthetic substrates. Plasma kallikrein

It has been shown earlier that human MG has a high affinity for red Sepharose (Sujatha and Pattabiraman, 1986). To test whether MG bound to protease will also behave similarly, the following experiment was performed. Plasma (50 μ l) was mixed with 20 μ g of bovine trypsin (in 10 μ l of 0.05 M phosphate buffer pH 7 containing 0.1 M NaCl). The mixture was diluted to 0.25 ml with the same buffer system and applied to a column of red Sepharose (bed volume 2 ml) equilibrated with the phosphate buffer. The column was washed with 10 ml of the buffer and the bound protein was eluted with 10 ml of 0.05 M phosphate buffer, pH 7 containing 1.5 M NaCl. Two ml fractions were collected at a flow rate of 10 ml/h and fractions were assayed for tryptic activity using BAPNA as substrate. The elution profile is shown in figure 1. Tryptic activity was distributed both in the washing and elution. The activity in the washing was inhibited by the trypsin inhibitor from *Adenanthera pavonia* seed (Prabhu and Pattabiraman, 1980) but the tryptic activity in the elution was not affected by the inhibitor. Since MG bound proteases are known not to interact with proteinaceous substrates and inhibitors (Sottrup-Jensen, 1989), it can be concluded that the protease activity in the bound fraction represents MG bound trypsin, indicating that protease bound MG also shows high affinity to red Sepharose. Recovery of tryptic activity in these studies was only 36%. This could be a reflection of partial inactivation of trypsin by other plasma protease inhibitors.

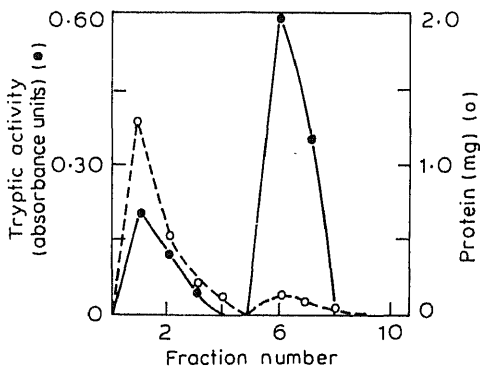


Figure 1. Chromatography of plasma:bovine trypsin mixture on red Sepharose CL 6B.

Red Sepharose chromatography of normal and venom treated plasma samples were performed similarly. The fractions were assayed for protease activity using S-2288, S-2266 as substrates.

Protein was determined by the method of Lowry *et al.* (1951) with bovine serum albumin as standard.

Results

Normal human plasma samples hydrolyzed the synthetic substrates to varying degrees and the highest activities were seen with S-2288, S-2302 and S-2266. Typical

2251, 4 with S-2586, 3 with S-2423, 2 with S-2484, 5 with STANA and 7 with BAPNA. In table 1, the data on the amidolytic activities on the 3 most active substrates by plasma samples are shown. The ratio of activities (S-2288:S-2302:1.01-1.82; S-2288:S-2266 0.74-1.14) varied over a narrow range. The ratios do agree with the reported ratios (S-2288:S-2302:S-2266) for plasma kallikrein (1.0:1.9:0.06), glandular kallikrein (1.0:10.0:13.0), plasmin (1.0:1.0:0.05), thrombin (1.0:0.11:0.02), trypsin (1.0:0.2:0.29) and factor Xa (1.0:0.48:0.01) (Kabi Vitco Product Information Bulletin, 1987). It is probable the amidolytic activities in plasma may represent more than one enzyme. However, based on the action on BAPNA, S-2586 and STANA, it can be concluded that tryptic, chymotryptic and elastase-like activities are negligible in plasma. Metal dependent elastase activity has been reported in human plasma (Franck and Byrjalsen, 1988). However, in our studies addition of Zn^{2+} (10^{-4} M) did not increase hydrolysis of STANA in plasma. *O. hannah* venom also hydrolyzed the synthetic substrates under similar conditions. The values (absorbance units/20 μ g weight) were 0.84 with S-2288, 0.80 with S-2302, 0.80 with S-2266, 0.34 with S-2238, 0.016 with S-2444, 0.02 with S-2222, 0.024 with S-2251, 0.028 with S-2423 and 0.0 with S-2484. However, at normal concentrations used (2 μ g/0.1 ml plasma) the venom contributed to about 3% of the activity with the most active substrate, S-2302.

Table 1. Amidolytic activity of plasma samples.

Substrate	Activity (absorbance units/ml plasma)	
	Mean	Range
S-2288	73.0	44-88
S-2302	77.0	71-86
S-2266	60.0	50-70

n = 6. Values are for 4 h incubation at 37°C.

In table 2, the amidolytic activities in fresh plasma, plasma incubated alone and venom-treated plasma are shown. While with plasma incubated alone no change in activities are marginal, drastic reduction was observed with venom-treated plasma. The decrease in activity was more with increase in concentration of venom. Patterns obtained with S-2586, S-2222, S-2251, S-2423 and S-2484 were similar (data not shown). The observations were quite contrary to expectation since if venom generated proteases, it should be reflected in increase in hydrolytic activity.

Table 2. Effect of venom on plasma amidolytic activity.

Substrate	Native plasma	Plasma incubated 12 h, 37°C	Venom + plasma incubated 12 h, 37°C	
			(2 μ g/0.1 ml)	(10 μ g/0.1 ml)
S-2288	0.71	0.66	0.17	0.07
S-2302	0.72	0.71	0.24	0.07
S-2266	0.70	0.65	0.09	0.0
S-2238	0.31	0.26	0.07	0.0
S-2444	0.12	0.11	0.03	0.0

Values are absorbance units for 10 μ l of plasma.

activities. Under similar conditions, the venom ($2\text{ }\mu\text{g}/0.1\text{ ml}$) caused nearly 90% loss of protease binding capacity of plasma MG. As observed with viper venom (Sujatha *et al.*, 1988), prior dilution of plasma with 0.02 M phosphate buffer, pH 7 abolished the action of *O. hannah* venom. Decrease in MG activity was 89% without dilution, 5.9, 0.0 and 0.0 respectively on 2-, 5- and 10-fold dilution when $2\text{ }\mu\text{g}/0.1\text{ ml}$ of venom was used.

In figure 2, the change in protease binding capacity of MG and amidolytic activity as functions of time of venom interaction are shown. The fall in the two activities were not parallel with time. Similar results were obtained with S-2302 and S-2288 (data not shown). This suggests that the two activities could be independent of each other and the amidolytic activities could be contributed by free proteases.

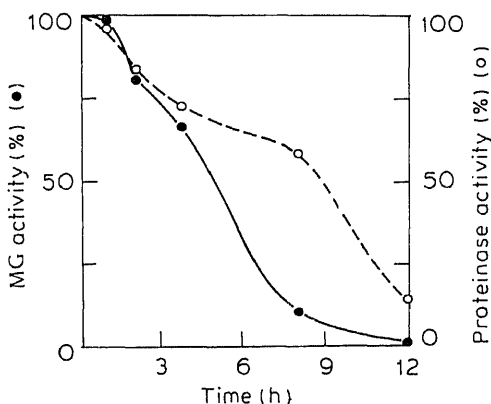


Figure 2. Effect of king cobra venom on plasma MG activity and hydrolysis of S-2266 as a function of time of inter-action. Plasma (0.1 ml) was incubated with venom ($5\text{ }\mu\text{g}$) in $10\text{ }\mu\text{l}$ of phosphate buffer pH 7 for different time intervals.

Plasma samples before and after venom treatment (12 h , $10\text{ }\mu\text{g}/0.5\text{ ml}$) were subjected to chromatography on Sephadex G-200. The results are shown in figure 3. With fresh plasma all the MG activity was eluted in the void volume region with 90–95% recovery. Major portion of amidolytic activity (with S-2302) was also eluted in the same region but slightly later than MG. In addition, a second minor

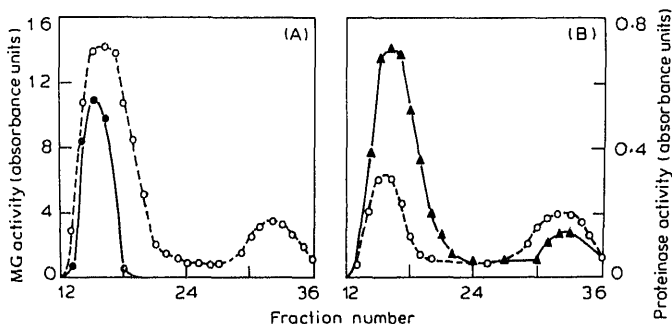


Figure 3. MG activity and proteinase (hydrolysis of S-2302) activity in plasma on gel

peak was seen much later (V_e 32 ml). However, the concentration of MG determined by immunoelectrophoresis showed a marginal decrease of not more than 15% (figure 4). Behaviour with S-2288 and S-2266 was also similar. Plasma kallikrein and bovine trypsin were eluted with V_e values of 26 and 28 ml respectively (data not shown). The results suggest that the major peak in plasma could represent proteases bound to MG. Fractions 15 and 16 were pooled and subjected to heat treatment at 60°C. After 5 and 20 min heat treatment, per cent loss of MG activity and amidolytic activity on S-2302 were respectively 13, 42 and 62, 88 indicating that the amidolytic activity is more susceptible to heat. Plasma incubated for 12 h at 37°C behaved similar to the native plasma on gel chromatography (figure 3B). On the other hand, with venom treated plasma, there was no detectable MG activity in the V_0 region. The amidolytic activity in the F_1 region was also drastically reduced. However, the minor peak showed a small increase in activity. The patterns with S-2288 and S-2266 were similar.

The recovery of protease activity during gel chromatography was around 70%. Fractions 29–33 separated from the venom treated plasma were pooled. On incubation with equal volume of fresh plasma, for 12 h at 37°C, the fraction did not



Figure 4. Immunoelectrophoretic estimation of plasma MG. From left to right—rockets 1 and 2, plasma incubated for 12 h at 37°C. Rockets 3 and 4, plasma incubated with venom (10 µg/0.1 ml) for 12 h at 37°C.

decrease MG activity. Similar results were obtained with the fraction concentrated 5 times by lyophilization.

Native plasma and venom treated plasma were subjected to chromatography on red Sepharose. The results are shown in figure 5. Small quantities of protease activity (S-2302) were found in the washings and bulk of the activity was bound to the matrix and eluted with high salt concentration, in normal plasma, suggesting that the major fraction of protease activity in plasma is bound to MG. On

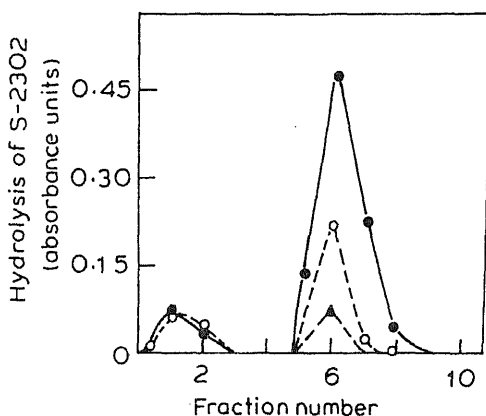


Figure 5. Hydrolysis of S-2302 by fractions obtained on chromatography on red Sepharose CL 6B. (●), Native plasma; (○) plasma treated with 2 µg/0.1 ml venom; (▲) plasma treated with 10 µg/0.1 ml venom.

Discussion

Press and Catanese (1981) suggested that venom proteases reacted slowly with MG and retained some of their proteolytic activities. Schapira *et al.* (1982) indicated that stability of MG to form complexes with proteases, is retarded in the presence of the substrates for the proteases. The present studies suggest that venom proteases can cause indirectly limited hydrolysis of MG as well as protease bound to MG leading to the inactivation of MG and the activity of the bound protease on small substrates. It is known that enzymes like proteinase C and neutrophil endopeptidase do not bind to MG (Marlar and Kressin, 1989; Painter *et al.*, 1988). Reddy *et al.* (1989) recently have shown that neutrophil and eosinophil proteases can cause functional inactivation of MG. The observation that venoms do not inactivate MG isolated from plasma unlike the activity in plasma *per se* indicates the mediation of factors in blood (Sujatha *et al.* 1988). This is also supported by the observation that action of *O. hannah* venom on MG is abolished by prior dilution of plasma. Further studies are needed to identify these factors. Proteolytic activity evidenced by hydrolytic action on synthetic substrates to a large extent was found to be associated with MG. The decrease in these activities in venom treated plasma would suggest that venom proteases or proteases generated by venom in plasma could hydrolyze and inactivate them. The exact nature of the amidolytic activity in plasma, that was not bound to MG and that was not decreased by the venom, is not known. The elution of this activity much later than kallikrein and trypsin would suggest that it is contributed by low molecular weight enzymes. However, anomalous behaviour of these proteases on Sephadex G-200 cannot be ruled out at this stage.

Acknowledgement

References

- Catanese, J. J. and Kress, L. F. (1985) *Comp. Biochem. Physiol.*, **80**, 507-512.
- Evans, H. J. and Guthrie, V. H. (1984) *Biochim. Biophys. Acta*, **784**, 97-101.
- Farid, T. M., Tu, A. T., Farid-el-Asmar, M. (1989) *Biochemistry*, **28**, 371-377.
- Franck, C. and Byrjalsen, I. (1988) *Biol. Chem. H.S.*, **369**, 679-689.
- Komori, Y., Nikai, T., Sakairi, Y. and Sugihara, H. (1988) *Int. J. Biochem.*, **20**, 387-392.
- Kress, L. F. (1986) *J. Cell. Biochem.*, **32**, 51-58.
- Kress, L. F. and Catanese, J. J. (1981) *Toxicon*, **19**, 501-507.
- Lowry, O. H., Rosebrough, N. J., Farr, A. L. and Randall, R. J. (1951) *J. Biol. Chem.*, **193**, 265-275.
- Mähar, A., Siigur, E. and Siigur, J. (1987) *Biochim. Biophys. Acta*, **925**, 272-281.
- Marlar, R. A. and Kressin, D. C. (1989) *Thromb. Res.*, **54**, 177-186.
- Nikai, T., Imai, K., Nagasaka, M. and Sugihara, H. (1988) *Int. J. Biochem.*, **20**, 1239-1245.
- Painter, R. G., Dukes, R., Sullivan, J., Carter, R., Erdos, E. G. and Johnson, A. R. (1988) *J. Biol. Chem.* **263**, 9456-9461.
- Prabhu, K. S. and Pattabiraman, T. N. (1980) *J. Sci. Food Agric.*, **31**, 967-980.
- Rao, N. R., Bhat, P. G. and Pattabiraman, T. N. (1984) *Biochem. Med.*, **32**, 357-364.
- Reddy, V. Y., Pizzo, S. V. and Weiss, S. J. (1989) *J. Biol. Chem.*, **264**, 13801-13809.
- Roche, M. and Pattabiraman, T. N. (1989) *Biochem. Arch.*, (in press).
- Schapira, M., Scott, C. F., James, A., Silver, L. D., Kueppers, J., James, H. L. and Colman, R. W. (1988) *Biochemistry*, **21**, 567-572.
- Sottrup-Jensen, L. (1989) *J. Biol. Chem.*, **264**, 11539-11542.
- Sujatha, S., Jacob, R. T. and Pattabiraman, T. N. (1988) *Biochem. Med. Metab. Biol.*, **39**, 217-225.
- Sujatha, S. and Pattabiraman, T. N. (1986) *Indian J. Clin. Biochem.*, **1**, 82-89.

Optimization of sodium orthovanadate to treat streptozotocin-induced diabetic rats

N. SEKAR, S. WILLIAM, N. BALASUBRAMANIAM,
P. KAMARAJAN and S. GOVINDASAMY

Department of Biochemistry, University of Madras, Guindy Campus, Madras 600 025,
India

MS received 16 October 1989; revised 9 April 1990

Abstract. Oral administration of sodium orthovanadate restored blood glucose to normal levels in streptozotocin-induced diabetic rats. To establish the safety dose and to evaluate the side effects of over dose, if any, different doses of vanadium were used in the present study. Low concentrations of vanadium (0.1 and 0.3 mg/ml in drinking water) restored blood glucose, urea, cholesterol and the status of liver pathophysiological enzymes to normal levels in experimental rats. High vanadate treatment proved to be toxic not only to diabetic but also to normal rats as evidenced from the observations on the blood urea, plasma and liver glutamate oxaloacetate transaminase and glutamate pyruvate transaminase. Low vanadate treatment restored body homeostasis of diabetic rats and was found to be nontoxic to normals.

Keywords. Vanadate optimization; diabetes; lipid peroxidation.

Introduction

Vanadium has been found to be essential for normal growth and development and vanadium deprivation causes reduced growth, increased plasma cholesterol levels, impaired reproductive performance and severe disorganization of the cells of the epiphysis with subsequent bone malformation in chick and rat (Golden and Golden, 1981).

Recently the role of vanadium in the biological system has been intensively studied because of its insulin mimetic effect. Heyliger *et al.* (1985) found that the inclusion of sodium orthovanadate in the drinking water (0.6–0.8 mg/ml) of streptozotocin-diabetic rats alleviated the symptoms of diabetes resulting in the normalization of blood glucose levels and the elimination of depressed cardiac performance. Gil *et al.* (1988) reported the insulin like effects of vanadate on glucokinase and fructose-2,6-bisphosphate levels in the liver of diabetic rats. High concentrations of orally administered vanadate (0.8 mg/ml in drinking water) reduced blood glucose levels within 2–4 days of administration and led to the appearance of hypoglycemia in test animals and impaired the liver functions. However lower concentration of vanadate (0.2 mg/ml in drinking water) lowered blood glucose levels within 4 days and did not impair the liver functions (Meyerovitch *et al.*, 1987). Hence an attempt has been made to evaluate the biological role of vanadium at various concentrations in normal and diabetic rats. The possible curative role of vanadate for streptozotocin-induced diabetes has been monitored.

Materials and methods

Male Wistar rats weighing 160–180 g were fasted for 24 h before inducing diabetes with streptozotocin (Sigma, USA). Animals were anesthetized with ether and injected via the tail vein with freshly prepared solution of streptozotocin (55 mg/kg body weight) in 0.1 M citrate buffer pH 4.5. Control animals received citrate buffer alone. Streptozotocin-treated animals were allowed to drink 5% glucose solution overnight to overcome drug induced hypoglycemia. Streptozotocin-treated control animals were allowed access to food and water *ad libitum*. The normal and overt diabetic rats (for a month) were divided into 4 groups each such as: normal (N), various concentrations of vanadate treated controls (0.1, 0.3 and 0.6 mg/ml; N₁, N₂, N₃ respectively), diabetic (D), and various concentrations of vanadate treated diabetic (0.1, 0.3, 0.6 mg/ml-D₁, D₂, D₃ respectively). Throughout this manuscript the groups N₁, N₂, D₁ and D₂ are referred as low vanadate treated and N₃ and D₃ are high vanadate treated rats. The normals and the streptozotocin-diabetic rats drank 0.5% of sodium chloride in water. The vanadate treated groups of rats drank 0.5% sodium chloride in water containing sodium orthovanadate (0.1, 0.3 and 0.6 mg/ml) prepared freshly, everyday. Sodium chloride was included in the diet known to reduce vanadium induced diarrhoea (Meyerovitch *et al.*, 1987).

After 15 days of vanadium treatment, the rats were sacrificed by cervical decapitation and blood was collected using EDTA as anticoagulant. The blood was precipitated with 10% trichloroacetic acid (TCA). After centrifugation, the supernatant was used for the estimation of glucose (Sasaki and Matsui, 1970), urea (Natelson *et al.*, 1951). Plasma cholesterol was estimated by the method of Parekh and Jung (1970). Plasma concentrations of vanadium were determined by Orion-960 Autochemistry system (USA). The lowest limit of detection of vanadium was 0.05 µg/ml. The diet fed to the experimental animals does not contain any measurable amount of vanadate.

The liver tissue of known weight was homogenized in 0.1 M Tris-HCl (pH 7.4) at 4°C in a Potter-Elvehjem homogenizer with a Teflon-pestle at 6000 rpm for 3 min. Plasma and liver homogenate glutamate oxaloacetate transaminase (GOT) and glutamate pyruvate transaminase (GPT) were assayed according to the method of Wooten (1965). TCA (20%) was used to precipitate plasma and liver homogenate protein. After centrifugation, the supernatants were used for estimation of lipid peroxides by measuring malondialdehyde (MDA) according to the method of Cynamon *et al.* (1985). Superoxide dismutase (SOD, Misra and Fridovich, 1972) and catalase (CAT, Takhara *et al.*, 1960) were also estimated in liver homogenate. The data were statistically analyzed and probabilities indicated.

Results

Changes in body weight are shown in figure 1, during the experimental period. Body weights were found to be increased in normals and low vanadate treated controls, decreased in diabetics and high vanadate treated diabetics and low vanadate treated control rats. Low vanadate treated diabetic groups regain body weight significantly when compared with diabetics.

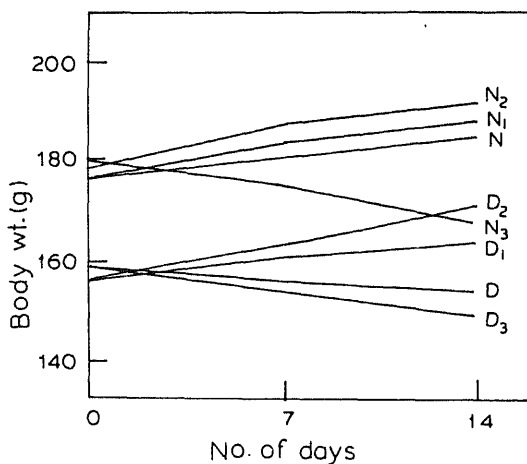


Figure 1. Body weight changes of normal, diabetic, vanadate treated control and diabetic groups of rats. N and D represent normal and diabetic rats. N₁N₂N₃ and D₁D₂D₃ represent 0.1, 0.3, 0.6 mg/ml vanadate treated control and diabetic groups respectively.

Table 1. Amount of fluid, vanadium intake and plasma vanadium levels in normal, vanadate (different concentrations) treated controls, diabetics and vanadate (different concentrations) treated diabetic rats.

Experimental groups	Fluid intake (ml/kg/day)	Vanadium intake (mg/kg/day)	Plasma vanadium levels (µg/dl)
N ₀	234.4 ± 23.2	—	—
N ₁	215.6 ± 14.4	21.6 ± 1.4	35.0 ± 4.8
N ₂	171.6 ± 15.2	51.5 ± 4.6	63.0 ± 5.4
N ₃	128.1 ± 14.6	77.6 ± 8.6	139.0 ± 9.8
D ₀	574.4 ± 49.0*	—	—
D ₁	312.2 ± 29.9*	30.3 ± 2.9*	42.0 ± 6.2
D ₂	208.8 ± 20.5*	62.6 ± 6.1*	76.0 ± 5.9*
D ₃	196.8 ± 20.8	120.0 ± 9.5*	184.0 ± 6.4*

Values are expressed as mean ± SD for animals in each group.

* $P < 0.05$; normals *vs* diabetes; different concentrations of vanadate treated controls *vs* different concentrations of vanadate treated diabetes.

vanadium concentrations were increased significantly in vanadate treated diabetic rats with respect to vanadate concentrations when compared to vanadate treated control rats. Previously Shechter and Karlsh (1980), have shown that vanadate elicits its effects *in vitro*, with ED₅₀ values between 2.4 µg/ml and 3.6 µg/ml vanadate. Assuming that the *in vivo* effects of vanadate are mediated through insulin-responsive tissues, the circulating concentration of vanadate in N₂ and D₂ groups have been found to be biologically effective and are on par with the ED₅₀ value of vanadate as assessed by *in vitro* studies. Hence the amount of vanadate administration (0.3 mg/ml) may be optimum and sufficient to maintain normoglycemia.

alterations in glucose, urea and cholesterol. However, high vanadate controls and diabetic rats exhibited hypolipidemic and hypoglycemic condition. The urea level was increased significantly in high vanadate treated controls. The increased glucose, urea and cholesterol observed in diabetic rats. The increased glucose, urea and cholesterol observed in condition reversed to normal levels in low vanadate treated diabetic group. Observations clearly show that low vanadate treatment in normal did not any of the observed body functions but corrected the biochemical alterations in diabetes and restored the body homeostasis.

Activities of GOT and GPT in plasma and liver of normals, vanadate treated controls, diabetic and vanadate treated diabetics are presented in table

Table 2. Levels of blood glucose, urea and plasma cholesterol in normals, vanadate (different concentrations) treated controls, diabetics and vanadate (different concentrations) treated diabetic rats.

	Glucose (mg/dl)	Urea (mg/dl)	Cholesterol (mg/dl)
N	87.3 ± 5.2	18.2 ± 2.8	82.6 ± 2.7
N ₁	84.4 ± 6.1	19.1 ± 2.2	80.9 ± 2.4
N ₂	82.6 ± 5.8	20.2 ± 3.1	78.8 ± 3.6
N ₃	73.2 ± 4.9	28.2 ± 2.4*	68.7 ± 3.2*
D	248.3 ± 6.9	26.4 ± 3.7	194.6 ± 4.7
D ₁	153.4 ± 6.4*	22.3 ± 2.6*	156.5 ± 5.4*
D ₂	122.6 ± 5.7*	20.8 ± 3.3*	124.1 ± 6.2*
D ₃	78.4 ± 5.5	37.7 ± 3.4*	73.6 ± 3.3*

Values are expressed as mean ± SD for 6 animals in each group.

* $P < 0.05$; Normals *vs* vanadate (different concentrations) treated controls. Diabetes *vs* Vanadate (different concentrations) treated diabetics.

Table 3. Activities of plasma (IU/l) and liver (nmol of pyruvate liberated/h/mg protein) GOT and GPT in normal, vanadate (different concentrations) treated control, diabetes and vanadate (different concentrations) treated diabetic rats.

	GOT		GPT	
	Plasma	Liver	Plasma	Liver
N	14.6 ± 1.2	612 ± 36	10.6 ± 0.8	956 ± 32
N ₁	14.8 ± 1.8	596 ± 47	10.2 ± 0.6	942 ± 29
N ₂	15.1 ± 0.8	580 ± 39	9.7 ± 1.0	936 ± 24
N ₃	19.3 ± 1.7*	649 ± 41	13.3 ± 1.2*	1027 ± 44*
D	17.3 ± 1.4	727 ± 35	21.3 ± 2.0	1046 ± 39
D ₁	16.6 ± 1.7	692 ± 29	19.5 ± 1.8	984 ± 28*
D ₂	15.8 ± 1.1	658 ± 33*	12.3 ± 1.2*	968 ± 33*
D ₃	20.6 ± 1.6*	714 ± 47	25.3 ± 1.6*	1084 ± 47

Values are expressed as mean ± SD for 6 animals in each group.

significantly elevated in high vanadate treated control and diabetic groups ($P < 0.05$). In control and diabetics, high vanadate treatment increased GPT in plasma and liver. In contrast, low vanadate treatment did not alter the transaminase activities in normals and restored the activity of GPT in diabetes to normal levels.

Table 4 depicts the levels of plasma and liver lipid peroxides, the activities of liver SOD and CAT of the experimental rats. The MDA content and the activities of SOD and CAT increased significantly ($P < 0.05$) in high vanadate treated experimental rats (controls and diabetics). Low vanadate treatment counteracted the alternations in the levels of MDA, SOD and CAT in diabetics and did not influence in controls.

Table 4. Levels of plasma and liver lipid peroxide (MDA) and the activities of liver SOD and CAT in normals, vanadate (different concentration) treated controls, diabetics and vanadate (different concentration) treated diabetic rats.

	Lipid peroxide (MDA)		Liver	
	Plasma nmol of MDA/ml	Liver nmol of MDA/ 100 mg protein	SOD	CAT
N	2.30 ± 0.32	139.2 ± 10.7	6.41 ± 0.8	68.7 ± 4.1
N ₁	2.41 ± 0.28	141.3 ± 11.5	6.62 ± 0.6	70.6 ± 4.8
N ₂	2.62 ± 0.23	146.3 ± 9.6	6.84 ± 1.1	71.8 ± 6.8
N ₃	4.26 ± 0.36*	175.6 ± 10.2*	4.16 ± 0.9*	46.4 ± 5.4*
D	5.68 ± 0.68	198.2 ± 12.3	3.12 ± 0.7	37.4 ± 4.7
D ₁	4.21 ± 0.46*	169.1 ± 11.4*	4.21 ± 1.0	44.8 ± 5.5*
D ₂	3.45 ± 0.61*	152.2 ± 9.8*	5.82 ± 1.1*	52.7 ± 4.2*
D ₃	6.21 ± 0.57	206.6 ± 12.7	2.82 ± 1.3	32.4 ± 5.3

The values are expressed as mean ± SD for 6 animals in each group.

* $P < 0.05$; Normals *vs* vanadate (different concentrations) treated controls. Diabetes *vs* vanadate (different concentrations) treated diabetics.

One unit of SOD activity is the amount of protein required to give 50% inhibition of adrenaline autooxidation. CAT activity is expressed as nmol of H₂O₂ decomposed/min/mg protein.

Histopathological studies revealed extensive alterations in diabetic liver (hyperaemia, multiple areas of necrosis, (figure 3D)), high vanadate treated diabetics [focal necrosis and mild fatty changes (figure 3D₃)] and in high vanadate treated control rats [multiple areas of necrosis cloudy swelling and nuclear pyknosis adjacent to the areas of necrosis (figure 2N₃)]. The pathomorphological changes induced in streptozotocin-diabetes become apparently normal during low vanadate treated diabetes (figure 3D₂). Low vanadate treated controls does not exhibit any pathomorphological alterations (figure 2N₂).

Discussion

The present study confirms the earlier observations of the hypoglycemic effects of vanadate treatment on streptozotocin diabetic rats (Hendler *et al.* 1985; Gil *et al.*

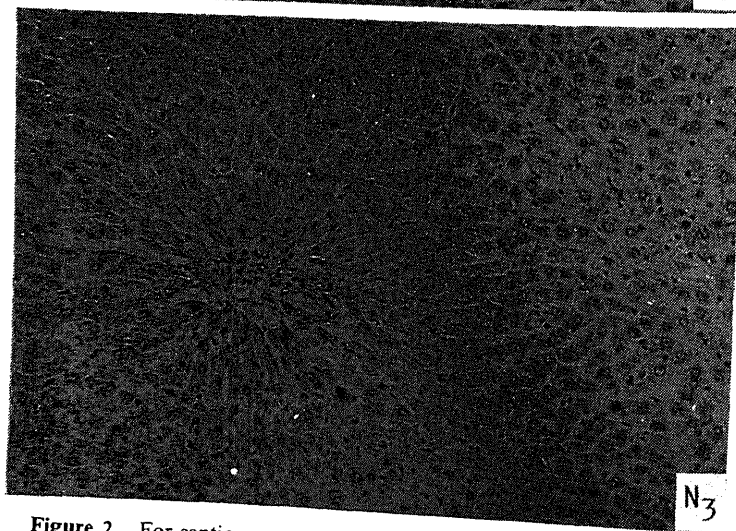
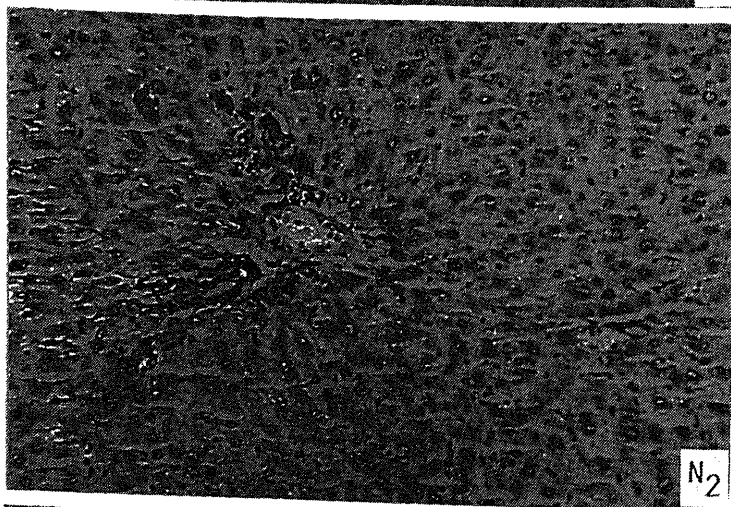
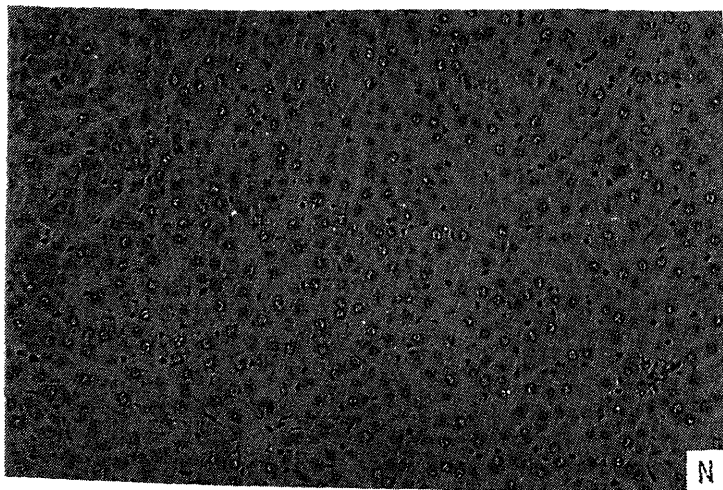
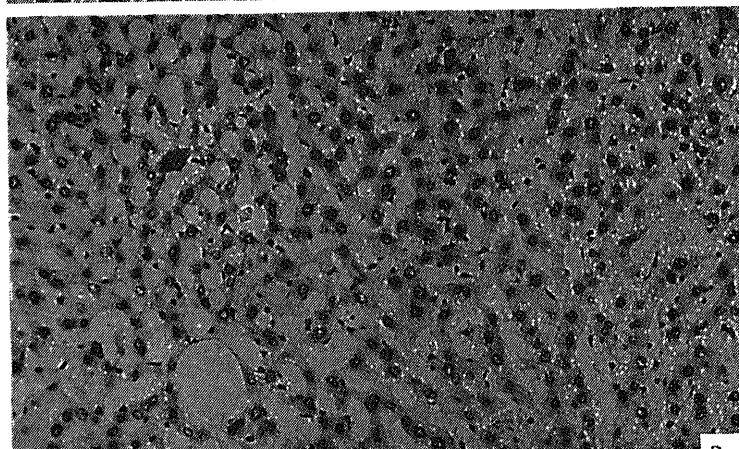
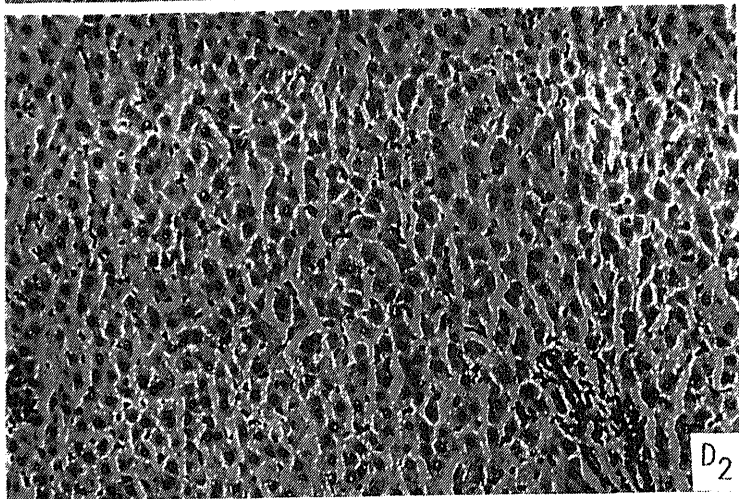
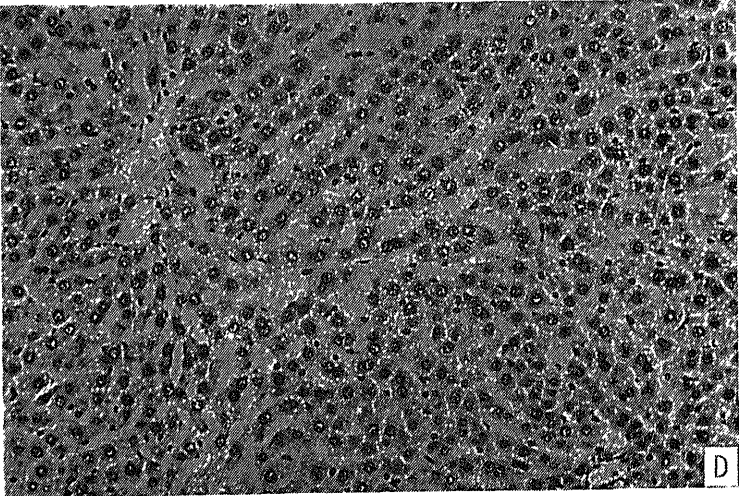


Figure 2. For caption, see p. 75.



cholesterol in diabetes mellitus (George and Augusti, 1978). In the streptozotocin-induced diabetic rats, the activities of urea cycle enzymes at least doubled over controls and the urea level was increased significantly (*et al.*, 1981). According to Feingold (1982), the *de novo* synthesis of cholesterol in the gut of diabetic rats increased 2-fold when compared to other organ systems and this may be the reason for the increase in plasma cholesterol. Kanthasamy *et al.* (1986) have reported that the increased cholesterol in diabetic rats were brought back to control levels during oral administration of vanadate. Addition of vanadium (50 $\mu\text{g}/100\text{ g}$ diet) to the diet enhanced the cholesterol level by over 40% than that of control rats (Schwarz and Milne, 1971).

Liver tissue contains 3 times the amount of GPT as heart muscle or kidney. A rise in GPT activity is almost always due to hepatocellular damage and is usually accompanied by a rise of GOT (Mohan Rao *et al.*, 1989). Moderately elevated activities of both GOT and GPT have been reported in spontaneous diabetic BB rats (Mohan Rao *et al.*, 1984). The mean activities of GOT and GPT of patients with severe complications and those with family history of diabetes were significantly higher than the normal. The elevated activities of GOT and GPT in diabetics after vanadate treatment may be due to hepatocellular damage followed by cardiac damage. Low vanadate treated diabetic rats maintained the normal GOT and GPT activities.

In many diseases, the lipid peroxides (MDA) formed, accumulated to a certain degree, leak from the organ or tissue into the blood stream and thereby increase the lipid peroxide level in the plasma. The increased lipid peroxide level in plasma could not be excreted as such into the urine and they circulate in the blood stream until they are decomposed by enzyme system such as glutathione peroxidase and glutathione reductase (Yagi, 1987). The plasma levels of lipid peroxide in diabetic patients were significantly higher than that of control which was reduced in controlled diabetic (Sato, 1979). In streptozotocin-induced diabetic rats, Wohaieb and Godin, (1987) have reported the alterations in the activities of antioxidant enzymes in several tissues and all were reversible by treatment with insulin. Decreased CAT and SOD activities have been noticed in streptozotocin-induced diabetic liver and kidney tissues where these enzyme activities are normally relatively high. The increased reactive oxygen radicals can thereby reduce the activity of these enzymes. The observed abnormalities of tissue antioxidant systems and plasma lipid peroxide of streptozotocin rats improved by low vanadate treatment seems indicative of their association with the process of diabetes (Laoven *et al.*, 1986). In low vanadate treated diabetic rats, an improvement in the defense system has been observed while the high vanadate treatment increased the lipid peroxides and decreased liver CAT and SOD.

The alterations of plasma and liver lipid peroxide, GOT, GPT and blood urea, plasma cholesterol and liver CAT and SOD in the diabetic condition have been counteracted after low vanadate treatment which indicate the insulinic action(s) of vanadate on diabetic rats. However high vanadate treatment potentiates the pathogenic state in diabetics as well as in controls.

Acknowledgement

One of the authors (N. S.) thank the Indian Council of Medical Research, Delhi, for the financial assistance in the form of a fellowship.

References

- Cynamon, H. A., Isenbrerg, J. N. and Nguyen Co. A. (1985) *Clin. Chim. Acta*, **151**, 169.
- Feingold, K. R., Fulford, M., Zsigmondgyula, M. H., Arthur, L. R., Steven, S. and Marvin, D. (1982) *Lessons Anim. Diabetes (Lect. Discus. Int. Workshop)* 556.
- George, K. A. and Augusti, K. T. (1978) *Indian J. Exp. Biol.*, **16**, 1952.
- Gil, J., Miralpeix, M., Carreras, J. and Bartrons, R. (1988) *J. Biol. Chem.*, **263**, 1868.
- Golden, M. H. N. and Golden, B. E. (1981) *Br. Med. Bull.*, **37**, 31.
- Heyliger, C. E., Tashiliani, A. G. and McNeil, J. H. (1985) *Science*, **227**, 1474.
- Jorda, A., Cado, J. and Grisolia, S., (1981) *Enzyme*, **26**, 240.
- Kanthasamy, A., Rathinavelu, A. and Govindasamy, S. (1986) *Contemp. Themes Biochem.*, **6**, 318.
- Loven, D., Schedl, H., Wilson, H., Daanbees, T. T., Stegink, D. L., Diekus, M. and Oberley, L. (1986) *Diabetes*, **35**, 503.
- Meyerovitch, J., Farfel, Z., Sack, J. and Shechter, Y. (1987) *J. Biol. Chem.*, **262**, 6658.
- Misra, H. P. and Fridovich, I. (1972) *J. Biol. Chem.*, **247**, 3170.
- Mohan Rao, G. M., Morghom, L. O., Kabur, M. N., Ben Mohmud, B. M. and Ashibani, K. (1989) *Indian J. Med. Sci.*, **5**, 118.
- Natelson, S., Scott, M. L. and Beffa, C. (1951) *Am. J. Clin. Pathol.*, **21**, 1423.
- Parekh, A. C. and Jung, D. H. (1970) *Anal. Chem.*, **42**, 1423.
- Sasaki, J. and Matsui, S. (1972) *Rinshu Kagaku*, **1**, 346.
- Sato, Y., Hotta, N., Sakamoto, N., Matusoka, S., Ohishi, N. and Yagi, K. (1979) *Biochem. Med.*, **21**, 104.
- Schwarz, K. and Milne, D. B. (1971) *Science*, **174**, 426.
- Scott, P. W., Trick, K. D., Lee, L. P. K., Hynie, I., Heick, H. M. C. and Nera, E. A. (1984) *Clin. Biochim.*, **17**, 270.
- Shechter, Y. and Karlsh, S. J. D. (1980) *Nature (London)*, **284**, 556.
- Takhara, S., Hamilton, B. H., Nell, J. V., Kobara, T. Y., Ogura, Y. and Nishimura, E. T. (1960) *J. Clin. Invest.*, **39**, 610.
- Wohaieb, S. A. and Godin, E. V. (1987) *Diabetes*, **36**, 1014.
- Wooten, I. D. P. (1965) *Microanalysis in medical biochemistry* (London: J and A Churchill Ltd.)
- Yagi, K. (1987) *Chem. Phys. Lipids*, **45**, 337.

Figure 2. Section of normal liver (N) low vanadate treated control (N₂) and high vanadate treated control (N₃) rat. Haematoxylin-Eosin × 240.

Figure 3. Section of diabetic liver (D) low vanadate treated diabetic (D₂) and high vanadate treated diabetic (D₃) rat. Haematoxylin-Eosin × 240.

Enzyme activities associated with developing wheat (*Triticum aestivum* L.) grain amyloplasts

R. MAHAJAN and RANDHIR SINGH*

Department of Chemistry and Biochemistry, Haryana Agricultural University, Hisar 125 004, India

MS received 19 December 1989; revised 24 April 1990

Abstract. Intact amyloplasts from endosperm of developing wheat grains have been isolated by first preparing the protoplasts and then fractionating the lysate of the protoplasts on percoll and ficoll gradients, respectively. Amyloplasts isolated as above were functional and not contaminated by cytosol or by organelles likely to be involved in carbohydrate metabolism. The enzyme distribution studies indicated that ADP-glucose pyrophosphorylase and starch synthase were confined to amyloplasts, whereas invertase, sucrose synthase, UDP-glucose pyrophosphorylase, hexokinase, phosphofructokinase-2 and fructose-2,6-P₂ase were absent from the amyloplast and mainly confined to the cytosol. Triose-P isomerase, glyceraldehyde-3-P dehydrogenase, phosphohexose isomerase, phosphoglucomutase, phosphofructokinase, aldolase, P_i-fructose-6-P-1 phosphotransferase, and fructose-1,6-P₂ase, though predominantly cytosolic, were also present in the amyloplast. Based on distribution of enzymes, a probable pathway for starch biosynthesis in amyloplasts of developing wheat grains has been proposed.

Keywords. Wheat; *Triticum aestivum*; amyloplasts; enzymes; carbohydrate metabolism.

Introduction

Starch synthesis in higher plants is confined to chloroplasts in green photosynthetic tissues and amyloplasts in non-green storage tissues such as the endosperm tissue of the developing wheat grain (Keeling *et al.*, 1988). The amyloplast consists of a starch granule and plastid stroma enclosed by a double membrane (Badenhuizen, 1969). Based on *in vitro* assays of enzymes presumed to be involved in starch synthesis, a biosynthetic pathway has been proposed for storage tissues including cereal grains (Singh and Mehta, 1986). Though the pathway proposed has received general acceptance, it does not take into account the intracellular compartmentation of starch synthesis within the amyloplast and the selective permeability of the plastid membranes. Hence, it could not be proved conclusively as to how translocated sucrose is converted to starch in storage tissues.

The transport properties of chloroplasts have been studied in detail (Heber, 1974; Heber and Heldt, 1981). However, parallel information is completely lacking for amyloplasts. This has been mainly because of the reason that intact amyloplasts from cereal grains could not be isolated till recently (Singh, 1989). However, techniques have now been developed and successfully employed for the isolation of intact amyloplasts from cereal grains (MacDonald and apRees, 1983a, b; Echeverria *et al.*, 1985; Entwistle *et al.*, 1988; Santha *et al.*, 1988). In our present attempt, we

*To whom all correspondence should be addressed.

have been successful in isolating intact amyloplasts from developing wheat grains. Furthermore, we have determined the activities of the enzymes involved in carbohydrate metabolism and starch synthesis associated with cytosol and amyloplastic fractions of wheat grains. Based on the distribution of enzymes, a probable mechanism for the biosynthesis of starch in amyloplasts of developing wheat grains has been proposed.

Materials and methods

Chemicals

All the biochemicals used in the present investigation were procured from Sigma Chemical Co., St. Louis, Missouri, USA. All other chemicals used were of high purity analytical grade obtained from BDH and/or E. Merck.

Plant material

Immature wheat grains were harvested from field grown wheat crop (cv. WH-157) at day 20 after anthesis, endosperms removed and stored in liquid nitrogen for further use.

Isolation of amyloplasts

Amyloplasts were isolated essentially by following the methods of Echeverria *et al.* (1985) and Emes and England (1986) with slight modifications. Unless stated otherwise, all steps were carried out at 0–4°C. Endosperm sections (1 g) were incubated for 18–20 h in 50 mM tricine-NaOH buffer (pH 7.9) containing 1 mM EDTA, 5 mM MgCl₂, 0.5 M sucrose, 0.1% bovine serum albumin (BSA), 2% cellulase (Onozuka, R-10), 1% pectinase (Sigma), 1% polyvinylpyrrolidone, 1 mM KCl, 1 mM CaCl₂ and 10 mM mercaptoethanol at 10°C. The endosperm sections were pressed gently with the help of fine brush. The homogenate was passed through a single layer of muslin cloth and underlaid with 50 mM of tricine-NaOH buffer (pH 7.9) containing 0.5 M sucrose, 1 mM EDTA, 5 mM MgCl₂, 0.1% BSA, 1 mM KCl, 1 mM CaCl₂, 10 mM mercaptoethanol and 10% percoll in the ratio of 1:1.

After allowing to stand for 1 h, the homogenate was centrifuged at 4000 *g* for 20 min in a swing out rotor (Hitachi model). The pellet was suspended in 50 mM tricine-NaOH buffer (pH 7.9) containing 0.5 M sucrose, 1 mM EDTA, 1 mM MgCl₂, 0.1% BSA and 10% mercaptoethanol. Amyloplasts were released by passing the above suspension through a 19 gauge syringe. The amyloplasts were then separated by layering the suspension on discontinuous ficoll gradient of 30–100% at 1×*g*. After setting at 1×*g* for 3 h, the amyloplasts appearing as bands were collected. The upper layer (30–50%) was free from amyloplasts contamination and centrifuged at 15,000 *g* for 20 min. The pellet obtained was dissolved in the supernatant after centrifugation in a swing-out rotor at 4000 *g*. This was recentrifuged at 15,000 *g* for 30 min to get rid of nuclei and mitochondria. The supernatant obtained at this step was referred to as cytosolic fraction.

For getting photographs under light microscope, the amyloplasts were stained with iodine solution. The length and width of amyloplasts were measured with the help of oculometer.

Enzyme assays

Ficoll gradient layer (60–70%) was collected and vigorously stirred on a vortex mixer for several seconds to rupture the amyloplast membranes. The suspension was centrifuged for 5 min at 1000 *g*. The supernatant obtained was used directly for enzyme assays except that of invertase for which the supernatants were dialyzed overnight at 4°C against 2 l of 5 mM phosphate buffer (pH 7) containing 5 mM EDTA.

All assays were carried out at 30°C, in the various reaction mixtures described below. Assays were conducted in the range of concentrations of enzyme where the activity increased linearly with increase in the amount of enzyme preparation and the reaction time. The background values were routinely taken as the activities obtained with denatured enzyme (the enzymes were denatured immediately after their addition to the reaction mixtures).

Triose phosphate isomerase (EC 5.3.1.1), aldolase (EC 4.1.2.13), fructose-1, 6-bisphosphatase (EC 3.1.3.11), phosphohexose isomerase (EC 5.3.1.9), and phosphoglucomutase (EC 2.7.5.1) were assayed spectrophotometrically following the procedures of MacDonald and apRees (1983a).

Hexokinase (EC 2.7.1.1), sucrose synthase (EC 2.4.2.13), invertase (EC 3.2.1.26), ADP-glucose pyrophosphorylase (EC 2.7.7.27), UDP-glucose pyrophosphorylase (EC 2.7.7.9) and starch synthase (EC 2.4.1.21) were assayed as described earlier (Kumar and Singh, 1984). Fructose-6-phosphate-1-phosphotransferase (PFP, EC 2.7.1.90), fructose-6-phosphate, 2-kinase (PFK-2, EC 2.7.1.105), fructose 2,6-P₂ase (EC 3.1.3.46), phosphofructokinase (PFK, EC 2.7.1.11) and glyceraldehyde-3-phosphate dehydrogenase (EC 1.2.1.12) were assayed as per the procedures of VanSchaftingen *et al.* (1982), Stitt *et al.* (1985), Kruger and Beevers (1985), Kelly and Latzko (1979) and Wu and Racker (1959), respectively.

Results and discussion

The amyloplast preparation obtained by the procedure detailed in methods was pure and not contaminated with cytosol as judged by the marker enzymes (ADP-glucose pyrophosphorylase and starch synthase). The length and width of these amyloplasts ranged from 13–39 and 10–34 μm , respectively and were ovoid or round in shape. Methods involving the use of sucrose gradients employed earlier by Gaynor and Galston (1983), MacDonald and apRees (1983a) and Nishimura and Beevers (1978) for isolating plastids were not successful in the present case. Our procedure for amyloplast separation took advantage of the relatively high density of the amyloplast which allowed them to settle through a ficoll gradient. The purity of the amyloplast fraction prompted us to further study the distribution of enzymes

The enzymes listed in table 1 could be divided into 3 main groups, i.e., (i) enzymes which were present only in cytosol, (ii) enzymes which were present only in amyloplast and (iii) the enzymes present in both fractions. The enzymes of sucrose hydrolysis and further metabolism, *viz.*, invertase, sucrose synthase, hexokinase and UDP-glucose pyrophosphorylase were absent in amyloplast and present only in cytosolic fraction, indicating these to be cytoplasmic. Similarly, PFK-2 and fructose-2,6-P₂ase were also mainly cytosolic. MacDonald and apRees (1983a) and Echeverria *et al.* (1988) obtained similar results for invertase and sucrose synthase in soybean suspension cultures and maize endosperm. However, UDP-glucose pyrophosphorylase which was absent from amyloplasts of rice (Nakamura *et al.*, 1989), soybean suspension cultures (MacDonald and apRees, 1983a) could be detected in the amyloplasts of maize endosperm (Echeverria *et al.*, 1988). Hexokinase was also absent from the amyloplasts of maize endosperm. Contrary to this, ADP-glucose pyrophosphorylase and starch synthase were present only in amyloplast. Similar localization for these enzymes has been suggested for storage tissue of rice (Nakamura *et al.*, 1989) and maize (Echeverria *et al.*, 1988).

Table 1. Enzymes of carbohydrate metabolism in the amyloplast and cytosol.

Enzymes	Amyloplast (n mol min ⁻¹ grain ⁻¹)	Cytosol
Invertase	—	7.81 ± 0.81
Sucrose synthase	—	10.80 ± 1.14
Hexokinase	—	15.12 ± 0.60
Phosphoglucosmutase	31.12 ± 0.67	436.88 ± 12.40
Phosphoglucoisomerase	32.64 ± 0.71	626.55 ± 18.70
PFK	1.42 ± 0.08	8.24 ± 0.99
Fructose-1,6-P ₂ ase	1.80 ± 0.11	42.01 ± 2.31
Aldolase	2.39 ± 0.67	8.40 ± 1.10
Triose phosphate isomerase	1.55 ± 0.04	6.60 ± 0.16
Glyceraldehyde-3-phosphate dehydrogenase	0.78 ± 0.04	3.86 ± 0.20
UDP-glucose pyrophosphorylase	—	16.48 ± 0.79
ADP-glucose pyrophosphorylase	8.88 ± 0.38	—
Starch synthase (Δ 540)	0.85 ± 0.04	—
PFK-2	—	1.21 ± 0.15
Fructose-2,6-P ₂ ase	—	16.60 ± 0.29
PFP	12.43 ± 0.72	329.76 ± 11.70

Each value is the mean of 6 replications.

Phosphoglucoisomerase, phosphoglucosmutase, PFK, aldolase, triose phosphate isomerase, fructose-1,6-P₂ase, glyceraldehyde-3P-dehydrogenase and PFP, though present predominantly in cytosolic fraction were also present in the amyloplast. Similar distribution for these enzymes has also been observed earlier in endosperm tissue of maize (Echeverria *et al.*, 1988) and soybean suspension cultures (MacDonald and apRees, 1983a). The confinement of starch synthase and ADP-glucose pyrophosphorylase to the amyloplast and of UDP-glucose pyrophosphorylase to the cytosol strongly suggests the ADP-glucose, rather than UDP-glucose, is the immediate precursor of starch. The absence of invertase, sucrose synthase and UDP-glucose pyrophosphorylase from amyloplasts indicates that this organelle

lacks any enzyme involved in sucrose metabolism. Thus sucrose cannot be considered as the substrate which could cross the amyloplast membrane but is metabolized in cytosol mainly by invertase, sucrose synthase, PFP and UDP-glucose pyrophosphorylase. Accordingly, the following pathway may be suggested for the conversion of sucrose to starch in developing wheat endosperm.

The pathway is mainly comprised of 3 sections/steps. First in the cytosol, sucrose is degraded to form triose-P (DHAP via reactions catalysed by invertase/sucrose synthase, UDP-glucose pyrophosphorylase, phosphoglucumutase, phosphohexose isomerase, fructokinase, PPi-PFK (and ATP-PFK), aldolase and triosephosphate isomerase (figure 1). DHAP is then translocated to amyloplast through phosphate translocator and converted to ADP-glucose (substrate for starch) through the reactions of triose phosphate isomerase, aldolase, fructose-1, 6-P₂ase, phosphohexoseisomerase, phosphoglucumutase and ADP-glucose-pyrophosphorylase. Finally, starch is synthesized from ADP-glucose through the reactions of starch synthase and Q enzyme. If this pathway is operational, we must expect atleast two forms each of triose phosphate isomerase, aldolase, fructose-1,6-P₂ase, phosphoglucumutase and phosphohexose isomerase. We have already demonstrated the presence of these forms in endosperm tissue of developing wheat grains (Anand and Singh, 1985; Sangwan and Singh, 1987a, b, 1988, 1989, 1990).

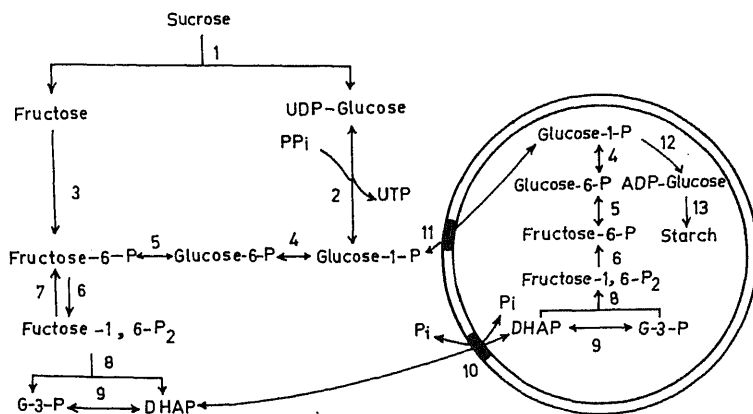


Figure 1. Proposed metabolic pathway for starch synthesis in amyloplasts of developing wheat grain. (1), Sucrose synthase; (2), UDP-glucose pyrophosphorylase; (3), hexokinase; (4), phosphoglucumutase; (5), phosphohexose isomerase; (6), PFK; (7), fructose-1, 6-bisphosphatase; (8), aldolase; (9), triose phosphate isomerase; (10), phosphate translocator; (11), hexose translocator; (12), ADP-glucose pyrophosphorylase; (13), starch synthase.

Involvement of triose-P in the biosynthesis of starch in non-photosynthetic tissues has been proposed by MacDonald and apRees (1983a, b), Singh and Mehta (1986) and by Echeverria *et al.* (1988). These results have been supported by the observations of Ngernprasirtairi *et al.* (1988) who found that, in the amyloplast envelope membrane from cultured sycamore cells, the Pi translocator like protein with molecular weight of 31 kDa was immunoreactive with an antibody raised against the pea chloroplast Pi translocator. In contrast, Keeling *et al.* (1988) and Tyson and apRees (1988) have reported glucose-1-P to be the preferred substrate

involved in translocation and synthesis of starch in amyloplasts of developing wheat grains. However, these authors were not sure whether this was the sole source of carbon for starch synthesis in wheat amyloplasts. Accordingly, in the present case we have shown the involvement of both triose-P and glucose-1-P in the synthesis of starch. The uncertainty as to which carbon compound is transported across the amyloplast membrane may only be resolved by studying transport properties of the isolated translocators from functional amyloplasts as has been done with chloroplast translocators. This aspect is currently being pursued in our laboratory.

Acknowledgement

The senior author is thankful to the Council of Scientific and Industrial Research, New Delhi, for financial assistance in the form of a fellowship.

References

- Anand, S. and Singh, R. (1985) *Plant Physiol. (Suppl.)*, **77**, 47.
- Badenhuizen, N. P. (1969) *Biogenesis of starch granules in higher plants* (New York: Appleton-Century-Crofts)
- Echeverria, E., Boyer, C. D., Liu, K. C. and Shannon, J. C. (1985) *Plant Physiol.*, **77**, 513.
- Echeverria, E., Boyer, C. D., Thomas, P. A., Liu, K. C. and Shannon, J. C. (1988) *Plant Physiol.*, **86**, 114.
- Emes, M. J. and England, S. (1986) *Planta*, **168**, 161.
- Entwistle, G., Tyson, R. H. and apRees, T. (1988) *Phytochemistry*, **27**, 993.
- Gaynor, J. J. and Galston, A. W. (1983) *Plant Cell Physiol.*, **24**, 411.
- Heber, U. (1974) *Annu. Rev. Plant Physiol.*, **25**, 393.
- Heber, J. and Heldt, H. W. (1981) *Annu. Rev. Plant Physiol.*, **32**, 139.
- Keeling, P. L., Wood, J. R., Tyson, R. H. and Bridges, I. G. (1988) *Plant Physiol.*, **87**, 311.
- Kelly, G. J. and Latzko, E. (1977) *Plant Physiol.*, **60**, 290.
- Kruger, N. J. and Beevers, H. (1985) *Plant Physiol.*, **77**, 358.
- Kumar, R. and Singh, R. (1984) *J. Agric. Food Chem.*, **32**, 806.
- MacDonald, F. D. and apRees, T. (1983a) *Biochem. Biophys. Acta*, **755**, 81.
- MacDonald, F. D. and apRees, T. (1983b) *Phytochemistry*, **22**, 1141.
- Nakamura, Y., Yuki, K., Park, S. Y. and Ohya, T. (1989) *Plant Cell Physiol.*, **30**, 833.
- Ngernprasirtairi, J., Harinasut, P., Macherel, D., Strzalka, K., Takabe, T., Akazawa, A. and Kojima (1988) *Plant Physiol.*, **87**, 371.
- Nishimura, M. and Beevers, H. (1978) *Plant Physiol.*, **62**, 40.
- Sangwan, R. S. and Singh, R. (1987a) *Indian J. Biochem. Biophys.*, **24**, 33.
- Sangwan, R. S. and Singh, R. (1987b) *Plant Physiol. Biochem.*, **25**, 745.
- Sangwan, R. S. and Singh, R. (1988) *Physiol. Plant.*, **73**, 21.
- Sangwan, R. S. and Singh, R. (1989) *J. Biol. Sci.*, **14**, 47.
- Sangwan, R. S. and Singh, R. (1990) *Indian J. Biochem. Biophys.*, **27**, 23.
- Santha, I. M., Swaroop, R. and Mehta, S. L. (1988) *Indian J. Biochem. Biophys.*, **25**, 532.
- Singh, R. (1989) in *Recent advances in plant biochemistry* (eds S. L. Mehta, M. L. Lodha and P. V. Saksena) (New Delhi: ICAR) p. 106.
- Singh, R. and Mehta, S. L. (1986) *J. Sci. Ind. Res.*, **45**, 336.
- Stitt, M., Cseke, C. and Buchanan, B. B. (1985) *Physiol. Veg.*, **23**, 819.
- Tyson, R. H. and apRees, T. (1988) *Planta*, **175**, 33.
- VanSchaftingen, E., Lederer, B., Batrons, R. and Hers, H. G. (1982) *Eur. J. Biochem.*, **129**, 191.
- Wu, R. and Racker, E. (1959) *J. Biol. Chem.*, **234**, 1029.

Control of ornithine decarboxylase activity in jute seeds by antizyme

MALABIKA PANDIT and BHARATI GHOSH

Department of Botany, Bose Institute, 93/1, Acharya Prafulla Chandra Road, Calcutta 700 009, India

MS received 8 January 1990; revised 10 May 1990

Abstract. The control of ornithine decarboxylase activity by antizyme was studied during early germination of jute seeds (*Corchorus olitorius*). When 2 mM of putrescine and spermidine were applied to the germinating medium, the enzyme activity was markedly inhibited (1.7-fold) during 16 h imbibition. This inhibition could be attributed to the formation of an inhibitory protein termed antizyme. The antizyme was partially purified from jute and barley seedlings. The activity of jute ornithine decarboxylase antizyme was weaker than that of barley.

Keywords. Antizyme; ornithine decarboxylase; polyamines; putrescine; spermidine.

Introduction

In animal (Canellakis *et al.*, 1978), bacteria (Heller *et al.*, 1983a) and certain plants putrescine is formed from ornithine by ornithine decarboxylase (ODC), L-ornithine decarboxylase (EC 4.1.1.17), a rate limiting enzyme for polyamine biosynthesis. Precise regulation of the enzyme has been reported in mammalian systems while in plants the information is scanty. In mammals, ODC is controlled by (i) post translation modification (Russell, 1981), (ii) changes in synthesis and turnover rate (Seely and Pegg, 1983) and (iii) modulation by antizyme (Fujita *et al.*, 1984). In lower plants like *Physarium polycephalum* there is evidence for phosphorylation of the enzyme (Atmar and Kuehn, 1981). Tyagi *et al.* (1981) observed post translation modification of ODC in *Saccharomyces cerevisiae* but in higher plants, there is one report showing the occurrence of ODC-antizyme (Kyriakidis 1983b).

ODC activity in most mammalian cells in culture declines rapidly after the addition of putrescine or polyamines by the formation of an inducible protein inhibitor (antizyme) to ODC (Heller *et al.*, 1983b). Antizyme has been isolated from rat liver (Heller *et al.*, 1977), H-35 cells (Fong *et al.*, 1976) and *Escherichia coli* (Canellakis *et al.*, 1981). The purification and partial characterization of ODC from jute embryos has been already reported from this laboratory (Pandit and Ghosh, 1988). The present paper describes the partial purification of ODC-antizyme and its effect on ODC activity in higher plants.

Materials and methods

Pyridoxal-5'-phosphate (PLP), dithiothreitol (DTT), Sephadex G-50 were purchased from Sigma Chemical Co., St. Louis, Missouri, USA. DL [1-¹⁴C]ornithine

hydrochloride (57 mCi/mol) were obtained from Radiochemical Centre, Amersham, UK. All other chemicals used were of analytical grade.

Plants

Pure line cultivars of jute and barley seeds were obtained from our experimental farm.

Germination of seeds

Jute and barley seeds after sterilization in 0.1% mercuric chloride (Hg_2Cl_2) were germinated on moistened filter paper in petridishes at $35^\circ \pm 1^\circ\text{C}$ and $26^\circ \pm 1^\circ\text{C}$ respectively.

Preparation and assay of ODC

ODC activity was assayed according to the method of Murakami *et al.* (1984). Briefly, the embryos were homogenised with 50 mM Tris-HCl buffer (pH 7.6), and the homogenate was centrifuged for 20 min at 26,000 *g* in a Sorvall refrigerated centrifuge. The supernatant was used as an enzyme source. The assay mixture contained: 50 mM Tris-HCl (pH 7.8), 20 μM PLP, 5 mM DTT, 0.5 mM DL-ornithine containing 0.1 μCi [$1\text{-}^{14}\text{C}$]ornithine-HCl and 0.2 ml of enzyme (0.5–2.0 mg of protein) in a volume of 1 ml. After incubating the mixture for 1 h at 37°C , the reaction was terminated by the injection of 0.5 ml of 4 N sulfuric acid (H_2SO_4). The released $^{14}\text{CO}_2$ was trapped with 0.5 ml of N KOH. Protein was estimated by the method of Lowry *et al.* (1951). One unit of ODC activity is defined as 1 nmol of $^{14}\text{CO}_2$ released/h/mg of protein.

Preparation and assay of ODC-antizyme

The 16 h germinated embryos (10 g fresh wt.) treated with 2 mM putrescine and spermidine were homogenized with homogenizing buffer 50 mM Tris-HCl, pH 7.6, 0.5 mM EDTA and centrifuged at 10,000 *g* for 20 min. The supernatant was dialyzed overnight against the same buffer at 4°C . The clarified extract was added to purified ODC from 16 h germinated seedlings (Pandit and Ghosh, 1988) and the residual enzyme activity was determined. Appropriate controls were always included.

Gel filtration on Sephadex G-50 from jute embryonic axis

The supernatant of embryo extract was subjected to 0.50% $(\text{NH}_4)_2\text{SO}_4$ and dialyzed for 24 h against the extraction buffer. The dialyzed supernatant after centrifugation was loaded over Sephadex G-50 column (23×1.7) preequilibrated with 50 mM Tris-HCl pH 7.6 containing 0.5 mM EDTA. The resulting fractions (4 ml each) were eluted at a flow rate of 0.3 ml/min.

Molecular weight determination

The molecular weight (M_r) of antizyme from jute embryos was estimated by gel filtration in a standardized column of Sephadex G-50 (Whitaker, 1965).

ODC-antizyme from barley

Antizyme was partially purified according to the method of Kyriakidis (1983a).

Protease assay

Protease activity was carried out according to Nair *et al.* (1978). The reaction mixture containing 0.1 M potassium phosphate buffer (pH 7.4), casein (100 mg/ml in 0.1 M phosphate buffer pH 4), 0.5 ml and enzyme preparation, 0.1–0.2 ml was incubated at 37°C for 30 min. The reaction was terminated by 20% trichloroacetic acid and centrifuged at 10,000 *g* for 15 min. The activity of enzyme was estimated at various time intervals.

Heat inactivation

The partially purified inhibitory protein, at a concentration of 0.2 mg/ml was split into 5 parts and heated individually on a thermostatic water bath maintained at 10–100°C. Aliquots were withdrawn every 10 min and assayed for inhibitory activity.

Results

Dose response curve for inhibition of ODC activity

The basal ODC activity increased with time during germination of jute seeds and maximum activity was obtained at 16 h. After 16 h germination the activity sharply declined. When the seeds were allowed to germinate in the presence of exogenous putrescine and spermidine, ODC activity was partially inhibited (figure 1) and the inhibition was dependent on the concentration of polyamine. At 1 mM no significant inhibition of ODC activity was observed. However, with increasing polyamine concentration, the inhibition is also increased (figure 2). The germination pattern and vigour of seedlings also changed with various concentration of putrescine and spermidine. However, for further experiments, we used 2 mM putrescine and spermidine for the induction of inhibitory protein where germination percentage and vigour of seedlings are normal. Similarly, inhibition of ODC activity in the presence of polyamines showed that inhibition of ODC is not due to the simple feed back inhibition but for the induction of antizyme (figure 3). Here we used 0.5 mM putrescine and spermidine as maximum inhibition was observed at 0.5 mM.

Mixing experiments of purified ODC (1 unit) with increasing amount of dialysed supernatant showed that the maximum amount of inhibition is obtained by 150 μ l

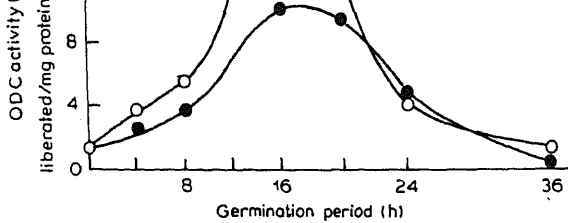


Figure 1. Effect of 2 mM putrescine and spermidine on ODC activity during germination of jute seeds.

The reaction mixture contained 40 mM Tris-HCl buffer pH 7.6, 20 μ M PLP, 5 mM DTT, 1.8 nmol of DL [1- 14 C] ornithine (Sp. activity 57 mCi/mmol) and dialyzed supernatant was incubated for 1 h at 37°C. (○), Control; (●), treated with spermidine and putrescine.

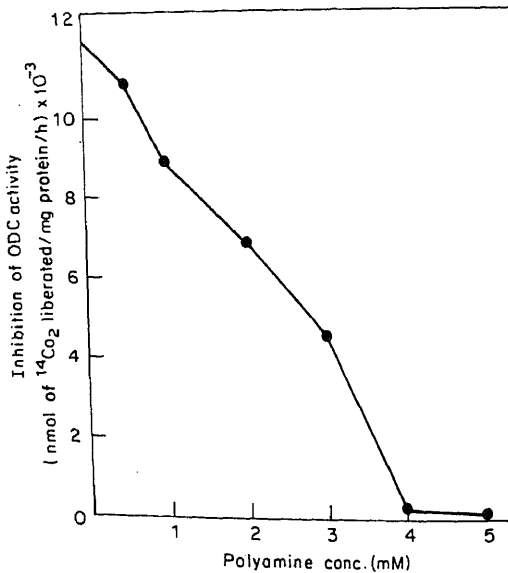


Figure 2. Dose response curve of varying concentrations of polyamine for the inhibition of ODC activity purified from 16 h germinated jute embryos.

Jute seeds were treated with different concentrations of polyamine and after 16 h germination antizyme activity was assayed as described in 'materials and methods'.

of extract containing 0.2 mg of protein. Such polyamine dependent inhibition was also reported in barley seed (Koromilas and Kyriakidis, 1988). On the other hand no such inhibition of ODC activity was observed by the dialysed supernatant of control extract which suggest that the antizyme was not induced without exogenous addition of putrescine and spermidine. However, antizyme, as a normal component

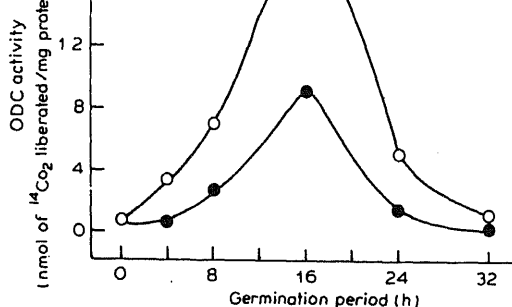


Figure 3. ODC activity in the presence of putrescine and spermidine.

The reaction mixture contained 40 mM Tris-HCl buffer pH 7.6, 20 μ M PLP, 5 mM DTT, 1.8 mmol of DL [1-¹⁴C] ornithine (Sp. activity 57 mCi/mmol) and dialyzed supernatant was incubated for 1 h at 37°C. (○), Control; (●), in the presence of 0.5 mM putrescine and spermidine.

of H-35 cells, has been reported (Heller *et al.*, 1977). Similar findings have also been reported in wheat leave extract (Smith and Marshall, 1988).

Table 1 summarizes the partial purification steps of antizyme. Though several active fractions were eluted in Sephadex G-50 column chromatography, purification of the most active fraction is presented. Further purification was not possible due to its instability.

Table 1. Partial purification of antizyme from jute seeds (*C. olitorius*).

Steps	Protein (mg)	Sp. activity (nmol of ¹⁴ CO ₂ liberated/mg of protein/h)	Purification fold	Recovery (%)
10,000 g supernatant	99	2×10^{-3}	1	100
(NH ₄) ₂ SO ₄ precipitation 0–50% saturation	15	9×10^{-3}	2	30
Sephadex G-50	2	4×10^{-2}	19.2	39

Antizyme was partially purified from jute seed using ammonium sulphate saturation and gel filtration on Sephadex G-50. About 19-fold purification of antizyme with a recovery of 39% was achieved.

Identification of inhibitory activity

To detect the presence of inhibitor in jute seeds, we measured ODC activity with various concentrations of combined putrescine and spermidine. Inhibition may be accounted for by the presence of antizyme in the extract as judged by the following experiments.

The inhibitory protein is heat labile at 60°C. About 80% of the activity at the end of 1 h. Trypsin inhibits the antizyme activity by 50 and 85% inhibition at 100 and 200 µg/ml trypsin respectively.

The partially purified inhibitory protein was tested for protease activity both the substrate like casein (hydrolysed) and albumin. No proteolytic activity was detected using phosphate buffer pH 7.4 and pH 4.

M_r of the antizyme

The *M_r* of jute antizyme was judged by the elution profile on Sephadex G-50. It has been estimated to be 25,700 (figure 4).

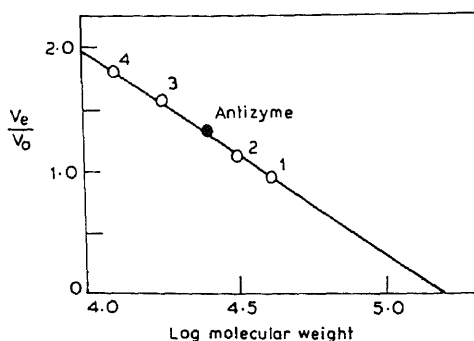


Figure 4. *M_r*-determination by gel filtration.

A portion of the partially purified inhibitory protein was chromatographed on a column of Sephadex G-50 (23 × 1.7 cm) using 0.01 M phosphate buffer (pH 7.6) containing 0.2 M NaCl with a flow rate of 12 ml/h. The column was standardized by using proteins of known *M_r*. The standard proteins were (1) Rnase-A, (2) cytochrome c, (3) pepsin and (4) ovalbumin.

Titration curve between ODC and antizyme

When increasing amounts of antizyme were added to 1 unit of ODC, the activity decreased linearly and the percentage of inhibition by the same amount of barley antizymes are 60 and 90% approximately (figure 5). The titration curve was almost identical to those reported from other systems.

Nature of inhibition

At different inhibitor concentrations, the inhibitory constant (*K_i*) was determined, which shows that the enzyme was inhibited non competitively. The *K_i* = 1.5×10^{-3} M (figure 6).

Specificity of interaction

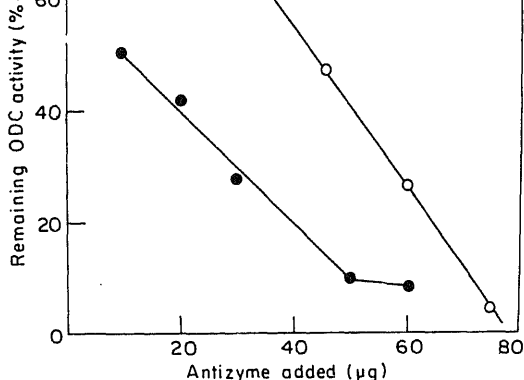


Figure 5. Titration curve of ODC purified from 16 h germinated jute embryo with antizyme from jute (○) and barley (●) respectively. Increasing amount of antizyme fractions from column chromatography were added to 1 unit of ODC. The activity was assayed under standard conditions.

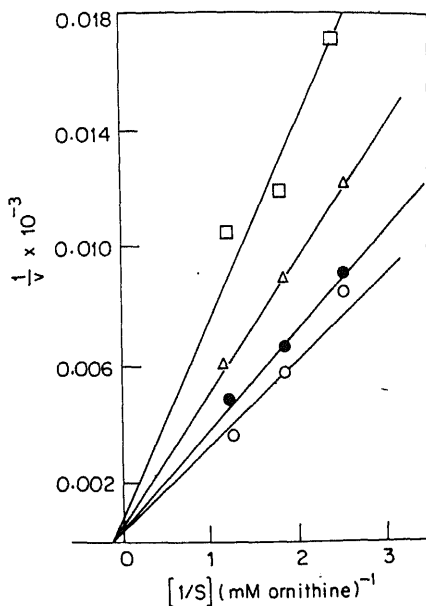


Figure 6. Effect of antizyme on the Lineweaver-Burk plot of ornithine decarboxylase reaction.

Each assay contained 1 unit of ODC supplemented with 27 μM (●), 54 μM (Δ) and 81 μM (□) antizyme.

interaction. Similar observations on acidic antizymes of *E. coli* inhibiting ODC activity in rat liver (Canellakis *et al.*, 1985) and *Tetrahymena pyriformis* (Sklaviadis *et al.*, 1985) respectively are available.

The existence of ODC antizyme has been confirmed in germinating jute seeds. Similar type of observations were also reported by others when polyamines were added to the culture medium of H-35 cells (Fong *et al.*, 1976), HTC cells (McCann *et al.*, 1977) rat hepatoma cell culture (Kallio *et al.*, 1977) and Hela cells (Branca and Herbst, 1980). The antizyme was partially purified by $(\text{NH}_4)_2\text{SO}_4$ saturation and Sephadex G-50 column chromatography. Previous workers have reported M_r of 22000 and 26500 ± 2000 respectively for the antizyme from rat liver and neuroblastoma cells (Heller *et al.*, 1977; Canellakis *et al.*, 1985). In the present study, the M_r of jute antizyme was estimated to be 25,700 from gel filtration data. It has been also observed that antizyme is a potent inhibitor of ODC and inhibits the enzyme in a non-specific way. However, there appears an underlying specificity of interaction of ODC with antizyme in a few systems. It is therefore possible that antizyme forms an inactive complex with the enzyme which would be a means of inactivating ODC and causing rapid degradation (Kyriakidis *et al.*, 1978). The presence of ODC-antizyme in unstimulated H-35 cells and in rat liver coupled with its induction by polyamines provide strong circumstantial evidence that it has some role in modulation of ODC *in vivo*.

In plants the characterization of the nature and function of antizyme in physiological processes remain unexplored. The elucidation of the mechanisms which are responsible for rapid down regulation and turnover of the enzyme during germination of higher plants is in progress.

Acknowledgements

Financial help from the Bose Institute was gratefully acknowledged. Authors thank Prof. A. K. Roychoudhury, for kind co-operation.

References

- Atmar, V. J. and Kuehn, G. D. (1981) *Proc. Natl. Acad. Sci. USA*, **78**, 5518.
- Branca, A. A. and Herbst, E. J. (1980) *Biochem. J.*, **186**, 925.
- Canellakis, E. S., Kyriakidis, D. A., Heller, J. S. and Pawlak, J. W. (1981) *Med. Biol.*, **59**, 279.
- Canellakis, E. S., Heller, J. S., Kyriakidis, D. A. and Chen, K. Y. (1978) *Adv. Polyamine Res.*, **1**, 17.
- Canellakis, E., Kyriakidis, D. A., Rinehart, C. A., Huang, A., Panagiotidis, E. and Fong, W. F. (1985) *Biosci. Rep.*, **5**, 189.
- Fong, N., Heller, J. S. and Canellakis, E. S. (1976) *Biochim. Biophys. Acta*, **428**, 456.
- Fujita, K., Matsufuji, S., Murakami, Y. and Hayashi, S. (1984) *Biochem. J.*, **218**, 557.
- Heller, J. S., Kyriakidis, A., Fong, W. F. and Canellakis, E. S. (1977) *Eur. J. Biochem.*, **81**, 545.
- Heller, J. S., Rostomily, R., Kyriakidis, A. and Canellakis, E. S. (1983a) *Proc. Natl. Acad. Sci. USA*, **80**, 5181.
- Heller, J. S., Kyriakidis, D. A. and Canellakis, E. S. (1983b) *Biochim. Biophys. Acta*, **760**, 154.
- Kallio, A., Lofman, M., Poso, H. and Janne, J. (1977) *Biochem. J.*, **177**, 63.
- Koromilas and Kyriakidis, A. (1988) *Phytochemistry*, **27**, 989.
- Kyriakidis, D. A. (1983a) *Adv. Polyamine Res.*, **4**, 427.
- Kyriakidis, D. A. (1983b) *Physiol. Plant.*, **57**, 499.
- Kyriakidis, A., Heller, J. S. and Canellakis, E. (1978) *Proc. Natl. Acad. Sci. USA*, **78**, 4699.
- Lowry, O. H., Rosebrough, N. J., Farr, A. L. and Randall, R. J. (1951) *J. Biol. Chem.*, **193**, 265.
- McCann, P. P., Tardif, E. and Mamont, P. S. (1977) *Biochem. Biophys. Res. Commun.*, **75**, 948.
- Murakami, Y., Fujita, K., Kameji, T. and Hayashi, S. (1984) *Biochem. J.*, **217**, 573.

- Nair, T. V. R. and Grover, H. L. and Abrol, Y. P. (1978) *Physiol. Plant.*, **42**, 293.
- Pandit, M. and Ghosh, B. (1988) *Phytochemistry*, **27**, 1609.
- Russell, D. H. (1981) *Biochem. Biophys. Res. Commun.*, **99**, 1167.
- Seely, J. E. and Pegg, A. E. (1983) *J. Biol. Chem.*, **258**, 2496.
- Smith, T. A. and Marshall, J. L. A. (1988) *Phytochemistry*, **27**, 703.
- Sklaviadis, T. K., Georgatsos, J. and Kyriakidis, D. A. (1985) *Biochim. Biophys. Acta*, **831**, 288.
- Tyagi, A. K., Tabor, C. W. and Tabor, H. (1981) *J. Biol. Chem.*, **256**, 12156.
- Whitaker, J. R. (1963) *Anal. Chem.*, **35**, 1950.

Lamellar dispersion and phase separation of chloroplast membrane lipids by negative staining electron microscopy

R. C. YASHROY

Biology Division, Carleton University and National Research Council, Ottawa, Canada
Present address: Biophysics, Electron Microscopy and Instrumentation Section,
A. N. Division (Bldg.), Indian Veterinary Research Institute, Izatnagar, Bareilly 243 122,
India

MS received 28 February 1990

Abstract. Aqueous dispersions of lipids isolated from spinach chloroplast membranes were studied by electron microscopy after negative staining with phosphotungstic acid. Influence of low temperature (5°C for 24 h) was also investigated. It was observed that when contacted with water, these lipids, as such, formed multilamellar structures. Upon sonication, these multilamellar structures gave rise to a clear suspension of unilamellar vesicles varying in size (diameter) between 250 and 750 Å. When samples of sonicated unilamellar vesicles were stored at 5°C for 24 h or more, they revealed a variety of lipid aggregates including liposomes, cylindrical rods (about 100 Å wide and up to 3600 Å long), and spherical micellar structures (100–200 Å in diameter)—thus indicating phase separation of lipids.

Keywords. Chloroplast; lipids; membranes; electron microscopy.

Introduction

Chloroplast membranes have an unusual lipid composition which includes chlorophylls, carotenoids, sterols, quinones, phospholipids and glycolipids (Benson, 1966, 1971). Unlike most other membranes in the biological world, phospholipids constitute only a minor fraction (about 10%) of the total chloroplast membrane lipids (Kates, 1970). Monogalactosyl-diacyl-diglycerol (MGDG), which constitutes the largest lipid component in the chloroplast membranes, does not form a lamellar structure; but instead it forms a reversed hexagonal liquid-crystalline phase. However, digalactosyl-diacyl-diglycerol (DGDG) forms an aqueous bilayer structure (Larsson and Puang-Ngern, 1979; Murphy, 1986). Larsson and Puang-Ngern (1979) assumed the lipid organization in thylakoid membranes to be a bilayer and opined against inverted-bilayer structure as proposed by Kreutz (1966) from X-ray diffraction studies. The present work was undertaken with the view to investigate the modalities as to how a variety of diverse lipids which constitute the chloroplast membranes may co-exist all together in aqueous lipid dispersions and how they undergo phase separation due to the effect of low temperature.

Materials and methods

Isolation of chloroplast membranes

Chloroplasts were isolated from chilled spinach leaves (without mid-ribs) by the

Extraction of membrane lipids

Lipids were extracted from the membrane-pellet following the procedure of Bligh and Dyer (1959). All solvents were bubbled with nitrogen gas before use and the routine drying and concentration of lipids was also accomplished under a stream of nitrogen gas. The final lipid-extract was dissolved in a mixture of chloroform and methanol (2:1 v/v), and stored at 10°C after sealing under an atmosphere of nitrogen gas.

Preparation of aqueous lipid dispersions

For preparation of aqueous lipid dispersions, an aliquot of lipid-extract was completely dried under a stream of nitrogen gas and then under vacuum (1–2 h), and was subsequently vortexed with a known volume (normally 1–2 ml) of distilled water for about 15 min at room temperature in a glass tube sealed under an atmosphere of nitrogen gas.

To prepare sonicated lipid-water dispersions, the vortexed aqueous lipid-dispersions were sonicated for about 10 min at 20°C in glass tubes sealed under an atmosphere of nitrogen gas, so as to obtain a clear (green-coloured) solution.

Electron microscopy

The aqueous lipid dispersions (sonicated or unsonicated) were stained with phosphotungstic acid by the method described by Lucy and Glauert (1964). Satisfactory results were also obtained by first drying (under nitrogen gas) a thin film of dilute lipid-extract (in chloroform-methanol 2:1 v/v) laid on a forvar-coated copper grid and then dipping it in distilled water for 2 min. The water-washed grid was then stained by placing a drop of 1% phosphotungstic acid on its coated-side for 2 min. Excess stain was soaked away by touching a filter paper strip. The grid was then dried under a stream of nitrogen gas and examined under Siemens Elmiskop I electron microscope at an instrument magnification of $\times 45,000$.

Results

Figure 1 shows the vortexed aqueous lipid dispersions prepared from the spinach chloroplast membranes. A typical multilamellar (liposomal) structure of these dispersions is clearly noticeable. Each lamella corresponds to a lipid bilayer structure. Rare spherical structures (arrow) about 100 Å in diameter are also seen in these preparations which correspond to spherical micellar structures.

When the liposomal suspensions are sonicated, a clear green-coloured solution results. On examination under the electron microscope after negative staining, it

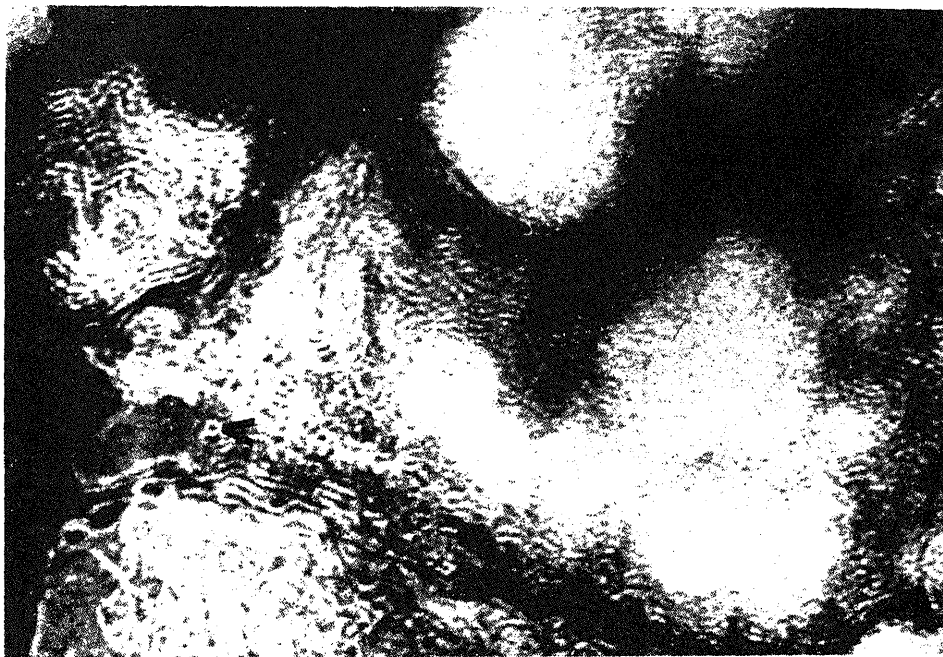


Figure 1. Electron micrograph of aqueous dispersion of lipids extracted from spinach chloroplast membranes after staining with phosphotungstic acid. Multilamellar (liposomal) structures are observable in the whole view. A few spherical structures (arrow-head) about 100 Å in diameter are also sparsely observable which are interpreted as spherical micelles ($\times 225,000$).



Figure 2. Electron micrograph of sonicated aqueous dispersion of lipids extracted from spinach chloroplast membranes after staining with phosphotungstic acid. Unilamellar microvesicles of diameter varying from 250–750 Å are observable ($\times 225,000$).

electron microscope. Figure 3 shows such an electron micrograph wherein a variety of lipid aggregates are seen. Structures like multilamellar liposomes cylindrical rods

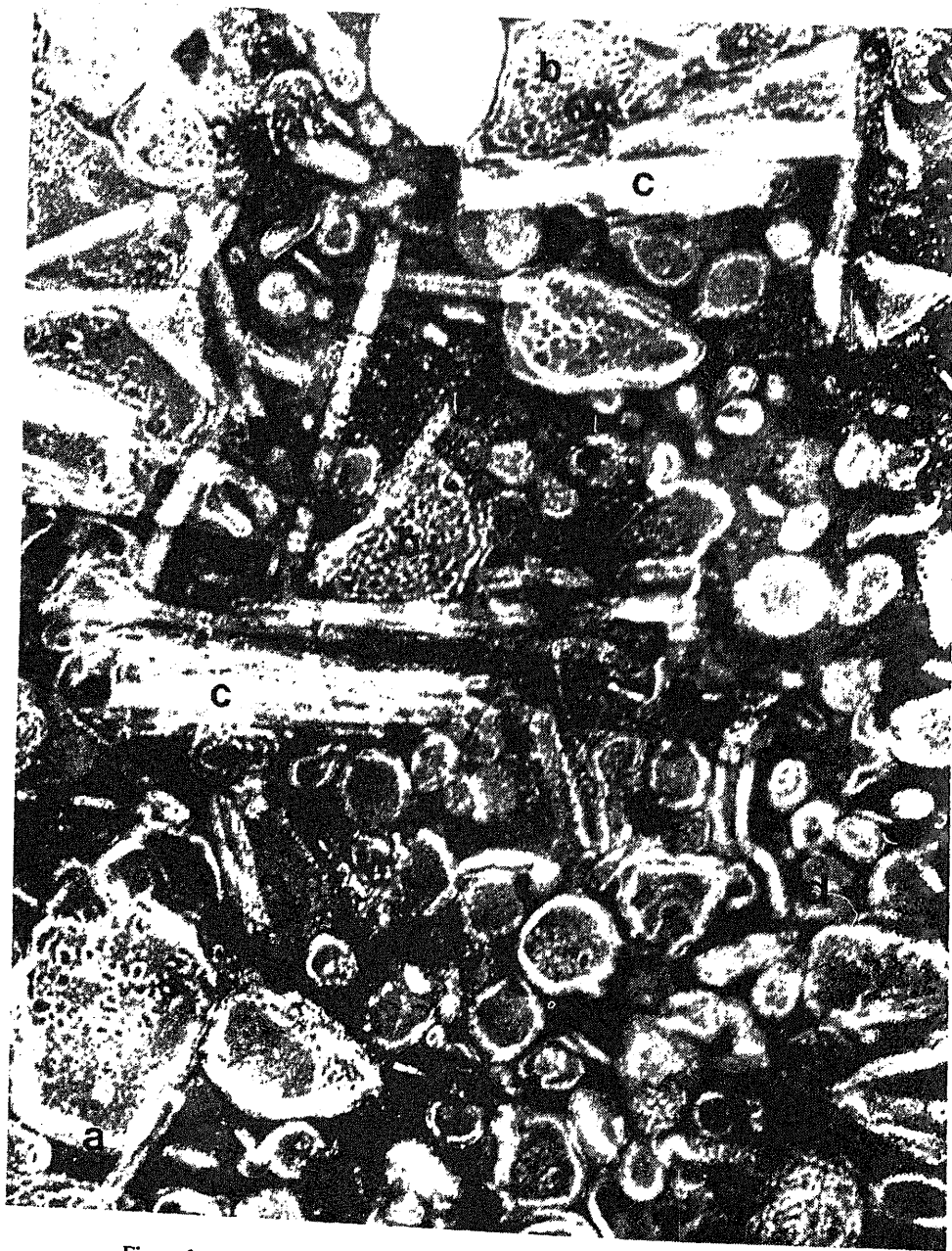


Figure 3. Electron micrograph of sonicated aqueous dispersion of lipids extracted from spinach chloroplast membranes after storage at low temperature (5°C for 24 h) and staining with phosphotungstic acid. Different lipid aggregates observable are (a) multi-lamellar vesicles, (b) spherical micelles of diameter ranging from 0.1 to 0.5 μm , and (c) cylindrical rods of diameter ranging from 0.1 to 0.5 μm .

and micelle-like spheres, besides the pre-existing unilamellar vesicles are indentifiable. The cylindrical rods have a diameter of approximately 100 Å.

Discussion

Chloroplast membranes contain a diverse variety of lipids and only a few of them are known to form a lipid bilayer structure (Murphy, 1986). The present studies (see figures 1, 2) reveal that many of the constituent lipids form non-bilayer lipid aggregates in isolation, but when they are mixed together, they form a fairly stable multibilayer structure (figure 1) which, upon sonication gives rise to unilamellar lipid micro-vesicles with diameter ranging between 250–750 Å. Such multilamellar aqueous lipid-dispersions and unilamellar microvesicles are known to represent a lipid-bilayer structure as has been revealed by studies on lipids from many other diverse sources (Kimmelberg, 1977; Huang, 1969; Bangham *et al.*, 1974). These observations also support the commonly accepted assumption that the lipid organisation in the chloroplast membranes, should be in the form of a bilayer. The chloroplast membranes and their extracted lipid-water dispersions show a high lipid-fluidity leading to the detection of sharp carbon-13 nuclear magnetic resonances arising from lipid fatty-acyl carbons (YashRoy 1987a, b). They also reveal gel-to-liquid crystalline phase transition around 18°C (YashRoy, 1990).

When samples of sonicated unilamellar vesicles (figure 2) were kept at temperature of 5°C for 24 h or more, marked changes were observed (figure 3) in the lipid organisation. Multilamellar liposomal-vesicles (figure 3a) were observed which were apparently formed by 'fusion' of unilamellar vesicles. In addition, structures like cylindrical rods (figure 3b) and spherical micelles (figure 3c) were also seen. It is clear that prolonged exposure to low-temperature of samples of these unilamellar vesicles results in the phase separation of the constituent lipids. Polarizing microscope and low-angle X-ray diffraction studies (Larsson and Puang-Ngern, 1979) of isolated chloroplast membrane-lipids taken individually, showed that when dispersed in water, the lipid, DGDG formed a lamellar phase. The lipid, sulphoquinovosyl-diacyl-glycerol is also known to form a lamellar phase with water (Murphy, 1986). On the other hand, the lipid, MGDG formed a reversed hexagonal liquid-crystalline phase with water. The latter phase seemingly appears as cylindrical rods under the electron microscope (figure 3). The spherical micelle-like structures (figure 3c) may well represent aggregates of molecules like chlorophyll, sterols etc.

The present investigation thus provides evidence that the diverse lipids of chloroplast membrane when dispersed in water all-together, form the lamellar (bilayer) structure under normal conditions. The lamellar structure is fairly stable. Under conditions of prolonged exposure to low-temperature (5°C), these lipid-water dispersions undergo phase separation giving rise to different kinds of lipid-aggregates (lamellar, micellar and cylindrical rods).

Acknowledgement

The author is thankful to the Canadian Commonwealth Scholarship and Fellowship Committee for financial support.

References

- Arnon, D. I., Allen, M. B. and Whatley, F. R. (1956) *Biochim. Biophys. Acta*, **20**, 449.
- Bangham, A. D., Hill, M. W. and Miller, N. G. A. (1974) in *Methods in membrane biology* (ed. E. D. Korn) (New York: Plenum) vol. 1, p. 1.
- Benson, A. A. (1966) *J. Am. Oil Chem. Soc.*, **43**, 265.
- Benson, A. A. (1971) in *Structure and function of chloroplasts* (ed. M. Gibbs) (Berlin, New York: Springer-Verlag) p. 129.
- Bligh, E. C. and Dyer, W. J. (1959) *Can. J. Biochem. Physiol.*, **37**, 911.
- Huang, C-H. (1969) *Biochemistry*, **6**, 344.
- Kates, M. (1970) *Adv. Lipid Res.*, **8**, 225.
- Kimelberg, H. K. (1977) in *Dynamic aspects of cell surface organisation. Cell surface reviews* (eds G. Poste and G. L. Nicolson) (Amsterdam, New York: North Holland) p. 205.
- Kreutz, W. (1966) in *Biochemistry of chloroplasts* (ed. T. W. Goodwin) (London, New York: Academic Press) vol. 1, p. 83.
- Larsson, K. and Puang-Ngern, S. (1979) in *Advances in biochemistry and physiology of plant lipids* (eds L.-A. Appelquist and C. Liljenberg) (New York: Elsevier/North Holland Biomedical Press) p. 27.
- Lucy, J. A. and Glauert, A. M. (1964) *J. Mol. Biol.*, **8**, 727.
- Murphy, D. J. (1986) *Biochim. Biophys. Acta*, **864**, 33.
- YashRoy, R. C. (1987a) *Indian J. Biochem. Biophys.*, **24**, 177.
- YashRoy, R. C. (1987b) *J. Biochem. Biophys. Methods*, **15**, 229.
- YashRoy, R. C. (1990) *J. Biochem. Biophys. Methods*, (in press).

In situ* study of chorion gene amplification in ovarian follicle cells of *Drosophila nasuta

P. K. TIWARI* and S. C. LAKHOTIA†

Cytogenetics Laboratory, Department of Zoology, Banaras Hindu University, Varanasi 221 005, India

*Present address: School of Studies in Zoology, Jiwaji University, Gwalior 474 011, India

MS received 26 February 1990; revised 26 May 1990

Abstract. The temporal and spatial pattern of replication of chorion gene clusters in follicle cells during oogenesis in *Drosophila melanogaster* and *Drosophila nasuta* was examined by [³H]thymidine autoradiography and by *in situ* hybridization with chorion gene probes. When pulse labelled with [³H]thymidine, the follicle cells from stage 10–12 ovarian follicles of both *Drosophila melanogaster* and *Drosophila nasuta* often showed intense labelling at only one or two sites per nucleus. *In situ* hybridization of chorion gene probes derived from *Drosophila melanogaster* with follicle cell nuclei of *Drosophila melanogaster* and *Drosophila nasuta* revealed these discrete [³H]thymidine labelled sites to correspond to the two amplifying chorion gene clusters. It appears, therefore, that in spite of evolutionary divergence, the organization and programme of selective amplification of chorion genes in ovarian follicle cells have remained generally similar in these two species. The endoreplicated and amplified copies of each chorion gene cluster remain closely associated but the two clusters occupy separate sites in follicle cell nucleus.

Keywords. Chorion genes; amplification; endoreplication; *Drosophila*; *in situ* hybridization.

Introduction

Unequal replication of different DNA sequences in endoreplicating cells appears to be a characteristic feature of *Drosophila* ontogeny (for recent reviews, see Spradling and Orr-Weaver, 1987; Raman and Lakhota, 1990). While in most cases certain sequences are under-replicated, at least one example is known where specific gene sequences, the chorion genes, are amplified in a developmental stage and cell type specific manner: the genome of *D. melanogaster* contains two clusters of chorion genes, one on X-chromosome and one on chromosome 3, which are selectively amplified in follicle cells between stages 8–14 of ovarian follicle growth (Spradling and Mahowald, 1980; Spradling *et al.*, 1980; Spradling, 1981). Studies on molecular organization of chorion genes in a number of *Drosophila* species (Martinez-Cruzado *et al.*, 1988) have shown that there are two clusters of chorion genes which show follicle-cell specific amplification in different species. In the present study, we have used a simple strategy to cytologically identify and compare the location and time course of amplification of chorion genes in ovarian follicle cells in *D. melanogaster* and *D. nasuta*. Phylogenetically, *D. nasuta*, belonging to the *immigrans* species group (Throckmorton, 1975), is more distantly related to *D. melanogaster* than those belonging to the *virilis/repleta* or the Hawaiian group of species examined by Martinez-Cruzado *et al.* (1988). Our present studies provide useful information on the cytology of amplifying chorion genes and also show that

the organization of chorion genes in *D. nasuta* is generally similar to *D. melanogaster*.

Materials and methods

[³H] Thymidine labelling of ovarioles

Ovaries from 3–4 days old healthy females of wild type *D. melanogaster* and *D. nasuta* were dissected out in Poels' salt solution (Lakhotia and Mukherjee 1981). Follicles between stages 9 and 12 were identified following the procedure described by King (1970), separated and transferred to fresh Poels' salt solution containing [³H] thymidine (100 µCi/ml; sp. act. 66 Ci/mM, Amersham) for 20 min at 25°C. The labelled follicles were washed with cold isotope-free salt solution, briefly fixed in cold aceto-methanol and squashed in 45% acetic acid. After removal of the excess acid, the preparations were autoradiographed using Kodak NTB-2 nuclear track emulsion. After 3–4 days of exposure, the autoradiograms were developed, fixed, stained with Giemsa and examined for labelling of the follicle cells in follicles of different stages.

In situ hybridization of chorion gene probes with follicle cell nuclei

Unlabelled squash preparations of ovarian follicles (stages 10–12 of *D. melanogaster* and stage 13 of *D. nasuta*) were hybridized *in situ* with two chorion gene probes derived from the X-chromosomal (p103) and autosomal (p302) gene clusters of *D. melanogaster*, respectively: the X-chromosomal probe includes the entire chorion gene cluster with its flanking 5' and 3' regions while the autosomal probe spans the entire cluster encompassing s18, s15 and s16 genes together with upstream region of the cluster (see Spradling, 1981 for details). The probe DNAs were nick-translated using [³²P] dNTPs (Amersham) to obtain specific activities ranging between 1–2 × 10⁸ c.p.m./µg DNA. The procedure for *in situ* hybridization to nuclear DNA was as described by Pardue (1986). While the ovarian follicle preparations of *D. melanogaster* were hybridized singly with either of the probes, those of the stage 13 follicles of *D. nasuta* were hybridized using both the labelled probes together. Hybridization was detected by autoradiography using Kodak NTB-2 emulsion. The slides were exposed for autoradiography for 2 weeks.

Results

Data on [³H] thymidine labelling of follicle cells are presented in table 1. Some examples are illustrated in figure 1. The frequency of labelled follicle cells remained high in ovarian follicles of stage 9 through 12; however, the frequency of nuclear labelling changed remarkably in later stages. Up to stage 10A, nuclei of follicle cells of both the species showed a uniform nuclear labelling (figure 1a). In some nuclei discrete clusters of labelling were also seen (figure 1b). In stage 12 of *D. nasuta*, the frequency of nuclei with clustered labelling was very high (figure 1c). In stage 10B of *D. melanogaster* could not be obtained. Since the numbers of grains per nucleus in this category of labelled nuclei from stages 9 to 10B varied and since the clusters were often not distinct (see figure 1b), no attempt was made to

Table 1. [^3H] Thymidine labelling of ovarian follicle cells of *D. melanogaster* and *D. nasuta* at different stages of ovarian follicle growth.

Stage	Species	Total nuclei	Nuclei unlabelled (%)	Labelling patterns (% among labelled)			
				Uniform	Clustered		
					1-5*	1	2
9-10A	<i>melanogaster</i>	151	2.0	81.1	18.9	*	*
	<i>nasuta</i>	355	7.6	74.6	15.2	*	*
10B	<i>nasuta</i>	110	13.6	8.4	91.6	*	*
11-12	<i>melanogaster</i>	632	13.8	1.6	4.0	70.6	10.1
	<i>nasuta</i>	301	19.6	0.7	2.0	34.5	43.2

Clustered labelling=labelling restricted to one or more discrete region(s) of the nucleus.

* Individual clusters of labelling not distinct.

these nuclei on the basis of the numbers of labelled cluster(s) seen per follicle cell nucleus: it may, however, be noted that in several of them only one or two distinct clusters of grains were seen. [^3H] Thymidine incorporation in follicle cells from stages 11 and 12 was found to be restricted, in most cases, to only one or two discrete sites (figure 1c, d). In nuclei with two labelled clusters, one was less labelled than the other. The chromocentre formed by fusion of pericentromeric heterochromatin of different chromosomes remained distinctly visible as a compact mass in nuclei of *D. nasuta* and this was always unlabelled.

Chorion gene probes were hybridized *in situ* to know location of the chorion gene clusters in follicle cell nuclei of the two species. When either of the two probes (X-chromosomal or autosomal, see 'materials and methods') were hybridized *in situ* with stage 10-13 follicle cells of *D. melanogaster*, a single site of dense labelling was seen in each follicle cell nucleus, although a few scattered silver grains were also occasionally present elsewhere in the nucleus. Figure 2a and b illustrate the patterns of hybridization seen with the X-chromosomal probe. The hybridization patterns with the autosomal probe were similar and therefore, not shown. When both the labelled probes were simultaneously hybridized *in situ* with stage 13 follicle cell nuclei of *D. nasuta*, two distinct sites of hybridization were seen in each nucleus. It is notable that the degree of hybridization of either of the *D. melanogaster* derived chorion gene probes was markedly less with *D. nasuta* than with *D. melanogaster* follicle cells.

Discussion

Extensive studies have been made at molecular level to analyze the process of selective amplification of chorion genes in ovarian cells of *D. melanogaster*: the follicle cells undergo a few cycles of endoreplication up to stage 9; in addition, the chorion gene clusters are selectively amplified beginning at stage 8 so that by stage 13-14, the X-chromosomal chorion genes are amplified by about 20x and those on the chromosome 3 by about 60-80x of the haploid copy number (Spradling and Mahowald, 1980; Spradling *et al.*, 1980; Spradling, 1981; Spradling and Orr-Weaver, 1987). The cytological organization of the two chorion clusters and their

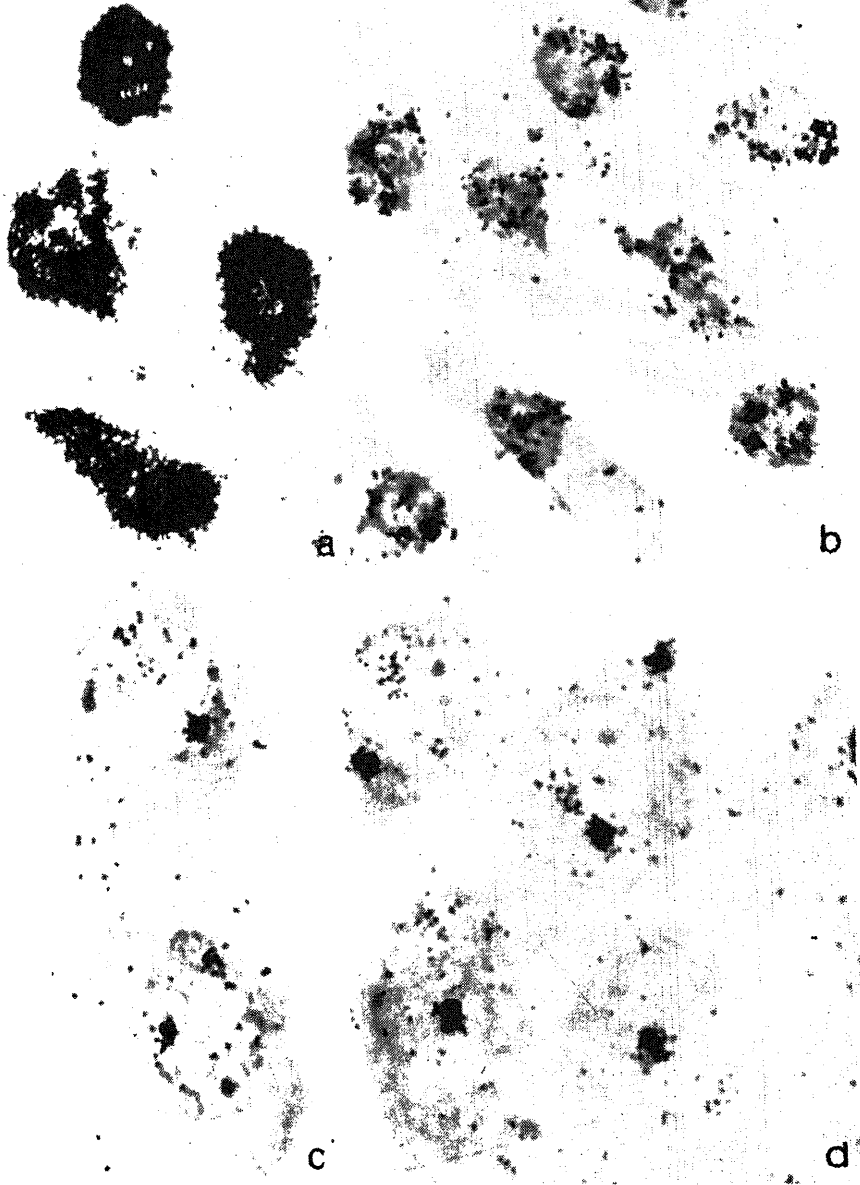


Figure 1. [^3H] Thymidine labelled autoradiograms of follicle cells of *D. nasuta* from ovarian follicles of stages 9 (a), 10B (b), 11 (c) and 12 (d). Note the labelling restricted to only one or two sites in nuclei from stage 11 (c) and 12 (d) with one site often more labelled than other.

amplified copies in follicle cell nuclei of *D. melanogaster* is, however, not known. Our present study provides some information on this aspect in *D. melanogaster* and *D. nasuta*.

[^3H] Thymidine labelling restricted to one or two discrete region(s) in a majority of follicle cell nuclei from stages 10B to 12 of both species is indicative of the

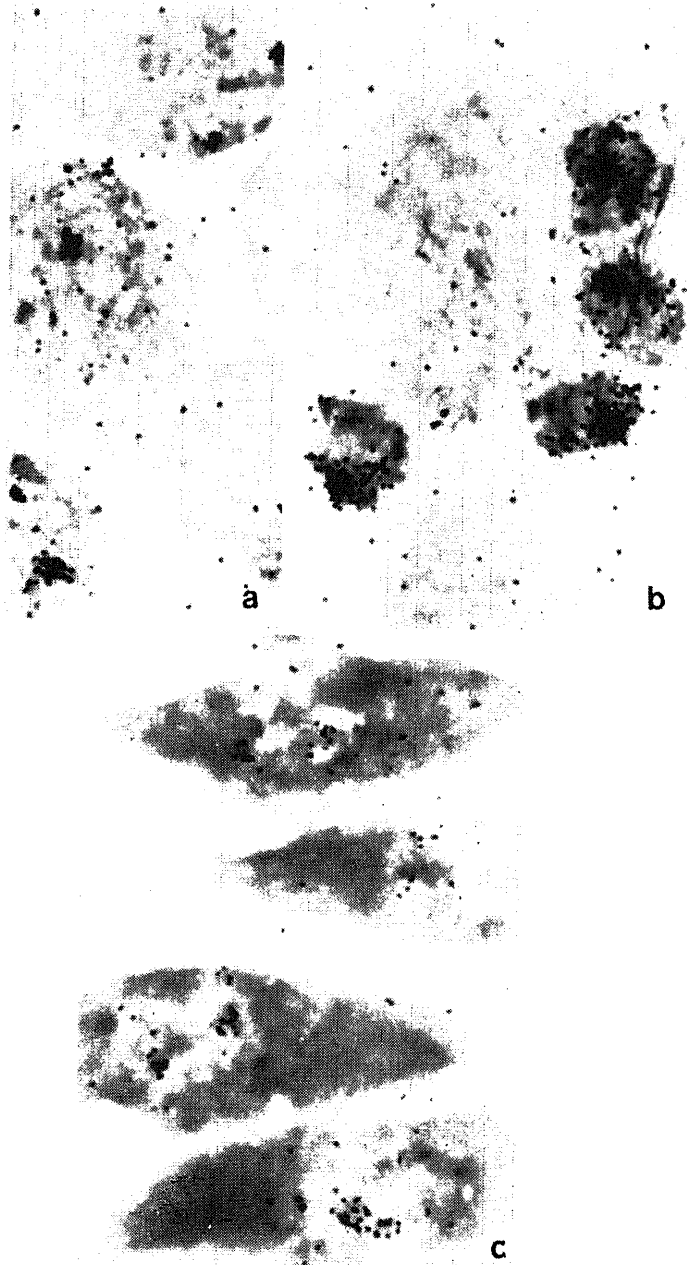


Figure 2. *In situ* hybridization of *D. melanogaster* chorion gene probes with follicle cells. (a) stage 10 and (b) stage 13 follicle cells of *D. melanogaster* hybridized with p103.47; (c) stage 13 follicle cells of *D. nasuta* hybridized with mixed p103.47 and p302.76 probes.

tion associated with amplification of chorion gene clusters. Some of the labelling restricted to a few regions in stages 9 to 10B may represent a phase of endoreplication cycles, perhaps analogous to the 2D and

1D type labelling patterns in salivary gland polytene nuclei (Lakhota and Sinha, 1983). However, following considerations show that the persistent [^3H] thymidine labelling at only 1 or 2 site(s) per nucleus in majority of stage 11–12 follicle cells is associated with amplification of chorion gene clusters rather than with [^3H] thymidine incorporation related to general endoreplication cycles: (i) these labelled region(s) do not correspond to late-replicating heterochromatin since the chromocentric heterochromatin was seen to be actually unlabelled in all cells as would be expected from the fact that heterochromatin regions remain grossly under-replicated in these cell types as in other endoreplicating nuclei (Hammond and Laird, 1985; Tiwari and Lakhota, 1990); (ii) in both species, in nuclei with two labelled sites, one was less labelled than the other—this agrees with the fact that of the two chorion gene clusters, one amplifies to a greater extent (Spradling, 1981) and is thus expected to incorporate more label; (iii) when hybridized *in situ* with the two *D. melanogaster* chorion gene probes together, the stage 13 follicle cell nuclei of *D. nasuta* displayed two distinct sites of hybridization while each probe singly hybridized predominantly to only 1 site of *D. melanogaster* follicle cell nucleus; moreover, the hybridization signal was found to increase from stage 10 to 12/13 follicle cell nuclei as may be expected with increasing copy numbers of chorion genes due to amplification during this period. Chorion gene sequences are known to be unique in *Drosophila* genome and to show cross-hybridization with analogous sequences in different species (Spradling, 1981; Martinez-Cruzado *et al.*, 1988; Spradling and Orr-Weaver, 1988). Therefore, the hybridization patterns leave no doubt that the [^3H] thymidine incorporation at 1 or 2 regions only in most of the stage 11–12 follicle cell nuclei was related to ongoing amplification of chorion genes.

Earlier studies on evolution of chorion gene clusters in several species of *Drosophila* (Martinez-Cruzado *et al.*, 1988) had shown a high conservation of overall organization of the autosomal chorion gene locus. *D. nasuta* belonging to the *immigrans* species group of the sub-genus *Drosophila* is phylogenetically more distant from *D. melanogaster* (Throckmorton, 1975) than any of the species examined by Martinez-Cruzado *et al.* (1988). The presence of two amplifying chorion gene loci in *D. nasuta* as in *D. melanogaster* thus provides further evidence for conservation of the organization of chorion gene loci in the genus *Drosophila*. Martinez-Cruzado *et al.* (1988) noted a high degree of sequence divergence in chorion genes in different species but a strong conservation of proximal 5' flanking and 5' region of the genes. The reduced hybridization of the *D. melanogaster* chorion gene probes with *D. nasuta* nuclei reflects this sequence divergence. However, since in our study, the probes spanned entire chorion genes, the regions of conservation or divergence cannot be identified. The difference in the relative frequencies of stage 11–12 follicle cell nuclei with one or two [^3H] thymidine labelled sites in *D. melanogaster* and *D. nasuta* seems to reflect small differences in the temporal programmes of amplification of the two chorion gene clusters in these two species.

The localization of replicating regions or specific gene sequences in intact nuclei in cytological preparations provides very useful information on the 3-dimensional organization of nucleus since the preparatory steps do not distort the general *in situ* structure. Using *in situ* hybridization to localize specific gene sequences in endoreplicated ovarian nurse and follicle cell nuclei of *D. melanogaster*, Hammond and Laird (1985) concluded that in these nuclei, the copies on endoreplicated

homologous strands remain associated to a varying degree of closeness depending upon the nature of the sequence examined. In this context, the present observations show that the endoreplicated and amplified copies of chorion genes maintain a fairly close association within each of the two clusters but the two clusters themselves appear to remain spatially distinct. In relation to the 3-dimensional organization of different gene sequences in nuclei, Hammond and Laird (1985) also considered the possibility if there was a functional compartmentalization such that similarly transcribed sequences stay together. Our observations suggest that such spatially distinct compartments may not be necessary since although the two chorion gene clusters are programmed to selectively amplify and transcribe in follicle cell nuclei within a limited time span, they are located in distinctly separate nuclear areas: if compartmentalization was required, one would expect to find the two chorion gene clusters in close vicinity rather than separate as seen in this study.

Acknowledgements

We gratefully acknowledge the generous gift of the chorion gene probes by Prof. A. C. Spradling. This work was supported by a research grant from the Department of Science and Technology, New Delhi to S.C.L. and by a Council of Scientific and Industrial Research, New Delhi research associateship to P.K.T.

References

- Hammond, M. P. and Laird, C. D. (1985) *Chromosoma*, **91**, 279.
 King, R. C. (1970) *Ovarian development in Drosophila melanogaster* (New York, London: Academic Press).
 Lakhota, S. C. and Mukherjee, T. (1980) *Chromosoma*, **81**, 125.
 Lakhota, S. C. and Sinha, P. (1983) *Chromosoma*, **88**, 265.
 Martinez-Cruzado, J. C., Swimmer, C., Fenerjian, M. G. and Kafatos, F. C. (1988) *Genetics*, **119**, 663.
 Pardue, M. L. (1986) in *Drosophila a practical approach* (ed. D. B. Roberts) (Oxford: IRL Press) p. 111.
 Raman, R. and Lakhota, S. C. (1990) in *Trends in chromosome research* (ed. T. Sharma) (Berlin: Springer-Verlag; New Delhi: Narosa) p. 69.
 Spradling, A. (1981) *Cell*, **27**, 193.
 Spradling, A., Digan, M. E. and Mahowald, A. P. (1980) *Cell*, **19**, 905.
 Spradling, A. and Mahowald, A. P. (1980) *Proc. Natl. Acad. Sci. USA*, **77**, 1096.
 Spradling, A. and Orr-Weaver, T. (1987) *Annu. Rev. Genet.*, **21**, 373.
 Throckmorton, L. H. (1975) in *Handbook of genetics* (ed. R. C. King) (New York: Plenum Press) vol. 3, p. 421.
 Tiwari, P. K. and Lakhota, S. C. (1990) in *DAE Symp. on advances in molecular biology* (Bombay: BARC) p. 237.

Regulation of cytochrome P-450 (b + e) and glutathione transferase (Ya + Yc) gene expression in rat liver

JARKI, V. S. N. K. FRANCIS and G. PADMANABAN*

Department of Biochemistry and Centre for Genetic Engineering, Indian Institute of Technology, Bangalore 560 012, India

Received 16 May 1990

The expression of cytochrome P-450(b+e) and glutathione transferase genes has been studied as a function of development in rat liver. The levels of the P-450(b+e) mRNAs and their transcription rates are too low for detection in the old fetal liver before or after phenobarbitone treatment. However, glutathione transferase (Ya+Yc) mRNAs can be detected in the fetal liver as well as their induction by phenobarbitone treatment can be demonstrated. These mRNAs contents as well as their inducibility with phenobarbitone are lower in maternal liver than that of adult non-pregnant female rat liver. Steroid hormone administration to immature rats blocks completely the phenobarbitone mediated induction of the two mRNA families as well as their transcription. It is suggested that steroid hormones constitute one of the factors responsible for the repression of the cytochrome P-450(b+e) and glutathione transferase genes in fetal liver.

* Cytochrome P-450; glutathione transferase; transcription; gene expression;

the cytochrome P-450 dependent mixed function oxygenase activity is very low in fetal liver and increase rapidly soon after birth. It is difficult to induce cytochrome P-450 in fetal liver, although 3-methylcholanthrene is capable of a selective but small level of induction. It has also been shown that phenobarbitone readily crosses the placental barrier and accumulates in the fetal liver at almost the same concentration observed in the adult liver. Phenobarbitone is quite effective in inducing cytochrome P-450 soon after birth (Kawanishi *et al.*, 1971; Guenther and Mannering, 1977; Cresteil *et al.*, 1979; Cresteil *et al.*, 1982).

Glutathione transferase, another important enzyme family of the drug metabolism, has been shown to be present at 10–20% of the adult levels in the fetal liver. The susceptibility of this enzyme family for induction at the fetal stage has not been studied, except that phenobarbitone induces this enzyme system soon after birth and the extent of induction remains constant throughout the fetal period (Neims and Neims, 1976; Neims *et al.*, 1976).

The mechanism of regulation of expression of these two gene systems in the fetal liver has not been well studied, except for a report that phenobarbitone induces cytochrome P-450b or e mRNA in 10- or 19-day old fetal liver. Significant levels of induction are seen on day 22 (Giachelli and Cresteil, 1985). In the present study, the induction of cytochrome P-450(b+e)

and glutathione transferase (Ya + Yc) mRNAs by phenobarbitone in fetal, postnatal and adult rat livers was examined using cloned cDNA hybridization probes. The transcription rates with isolated nuclei were measured. The effects of circulating steroid hormones on these parameters were also studied and the suggestion is that these hormones constitute one of the factors responsible for maintaining genes in the repressed state in fetal liver.

Experimental procedures

Treatment of animals

Pregnant rats (200 g body weight) of the Institute strain were given one, two or three intraperitoneal injections of phenobarbitone (8 mg/100 g body weight) on day 17 or 19. The animals were killed 12 h after the last injection. Injections of steroid hormones were given intraperitoneally at a dose of 1 mg/kg 15 min before the drug administration.

Quantification of cytochrome P-450(b + e) and glutathione transferase (Yc) mRNA

Polysomal RNA was isolated from the pooled livers of rats by the magnetic precipitation procedure of Palmiter (1974). Poly (A)-containing RNA was isolated using oligo-dT cellulose chromatography. Specific mRNA concentration was estimated by dot blot hybridization using specific nick-translated cloned cDNA probes. In these studies 500 ng to 1 µg of poly (A)-containing RNA or 10–20 µg total polysomal RNA was loaded onto nitrocellulose filters. In northern blot experiments 10 µg of polysomal RNA was used. The dot blot and northern blot hybridizations were carried out as described by Thomas (1980). Agarose (1%) formaldehyde gels were used for RNA analysis (Maniatis *et al.*, 1982). The probes used were inserts from the plasmids pP-450 91 (Ravishankar and Padmanabhan, 1985) and pGST 19 (Francis *et al.*, 1986) for quantifying cytochrome P-450 and glutathione transferase (Ya + Yc) mRNAs respectively. The probes contain more than 2/3 of cytochrome P-450e and glutathione transferase Ya and Yc mRNAs respectively from 3' ends. Cytochrome P-450 e and b mRNAs and glutathione transferase Yc and Ya subunit mRNAs have extensive region of homology (Mizukami *et al.*, 1983; Pickett *et al.*, 1984). Albumin mRNA was quantified with the albumin cDNA probe (Sathyabhama *et al.*, 1986). ³²P translation was carried out in the presence of [α ³²-P]dCTP and a labelled protein of 5 × 10⁷ to 10⁸ cpm/µg DNA was routinely obtained. After carrying out dot blot hybridization and washing procedures, the blots were exposed to X-ray film and the corresponding dots were punched out from the nitrocellulose blots and radioactivity measured using 0.5% (w/v) PPO in toluene as the scintillation fluid. The responses were obtained in the concentration range up to 1.5 µg for poly (A)-containing RNA and 20 µg for total polysomal RNA. The experiment was repeated 4 times and the pattern of results was reproducible. However, the radioactivity in the dots varied between experiments depending on the activity of the probe used.

transcription

ed from the livers of rats given the various treatments and cell- was carried out in the presence of [α^{32} -P] UTP as described by Padmanaban (1985) based on the reaction conditions given by 83). The RNA transcribed *in vitro* (10^7 cpm) was hybridized to pP-450 91 or pGST 19 or pAlb 6 DNA. About 5 μ g of the DNAs lters. After hybridization and washing the filters were dried and sured. Addition of α -amanitin (1 μ g/ml) to the transcription 1 to inhibit total transcription by about 50%, but hybridization to used was found to be inhibited by 96–98%. Non-specific hybridiza- DNA was of the order of 10% of specific hybridization and this ted in the final data presented.

of cytochrome P-450(b + e) and glutathione transferase (Ya + Yc) barbitone in fetal, pup and adult livers were examined by dot blot d the quantitative values are presented in table 1. The results stable levels of cytochrome P-450(b + e) mRNA are not present in . The mRNAs can be detected in the livers of 5-day old pups, n-pregnant female adult livers. Phenobarbitone administration to o induce these mRNAs in fetal liver. This is irrespective of whether ceived 1, 2 or 3 injections of the drug. There is about 10–12-fold 5-day old pup and pregnant mother.

.. Cytochrome P-450 and glutathione transferase (Ya + Yc) mRNA s in rat liver as a function of development.

	P-450 (b + e) mRNA		GST (Ya + Yc) mRNA	
	Control	PB	Control	PB
	(cpm hybridized)			
prenatal	ND	ND	33	55
	18	190	50	85
adult	24	256	80	152
(non-pregnant female)	30	626	135	301

en-day old pregnant rats as well as the other groups received a single n of phenobarbitone and the animals were killed after 12 h. Poly (A)- ing RNA (1 μ g) isolated from the magnesium-precipitated liver osomes was loaded onto nitrocellulose filters and hybridized with the anslated probes. The values presented are those obtained in a typical ment.

Not detectable.

n is nearly 20-fold in the non-pregnant adult female. Unlike 50(b + e) mRNAs, glutathione transferase (Ya + Yc) mRNAs can be

fold in control pup, pregnant and non-pregnant female livers respectively. Phenobarbitone administration results in a small but consistent pattern of induction of glutathione transferase (Ya+Yc) mRNAs in fetal liver. The induction is around 1.5-fold in pups, 2- and 2.5-fold in the pregnant and non-pregnant adult females respectively 12 h after a single injection of phenobarbitone. The northern blot presented in figure 1 confirms the pattern of data presented in table 1. In particular, it is clear that glutathione transferase (Ya+Yc) mRNAs are present in the fetal liver and are induced by phenobarbitone (figure 1, lanes 3 and 6). It may be pointed out that for northern blot analysis, RNA was isolated from animals which had received 3 injections of the drug and the glutathione transferase (Ya+Yc) mRNA induction obtained is nearly 7–10-fold of the levels observed in control rats. In separate hybrid selection experiments, pGST-19 has been found to pick up mostly Ya mRNA and therefore these results would mostly reflect changes in the concentration of Ya mRNA. On the basis of the mobility of the size markers, it appears that these have a size range of 900 ± 50 nucleotides which is around the value reported earlier (Pickett *et al.*, 1983). Giachelli and Omiecinski (1986) have

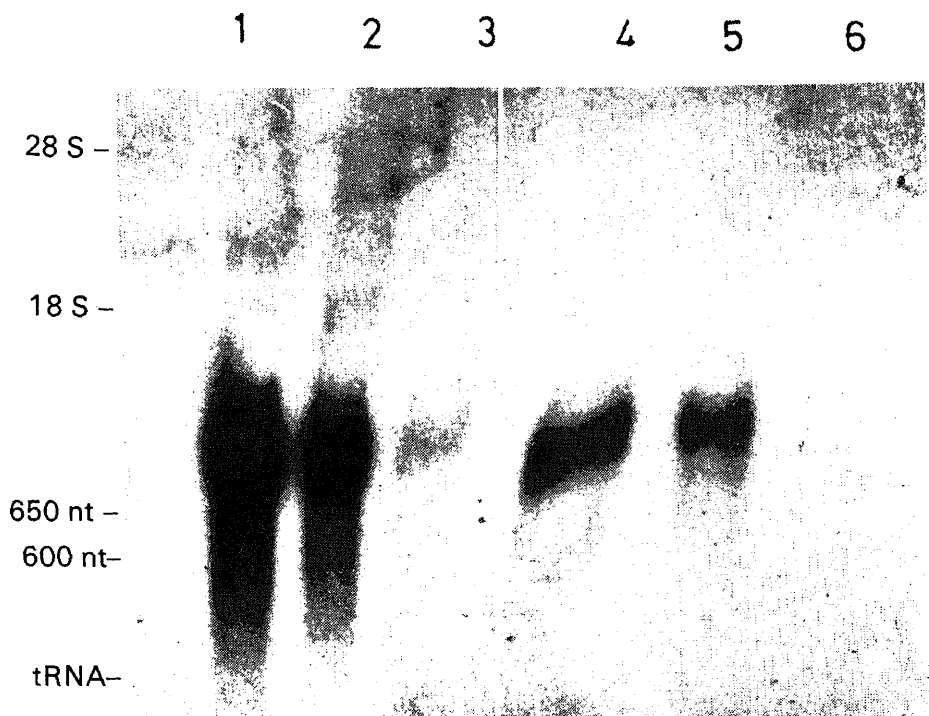


Figure 1. Northern blot analysis of glutathione transferase (Ya+Yc) mRNAs during development and phenobarbitone treatment. The animals received 3 injections of phenobarbitone one each at 24 h intervals. The first injection was given to 17-day old pregnant rats and the maternal and fetal livers were isolated on day 19. Total polysomal RNA (10 μ g) was subjected to northern blot analysis using nick-translated fragment from pGST-19 as probe. 28 S and 18 S ribosomal RNAs, globin mRNA and tRNA were used as

reported that the size of cytochrome P-450e mRNA remains around 1.8 kb throughout development.

In view of the findings that phenobarbitone fails to induce cytochrome P-450(b+e) mRNAs and induces glutathione transferase (Ya+Yc) mRNAs to a lower extent in fetal livers than in the adult and that the induction of these mRNA families in the pregnant mother is lower than that of the non-pregnant female, the effects of circulating steroid hormones on the phenobarbitone-mediated induction of these mRNAs were investigated. Figure 2 indicates that estradiol and progesterone administration block significantly the phenobarbitone mediated induction of cytochrome P-450(b+e) mRNAs in the 5-day old pup. Surprisingly, the hormones fail to block the induction in adult male rats. In fact, a certain level of synergism is seen between the hormones and the drug. Detailed quantitative results for cytochrome P-450(b+e) and glutathione transferase (Ya+Yc) mRNAs are presented in table 2. The hormones estradiol, progesterone, testosterone and dexamethasone inhibit the phenobarbitone-mediated induction of both mRNA families by 50–70% in the 5-day old pup liver.

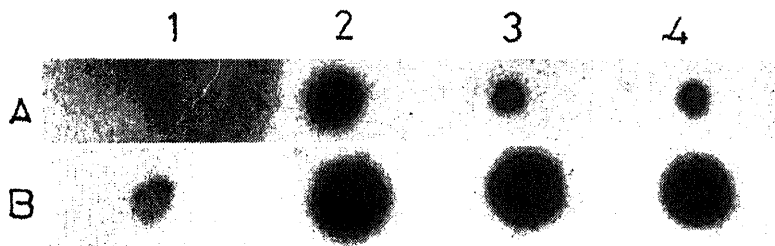


Figure 2. Dot blot analysis of cytochrome P-450(b+e) mRNAs after phenobarbitone and steroid treatments. Five-day old pups and adult male rats received single injections of phenobarbitone along with estradiol and progesterone. Poly (A) containing RNA (1 µg) was used for the dot blot analysis using nick-translated fragment from pP-450 91 as probe. Lane A (pup): (1), control; (2), phenobarbitone; (3), phenobarbitone + estradiol; (4), phenobarbitone + progesterone. Lane B (adult): (1), control; (2), phenobarbitone + estradiol; (3), phenobarbitone + progesterone; (4), phenobarbitone.

Table 2. Effect of steroid hormones on the induction of cytochrome P-450(b+e) and glutathione transferase (Ya+Yc) mRNAs by phenobarbitone.

Treatment	Pup		Adult (male)	
	P-450 (b+e) mRNA	GST (Ya+Yc) mRNA	P-450 (b+e) mRNA	GST (Ya+Yc) mRNA
	(cpm hybridized)			
Control	21	63	32	175
PB	196	126	750	420
PB + estradiol	75	85	855	510
PB + progesterone	96	89	825	435
PB + testosterone	66	79	793	556
PB + dexamethosone	71	75	835	456

The treatment conditions and other experimental details are as described in the text and table 1. The results presented are those obtained in a typical experiment.

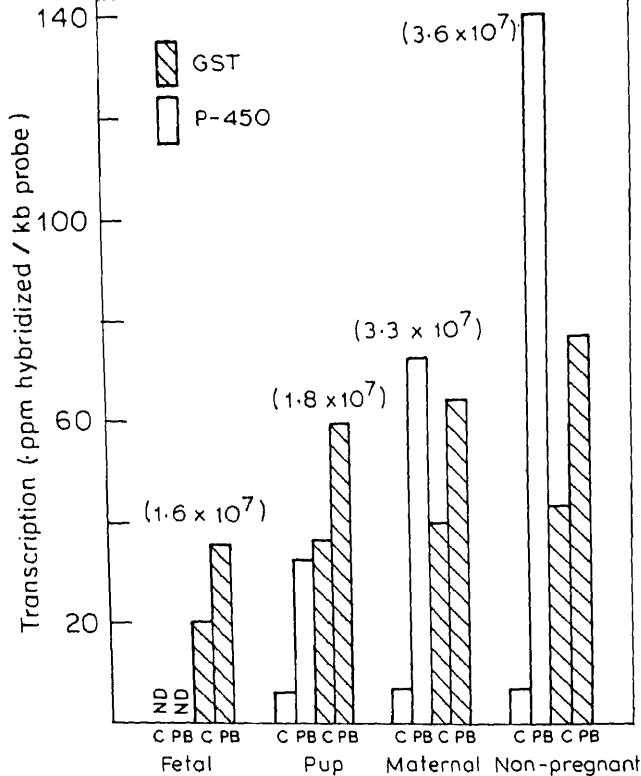


Figure 3. Transcription rates of cytochrome P-450(b+e) and glutathione transferase (Ya + Yc) mRNAs as a function of development. The nuclei isolated from the livers of rats at different developmental stages were incubated for 45 min at 25°C and other components with [α - 32 P]UTP and the transcribed RNA was hybridized to the probes. The total RNA transcribed, expressed in cpm in the case of each nuclear preparation, is indicated in parenthesis. The specific transcription rates presented as bars are an average from two independent experiments and are expressed as ppm of RNA hybridized/kb of the probe used. The other details are given in the text. (C), Control; (PB), phenobarbitone., (ND), not detectable.

The results presented in figure 3 indicate that the total RNA transcription rates obtained for fetal and pup livers is consistently around 50% of the adult livers. In the case of cytochrome P-450(b+e) mRNAs, phenobarbitone administration results in about 5-, 10- and 20-fold increase in transcription rates for pup, pregnant and non-pregnant livers. Transcription of these mRNAs cannot be detected in control or phenobarbitone-treated fetal liver nuclei. In the case of glutathione transferase (Ya + Yc) mRNAs, significant level of transcription is detectable in control fetal liver nuclei. With development, this increases by nearly 2-fold in the adult. Phenobarbitone administration results in a small but consistently detectable increase in the transcription rates in the fetal liver nuclei. The increase obtained with the pup, pregnant and non-pregnant liver nuclei is less than 2-fold of the values obtained with control animals, 12 h after a single injection of the drug.

Since estradiol and progesterone significantly inhibited the induction of cytochrome P-450(b+e) mRNAs and glutathione transferase (Ya + Yc) mRNAs in

inhibit the phenobarbitone-mediated increase in the transcription rates of the two mRNA families by 50–60%. It is of interest to point out that albumin mRNA transcription rates measured under these conditions also show significant changes. First of all, phenobarbitone administration *per se* decreases albumin transcription rate in the pup. Estradiol as well as testosterone treatments, further decrease the albumin mRNA transcription rates. The albumin mRNA transcription rate observed in the normal pup is around 40% of that seen with the adult (data not presented). It should, however, be pointed out that none of the treatments affects total RNA transcription rates to any significant extent.

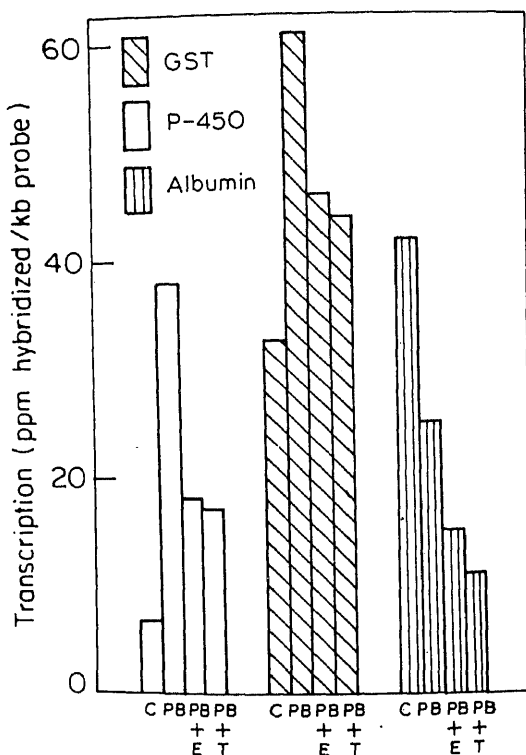


Figure 4. Effect of steroid hormones on the phenobarbitone-mediated increase in transcription rates of cytochrome P-450(b+e), glutathione transferase (Ya+Yc) and albumin mRNAs in pup liver. Nuclei were isolated from the livers of pups given the different treatments. The experimental details are given in figure 3 and text. The values depicted are an average obtained from two independent experiments. (C), Control, (PB), phenobarbitone; (E), estrogen; (T), testosterone.

Discussion

Several interesting features of developmental regulation of the hepatic cytochrome P-450(b+e) and glutathione transferase (Ya+Yc) gene systems are apparent from this study. First of all, detectable levels of expression of the cytochrome P-450(b+e)

mRNAs in control or phenobarbitone-treated 19–20-day old fetal livers are not manifest, confirming the report of Giachelli and Omiecinski (1986). However, glutathione transferase (Ya + Yc) mRNAs are expressed as well as induced in fetal livers.

Steroid hormones appear to exert a negative control in regulating the expression of both cytochrome P-450(b + e) and glutathione transferase (Ya + Yc) mRNAs in fetal liver. The poor or non-expression of the former and the lower level of expression of the latter gene systems in fetal liver in the presence or absence of the inducer, the inhibitory effects of the steroid hormones on phenobarbitone mediated induction of the two mRNA families in the immature animal and the lower levels of these mRNAs in the drug-treated pregnant mother compared to the non-pregnant adult female, all point to the role of circulating steroid hormones in exerting a negative control on the expression of these two gene systems in fetal and pregnant rat livers. It has not been possible to examine the effect of steroid hormones on cytochrome P-450(b + c) gene transcription directly in fetal liver in view of poor expression. The possibility of factors in the fetomaternal environment suppressing the phenobarbitone-mediated induction of the drug-metabolizing enzymes in fetal liver has been suggested by Guenther and Mannering (1977). Further studies are needed to examine the hormone-dependent changes in the expression of these genes during different phases of the estrous cycle in non-pregnant female adult rats.

It is also clear that the responsiveness of the gene involved for interaction with the environment also changes during development. For example, in the adult male the steroid hormones fail to repress the phenobarbitone-mediated induction of these mRNAs. We have recently shown that dexamethasone inhibits phenobarbitone-mediated increase in the transcription of cytochrome P-450(b + e) genes both in adult and pup livers. However, dexamethasone inhibits the drug mediated induction of cytochrome P-450(b + e) mRNAs only in pup livers, but actually shows synergism with the drug in adult livers (table 2; Venkateswara Rao *et al.*, 1990). Thus, development dependent post-transcriptional mechanisms are also involved in determining the ultimate levels of the functional mRNA and perhaps of the protein species as well. This is further indicated by the lack of a strict correlation between changes in transcription rates and mRNA contents under different developmental and physiological states.

Two other features of this study are of interest. One is that all the 4 steroid hormones examined share the ability to inhibit phenobarbitone-mediated increase in the transcription of cytochrome P-450(b + e) and glutathione transferase (Ya + Yc) genes. Steroid receptors belong to a super family and are related structurally. The DNA consensus elements, involved in receptor binding are also similar, but distinct identity is maintained in mediating transcriptional activation by the individual steroids (Evans, 1988; Green and Chambon, 1988). However, the DNA consensus elements involved in mediating the negative modulatory effects of steroids have not been well characterized. The negative glucocorticoid receptor element does not appear to share much of homology with the positive element or with the negative elements detected in different gene systems (Sakai *et al.*, 1988). It is possible that the negative steroid elements are degenerate and recognise more than one steroid receptor *in vitro*. The second feature is that the steroids used

ver. Thus, the role of steroids as negative modulators of the
er proteins in fetal liver is indicated and would need further

out in a project supported by the Indian Council of Medical
The centre for Genetic Engineering is supported by the
nology, New Delhi. Thanks are due to Ms P. G. Vatsala for

- Pfister, A. and Leroux, J. -P. (1979) *Biochem. Pharmacol.*, **28**, 2057.
2, **240**, 889.
xi, V. J. and Padmanaban, G. (1986) *Nucleic Acids Res.*, **14**, 2497.
inski, C. J. (1986) *J. Biol. Chem.*, **261**, 1359.
. (1988) *Trends Genet.*, **4**, 309.
mering, G. J. (1977) *Biochem. Pharmacol.*, **26**, 567.
owiak, J., Anderson, A. and Belanger, L. C. (1983) *Biochemistry*, **22**, 4296.
H. (1976) *Biochem. J.*, **160**, 231.
' and Sambrook, J. (1982) *Molecular Cloning—A Laboratory manual* (New
bor Laboratory).
, Suwa, Y., Muramatsu, M. and Fujii-Kuriyama, Y. (1983) *Proc. Natl. Acad.*

, Lang, M. A., Hjemeland, L. M. and Eisen, H. J. (1982) *Adv. Genet.*, **21**, 1.
Langhman, P. M. and Aranda, J. V. (1976) *Annu. Rev. Pharmacol. Toxicol.*, **16**,
chemistry, **13**, 3601.
-Hopkins, C. A., Donohue, A. and Lu, A. Y. H. (1983) *Arch. Biochem. Biophys.*,

i-Hopkins, C. A., Ding, G., Argenbright, L. and Lu, A. Y. H. (1984) *J. Biol.*

manaban, G. (1985) *J. Biol. Chem.*, **260**, 1588.
Carlstedt-Duke, J., Gustaffson, J. A., Rottman, F. M. and Yamamoto, K. R.
.144.
R. S. and Padmanaban, G. (1986) *Biochemistry*, **25**, 4508.
2. *Natl. Acad. Sci. USA*, **77**, 5201.
angarajan, P. N. and Padmanaban, G. (1990) *J. Biol. Chem.*, **265**, 5617.
in, W. L. (1971) *Biochem. Pharmacol.*, **21**, 547.

ed to bring out this issue consisting of the papers presented at
ference on Structure and Function of Biomembranes held at
lcutta during November 28–December 2, 1989. The Editorial
ly like to acknowledge the help rendered by Prof. Parul
or), Dr Jyoti Basu (Joint Convenor) and Dr Manikuntala
nor) who acted as Guest Editors for reviewing the papers
3.

Editor

Nuclear magnetic resonance and thermal studies of drug doped dipalmitoyl phosphatidyl choline-H₂O systems

K. USHA DENIZ†§, P. S. PARVATHANATHAN†, GEETA DATTA††, C. L. KHETRAPAL, K. V. RAMANATHAN, N. SURYAPRAKASH and S. RAGHOTAMA

Sophisticated Instrument Facility, Indian Institute of Science, Bangalore 560 012, India

†Nuclear Physics Division and ††Biochemistry Division, Bhabha Atomic Research Centre, Trombay, Bombay 400 085, India

Abstract. The influence of the sulfone drugs, diamino diphenyl sulfone and diamino monophenyl sulfone on the phase transitions and dynamics of dipalmitoyl phosphatidyl choline-H₂O/D₂O vesicles have been investigated using differential scanning calorimetry and nuclear magnetic resonance. Our results show that diamino diphenyl sulfone interacts quite strongly with the headgroups of dipalmitoyl phosphatidyl choline whereas the diamino monophenyl sulfone-dipalmitoyl phosphatidyl choline interaction is quite weak. This is attributed to the difference in the structure and hydrophobic character of the two drugs.

Keywords. Dipalmitoyl phosphatidyl choline; drug-membrane interaction; differential scanning calorimetry; ¹H NMR; ³¹P NMR.

Introduction

Study of interactions of drugs with biomembrane is of great importance. Biomembranes being very complex, one studies interactions of drugs with model-membranes as a first step towards understanding drug-biomembrane interactions. In the present work, we have carried out differential scanning calorimetry (DSC) and nuclear magnetic resonance (NMR) (¹H and ³¹P) experiments at temperatures in the vicinity of the chain melting (CM) transition to observe the interaction of the sulfone drugs, diamino diphenyl sulfone (DDS or Dapsone) and diamino monophenyl sulfone (DMS or sulfanilamide) with the model membrane, dipalmitoyl phosphatidyl choline (DPPC)-H₂O/D₂O, in vesicle form. These drugs are expected to possess distorted tetrahedral structures (figure 1). Though DDS has been in use as an antileprosy drug for a few decades, hardly any information about its interactions with membranes was available until recently (Deniz *et al.*, 1983, 1989). While our main interest was in DDS-membrane interactions, DMS was used in order to understand how structural differences affect these interactions.

Materials and methods

DPPC and DMS were purchased from Sigma Chemical Company, St. Louis, Missouri, USA, while DDS was a gift from Burroughs Wellcome India. These were

§To whom all the correspondence should be addressed.

Abbreviations used: DSC, Differential scanning calorimetry; NMR, nuclear magnetic resonance; CM, chain melting; DDS, diamino diphenyl sulfone; DPPC, dipalmitoyl phosphatidyl choline; PT, pre-transition

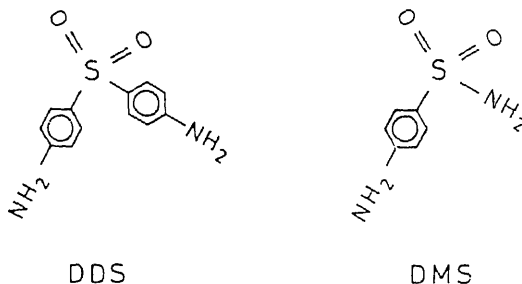


Figure 1. The structure of molecules, DDS and DMS.

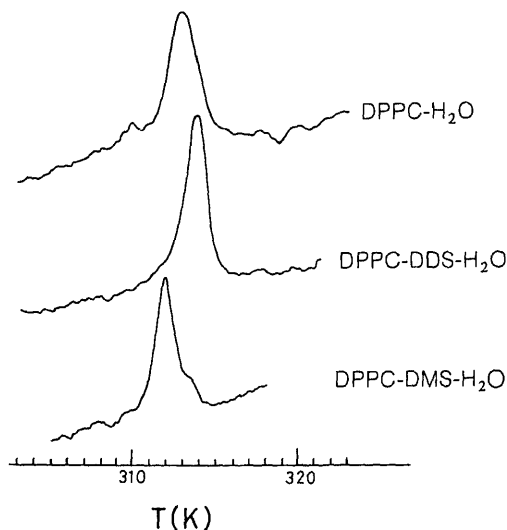
used without further purification. The vesicles of DPPC and drug-DPPC prepared by hydrating their films with $\text{H}_2\text{O}/\text{D}_2\text{O}$ at 45°C , vorticising then subsequently sonicating at 45°C for 45 min, using a microtip. DPPC concentration [DPPC], of 50 mM and a molar ratio, R_m , of drug to DPPC of 0.1 were used. DSC studies were carried out on a Perkin Elmer DSC-2C instrument. Sample weights ranged from 10–16 mg and the scans were carried out at rates of 2.5–10 K/min. ^1H NMR at 270 MHz was carried out on a Bruker WM 270 instrument with sodium-3-trimethylsilyl (2,2,3,3- ^2H) propionate (TSP) as reference and ^{31}P NMR at 121.44 MHz was done on a Bruker MSL 300 instrument with phosphoric acid as reference.

Results and discussion

DSC

The model membrane, DPPC- $\text{H}_2\text{O}/\text{D}_2\text{O}$ exhibits an ordered lamellar gel phase at room temperature. On heating, a pre-transition (PT) occurs to a phase ($P_{\beta'}$) (Janiak *et al.*, 1976; Scott, 1981). This is followed by a CM transition into a disordered liquid crystalline (L_α) phase. This transition is of physiological importance, since the chain mobility (membrane function) is related to it.

DSC scans through the CM transitions for the 3 systems are shown in figure 1. We find that (i) T_{CM} is slightly increased in the presence of DDS but is slightly decreased by DMS and (ii) PT (not seen in the figure) is suppressed completely by DDS but only partially by DMS. This can be explained in the following way. Due to the tetrahedral structure of the DDS molecule and its amphiphilic nature, one would expect [in the light of De Verteuil *et al.* (1981) theory] a significant decrease in T_{CM} , if DDS were to be located in the acyl chain region. Since it is not observed, DDS must be located at the DPPC- H_2O interface, interacting with the polar group of the lipid and enhancing the effective DPPC head group-head group interaction. This can account for the observed increase in T_{CM} (De Verteuil *et al.*, 1981). DMS being more polar than DDS, is less likely to enter the acyl chain region. However, it must be decreasing slightly, the effective interaction between DPPC head groups, leading to the observed decrease in T_{CM} . The values of T_{CM} and ΔH_{CM} measured with stacked bilayers (Deniz *et al.*, 1983) of the 3 systems, differ from those obtained in the present measurements with vesicles.



DSC scans of the 3 model membranes, DPPC-H₂O, DPPC-DDS-H₂O and DPPC-DMS-H₂O showing the CM transition (scan rate: 2.5 K/min).

T_{CM} and ΔH_{CM} for various model membrane

	Stacked bilayers		Vesicles	
	T_{CM} (K)	ΔH_{CM} (KCal/mol)	T_{CM} (K)	ΔH_{CM} (KCal/mol)
DPPC-H ₂ O	313.7	8.44	312.8	4.42
DPPC-DDS-H ₂ O	312.4	9.56	314.8	5.39
DPPC-DMS-H ₂ O	312.9	8.41	314.0	7.01

which are unilamellar or made up of only a few lamellae (i) it is possible to have access to the DPPC-head group than in stacked bilayer environment for (a), (ii) increased fluctuations in the order parameter of the DPPC chain reduces ΔH_{CM} resulting in (b) and (iii) these order parameter fluctuations can be reduced by the drug-DPPC interactions leading to $\Delta H_{CM} > \Delta H_{CM}(\text{DPPC-H}_2\text{O})$ (observation (a)).

The ¹H NMR spectra of DPPC in the 3 model membranes are shown in figure 3. In figure 3A, the chain resonances, (1)–(4) and the choline group are clearly visible at 315 K. The chain resonances are seen to be resolved at 310 and 312 K. They begin to get resolved at 313 K, $310 < T < 313$ K. The N⁺(CH₃)₃ resonance, (5) is sharp even at 310 K. The DPPC in the 3 model membranes is in the liquid phase at 315 K. The ¹H NMR spectra of DPPC in the 3 model membranes are shown in figure 3. In figure 3A, the chain resonances, (1)–(4) and the choline group are clearly visible at 315 K. The chain resonances are seen to be resolved at 310 and 312 K. They begin to get resolved at 313 K, $310 < T < 313$ K. The N⁺(CH₃)₃ resonance, (5) is sharp even at 310 K. The DPPC in the 3 model membranes is in the liquid phase at 315 K.

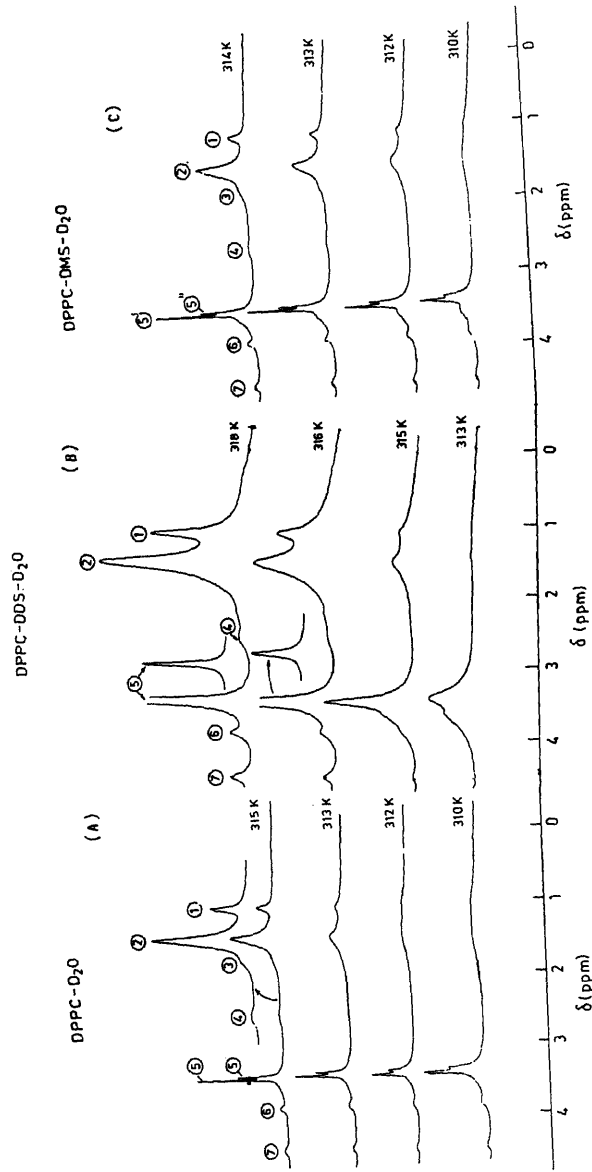
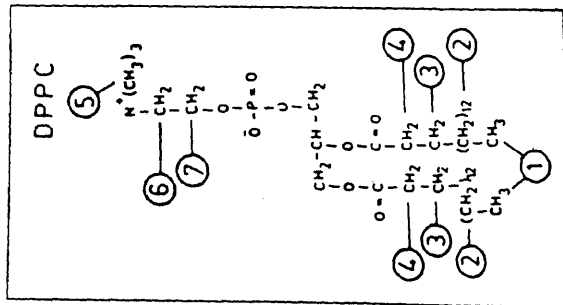


Figure 3. ^1H NMR spectra of (A) DPBC- D_2O , (B) DPBC-DDS- D_2O and (C) DPBC-DMS- D_2O taken at different temperatures in the neighbourhood of T_{CM} . The assignments to the various groups in DPBC are shown in the insert.

The spectra for DPPC-DMS-D₂O (figure 3B) closely resemble those of DPPC-D₂O except that T_{CM} is slightly decreased ($T_{CM} \approx 312$ K). The spectra for DPPC-DDS-D₂O (figure 3C) shows the following: (i) The chain resonance (1), (2) and (4) can be seen at 318 K, but resonance (3) is not observed, possibly due to the broadening of the (CH₂)_n resonance. (ii) The CM transition in this case, occurs between 315 and 316 K, *i.e.*, T_{CM} (DPPC-DDS-D₂O) > T_{CM} (DPPC-D₂O). (iii) Although all the 3 choline resonances, (5)–(7) can be seen, (5) is a single peak even at $T > T_{CM}$, unlike in the other two cases. This would mean that the chains and the N⁺(CH₃)₃ groups become more rigid in the presence of DDS. These results suggest that DDS interacts with the choline groups and perhaps also the carbonyl group of DPPC, the latter leading to decreased chain mobility.

The ¹H NMR spectra of the aromatic protons of (i) DDS in D₂O, (ii) DDS in DPPC-D₂O and (iii) DMS in DPPC-D₂O are shown in figure 4, the latter two for temperatures in the vicinity of T_{CM} . The aromatic proton spectra for DDS in D₂O and DMS in D₂O are similar, consisting of two doublets. This doublet structure (the spin coupling constant) is temperature independent for the temperature range used in these experiments. In DPPC-DMS-D₂O, the doublet structure is hardly changed. However, in DPPC-DDS-D₂O, these resonances are broadened and the doublets cannot be resolved, showing that the aromatic rings of DDS are also interacting with DPPC.

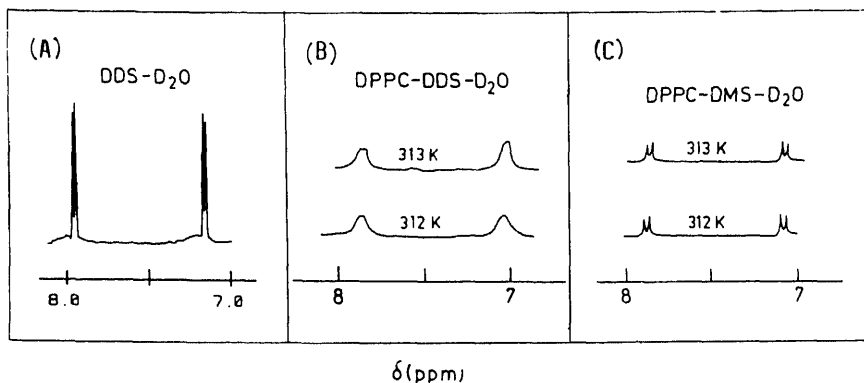


Figure 4. ¹H NMR spectra of the aromatic protons in (A) DDS-D₂O, (B) DPPC-DDS-D₂O and (C) DPPC-DMS-D₂O. (B) and (C) are given for temperatures $\approx T_{CM}$.

³¹P NMR

A ³¹P NMR study of DPPC-D₂O and DPPC-DDS-D₂O was carried out as a function of temperature. Typical spectra for $T < T_{CM}$ and $T > T_{CM}$ are shown in figure 5. For the drug-free system, the resonance is very sharp for both the temperatures, whereas in the presence of DDS, these resonances are broadened considerably even for $T > T_{CM}$. This indicates that DDS (NH₂ group) interacts with the phosphate group of DPPC.

Our results show that DDS-DPPC interaction is much stronger than that of

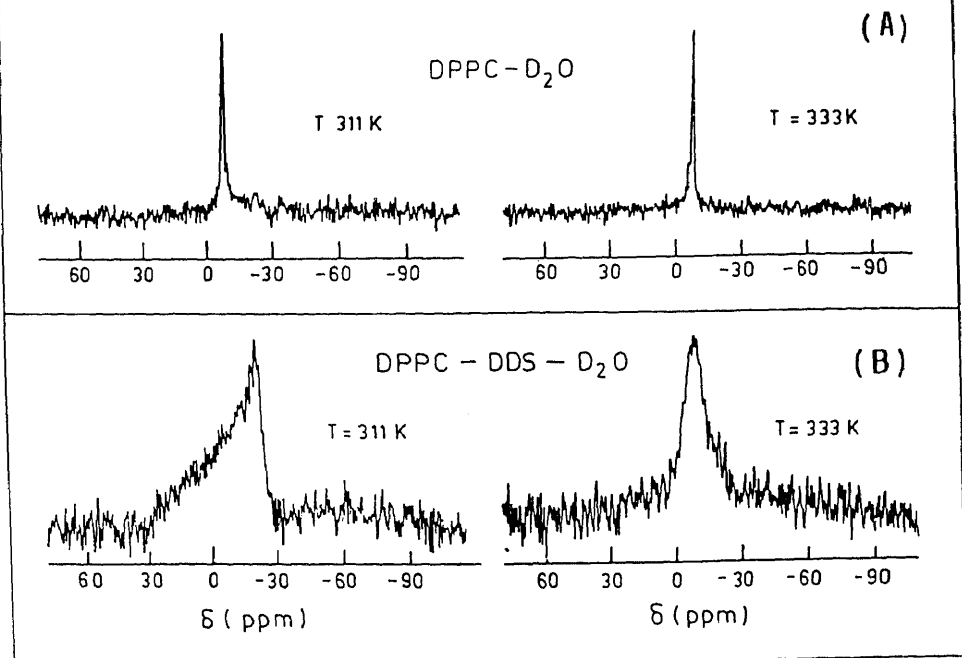
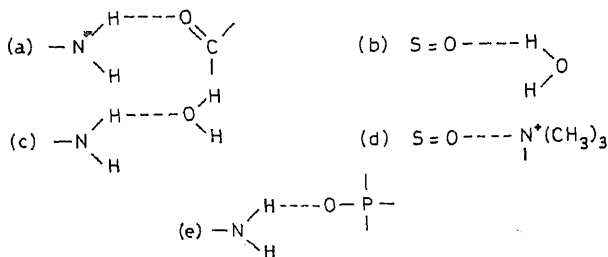


Figure 5. ^{31}P NMR spectra of (A) DPPC- D_2O and (B) DPPC-DDS- D_2O , for $T < T_{\text{CM}}$ and $T > T_{\text{CM}}$.

DMS with DPPC. The aromatic as well as polar groups of DDS interact with DPPC head group. The most likely interactions are shown below:



Probable combinations of these are (a)+(b), (c)+(d) and (a)+(d).

The difference between the DDS-DPPC and DMS-DPPC interactions could be due to (i) more polar character of DMS leading to its greater solubility in water and weaker interactions with DPPC and (ii) molecular structure of DDS which would allow its interactions with the head groups of neighbouring DPPC molecules whereas the same would not be possible with DMS.

Acknowledgement

We are grateful to Burroughs Wellcome India Ltd. for the gift of DDS.

- hanathan, P. S., Mirza, E. B., Amirthalingam, V., Muralidharan, K. V. and
Mol. Cryst. Liq. Cryst., **98**, 163.
- anathan, P. S., Datta, G. and Mirza, E. B. (1989) in *Surfactants in solution* (ed.
York: Plenum) vol. 8, p. 203.
- D. A., Vadas, E. B. and Zuckermann, M. J. (1981) *Biochim. Biophys. Acta*, **640**, 207.
- J. M. and Shipley, G. G. (1976) *Biochemistry*, **15**, 4575.
-) *Biochim. Biophys. Acta*, **643**, 161.

ce methods for studying intact spermatozoa

3. PHADKE, SUDHA SRIVASTAVA and
I GOVIL*

Physics Group, Tata Institute of Fundamental Research, Bombay 400 005, India

Motility is used as a routine parameter for assessing spermatozoa activity. The techniques adopted are based on electron or optical microscopy. However, these depend on gross structural and dynamical features of sperm cells and do not provide information on metabolic activity of intact cells. Lately, biochemical assays are popular. Such methods are cumbersome and destroy the samples. Magnetic resonance methods offer a non-invasive method for studies on intact sperms. We have studied respiration, maturation and *in vitro* capacitation of sperms from human and sperms extracted from goat reproductive organ using electron spin resonance, spin labelling and [^{31}P] nuclear magnetic resonance methods. These studies establish the advantages of magnetic resonance in studies related to metabolic processes in sperms.

Sperms; ESR spin labelling; [^{31}P] NMR; human semen; goat reproductive organ; electron transport chain; cold shock.

Spermatozoa has been extensively used as a parameter to assess viability (Mann, 1977). However, research in male reproductive biology has shown that although being motile, the spermatozoa should possess several other characteristics to exhibit their full potential during the act of procreation (Mann, 1977; Phillips, 1975). These methods provide information on structural features and hence about the gross structural features. The methods on the other hand, provide clues about the functional level (Mann and Mann, 1981). These experiments are difficult to perform. Moreover, the cells have to be sacrificed in the process of using these techniques. Magnetic resonance techniques ([^{31}P] nuclear magnetic resonance, electron spin resonance, ESR) are unique as they are non-invasive by nature and can be gainfully utilised for the study of a variety of biological conditions (Gadian, 1982; Gelerinter *et al.*, 1982). These techniques can provide detailed information on motility, metabolic activity, intracellular events and environment. We have used magnetic resonance techniques for studies of sperm cells. In studies of sperm cells, requirement of circulating growth media and oxygen to keep the cells alive are problems and special arrangements are required (Cohen, 1987). The viability of sperms is supported by anaerobic glycolysis, such

*Correspondence should be addressed.

JMR, Nuclear magnetic resonance; ESR, electron spin resonance; TEMPO, 2,2,6,6-tetramethyl-1-piperidine-N-oxyl; ETC, electron transport chain; G6P, glucose-6-phosphate; GPC, glycerol-3-phosphate; PG, phosphoglyceric acid.

120 Prasad et al.
problems do not pose difficulties. Here, we report our findings on freshly obtained human semen and sperms recovered from goat reproductive organs.

Materials and methods

2,2,6,6-Tetramethyl piperidine-N-oxyl (TEMPO) was purchased from SYVA Research Chemicals, USA. Rotenone and antimycin-A were bought from Sigma Chemical Co., St. Louis, Missouri, USA. All other reagents were of AnalaR grade.

Human semen samples were collected from volunteers, preserved in ice and brought to the laboratory within 2 h. Ejaculates exhibiting more than 60% motility were used for experimentation. In order to increase sperm concentration, ejaculates were pooled and centrifuged at 80 *g* for 5 min in a REMI R8C laboratory centrifuge. The pellet was resuspended in tyrode buffer.

Goat reproductive organs were procured from the slaughter house and kept refrigerated until use. The epididymes were segmentally dissected into their caput, corpus and cauda regions. Each segment was mechanically dissociated by gentle mincing and tweezing followed by repeated washing by buffer. Tissue was removed by settling. The overlaying cells were washed, pelleted by centrifugation and resuspended in buffer in the desired concentrations of cells.

The viability and concentration of cells was checked from time to time using light microscope. The sperms exhibiting more than 60% motility were used for further experimentation. The motility was checked immediately before and after the experiment. Whenever the quantity of sperms was not sufficient to carry out a series of experiments, sperms from more than one animal were pooled together. Justification for this was obtained from a separate experiment where it was observed that the ability of sperms from different animals to reduce spin labels was same, within experimental errors.

The buffers were subjected to 1 h of nitrogen bubbling prior to use, to avoid the effects of dissolved oxygen radicals. All experiments were carried out at 300 K unless stated otherwise. The variation in concentration was achieved by centrifuging at 80 *g* using REMI R8C laboratory centrifuge and resuspending the pellet so obtained in requisite amount of buffer. After each experiment, sperm concentration was determined using a cytometer. Appropriate controls were run to ensure that the observed effects are solely due to sperms. The concentration of spin label TEMPO in each sample was carefully adjusted to 1 mM final concentration. Concentrations higher than 1 mM were avoided to circumvent ESR signal broadening arising from spin-spin interactions. A timer was started at the initial contact of the sperms with the spin label. Sample was thoroughly mixed by subjecting to mild vortexing for 10 s and then transferred to 50 μ l glass capillary sealed at one end. ESR spectra were recorded at regular intervals of time. The observations were normalised to 10^9 cells to enable comparative assessment of the results. The experimental error was less than 1% in all the measurements.

X-Band ESR spectrometer having a Varian 12 inch electromagnet and Varian V-45601 100 KHz field modulation and detection unit was used. [^{31}P] NMR work was carried out on Bruker AM-500 FT-NMR spectrometer interfaced with Aspect 3000. The resonance frequency of [^{31}P] at the magnetic field of 11.7 T is 202.5 MHz. The pulse width used was 40 μ s. The relaxation delay of 1 s and broad-band power gated proton decoupling were used.

ESR spin labelling

Spin labels are stable molecules with unpaired electrons and can be easily monitored by ESR. These molecules are known to undergo reduction when in contact with biological systems, leading to the decay of ESR signal (Baldassare *et al.*, 1974). The process of spin label reduction has been attributed to electron-donating capability of live cells (Chapman *et al.*, 1985). In these studies, we have used TEMPO which is a spherical amphipathic spin label which partitions into aqueous and lipid medium. Figure 1a shows a typical ESR spectrum of TEMPO in buffer. It consists of 3 sharp lines which are characteristic of rapidly tumbling spin labels. The signal height starts decreasing when mixed with intact semen (figure 1b). The signal builds up again on adding oxidizing agents such as potassium dichromate, thus indicating that the sperms do not chemically destroy spin label molecules.

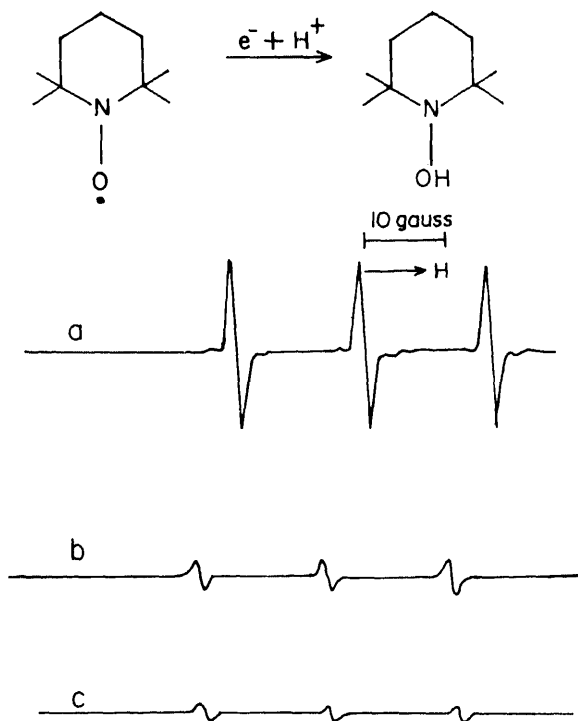


Figure 1. X-Band ESR spectrum of TEMPO (1 mM) (a) in buffer, (b) and (c) after contact with sperms for 1 and 1.5 h, respectively.

In order to understand the origin for TEMPO reductions, the spermatozoa were separated from seminal plasma by centrifugation. The seminal plasma itself does not cause reduction of spin label even after several hours of incubation. Also, the medium alone does not reduce spin labels. The spermatozoa free of seminal fluid

and suspended in buffer exhibited as much reducing capacity as the intact semen. Sperm with reduced motility (<30%) show decrease in their ability to reduce spin labels. Dead sperm caused no reduction. These experiments therefore establish that the ability of sperm to donate electrons and cause spin label reduction is closely associated with their metabolic activity. The mid piece region containing mitochondria reduces spin labels while head and tail regions are ineffective (Chapman *et al.*, 1985).

Since the ESR signals are sharp and do not show changes in line width, one is justified to use the signal height as a parameter representing the concentration of spin labels. The decrease of ESR signal height with time (figure 2) has been found to fit to a single exponential function of the type $h(t) = h(o) e^{-kt}$ where $h(o)$ and $h(t)$ are signal heights at time 'o' and 't' respectively. The fitting has been done using least squares methods. The fit was excellent with CQ 99.99. Thus, the process of spin label reduction by sperm follows first order kinetics with respect to spin-label concentration.

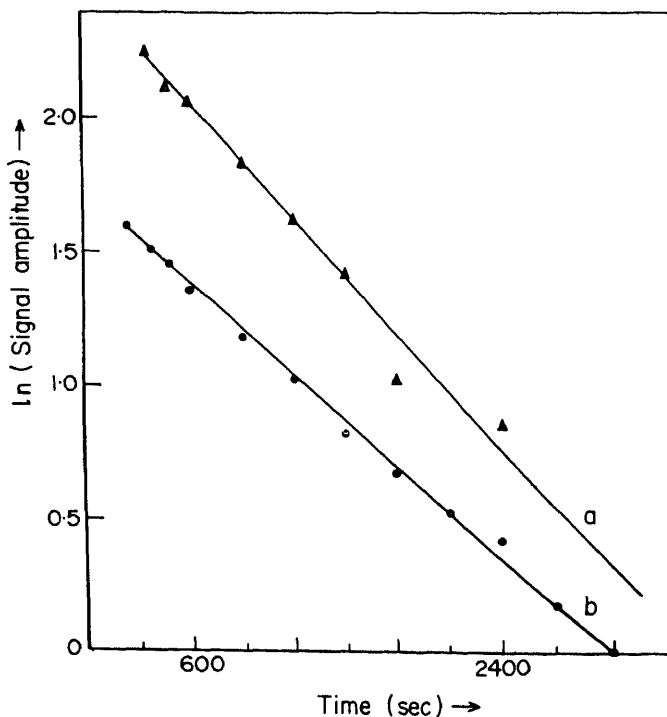
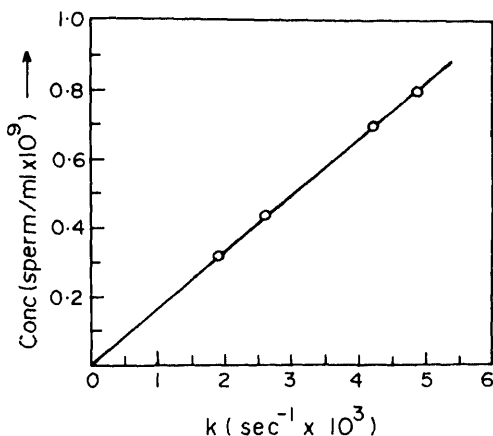


Figure 2. ESR signal height of TEMPO at various times following contact with sperm from (a) cauda and (b) caput regions.

The rate constant (k) can be used as a parameter to investigate the influence of different external conditions on the sperm cells. In the case of goat samples, sperm originating from caput (A2), corpus (O3) and cauda (U4) reduced spin labels to different extent. However, in all cases, the estimated k values vary linearly with sperm concentration.

k on the concentration of sperms in the sample is shown in Figure 3. The rate constant for ESR signal decay was found to be linearly dependent on the concentrations of similarly treated samples. The samples drawn from the same human on different days exhibit similar k values. However, in every case, the values show linear dependence on concentrations. Thus the rate of spin-label reduction follows both with respect to sperm and the spin-label concentrations.



The reduction rate constant k of TEMPO ESR signal as a function of human sperm concentration in the medium.

These observations hold equally true for sperms originating from different sources, including 4) of goat reproductive organ. These observations justify the linear relationship between the values with respect to 10^9 cells/ml in all experiments.

Experiments

Experiments were carried out to understand the process of respiration (aerobic) and glycolysis. To understand these, following experiment was done. The human samples were divided in 3 parts. Nitrogen was bubbled through one for 10 minutes, through the other for the same length of time. The third portion was kept as control. The rate constant was the same as the control for the control sample. The nitrogen bubbled sample gave a larger initial signal on observation as the process of bubbling nitrogen leads to the formation of free radicals and helps in build-up of ESR signal. Moreover, the rate of reduction was increased by 13%. These experiments indicate that the process of nitrogen increases higher electron donating capacity to spermatozoa (figure 4). The results of (U4) region of goat show similar behaviour.

k

These findings have implications for artificial insemination and *in vitro* fertilization,

GOAT

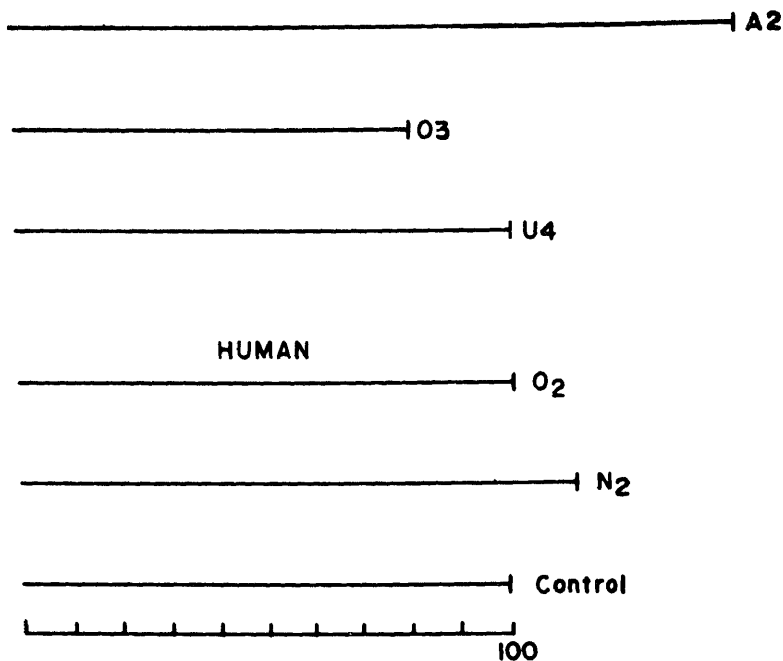


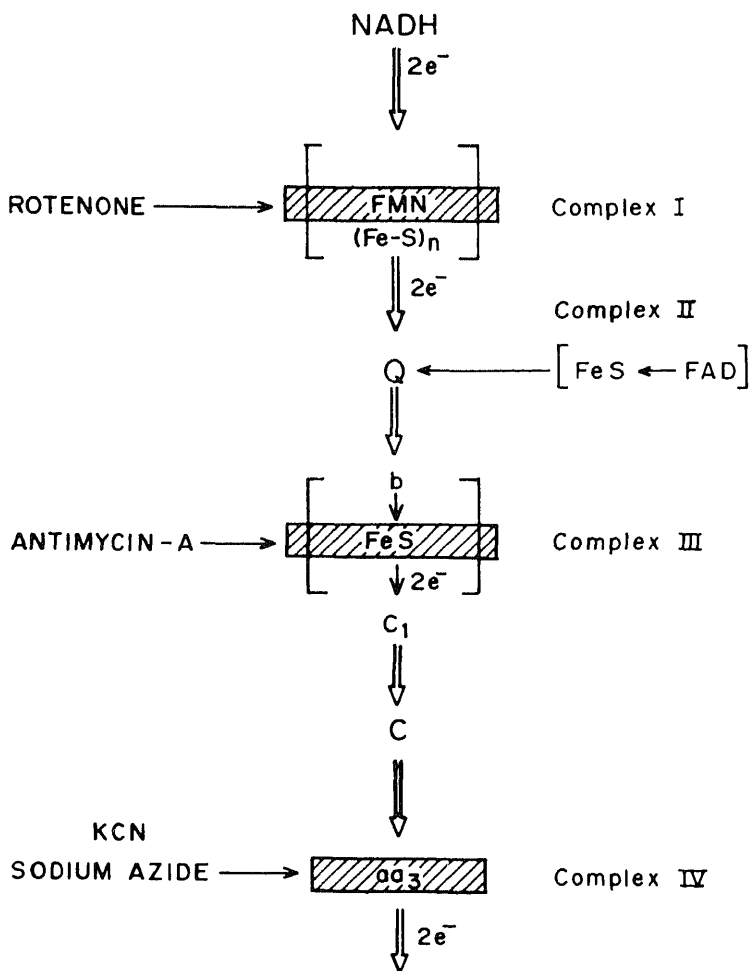
Figure 4. Rate of TEMPO reduction by sperms in the presence of oxygen and nitrogen gases. Data has been normalised to 10^9 sperms in control sample. Results have also been shown for goat sperms from caput (A2), corpus (O3) and cauda (U4).

preservation of semen without loss in its potential to become fully motile and fertile at the end of the storage period, has attained immense importance. Rapid cooling of semen by dipping it in liquid nitrogen has been reported to be a safe method (Pogle, 1979). To assess the effect of cold-shock, experiments have been carried out on a sample which was rapidly cooled by dipping in liquid nitrogen for 1 min and then warmed to 295 K. Remaining semen from the same pool which was not subjected to the above treatment serves as control. The behaviour of the two samples (as indicated by rate of reduction) is identical except that there is an overall gain in ESR signal which may be attributed to expulsion of oxygen and its radicals (O_2^-/OH^- /singlet O_2) during cooling. Peroxidation has been carried out on intact semen by adding 0.6% H_2O_2 and then subjecting to cold shock. Both samples show higher rate of reduction as compared to normal cells. A control experiment with H_2O_2 and spin label has been carried out to verify that H_2O_2 itself does not reduce spin labels.

Effects of inhibitors of electron transport chain

The trends in the influence of inhibitors of electron transport chain (ETC) such as rotenone, antimycin A and sodium azide which inhibit ETC at different levels are

shown in (figure 5) (Lehninger, 1982). Rotenone (200 $\mu\text{g/ml}$) reduces the rate of reduction to 73%; antimycin A (100 $\mu\text{g/ml}$) and sodium azide (1 mM) increase the rate of reduction to about 150%. Thus, the influence of rotenone block is in opposite sense to that due to the other two. Taking into account the fact that rotenone, antimycin A and sodium azide cause blockage at site I (flavoprotein), site II (cyt b) and site III (cyt a) respectively, one can infer that the spin label reduction occurs somewhere between site I and II, *i.e.* at the ubiquinone level. The blockage of site I restricts the influx of electrons in ubiquinone systems and causes lowering of the rate of the spin label reduction. Blockage at site II or site III prevents the passage of electrons to molecular oxygen leading to flooding of ubiquinone site by electrons. These electrons are readily available for spin label reduction.



The capacity to reduce spin labels exhibited by sperms from cauda region (U4) by the sperms which are fully matured is assumed to be 100. The observations of sperms from other regions and under different conditions are expressed in terms of this number (figure 4). The sperms from corpus (O3) region show 80% activity while those from caput (A2), (i.e., least mature sperm) show increased activity of 100. These observations are not consistent with the reported profile of maturation. It is generally believed that the sperms acquire higher maturity during their descent from caput → corpus → cauda of epididymal tract. One may therefore expect that the electron donating capacity of the sperms shall also increase in this order. However, it is also known that the sperms acquire their lipid coat in the corpus region (Guraya, 1987). In caput region, the mitochondrial part of the sperms which is responsible for reduction of spin labels is better exposed and therefore more accessible to spin labels. This fact may be responsible for the faster reduction kinetics. The fully matured cauda region sperms, exhibit larger activity than those from O3. No definite conclusions could be drawn regarding sperms from T₁ (testis) region, since the sperm suspension gets contaminated with pieces of neighboring tissues.

Capacitation in the female tract is known to be essential for the act of fertilization (Mann and Mann, 1981). We subjected the sperms from cauda (U4) region to a medium which is similar to secretions of female tract. The sperms incubated for 24 h in the medium acquire 5 times higher electron donating capacity than the control samples. Incubating for longer time has been found to be detrimental.

[³¹P] NMR

Very little is known of the physiological changes associated with sperm maturation during the descent in the epididymidis. We describe below the usefulness of [³¹P] NMR in such studies. To obtain requisite quantities, sperms from more than 100 animals were pooled together and subjected to mild centrifugation (~1000 rev/min) for 10 min. The resulting pellet was resuspended in buffer. ²H₂O (10%) was added to facilitate field-frequency locking. External phosphocreatine was used as reference. One observes a large number of [³¹P] peaks originating from cauda region sperm cells (figure 6). The assignment of these signals has been done by adding successively increasing amount of phosphorous containing compounds such as ATP, ADP, AMP, glucose-6-phosphate (G6P), glyceryl phosphocholine (GPC), phosphoglyceric acid (PGA), and other mono- and diphosphates to the homogenates of the sperm cells. The signals arising from these compounds have been compared with the spectra obtained from the intact sperms and identification of peaks have been achieved. ATP signals are prominent for cauda sperms but are weak for caput and corpus. Samples from these regions show intense peaks corresponding to inorganic phosphate and phospholipids. Noteworthy is the absence of creatine phosphate and any other mono- and dinucleotides.

The extruded epididymal fluid from caput, corpus and cauda regions has been subjected to centrifugal fractionation. The supernatant so obtained shows several resonance peaks corresponding to inorganic phosphate and phosphocholine glycerol (figure 7), in agreement with similar studies using biochemical methods in the

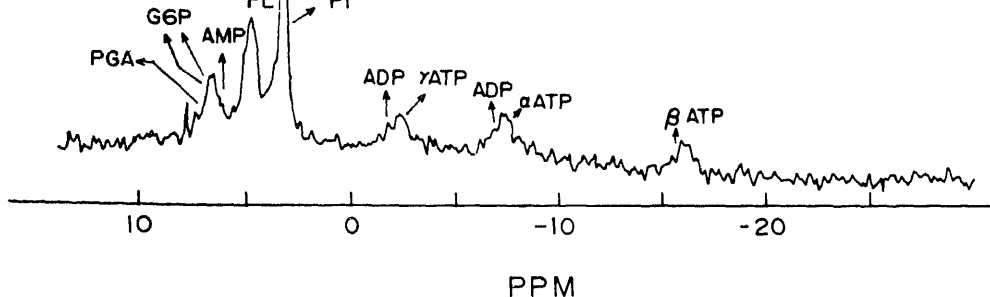


Figure 6. [^{31}P] NMR spectra of goat sperm cells obtained from cauda region of epididymis. The signals for ATP, ADP, inorganic phosphate, phospholipid, AMP, G6P and PGA have been assigned as discussed in text.

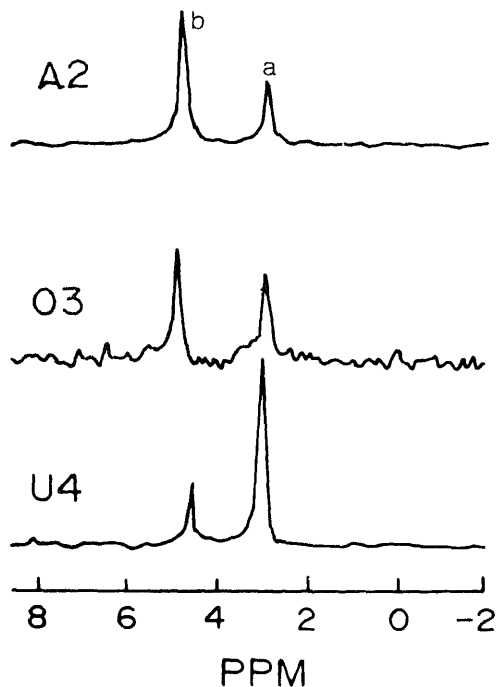


Figure 7. [^{31}P] NMR spectrum of excretions in the goat epididymis obtained from different regions-U4-cauda, O3-corpus and A2-caput. Signals are (a), inorganic phosphate and (b) glyceryl phosphocholine.

of bovine and other species. It is thus clear that [^{31}P] NMR can provide important clues about intra- and intercellular components residing in respective regions. Noteworthy is the ease and speed with which constituent molecules could be identified using [^{31}P] NMR without recourse to the cumbersome chemical assay

procedures. However, NMR is not a sensitive method and cannot detect compounds with concentrations less than mM levels. During the process of *in vitro* capacitation of cauda sperms for increasing periods, one observes build-up of ATP signals at the expense of inorganic phosphate and GPC. A period of 3 h capacitation appears to be optimum as the ATP signals start deteriorating thereafter.

It may be useful to compare this with the ESR spin labelling results which also show that the sperms acquire maximum electron donating ability at 3 h capacitation and longer capacitation periods prove detrimental. This indicates that although capacitation in female tract is an essential part of the act of fertilization, the duration of this process has to be optimum.

Sperms from cauda region have been subjected to fructose starvation for about 2 h; 20 mg of fructose was then added. The spectra were accumulated for 11 min at regular intervals. At $t=0$, the sperms are quiescent having less ATP, which builds up gradually with time and persists for 90 min and longer. This provides evidence for sperm capability to withstand starvation and activation by fructose in concurrence with earlier reports.

To sum up, the use of magnetic resonance methods is at the threshold of opening a new era in research in reproductive biology as these methods provide information on metabolic aspects of the cells. Further research needs to be done on different animal systems before these methods can attain the status of quality rating method.

Acknowledgements

The authors are thankful to Prof. B. Venkataraman and Shri V. R. Bhagat for use of ESR spectrometer. The facilities provided by the 500 MHz FT-NMR National Facility supported by the Department of Science and Technology, T.I.F.R., Bombay, are gratefully acknowledged.

References

- Baldassare, J. J., Roberston, D. E., McAfee, A. G. and Ho, C. (1974) *Biochemistry*, **13**, 5210.
- Chapman, D. A., Killian, G. J., Gelerinter, E. and Jarrett, M. T. (1985) *Biol. Reprod.*, **32**, 884.
- Cohen, S. M. (1987) *Physiological NMR spectroscopy from isolated cells to man* (New York: New York Academy of Sciences).
- Fawcett, D. W. (1977) in *Frontiers in reproduction and fertility control* (eds R. O. Greep and M. A. Koblinsky) (Cambridge: MIT Press) p. 353.
- Gadian, P. G. (1982) *Nuclear magnetic resonance and its applications to living systems* (Oxford: Clarendon Press).
- Gelerinter, E., Narra, S. and Killian, G. J. (1980) *Biol. Reprod.*, **23**, 513.
- Curaya, S. S. (1987) *Biology of spermatogenesis and spermatozoa in mammals* (Berlin: Springer-Verlag).
- Lehninger, A. L. (1982) in *Principles of biochemistry* (New York: Worth Pub.) pp. 474 and 482.
- Mann, T. (1975) in *Handbook of physiology* (eds D. W. Hamilton and R. O. Greep) (Washington D.C.: Am. Physiol. Soc.) Section 7, vol. 5, p. 461.
- Mann, T. and Mann, C. L. (1981) *Male reproductive function and semen* (Berlin: Springer-Verlag).
- Phillips, D. M. (1975) in *Handbook of physiology: Endocrinology* (eds R. O. Greep and E. B. Astwood) (Washington, D.C.: Am. Physiol. Soc.) Section 7, vol. 5, p. 405.
- Poole, C. (1979) in *Frozen human semen* (eds E. Richardson, D. Jarrett, M. S. G. and R. O. Greep) (New York: Academic Press) p. 10.

Erythrocyte stability under imposed fields

V. SITARAMAM

Biotechnology, Department of Zoology, University of Poona, Pune 411 007, India

Abstract. Lysis of erythrocytes offers an unique opportunity to probe the fine structure of the bilayer as a function of its state of energization. Critical monitoring of the volumes, ion fluxes and related measures in erythrocytes exposed to a variety of milieu and treatments showed that one can critically distinguish the nature of the prelytic perturbations and the proximate forces actually responsible for the disruption of the membranes among surface charge density, elastic energy etc.

Keywords. Osmolysis; erythrocytes; detergents; pores; polyols; ionophores; ionic strength.

Introduction

The bimolecular leaflet structure of the biological membranes is an equilibrium structure in the strict thermodynamic sense (Israelachvili *et al.*, 1980). This planar, smectic mesophase offers the expedient solution to pack amphiphilic lipid molecules which are characterized by bulky acyl chain moieties compared to their relatively small head groups. As a consequence, any imposed field of adequate magnitude could affect this equilibrium state, the end result being a disruption of the membrane (Sitaramam, 1981). Two thoughts of considerable importance need to be entertained: firstly, a shift in the equilibrium state must necessarily be identified with enhanced internal energy of the system since,

$$\Delta G = -RT \ln K_{eq},$$

such that disruption of membranes represents a most conclusive evidence for a change in the internal energy of the system ($dU \neq 0$); secondly, disruption not only entails flux of molecules across the bilayer barrier, but also entails and is preceded by a flux of lipid molecules within the bilayer (Sitaramam 1988a; Mathai and Sitaramam, 1989; Sitaramam *et al.*, 1989). The central question is whether such a flux of lipid molecules in the prelytic domain is continuous or catastrophic. If catastrophic, the membrane would exhibit an abrupt enhancement of conductance at a critical field intensity without any evidence for prelytic disturbances in conductance. If continuous, two consequences arise: firstly, the prelytic domain would be characterized by enhanced porosity of the membrane; secondly, and most importantly, this enhanced porosity necessarily accompanies and is a forerunner of disruption in any situation of imposed fields, including even the physiological energy transduction mechanisms (Mathai and Sitaramam, 1989; Sitaramam *et al.*, 1989).

In recent years, it has been demonstrated that disruption is but an extreme case of variable porosity in membranes with several kinds of imposed fields, *e.g.*, gravitational fields (Sitaramam and Sarma, 1981; Sarma and Sitaramam, 1982), respiration (Sambasivarao and Sitaramam, 1985), ATP hydrolysis (Sambasivarao *et al.*, 1988), electrostatic fields created by the unscreened fixed charges on the RBC membranes when acutely suspended in media of low ionic strength (Sambasivarao

et al., 1986; Sitaranam *et al.*, 1988). Comparable evidence exists in the case of pulses of electrical fields (Teissie and Tsong, 1977), action potentials (Villegas *et al.*, 1966) etc. The erythrocyte offered an excellent tool since its lysis can be monitored readily. A systematic investigation led to a number of insights into the nature of disruption and the proximate fields responsible for it, often at variance with the generally held beliefs. The results on osmotic lysis, 'hypertonic lysis' in non-electrolyte media, lysis by detergents and lysis by ionophores are briefly discussed.

Materials and methods

These are as indicated in the legends to figures and in the corresponding cross references.

Results and discussion

Hypotonic lysis of erythrocytes

Erythrocytes, when suspended in hypotonic media, would swell with consequent increase in the elastic energy of the membrane. The elastic energy of the membrane would be parabolically related to the change in the average interfacial area of the head groups of the lipids (Israelachvili *et al.*, 1980); when the elastic energy exceeds the intermolecular cohesive forces that define the bilayer geometry, the cell disrupts. The specific conclusions borne out by the experiment were (i) an increase in the (elastic) free energy of the membrane would affect the equilibria of the component protein molecules of the membrane, as demonstrated by a prelytic increase in the conductance of the potassium *via* calcium-independent, potassium channels (Sambasivarao *et al.*, 1986); (ii) the onset of lysis would correspond to the maximal volume of the cells to lysis, as seen by Coulter profiles of cell radii (figure 1A); (iii) treatment with certain ionophores would lead to loss of internal potassium as well as a corresponding shift in the onset of lysis to lower tonicities; whereas enhanced permeation to the external NaCl by other ionophores would lead to a shift of the onset to greater tonicities (figure 1B); (iv) this would be due to preferential loss of internal potassium or gain in sodium from without, as can be demonstrated by light scatter studies on volume changes (figure 1C,D); (v) the light scatter studies exhibit a precise relationship between potassium loss (=volume change) and turbidity changes, whose limits can be determined critically in a simultaneous measurement of potassium loss and turbidity (figure 1E). Thus, the hypotonic lysis could be precisely defined in terms of the component physical changes; the field responsible could be identified unequivocally as the elastic energy profile as a slave variable tracking the osmotic gradient. Variations in elastic energy were seen to have their own consequence of affecting the structural/dynamic K_{eq} of the potassium channel towards greater conductance (Sambasivarao *et al.*, 1986). The missing link was the fact that progressive lysis occurs even in saline media albeit to a small degree; and what could be the reason for it?

Lysis in non-electrolyte media

The phenomenon of hypertonic disruption of erythrocytes in non-electrolyte media

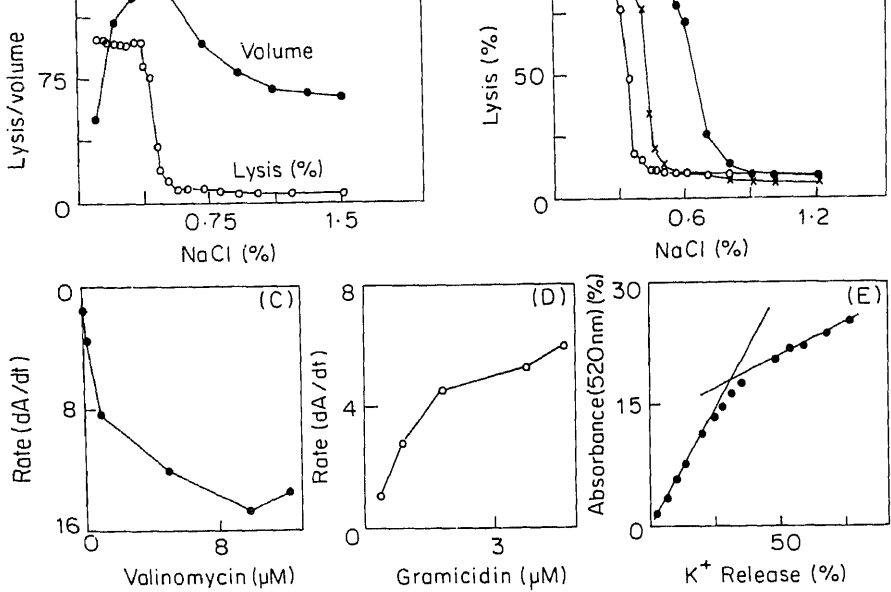


Figure 1 (A) The mode of the frequency distributions of the volume profiles (in femtolitres) of rat erythrocytes obtained with Coulter Counter ZM with Channelyzer C256 at varying NaCl concentrations was plotted along with per cent lysis profiles (hemoglobin released into cellfree supernatants). Note that the maximal volume corresponds to the onset of lysis, but the completion of lysis does not correspond to the least volume. (B) Per cent lysis profiles in control (\times), 1 μ M valinomycin-treated (O) and 10 μ M gramicidin A-treated (\bullet) rat erythrocytes. Note the concordant shift in the onset and completion of lysis corresponding to the efflux and influx of the solute with each ionophore. (C) Rate of change in absorbance of constantly stirred samples of rat erythrocytes at 520 nm as a function of the varying concentrations of valinomycin. The direction was reversed in this and the next (D) plots to keep it parallel to the volume changes. Note the saturation kinetics. (D) Rate of change of absorbance in rat erythrocytes with gramicidin, plotted as in (C). (E) The efflux of potassium was measured with an Orion potassium electrode and an Orion 901 Ionalyzer. The change in absorbance was simultaneously monitored in a parallel sample. Both measurements were plotted as a function of time after addition of 1 μ M valinomycin to the stirred suspensions. The lines were obtained by the least square linear regression analysis to show that up to 15% change in turbidity reliably measures volume changes due to solute fluxes.

has been characterized as one of disaffected equilibrium state of the erythrocyte membranes due to decreased screening of the external fixed negative charges (Sambasivarao *et al.*, 1986; Sitaramam *et al.*, 1988). The consequent increase in self-potential of the charged 'sphere' would account for a variety of dynamic fluxes of ions and solutes including an instability in the bilayer (Sitaramam *et al.*, 1988). Figure 2A shows the phenomenon of hypertonic disruption in an osmometric profile of erythrocyte lysis (= hemoglobin release) in sucrose media. Figure 2B also shows a parallel increase in lysis in NaCl media with time and this increase was inversely proportional to the ionic strength of the media. Thus, lysis during prolonged periods in NaCl media was shown to be entirely due to the exposure of

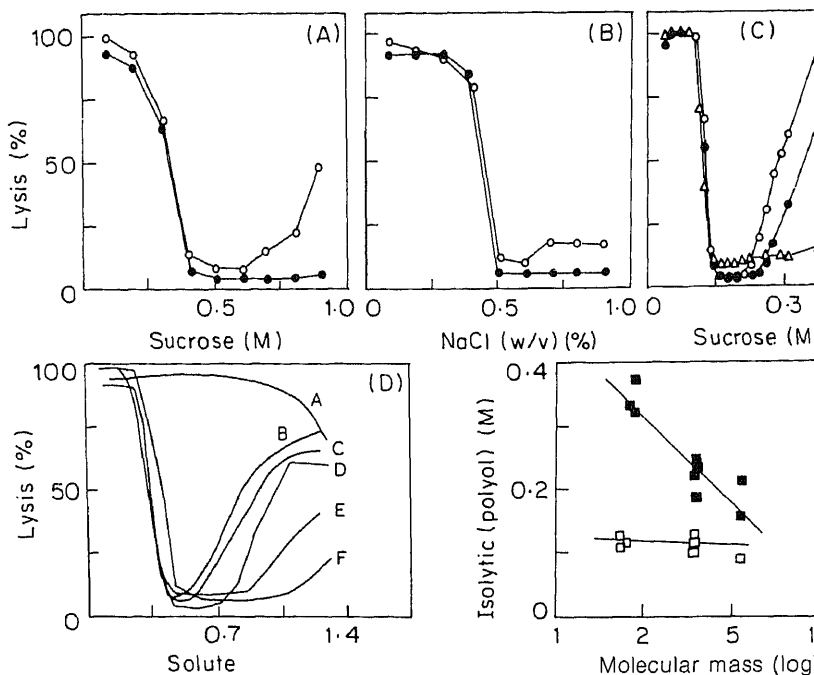


Figure 2. (A) Per cent lysis (as in figure 1A) at 15 min (●) and 4 h (○) in sucrose media of varying tonicity. Note that the enhanced lysis at 4 h also enhances with osmolarity of the media, hence the name 'hypertonic disruption'. (B) Per cent lysis in NaCl media (as in A). Note that NaCl media also exhibit finite lysis at hypertonicities similar to sucrose media. (●), 15 min; (○), 4 h incubations. (C) Effect of ionic detergents on erythrocyte disruption profiles in sucrose media at 4 h (as in A). (●), Control; (○), 34 μM CTAB; (Δ), 2.74 μM CTAB. Note that nonionic detergents had no effect and the pronounced stimulatory and inhibitory effects of these detergents of opposing osmolarity without any influence in the hypotonic domain or the basal lysis in the same media. (D) Hypertonic disruption profiles in polyols of different molecular masses. A, Erythritol; B, lactose; C, maltose; D, sucrose; E, mannitol and F, glucose. Note that there is no distinction in the extent of lysis in the hypotonic domain among the polyols with the marginal exception of glucose. Per cent lysis was plotted against the concentration equivalents of NaCl % w/v for each polyol (Sitaramam *et al.*, 1988). (E) Plot of molecular mass on per cent lysis in the hypertonic and hypotonic domains. (●), concentration corresponding to 20% lysis in the hypertonic domain; (○), concentration corresponding to 50% lysis in the hypotonic domain. The line represents linear regression by least squares. Data from an extended version of (D).

fixed charges on the surface of erythrocytes and these charges are most likely proteinaceous in origin and not from the glycocalyx. Figure 2C shows that hypertonic disruption is due to externally faced negative charges since it is inhibited by cetyltrimethylammonium bromide (CTAB), a cationic detergent, whereas it was accentuated by sodium dodecyl sulfate (SDS), an anionic detergent. Erythrocyte lysis offers an exquisite example of the consequences of enhanced energy of the membrane in terms of the strict molecular weight dependence of the inferred permeability to polyols. Figure 2D shows the effect of various polyols on

lysis *vis-a-vis* the molecular weight of the external polyol showing the behaviour of the erythrocyte membrane as a perfect molecular sieve under these conditions of disaffected equilibrium state.

Disruption of erythrocytes in the presence of detergents

Figure 3A, B shows the effect of CTAB and SDS on lysis of erythrocytes in sucrose and NaCl media. These data on the minimal lytic concentrations for these ionic detergents (since non-ionic detergents did not exhibit dependence on the ionic strength of the medium) can be critically accounted for in terms of charge repulsion/attraction and charge screening. A negatively charged membrane exhibits greater interfacial concentration of the detergent of opposite charge in the unscreened state, *i.e.*, in non-electrolyte media, rather than in electrolyte media. Figure 3C shows that the effect of CTAB is 2-fold in nonelectrolyte media: it causes inhibition of lysis at lower concentrations and enhances lysis at higher concentrations by its detergent action. Preliminary studies indicate that the lysis by different ionic detergents in RBC is not comparable; the anionic detergents cause lysis primarily by a charge-mediated instability in the membrane rather than by detergency, whereas the cationic detergents appear to cause lysis only by detergency. The osmotic dependence of such lysis appears to suggest that the prelytic hole produced by anionic detergents is much smaller than that by the cationic detergents as evidenced by the lysis profiles in polyols of varying magnitude (data not given). These studies indicate that the proximate cause of lysis is different for different detergents, depending on their charge as well as on the net charge density on the membrane.

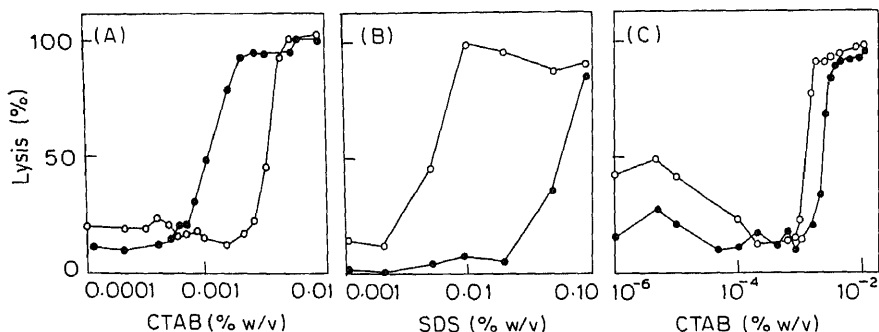


Figure 3. (A) Per cent lysis (release of hemoglobin into cell-free supernatants) in rat erythrocytes suspended in 0.31 M sucrose (●) and 0.155 M NaCl (○) media in the presence of various concentrations of CTAB. (B) Per cent lysis in rat erythrocytes suspended in 0.31 M sucrose (●) and 0.155 M NaCl (○) media in the presence of various concentrations of SDS. (C) Effect of CTAB on per cent lysis of rat erythrocytes in sucrose media at 15 min (as in A and B) (●) and at 4 h (○), both at room temperature. Note that the 4 h incubation refers to hypertonic disruption demonstrated in figure 2, which increases with time and sucrose concentration. CTAB has a marked biphasic effect at 4 h due to its dual role as a charged species (protective) and a detergent (lytic).

Lysis of erythrocytes in the presence of ionophorous antibiotics

Primarily, any antibiotic that enhances the net permeability of the membrane to the

external osmolyte will cause lysis equivalent to hypotonic lysis. This was critically investigated by a combination of osmolysis profiles and Coulter profile volume/diameter of these cell populations. Our very first attempts at demonstration of the action of valinomycin and gramicidin D on such populations exhibited a major contradiction worthy of note. The gramicidin-treated cells exhibited loss of internal potassium, increase in cell volume indicating larger influx of sodium ions from the medium such that the onset of lysis still corresponded to the maximal volume of the cells, *i.e.*, hematocrit. The same was not true of valinomycin-treated cells. The cells contracted due to loss of potassium from within. However, the onset of hypotonic lysis was not accompanied by volume expansion, indicating the most odd situation of hypotonic lysis without elastic stretch (figure 4). The cause of this hypotonic lysis cannot be due to volume-dependent elastic stress. Studies on the ionic dependence as well as studies with all other known monovalent selective cationophores indicated that the cause of lysis was the expression of internal charges on the inner leaflet of the cell membrane and the mechanism was once again a charge-mediated instability in the membrane.

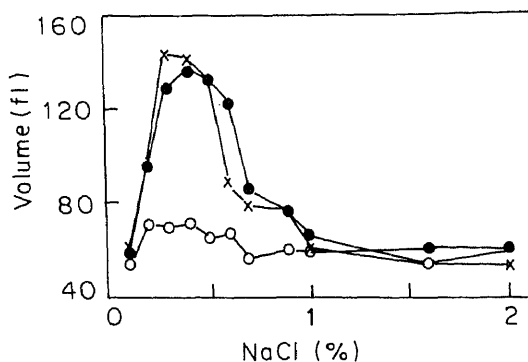


Figure 4. Mode of the frequency distributions of the volume profiles (in femtoliters) of erythrocytes obtained with Coulter Counter ZM with Channelyzer C256 at varying NaCl concentrations. (x), Control; (●), 10 μ M gramicidin-treated; (○), 1 μ M valinomycin-treated. The cells were washed thrice in 0.9% NaCl, pre-treated with the ionophore in small aliquots and diluted into NaCl media of varying tonicity for Coulter measurement. Lysis results for these erythrocytes were as in figure 1B.

Lysis is a result of major deviation of the resting membrane from its equilibrium structure, with defined and measurable prelytic events. Most current literature attempts to view the bilayer and its components as of invariant interactions with themselves and with each other in the structural, kinetic as well as dynamic aspects. Each subsystem in the membrane relaxes, when challenged with an increase in energy, with its own characteristic relaxation time. This gives rise to complex dynamics whose causality is however entirely definable and tractable. The question ultimately relates to whether we wish to view the bilayer as isothermally and planar, or, negentropic capable of structural evolution, since the latter would violate the traditional notions in chemical thermodynamics. These questions relate to the definition of the chemical potential of a species on the assumption of invariant or negligible changes in entropy, internal energy and volume work.

studies on erythrocytes and mitochondria have given lie to this generally held assumption, requiring an active investigation in the identification of the proximate cause-effect relationship of the same event such as lysis under diverse conditions.

Acknowledgement

This work was supported by a grant from Department of Science and Technology, New Delhi.

References

- Israelachvili, J. N., Marcelja, S. and Horn, R. G. (1980) *Q. Rev. Biophys.*, **13**, 121.
 Mathai, J. C. and Sitaramam, V. (1989) *Biochim. Biophys. Acta*, **976**, 214.
 Sambasivarao, D. and Sitaramam, V. (1985) *Biochim. Biophys. Acta*, **806**, 195.
 Sambasivarao, D., Rao, N. M. and Sitaramam, V. (1986) *Biochim. Biophys. Acta*, **857**, 48.
 Sambasivarao, D., Kramer, R., Rao, N. M. and Sitaramam, V. (1988) *Biochim. Biophys. Acta*, **933**, 200.
 Sarma, M. K. J. and Sitaramam, V. (1982) *Biochem. Biophys. Res. Commun.*, **105**, 362.
 Sitaramam, V. (1981) *Indian J. Biochem. Biophys.*, **18**, 96.
 Sitaramam, V. (1988a) *J. Sci. Ind. Res. India*, **47**, 395.
 Sitaramam, V. (1988b) *Indian J. Biochem. Biophys.*, **25**, 172.
 Sitaramam, V. and Sarma M. K. J. (1981) *Proc. Natl. Acad. Sci. USA*, **78**, 3441.
 Sitaramam, V., Sambasivarao, D. and Rao, N. M. (1988) *Indian J. Biochem. Biophys.*, **25**, 590.
 Sitaramam, V., Sambasivarao, D. and Mathai, J. C. (1989) *Biochim. Biophys. Acta*, **975**, 252.
 Teissie, J. and Tsong, T. Y. (1977) *Proc. Natl. Acad. Sci. USA*, **74**, 1923.
 Villegas, R., Villegas, G. M., Blei, M., Herrara, F. C. and Villegas, J. (1966) *J. Gen. Physiol.*, **50**, 43.

Depth profiling in membranes by fluorescence quenching

AMITABHA CHATTOPADHYAY

Centre for Cellular and Molecular Biology, Uppal Road, Hyderabad 500 007, India

Abstract. Membrane penetration depth is an important parameter in relation to membrane structure and organization. A methodology has been developed to analyze the membrane penetration depths of fluorescent molecules or groups utilizing differential fluorescence quenching caused by membrane embedded spin-label probes located at different depths. The method involves determination of the parallax in the apparent location of fluorophores, detected when quenching by phospholipids spin-labelled at two different depths is compared. By use of relatively simple algebraic expressions, the method allows calculation of depth in Å. This method has been used to determine the location of fluorophores in NBD-labelled lipids and anthroyloxy-labelled fatty acids in model membranes and of the membrane embedded tryptophan residues in the reconstituted nicotinic acetylcholine receptor.

Keywords. Fluorescence quenching; spin labelled phospholipids; membrane penetration depth.

Fluorescence quenching is a powerful tool for analysis of membrane structure. Fluorescence quenching by spin-labelled probes has been used to investigate lipid-protein and protein-protein interactions in membranes (London, 1982). Such quenching interactions are short ranged and thus convenient for structure analysis on the scale of molecular dimensions. An important application of quenching in membranes is the determination of the distance (depth) of membrane-bound groups or molecules from the membrane surface (London, 1982; Blatt and Sawyer, 1985). Knowledge of the precise depth of a molecule or group should help define the conformation and topology of membrane probes and proteins.

Recently a method has been developed for measuring the membrane penetration depth utilizing fluorescence quenching by spin-labelled phospholipids and it has been applied to determine penetration depths of the fluorescent groups in a series of NBD-labelled lipids (Chattopadhyay and London, 1986, 1987), anthroyloxy-labelled fatty acids (Chattopadhyay, 1987), and of the membrane embedded tryptophan residues in the reconstituted nicotinic acetylcholine receptor (Chattopadhyay and McNamee, 1989). Analysis of depth in this way is quantitative, yet less complicated than methods utilizing fluorescence energy transfer. In addition, spin labels, unlike other types of quenchers, have the advantage of being quenchers of a wide range of fluorophores including tryptophans.

Two sets of samples are prepared for such depth measurements. The first set contains membranes containing the fluorophore, variable concentrations of a lipid labelled with the quencher at one depth (to be called the shallow quencher), and an unlabelled lipid dioleoyl phosphatidylcholine). The other set contains the same fluorophore, variable concentrations of a different quencher lipid labelled at a

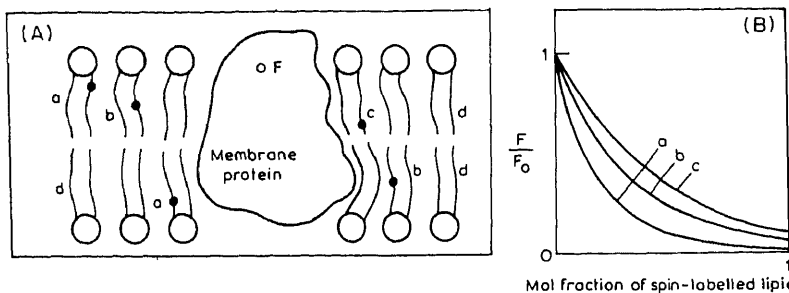


Figure 1. (A) A schematic diagram of an integral membrane protein containing an ordinary (non quenching) lipid fluorophore (F) in a bilayer containing an ordinary (non quenching) lipid. Three quenching lipids (a, b, c) in which the quencher group on the lipid is placed at different depths in the membrane. Notice that the vertical distance (depth) of the fluorophore from the most shallow quencher (a) is the least of the 3 depths. It should be mentioned that in an actual experiment each sample will have only one kind of quenching lipid in the bilayer and an ordinary lipid. (B) Differential fluorescence quenching curves for the system shown in (A). The ordinate is the ratio of fluorescence in the presence (F) and absence (F₀) of the quencher. Note that the strongest quenching is obtained with the most shallow quencher (a).

$$Z_{cf} = L_{c1} + \left[\left(-\frac{1}{\pi C} \ln F_1/F_2 - L_{21}^2 \right) / 2L_{21} \right],$$

where Z_{cf} = depth of the fluorophore from the center of the bilayer, L_{c1} = distance from the center of the bilayer from the shallow quencher 1, L_{21} = difference in depth between the two quenchers, C = two-dimensional quencher concentration in the plane of the membrane, and F_1/F_2 is the ratio of fluorescence intensity for two sets of samples for the same quencher concentration C . The above equation is derived from an extended version of the Perrin (1924) quenching equation which is applicable to quenching occurring in membranes where fluorophores and quenchers are randomly distributed in the plane of the membrane. It can also be shown that by combining two experiments in this way the effect of restrictions on the free lateral approach of fluorophore and quencher is cancelled. Determination of depth of a fluorophore in a membrane protein by this approach is schematically shown in figure 1. Analysis of depth in this way can also be applied to quenching by probes other than spin labels. Future applications of this method include investigation of the conformation and orientation of hydrophobic molecules and other membrane active molecules in the membrane bilayer.

References

- Blatt, E. and Sawyer, W. H. (1985) *Biochim. Biophys. Acta*, **822**, 43.
- Chattopadhyay, A. (1987) *A novel fluorescence quenching method for measurement of lipid penetration dept*, Ph.D. thesis, State University of New York, Stony Brook, New York.
- Chattopadhyay, A. and London, E. (1986) *Biophys. J.*, **49**, 308a.
- Chattopadhyay, A. and London, E. (1987) *Biochemistry*, **26**, 39.
- Chattopadhyay, A. and McNamee, M. G. (1989) *Biophys. J.*, **55**, 149a.
- London, E. (1982) *Mol. Cell. Biochem.*, **45**, 181.
- Perrin, F. (1924) *C. R. Hebd. Seances Acad. Sci.*, **178**, 1978.

Role of nicotinic acid as modulator of liposomal microviscosity

M. CHATTERJEE*, R. BASU and P. NANDY†

Department of Physics, Jadavpur University, Calcutta 700 032, India

*Present address: Guha Institute of Biochemistry, 55/5 Purna Das Road, Calcutta 700 029, India

Abstract. Using the fluorescent probe 1,6-diphenyl-1,3,5 hexatriene, we have investigated the effect of nicotinic acid, a derivative of the toxic alkaloid nicotine, on the fluidity profile and activation energy of diffusion in the liposomal system of several lipids. We have also studied how the fluidizing property of nicotinic acid affects the intermediate fluid condition induced by cholesterol in these liposomal systems.

Keywords. Nicotinic acid; phospholipid; fluidity; phase transition.

Introduction

Nicotinic acid (NA), a drug clinically used as vasodilatory agent, can lower serum cholesterol level when administered to man in large doses (Miller and Hamilton, 1964). From the observations in *in vivo* systems, it was concluded that the dilating effect is not correlated to the carboxyl group and the ring configuration probably is necessary in order to slow down the cholesterol biosynthesis. However, the exact mechanism of this drug is not clearly known as yet (Yovos *et al.*, 1982).

In order to investigate how this drug affects the membrane systems, we have recently studied its effect on the fluidity profile and activation energy of diffusion of several liposomal systems mimicking the actual biological membrane. These are liposomal systems of (i) dipalmitoyl phosphatidyl choline (DPPC) (Bhattacharyya *et al.*, 1988), (ii) egg lecithin (Bhattacharyya *et al.*, 1988), (iii) total lipid isolates of erythrocyte ghost membrane (Bhattacharyya and Nandy, 1986), (iv) sphingomyelin (Sph) (Bhattacharyya and Nandy, 1989) and (v) mixed lipid of Sph and DPPC (1 : 4 molar ratio) (Bhattacharyya and Nandy, 1989). The latter was chosen as it has lipid composition similar to that of rat liver plasma membrane (Bhattacharyya and Nandy, 1989).

For this study we have used the fluorescent probe 1, 6-diphenyl-1,3,5-hexatriene (DPH) whose polarisation when embedded in the membrane is an index of fluidity of its environment and thus any change in fluidity induced by an external agent can be detected (Shinitzky and Barenholtz, 1978). Our study indicates that this drug modifies the membrane fluidity, probably by mechanical interaction between the drug and membrane constituent molecules as there is no evidence of strong complex formation from spectral studies. We have also shown that the drug can disrupt the intermediate fluid condition induced by cholesterol in the cholesterol incorporated liposomal system.

Materials and methods

Spectral grade solvents and AR grade chemicals were used. DPH, Sph and (Sigma, USA) were used. Liposomes were prepared by sonication of an dispersion of measured amounts of lipids (Bhowmik *et al.*, 1986). Cholesterol drugs were incorporated into the liposomes (Bhattacharyya *et al.*, 1986). Fluorescence measurements were performed with a Perkin-Elmer Model 560 spectrofluorometer using a thermostated cell. Free drug was removed by filtration.

Results and discussion

DPH, when incorporated in lipid bilayers, becomes an integral part of the bilayer regardless of its phase or composition and from the measurement of polarization of this probe in the liposome, an approximate evaluation of viscosity ($\bar{\eta} \pm 15\%$) of the probe environment can be made (Shinitzky and Barenholtz, 1978).

From the viscosity temperature relation (Shinitzky and Barenholtz, 1978), the activation energy E can be calculated. When $\ln \bar{\eta}$ is plotted with respect to temperature, a straight line is expected if the probe environment maintains the same structure. Deviation from linearity indicates a change in phase and/or structure (Shinitzky and Barenholtz, 1978).

Table 1. Effect of the drug nicotinic acid on the fluidity profile of some lipid systems*.

Liposomal systems	Lipid: cholesterol: NA	Viscosity (in poise)		Max activation energy (ev)	V of of bl
		20°C	40°C		
DPPC**	1:0:0	14.73	3.32	1.63	
	1:1:0	6.63	5.58	—	
	1:1:1	9.77	5.57	—	
	1:0:1	5.36	2.31	1.54	
EPC**	1:0:0	1.55	0.70	0.95	(C
	1:1:0	4.39	2.71	—	
	1:1:1	3.59	1.68	—	
	1:0:1	1.00	0.37	0.69	(C
Sphingomyelin	1:0:0	12.50	2.58	1.17	(C
	1:1:0	8.80	6.20	—	
	1:1:1	14.15	6.68	0.47	
	1:0:1	8.37	1.91	1.14	(C
Mixed lipid of Sph and DPPC (1:4 molar ratio)†	3:0:0	9.97	2.7	2.32	(C
	3:1:0	7.76	3.50	0.72	
Total lipid isolates of erythrocyte ghost membrane††	3:1:1	9.02	4.37	1.50	
	3:0:3	8.50	1.82	2.16	(C
	1:0:0	9.02	2.41	1.02	(C
	1:0:1	7.53	2.13	0.88	(C

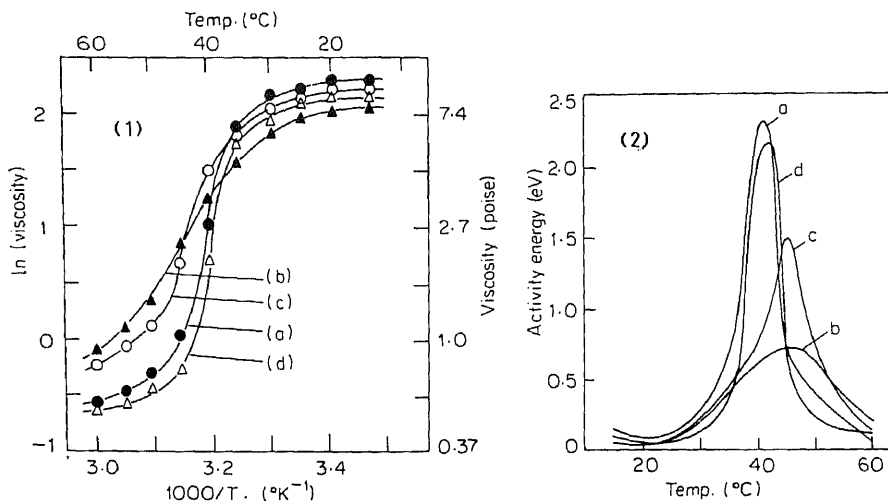
The fluidity profiles of these liposomal systems have a common feature though the absolute value of viscosity varies from system to system (table 1). Out of all these systems, let us consider as a representative one, the liposome of mixed lipids of DPPC and Sph in the molar ratio 4:1 (Bhattacharyya *et al.*, 1989). In figure 1 (curve a) we have shown how the liposomal microviscosity varies with temperature. Addition of cholesterol induces an intermediate fluid condition (figure 1, curve b). When NA is added to the cholesterol incorporated system, the original fluidity profile is brought back to some extent (figure 1, curve c). Addition of NA alone to the liposome merely fluidizes the system (figure 1, curve d).

In figure 2, we have plotted the calculated values of activation energy as a function of temperature and the empirical relation is

$$E = E_0 \exp(-b(\Delta T)^2),$$

where $\Delta T = T - T_c$, T_c being the critical temperature for each system and b is a constant for the system. Values of E_0 and b for the different liposomal systems are given in table 1.

Comparison of the results of mixed lipid liposomes with those in cases of individual lipid components shows that NA affects the fluidity of model membrane liposomes prepared from DPPC or Sph or mixture of both. The fatty acyl chains and the head group of lipid molecules probably interact mechanically with NA molecules as there is no spectral evidence of complex formation. E , the activation energy which is the energy barrier that must be overcome before the elementary flow process can occur, also reduces in the presence of NA. The observed vasodilatory effect of NA *in vivo* may be a natural consequence of the fluidizing effect recorded *in vitro*.



Figures 1 and 2. (1) Microviscosity vs. temperature curves and (2) activation energy vs. temperature for DPH-probed mixed lipid liposome. Concentration of DPPC, 10^{-4} M. Molar ratio of Sph and DPPC is 1:4. (a) liposome only, (b) cholesterol added to (a) in molar ratio 1:1, (c) NA added to (b) molar ratio of lipid, cholesterol and NA is 1:1:1, (d)

Acknowledgement

Financial assistance from the Council of Scientific and Industrial Research, Delhi, is thankfully acknowledged.

References

- Bhattacharyya, M., Bhowmik, B. B. and Nandy, P. (1988) *Arch. Biochem. Biophys.*, **263**, 117.
Bhowmik, B. B., Chatterjee, I. and Nandy, P. (1986) *Chem. Phys. Lipids*, **39**, 271.
Bhattacharyya, M. and Nandy, P. (1986) *Indian J. Pharm.*, **48**, 200.
Bhattacharyya, M. and Nandy, P. (1989) *Arch. Biochem. Biophys.*, (in press).
Miller, O. N. and Hamilton, J. G. (1964) in *Lipid pharmacology* (ed. R. Paolette) (New York: Press) p. 275.
Shinitzky, M. and Barenholtz, Y. (1978) *Biochim. Biophys. Acta*, **515**, 367.
Yovos, J. G., Patel, S. T., Falko, J. M., Newman, H. A. I. and Hill, D. S. (1982) *J. Clin. E. Metab.*, **54**, 1210.

Fluidity of detergent micelles plays an important role in muscarinic receptor solubilization

ANU KÕIV, AGO RINKEN and JAAK JÄRV*

Laboratory of Bioorganic Chemistry, Tartu University, Tartu, Estonia, USSR

Abstract. In order to find a suitable reagent for extracting the muscarinic receptor from rat brain membranes 14 different detergents were tested. Only the plant glycoside digitonin efficiently solubilized the receptor protein in its native form. At the same time microviscosity of detergent micelles was determined by measuring the fluorescence polarization of a hydrophobic fluorescent probe diphenylhexatriene incorporated into the micelles. In the case of digitonin the polarization value was close to the corresponding value obtained for rat brain membrane fragments, while for the other detergents studied it remained considerably lower. The results obtained indicate that the fluidity of detergent micelles may play an important role in retaining the active conformation of the solubilized muscarinic receptor.

Keywords. Muscarinic receptor; receptor solubilization; diphenylhexatriene; fluorescence polarization; micelle fluidity.

Introduction

The muscarinic acetylcholine receptor is located in synaptic membranes of the central nervous system and several peripheral tissues (Snyder *et al.*, 1975). Solubilization of this integral membrane protein is an important step in the procedure of its purification and molecular characterization. However, there seems to be a very limited number of solubilizing agents able to extract the muscarinic receptor from biomembranes without a considerable loss of its activity (Aronstam *et al.*, 1978; Sokolovsky, 1984). The best results so far have been obtained using the plant glycoside digitonin (Rinken *et al.*, 1987; Raidaru *et al.*, 1989) but the physico-chemical basis of its action is not known. Therefore it is important to evaluate the properties of detergents essential for their ability to solubilize the receptor protein retaining its ability to specifically bind ligands. In the present study we compare some physico-chemical characteristics of detergent micelles, critical micellar concentration (CMC), aggregation number and fluidity with the ability of these agents to solubilize the native receptor.

Materials and methods

Suspension of rat brain membranes in 50 mM K-phosphate buffer (pH 7.4) was prepared as described by Langel *et al.* (1982).

Solubilization of the native receptor was carried out as follows: suspension of rat brain membrane fragments (approximately 1 mg protein/ml) was incubated with detergent solutions of different concentrations for 30 min at 0°C and centrifuged at

*To whom all the correspondence should be addressed.

Abbreviations used: CMC, Critical micellar concentration; QNB quinuclidinyl benzilate; DPH, diphenylhexatriene; CHAPS, 3-[(3-cholamidopropyl)-dimethylammonio]-1-propanesulfonate; SDS,

100,000 g for 1 h. Components remaining in the supernatant were considered solubilized.

The amount of solubilized receptor was determined by specific binding of 3 nM [^3H] quinuclidinyl benzilate (QNB) (43 Ci/mmol, Amersham) at 25°C. Receptor-QNB complex was separated from the excess of free ligand on Sephadex G-50 columns in the case of solubilized receptor and on GF/B glass-fibre filters (Whatman) in the case of membrane-bound receptor.

In order to solubilize the receptor-ligand complex the membrane fragments were incubated with 3 nM [^3H]QNB for 30 min prior to adding the detergent solution.

Non-specific binding of [^3H]QNB was determined in the presence of 10 μM atropine sulphate (Merck).

Protein concentration was determined by the modified method of Lowry (Peterson, 1977) using bovine serum albumine as standard.

Microviscosity of detergent micelles was estimated by means of measuring the fluorescence polarization of a hydrophobic fluorescent probe diphenylhexatriene (DPH) incorporated into the micelles. Two μl of DPH dissolved in tetrahydrofuran was added into a detergent solution to achieve a final concentration of the probe of 1 μM . The mixture was incubated for 30 min at room temperature and the fluorescence polarization of DPH was measured on Hitachi-850 spectro-fluorimeter at excitation and emission wavelengths of 358 and 430 nm, respectively. In all cases, detergent concentrations well above their CMCs were used. Digitonin was obtained from Merck, 3-[(3-cholamidopropyl)-dimethylammonio]-1-propanesulfonate (CHAPS) from Calbiochem and other detergents from Sigma.

Results and discussion

Out of the 14 detergents, studied only the plant glycoside digitonin was able to effectively solubilize the native muscarinic receptor with an yield of 34%. Besides digitonin, CHAPS was also able to solubilize the native receptor to a certain extent, the maximal yields reaching only 6–8%. In the case of sodium dodecyl sulphate (SDS), cholates and detergents of Triton X and Tween series no muscarinic ligand binding activity could be detected in the solution although they were able to extract major part of the protein present in the membrane (table 1).

As both digitonin and CHAPS contain the steroid core, its presence in the detergent molecule can be considered important in retaining the active conformation of the muscarinic receptor. However, the presence of this structural element is not sufficient as cholate and deoxycholate turned out to be ineffective. In the latter cases the ionic charge situated near the steroid core probably facilitates the denaturation of the receptor by these detergents while CHAPS, being a zwitterionic molecule, where the ionic charges are separated from the steroid core by several methylene groups, is a much weaker denaturing agent allowing the solubilization of the muscarinic receptor at low detergent concentrations.

In addition to digitonin and CHAPS the receptor-QNB complex could also be solubilized with Triton X-100, X-102, X-114, X-165 and SDS (table 1). In all these cases the complex solubilization yields did not exceed 50% of its total amount in the membrane. This value could not be increased using mixtures of the studied

Table 1. Muscarinic receptor solubilization yields and micelle-characterizing parametres for some detergents.

Detergent	CMC (mM)*	Aggregation number*	Fluorescence polarization of DPH	% Solubilization of		
				native receptor	receptor [^3H] QNB complex	protein yield**
Digitonin	0.16	60	0.359 ± 0.004	34 ± 4	41 ± 5	70 (0.6%)
CHAPS	8-10	4-14	0.167 ± 0.003	6 ± 1	8 ± 2	-
Sodium cholate	13-15	2-4	0.102 ± 0.005	0	0	50 (1%)
Sodium deoxycholate	4-6	4-10	0.132 ± 0.004	0	0	100 (1%)
Triton X-45	0.11	-	-	0	0	-
Triton X-100	0.24	140	0.153 ± 0.004	0	50 ± 6	50 (0.3%)
Triton X-102	0.3-0.4	-	-	0	45 ± 3	40 (0.3%)
Triton X-114	0.2	-	-	0	30 ± 4	65 (0.5%)
Triton X-165	0.43	-	0.164 ± 0.004	0	47 ± 2	90 (0.5%)
Triton X-305	-	-	0.167 ± 0.002	0	0	-
Tween 20	0.059	-	-	0	0	35 (1%)
Tween 40	0.029	-	-	0	0	-
Tween 60	0.027	-	-	0	0	-
Tween 80	0.012	58	0.114 ± 0.002	0	0	-
SDS	8.2	62	0.094 ± 0.004	0	50 ± 5	60 (0.03%)

*Data are taken from Helenius and Simons (1975), Chattopadhyay and London (1984) and *A guide to the properties and uses of detergents in biology and biochemistry* (San Diego: Calbiochem) (1987).

**Data correspond to the detergent concentrations (shown in parentheses) giving the highest receptor solubilization yield.

Consequently, about half of the complex dissociates during the solubilization. As in the absence of detergents the receptor-QNB complex dissociation process is very slow (Sokolovsky, 1984), its loss is caused by denaturation of the receptor protein.

Examining the CMCs and aggregation numbers of the detergents used, no relationship between their values and the ability to solubilize the muscarinic receptor could be observed. Thus, these parameters of detergents are not essential for receptor solubilization.

Determination of the fluorescence polarization values of several fluorescent probes, most often DPH, have been used to monitor the fluidity of the probe environment (Shinitzky and Barenholz, 1974; Masturzo *et al.*, 1985). In the present study DPH was used for this purpose. Fluorescence polarization values were measured for DPH incorporated into detergent micelles as well as for DPH incorporated into the native membrane containing the muscarinic receptor. In the case of digitonin the polarization value obtained was close to the corresponding value for the membrane (0.28-0.30): for all other studied detergents it remained considerably lower (table 1). Consequently, fluidity of native receptor microenvironment seems to be important for supporting its active conformation in solution. The receptor-QNB complex can also be solubilized with the help of some detergents

References

- Aronstam, R. S., Schussler, D. C. and Eldefrawi, M. E. (1978) *Life Sci.*, **23**, 1377.
- Chattopadhyay, A. and London, E. (1984) *Anal. Biochem.*, **139**, 408.
- Helenius, A. and Simons, K. (1975) *Biochim. Biophys. Acta*, **415**, 29.
- Langel, U. L., Rinken, A. A., Tähepold, L. J. and Jarv, J. L. (1982) *Neirokhimiya*, **1**, 343.
- Masturzo, P., Salmona, M., Nordstrom, O., Consolo, S. and Ladinsky, H. (1985) *FEBS. Lett.*,
- Peterson, G. L. (1977) *Anal. Biochem.*, **83**, 346.
- Peterson, G. L. and Schimerlik, M. I. (1984) *Prep. Biochem.*, **14**, 33.
- Raidaru, G., Rinken, A., Jarv, J. and Lohmus, M. (1989) *Proc. Acad. Sci. Estonian SSR Chem.*.
- Rinken, A. A., Jarv, J. L. and Langel, U. L. (1987) *Biokhimiya*, **52**, 303.
- Shinitzky, M. and Barenholz, Y. (1974) *J. Biol. Chem.*, **249**, 2652.
- Snyder, S. H., Chang, K. J., Kuhar, M. J. and Yamamura, H. I. (1975) *Fed. Proc.*, **34**, 1915.
- Sokolovsky, M. (1984) *Int. Rev. Neurobiol.*, **25**, 139.

Peptide induced polymorphism in model membranes

RATNA S. PHADKE, SUDHA SRIVASTAVA and
GIRJESH GOVIL*

Chemical Physics Group, Tata Institute of Fundamental Research, Bombay 400 005, India

Abstract. Lipids in biological membranes generally adopt bilayer structures. However, incorporation of peptides may induce alterations in such structures. We have studied the influence of tryptophan, leucine, Trp-Leu, luteinizing hormone releasing hormone and renin inhibitor peptide on lipid organisation in liposomes. It has been observed that the effect is specific to the peptide molecule as a whole and does not have direct correlation to the constituent amino acids or the conformation of the molecule.

Keywords. Peptides; phosphorous NMR; polymorphism; electron microscopy; liposomes.

It is well known that the major constituents of biological membranes are lipids and proteins. The relative proportion of these two classes of molecules is closely related to the specific functions of the membrane. For instance, whereas the mitochondrial membranes are rich in protein content, the plasma membranes have preponderance of lipids. In general, lipids provide a fluid matrix while the specific functions of the membranes are dependent to a large extent on the chemistry, structure and dynamics of lipids, proteins and the interactions between these molecules (Singer and Nicolson, 1972). While the membrane lipids are usually organized in bilayer form, morphological and structural studies indicate existence of non-bilayer and/or transient structures (Navarro *et al.*, 1984; Jensen and Schutzbach, 1985) as a consequence of lipid-protein interaction. Such modulations may permit specific processes to occur at discrete sites.

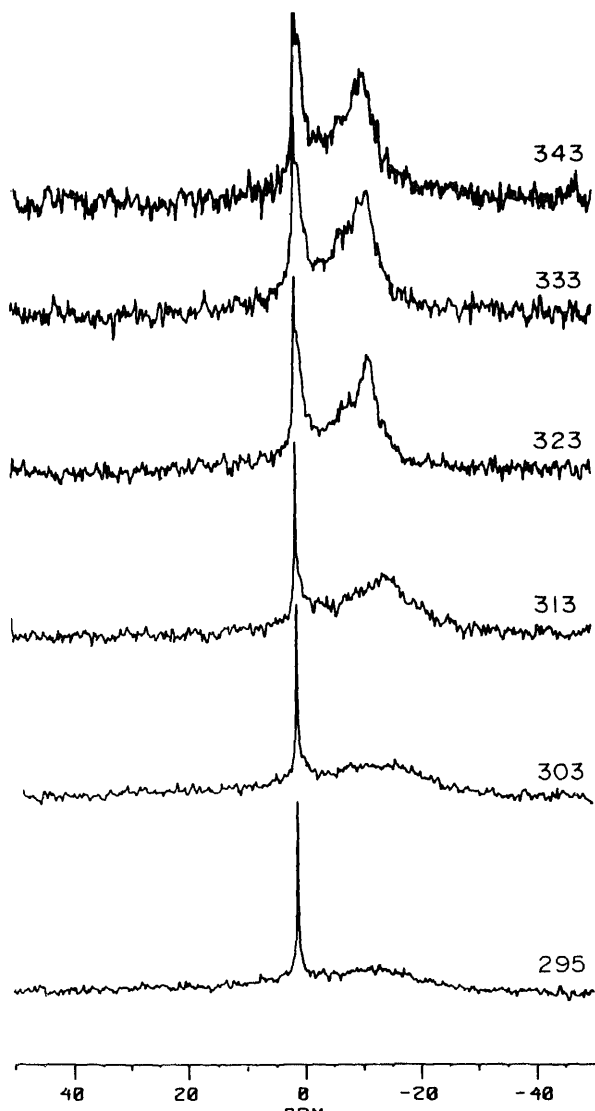
A number of methods have been used to study lipid-protein interactions. X-ray diffraction (Luzzati, 1968), neutron diffraction (Worcester, 1976) and electron microscopy (Deamer *et al.*, 1970) methods have the common drawback that they provide only static information. Spin labelling electron spin resonance (ESR) have been extensively used (Berliner, 1976) but this method has certain limitations. Recently, [^{31}P] nuclear magnetic resonance is being used (Seelig, 1978). The main advantage is that it does not require incorporation of external probes as in ESR spin labelling. Moreover, structural as well as dynamic aspects are reflected in the [^{31}P] resonance pattern.

We have incorporated certain peptides in the normal bilayer structures of dipalmitoyl phosphatidyl choline (DPPC) and have studied polymorphic changes in lipid assemblies brought by such peptides. Since, our aim is to understand the alterations induced by peptides in lipid matrix, we have used higher concentrations of peptides than those encountered in biological systems. A single type of lipid (DPPC) has been used to circumvent difficulties encountered while interpreting the results due to chemical diversity of constituents in real biological membranes.

A large class of membrane proteins react with the polar and apolar parts of the lipid bilayer and destabilize bilayer structure. For instance, gramicidin can dramatically influence the barrier properties of membranes (Killian and de Kruijff, 1988). In the 15 residues of gramicidin, 4 each are tryptophan and leucine. In a previous communication we have reported that the presence of tryptophan promotes a nonbilayer structure in liquid crystalline phase of the lipid (DPPC) (Srinivasan et al., 1988). Leucine on the other hand stabilizes the bilayer structure. We now report the results of experiments present in 1:5 peptide-lipid molar ratio even at high temperatures as j



[^{31}P] chemical shift anisotropy (CSA) pattern (figure 1). In the gel phase ($T < 313\text{K}$) the characteristic bilayer pattern consisting of an intense peak separated by a broad shoulder is clearly visible ($\Delta\sigma = 48\text{ ppm}$). With increasing temperatures, the width of the intense peak decreases, the broad shoulder becomes less prominent and the CSA ($\Delta\sigma$) value decreases. Such behaviour is expected because higher temperatures increase overall tumbling rates of the vesicles and also increase rotational as well as segmental motions of the lipid molecules. All these add to decrease anisotropy experienced by the phosphate moiety. Additional support regarding structural



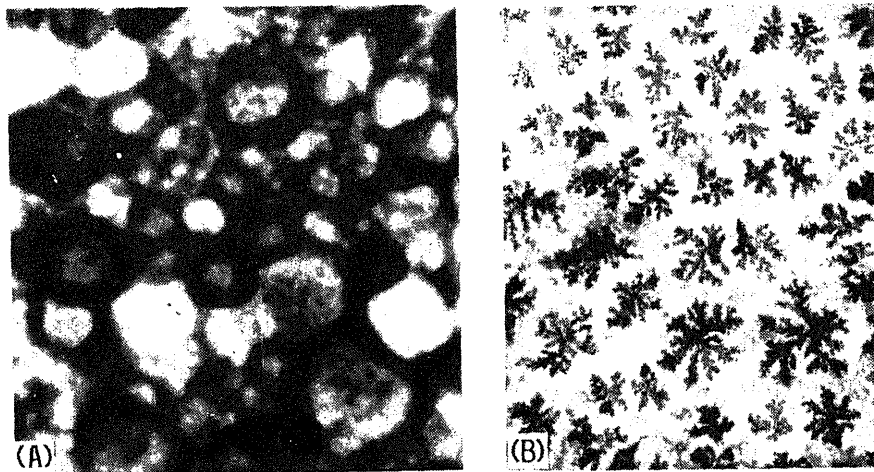


Figure 3. Electron micrograph ($\times 10,000$) of DPPC-peptide system (2:1 mol) indicating a change in lipid packing. (A), DPPC; (B), DPPC + RIP.

aspects is obtained by electron microscopy which shows that the normal liposomal organization remains unchanged on incorporation of leucine.

Exactly identical behaviour have been observed for liposomes containing dipeptide Trp-Leu. Gramicidin, on the other hand, has been reported to induce hexagonal phase formation for lipids with phosphocholine head group (Kilb and de Kruijff, 1986). This indicates that the polymorphism of lipid assemblies is determined by the peptide molecule as a whole and does not totally depend on constituent amino acids.

It has been reported earlier that the shape of the peptide molecules plays a major role in inducing polymorphism (de Kruijff *et al.*, 1985). Our earlier studies have shown that luteinizing hormone releasing hormone (LHRH) (Srivastava, 1986) and an inhibitor polypeptide (RIP) assume random coil conformations when in solution and ordered structures in lipid phase. We have incorporated these hormones in DPPC liposomes. In the presence of LHRH the normal bilayer structure remains unaltered as indicated by $[^{31}\text{P}]$ CSA pattern but RIP induces mixed phase formations. In the latter case, the CSA pattern in gel consists of a sharp peak at 0.4 ppm and a broad peak centered around 1.0 ppm (figure 2). The CSA sign is reverse to that for bilayer structure and the intensity is almost half. With increasing temperatures the broad peak builds up and the sharp peak decreases. Figure 3A shows normal bilayer assemblies which in the presence of RIP transform into complex patterns consisting of rods joined together (figure 3B). One observes that although both peptides assume similar shapes they induce different organizations in DPPC liposomes indicating that shape of the peptide is not the sole decisive criteria.

Acknowledgement

References

Berliner, L. J. (1976) *Spin labelling: Theory and applications* (New York: Academic Press).

Deamer, D. W., Leonord, R., Tardien, A. and Branton, D. (1970) *Biochim. Biophys. Acta*, **219**, 47.

De Kruijff, D., Cullis, P. R., Verkleij, A. J., Hope, M. J., Van Echteld, A. and Taraschi, T. F. (1985) *Membrane structure and dynamics*, volume 1 (New York: Plenum).

Jensen, J. W. and Schutzbach, J. S. (1985) *Eur. J. Biochem.*, **153**, 41.

Killian, A. and de Kruijff, B. (1986) *Chem. Phys. Lipids*, **40**, 259.

Luzzati, V. (1968) *Biol. Membr.*, **1**, 71.

Navarro, J., Kinnucan, M. T. and Racker, E. (1984) *Biochemistry*, **23**, 130.

Seelig, J. (1978) *Biochim. Biophys. Acta*, **515**, 105.

Singer, S. J. and Nicolson, G. C. (1972) *Science*, **175**, 720.

Srivastava, S., Phadke, R. S. and Govil, G. (1988) *Indian J. Biochem. Biophys.*, **25**, 283.

Srivastava, S. (1986) *Interaction of vitamins, drugs and hormones with model membranes*, Ph.D. thesis, Bombay University, Bombay.

Worcester, D. L. (1976) *Biol. Membr.*, **3**, 1.



Kinetic mechanisms of mitochondrial carriers catalysing exchange reactions

F. E. SLUSE, A. EVENS, C. DUYCKAERTS and
C. M. SLUSE-GOFFART

Laboratory of Bioenergetics, University of Liège, Place du 20-Août 7, 4000 Liège, Belgium

Abstract. The single-binding site or ping-pong mechanism is widely accepted for exchange reactions, catalysed by mitochondrial carriers.

However, when the most relevant approach to discriminate between mechanisms, *i.e.*, kinetic study is used, the ping-pong mechanism is eliminated in favour of the sequential or ternary complex mechanism implying two binding sites simultaneously accessible to both internal and external substrates. This is the case for the oxoglutarate carrier, the aspartate/glutamate carrier and there are very strong presumptive evidences for the adenylic carrier.

Keywords. Mitochondrial carriers; kinetics; ping-pong mechanism.

Introduction

Elucidation of the whole molecular mechanism from structure/function relationship is far from being solved for any biomembrane carrier. As available structural informations cannot be interpreted unequivocally in terms of mechanism of action the most powerful approach to discriminate between mechanisms remains kinetic study. Mechanistic informations obtained from kinetics define the precise limits in which interpretations of structural and molecular data must be restricted.

Translocations by exchange through membranes must obey one of the two general types of kinetic mechanisms for a two-substrate reaction: the ping-pong mechanism or the ternary complex (sequential) mechanism.

If translocation follows a ping-pong mechanism the carrier possesses a single binding site for its substrates and it exists in two forms, one that can be loaded by the internal substrate and the other that can be loaded by external substrate. Since the transformation of one form into the other can only occur if the carrier is loaded with one substrate, the carrier performs an obligatory one-to-one exchange by binding alternately both its substrates without formation of a ternary complex S_{ext} -carrier- S_{int} . If the translocation follows a sequential mechanism the carrier possesses two binding sites, one accessible to the internal substrate and the other accessible to the external substrate and the two substrates must bind to the translocator, forming the active ternary complex, before the exchange occurs. It appears that discrimination between the two types of mechanisms gives at least direct informations on the minimum number of sites simultaneously accessible to substrates.

An initial-rate analysis permits to distinguish between the two types of mechanisms: in Lineweaver-Burk plots, a ping-pong mechanism leads to a pattern

second substrate while a ternary complex mechanism exhibits straight-lines having a common point of intercept somewhere to the left of the origin. The conclusions coming from such an analysis must be warranted by the measurements of actual initial rates (V_O) and by the knowledge of the true free-substrate concentrations to which the binding sites are exposed, at least on one side of the membrane. Moreover, the exchange under study must be catalysed by only one translocator species so that the rate is not the sum of different translocation activities and only one exchangeable substrate must be present on each side of the membrane.

Kinetic studies of mitochondrial carriers, *in situ*, have been underrated because of the technical problems that make difficult the initial-rate measurements at various concentrations of both internal and external exchangeable substrates.

An ideal situation was encountered with the oxoglutarate translocator in rat-heart mitochondria: all conditions to measure and use the initial rates properly are fulfilled and have allowed not only to eliminate the ping-pong mechanism but also to infer that the mechanism is rapid-equilibrium random and that the internal sites and the external sites are independent as shown by the convergence on the abscissa axis in double reciprocal plots. Moreover, extensive kinetic data with external oxoglutarate and malate show that the oxoglutarate translocator has an oligomeric structure, that several conformational changes occur during its activity and that the behaviour of the translocator is intrinsically asymmetrical regarding both sides of the membrane and both exchanged substrates (Sluse-Goffart and Sluse, 1986).

Initial-rate study has also allowed to eliminate the ping-pong mechanism for the aspartate-glutamate carrier (Dierks *et al.*, 1988).

The adenyllic carrier has been intensively studied through the molecular approach by the group of Klingenberg in Germany and the group of Vignais in France, leading to an intriguing situation where no proper kinetic data were available. The occurrence of high-affinity inhibitors binding selectively either from the inside (bongkrekate) or from the outside (atractylate) has permitted an early proposal, 18 years ago, on the transport mechanism at a so-called molecular level: it was the single-binding-center gated pore mechanism with two conformational states of the carrier, the cytosol-state and the matricial-state, and this corresponds to a ping-pong mechanism. This has been claimed to be the most widespread, mechanism through which carriers translocate solutes across membranes (Klingenberg, 1989).

Methods

As isolated mitochondria contain both ADP and ATP, the first challenge to take up was to vary to a large extent the internal concentration of a single adenine nucleotide. It was reached by a depletion with pyrophosphate followed by ADP-Mg reloading procedure that leads to a wide range of ADP-concentrations (from 0 to 2.5 mM). Then, the homologous exchange $[^{14}\text{C}] \text{ADP}_{\text{out}}/\text{ADP}_{\text{in}}$ could be studied. The efficiency of the inhibitors was checked using different concentrations of carboxyatractylate (CAT) between 10 and 500 μM . If 10 μM CAT is large enough to block completely the exchange it does not act instantaneously. Indeed the $[^{14}\text{C}]$ ADP content of the mitochondrial pellet is higher if CAT is added simultaneously

with ADP than if CAT is added 5 s before ADP. At 100 μM CAT there is no more difference showing that at this concentration the inhibitor acts as fast as possible.

Results and discussion

The time courses of [^{14}C] ADP accumulation in mitochondrial pellet seem to be linear between 0.3 and 1 s. The [^{14}C] uptake extrapolated to $t=0$ increases with internal ADP concentrations for a given external [^{14}C] ADP concentration. This is due to a burst at the early periods of the progress curve as shown by fast kinetic experiments (from 35 ms) using a quench flow apparatus. The time course shows an astonishing complexity: a 10-ms lag followed by a burst lasting about 200 ms then by a quasi-linear phase (till 1 or 2 s) and lastly by a rate-decreasing phase.

The amplitude and the duration of the burst increase when external [^{14}C] ADP concentration increases at a given internal ADP concentration and increase with internal ADP concentration at a given external [^{14}C] ADP concentration. If the concentrations are low inside ($<0.2\text{ mM}$) and outside ($<2\text{ }\mu\text{M}$) the burst disappears and is replaced by a long duration lag. It must be noticed that if a rapid-equilibrium ping-pong mechanism can exhibit a burst due to the reorientation of sites induced by the addition of the external substrate such a burst would have to increase when the internal substrate content decreases contrary to our observation.

The derivative of the time course giving the uptake rate as a function of time (figure 1) clearly shows a transient phase in which the rate varies very rapidly followed by a more stable phase. As a first approximation, we have considered that the rates between 0.3 and 1 s are initial steady-state rates. Double reciprocal plots exhibit linear relationships and the straight-lines obtained for the 8 different mitochondrial contents have a common intersection point below the abscissa ($0.77\text{ }\mu\text{M}^{-1}$, $0.012\text{ }\mu\text{mol}^{-1}\text{ s}\cdot\mu\text{l mito}$) suggesting that the translocator follows a ternary complex mechanism.

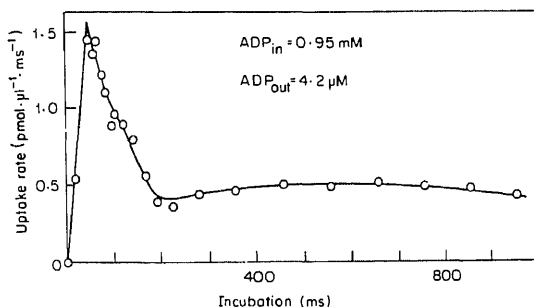


Figure 1. Time-derivative of the progress curve.

In conclusion, among the 3 mitochondrial carriers that have been studied seriously by the kinetic approach two have been proved to follow a ternary complex mechanism, oxoglutarate (Sluse-Goffart and Sluse, 1986) and aspartate-glutamate carriers (Dierks *et al.*, 1988) and we have very strong presumptive evidence for the adenylic carrier. It seems clear that a fresh look at carrier mechanisms needs to be taken.

Acknowledgement

The authors wish to thank the Fonds de Recherche de la Faculte de Medecine de l'Universite de Liege and the Fonds Special pour la Recherche dans les Universites de la Region wallonne.

References

Dierks, T., Riemer, E. and Kramer, R. (1988) *Biochim. Biophys. Acta*, **943**, 231.

Klingenberg, M. (1989) *Arch. Biochem. Biophys.*, **270**, 1.

Sluse-Goffart, C. M. and Sluse, F. E. (1986) *Dynamics of biochemical systems* (Amsterdam: Elsevier).

Identification and isolation of ATP transport protein in mycobacillin sensitive *Aspergillus niger*

BHABADEB CHOWDHURY and S. K. BOSE*

Department of Biochemistry, University College of Science, 35, Ballygunge Circular Road, Calcutta 700 019, India

Abstract. The temperature sensitive release and uptake of ATP through the *Aspergillus niger* G₃Br membrane vesicles followed saturation kinetics. Both the processes which occurred in the absence of mycobacillin were greatly enhanced by its presence. Liposomes prepared with antifilipin sterol and lipid showed the release and uptake of ATP in the presence of filipin, but no such uptake and release was seen with antimycobacillin sterol and lipid in the presence of mycobacillin. However the liposomes supplemented with *Aspergillus niger* membranes protein (s) showed the release and uptake of ATP, implicating membrane protein as a carrier in the transport process.

Keywords. Membrane vesicles; liposome; reconstituted liposome; isolation of ATP transport protein; uptake and release of ATP.

Introduction

It is generally believed that cell membranes are impermeable to ATP (Glynn, 1968) although there are indications in the literature that ATP might be able to cross the cell membrane. Weideman *et al.* (1969) suggested that rat kidney cortical cells are permeable to ATP. Chaudry and Gould (1970) reported the entry of ATP into intact skeletal muscles, liver and kidney cells and further suggested that this entry might be a carrier-mediated process (Chaudry *et al.*, 1976). Release of ATP from motor nerve terminals on indirect stimulation of the mammalian nerve-muscle preparation was observed by Silinsky and Hubbard (1973). The position regarding the release and uptake of ATP is however very unclear for prokaryotic systems. Previous work from our laboratory has shown that mycobacillin (Majumdar and Bose, 1958) caused enhanced release as well as uptake of ATP along with other cell constituents in case of the sensitive strain *Aspergillus niger* G₃Br (Das *et al.*, 1986a) which we suggested to be a carrier mediated process (Das *et al.*, 1986b). In view of this we further studied using membrane vesicles to show that the release and uptake of ATP might implicate a protein. This putative protein was isolated from the *A. niger* membrane vesicles and incorporated into liposome to identify that it is a ATP transport protein.

Materials and methods

Mycobacillin was prepared from the culture filtrate of *Bacillus subtilis* B₃ by the method of Majumdar and Bose (1960). Helix pomatia was purchased from L. industrie Biologique Francaise Gennevilliers, France. Filipin was kindly provided by

*To whom all the correspondence should be addressed.
Abbreviation used: DCP, Dicetyl phosphate.

Dr. G. B. Whitfield, Upjohn Company, Kalamazoo, Michigan, USA. RNase, glutathion, lecithin, cholesterol, dicetyl phosphate (DCP), EDTA, DDT, and were obtained from Sigma Chemical Co., St. Louis, Missouri, USA. [^3H]ATP purchased from Bhabha Atomic Research Centre, Bombay. All other chemicals used were of reagent grade and obtained from commercial sources.

Microorganism

A sensitive strain of *A. niger* was used through out the experiments. Mycelial growth (as spherules) of log phase cells (2 days old) grown in Czapek broth at $32 \pm 1^\circ\text{C}$ with shaking was used.

Preparation of membrane vesicles from the sensitive strain of A. niger

Membrane vesicles from the sensitive organism *A. niger* were prepared from protoplasts of *A. niger* by the method of Kaback (1974). Purity of the membrane fraction was checked by Chit in synthetase (Duran *et al.*, 1975).

Preparation of depleted membrane vesicles

Depleted membrane vesicles were prepared with the addition of Tris/maleate buffer, pH 7 at a concentration of 10 mg of membrane protein/ml buffer and incubated for 90 min with gentle shaking at 37°C . The amount of membrane concentration was measured in terms of their protein content.

ATP uptake by depleted and release from preloaded membrane vesicles

ATP uptake by depleted membrane vesicles was studied according to the method of Chaudry and Baue (1980). The reaction mixture (1 ml) contained 4 mg membrane protein, 100 mM Tris/maleate buffer (pH 7), $100\ \mu\text{l}$ of mycobacillin (2500 Ci/mmol), 10 mM ATP containing $2\ \mu\text{Ci}$ of [^3H]ATP specific radioactivity 2500 Ci/mmol. In order to perform ATP release experiments, membrane vesicles were depleted of ATP and then preloaded in 100 mM Tris/maleate buffer, pH 7, containing 10 mM labelled ATP and $2\ \mu\text{Ci}$ of [^3H]ATP specific radioactivity 2500 Ci/mmol. The vesicles were incubated with gentle shaking at 37°C for 2 h. At the end of incubation the membrane suspension was separated by rapid centrifugation. Uptake and release of ATP were expressed as the amount of substrate incorporated in nmol/mg membrane protein being calculated from the observed radioactivity (cpm)/mg membrane protein and the specific radioactivity *i.e.*, cpm per nmol of the substrate.

Recovery of membrane protein from membrane vesicles

For reconstitution studies the membranes were solubilized by 1% Triton X-100. Solubilized membrane proteins were precipitated by the addition of $(\text{NH}_4)_2\text{SO}_4$ to 80% saturation and the precipitate washed twice to remove

detergent. Dialysis buffer (50 mM phosphate buffer pH 6.8) was used to free $(\text{NH}_4)_2\text{SO}_4$ and detergent if any from protein suspension.

Preparation of liposomes and incorporation of membrane protein in its lipid bilayer

Liposomes were prepared with a mixture of phospholipid/cholesterol/DCP in a molar ratio 7:2:1 according to the method of Gregoriadis and Ryman (1972). During the preparation of liposome, antimycobacillin sterol (cholesterol) and lipid (lecithin) were used (Halder and Bose, 1971, 1973). The resulting liposomes were incubated with different concentrations of membrane protein separately for 30 min at room temperature containing 10 mM MgCl_2 . The liposomes with entrapped ATP were separated from the untrapped material by centrifugation at 105,000 *g* and repeated washing in buffer.

Results

Kinetics of uptake and release of ATP through membrane vesicles in the presence and absence of mycobacillin showed a linear increase with time till they attained the peak values (figure 1A). The presence of mycobacillin hastened the uptake as well as the release process. The temperature profiles of the kinetics of uptake and release of ATP through membrane vesicles under the above specified condition, further showed that both the processes were temperature sensitive, being adversely affected by high temperature (figure 1B).

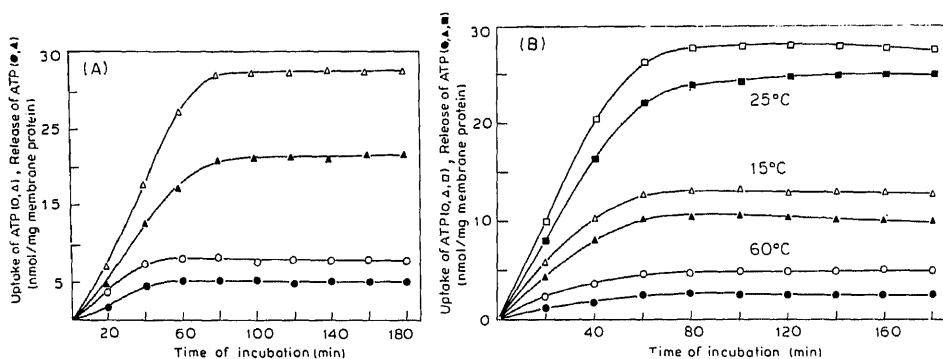


Figure 1. (A) Effect of mycobacillin on the kinetics of uptake and release of ATP through membrane vesicles. The process of uptake and release of ATP was followed by the gain or loss of radioactivity by membrane vesicles. (Δ , \circ) Uptake and (\blacktriangle , \bullet) release of ATP in the presence and absence of mycobacillin. (B). Temperature profiles on the kinetics of uptake and release of ATP through membrane vesicles. The reaction mixtures were incubated with shaking at 15°, 25° and 60°C separately in the presence of mycobacillin for different lengths of time.

Uptake and release of ATP through membrane vesicles as a function of ATP concentration in the presence and absence of mycobacillin showed that the uptake as well as release of ATP increased gradually with increase in ATP concentrations till it attained a maximum value. The amount of ATP taken up was 40 nmol in the

action of the antibiotic (figure 2).

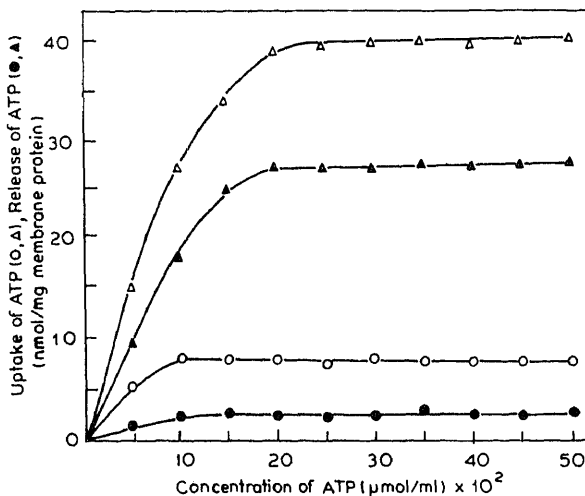


Figure 2. Effect of different concentrations of substrate (ATP) on uptake and release through membrane vesicles. Uptake was followed by depleted and release by preloaded membrane vesicles in the presence of varying concentrations of ATP. (Δ , \circ). Uptake and (\blacktriangle , \bullet) release of ATP in the presence and absence of mycobacillin.

Effect of different concentrations of mycobacillin on the uptake and release of ATP through membrane vesicles in the presence of an optimum concentration of ATP showed that release recorded a linear increase with increasing concentrations of mycobacillin till it become constant at $150 \mu\text{g/ml}$ of antibiotic. Uptake also recorded a linear increase up to $25 \mu\text{g/ml}$ beyond which a rapid decline was observed due to simultaneous release of accumulated ATP caused by mycobacillin (figure 3).

Table 1 indicates that mycobacillin had no effect on the release or uptake of ATP by liposome. However filipin could cause release (65%) and uptake (72%) of ATP from this liposome without being supplemented with membrane protein. Experiments relating the effect of mycobacillin on the uptake and release of ATP from liposome supplemented with membrane protein(s) showed that both uptake and release of ATP from liposome in which membrane protein(s) were incorporated in its lipid bilayer was increased with increasing concentrations of membrane protein in the presence of mycobacillin (data not shown).

Discussion

In continuation of our previous work (Das *et al.*, 1986a, b, 1987) which showed the release and uptake of ATP by the whole cells of a sensitive strain of *A. niger* to be a carrier mediated process, we carried out the study with membrane vesicles and liposomes instead of whole cells to provide additional evidence. These studies showed that release and uptake of ATP by membrane vesicle were enhanced by

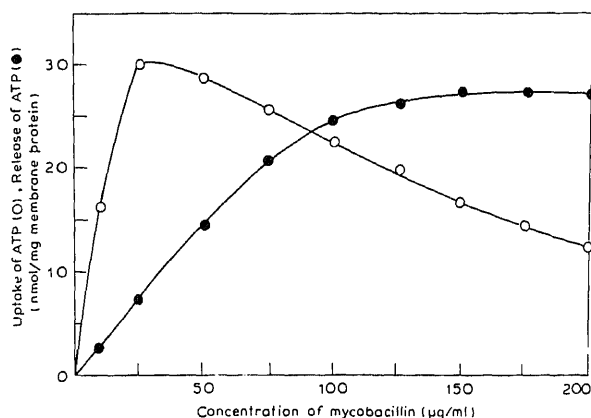


Figure 3. Effect of different concentrations of mycobacillin on the uptake and release of ATP through membrane vesicles. The effect of mycobacillin concentrations on uptake (○) and release (●) of ATP was studied under conditions (controlling parameter, peak concentration of ATP from figure 2, and maximum time incubation from figure 1) of maximum uptake and release.

Table 1. Uptake and release of ATP from liposome in the presence of mycobacillin, filipin and detergent. Triton X-100.

Release of entrapped [^3H] ATP			Uptake of [^3H] ATP by liposome		
System	Radioactivity in liposomes at the end of incubation period	Release (%)	System	Radioactivity in liposomes at the end of incubation period	Uptake (%)
Liposome with entrapped [^3H] ATP + mycobacillin	1735	2.52	Liposome + [^3H] – ATP + mycobacillin	120	1.76
Liposome with entrapped [^3H] ATP + filipin	620	65.1	Liposome + [^3H] – ATP + filipin	4878	71.8
Liposome with entrapped [^3H] ATP + Triton X-100	75	95.7	Liposome + [^3H] – ATP + Triton X-100	175	2.5

Uptake and release of ATP was followed under conditions as stated in the text. For the study of release, [^3H] ATP was entrapped into the liposome whose initial radioactivity was 1,780 cpm. For the study of uptake, [^3H] ATP was added to the suspension buffer whose initial radioactivity was 6790 cpm. Concentrations of mycobacillin, filipin and Triton X-100 used were 250 $\mu\text{g/ml}$, 1 mg/ml and 0.1% (v/v) respectively. The concentration of liposome used was of OD 0.612 at 660 nm.

mycobacillin. The uptake of ATP followed saturation kinetics (figure 2) implicating a carrier in the process which was further supported by the temperature sensitivity of both the processes (figure 1B).

The uptake and release were further studied with liposome using antimycobacillin and antifilipin cholesterol and lecithin. These studies showed that

ATP as usual. The putative membrane protein was thereafter isolated and incorporated into liposome. When liposome was supplemented with membrane protein in its lipid bilayer, the release of ATP occurred as usual in the presence of mycobacillin. This action of mycobacillin which differed from that of filipin might be due to action of mycobacillin on membrane protein in the lipid bilayer of liposome. Previously we reported that mycobacillin action was antagonized by cholesterol and lecithin. Hence the inaction of mycobacillin towards lipid bilayer in absence of protein while its positive action toward liposome supplemented with membrane protein isolated from *A. niger* membrane vesicles, is a clear indication that ATP was transported by a carrier protein and that the enhancing action of mycobacillin might be due to its action on this lipo-protein complex. The induced conformational change might be responsible for the release and uptake of ATP.

Acknowledgement

We thank the Council of Scientific and Industrial Research, New Delhi for financial assistance.

References

- Chaudry, I. H. and Gould, M. K. (1970) *Biochim. Biophys. Acta*, **196**, 320.
- Chaudry, I. H., Sayeed, M. M. and Baue, A. E. (1976) *Can. J. Physiol. Pharmacol.*, **54**, 742.
- Chaudry, I. H. and Baue, A. E. (1980) *Biochim. Biophys. Acta*, **628**, 336.
- Das, S. K., Basu, S., Majumder, S., Mukherjee, S. and Bose, S. K. (1986a) *J. Antibiot.*, **39**, 581.
- Das, S. K., Basu, S., Majumder, S. and Bose, S. K. (1986b) *Biochem. J.*, **239**, 317.
- Das, S. K., Mukherjee, S., Majumder, S., Basu, S. and Bose, S. K. (1987) *J. Antibiot.*, **40**, 1036.
- Duran, A., Bowers, B. and Cabib, E. (1975) *Proc. Natl. Acad. Sci. USA*, **72**, 3952.
- Glynn, I. M. (1968) *Br. Med. Bull.*, **24**, 165.
- Gregoriadis, G. and Ryman, B. E. (1972) *Biochem. J.*, **129**, 123.
- Halder, A. and Bose, S. K. (1971) *J. Antibiot.*, **24**, 779.
- Halder, A. and Bose, S. K. (1973) *J. Antibiot.*, **26**, 358.
- Kaback, H. R. (1974) *Methods Enzymol.*, **31**, 609.
- Majumdar, S. K. and Bose, S. K. (1958) *Nature (London)*, **181**, 134.
- Majumdar, S. K. and Bose, S. K. (1960) *Arch. Biochem. Biophys.*, **90**, 154.
- Silinsky, E. M. and Hubbard, J. I. (1973) *Nature (London)*, **243**, 404.
- Weideman, M. J., Hems, D. A. and Krebs, H. A. (1969) *Biochem. J.*, **115**, 1.

pH-Dependent membrane interactions of diphtheria toxin: A genetic approach

R. JOHN COLLIER

Department of Microbiology and Molecular Genetics and Shipley Institute of Medicine, Harvard Medical School, Boston, Massachusetts 02115, USA

Abstract. A genetic approach is described for exploring the mechanism by which diphtheria toxin undergoes pH-dependent membrane insertion and transfer of its enzymic A fragment into the cytoplasm of mammalian cells. The cloned toxin expressed in *Escherichia coli* is secreted to the periplasmic space, where it is processed normally and folds into a native structure. When bacteria synthesizing the toxin are exposed to pH 5, they die rapidly. The toxin undergoes a conformational change that is believed to allow it to be inserted into the bacterial inner membrane and form channels, which proves lethal for the cell. The membrane insertion event mimics the process by which the toxin inserts into the endosomal membrane of mammalian cells, leading to release of the enzymic A fragment into the cytoplasm. The observation of pH-dependent bacterial lethality provides the basis for a positive genetic selection method for mutant forms of the toxin that are altered in ability to undergo membrane insertion or pore formation.

Keywords. Diphtheria toxin; enzymic A; pH-dependent lethality.

Introduction

Diphtheria toxin (DT) is representative of a group of toxic proteins of bacterial or plant origin that act by covalently modifying substrates within the cytoplasm of mammalian cells (Collier, 1975; Pappenheimer, 1980). Members of this group function as an unusual group of enzymes, which undergo a complex series of events, leading to the introduction of an enzymic moiety of the toxin into the cytosol. Although the mechanism of entry has not been described in detail for any of these toxins, DT has been studied intensively in this regard, and a good working model for entry now exists. In this communication a novel genetic approach that may permit us to isolate mutant forms of the toxin that are defective in their membrane interactions has been reported.

Mechanism of DT action

DT (535 residues) kills mammalian cells by inhibiting protein synthesis. Before or soon after the toxin binds to cells it is proteolytically processed into 2 chains, termed fragments A and B. The enzymic moiety of the toxin (fragment A, or DTA; 193 residues) is delivered to the cytosol by a process that begins with receptor-mediated endocytosis. After binding to cell surface receptors, the toxin is conveyed to an intracellular acidic compartment (endosome) where the acidic conditions induce a conformational change in the protein. This exposes hydrophobic regions within fragment B (DTB), which leads to insertion of the toxin into the endosomal membrane. Concurrently or subsequently DTA is translocated across the

endosomal membrane into cytosol, where it catalyzes the ADP-ribosylation of elongation factor-2 (EF-2). The factor is thereby inactivated and protein synthesis ceases.

The mechanisms responsible for intoxication by DT are slowly emerging at a highly detailed level. For example, an amino acid residue that is believed to participate in catalysis has been identified (Glu-148) (Carroll and Collier, 1985; Carroll *et al.*, 1985). By contrast, the process of membrane insertion/translocation remains largely unexplored at a detailed level. It is known that DT and its fragments form ion-conductive channels in artificial lipid bilayers under acidic conditions (Donovan *et al.*, 1981; Kagan *et al.*, 1981) and recent reports suggest that similar channels are formed during toxin translocation in mammalian membranes (Sandvig and Olsnes, 1988). Although it is clear that central regions of DTB contain highly hydrophobic sequences that almost certainly participate in insertion/translocation, there are few data regarding the roles of specific residues in these regions.

An approach to isolate mutant forms of DT toxin

Here an attempt has been made to isolate mutant forms of DT that are defective in membrane interactions at acidic pH. It has been found that *E. coli* cells in which cloned DT is synthesized and secreted to the periplasm are killed by exposure to acidic conditions (O'Keefe and Collier, 1989). An enzymically attenuated form of the toxin, DT-E148S, has been used in order to comply with the recombinant DNA guidelines. Mutagenesis of the toxin gene followed by selection at acidic pH should yield mutant forms of the toxin that are nonlethal to *E. coli* due to defects in their ability to interact with membranes. A subset of these mutants, at a minimum, would be expected to exhibit defects in ability to interact with mammalian cells.

The notion that DT within the periplasmic compartment might prove lethal to the producing cells under acidic conditions derives directly from the finding that DT inserts and forms channels in artificial lipid bilayers at acidic pH. Thus, if the toxin were to form a pore in the inner membrane of *E. coli*, this would presumably cause a loss of membrane potential and permit leakage of ions and perhaps small molecules of the cytoplasm. Lethality for the bacteria would therefore be independent of the ADP-ribosyltransferase function of the toxin; and indeed, it is known that bacterial protein synthesis, in contrast to that in mammalian cells, is not inhibited by the toxin.

The pH-dependent lethality of the toxin in *E. coli* may be demonstrated by plating toxin-producing cells on agar media at a variety of pHs (O'Keefe and Collier, 1989). Cells synthesizing DT-E148S showed drastic loss of viability at low pHs, with only 1 in 10^7 cells surviving at pH 5. Cells producing the corresponding fragment A showed no loss of viability at low pH. Production of a toxin fragment termed F2, which contains all of DTA and part of DTB (including most of the central hydrophobic domain) also showed loss of viability under acidic conditions.

When the physiological consequences of producing DT-E148S or DTA-E148S were examined under acidic conditions, it was found that cells synthesizing the whole toxin lost membrane potential, the capacity to import proline by active transport, and the ability to retain intra-cellular ^{86}Rb (O'Keeffe and Collier, 1989). Cells producing only the A chain were unaffected.

Mutagenesis of the toxin gene followed by transformation of *E. coli* and selection of clones that survive at pH 5 provides a potential route to the direct selection of mutant forms of the toxin that are deficient in the ability to insert into membranes and/or form transmembrane channels in a pH-dependent manner. This method, which provides a unique approach to identifying specific amino acids that are functional in membrane insertion or channel formation, should complement biophysical and biochemical that have been applied to such questions to date. The method may be applicable to other toxins, and possibly to mammalian viruses, that undergo pH-dependent steps in entry into the cell, and it could yield information relevant to broader questions concerning the insertion of other classes of proteins into membranes.

Acknowledgement

This work was supported by National Institute of Health Grants AI-22021 and AI-22848.

References

- Carroll, S. F. and Collier, R. J. (1984) *Proc. Natl. Acad. Sci. USA*, **81**, 3307.
Carroll, S. F., McCloskey, J. A., Crain, P. F., Oppenheimer, N. J., Marschner, T. M. and Collier, R. J. (1985) *Proc. Natl. Acad. Sci. USA*, **82**, 7237.
Collier, R. J. (1975) *Bacteriol. Rev.*, **39**, 54.
Donovan, J. J., Simon, M. I., Draper, R. K. and Montal, M. (1981) *Proc. Natl. Acad. Sci. USA*, **78**, 172.
Kagan, B. L., Finkelstein, A. and Colombini, M. (1981) *Proc. Natl. Acad. Sci. USA*, **78**, 4950.
O'Keeffe, D. O. and Collier, R. J. (1989) *Proc. Natl. Acad. Sci. USA*, **86**, 343.
Pappenheimer, A. M. Jr. (1980) *Harvey Lect.*, **76**, 45.
Sandvig, K. and Olsnes, S. (1988) *J. Biol. Chem.*, **263**, 12352.

Iron-regulated membrane proteins and bacterial virulence

E. GRIFFITHS

National Institute for Biological Standards and Control, Blanche Lane, South Mimms, Potters Bar, Hertfordshire EN6 3QG, England

Abstract. The amount of iron that might be readily available to bacteria in body fluids is extremely small. This iron restricted environment induces phenotypic changes in the metabolism and in the composition of the membrane proteins of bacteria growing *in vivo*. These changes are now providing a fresh insight into the capabilities of bacteria to multiply in host tissues and are suggesting new possibilities for targeting therapeutic and prophylactic measures.

Keywords. Bacterial virulence; iron-regulated membrane proteins.

Introduction

The ability of an invading pathogen to multiply successfully under the conditions found in the host is an essential factor in any infection. Here bacteria must produce the full complement of virulence determinants required for pathogenicity. It is, of course, well known that bacteria can alter their metabolism rapidly in response to environmental changes, and they are capable of existing in a variety of physiological states which can be quite different from one another. However, in the past the effect of the host environment on pathogenic bacteria has generally been ignored. We thus find that most investigations into bacterial virulence have been carried out with organisms grown *in vitro* under conditions that do not necessarily reflect microbial behaviour *in vivo*; this is likely to give at best only a partial picture of bacterial characteristics associated with virulence and with immune responses important for protection. The situation is now changing rapidly and we are becoming more and more aware that specialized determinants are induced only when a pathogen encounters its host.

Host factors that might be expected to influence bacterial characteristics and their ability to multiply *in vivo* include temperature, pH, osmotic pressure, oxygen tension and the availability of essential nutrients. Perhaps the best-understood property of the environment encountered by pathogens in host tissues, and its effects on bacterial properties and growth, is the availability of iron. Our understanding of the way the host normally restricts the availability of this metal and the effect of its restriction on bacterial metabolism and multiplication has increased enormously in recent years and there is now a considerable literature on the relationship between iron and pathogenicity (Bullen and Griffiths, 1987).

Availability of iron *in vivo*

Although there is a considerable amount of iron present in the body fluids of humans and animals, it is known that the amount of free iron which might be readily available to bacteria, is normally extremely small (Bullen and Griffiths, 1987). Most is found intracellularly, in ferritin, haemosiderin or haem, and extra-

cellular iron in body fluids is attached to high affinity iron binding glycoproteins, transferrin in serum and lymph, and lactoferrin in external secretions and milk. A related protein called ovotransferrin is found in avian egg white. These proteins bind iron extremely tightly and ensure that virtually no free iron is available to invading bacteria.

Nevertheless, pathogenic bacteria can multiply successfully under these conditions to establish extracellular infections. They must therefore be able to overcome this iron-restricted environment and produce mechanisms for assimilating protein-bound iron or for acquiring it from liberated haem. So far little is known about the availability of iron inside cells, although it seems in some cells that iron is freely available (Lawlor *et al.*, 1987).

Siderophore-mediated iron uptake systems

The best-understood systems whereby bacterial pathogens assimilate iron from iron-binding proteins are those which depend on the production of soluble, low molecular mass, high affinity iron-chelating compounds known as siderophores (Bullen and Griffiths, 1987; Crosa, 1989). Some siderophores are able to release iron from iron-binding proteins and the best understood of these are those used by enteric organisms. For example *Escherichia coli*, *Salmonella typhimurium* and *Klebsiella pneumoniae* produce a phenolate chelator called enterobactin (enterochelin) under conditions of iron restriction. Some strains produce, in addition, a hydroxamate chelator called aerobactin. In particular many strains of *E. coli* and *K. pneumoniae* that cause septicaemias produce aerobactin, the genes for which may be located in the chromosome or on a plasmid (Crosa, 1989). It is not entirely clear why acquiring the ability to make this second siderophore confers a selective advantage on bacteria that can already make enterobactin although there have been a number of hypotheses (Bullen and Griffiths, 1987; Crosa, 1989). Mutants unable to produce relevant siderophores are unable to multiply in the presence of an iron-binding protein.

An integral part of the high-affinity iron-uptake systems based on chelators is the production of outer membrane proteins which act as receptors for the siderophores, as well as mechanisms for the release of chelator-bound iron (Bullen and Griffiths, 1987; Crosa, 1989; Ecker *et al.*, 1986; Neilands, 1982). The requirement for outer membrane receptor proteins in siderophore-mediated iron uptake is shown by the fact that mutants lacking such proteins are completely devoid of transport activity (Crosa, 1989; Neilands, 1982; Grewel *et al.*, 1982). Although the outer membrane receptors are siderophore specific, inner membrane components, also necessary for siderophore-mediated iron transport are also siderophore specific.

The enteric bacteria produce several new outer membrane proteins under iron-restricted conditions but so far only some have been identified as ferric siderophore receptors. For example, an 81 kDa protein in *E. coli* functions as the receptor for ferric enterobactin (Neilands, 1982; Hollifield and Neilands, 1978), and a colicin plasmid-encoded 74 kDa protein functions as the receptor for aerobactin (Crosa *et al.*, 1982; Bindereif *et al.*, 1982). Most of the work on the iron-regulated outer membrane proteins of *E. coli* has been carried out with laboratory strains such as *E. coli* K12. However, the outer membrane proteins of *E. coli* O157:H7, a

proteins when grown *in vitro* in the presence of iron-binding proteins, and *in vivo* during infection (Griffiths *et al.*, 1983; Chart and Griffiths, 1985; Chart *et al.*, 1988). Results also show considerable qualitative and quantitative variation in the expression of iron-regulated membrane proteins by different strains of pathogenic *E. coli*; some strains produce larger amounts of these proteins than *E. coli* K12, and some produce iron-regulated proteins not seen in laboratory strains (Griffiths *et al.*, 1983; Chart *et al.*, 1988).

Although much of our understanding of iron-sequestering systems based on siderophores and outer membrane protein receptors, and of their role in bacterial virulence, has come from studies on enteric bacteria, there is increasing evidence that similar systems play an equally important role in the pathogenicity of other bacteria (Bullen and Griffiths, 1987; Crosa, 1989). Iron-regulated siderophores, membrane proteins and other iron-regulated properties have been found in many pathogens and the list continues to grow (Poole and Braun, 1988; Williams *et al.*, 1988; Carniel *et al.*, 1989; Domingue *et al.*, 1989; Fernandez-Beros *et al.*, 1989; Paul *et al.*, 1989). In many cases the function of the iron-regulated membrane proteins is unknown, although some are known to be ferric siderophore receptors. The synthesis of several factors, like bacterial toxins, is also regulated by iron (Bullen and Griffiths, 1987; Crosa, 1989).

Siderophore-independent receptor mediated iron-uptake systems

The best-understood systems used by pathogenic bacteria to assimilate iron from host iron-binding proteins are those which depend on the production of siderophores and outer membrane ferric-siderophore receptors. However, the fact that such systems are the best-understood at present does not mean that they are the most common, nor indeed the most efficient systems for sequestering iron *in vivo*. Some pathogens, like the *Neisseria* and *Haemophilus* species, use a mechanism which depends on the direct interaction between the bacterial cell surface and the iron-binding protein in a manner analogous to the reaction occurring between transferrin and the mammalian cell (Crichton and Charleaux-Wauters, 1987; Huebers and Finch, 1987); no siderophore is involved. Perhaps the most significant feature of these systems, which distinguishes them from the known siderophore-mediated mechanisms, is the highly specific nature of the process (Mickelsen and Sparling, 1981; Mickelsen *et al.*, 1982; Simonson *et al.*, 1982; Schryvers and Morris, 1988; Morton and Williams, 1989; Schryvers and Lee, 1989). Thus the iron uptake system of *N. meningitidis* is highly specific for human transferrin and human lactoferrin and discriminates against lactoferrin and transferrin from other species. This has obvious implications for explanations of host specificity of *N. meningitidis* and for the development of an animal model (Schryvers and Gonzalez, 1989).

Although molecular mechanisms involved in iron-uptake by these organisms are not understood, it is thought that membrane receptors specific for transferrin or lactoferrin are involved. Recently, iron-regulated lactoferrin- and transferrin-binding

Molecular mechanisms regulating iron-controlled functions

In *E. coli* the expression of chromosomal and plasmid encoded systems controlled by iron, including some toxins, are negatively regulated *via* a global repressor protein called Fur, which uses ferrous iron as a co-repressor (Bagg and Neilands, 1987); Fur is the product of a regulatory gene *fur*. A *fur*-like system operates in several pathogens, including *Corynebacterium diphtheriae*, where it controls the synthesis of diphtheria toxin as well as other iron responsive determinants (Taylor and Holmes, 1988). Binding sites for the Fur repressor protein, called the "iron box", have been identified in several iron-regulated promoters (Bagg and Neilands, 1987; Poole and Braun, 1988; Tai and Holmes, 1988). The consensus sequence consists of a highly AT-rich palindrome and deletions that disrupt the palindromic structure make the promoter unresponsive to regulation by iron (Calderwood and Mekalanos, 1988). An additional global regulatory system, based on the undermodification of several transfer RNAs, also appears to operate in *E. coli* and *S. typhimurium* (Bullen and Griffiths, 1987). Much less is known about the molecular mechanisms of iron regulation of virulence determinants in other organisms.

Conclusion

Without doubt, current developments are rapidly increasing our understanding of the critical role of iron, or the lack of it, in infection, and are producing new insight into the capacity of bacteria to multiply *in vivo* and to cause disease. This information has important practical implications for vaccine production and the development of new therapeutic measures for treating bacterial infection. For example, the identification and characterization of determinants expressed in certain niches in the host, such as those produced under iron restricted conditions, offer the possibility of producing novel or improved vaccines containing immunogenic host-induced antigens. These may be much more relevant to host protective immunity than antigens found on organisms grown in the usual laboratory media.

References

- Bagg, A. and Neilands, J. B. (1987) *Microbiol. Rev.*, **51**, 509.
- Bindereif, A., Braun, V. and Hantke, K. (1982) *J. Bacteriol.*, **150**, 1472.
- Bullen, J. J. and Griffiths, E. (1987) *Iron and infection: Molecular, physiological and clinical aspects* (London: John Wiley).
- Calderwood, S. B. and Mekalanos, J. J. (1988) *J. Bacteriol.*, **170**, 1015.
- Carniel, E., Mercereau-Puijalon, O. and Bonnefoy, S. (1989) *Infect. Immun.*, **57**, 1211.
- Chart, H. and Griffiths, E. (1985) *J. Gen. Microbiol.*, **131**, 1503.
- Chart, H., Stevenson, P. and Griffiths, E. (1988) *J. Gen. Microbiol.*, **134**, 1549.
- Crichton, R. R. and Charleaux-Wauters, M. (1987) *Eur. J. Biochem.*, **164**, 485.
- Crosa, J. H. (1989) *Microbiol. Rev.*, **53**, 517.
- Domingue, P. A. G., Lambert, P. A. and Brown, M. R. W. (1989) *FEMS Microbiol. Lett.*, **59**, 1.
- Ecker, D. J., Matzanke, B. F. and Raymond, K. N. (1986) *J. Bacteriol.*, **167**, 666.
- Fernandez-Beros, M. E., Gonzalez, C., McIntosh, M. A. and Cabello, F. C. (1989) *Infect. Immun.*, **57**, 1271.
- Grewel, K. K., Warner, P. J. and Williams, P. H. (1982) *FEBS Lett.*, **140**, 27.
- Griffiths, E., Stevenson, P. and Joyce, P. (1983) *FEMS Microbiol. Lett.*, **16**, 95.

- Griffiths, E., Stevenson, P. and Ray, A. (1990) *FEMS Microbiol. Lett.*, **69**, 31.
- Hollifield, W. C. Jr. and Neilands, J. B. (1978) *Biochemistry*, **17**, 1922.
- Huebers, H. A. and Finch, C. A. (1987) *Physiol. Rev.*, **67**, 520.
- Lawlor, K. M., Daskaleros, P. A., Robinson, R. E. and Payne, S. M. (1987) *Infect. Immun.*, **55**, 594.
- Mickelsen, P. A. and Sparling, P. F. (1981) *Infect. Immun.*, **33**, 555.
- Mickelsen, P. A., Blackman, E. and Sparling, P. F. (1982) *Infect. Immun.*, **35**, 915.
- Morton, D. J. and Williams, P. (1989) *FEMS Microbiol. Lett.*, **65**, 123.
- Neilands, J. B. (1982) *Annu. Rev. Microbiol.*, **36**, 285.
- Paul, T. R., Smith, S. N. and Brown, M. R. W. (1989) *J. Med. Microbiol.*, **28**, 93.
- Poole, K. and Braun, V. (1988) *Infect. Immun.*, **56**, 2967.
- Schryvers, A. B. (1989) *J. Med. Microbiol.*, **29**, 121.
- Schryvers, A. B. and Gonzalez, G. C. (1989) *Infect. Immun.*, **57**, 2425.
- Schryvers, A. B. and Lee, B. C. (1989) *Can. J. Microbiol.*, **35**, 409.
- Schryvers, A. B. and Morris, L. J. (1988) *Mol. Microbiol.*, **2**, 281.
- Simonson, C., Brener, D. and DeVoe, I. W. (1982) *Infect. Immun.*, **36**, 107.
- Tai, S. P. S. and Holmes, R. K. (1988) *Infect. Immun.*, **56**, 2430.
- Williams, P., Denyer, S. P. and Finch, R. G. (1988) *FEMS Microbiol. Lett.*, **50**, 29.

Inhibition of anion transport in the red blood cell membrane by anionic and non-anionic arginine-specific reagents

LAILA ZAKI

Max-Planck-Institut für Biophysik, Heinrich-Hoffmann-Straße 7, 6000 Frankfurt am Main 71, FRG

Abstract. Arginine specific reagents are found to be powerful inhibitors of anion exchange in the red blood cell membrane. Some of these inhibitors such as cyclohexandione, phenylglyoxal and 2, 3-butanedione are found to produce their inhibition by interacting covalently with band 3. In contrast to the action of these compounds, the inhibition caused by the phenylglyoxal derivative 4-hydroxy-3-nitrophenyl-glyoxal has been found to be completely reversible. In extending the studies on the mode of action of these compounds on sulfate exchange and to get some more information about their binding site, the degree of inhibition caused by different phenylglyoxal derivatives which have a similar core but differ in their substituent groups have been compared. The interaction between the binding sites of these compounds and other anion transport inhibitors have also been studied.

Keywords. Red blood cell; anion transporter; arginine-specific reagents.

Introduction

During the last 20 years many important discoveries have been made in the field of membrane research. One of these important discoveries was the identification of band 3 protein as the protein which catalyses the exchange of anion across the red blood cell membrane (Cabantchik and Rothstein, 1974; Zaki *et al.*, 1975). The method which was used and which enabled to characterize this protein among the complex mixture of the membrane components was based on chemical modification. The interactions between two types of anion transport inhibitors have been studied. One of these inhibitors is 4-acetamido-4'-isothiocyano 2,2-stilbene disulfonate (SITS), which is a nonpenetrating, very specific anion transport inhibitor. The other one is flouro-2,4-dinitrobenzene (DNFB). The common covalent binding site of DNFB, SITS and 4,4'-diisothiocyanodihydrostilbene-2,2'-disulfonate (H_2DIDS) is a lysine residue which is located in the 60 kDa fragment of band 3 protein (Brazilay *et al.*, 1979). Kinetic studies have shown that this lysine does not participate in the substrate binding site (Passow *et al.*, 1980). α -Dicarbonyl reagents which are known to react selectively with guanidyl residues in proteins are found to be potent inhibitors of sulfate exchange across the red blood cell membrane (Zaki, 1981, 1983, 1984; Zaki and Julien, 1985; Julien and Zaki, 1987). Complete inhibition of anion-transport is accompanied by modification of 2 to 3 arginine residues (Zaki, 1984). The results with the reversible binding phenylglyoxal derivative 4-hydroxy-3-

nitrophenylglyoxal (HNPG), suggest that these reagents are interacting with the substrate binding site (Julien and Zaki, 1988).

Materials and methods

All experiments were performed with human erythrocytes from healthy donors. Blood was obtained from the Red Cross in Frankfurt/Main and stored at 4°C in acid/citrate/dextrose buffer. The cells were used after no more than 4 days of storage. Resealed ghosts were prepared essentially as described by Zaki *et al.* (1975).

Cells were hemolyzed at 0°C at a cell/medium ratio of 1:20 in medium containing 4 mM MgSO₄ and 1.45 mM acetic acid. Five minutes after hemolysis, sucrose, gluconate, citrate and HEPES were added from a concentrated stock solution to obtain a final concentration of 200 mM sucrose, 27 mM gluconate, 25 mM citrate and 5 mM HEPES in the hemolysate.

After centrifugation, the ghosts were resuspended and resealed in standard medium containing (mM): 200 sucrose, 27 gluconate, 25 citrate, 5 HEPES and 1 Na₂SO₄. The pH was either 7.4 or 8. Modification of resealed ghosts was done with HNPG. The reaction of the resealed ghosts with HNPG was carried out at a hematocrit of 10% in standard medium at 37°C.

Flux measurements and calculation of the rate constants were done as described previously (Zaki *et al.*, 1975). Calculation of SO₄²⁻ flux was done according to Schnell (1972). Transport is expressed as per cent of the residual activity relative to a control value in the same media used for the reaction but without the inhibitor.

The kinetic data were fitted with a least-squares method by a nonlinear regression.

Phenylglyoxal was obtained from Serva. Phenylglyoxal (PG) derivative HNPG was synthesised according to Julien and Zaki (1988); other derivatives according to Julien *et al.* (1990). All other substances were from Merck, Darmstadt.

Results

Labelling pattern of resealed ghosts with DNFB in the presence and absence of SITS.

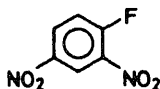
Treatment of the erythrocytes with [¹⁴C] DNFB causes labelling of all the membrane protein and retreatment of the cells with 0.5 mM SITS caused protection of band 3 against dinitrophenylation figure 1.

Inactivation course of sulfate equilibrium exchange by 4-hydroxyphenylglyoxal and 4-methylphenylglyoxal

Figure 2 shows the inactivation course of sulfate equilibrium exchange by *p*-hydroxyphenylglyoxal (OH-PG) and *p*-azidophenylglyoxal (CH₃-PG) at pH 7.4. It also shows that the activity loss followed pseudo first-order kinetics and the degree of inhibition is dependent on reagent concentration.

DNFB

(2,4 - dinitrofluorobenzene)



SITS

(4 - acetamido - 4' - isothiocyano - 2 - 2' - disulfonic - stilbene)

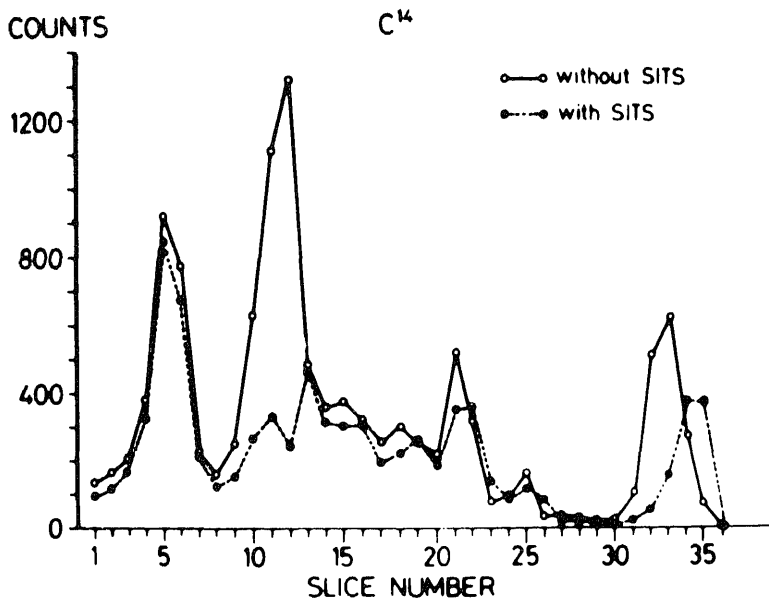
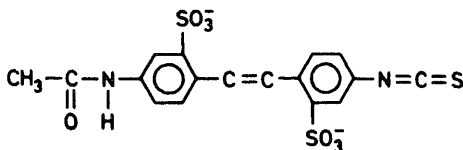


Figure 1. Labelling pattern of resealed ghosts with $[^{14}\text{C}]$ DNFB in the absence (\circ) and in presence (\bullet) of 0.5 mM SITS. Dinitrophenylation was done at pH 7.2 for 30 min at 25°C.

Inactivation of sulfate exchange in resealed ghosts by different derivatives of phenylglyoxal at pH 8

To evaluate the chemical properties of the binding site of arginine-specific reagents, different derivatives of phenylglyoxal which have a similar core but different substituent groups have been synthesised.

The degree of inhibition of the sulfate exchange by the various derivatives has

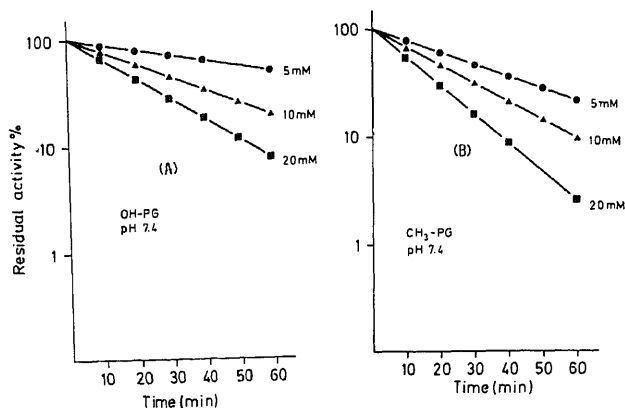


Figure 2. Kinetics of inactivation of sulfate exchange in resealed ghosts by OH-PG (A) and CH₃-PG (B). The ghosts were incubated with different concentrations of the reagent at pH 7.4. The transport activity was assayed in aliquots. The observed pseudo-first order rate constant values were calculated from the data presented.

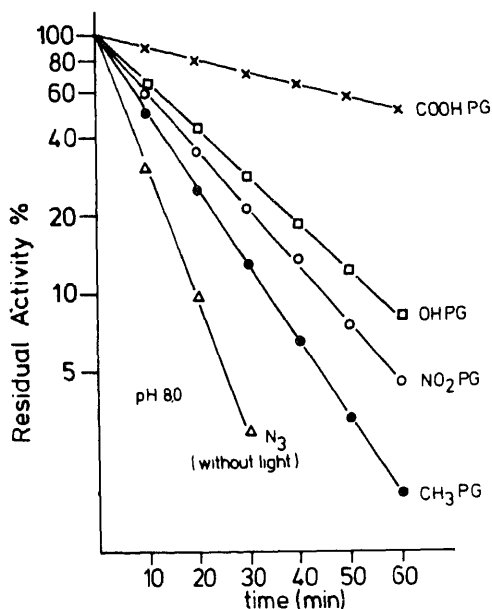


Figure 3. Time course of the inhibition of sulfate transport with differed PG derivatives. Resealed ghosts were modified with 10 mM of COOH-PG, OH-PG, NO₂-PG, CH₃-PG and N₃-PG.

been compared. Figure 3 presents the time course of inactivation of sulfate equilibrium exchange by *p*-carboxyphenylglyoxal (COOH-PG), OH-PG, N₃-PG and *p*-methylphenylglyoxal (CH₃-PG). The concentration of the inhibitors was 10 mM, and the pH of the reaction medium was 8. N₃-PG was found to be the

thin-layer partition chromatography according to Motais and Cousin (1976) as shown in figure 4.

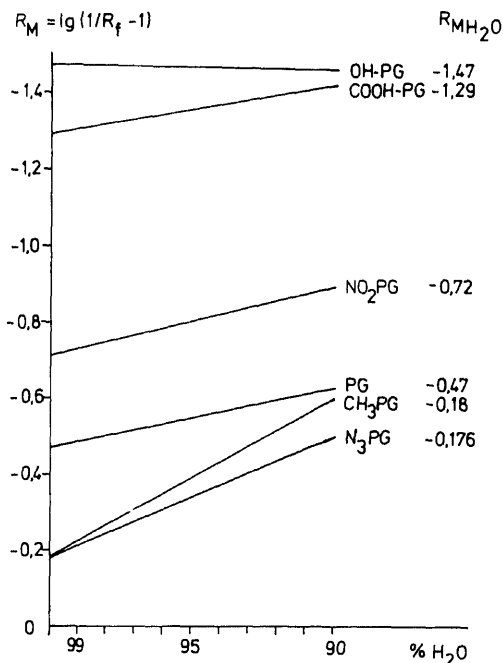


Figure 4. Lipophilic character of the PG derivatives. The lipophilic properties of the different PG derivatives were determined by thin-layer partition chromatography. Silica gel was the stationary phase, a mixture of water and acetic acid was the mobile phase. Ordinate the R_M values where $R_M = \lg (1/R_f - 1)$. Abscissa: % of H_2O in the mobile phase. The intercept of the straight lines with the ordinate yielded the R_M value for pure H_2O .

Under the experimental conditions used, the half time of inactivation of sulfate exchange by N_3 -PG was found to be 5.9 min. This value is equal to the half time of inactivation of the system by PG.

These results show that the hydrophobic properties of these probes do not correlate with their inhibitory potency.

Effect of 4,4'-dinitrostilbene-2,2'-disulfonate and flufenamate on 4-hydroxyphenylglyoxal binding site

Resealed ghosts were first incubated with the reversible acting inhibitors (table 1).

Table 1. Effect of DNDS and Flufenamate on the rate of transport inactivation by OH-PG at pH 8.

Conditions	Residual activity (%)
5 mM OH-PG	33 ± 1.74
5 mM OH-PG in the presence of 50 μ M DNDS	67 ± 4.80
5 mM OH-PG in the presence of 50 μ M Fufenamate	76 ± 4.90

After 5 min of incubation OH-PG was added and the ghosts were further incubated for 45 min at 37°C. After removal of the reversible-acting inhibitors and the excess of PG derivative by washing, flux measurements were performed.

The results in table 1 show that the reversible-acting anion transport inhibitors are able to protect the transport system against inhibition with the phenylglyoxal derivative OH-PG.

Discussion

The present data show that both anionic and non-anionic PG derivatives are able to inhibit sulfate exchange across the red blood cells.

Previous results (Zaki and Julien, 1986) have shown that the binding site of these inhibitors is mutually exclusive to the binding site of PG and HNPG.

The structural activity studies show that neither the lipophilic nor the electronic properties of PG derivatives seem to play a role in their inhibitory potency. This is not the case found in the structural activity studies done with the stilbene disulfonate derivatives (Brazilay *et al.*, 1979). We have also been able to show that the binding of PG does not effect the $^3\text{H}_2$ DIDS binding to band 3.

These findings suggest that the essential arginine(s) in band 3 protein is not located in the segment of the peptide chain that contains the stilbene disulfonate binding site.

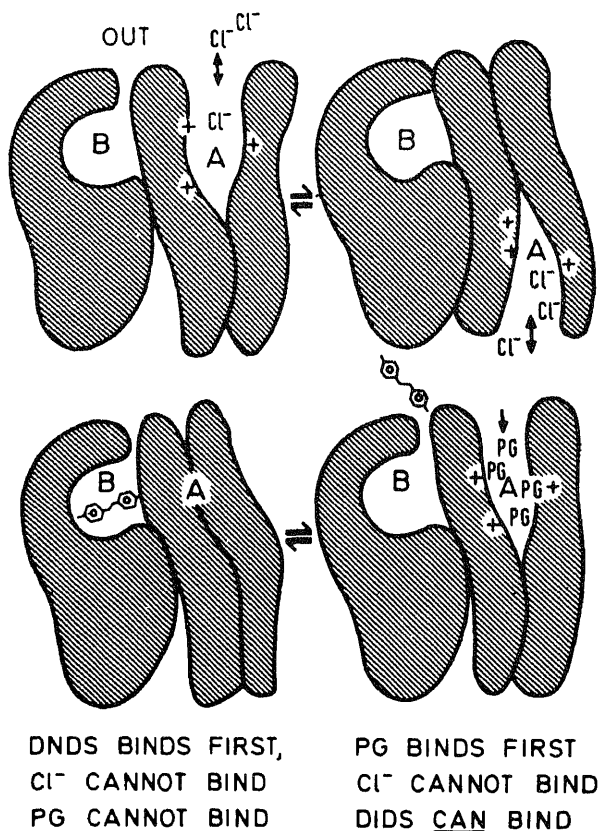


Figure 5. Cascade model.

On the other hand, allosteric interaction between the two binding sites is shown in table 1.

Cascade model

Figure 5 shows the interaction between the two binding sites and transportable anions. The anion transport site which reacts with PG or its derivatives (one or several arginine residues) may be located in a segment of band 3 designated A. The binding site of the stilbene disulfonate may be located in an adjacent transmembrane segment in a hydrophobic niche called B. Site A is likely to exist in a cleft which is inaccessible to positively charged probes and less accessible to probes which are bulky and negatively charged. The rate of inactivation of sulfate flux with these latter reagents is much slower than with PG and other derivatives presented in this work.

The binding of the bulky and negatively charged stilbene derivative to site B causes a large conformational change in band 3 and its environment (Singer and Morrison, 1980). These changes may lead to the burial of the transport site and make it incapable of reacting with PG or with the substrate anion. When phenylglyoxalation of the resealed ghosts is done first, the stilbene disulfonate binding site remains essentially unchanged since it is known that PG reaction with protein causes no perturbation of their tertiary structure (Catherine and HSV, 1983). DNDS can still bind, but the substrate anion cannot bind.

In the presence of SO_4^{2-} or Cl^- , the site A is loaded with the substrate anion and translocation takes place. This may be accompanied by changing the orientation of the transporter from facing outward to inward. This conformational change causes the DIDS-binding site to be buried. PG is also prevented from binding, hence the site is occupied by a substrate anion.

References

- Brazilay, M., Ship, S. and Cabantchik, Z. I. (1979) *Membr. Biochem.*, **2**, 227.
- Cabantchik, Z. and Rothstein, A. (1974) *J. Membr. Biol.*, **15**, 207.
- Catherine, M. V. and HSV, R. Y. (1983) *Arch. Biochem. Biophys.*, **225**, 296.
- Julien, T., Betakis, E. and Zaki, L. (1990) *Biochim. Biophys. Acta*, **1026**, 43.
- Julien, T. and Zaki, L. (1987) *Biochim. Biophys. Acta*, **900**, 169.
- Julien, T. and Zaki, L. (1988) *J. Membr. Biol.*, **102**, 217.
- Motais, R. and Cousin, T. L. (1976) *Am. J. Physiol.*, **231**, 1485.
- Passow, H., Fasold, H., Gartner, E., Legrum, B., Ruffing, W. and Zaki, L. (1980) *Ann. N. Y. Acad. Sci.*, **341**, 361.
- Schnell, K. F. (1972) *Biochim. Biophys. Acta*, **282**, 265.
- Singer, J. and Morrison (1980) *Biochim. Biophys. Acta*, **598**, 40.
- Zaki, L. (1981) *Biochem. Biophys. Res. Commun.*, **99**, 234.
- Zaki, L. (1983) *Biochem. Biophys. Res. Commun.*, **110**, 616.
- Zaki, L. (1984) *FEBS Lett.*, **169**, 234.
- Zaki, L., Fasold, H., Schumann, B. and Passow, H. (1975) *Cell. Physiol.*, **86**, 471.
- Zaki, L. and Julien, T. (1985) *Biochim. Biophys. Acta*, **818**, 325.
- Zaki, L. and Julien, T. (1986) *8th School on Biophysics of Membrane Transport Proceedings*, Agricultural University of Wroclaw, Poland.

Functional and pathological significance of phospholipid asymmetry in erythrocyte membranes

ROBERT A. SCHLEGEL[†], SUSAN KEMPER and
PATRICK WILLIAMSON*

Department of Molecular and Cell Biology, The Pennsylvania State University, University Park, PA 16802, USA

*Department of Biology, Amherst College, Amherst, MA 01002, USA

Abstract. The normal asymmetric distribution of phospholipids in the plasma membrane is perturbed in erythrocytes from patients with chronic myelogenous leukemia. Since experimentally-produced lipid-symmetric erythrocytes are more interactive with cells of the reticuloendothelial system than are their lipid-asymmetric counterparts, the biological recognition of chronic myelogenous leukemia erythrocytes by the reticuloendothelial system was examined. With one exception, all erythrocyte samples from patients with chronic/benign chronic myelogenous leukemia were more adherent to endothelial cells and more readily phagocytosed by macrophages *in vitro* than were normal erythrocytes. Thus, these naturally occurring pathological erythrocytes display the same dysfunctional intercellular interactions as the laboratory models.

Keywords. Erythrocyte membrane; phospholipid asymmetry; chronic myelogenous leukemia; lipid packing; phosphatidylserine; cellular interactions; reticuloendothelial system; liposomes; annexins.

Introduction

In erythrocytes, the phospholipids of the plasma membrane are asymmetrically distributed across the bilayer (Op den Kamp, 1979). Lysis and resealing of the cells under specified conditions allows production of populations with either lipid-symmetric or lipid-asymmetric membranes (Williamson *et al.*, 1985), which have been used to test the functional consequences of loss of asymmetry in erythrocytes. Structurally, lipid-symmetric erythrocytes have more loosely-packed phospholipids in their exterior leaflet (Williamson *et al.*, 1985) and display a more hydrophobic surface (McEvoy *et al.*, 1986) than their asymmetric counterparts, besides an increase in the amount of phosphatidylethanolamine and phosphatidylserine (PS) in their outer leaflet. These alterations are associated with changes in the functional characteristics of the cell: lipid-symmetric erythrocytes are more adherent to endothelial cells (Schlegel *et al.*, 1985a) and are more readily phagocytosed by monocyte-derived macrophages (McEvoy *et al.*, 1986) and cells of the J774A.1 macrophage line (Schlegel *et al.*, 1985b) than are lipid-asymmetric cells.

Kumar and Gupta (1983) were the first to recognize that the distribution of membrane phospholipids is altered in erythrocytes from patients with chronic myelogenous leukemia (CML). To determine whether phospholipid packing in the membranes of these pathological erythrocytes was also perturbed, the fluorescent probe merocyanine 540 (MC540), which binds more avidly to loosely packed bilayers (Williamson *et al.*, 1983), was applied. Not only did erythrocytes from all

but so too did erythrocytes from patients with other myeloproliferative disorders (Reed *et al.*, 1987). These properties of CML erythrocytes predict that their biological recognition may be altered just as in the case of experimentally-produced lipid-symmetric erythrocytes. To test this prediction we have examined the adherence of CML erythrocytes to human endothelial cells and their phagocytosis by J774A.1 macrophages.

Materials and methods

To assess variability among normal samples, blood from multiple normal volunteers was collected and erythrocytes examined in side-by-side assays. As shown in table 1, when the adherence values for 3 samples (1-3) were averaged

Table 1. Cellular recognition of CML erythrocytes.

Condition	Sample	Adherence ratio ^a	Phagocytosis ratio ^a
Normal			
Pennsylvania ^b	1	1.0	
	2	0.9	
	3	1.1	
	4		1.2
	5		0.8
	6		1.0
	7		0.9
	8		1.1
Texas	1643		1.0
	1679	1.3	
	1680	1.2	
CML			
Benign/chronic	1301	2.9	1.5
	1302	1.5	1.6
	1319		3.2
	1320		2.2
	1321	5.2	2.1
	1322	4.3	1.6
	1330		2.0
	1397	3.1	1.6
	1398	2.4	1.7
	1412	2.0	
	1414	1.7	
	1479		2.8
	1480		4.2
	1571		0.7
Accelerated	1572		1.0
	1573		1.2
Other hematological disorders			
Essential thrombocytosis	1331		1.5
CML Ph ⁻ (BCR ⁺)	1411		0.9
CMML Ph ⁻	1478		3.3
AUL	1570		0.9

^aAssays were performed as described by Pradhan *et al.* (1990).

^bIndividual ratios for samples 1-3, 4-5, 6-8 were calculated against the average within these groups.

adherence ratios computed against the average for each sample, little variability among samples was seen. The same was true for phagocytosis ratios determined for samples 4 and 5 and 6-8.

Samples from patients were shipped overnight on ice from M. D. Anderson Cancer Center, Houston, Texas and examined within 24 h of collection. Normal samples, against which patient samples were compared, were collected in Pennsylvania identically and on the same day as patient samples and stored overnight on ice. However, to assure the veracity of these normal samples, several samples collected from normal volunteers in Texas were compared against normal samples collected in Pennsylvania and expressed as adherence ratios. As seen in table 1, neither adherence or phagocytosis ratios differed much from unity for any of these samples.

Results and discussion

Erythrocytes from 14 different patients with Philadelphia chromosome positive, benign/chronic CML, all undergoing therapy, were examined in the study. Because endothelial cells were never passaged more than twice before use, they were not always available for assays, accounting for the smaller number of adherence ratios obtained. However, as seen in table 1, all samples which could be examined were more adherent than normal controls. Because J744A.1 macrophages are a continuous line, they were always available for phagocytosis assays. As seen in table 1, with the exception of sample 1571, all phagocytosis ratios were greater than any value obtained with normal erythrocytes. Perhaps surprisingly, the phagocytosis ratios for the only two patients in accelerated CML, or blast crisis, deviated little from the norm. In addition to the samples from CML patients, a limited number of samples from patients with other hematological disorders were examined. One patient with Philadelphia chromosome negative chronic myelomonocytic leukemia showed a markedly elevated phagocytosis ratio, and one patient with essential thrombocytosis had a somewhat increased ratio. A Philadelphia chromosome negative, but breakpoint chromosome region positive, CML patient and a patient with adult undifferentiated leukemia had ratios within the normal range.

These results indicate that with one exception CML erythrocytes from all patients showed increased adherence to endothelial cells and increased phagocytosis by macrophages. It would have been of interest to determine whether the samples with the highest phagocytosis ratios also had the highest adherence ratios. Unfortunately, adherence ratios were not obtained for the samples which had the highest phagocytosis ratios. It would also be of interest to determine whether the presence of the Philadelphia chromosome is required for increased adherence and phagocytosis, and whether these altered properties of erythrocytes are present in a wider range of hematological disorders. These and other questions can be pursued in future studies of a larger patient population.

The effector mechanisms responsible for maintenance and loss of phospholipid asymmetry, and the effector mechanisms responsible for enhanced cellular recognition following loss are under intensive investigation in numerous laboratories. With regard to effector mechanisms, several signals have been proposed for recognition of lipid-symmetric erythrocytes by cells of the reticuloendothelial system (RES): loosened packing of surface phospholipids (McEvoy *et al.*, 1986) and exposure of PS on the outer surface of the cell (Tanaka

and Schroit, 1983; Schroit *et al.*, 1985). Since these properties cannot be dissected in lipid-symmetric erythrocytes, liposomes modeled after the erythrocyte membranes which circulate for extended periods in mice were used to test these alternatives separately. By systematically altering the composition of the liposomes and assessing the effects on their ability to remain in circulation, it was concluded that both tight packing of phospholipids and exclusion of PS from the surface are required to prevent enhanced clearance by the RES (Allen *et al.*, 1988).

The relative importance of the cytoskeleton and the aminophospholipid translocase as effector mechanisms is being closely scrutinized (see, for example, Williamson *et al.*, 1987; Middelkoop *et al.*, 1989). In CML erythrocytes, a potential role for the cytoskeleton in the perturbations of phospholipid distribution has emerged from the finding of abnormalities in the architecture of the spectrin underlying the membrane of these cells (Basu *et al.*, 1988). Another potential contributing factor has been uncovered in investigations of the finding that elevation of intracellular Ca^{2+} levels in normal erythrocytes results in loss of phospholipid asymmetry (Williamson *et al.*, 1985; Chandra *et al.*, 1987). The few years have seen the discovery of a new class of Ca^{2+} -sensitive, potentially regulatory proteins in the annexins, which bind to membranes in a Ca^{2+} -dependent fashion (Burgoyne and Geisow, 1989). If annexins are involved in maintenance of loss of lipid asymmetry, their levels and/or distribution might be altered in CML erythrocytes. We have recently established that a 67 kDa annexin is present in the cytoplasm of normal human erythrocytes and is translocated to the membrane in the presence of Ca^{2+} . This 67 kDa protein, and also other proteins of 33 and 38 kDa which react with antisera to annexins, are present in CML erythrocytes as well. However, the 67 kDa protein is found on the membranes of the CML erythrocytes even in the absence of Ca^{2+} (Fujimagari *et al.*, 1990). Whether the abnormal amount and distribution of annexins play a role in the perturbations of phospholipid asymmetry in CML membranes is currently under investigation.

In summary, the use of both laboratory and naturally occurring pathological models in which phospholipid asymmetry has been perturbed has allowed insight into the mechanisms of maintenance and loss of phospholipid asymmetry and the functional consequences of the failure of those mechanisms.

Acknowledgements

We are indebted to Dr. A. Deisseroth of the University of Texas M. D. Anderson Cancer Center, Houston, Texas for providing patient samples. We wish to particularly thank Dr. O. M. Zack Howard for her generous help in coordinating transport of the samples and expert advice on patient evaluation. This work was supported by United States Public Health Service Grant CA28921.

References

- Allen, T. M., Williamson, P. and Schlegel, R. A. (1988) *Proc. Natl. Acad. Sci. USA*, **85**, 8067.
- Basu, J., Kundu, M., Rakshit, M. M. and Chakrabarti, P. (1988) *Biochim. Biophys. Acta*, **945**, 12.
- Burgoyne, R. E. and Geisow, M. J. (1989) *Cell Calcium*, **110**, 1.
- Chandra, R., Joshi, P. C., Bajpai, V. K. and Gupta, C. M. (1987) *Biochim. Biophys. Acta*, **902**, 23.
- Fujimagari, M., Williamson, P. and Schlegel, R. A. (1990) *Blood*, **75**, 1337.

- Kumar, A. and Gupta, C. M. (1983) *Nature* (London), **303**, 632.
- Kumar, A., Daniel, S., Agarwal, S. S. and Gupta, C. M. (1987) *J. Biosci.*, **11**, 543.
- McEvoy, L., Williamson, P. and Schlegel, R. A. (1986) *Proc. Natl. Acad. Sci. USA*, **83**, 3311.
- Middelkoop, E., Van der Hock, E. E., Bevers, E. M., Comfurius, P., Slotboom, A. J., Op den Kamp, J. A. F., Lubin, B. H., Zwaal, R. F. A. and Roelofsens, B. (1989) *Biochim. Biophys. Acta*, **981**, 151.
- Op den Kamp, J. A. F. (1979) *Annu. Rev. Biochem.*, **48**, 47.
- Pradhan, D., Weiser, M., Lumley-Sapanski, K., Frazier, D., Kemper, S., Williamson, P. and Schlegel, R. A. (1990) *Biochim. Biophys. Acta*, **1023**, 398.
- Reed, J. A., Kough, R. H., Williamson, P. and Schlegel, R. A. (1985) *Cell Biol. Int. Rep.*, **9**, 43.
- Reed, J. A., Green, R., Yamada, Y., Kough, R., Williamson, P. and Schlegel, R. A. (1987) *Cell Biol. Int. Rep.*, **11**, 55.
- Schlegel, R. A., Prendergast, T. W. and Williamson, P. (1985a) *J. Cell Physiol.*, **1123**, 215.
- Schlegel, R. A., McEvoy, L. and Williamson, P. (1985b) in *Red blood cells as carriers for drugs* (eds J. DeLoach and U. Sprandel) (Basel: Karger) p. 134.
- Schroit, A. J., Madsen, J. W. and Tanaka, Y. (1985) *J. Biol. Chem.*, **260**, 5131.
- Tanaka, Y. and Schroit, A. J. (1983) *J. Biol. Chem.*, **260**, 11335.
- Williamson, P., Mattocks, K. and Schlegel, R. A. (1983) *Biochim. Biophys. Acta*, **732**, 387.
- Williamson, P., Algarin, L., Bateman, J., Choe, H. R. and Schlegel, R. A. (1985) *J. Cell. Physiol.*, **123**, 209.
- Williamson, P., Antia, R. and Schlegel, R. A. (1987) *FEBS Lett.*, **219**, 316.

Calcium and magnesium induced changes in the relative fluidity of phosphatidylcholine liposomes

R. K. MISHRA and GAURI S. SINGHAL

School of Life Sciences, Jawaharlal Nehru University, New Delhi 110 067, India

Abstract. The effect of Ca^{2+} and Mg^{2+} on relative fluidity of phosphatidylcholine liposomes was studied by measuring the degree of chlorophyll fluorescence polarization. An increase in the degree of fluorescence polarization was observed on incubation of liposomes with different concentrations of Ca^{2+} or Mg^{2+} . The results have been interpreted on the basis of increase in the size of liposomes which could be brought about by calcium or magnesium induced fusion of small unilamellar liposomes to form larger vesicles. Fusion of liposomes has also been confirmed by the experiments on efficiency of energy transfer from chlorophyll b to chlorophyll a, and transmission electron microscopy of liposomes before and after incubation with Ca^{2+} and Mg^{2+} .

Keywords. Liposomes; fluidity; fluorescence polarization; phosphatidylcholine.

Introduction

Fluidity of the lipid bilayer plays a role in the membrane fusion. Small sonicated vesicles, because of their large curvature are known to exhibit different physical properties from large bilayer vesicles and multilamellar liposomes (Scheetz and Chan, 1972). In particular, small sonicated vesicles have intrinsically greater tendency to fuse as compared to the larger vesicles (Prestegard and Fellmeth, 1974; Miller and Racker, 1976; Liao and Prestegard, 1979). Fusion of vesicles of pure phospholipids incubated above their phase transition temperatures is considerably less due to the repulsive forces at the interface of the membranes of neutral phospholipids (LeNeveu *et al.*, 1978, Parsegian and Rand 1983).

However, rapid fusion of phosphatidylcholine vesicles occurs at the phase transition temperatures of these lipids (Prestegard and Fellmeth, 1974; Taupin and McConnel, 1972). Fusion between mixed (unsaturated) vesicles (Maeda and Ohnishi, 1974) and heterofusion between saturated and unsaturated phosphatidylcholine vesicles have also been reported.

The purpose of the present work was to study the effect of Ca^{2+} and Mg^{2+} on the fluidity of small unilamellar vesicles of phosphatidylcholine, in acidic and neutral environment. Based on our results, we suggest that the decrease in the relative fluidity of phosphatidylcholine liposomes, after incubation with $\text{Ca}^{2+}/\text{Mg}^{2+}$, is due to the formation of large multilamellar vesicles.

Materials and methods

L- α -phosphatidylcholine (from egg yolk) was purchased from CSIR Centre for Biochemicals, Delhi. CaCl_2 and MgCl_2 were from E. Merck, Germany and Glaxo, India respectively. Chlorophylls were extracted from fresh spinach leaves in methanol-petroleum ether (2:1 v/v) and were transferred into diethyl ether. The concentration of chlorophylls was determined according to Arnon (1949).

Small unilamellar vesicles of phosphatidylcholine were prepared in 0.1 M NaCl, 0.1 mM EDTA and 0.5 mM Tris(hydroxymethyl) methylamine buffer, pH 7.4 and 5.5. The lipid (10 mM) was dispersed in the buffer and was sonicated in a bath-type sonicator for 75 min. The preparation was subsequently ultracentrifuged at 115,000 *g* for 1 h in Beckman SW 50.1 rotor to remove the large vesicles and/or aggregates.

Vesicles with chlorophylls within the lipid bilayer were prepared as described by Mishra *et al.* (1988). The ratio of lipid:chlorophylls was always kept constant at 50:1 (w/w). The suspension of liposomes after sonication and ultracentrifugation was passed through a Sephadex G-25 column (25 × 1.5 cm) in order to remove the non-incorporated chlorophyll molecules.

Solutions of CaCl₂ or MgCl₂ were added to the liposomal suspension to give different concentrations. The fusion mixture was incubated at room temperature for 3 h and then excess of EDTA was added to chelate the metal ions. The mixture was again incubated for 1 h at room temperature before measuring the fluorescence emission and degree of fluorescence polarization. The samples were excited at 468 nm and the emission was measured at 658, 677 and 700 nm respectively on a Shimadzu RF-450 spectrofluorometer (Japan). The efficiency of energy transfer from Chl b to Chl a was given by $(F_{677}-F_{700})/(F_{658}-F_{700})$ (Gad and Eytan, 1983).

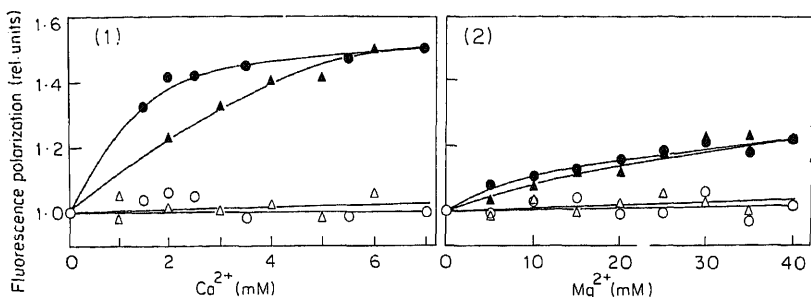
The measurement of steady-state fluorescence polarization was done by setting the excitation and emission wavelengths at 468 and 677 nm. The relative intensities of the 4 combinations of vertical and horizontal excitation and emission beams were recorded on a Shimadzu RF-540 spectrofluorometer (Japan). The steady-state fluorescence polarization was calculated as reported earlier (Dale and Eisinger, 1975; Dale *et al.*, 1977). All the experiments were carried out at two different pH *i.e.*, one at neutral pH 7.4 and the other at acidic pH 5.5.

The liposomes were negatively stained with 2% phosphotungstic acid for transmission electron microscopy. The pH of the stain solution was adjusted to 7.4 using 1 M NaOH. The liposomal suspension was taken on a copper grid (300 mesh size), coated with carbon-formvar and stained directly by putting a drop of 2% phosphotungstic acid solution on the grid (Munn, 1974). Staining was done for 3–4 min and the grid was blotted from side with a filter paper. After air drying the grid was mounted and viewed at a magnification of 135000 X in a transmission electron microscope (CM 10, Philips, The Netherlands).

Results

On incubation of liposomes with Ca²⁺ at pH 5.5 at room temperature, a sharp increase in the degree of fluorescence polarization was observed as the concentration of Ca²⁺ was raised from 0–2 mM. It maintained almost the same level between the Ca²⁺ concentration of 2 and 7 mM (figure 1). Results of experiments at pH 7.4 also showed a similar pattern but the increase in fluorescence polarization was slower (figure 1). No significant change was observed on incubation of liposomes without Ca²⁺ either at pH 5.5 or 7.4. Incubation of liposomes with Mg²⁺ also resulted in an increase in the fluorescence polarization value both at pH 5.5 and 7.4. The increase was, however, slower at pH 7.4 than that at pH 5.5 (figure 2).

The fusion of pigmented liposomes with the non-pigmented ones was monitored



Figures 1 and 2. Changes in the degree of fluorescence polarization of the mixture of pigmented and non-pigmented liposomes of phosphatidylcholine before (O, Δ) and after (●, \blacktriangle) incubation with Ca^{2+} (1) and Mg^{2+} (2) at pH 5.5 (O, Δ) and 7.4 (●, \blacktriangle). The samples were excited at 468 nm and the fluorescence emission was detected at 677 nm.

by the changes in efficiency of energy transfer from Chl b to Chl a as described by Gad and Eytan (1983) and Mishra *et al.* (1988). Table 1 shows the changes induced

Table 1. Efficiency of energy transfer from Chl b to Chl a in the mixture of pigmented and non-pigmented liposomes of phosphatidylcholine before and after incubation with different concentrations of Ca^{2+} and Mg^{2+} at pH 5.5 and 7.4 (see 'materials and methods' for details).

Ca^{2+} [mM]	pH 5.5		Ca^{2+} [mM]	pH 7.4		Mg^{2+} [mM]	pH 5.5		pH 7.4	
	Before	After		Before	After		Before	After	Before	After
0.0	1.64	1.45	0.0	2.68	1.64	0	1.59	1.50	1.14	1.12
1.5	1.65	1.24	1.0	1.66	1.49	5	1.57	1.38	1.22	1.08
2.0	1.55	1.17	2.0	1.55	1.52	10	1.66	1.35	1.15	1.09
2.5	1.55	1.17	3.0	1.61	1.49	15	1.52	1.35	1.13	1.09
3.5	1.51	1.19	4.0	1.60	1.49	20	1.50	1.30	1.13	1.09
5.5	1.55	1.25	5.0	1.65	1.47	25	1.55	1.28	1.17	1.08
7.0	1.50	1.21	6.0	1.63	1.43	30	1.59	1.23	1.15	1.06
			7.0	1.63	1.56	35	1.59	1.27	1.14	1.06

by various concentrations of Ca^{2+} at pH 5.5 and 7.4 respectively. It is apparent from the table that reduction in the efficiency of energy transfer is more at pH 5.5 than that at pH 7.4. The changes were less when liposomes were incubated with Mg^{2+} . However, acidic pH still favoured the reduction in energy transfer at all concentrations of Mg^{2+} (table 1). The fusion of liposomes induced by Ca^{2+} and Mg^{2+} were also confirmed by electron microscopy before and after incubation with Ca^{2+} or Mg^{2+} . Figure 3 shows the increase in the size of phosphatidylcholine vesicles after incubation with 5 mM CaCl_2 and 35 mM MgCl_2 .

Discussion

Our results show that Ca^{2+} brings about increase in the degree of chlorophyll fluorescence polarization more than Mg^{2+} . The degree of fluorescence polarization is considered to be a measure of mobility of the fluorophore, the chlorophyll molecule, within the lipid bilayer. Mobility of the fluorophore is affected by 3 major

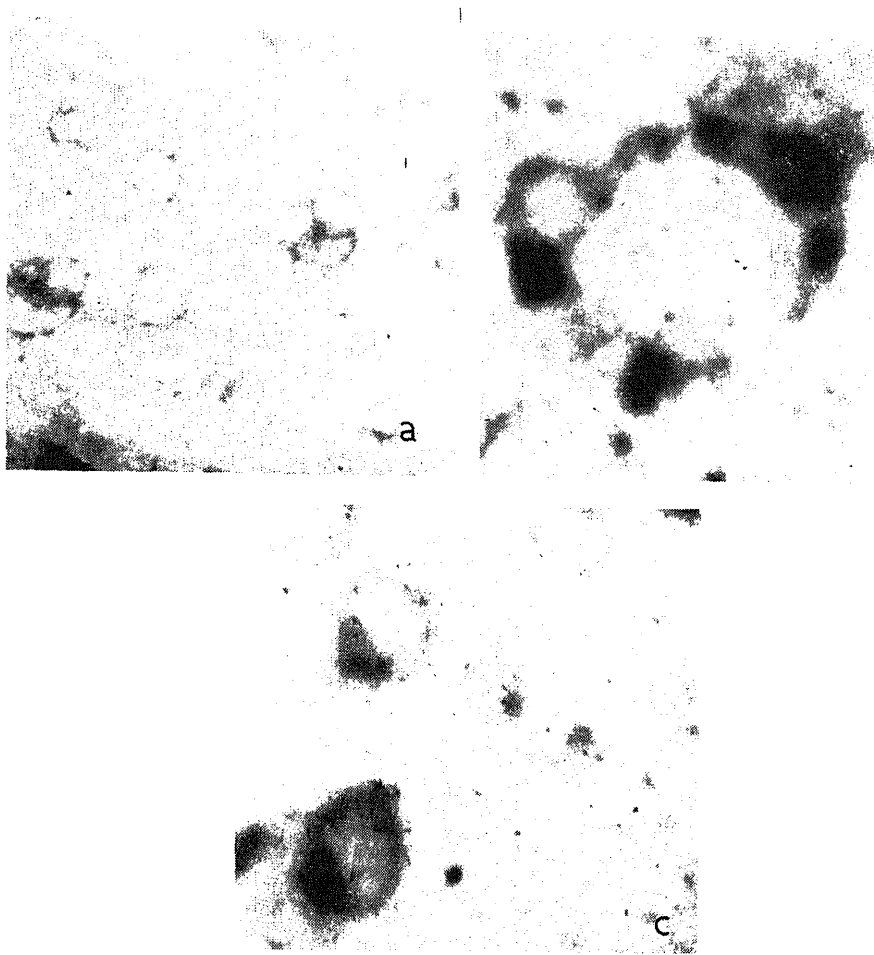


Figure 3. Electron micrographs of negatively stained liposomes before incubation (a), after incubation with 5 mM CaCl_2 (b) and 35 mM MgCl_2 (c) at 405,000 X magnification (see 'materials and methods' for details).

factors *viz.*, temperature, viscosity of the medium and, size and shape of the liposomes containing the fluorophore. Considering the experimental conditions, changes in fluorescence polarization could only be expected in the lipid bilayers containing chlorophyll molecules.

The results could be interpreted on the basis of an increase in the size of the liposomes after incubation with Ca^{2+} or Mg^{2+} , which could happen only by the fusion of small sonicated liposomes to form large multilamellar vesicles. It is known that small unilamellar vesicles form larger structures in a period of several hours when incubated at appropriate temperatures (Taupin and McConnell, 1972). Taupin and McConnell (1972) were the first to suggest that this process involves liposome fusion, which was further substantiated by other reports (Dietrich and

interpreted in terms of simple molecular exchange of the type described earlier (Sano and Huang, 1975; Lawaczek *et al.*, 1975, 1976). The greater ability of Ca^{2+} over Mg^{2+} in bringing about changes in the relative fluidity of liposomes has not been understood well and it needs further investigation. Reasons do exist for divalent cations induced fusion of liposomes of charged phospholipids but so far there is no conclusive evidence to show the binding of Ca^{2+} or Mg^{2+} to phosphatidylcholine liposomes. Thus the mechanism of Ca^{2+} / Mg^{2+} induced decrease in the bilayer fluidity and liposome fusion seems to be indirect to give apparent results presented here; but this mechanism appears to be sensitive to its ionic environment as the effects are more pronounced in the acidic medium.

Acknowledgements

The authors are thankful to All India Institute of Medical Sciences, New Delhi for electron microscopy facility. This work was supported in part by USDA-ICAR project grant no. FG-In-574. One of the authors (R.K.M.) gratefully acknowledges the award of a fellowship from the Council of Scientific and Industrial Research, New Delhi.

References

- Branton, D. I. (1949) *Plant Physiol.*, **24**, 1.
- Lawaczek, R. E., Chan, L. A. and Brand, L. (1977) *J. Biol. Chem.*, **252**, 7500.
- Lawaczek, R. E. and Eisinger, J. (1975) in *Biochemical fluorescence: Concepts* (eds R. F. Chen and J. Edelhoch) (New York: Marcel Dekker) vol. 1, p. 115.
- Lawaczek, R. E. and Eytan, G. D. (1983) *Biochim. Biophys. Acta*, **727**, 172.
- Lawaczek, R. E., Kishano, N. and Chan, S. I. (1976) *Biochim. Biophys. Acta*, **443**, 313.
- Lawaczek, R. E., Kishano, N., Girardet, J. L. and Chan, S. I. (1975) *Nature (London)*, **256**, 584.
- Lawaczek, R. E., Rand, R. P., Parsegian, G. M. and Gingell, D. (1978) *Nature (London)*, **259**, 601.
- Lawaczek, R. E. and Prestegard, J. H. (1979) *Biochim. Biophys. Acta*, **550**, 157.
- Lawaczek, R. E., T. and Ohnishi, S.-I. (1974) *Biochem. Biophys. Res. Commun.*, **60**, 1509.
- Lawaczek, R. E., C. and Racker, E. (1976) *J. Membr. Biol.*, **30**, 276.
- Lawaczek, R. E., Rajeswari, M. R. and Singhal, G. S. (1988) *Biochem. Int.*, **16**, 1137.
- Lawaczek, R. E. (1974) *Methods Enzymol.*, **32B**, 20.
- Lawaczek, R. E. and Huang, L. (1975) *J. Cell Biol.*, **67**, 49.
- Lawaczek, R. E., Hadjopoulos, D., Vail, W. J., Newton, C., Nir, S., Jacobson, K., Poste, G. and Lazo, R. (1972) *Biochim. Biophys. Acta*, **465**, 579.
- Lawaczek, R. E., V. A. and Rand, R. P. (1983) *Annal. N. Y. Acad. Sci.*, **416**, 1.
- Lawaczek, R. E., J. H. and Fellmeth, B. (1974) *Biochemistry*, **13**, 1122.
- Lawaczek, R. E., M. P. and Chan, S. I. (1972) *Biochemistry*, **11**, 4573.
- Lawaczek, R. E., C. and McConnel, H. M. (1972) in *Membrane fusion in mitochondria: Biomembranes* (FEBS Symposium, 8th Meeting, Amsterdam) (Amsterdam: Elsevier) p. 129.

Expression of 5-amino levulinic acid induced photodynamic damage to the thylakoid membranes in dark sensitized by brief pre-illumination

N. CHAKRABORTY and B. C. TRIPATHY*

School of Life Sciences, Jawaharlal Nehru University, New Delhi 110 067, India

Abstract. The 5-amino levulinic acid treated cucumber (*Cucumis sativus* L., CV. Pointsette) plants upon exposure to light ($\approx 30,000$ lux) wilted within 6 h and died after 36 h due to photodynamic reactions. Thylakoid membranes, the site of accumulation of porphyrins, were damaged due to photodynamic reactions leading to the inhibition of membrane linked functions of photosystem II, photosystem I and the whole chain electron transport. Photosystem II was more susceptible to photodynamic damage than photosystem I. The exogenous electron donors Mn^{2+} , diphenyl carbazide and NH_2OH failed to donate electrons to photosystem II suggesting that the damage has taken place close to P680. The 5-amino levulinic acid treated plants exposed to 30 min of light did not show any damage to the thylakoid membranes. However, when the above plants were transferred to dark for 12 h there was substantial damage to the thylakoid membrane system.

Keywords. 5-Amino levulinic acid; thylakoid membrane; photosystem.

Introduction

Biological tissues, which accumulate tetrapyrroles, are sensitive to photodynamic action of light (Rebeiz *et al.*, 1984, 1987a, b; Witkowski and Halling, 1988). 5-Amino levulinic acid (ALA) is a metabolite present in all living cells. The chlorophyll (Chl) molecules are synthesized from ALA *via* predominantly monovinyl and divinyl monocarboxylic acid routes (Tripathy and Rebeiz, 1986, 1988). The plants treated with ALA in dark accumulate an excess amount of tetrapyrroles of protoporphyrin IX, Mg protoporphyrin IX and protochlorophyllide (Rebeiz *et al.*, 1984, 1987a, b). When the ALA treated plants are exposed to light these excess tetrapyrroles absorb light that is not utilized in the photochemical reactions; rather it may be utilized to photosensitize the production of singlet oxygen (Hopf and Whitten, 1978). It is proposed that the latter oxidizes the unsaturated membrane lipids and generates free radicals leading to membrane peroxidation and death of the plants (Haworth and Hess, 1988). Recently it has been reported that the treatment of plants with the herbicides, diphenyl ether and oxadiazon causes excess accumulation of protoporphyrin IX, the photodynamic pigment (Lydon and Duke, 1988; Becerril and Duke, 1989; Duke *et al.*, 1989). This pigment may act as sensitizer for the production of singlet oxygen in the plants leading to their death.

The primary target of the photodynamic damage should be the thylakoid membranes where most of the tetrapyrroles are localized. In the present paper, we demonstrate that the ALA induced photodynamic reactions damage the thylakoid membranes and this damage can be accomplished by exposing the ALA treated plants to light for a brief period followed by darkness.

Cucumber (*Cucumis sativus* L. CV. Pointsette) seeds were grown in petri (14.5 cm diameters) on moist germination paper at 25°C as described (Tripathy and Mohanty, 1980). Five ml of aqueous ALA solution (20 mM, pH 4) was spread on each petri plate having 6–8-day old cucumber plants. A glass sprayer (atomizer) was used for spraying ALA. After the ALA spray, the plants were kept in the dark for 15 h. The control plants were sprayed with distilled water (pH 4) and kept for the same period in dark. After 15 h of dark period, the ALA treated plants as the control plants were exposed to light ($\approx 30,000$ lux) at 25°C in a plant growth chamber (Heraeus Votsch VEPHO 5/2000). The cotyledons were harvested after a desired time period for chloroplast isolation as described before (Tripathy and Mohanty, 1980). Chlorophyll was determined according to Arnon (1969). Carotenoids were estimated according to Wellburn and Lichenthaler (1978). Protein content was estimated according to the method of Bradford (1976).

The electron transport activity through photosystem II (PSII) was monitored spectrophotometrically as well as polarographically. The spectrophotometric measurement of dichlorophenol indophenol (DCIP) photoreduction was measured at 600 nm as described before (Tripathy and Mohanty, 1980). $K_3Fe(CN)_6$ and *p*-phenylenediamine supported oxygen evolution was measured polarographically by model 53 Clark type oxygen electrode connected to a recorder (Tripathy and Mohanty, 1980). Electron transport through the whole chain of photosynthesis from H_2O to methyl viologen (MV) (O_2 uptake) was measured polarographically (Tripathy and Mohanty, 1980). The partial electron transport chain through ascorbate/DCIP to MV was also measured polarographically in terms of O_2 uptake (Tripathy and Mohanty, 1980). The Chl fluorescence induction kinetics in the dark adapted chloroplasts were measured after Renganathan and Bose (1978) using a laboratory built apparatus.

ALA, DCIP, 3-(3,4-dichlorophenyl)-1, 1-dimethyl urea (DCMU), 4-(2-hydroxyethyl)-1-piperazineethanesulfonic acid (Hepes) and NH_2OH were obtained from Sigma (USA). DPC was obtained from E. Merck (FRG).

Results

There was no damage to the ALA treated cucumber plants kept in dark for 15 h. Upon transfer to light ($\approx 30,000$ lux) the above plants wilted within 6 h and died after 36 h.

Effect of photodynamic damage on pigments and protein content

Upon exposure of ALA treated plants incubated in dark for 15 h, the leaves followed by the appearance of prominent necrotic patches. Due to desiccation the moisture content of the leaves reduced by 4–20% after 6–12 h of light exposure. The estimation of the pigment (per g fresh weight) in light exposed ALA treated plants was corrected for the decrease in fresh weight. The total Chl content was reduced by 33–49% after 4–12 h of exposure (figure 1). However, the loss of Chl *a* was higher (56%) than that of Chl *b* (30%) after 12 h of light exposure. Hence Chl *a/b* ratio decreased from 2.8 at 0 h to 1.8 after 12 h of light treatment.

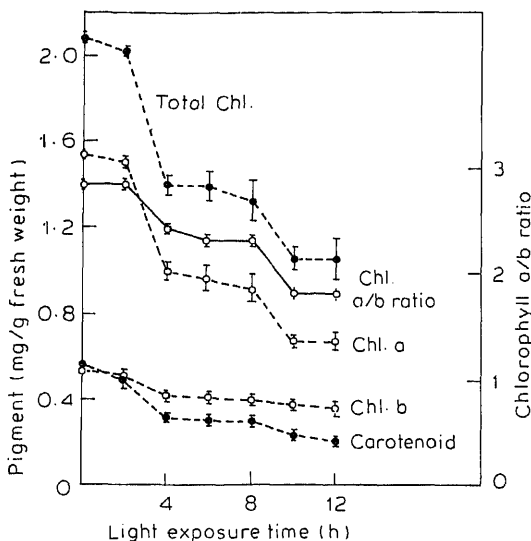


Figure 1. Effect of photodynamic damage on pigment content of the leaves as a function of time of exposure to light ($\approx 30,000$ lux) at 25°C . The error bars represent standard deviation.

carotenoid content declined by 59% after 12 h. Under identical conditions, there was no decline in Chl and carotenoid content of control plants (data not shown).

The protein content of the leaves in control plants was almost the same throughout the treatment. However, in ALA treated plants, the protein content of the leaves declined by 13–45% after 4–12 h of light exposure (figure 2). The protein content was also corrected for the decrease in fresh weight due to photodynamic damage.

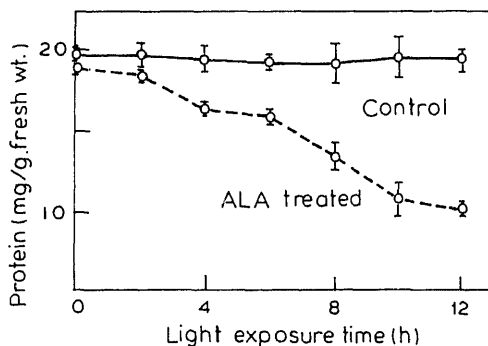


Figure 2. Effect of light exposure for various time period on protein content of control (—) and ALA treated (---) cucumber plants. The error bars represent SD.

photosystems. Table 1 shows the electron transport rate in chloroplasts isolated from control and treated plants exposed to light for 6 and 12 h. The $K_3 Fe(CN)_6$ -supported PSII dependent O_2 evolution inhibited by 35% within 6 h of exposure. After 12 h of exposure the PSII activity reduced by 70%. The PSI activity less susceptible to photodynamic damage. The PSI activity reduced by 18% after 6 and 12 h respectively. The whole-chain electron transport measured in terms of O_2 uptake reduced by 38 and 65% after 6 and 12 h of light exposure respectively.

Table 1. Effect of photodynamic damage on the photochemical reactions of the thylakoid membrane.

		T6	T12
Photochemical reactions	Control	$\mu\text{mol O}_2/\text{mg}$	Chl/h
PSII assay			
$\text{H}_2\text{O} \rightarrow \text{K}_3 \text{Fe}(\text{CN})_6$	45 ± 2	29 ± 1(35)	14 ± 1(70)
PSI assay			
$\text{DCIPH}_2 \rightarrow \text{MV}$	327 ± 14	239 ± 19(27)	199 ± 17(39)
Whole chain assay			
$\text{H}_2\text{O} \rightarrow \text{MV}$	34 ± 5	21 ± 1(38)	11 ± 1(65)

The cucumber plants sprayed with ALA were incubated in dark for 15 h. They were exposed to light ($\approx 30,000$ lux) for 6 h (T6) and 12 h (T12) at 25°C. The cotyledons were harvested immediately after the light treatment and their chloroplasts were isolated. Polarographic measurement of electron transport through PSII (O_2 evolution), PSI (O_2 uptake) and the whole chain (O_2 uptake) were measured as described before. The per cent inhibitions are given in parentheses. Each observation is the mean of 3 replicates.

The water splitting enzyme system of PSII is labile and most likely destroyed by the photodynamic damage of the thylakoid membranes. To assess if the decrease of PSII activity was only due to the impairment of the water splitting enzyme system or also due to the inactivation of PSII reaction centre, the effect of exogenous electron donors on PSII-supported DCIP reduction was measured. Mn^{2+} , DPC and NH_2OH donate electrons at the oxidizing side of PSII at different sites (Ghanotakis and Babcock, 1983; Tripathy and Mohanty, 1980). None of the above electron donors could restore the PSII mediated DCIP-photoreduction in photodynamically damaged chloroplasts (data not shown). DPC also failed to restore PSII-supported DCIP reduction in the above chloroplasts treated with ALA as before (Tripathy and Mohanty, 1980). The variable Chl a fluorescence level in chloroplasts decreased due to the photodynamic damage to the thylakoid membranes. As expected from the electron transport data the exogenous electron donors, Mn^{2+} , DPC and NH_2OH could not restore the lost variable fluorescence (data not shown).

The ALA treated plants exposed to light ($\approx 30,000$ lux) for 10–30 min did not exhibit any visual symptom of injury or any damage to the thylakoid membrane functions. Upon return of 10 min light treated plants to darkness for 12

expected, there was no damage to the thylakoid membrane functions. However, upon dark incubation of 30 min light exposed plants, the plants wilted in 8–12 h. The assay of photochemical functions revealed no inhibition of photochemical reactions after 1 h of dark treatment. The PSII, PSI and whole-chain electron transport activities damaged by 55, 50 and 27% respectively after 8 h of dark incubation (table 2). After 12 h in the dark, PSII, PSI and whole-chain electron transport rates damaged by 65, 60 and 35% respectively. The extent of above damage to the thylakoid membrane was slightly less than in continuous light treatment for 12 h.

Table 2. Post dark treatment of 30 min light exposed ALA sprayed cucumber plants.

Assay condition	Control	TO	DT1	DT8	DT12
	$\mu\text{mol O}_2/\text{mg Chl/h}$				
PSII assay					
$\text{H}_2\text{O} \rightarrow \text{K}_3\text{Fe}(\text{CN})_6$	82 ± 6	82 ± 6	80 ± 5	$37 \pm 4(54)$	$29 \pm 1(65)$
PSI assay					
$\text{DCIPH}_2 \rightarrow \text{MV}$	191 ± 20	187 ± 10	190 ± 10	$136 \pm 12(27)$	$117 \pm 8(37)$
Whole chain assay					
$\text{H}_2\text{O} \rightarrow \text{MV}$	44 ± 2	47 ± 2	48 ± 1	$23 \pm 2(50)$	$19 \pm 1(60)$

The cucumber plants sprayed with ALA were incubated in dark for 15 h. They were then exposed to light ($\approx 30,000$ lux) for 30 min (TO) followed by dark treatment of 1 h (DT1), 8 h (DT8) and 12 h (DT12). The photochemical reactions of isolated chloroplasts were measured as described before. The per cent inhibitions were calculated from TO and are given in parentheses. Each observation is the mean of 3 replicates.

Discussion

There is significant loss of Chl due to photodynamic damage. The loss of Chl a is higher than that of Chl b. The rate of Chl b degradation is also slower, which results in the progressive decrease in Chl a/b ratio. This suggests preferential loss of Chl a enriched light harvesting Chl-protein (LHCP) complex I over Chl b enriched LHCP complex II (Staehelin, 1986). The loss of protein due to photodynamic damage suggests the destruction of primary structure of protein.

The inhibition of PSII and PSI electron transport suggests that the photodynamic action damages the thylakoid membranes. PSII is more susceptible than PSI. The latter is usually more resistant to stresses such as drought, heavy metal etc. (Hsiao, 1973; Tripathy *et al.*, 1981, 1983). NH_2OH at low concentration inhibits not only water oxidizing enzyme system but also the site between Z and P680. Higher concentration of NH_2OH donates electron to PSII and its donating site is after the inhibition site between Z and P680 (Ghanotakis and Babcock, 1983). The failure of NH_2OH to donate electrons to PSII suggests that the damage occurs either to P680 or extremely close to P680.

The damage to the thylakoid membrane in the dark following sensitization by 30 min preillumination is of interest. The loss of photochemical reactions appears

on in the dark following the production of singlet oxygen in the presence of light. The extent of damage to the thylakoid membrane in the dark is slightly lower than that in continuous light treatment. This suggests that production of a certain amount of active species (singlet oxygen and free radicals) is enough to damage the thylakoid membrane. The absence of damage to the thylakoid membrane in light exposed ALA treated plants suggests that a certain threshold level of active species should be produced for the onset of photodynamic membrane damage. The mechanism of cell and plant death is under investigation.

Acknowledgement

This work was supported by the Department of Science and Technology, New Delhi.

References

- Arnon, D. I. (1949) *Plant Physiol.*, **24**, 1.
- Becerril, J. M. and Duke, S. O. (1989) *Plant Physiol.*, **90**, 1175.
- Bradford, M. M. (1976) *Anal. Biochem.*, **72**, 248.
- Duke, S. O., Lydon, J. and Paul, R. N. (1989) *Weed Sci.*, **37**, 152.
- Ghanotakis, D. F. and Babcock, G. T. (1983) *FEBS Lett.*, **153**, 231.
- Haworth, P. and Hess, F. D. (1988) *Plant Physiol.*, **86**, 672.
- Hopf, F. R. and Whitten, D. G. (1978) in *The porphyrins* (ed. D. Dolphin) (New York: Academic Press) Vol. 2, p. 161.
- Hsiao, T. C. (1973) *Annu. Rev. Plant Physiol.*, **24**, 519.
- Lydon, J. and Duke, S. O. (1988) *Pestic. Biochem. Physiol.*, **31**, 74.
- Renganathan, M. and Bose, S. (1989) *Biochim. Biophys. Acta.*, **974**, 247.
- Rebeiz, C. A., Montazer-Zouhoor, A., Hopen, H. J. and Wu, S. M. (1984) *Enzyme Microb. Technol.*, **6**, 390.
- Rebeiz, C. A., Montazer-Zouhoor, A., Mayasich, J. M., Tripathy, B. C., Wu, S. M. and Rebeiz, C. A. (1987a) *CRC Crit. Rev. Plant Sci.*, **6**, 385.
- Rebeiz, C. A., Montazer-Zouhoor, A., Mayasich, J. M., Tripathy, B. C., Wu, S. M. and Rebeiz, C. A. (1987b) in *ACS Symposium series*, No. 339 (eds J. R. Heitz and K. R. Douenun) (Washington: American Chemical Society) p. 295.
- Staelin, L. A. (1986) *Encycl. Plant Physiol.*, **19**, 1.
- Tripathy, B. C., Bhatia, B. and Mohanty, P. (1981) *Biochim. Biophys. Acta.*, **638**, 217.
- Tripathy, B. C., Bhatia, B. and Mohanty, P. (1983) *Biochim. Biophys. Acta.*, **722**, 88.
- Tripathy, B. C. and Mohanty, P. (1980) *Plant Physiol.*, **66**, 1174.
- Tripathy, B. C. and Rebeiz, C. A. (1986) *J. Biol. Chem.*, **261**, 13556.
- Tripathy, B. C. and Rebeiz, C. A. (1988) *Plant Physiol.*, **87**, 89.
- Wellburn, A. R. and Lichenthaler, H. (1984) in *Advances in photosynthesis research* (ed. C. S. Yocum) (The Hague, Boston, Lancaster: Martinus Nijhoff/Dr. W. Junk Publishers) vol. 2, p. 9.
- Witkowski, D. A. and Halling, B. P. (1988) *Plant Physiol.*, **87**, 632.

Polyvanadate acts at the level of plasma membranes through α -adrenergic receptor and affects cellular calcium distribution and some oxidation activities

T. RAMASARMA, SHARADA GULLAPALLI, VIDYA SHIVASWAMY
and C. K. RAMAKRISHNA KURUP

Department of Biochemistry, Indian Institute of Science, Bangalore 560 012, India

Abstract. The activities of calcium-stimulated respiration, calcium uptake, α -glycerophosphate dehydrogenase and rates of oxidation in state 3 and of H_2O_2 generation, were found to increase and that of pyruvate dehydrogenase decrease in mitochondria isolated from livers of rats administered intraperitoneally or perfused with polyvanadate. Phenoxybenzamine, an antagonist of α -adrenergic receptor, effectively prevented these changes. It was also found that perfusion of the liver with polyvanadate reproduced one of the best characterized events of α -adrenergic activation—stimulation of protein kinase C in plasma membrane accompanied by its decrease in cytosol. These experiments indicate for the first time the α -adrenergic mimetic action of polyvanadate.

Keywords. Polyvanadate; α -adrenergic receptor; calcium; oxidation.

Introduction

Consistent with vanadium being a micronutrient, salts of vanadate are shown to influence metabolic processes (Ramasarma and Crane, 1981; Boyd and Kustin, 1984) and to possess insulin-mimetic (Tamura *et al.*, 1984) and noradrenaline mimetic (Schawabe *et al.*, 1979) properties. These actions of vanadate are obtained through its abilities other than the well known inhibition of a variety of phosphatases, including Na, K-ATPase (Cantley *et al.*, 1977).

A role of calcium in the mechanism of action of α -adrenergic receptor system is now well-documented (Taylor *et al.*, 1987). Based on pharmacological potency and radioligand binding, the catecholamine receptors are classified as α - and β -types. While the activation of β -adrenergic receptor is now identified to act through adenylyl cyclase, cAMP and cascade of phosphorylations, the action of α -type receptor is unclear. A number of effects of glycogenolysis, gluconeogenesis, respiratory activity and phosphatidylinositol turnover obtained on treatment with noradrenaline or the agonists are considered to be due to redistribution of calcium, both extra and intracellular stores. All these effects are prevented by pretreatment with phenoxybenzamine, a general antagonist of α -adrenergic system.

We found that 3 mitochondrial activities— H_2O_2 generation, α -glycerophosphate dehydrogenase and calcium-stimulated oxygen uptake—were stimulated, and also depletion of mitochondrial calcium on treatment of rats with noradrenaline (Sivaramakrishnan and Ramasarma, 1983; Swaroop *et al.*, 1983) or vanadate (Gullapalli *et al.*, 1989a,b). These effects were prevented by phenoxybenzamine. These results suggest that vanadate can act as an agonist of α -adrenergic receptor.

Calcium-stimulated oxygen uptake, calcium redistribution and mitochondrial enzymes in polyvanadate-treated animals

A transient (about 20 s) spurt of oxygen uptake occurs when small amounts of calcium ions are added to tightly coupled mitochondria. This is accompanied by

isolated from livers of rats injected intraperitoneally with polyvanadate (4 μ mol/kg, 1 h), and also metavanadate, showed significantly higher rates of this activity than the net oxygen uptake (table 1). This increase was prevented by pretreatment with phenoxybenzamine, but not propranolol or in sympathectomized rats (table 1). These results suggested that polyvanadate is acting through α -adrenergic receptors and probably not *via* increasing endogenous noradrenaline.

The increase in calcium-stimulated respiration is an indication of depletion of calcium from mitochondria. On measuring the distribution of calcium in mitochondrial and cytosolic fractions obtained by differential centrifugation in sucrose medium or rapidly in percoll gradient, decrease in mitochondrial calcium and increase in cytosol were demonstrated (table 1). The redistribution pattern was further confirmed by increase of ^{45}Ca -uptake in mitochondria with corresponding decrease in cytosol (table 1).

Table 1. Effect of treatment with vanadate on calcium redistribution and mitochondrial activities.

	Control	Vanadate	% control
Ca²⁺-stimulated oxygen uptake			
Polyvanadate (PV)	7.3 \pm 1.0	13.1 \pm 1.5	179
Metavanadate	7.4 \pm 1.2	13.2 \pm 2.5	178
PV + phenoxybenzamine	7.5 \pm 0.8	7.2 \pm 1.5	96
PV + propranolol	5.0 \pm 1.6	10.1 \pm 2.2	202
PV in sympathectomy	6.9 \pm 1.1	11.0 \pm 0.9	159
Calcium distribution			
Mitochondrial (sucrose)	17.7 \pm 1.5	11.3 \pm 0.4	63
Cytosolic (sucrose)	9.1 \pm 1.6	14.1 \pm 2.6	154
Mitochondrial (percoll)	18.9 \pm 2.0	9.7 \pm 1.8	51
Cytosolic (percoll)	11.9 \pm 1.4	19.7 \pm 2.4	168
^{45}Ca-uptake			
Mitochondrial	30.8 \pm 1.4	40.3 \pm 0.6	130
Cytosolic	33.8 \pm 2.8	21.6 \pm 0.7	63
Mitochondrial enzymes			
State 3 respiration (succinate)	92 \pm 10	125 \pm 16	136
+ phenoxybenzamine	100 \pm 4	96 \pm 15	96
α -Glycerophosphate dehydrogenase	11.6 \pm 2.1	17.7 \pm 2.4	152
+ phenoxybenzamine	14.7 \pm 1.5	13.3 \pm 1.4	90
Pyruvate dehydrogenase	10.8 \pm 1.5	5.3 \pm 0.9	49
+ phenoxybenzamine	12.7 \pm 4.2	11.3 \pm 3.2	83
H ₂ O ₂ generation (succinate)*	0.12 \pm 0.03	0.20 \pm 0.03	167

The experimental details are given in Gullapalli *et al.* (1989a,b). Polyvanadate (or metavanadate) was given intraperitoneally at a dose of 4 μ mol/rat, 1 h before killing and livers were processed for various estimations. Where mentioned, phenoxybenzamine (2.5 mg/rat) or propranolol (1.7 mg/rat) was given 20 min before polyvanadate.

*Experiments with phenoxybenzamine in this case were not done.

The mitochondrial enzyme activities of state 3 respiration with succinate as substrate, α -glycerophosphate dehydrogenase and succinate-dependent

generation increased and that of pyruvate dehydrogenase decreased on vanadate treatment (table 1). These changes were also obtained on treatment with noradrenaline and were sensitive to pretreatment with phenoxybenzamine, pointing to the participation of α -adrenergic receptor.

Experiments on perfusion with polyvanadate confirm direct action on liver tissue

Perfusion of livers at slow rates with unbuffered 0.25 M sucrose ensured removal of blood from the organ without affecting the structural integrity of subcellular organelles and avoided any possible salt effects. Perfusion of livers with a medium containing 100 μ M of polyvanadate for short periods of 5–10 min gave effects similar to the experiments with intraperitoneal administration. Polyvanadate, but not metavanadate, increased calcium-stimulated oxygen uptake and this effect was sensitive to phenoxybenzamine, but not propranolol (table 2).

Table 2. Effect of perfusion of livers with polyvanadate on calcium distribution, mitochondrial activities and protein kinase C.

	Control	Polyvanadate	% control
A. Ca^{2+}-stimulated oxygen uptake			
	ng atom O/mg protein		
Polyvanadate (PV)	8.2 \pm 0.9	11.8 \pm 1.4	144
Metavanadate	7.1 \pm 1.0	7.0 \pm 1.3	99
PV + phenoxybenzamine	7.3 \pm 0.7	7.3 \pm 0.8	100
PV + propranolol	8.2 \pm 0.8	11.5 \pm 1.0	140
B. Mitochondrial enzymes			
	nmol/min/mg protein		
State 3 respiration (succinate)	87 \pm 9	82 \pm 5	95
+ phenoxybenzamine	87 \pm 8	85 \pm 9	98
α -Glycerophosphate dehydrogenase	13.5 \pm 1.2	21.3 \pm 2.3	158
+ phenoxybenzamine	15.1 \pm 1.4	14.4 \pm 2.4	95
Pyruvate dehydrogenase	6.3 \pm 0.4	3.2 \pm 1.0	51
C. Protein kinase C			
	pmol/min/mg protein		
Plasma membrane	27 \pm 6	165 \pm 20	611
+ Phenoxybenzamine	13 \pm 4	11 \pm 2	84
+ Propranolol	17 \pm 8	125 \pm 12	735
Cytosol	132 \pm 22	19 \pm 2	14
+ Phenoxybenzamine	116 \pm 21	121 \pm 25	104
+ Propranolol	97 \pm 27	11 \pm 3	11

The livers were perfused with 100 μ M polyvanadate (or metavanadate) in 0.25 M sucrose for 10 min in experiments A and B and for 5 min in experiment C. The experimental details are given in Gullapalli *et al.* (1988a,b, 1990). Where mentioned, the blocking agents were present in the perfusion medium at a concentration of 70 μ g/ml. Protein kinase C activity is measured by the transfer of [γ - 32 P]-ATP to histone H₁ in the presence of Ca^{2+} , phosphatidyl serine and diglyceride.

Of the mitochondrial enzyme activities, state 3 respiration with succinate as the substrate did not respond to polyvanadate perfusion, unlike intraperitoneal experiments. Phenoxybenzamine-sensitive increase in α -glycerophosphate dehydrogenase and decrease in pyruvate dehydrogenase were reproduced (table 2).

Increase in plasma membrane and decrease in cytosol of the activity of calcium- and lipid-dependent protein kinase C are the well-characterized effects of activation of α -adrenergic receptor (Kikkawa and Nishizuka, 1986). On perfusion for 5 min, polyvanadate mimicked these effects apparently acting as an α -adrenergic agonist (table 2). Phenoxybenzamine prevented the changes of both the increase in plasma membrane and decrease in cytosol of protein kinase C while propranolol was unable to do so (table 2). These changes in protein kinase C activity are consistent with a plasma membrane-level of action of polyvanadate similar to that of an α -adrenergic agonist (Gullapalli *et al.*, 1990).

Polyvanadate must be acting at the level of plasma membrane

One other compelling reason to believe plasma membrane level of action is the finding that vanadium could not be detected in the liver tissue by atomic absorption spectroscopic analysis under the experimental conditions used. Addition of polyvanadate to mitochondria *in vitro* did not elicit similar results. One interesting difference with vanadate treatment is the lack of mobilization of calcium from endoplasmic reticulum (Taylor *et al.*, 1987). It appears that the accumulation of calcium in cytosol is due to inhibition of calcium pump by vanadate (Delfert and McDonald, 1985). The effects on redistribution of calcium and other redox enzymes appear to be indirect and the intracellular mechanism responsible must be generated by activation of the α -adrenergic receptor.

We tested the effect of vanadate treatment on incorporation of ^{32}P (100 μCi , intraperitoneally 1 h before vanadate) into inositol phosphatides (PIP2, PIP3, and phosphatidic acid) and found little change in the pattern (data not shown), indicating that their altered turnover was not involved. Some other mechanism of signal transduction may be utilized in vanadate action.

Vanadate-stimulated NADH oxidation in plasma membranes

An example of a polyvanadate-specific activity in plasma membranes is NADH oxidation discovered in our laboratories (Ramasarma *et al.*, 1981; Vijayaraj *et al.*, 1984). The properties of this system in rat liver plasma membranes are summarized in table 3. This activity will generate H_2O_2 with high rates and can be turned on only if vanadate is converted to the polymeric form by local acid conditions. It is possible to obtain by proton gradients. Independently it appears vanadate in this system can generate hydroxyl radicals as the ESR spectra of DMPO-OH radical adduct.

Table 3. Vanadate-stimulated NADH oxidation in rat liver plasma membrane.

Specific to NADH, K_m 36 μM ; low activity with NADPH
Stoichiometry of $\text{NADH}:\text{O}_2:\text{H}_2\text{O}_2$ is 1:1:1; rapid generation of H_2O_2
Phosphate (50 mM) is required for maximal activity
Activity increases in acid pH up to 5.0
Decavanadate, a polymeric form of vanadate produced in acid pH, is most active
maximal activity obtained at 5 μM (V_{10})
Hydroxyl radicals are produced during reaction

The activity of NADH oxidation was measured by the decrease in absorbance at 340 nm. The experimental details are given in Ramasarma *et al.* (1981).

identified by us earlier (Vijaya *et al.*, 1984) are now considered to be due to hydroxyl radicals but not superoxide (Kuppusamy and Zweir, 1989). Will some of the vanadate-specific reactions occur on using H_2O_2 or hydroxyl radicals as secondary signals?

In this context it is interesting to recall some related effects of vanadate and H_2O_2 such as insulin mimetic action (Tamura *et al.*, 1984), insulin receptor protein-tyrosine phosphorylation (Haffetz and Zick, 1989), selective activation and inactivation by H_2O_2 of protein-kinase C (Gopalakrishna and Anderson, 1989).

Comparison of effects and structures of noradrenaline and decavanadate

We have been able to identify that a number of metabolic effects obtained by vanadate are similar to that by noradrenaline (Sivaramakrishnan and Ramasarma, 1983; Swaroop *et al.*, 1983). Among these are increases in calcium stimulated oxygen uptake in mitochondria, calcium concentration in cytosol, α -glycero-phosphate dehydrogenase and H_2O_2 generation in mitochondria (Gullapalli *et al.*, 1989a,b) and protein kinase C in plasma membrane, and also decreases of calcium concentration and pyruvate dehydrogenase in mitochondria and of protein kinase C in cytosol. All these effects appear to be mediated by α -adrenergic receptor, possibly the α_1 -type, albeit not necessarily through inositol phosphatides. The effective form of vanadate is believed to be decavanadate ($\text{V}_{10}\text{O}_{28}^{6-}$) which

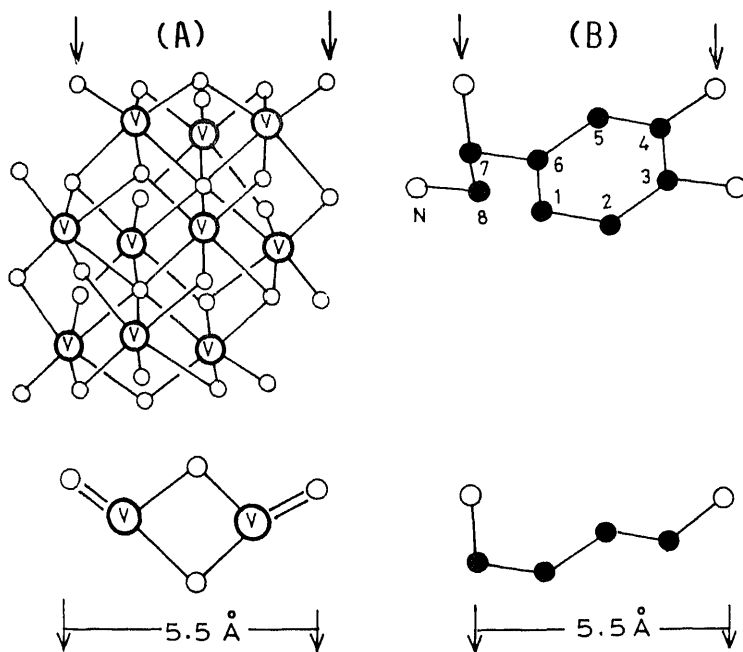


Figure 1. Comparison of structures of decavanadate (A) and noradrenaline (B). The structures were adapted from Debaerdemaeker *et al.* (1982) and Carlstrom and Bergin (1967) for decavanadate and noradrenaline, respectively. The pair of oxygens marked by arrows are at an approximate distance of 5.5 Å as shown in the abstracted portions shown below each structure and offer a common feature.

acquires on polymerization the characteristic structural feature $\text{O}=\text{V}-\text{O}$ which seems to account for the 985 cm^{-1} IR band and a 3 banded NMR spectrum. It is difficult to explain how a simple inorganic polymer with nothing more than phosphate groups can stimulate actions of a catecholamine. On comparison of the structures of decavanadate (Debaerdemaeker *et al.*, 1982) and noradrenaline (Carlstrom and Bergin, 1967), already available in literature, we found the presence of two oxygens at a distance of 5.5 \AA (figure 1). Will these positioned oxygens be responsible for ionic or H-bonded interactions with a similarly positioned counter-atoms in a plasma membrane protein? Do the different activation responses of polyvanadate have a common transducing mechanism? Will H₂O₂ and hydroxyl radicals be used as signal transducers in the redistribution of calcium? protein kinase C? Investigations on these and other questions will unravel the multifaceted biological functions of vanadate.

Acknowledgement

Financial assistance from the Department of Science and Technology, New Delhi is acknowledged.

References

- Boyd, D. W. and Kustin, K. (1984) *Adv. Inorg. Biochem.*, **6**, 311.
- Cantley, L. C. Jr., Josephson, L., Warner, R., Vanagisawa, M., Lechene, C. and Guidotti, C. (1989) *J. Biol. Chem.*, **264**, 7421.
- Carafoli, E. and Sottocasa, G. (1984) *Bioenergetics* (Amsterdam: Elsevier)
- Carlstrom, D. and Bergin, R. (1967) *Acta. Crystallogr.*, **23**, 313.
- Debaerdemaeker, T., Arrieta, J. M. and Amigo, J. M. (1982) *Acta. Crystallogr.*, **B38**, 2465.
- Delfert, D. M. and McDohald, J. M. (1985) *Arch. Biochem. Biophys.*, **241**, 665.
- Gopalakrishna, R. and Anderson, W. B. (1989) *Proc. Natl. Acad. Sci. USA*, **86**, 6758.
- Gullapalli, S., Shivaswamy, V., Ramasarma, T. and Ramakrishna Kurup, C. K. (1989a) *Biochem. Biophys.*, **26**, 227.
- Gullapalli, S., Shivaswamy, V., Ramasarma, T. and Ramakrishna Kurup, C. K. (1989b) *Mol. Biochem.*, **90**, 155.
- Gullapalli, S., Ramakrishna Kurup, C. K. and Ramasarma, T. (1990) *FEBS Lett.*, **267**, 93.
- Haffetz, D. and Zick, Y. (1989) *J. Biol. Chem.*, **264**, 10126.
- Kikkawa, U. and Nishizuka, Y. (1986) *Annu. Rev. Cell. Biol.*, **2**, 149.
- Kuppusamy, P. and Zweir, J. L. (1989) *J. Biol. Chem.*, **264**, 9880.
- Ramasarma, T. and Crane, F. L. (1981) *Curr. Top. Cell. Regul.*, **20**, 248.
- Ramasarma, T., Mackellar, W. and Crane, F. L. (1981) *Biochim. Biophys. Acta*, **646**, 88.
- Schawabe, U., Puchstein, C., Hannemann, H. and Sochtig, E. (1979) *Nature (London)*, **277**, 143.
- Sivaramakrishnan, S. and Ramasarma, T. (1983) *Indian J. Biochem. Biophys.*, **20**, 16.
- Swaroop, A., Patole, M. S., Puranam, R. S. and Ramasarma, T. (1983) *Biochem. J.*, **214**, 745.
- Tamura, S., Brown, T. A., Whipple, J. H., Yaaguchi, Y. F., Dubbler, R. E., Cheng, K. and Iversen, P. W. (1984) *J. Biol. Chem.*, **259**, 6650.
- Taylor, W. M., Reinhart, P. H. and Bygrave, F. L. (1987) *The role of calcium in drug action* (Pergamon Press).
- Vijaya, S., Crane, F. L. and Ramasarma, T. (1984) *Mol. Cell. Biochem.*, **62**, 175.

Membrane lipid peroxidation by ultrasound: Mechanism and implications

A. K. JANA, S. AGARWAL and S. N. CHATTERJEE*

Biophysics Division, Saha Institute of Nuclear Physics, 37 Belgachia Road, Calcutta 700 037, India

Abstract. Ultrasonic radiation produced a dose-dependent linear increase in lipid peroxidation in the liposomal membrane as reflected in the measurement of conjugated dienes, lipid hydroperoxides and malondialdehydes. Ultrasound induced malondialdehyde production could not be inhibited by any significant degree by superoxide dismutase or histidine or dimethyl furan but was very significantly inhibited by butylated hydroxytoluene, cholesterol, sodium benzoate, dimethyl sulphoxide, sodium formate and EDTA. The scavenger studies indicated the functional role of hydroxyl radicals in the initiation of ultrasound induced lipid peroxidation.

Keywords. Ultrasound; liposomes; lipid peroxidation; hydroxyl radicals; scavengers.

Introduction

Ultrasound is being increasingly used in biology and medicine for clinical diagnosis, physiotherapy and also in hyperthermic cancer therapy (Kremkau, 1979). The biophysical effects of ultrasound in aqueous solutions can be classified as thermal effects, cavitation and the direct effects (Hill, 1968). The thermal effects of ultrasound are utilized for hyperthermia. The effects of its non-thermal modes of action have not been investigated. Although degradation of DNA in aqueous solution and breaking of cells are induced by ultrasound mostly by shearing stress of cavitation (Coakley and Nyborg, 1978), the chemical effects of free radicals produced during collapse of ultrasound induced cavitation bubbles have mostly remained unexplored. In the context of the important and increasing use of ultrasound and in view of the advantages offered by liposomal systems (Chatterjee and Agarwal, 1988) in the study of free radical-mediated membrane damage, this study has used liposomes to show that ultrasound induces a free radical-mediated and dose-dependent lipid peroxidation. Preliminary results were published elsewhere (Jana *et al.*, 1986).

Materials and methods

Multilamellar liposomes were prepared using egg lecithin (obtained from V. P. Chest Institute, Delhi) by the method described earlier (Chatterjee and Agarwal, 1988). Liposomes in the presence or in absence of scavengers/quenchers were exposed to 20 KHz ultrasound (Labsonic 1510, Braun, Melsungen AG, Germany) by the method of Jana *et al.* (1986). Ultrasound dose rate was measured by Fricke Dosimetry (Fricke and Hart, 1966). Ultrasound induced lipid peroxidation was estimated by the simultaneous measurement of malondialdehyde (MDA),

conjugated dienes and hydroperoxide by the method of Chatterjee and (1988). Electron microscopy of liposomes, sonicated or non-sonicated, was the negative staining technique (Banerjee and Chatterjee, 1983).

Results

Figure 1A shows the electron micrograph of the nonirradiated liposomes illustrating the presence of multi bilayers of lipid. After exposure to ultrasound dose 913 J/m^2 the liposomes got fragmented as evident in figure 1B. Many small spherules (presumably unilamellar liposomes) of diameter $\approx 300\text{ \AA}$ are seen in figure 1B as fragmentation products. Exposure of liposomal suspension to ultrasound radiation (20 KHz) caused free radical-mediated lipid peroxidation as estimated by measurement of at least 3 reaction products, viz., conjugated dienes, lipid hydroperoxides and MDA. A linear dose-effect relation was observed in figure 2. Production of MDA was confirmed by spectrophotometric and spectrofluorometric methods including the detection of the excitation (360 nm) and emission (435 nm) maxima characteristic of MDA-glycine adduct formation. Addition of glycine in the system. Different radical scavengers, antioxidants and quenchers were introduced one by one and their effects on the ultrasound induced lipid peroxidation were noted. The use of different radical scavengers and antioxidants did not change the nature of the dose-response relation but significantly the slope of the line thereby indicating significant inhibition of lipid peroxidation reaction. Table 1 shows the values of maximum inhibition of lipid peroxidation by the different inhibitors used and the corresponding inhibitor concentrations. Cholesterol and butylated hydroxy toluene produced maximum inhibition (90%), dimethyl sulphoxide (DMSO) and sodium benzoate produced about 80% inhibition of ultrasound induced lipid peroxidation. Sodium formate also produced comparatively less but very significant inhibition (64%) of lipid peroxidation. Histidine, dimethylfuran and superoxide dismutase (SOD) did not produce any significant inhibition of the ultrasound induced lipid peroxidation.

Discussion

This study has thus shown that ultrasonic radiation can cause lipid peroxidation of the liposomal membrane and that the yield was significantly reduced by the addition of antioxidant, BHT, OH^* radical scavenger, sodium formate, metal ion chelator EDTA and cholesterol. Also, all the 3 reaction products of lipid peroxidation, viz., conjugated dienes, lipid hydroperoxides and MDA, were detected in the ultrasound exposed liposomal membrane. The ultrasound induced lipid peroxidation appeared to be the result of free radicals and oxygen mediated chain reaction (Chatterjee and Agarwal, 1988) and which basically involves the following steps: (i) abstraction of hydrogen atom, (ii) formation of lipid free radical (R^*), (iii) reaction of lipid-peroxyl free radical (ROO^*), (iv) formation of lipid hydroperoxide and (v) formation of conjugated dienes.

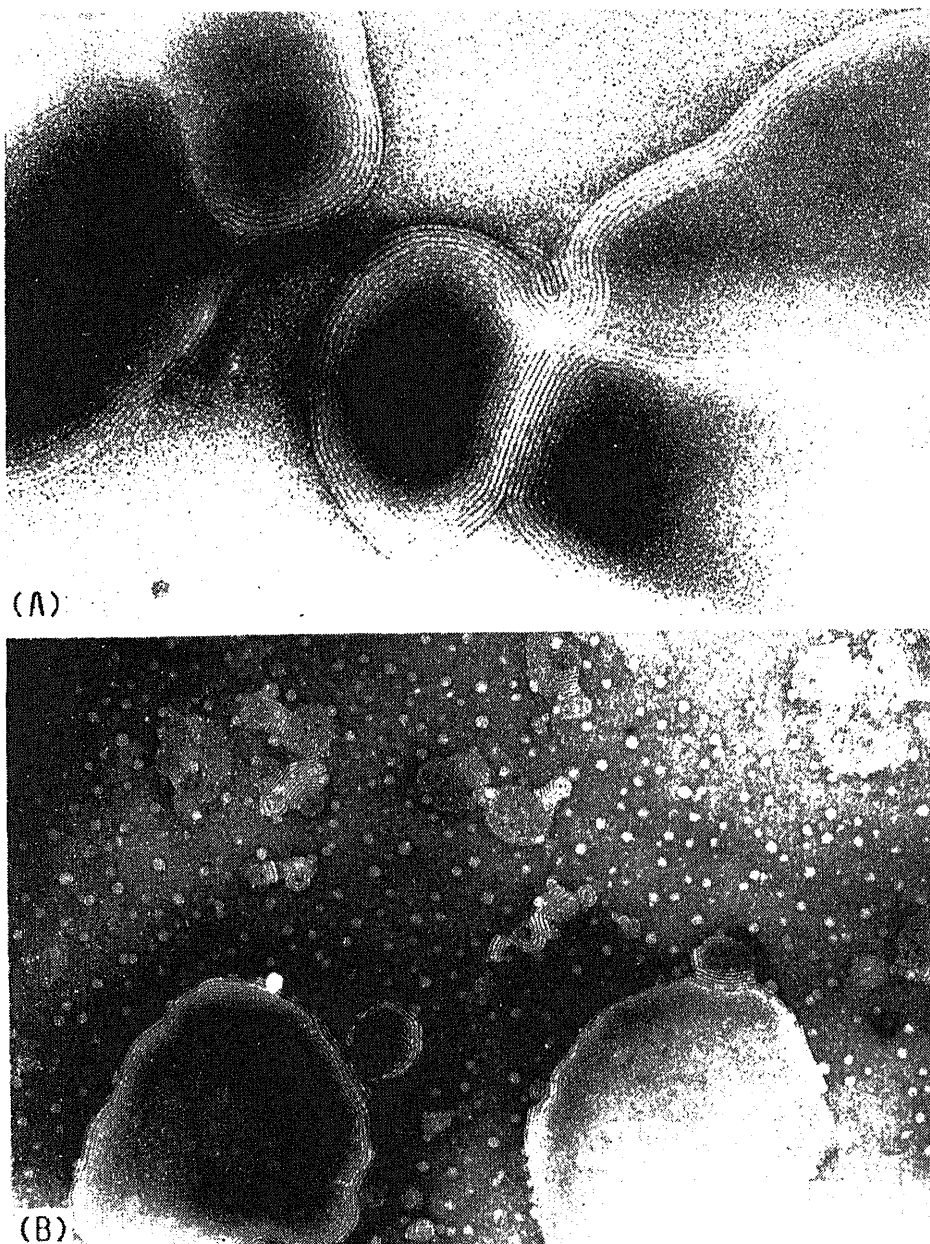


Figure 1. Egg lecithin liposomes negatively stained with PTA. (A), Nonirradiated ($\times 150,000$) and (B), irradiated with ultrasound of dose 913 J/m^2 ($\times 65,600$).

using any one of the assay methods may easily be misleading. With a view to obtaining greater confidence 3 reaction products, e.g., conjugated dienes, hydroperoxides and MDA, were assayed in parallel in this study. It is of interest to note that all the 3 methods of assay presented similar dose-dependent pattern of ultrasound induced lipid peroxidation.

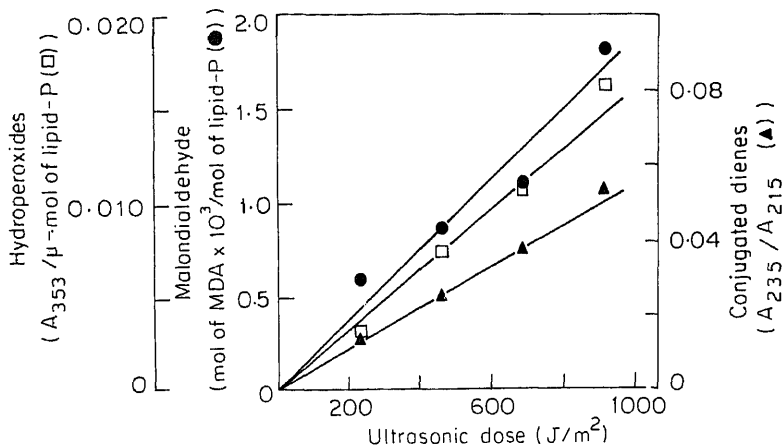


Figure 2. Increase in the production of conjugated dienes (A_{235}/A_{215} , ▲), hydroperoxides ($A_{353}/\mu\text{mol}$ of lipid-P, □) and MDA (●) in the liposomal membrane with increasing of ultrasound (dose rate $7.61 \text{ J/m}^2/\text{s}$).

Table 1. Inhibition of ultrasound-induced lipid peroxidation.

Additions	Malonaldehyde content (mol of MDA $\times 10^3$ /mol lipid-P)	Inhibition
Liposome + ultrasound of dose 913 J/m^2 (control)	1.94	—
Control + cholesterol (1 mol/mol lipid-P)	0.136	93
Control + BHT (0.41 mol/mol lipid-P)	0.233	88
Control + sodium benzoate (1.67 mol/mol lipid-P)	0.388	80
Control + DMSO (27.59 mol/mol lipid-P)	0.407	79
Control + sodium formate (14.22 mol/mol lipid-P)	0.698	65
Control + EDTA (1.35 mol/mol lipid-P)	0.698	65
Control + SOD (44.77 units/ μmol lipid-P)	1.878	3
Control + DMF (4.57 mol/mol lipid-P)	1.9	2
Control + L-histidine (1.44 mol/mol lipid-P)	1.949	2

In a preliminary report (Jana *et al.*, 1986) we have shown evidence for the involvement of OH^* radicals as the initiator of ultrasound-induced lipid peroxidation. This study has presented additional evidence in confirmation of our report. Although the production of OH^* radicals and hydrogen atoms in aqueous media by ultrasound of different frequencies was demonstrated by electron spin resonance and spin trapping studies (Makino *et al.*, 1983; Edmonds and Samson 1983), these demonstrations do not necessarily prove the functional role of these radicals (Valenzano, 1987). To determine a functional role, experiments aimed at demonstrating modulation of the reactants by use of radical scavengers are appropriate (Valenzano, 1987) and have been widely used (Chatterjee and Aggarwal 1988). In this study, no significant inhibition of lipid peroxidation resulted by SOD or histidine or DMF. The involvement of superoxide radicals (O_2^-) or singlet oxygen ($^1\text{O}_2$) in the ultrasound-induced lipid peroxidation thus appears unlikely. BHT and cholesterol produced nearly 90% inhibition of lipid peroxidation. B

a nonspecific scavenger of lipid free radicals (Chatterjee and Agarwal, 1988) and hence no specific information could be derived there from about the initiation mechanism. The role of cholesterol in the inhibition of lipid peroxidation has been debated by many investigators and several possible mechanisms were suggested (Szebeni and Toth, 1986). However, none of the mechanisms suggested are so specific as to suggest the involvement of any particular radical in the initiation of lipid peroxidation. On the other hand, each one of the agents, sodium formate, sodium benzoate, DMSO and EDTA, produced significant inhibition of ultrasound induced lipid peroxidation. Sodium formate, sodium benzoate and DMSO are already known as scavengers of OH* radicals (Chatterjee and Agarwal, 1988). EDTA is known to inhibit metal catalyzed lipid peroxidation (Tien *et al.*, 1982), although under some circumstances EDTA was also reported to stimulate lipid peroxidation (Tien *et al.*, 1982). On the other hand, EDTA is also known to act as a good quencher of OH* radicals (Blazek and Peak, 1988). Although the exact role of EDTA in the present case may be debated, parallel use of these agents, sodium formate, sodium benzoate, DMSO and EDTA, lends greater support to the finding that OH* radical is involved in the ultrasound induced lipid peroxidation.

This study has thus shown that OH* radicals are involved in the initiation of ultrasound-induced lipid peroxidation. Considerable evidence has by now accumulated to indicate that the products of lipid peroxidation are toxic, mutagenic and carcinogenic (Pryor, 1976; Yagi, 1982; Chatterjee and Agarwal, 1988). In view of the wide use of ultrasound in human diagnosis and therapy, the present finding should have wider and important relevance and should sound a note of caution against indiscrete use of this radiation.

References

- Banerjee, S. and Chatterjee, S. N. (1983) *Z. Naturforsch.*, **38c**, 302.
 Blazek, E. R. and Peak, M. J. (1988) *Int. J. Radiat. Biol.*, **53**, 237.
 Chatterjee, S. N. and Agarwal, S. (1988) *Free Radical Biol. Med.*, **4**, 51.
 Coakley, W. T. and Nyborg, W. L. (1978) in *Ultrasound: Its applications in medicine and biology* (ed. F. J. Fry) (Amsterdam: Elsevier) p. 77.
 Edmonds, P. D. and Sancier, K. M. (1983) *Ultrasound Med. Biol.*, **9**, 635.
 Fricke, H. and Hart, E. J. (1966) in *Radiation dosimetry* (eds F. H. Attix and W. C. Roesch) (New York: Academic Press) vol. 2, p. 167.
 Hill, C. R. (1968) *Br. J. Radiol.*, **41**, 561.
 Jana, A. K., Agarwal, S. and Chatterjee, S. N. (1986) *Radiat. Environ. Biophys.*, **25**, 309.
 Kremkau, F. W. (1989) *J. Clin. Ultrasound*, **7**, 287.
 Makino, K., Mossaba, M. M. and Riesz, P. (1983) *J. Phys. Chem.*, **87**, 1369.
 Pryor, W. A. (1976) *Free radicals in biology*, volumes 1-5 (New York: Academic Press).
 Szebeni, J. and Toth, K. (1986) *Biochim. Biophys. Acta*, **857**, 139.
 Tien, M., Morehouse, L. A., Bucher, J. R. and Aust, S. D. (1982) *Arch. Biochem. Biophys.*, **218**, 450.
 Valenzano, D. P. (1987) *Photochem. Photobiol.*, **46**, 147.
 Yagi, K. (1982) *Lipid peroxides in biology and medicine* (New York: Academic Press).

Dephosphorylation of cell-surface phosphoproteins of goat spermatozoa

M. BARUA and G. C. MAJUMDER

Indian Institute of Chemical Biology, 4, Raja S. C. Mullick Road, Jadavpur, Calcutta 700 032, India

Abstract. Multiple ecto-phosphoproteins of the goat cauda-epididymal intact spermatozoa have been shown to undergo dephosphorylation *in vitro* by endogenous phosphoprotein phosphatase(s) located on the sperm outer surface. The major ecto-phosphoproteins that are dephosphorylated have molecular masses of 27, 40, 70, 116 and 205 kDa. The cell surface dephosphorylation reaction is not dependent on bivalent metal ions. Mg^{2+} (5 mM), Mn^{2+} (5 mM), orthovanadate (200 μ M) and cAMP (5 μ M) have no effect on this surface reaction whereas it is inhibited nearly 50% by Co^{2+} or Zn^{2+} (1 mM). Spermidine (5 mM), or Ca^{2+} (1 mM) inhibited to a small extent (approx. 25%) the cell surface dephosphorylation of proteins.

Keywords. Ecto-protein; spermatozoa; phosphoproteins; protein dephosphorylation; proteinphosphatase; cell-surface.

Introduction

Phosphoproteins have been demonstrated on the surface of the mammalian cells and they have been implicated to have important role in regulating cell functions (Majumder and Turkington, 1972; Rubin and Rosen, 1973; Uno *et al.*, 1977; Kübler *et al.*, 1982; Blackshear *et al.*, 1988). Goat epididymal spermatozoa possess a cAMP-independent protein kinase (CIK) on the outer cell surface that causes phosphorylation of multiple endogenous ecto-phosphoproteins of the intact cells (Haldar and Majumder, 1986). A phosphoprotein phosphatase (PPase) has also been demonstrated on the sperm outer surface that causes dephosphorylation of exogenous [^{32}P]labelled proteins such as histones, protamine, casein and phosvitin (Barua *et al.*, 1985; Barua and Majumder, 1987). Several lines of evidence have been provided to show that the observed ecto-PPase activity is not due to leaky/damaged spermatozoa (Barua *et al.*, 1985; Haldar and Majumder, 1986; Barua and Majumder, 1987). The specific activity of ecto-PPase was markedly higher in the intact forward-motile spermatozoa than the composite cells from where the former cells were isolated, suggesting thereby that the ecto-enzyme may have an important role in regulating sperm motility (Barua and Majumder, 1987). Recently it has been observed that the ecto-phosphoprotein(s) of the intact sperm undergo dephosphorylation by the endogenous ecto-PPase (Barua *et al.*, 1990). The present study describes some characteristics of the sperm ecto-PPase(s) and identifies their physiological substrates located on the sperm surface. The present study shows that the sperm ecto-PPase is capable of dephosphorylating multiple sperm ecto-phosphoproteins.

cAMP, ATP (horse muscle), sodium dodecyl sulphate (SDS), spermidine, and SDS-marker proteins (cross-linked haemoglobins and albumins, SDS-70L and 200) were obtained from Sigma Chemical Company, St. Louis, Missouri. Spermatozoa were extracted from the goat cauda-epididymides within 2–4 h after slaughter of the animals in the local slaughter houses. [γ - 32 P]ATP was prepared as described earlier (Majumder and Biswas, 1979).

Isolation of epididymal spermatozoa

Highly motile spermatozoa were extracted from goat cauda-epididymides in medium A (119 mM NaCl, 5 mM KCl, 1.2 mM MgSO₄, 10 mM glucose, 16 mM K-phosphate, pH 6.9 and 50 U/ml penicillin) as described earlier (Barua, 1985). Spermatozoa were sedimented at 500 *g* for 5 min at room temperature (29 ± 2°C) and the pellet was washed twice with medium A. The washed cells were finally dispersed in the same medium.

Dephosphorylation of sperm outer surface proteins

The sperm outer surface phosphoproteins were phosphorylated by the endogenous spermatozoal kinase (ecto-CIK (Haldar and Majumder, 1986) prior to estimating the degree of dephosphorylation of the surface proteins by the intact-cell ecto-PPase. Spermatozoa (15–30 × 10⁷ cells) were incubated with 75 nmol of [γ - 32 P]ATP (approx. 2 × 10⁷ cpm), 30 μ mol of MgCl₂, 3 μ mol of EGTA in a total volume of 1 ml of medium A. Incubation was carried out at 37°C for 3 min and the kinase reaction was arrested with 5 mM non-radioactive ATP. Spermatozoa were sedimented immediately by low speed centrifugation and the cells were washed with medium A. The medium which is same as medium A except that it is buffered with 20 mM HCl, pH 7.2 rather than K-phosphate. The [32 P]labelled cells were finally dispersed in RTS medium and immediately incubated at 37°C for 10 min for dephosphorylation reaction. The reaction was stopped with the addition of 5% 10% trichloroacetic acid (TCA) and the protein precipitates were processed for assay of [32 P]radioactivity (Haldar and Majumder, 1986). One zero-min time point after the dephosphorylation reaction served as control showing initial total radioactivity of the sperm ecto-proteins. The degree of dephosphorylation of sperm ecto-proteins was measured by estimating the amount of loss of [32 P] from the cell surface proteins.

Analysis of sperm ecto-phosphoproteins which undergo dephosphorylation

The intact-sperm ecto-proteins were first phosphorylated by the ecto-CIK and then dephosphorylated by the ecto-PPase as described above. As shown earlier (Haldar and Majumder, 1986) under this condition of protein kinase reaction, only the sperm outer surface proteins undergo phosphorylation (Haldar and Majumder, 1986). The TCA-precipitated

the [^{32}P]labelled proteins were collected and washed with 5% TCA. The protein pellet was dissolved in SDS-sample buffer and centrifuged in an Eppendorf centrifuge for 15 min. Protein contents of the resulting supernates were estimated according to Bensadoun *et al.* (1976). The [^{32}P]labelled proteins were analysed by gel electrophoresis and autoradiography (Haldar, 1988). The labelled proteins were subjected to 10% SDS-polyacrylamide gel electrophoresis (Laemmli, 1970). Duplicate gels were run for each sample. One gel was stained with Coomassie blue whereas the other was subjected to fluorographic treatment, dried in an automatic gel dryer and finally exposed to X-ray film for autoradiography. Marker proteins: myosin (205 kDa), β -galactosidase (116 kDa), phosphorylase b (97 kDa), bovine serum albumin (66 kDa), ovalbumin (45 kDa) and carbonic anhydrase (29 kDa), were also electrophoresed side by side.

Results

The intact spermatozoa with the [^{32}P]labelled proteins on the outer cell surface, have been found to lose radioactivity when incubated at 37°C. Analysis of the [^{32}P]labelled products of incubation of the labelled cells, in the TCA-soluble fraction by paper electrophoresis (Barua and Majumder, 1987) showed that ^{32}Pi is released from the surface protein(s) indicating that the sperm ecto-PPase(s) cause dephosphorylation of the ecto-phosphoprotein(s) (Barua *et al.*, 1990).

As shown in table 1, the sperm ecto-PPase is not dependent on any bivalent metal ions for its activity to cause dephosphorylation of the surface proteins. Mg^{2+} or Mn^{2+} (5 mM) had little effect on the PPase activity. However, Co^{2+} or Zn^{2+} (1 mM) caused nearly 45% inhibition of the enzymic activity whereas Ca^{2+} at 5 mM level inhibited approx. 40% of the dephosphorylation reaction, and all these metal ion-mediated inhibitions were statistically significant ($P < 0.05$). cAMP (5 μM)

Table 1. Effect of various reagents on the dephosphorylation of intact-sperm ecto-proteins by the endogenous ecto-PPase.

Exp.	Additions	^{32}Pi liberated from protein (pmol) Mean \pm SEM
I	Nil (Control)	2.5 \pm 0.4
	+ cAMP, 5 μM	2.4 \pm 0.3
	+ Sodium orthovanadate, 200 μM	2.3 \pm 0.7
	+ Spermidine, 5 mM	1.8 \pm 0.1
II	Nil (Control)	1.8 \pm 0.3
	+ MgCl_2 , 5 mM	1.7 \pm 0.3
	+ CaCl_2 , 1 mM	1.4 \pm 0.3
	+ CaCl_2 , 5 mM	1.1 \pm 0.2
	+ MnCl_2 , 5 mM	1.5 \pm 0.3
	+ CoCl_2 , 1 mM	1.0 \pm 0.2
	+ ZnCl_2 , 1 mM	1.1 \pm 0.2

Standard assay method was used for the dephosphorylation of sperm ecto-proteins except for the additions indicated above (Exp. I). For Exp. II, the [^{32}P]labelled cells were dispersed in RTS medium devoid of bivalent metal ions. The data shown are for 4 experiments.

and orthovanadate (200 μ M) had no appreciable effect on the ecto-PPase activity, whereas spermidine (5 mM), a polyamine inhibited to a small extent (approximately 20%) the ecto-enzymic activity.

As shown earlier using gel electrophoretic and autoradiographic techniques (Haldar and Majumder, 1986; Haldar, 1988), multiple sperm surface proteins are phosphorylated by the intact-cell ecto-CK (Haldar and Majumder, 1986). Investigation was carried out to examine the specificity of the ecto-PPase(s) in dephosphorylating surface protein phosphorylation (figure 1). All the [32 P]labelled sperm surface proteins of the intact cells were dephosphorylated by the endogenous ecto-PPase(s). The major ecto-phosphoproteins undergoing dephosphorylation have molecular masses of 205, 116, 70, 40 and 27 kDa.

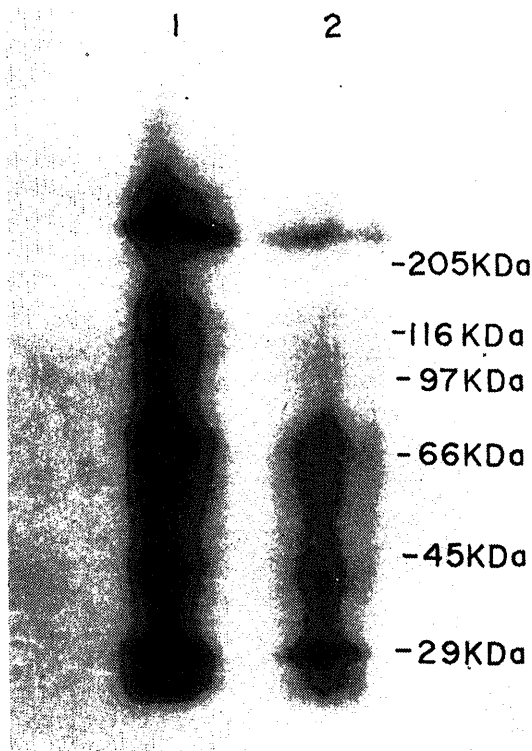


Figure 1. Autoradiogram of sperm ecto- $[^{32}\text{P}]$ proteins (lane 1) dephosphorylated for 10 min (lane 2) by the endogenous ecto-PPase(s) of intact cauda-spermatozoa. [^{32}P]labelled sperm protein (200 μ g; 27,000 cpm); lane 2, partially dephosphorylated [^{32}P]labelled sperm protein (200 μ g; 14,000 cpm).

Discussion

Ecto-phosphoproteins have been demonstrated on the surface of mammalian cells and they are phosphorylated by the endogenous ecto-kinases of the intact cells (Kübler *et al.*, 1982; Kang *et al.*, 1978; Sommarin *et al.*, 1981). Ecto-PPase has been localized in fibroblasts that dephosphorylate

exogenous histones (Makan, 1979). As mentioned above, previous study from our laboratory demonstrated an ecto-PPase on the goat sperm surface that dephosphorylates exogenous [^{32}P]labelled protein substrates (Barua *et al.*, 1985; Barua and Majumder, 1987). This study shows that the sperm ecto-PPase also causes dephosphorylation of multiple ecto-phosphoproteins of the sperm surface. The ecto-PPase may thus modulate the phosphorylated states of the sperm surface proteins and thereby serve an important role in regulating the structure and functions of the sperm plasma membrane. Exogenous Ca^{2+} has been implicated to have an important role in sperm motility (Feng *et al.*, 1987; McGrady *et al.*, 1974) and acrosomal reaction (Yanagimachi and Usui, 1974), although the biochemical basis of this action of Ca^{2+} is largely unknown. It is possible that Ca^{2+} modulation of the phosphorylated state of ecto-phosphoproteins (table 1), may mediate at least in part the regulatory role of this metal ion in sperm physiology.

At present it is difficult to ascertain as to whether the same ecto-PPase is responsible for the dephosphorylation of the exogenous protein substrates (Barua and Majumder, 1987) and the endogenous ecto-phosphoproteins. Both the PPase activity profiles in response to various reagents were similar. A significant difference between these enzymic activities is that the PPase causing dephosphorylation of histone was more sensitive to Zn^{2+} (Barua and Majumder, 1987), than the enzyme that dephosphorylates endogenous ecto-proteins (table 1). The data suggest that there may be more than one PPase species on the sperm surface differing in their enzymic properties with special reference to substrate specificity.

Acknowledgements

The authors are thankful to Dr. S. C. Pakrashi for his interest in this study. One of the authors (M. B.) is grateful to the Council of Scientific and Industrial Research, New Delhi for a fellowship.

References

- Barua, M., Bhattacharyya, U. and Majumder, G. C. (1985) *Biochem. Int.*, **10**, 733.
- Barua, M. and Majumder, G. C. (1987) *Biochem. Cell Biol.*, **65**, 602.
- Barua, M., Haldar, S. and Majumder, G. C. (1990) *Biochem. Int.*, **20**, 1089.
- Bensadoun, A. and Weinstein, D. (1976) *Anal. Biochem.*, **70**, 241.
- Blackshear, P. J., Narin, A. C. and Kuo, J. F. (1988) *FASEB J.*, **2**, 2957.
- Feng, B., Bhattacharyya, A. and Yanagimachi, R. (1987) *Andrologia*, **20**, 155.
- Haldar, S. (1988) Studies on the phosphorylation of goat sperm ecto-phosphoproteins by the endogenous ecto-protein kinase, Ph. D. thesis, Jadavpur University, Calcutta.
- Haldar, S. and Majumder, G. C. (1986) *Biochim. Biophys. Acta*, **887**, 291.
- Kang, E. S., Gates, R. E. and Farmer, D. M. (1978) *Biochem. Biophys. Res. Commun.*, **83**, 1561.
- Kübler, D., Pyerin, W. and Kinzel, W. (1982) *J. Biol. Chem.*, **257**, 322.
- Laemmli, U. K. (1970) *Nature (London)*, **227**, 680.
- Majumder, G. C. and Biswas, R. (1979) *Biochem. J.*, **183**, 737.
- Majumder, G. C. and Turkington, R. W. (1972) *J. Biol. Chem.*, **247**, 7207.
- Makan, N. R. (1979) *Biochim. Biophys. Acta*, **585**, 360.
- McGrady, A. V., Nelson, L. and Ireland, M. (1974) *J. Reprod. Fertil.*, **40**, 71.
- Rubin, C. S. and Rosen, O. M. (1973) *Biochem. Biophys. Res. Commun.*, **50**, 421.
- Sommarin, M., Henriksson, T. and Jergil, B. (1981) *FEBS Lett.*, **127**, 285.
- Uno, I., Veda, T. and Greengard, P. (1977) *J. Biol. Chem.*, **252**, 5164.
- Yanagimachi, R. and Usui, N. (1974) *Exp. Cell Res.*, **89**, 161.

Activities of myelin bound cytidine 5'-diphosphate-choline 1,2 diacylglycerol choline phosphotransferase and uridine 5'-diphosphate-galactose-ceramide galactosyltransferase under restricted food intake

S. PADMINI and P. SRINIVASARAO

National Institute of Nutrition, Hyderabad 500 007, India

Abstract. Activities of cytidine 5'-diphosphate-choline glycerol choline phosphotransferase and uridine 5'-diphosphate galactose-ceramide galactosyltransferase were determined in isolated myelin in different brain regions of control, and rats with restricted food intake. Kinetic experiments indicated an increase in K_m value of phosphocholinetransferase in brain stem of undernourished rats, without significant change in the specific activity of this enzyme. Stimulation of this myelin bound enzyme activity was also evident in the animals when myelin was treated with the detergent: Tween CF. 54. Though specific activities of galactosyl transferase in myelin of undernourished rats were significantly diminished, the K_m of this enzyme was unaltered. These studies point to an adverse effect of early nutritional stress on the activities of enzymes bound to myelin membrane which has hitherto been considered metabolically inert.

Keywords. Myelin; UDP-galactose-ceramide galactosyltransferase; CDP-choline; nutritional stress.

Introduction

Maternal feed inadequacy instituted during gestation, and continued through lactation in dams, was found to result in marked impairments in the activities of microsomal cytidine 5'-diphosphate (CDP) choline: 1,2-diacyl-sn-glycerol choline phosphotransferase (EC 2.7.8.2) and uridine 5'-diphosphate (UDP) galactose: ceramide galactosyltransferase (EC 2.4.1.45) in developing brains of the offspring nursed by such feed restricted animals. The presence of enzymes needed to convert diacylglycerol to phosphatidylcholine and ethanolamine, in highly purified myelin is well established. In view of the proposed role of some of these enzymes in myelin maintenance and remodelling (Leeden *et al.*, 1985), a detailed study was undertaken to enable us to obtain an insight into the developmental profiles of these 2 myelin enzymes in different regions of the rat brain under nutritional stress.

Materials and methods

Typically, undernutrition was imposed by feed restriction (experimental animals fed 50% of the amount consumed by control animals on an ad-lib regimen of a 22% protein diet adequate with respect to all other constituents) through gestation and lactation, in 10-day old pregnant Wistar strain rats. Pups nursed by these 2 groups of dams were considered as experimental and control respectively, litters pooled to a size of 8 numbers at birth, and used at 14 and 21 days of postnatal age. Myelin and microsomes were isolated from pooled rat brain regions by the method of Wu and Ledeen (1980). A second procedure utilizing EGTA (DeVries, 1976) to obtain

myelin free from axolemmal contamination was also employed. Choline phosphotransferase and galactosyltransferase were assayed by the method of Ledeen (1980) and Costantino-Ceccarini *et al.* (1979) respectively. Membrane subfractions were routinely checked for purity by assaying succinate dehydrogenase (mitochondrial marker) glucose-6-phosphatase and NADH cytochrome C reductases (microsomal markers) by the methods of Morre and Takeshita *et al.* (1982).

Results and discussion

The myelin choline phosphotransferase activity was activated in the presence of Triton CF-54 in both groups of animals. Interestingly, however, the activation was higher in myelin obtained from control cerebella and brain stems; myelin from control brain stems exhibited an 8-fold increase in the presence of 60 μg of CF-54, while experimental brain-stem myelin yielded around 6.5-fold stimulation (figure 1). The results of varying substrate concentrations (table 1) re-

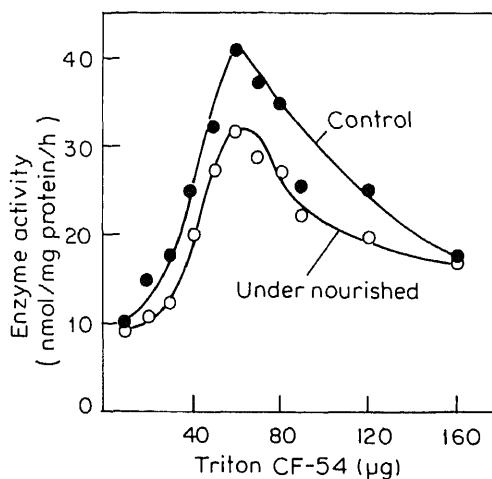


Figure 1. Effect of Triton CF-54 concentration on brain stem myelin choline phosphotransferase activity.

Table 1. K_m values for choline phosphotransferase and UDP-galactosyl transferase of brain stem-myelin of control and undernourished weanling rats.

Enzyme	Substrate		K_m
Choline phosphotransferase	Diolein	C	$2.6 \pm 0.3 \times 10^{-4} \text{M}$
		E	$4.4 \pm 0.3 \times 10^{-4} \text{M}$
	CDP-choline	C	$3.6 \pm 0.6 \times 10^{-4} \text{M}$
		E	$6.5 \pm 0.6 \times 10^{-4} \text{M}$
UDP-galactosyl transferase	Hydroxy ceramide	C	$2.1 - 2.4 \times 10^{-4} \text{M}$
		E	$2.2 \pm 2.4 \times 10^{-4} \text{M}$
		C	$2.7 \pm 3.4 \times 10^{-5} \text{M}$
		E	$2.6 - 3.5 \times 10^{-5} \text{M}$

C, Control; E, experimental.

Table 2. Myelin UDP galactose: ceramide galactosyltransferase in the developing rat brain.

	Enzyme activity (nmol/mg protein/h)		
	Cerebrum	Cerebellum	Brain stem
14 day control	24.5 ± 2.66	27.1 ± 2.07	32.3 ± 1.07
14 day experimental	17.7 ± 2.96*	18.4 ± 2.65***	22.8 ± 1.80***
21 day control	16.7 ± 1.44	19.1 ± 1.84	21.5 ± 3.04
21 day experimental	10.1 ± 1.67**	9.7 ± 1.49**	10.6 ± 2.99***

* $P < 0.05$; ** $P < 0.01$; *** $P < 0.001$.

significant differences in the K_m of the myelin enzyme for both, diolein and CDP-choline in experimental brain stems at the 21-day stage, as compared to corresponding control values. One plausible explanation of the differences (in response to detergent activation) of enzyme activity, between myelin derived from control and experimental animals could be attributed to the fact that myelin membrane acyl phospholipid composition is appreciably different in brain stem from undernourished rat pups (Shantaram and Srinivasa Rao, 1989).

The activity of myelin choline phosphotransferase is not altered in experimental animals. In contrast to this, the specific activities of myelin galactosyltransferase were drastically diminished (table 2) as compared to control values, in all 3 regions of the brain, during the third week of postnatal life. The K_m of myelin galactosyltransferase for either UDP-galactose or hydroxy fatty acid ceramides did not vary in myelin membrane from control and experimental brains (table 1) irrespective of age or regions. This observation supports the hypothesis that hypomyelination observed in the developing brains of undernourished animals may be a consequence of decreased synthesis of galactosylceramides, since these lipids are localised on the external surface of myelin membrane and are known to contribute to the stability of the myelin sheath.

References

- Costantino-Cecarini, E., Cestelli, A. and DeVries, G. H. (1979) *J. Neurochem.*, **32**, 1175.
 DeVries, G. H. (1976) *Neurosci. Lett.*, **3**, 117.
 Ledeen, R. W., Kunishita, T., Wu, P. S., Haley, J. E. and Novak, G. P. (1985) *Phospholipid synthesis in myelin*, Vol. 2, (New York: Raven Press)
 Mörré, D. J. (1971) *Methods Enzymol.*, **9**, 130.
 Shantharam, P. and Srinivasa Rao, P. (1989) *Biochim. Biophys. Acta*, **982**, 115.
 Takeshita, M., Miki, M. and Yubisui, T. (1982) *J. Neurochem.*, **39**, 1047.
 Wu, P. S. and Ledeen, R. W. (1980) *J. Neurochem.*, **35**, 659.

Desmosome and intermediate filament assembly during differentiation and stratification of epithelial cells

ASIMA LAHIRI MAJUMDER*† and CHARLES F. SHULER

College of Dentistry, Ohio State University, Columbus, Ohio 43210, USA

*Present address: Biochemistry Laboratory, Department of Botany, Visva-Bharati University, Santiniketan 731 235, India

Abstract. In the present investigation the sequential expression and organization of keratin intermediate filament proteins were studied in the developing rat palatal epithelia starting from early gestation period to the adult. The distribution and organization of keratin proteins were correlated with the formation and elaboration of desmosomes during differentiation and stratification of the epithelia.

Keywords. Intermediate filaments; keratin; desmosome; differentiation; stratification; antikeratin antibodies; immuno-electron microscopy.

Introduction

The differentiation of stratified squamous epithelia is associated with a precise series of morphologic and molecular changes in the cells. Intermediate filament (10 nm in diameter) keratins are the most complex, heterogeneous group of 40–70 kDa proteins that are epithelium specific and developmentally regulated (Moll *et al.*, 1982). Though all the functions of intermediate filaments are still not clear they seem to interact with plasma membrane and other cellular organelles and have been implicated to be influential factors in the specialization, differentiation and conformation of epithelial cells (Franke *et al.*, 1981; Sun *et al.*, 1983; Traub, 1985).

Keratin filaments specifically interact with the specialized plasma membrane domains termed as desmosomes (Arnn and Staehelin, 1981; Gorbiskey and Steinberg, 1981; Cowin *et al.*, 1985; Franke *et al.*, 1986; Goldman *et al.*, 1986; Suhrbier and Garrod, 1986). As evident from standard electron microscopic structure, desmosomes possess characteristic morphology in which the plasma membranes of two contacting cells associate closely being separated by a narrow gap containing glycoproteins (desmogleins). Dense plaques composed of several desmoplakin proteins are present on the cytoplasmic face of the membranes to which bundles of keratin filaments are attached (Cowin *et al.*, 1985; Garrod, 1986; Suhrbier and Garrod, 1986; Sun *et al.*, 1983). Desmosomes are thus thought to provide link between the intermediate filament systems of adjacent epithelial cells. The nature and mechanism of the interaction between these components are not clear.

Most of the studies of keratins in differentiation are derived from cells and tissues of neonatal and adult epidermis and cells propagated *in vitro*. Since the initial or primary differentiation of any stratified squamous epithelium occurs during fetal development, it seemed logical to us to investigate the ultimate progenitor epithelial cells in the prenatal state where differentiation and developmental events are most obvious and initially observed. In the present investigation the sequential

†To whom all the correspondence should be addressed.

expression and organization of keratin intermediate filament and desmosomes were studied during differentiation and stratification of rat palatal mucosa.

Materials and methods

Palatal mucosa from Sprague Dawley rats of 15–19-day of gestation period and that from the adult were used as tissue source in this study.

Transmission electron microscopy

Tissues were fixed in 2.5% glutaraldehyde in phosphate buffered saline (PBS) (pH 7.4) and embedded in spur. Thick sections (0.5 μm) were used for light microscopic study of histodifferentiation at different stages of fetal development and that of the adult. Thin sections were cut and stained in uranyl acetate and lead citrate for electron microscopic visualization.

Immuno-electron microscopic study with frozen section

Tissue preparation for ultra thin frozen section: Palatal mucosae were fixed in 4% paraformaldehyde in PBS (pH 7.4) with 4% sucrose for 2 h at room temperature. The tissue was subsequently washed in PBS with 4% sucrose and stored in 2.3 M sucrose in PBS overnight at 4°C. The tissues were placed on a cryo-ultramicrotome specimen holder and frozen in liquid N₂. Thick frozen sections (0.5–0.7 μm) were cut in a Reichert Jong Ultracut F4D ultra-microtome, picked up with a drop of sucrose (2.3 M) on a wire loop and placed on slides. The sections were either stained with toluidine blue for immediate visualization or stored at –20°C until used for immunocytochemistry. Thin sections (70 nm) were cut and transferred to the grids. The grids were transferred to gelatin/agarose coated plates with a few drops of PBS to wash away the sucrose.

Immunoreagents

Pooled mouse AE1/AE3 monoclonal antibodies (Hybritech Inc., USA) to human epithelial keratins were used for positive identification of epithelial intermediate filament protein. The AE1/AE3 combination will recognize all members of the acidic and basic keratin subfamilies.

Immunogold localization

The sections were washed in PBS for 10 min. Non-specific binding of the antisera to the tissue was blocked by treating the sections with 1% bovine serum albumin. The grids with tissue were then directly incubated in the primary antiserum for 2 h at 37°C. Grids either without primary antiserum or with preimmune serum served as controls. The grids were subsequently extensively washed and incubated with the secondary gold conjugated antibody (rat antimouse IgG-Gold. GAM 10 Bioclinical Services Ltd.) for 1 h at 37°C. The tissues were washed in 0.1 M phosphate buffer,

washing the sections were stained with 2% neutral uranyl acetate at room temperature and embedded in methyl cellulose (0.02% aqueous uranyl acetate/0.1% methyl cellulose) at 4°C for 15 min. The excess embedding medium was removed from the grids, and after drying they were examined under a Philips 300 electron microscope at either 60 or 80 kv.

Results and discussion

At earliest stages the palatal epithelia were simple columnar (day 15) with stratification generally evident at 16-day *in utero*, by 17-day of gestation strata germinativum, spinosum and some granulosum were easily identified. Four layered adult type strata containing germinativum (basal), spinosum, granulosum and corneum were prominent by 19th day of gestation. Thus, in fetal rat, palate at

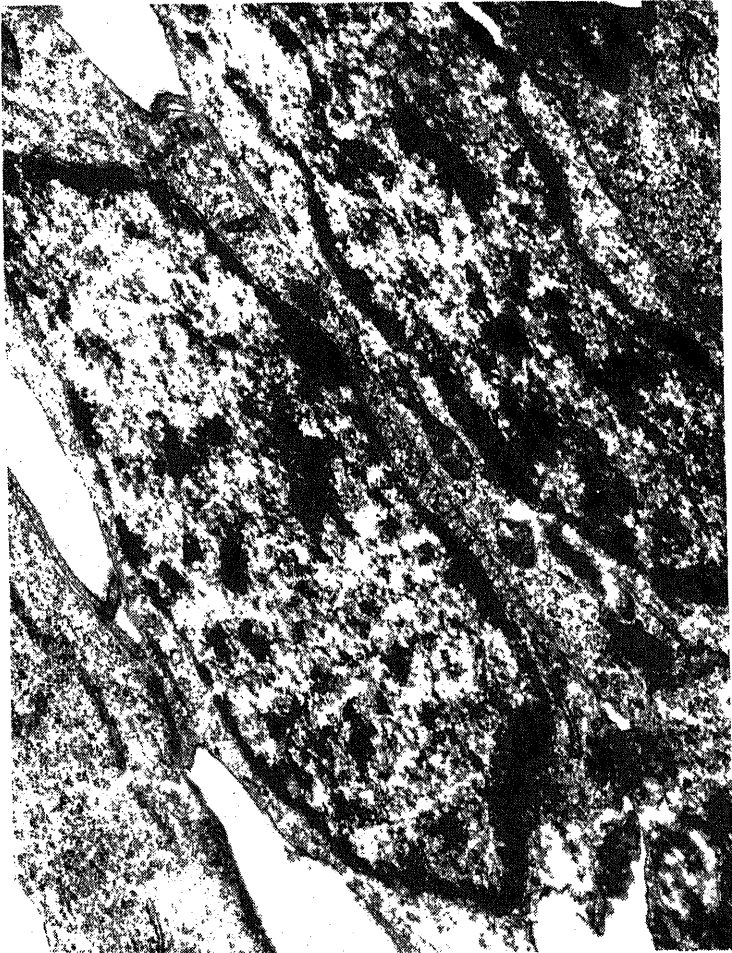
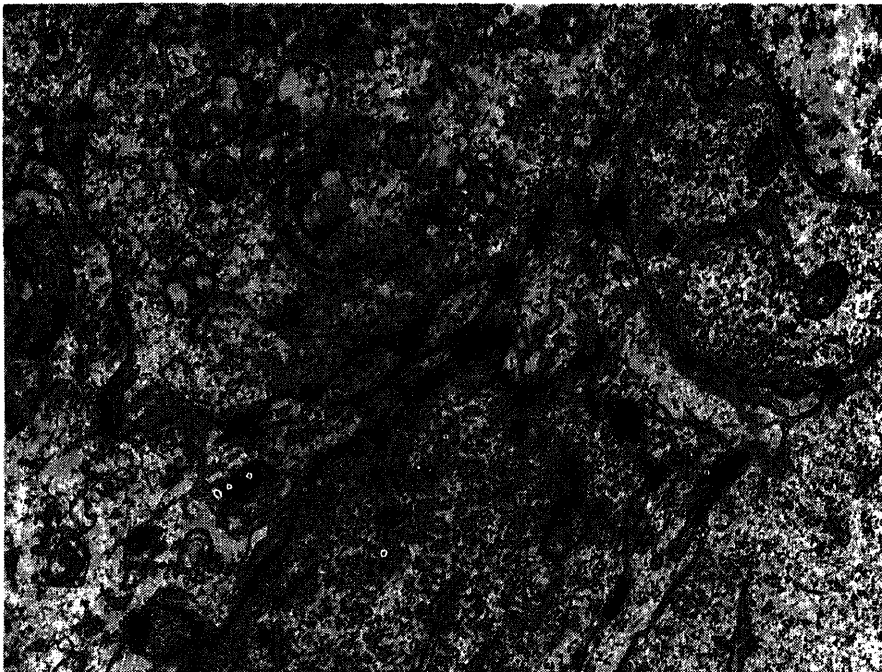


Figure 1. Basal cell from 15-day fetal palatal epithelium ($\times 18,250$).

different gestational stages serves as accurate indicator for the degree of histological differentiation of this tissue.

Ultrastructurally, at day 15 of fetal development in basal cells (figure 1) filamentous keratins were almost negligible compared to that of the intermediate cells. In the stratum corneum, desmosomal contacts were not well developed, peridermal cells contained filaments and some keratin label was observed near the cell contact points in the stratum corneum section. At day 16, with the onset of stratification, desmosomal contacts were observed mostly in the suprabasal cells and keratin filaments were present in intermediate cells; immunolabelling with antikeratin antibodies revealed gold label near the desmosomal area. With the progression of stratification increased amounts of aggregated keratin filaments in all the cell layers together with desmosomes were observed. Dramatic increase in the formation of desmosomes were observed at day 17 *in utero* in the stratum spinosum cells (figure 2) and they were morphologically well defined, keratin filaments were also abundant in all the cells of different layers. Eighteen-day fetal palate continued to demonstrate the same and by day 19 all strata including granular and cornified cells showed typical keratin distribution as in the adult; this is also evident by immunoelectron microscopy. Morphologically a typical desmosome with attached keratin filament is shown in figure 3; the localization of keratins were observed in the filament bundles and keratohyalin granules as in figure 4. In the adult palatal epithelia (unlike the earlier stages) basal cells (distinct from 15-day basal cells) basal cells demonstrated bundles of



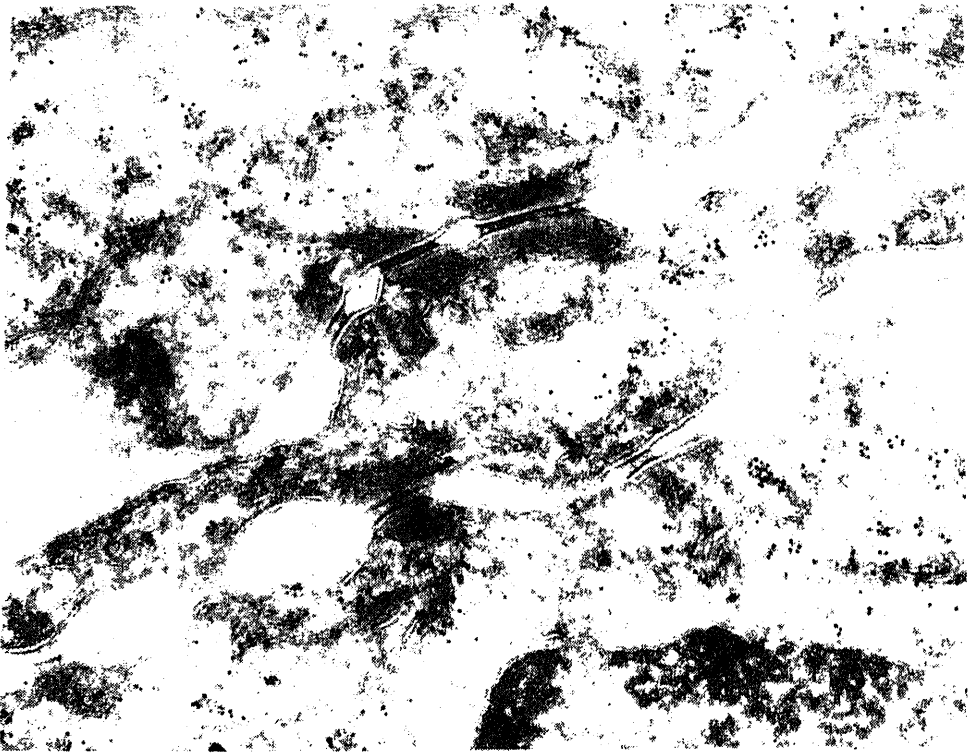


Figure 3. Localization of keratin proteins with gold-conjugated antibody in the keratin filaments and keratohyaline granules in the frozen section of 19-day fetal palate ($\times 45,125$).

filaments distributed throughout the cell and near the plasma membrane (figure 4), well developed desmosomes were present though desmosomal contacts were more abundant in the spinous cells. Immuno-gold labelling of keratins were found to be highly specific as shown in figure 5. General distribution of keratins in spinous cells is shown in figure 6 demonstrating immunolabel at the desmosomal area.

Despite numerous studies indicating interactions of keratin filaments with desmosomes and other cell components, no nucleation or organization sites have been identified for these filaments inside the cell and the nature and mechanism of these interaction are very poorly understood. The highly specific localization of keratin filament proteins supports that the general distribution of these proteins appears in a differentiation dependent manner; moreover in the ultrathin frozen sections the morphology of the cells was sufficiently well maintained to study the interaction between the filaments and plasma membrane and other organelles. From isolated bovine nasal epithelium, the protein and glycoprotein composition of the desmosomes were established. The exact location of all the proteins and glycoproteins in the desmosome is still not very clear but desmoplakins are established to be the specific membrane domains for intermediate filament attachment. Of the 4 desmoplakins so far identified, desmoplakin I (molecular weight 25,000) and desmoplakin II (molecular weight 215,000) are the most abundant components (Cowin *et al.*, 1985; Franke *et al.*, 1986) and they are

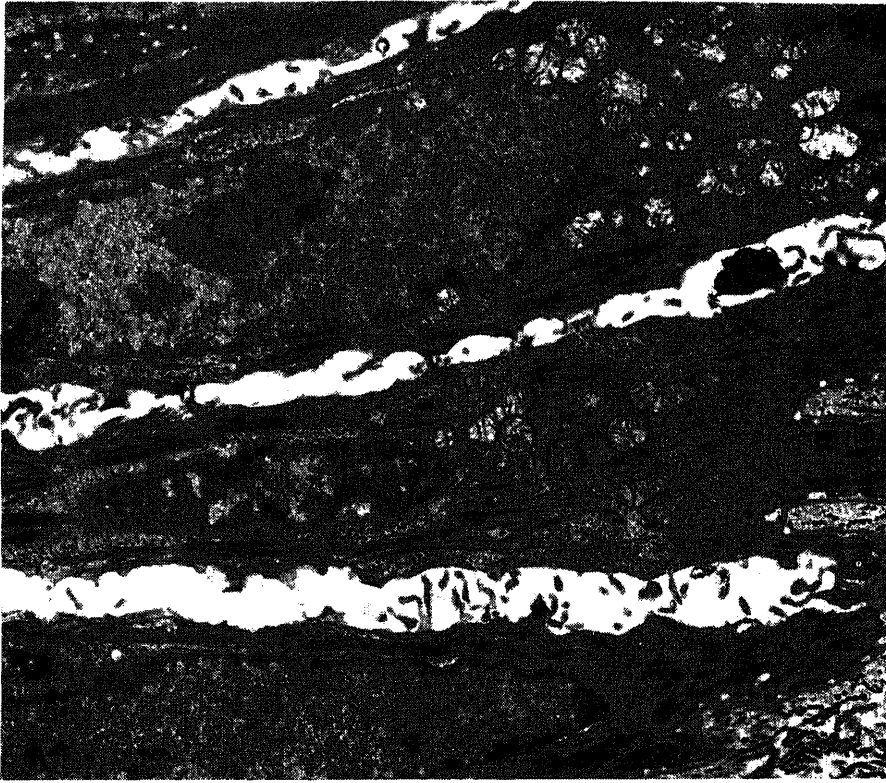


Figure 4. Basal cell from adult palatal mucosa showing general architecture and distribution of keratin filaments ($\times 12,375$).

biochemically and immunologically related to each other. The dynamic of desmosome formation have been investigated using several cell culture systems by several workers. Hennings and Holbrook (1983) studied the calcium-modulated desmosome formation and stratification of mouse epidermal cells in culture. Bologna *et al.* (1986) suggested that desmosome formation was a prerequisite for the organization of the intermediate filaments in rat mammary epithelial cells. and Goldman (1985) studied the mouse epidermal keratinocyte where the organization of the keratin IF and desmosome formation could be manipulated by varying the exogenous levels of Ca^{2+} . Double label immunofluorescence studies suggested that desmoplakin was preformed in the cytoplasm and associated with the intermediate filament system in perinuclear position in low Ca^{2+} . Following stimulation from the environment (appropriate Ca^{2+} levels and cell-cell contact formation), desmoplakin was redistributed towards the cell membrane where desmosome morphogenesis progressed; their data suggested that the movement of interm-

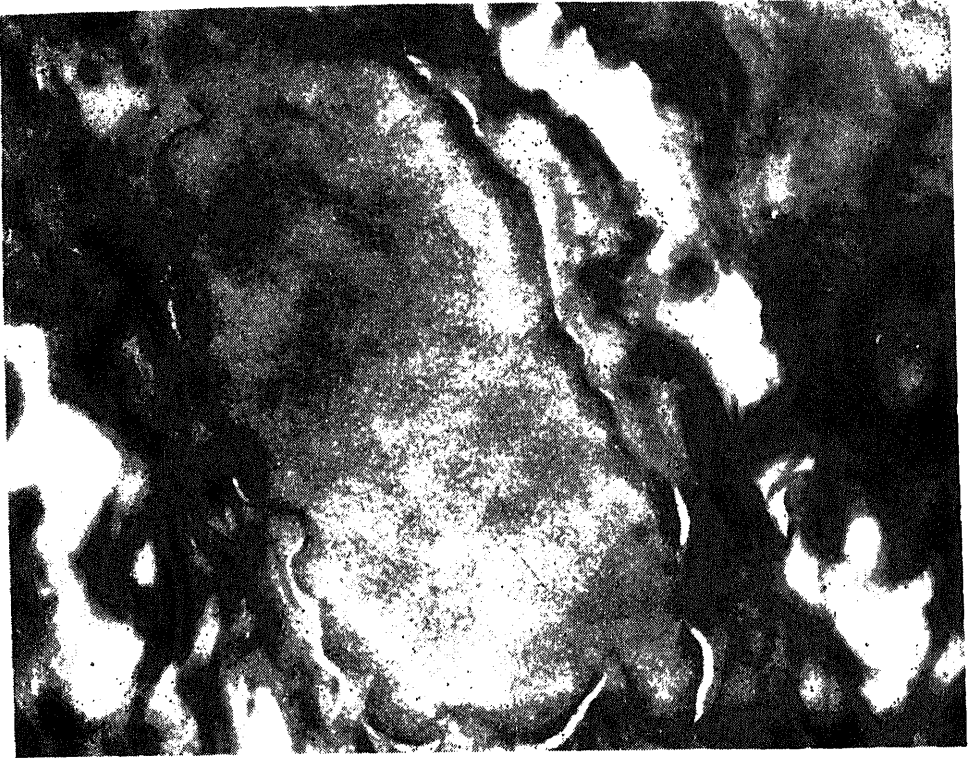
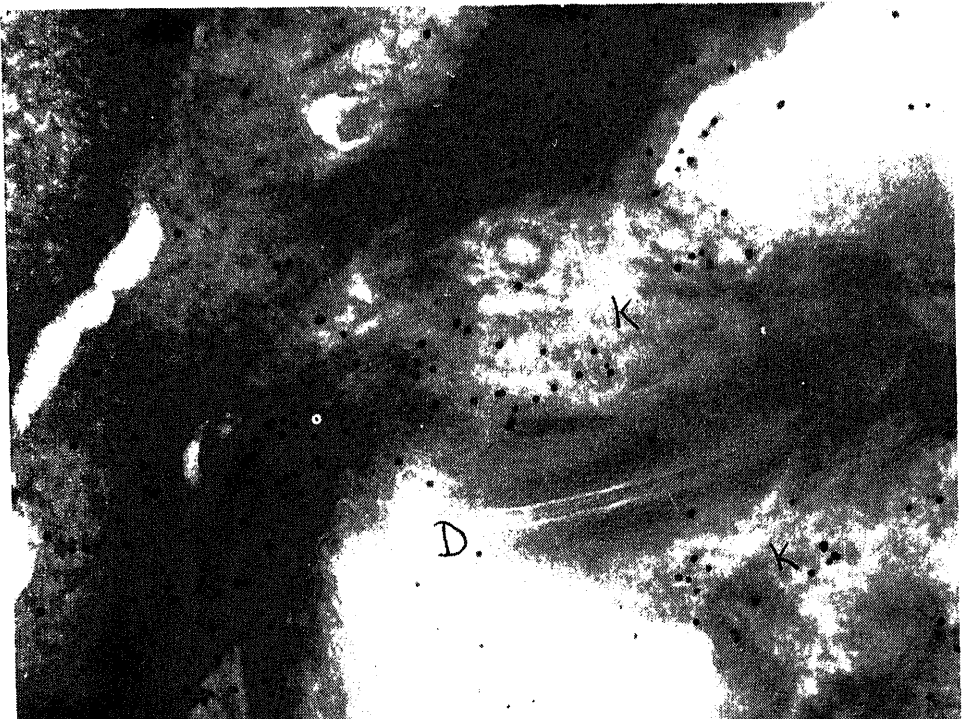


Figure 5.



filament bundles and preformed desmosomal components to the cell surface are important events in desmosome formation. The results from other studies suggest a general pattern of intermediate network that radiate from the nuclear surface to the cell surface and they interact with microtubules and microfilaments (Bridgman *et al.*, 1986; Hennings and Holbrook, 1983). Pasdar and Nelson (1988) support the view that cytokeratin intermediate filaments may function as a nucleation site for the assembly of desmoplakin I and II in the cytoplasm and upon cell-cell contact the insoluble complexes of desmoplakin I and II move rapidly to the plasma membrane in association with, or along individual bundles of intermediate filaments and organize into desmosomes in regions of cell-cell contact.

We presented here a unique *in vivo* model system with developing fetal epidermis which could be used for further study in resolving some of the disputes regarding the mechanism of interaction between keratin filaments and desmosomal proteins. With the help of antikeratin and antidesmoplakin antibodies. The interaction of these two epithelial proteins might play a significant role in the differentiation and stratification of epithelial cells.

References

- Arnn, J. and Staehelin, L. A. (1981) *Dermatology*, **20**, 330.
- Bologna, M., Allen, R. and Dulbeco, R. (1986) *J. Cell Biol.*, **102**, 560.
- Cowin, P., Franke, W. W., Grund, C., Kapprell, H. P., Kartenbeck, J. (1985) in *The cell in contact* (Edelman and J-P. Thiery) (New York: Wiley) p. 427.
- Franke, W. W., Schmid, E., Grund, C., Muller, H., Engelbrecht, I., Moll, R., Stadler, J. and Jarasch, R. (1981) *Differentiation*, **20**, 217.
- Franke, W. W., Cowin, P. A., Schmetz, M. and Kapprell, H. (1986) in *Junctional complexes of epithelial cells*, (Ciba Foundation Symposium 125) (Chichester: Wiley) p. 26.
- Garrod, D. R. (1986) *J. Cell. Sci. Suppl.*, **4**, 221.
- Goldman, R. D., Goldman, A. E., Green, K. J., Jones, J. C. R., Jones, S. M. and Yang, H. Y. (1985) *Cell. Sci., Suppl.*, **5**, 69.
- Gorbskey, C. and Steinberg, M. S. (1981) *J. Cell. Biol.*, **90**, 243.
- Hennings, H. and Holbrook, K. A. (1983) *Exp. Cell Res.*, **143**, 127.
- Jones, J. C. R. and Goldman, R. D. (1985) *J. Cell. Biol.*, **101**, 506.
- Moll, R., Franke, W. W., Schiller, D. L., Geiger, B. and Krepler, R. (1982) *Cell*, **31**, 11.
- Pasdar, M. and Nelson, W. J. (1988) *J. Cell. Biol.*, **106**, 687.
- Suhrbier, A. and Garrod, D., (1986) *J. Cell. Sci.*, **81**, 223.
- Sun, T. T., Eichner, R., Nelson, W. G., Tseng, S. C. G., Weiss, R. A., Jarvinnen, M. and Woloszewicz, J. (1983) *J. Invest. Dermatol.*, **81**, 109.
- Traub, P. (1985) *Intermediate filaments—review* (Berlin; Springer-Verlag).

Coupling of proteins to liposomes and their role in understanding delayed type of hypersensitivity in human and mice

U. SENGUPTA, SUDHIR SINHA, V. CHATURVEDI,
R. B. NARAYANAN*, SREEVATSA and C. M. GUPTA**

Central JALMA Institute for Leprosy, Taj Ganj, Agra 282 001, India

*Department of Immunology, Walter Reed Army Medical Centre, Walter Reed Army Institute of Research, Washington DC 20307-5100, USA

**Division of Membrane Biology, Central Drug Research Institute, Lucknow 226 001, India

Abstract. Liposome-coupled lepromin was found to elicit a 3-week skin reaction in leprosy patients similar to that elicited by whole *Mycobacterium leprae*. The present study suggests that the presentation of antigens in a specific orientation is necessary for evoking delayed type hypersensitivity response in humans.

Keywords. Liposome-coupled lepromin; delayed type hypersensitivity.

Introduction

Lepromin test is a delayed type of hypersensitivity (DTH) test which is elicited as skin reaction after intradermal inoculation of lepromin. When whole *Mycobacterium leprae* remain as an integral component in lepromin, it elicits two types of skin reaction—early, Fernandez reaction (24–48 h reaction) and late, Mitsuda reaction observed after 3 to 4 weeks (Rees, 1964). However, when *M. leprae* are sonicated and the soluble components are injected, they evoke only an early reaction (Sinha *et al.*, 1979; Smelt *et al.*, 1981). Quite likely, if *M. leprae* soluble antigens are also made to present antigens in a manner mimicking the antigen presentation by *M. leprae* to the host then they may also evoke a late reaction. To investigate this possibility, we have coupled *M. leprae* soluble antigens to liposomes and used these as skin test antigens.

Materials and methods

Antigens

- (i) *M. leprae* soluble antigens [MLSA, prepared by the described method (Smelt *et al.*, 1981)] was a kind gift from Dr. R. J. W. Rees, NIMR, London.
- (ii) Standard Dharmendra lepromin (DL) was prepared as described (Sengupta *et al.*, 1979).

Antisera

Commercially available monoclonal antibodies against pan, helper and suppressor T cells, Langerhans cells, Ia antigens were obtained from Becton Dickinson, USA

and Ortho Pharmaceuticals. FITC conjugated sheep antimouse Ig F(ab')₂ u second antibody was obtained from New England Nuclear, Boston, USA.

Liposomes

Liposomes were prepared from egg lecithin (45 μ M), cholesterol (45 μ M) gangliosides (9 μ M) in 2 ml borate-buffered saline (pH 8.4) by sonication fractionation (Gupta and Bali, 1981).

Liposome coupling with antigens

The soluble protein of MLSA was covalently coupled to the liposome s according to a standard method (Heath *et al.*, 1981).

Skin biopsies

The patients with leprosy were selected from the outpatient clinic of C JALMA Institute for Leprosy, Agra. They were intradermally injected with (1×10^6 bacilli in 100 μ l); MLSA (1 μ g in 100 μ l); MLSA coupled to liposome in 100 μ l); liposomes in saline (100 μ l). The diameter of skin indurations recorded in mm at 48 h and 21 days after injection. An induration of 5 mm or more was regarded as positive for the 21-day skin reaction. For immunofluorescence studies, the biopsies were collected from a separate group of patients.

DTH in mice

BALB/c mice were sensitized by intracutaneous injection of 2 mg of bovine albumin (BSA) with incomplete Freund's adjuvant at the base of the tail. At 7 days the DTH reactions were elicited by foot pad inoculations with 0.03 ml of BSA solution (600 μ g) and liposomised BSA solution (15 μ g) respectively. The administered dose of free BSA was selected according to published reports while the dose of liposomised BSA was selected arbitrarily.

Results and discussion

Skin reaction in 10 borderline tuberculoid patients at 48 h and at 21 days after sensitization by different antigens are depicted in table 1. While MLSA elicited only early reaction, DL elicited mostly 48 h and 3-week reactions. In all these patients liposomised antigen elicited both early and late reactions similar to those elicited by free antigen. Control liposomes induced insignificant reactions at 48 h in 4 patients. Lepromatous leprosy patients showed negative skin reaction to these antigens.

Elicitation of a 3-week skin reaction with liposome-coupled lepromin supports the hypothesis that the presentation of eliciting antigens in a specific orientation is required for the development of late reaction. To find out whether the

Table 1. Skin reactions with different antigen preparations in borderline tuberculoid leprosy patients.

Patient	Antigens							
	MLSA (10 µg/ml)		DL (10 ⁷ bacilli/ml)		Liposomised MLSA		C	
	48 h	3 weeks	48 h	3 weeks	48 h	3 weeks	48 h	3 weeks
1	29	0	28	10	28	10	0	0
5	20	0	25	7	27	7	5	0
3	28	0	22	0	32	0	5	0
4	0	0	0	6	15	0	5	0
5	23	0	18	0	30	0	5	0
6	12	0	12	0	13	0	0	0
7	15	0	12	5	12	5	0	0
8	26	0	24	12	27	6	0	0
9	30	0	22	5	19	10	0	0
10	18	0	16	5	14	6	0	0

Numbers in this table represent the diameter of skin indurations in mm.

C, Control liposomes.

analysis. It was noted that the 48 h skin reaction yielded a classical DTH picture, a predominant lymphocytic infiltration interspersed with a few polymorphonuclear cells. The 21-day reaction with liposomised MLSA also revealed a histological picture resembling the DTH reaction induced by DL with focal collection of epithelioid and giant cells (table 2).

Table 2. Cellular characteristics of the DTH skin reactions.

Cell type	DL lepromin		Liposomised MLSA	
	48 h	3 weeks	48 h	3 weeks
Ly ^a	+	+	+	+
PMN ^b	+	—	+	—
EC ^c	—	+	—	+
Ratio Leu 3a + / T8+ (mean±SD)	1·18±0·18	4·0±1·5	1·21±0·25	3·12±1·3
Distribution	No pattern	Diffused in	No pattern	Diffused in
Ly Leu 3a +		EC granuloma		EC granuloma
T8 +	No pattern	Periphery of	No pattern	Periphery of
		EC granuloma		EC granuloma
T6+ cells	+	+	+	+
Macrophages	—	Ia +, T6 +	—	Ia +, T6 +

^a Ly, Lymphocyte; ^b PMN, polymorphonuclear leucocytes; ^c EC, epithelioid cell.

Immunohistologically, the 48 h skin reaction induced by liposomised MLSA was again akin to the 48 h reaction induced by DL with infiltration of activated T

evoked by liposomised MLSA the granuloma cell infiltration was similar to the day skin reaction induced by DL. The predominant lymphocytes in granulomas were activated T cells expressing Leu 4 and Ia like antigens. Epithelioid cell granulomas were surrounded by Leu 4+ positive cells. OKT8+ cells were lesser in number. The ratio of Leu 3a+ /OKT8+ cells were 3.2 ± 1.3 . Leu 3a+ cells were found scattered amongst the epithelioid cells. OKT8+ cells were localised 'ring' in the periphery of the granuloma (table 2).

This study substantiates the fact that covalent liposomisation of protein molecules of MLSA presented the antigens in a manner similar to those of integral *M. leprae*. It was, however, not possible to define the molecules involved in the development of DTH reactions.

As the above *in vivo* experiments are very difficult to perform on patients because of the difficulty in obtaining their consent, an attempt was further made to establish an experimental model in mice using a simple protein like BSA. It was noted that liposomised BSA was capable of inducing larger 48 h reaction than BSA alone in BSA-sensitized mice. This was despite the fact that the administered dose of liposomised BSA was 40 times lesser than that of free BSA, indicating that liposomization enhanced the immunogenicity of BSA. However liposomised BSA did not elicit a 3-week reaction in mice. This could be due to the different nature of antigen or the host involved. Further studies on these lines are needed.

References

- Gupta, C. M. and Bali, A. (1981) *Biochim. Biophys. Acta*, **663**, 506.
Heath, T. D., Macher, B. A. and Papahadjopoulos, D. (1981) *Biochim. Biophys. Acta*, **640**, 66.
Narayanan, R. B., Ramu, G., Malaviya, G. N., Sengupta, U. and Desikan, K. V. (1985) *Indian J. Lepr.*, **57**, 265.
Rees, R. J. W. (1964) *Prog. Allergy*, **8**, 224.
Sengupta, U., Ramu, G. and Desikan, K. V. (1979) *Lepr. India*, **51**, 316.
Sinha, S., Sengupta, U., Ramu, G. and Desikan, K. V. (1979) *Lepr. India*, **51**, 323.
Smelt, A. H. M., Rees, R. J. W. and Liew, F. Y. (1981) *Clin. Exp. Immunol.*, **44**, 501.

Editorial

als go through critical stages of evolution. We have reached such a stage in evolution of journals related to research in life sciences in the country. There is perceptible increase in the quality and quantity of research output in biology in years in the country. It is all our concern to examine whether the Indian journals are able to reflect this transformation.

Academy first published papers in life sciences in the Proceedings of the Academy of Sciences, Section B (monthly) in 1934. In 1978, Section B was split into *Proceedings—Animal Sciences*, *Proceedings—Plant Sciences* and *Experimental Biology*, each published once in three months. The section on *Experimental Biology* became the *Journal of Biosciences* in 1979.

Journal of Biosciences has done reasonably well, having the highest impact among journals devoted to life sciences in the country. It has been our dream to make it truly an international journal aspiring for international standards. While the journal received a large number of papers, it has not been easy to maintain the high standards in terms of the quality of papers published. One reason is of course the flight of good papers to foreign journals. Another reason is perhaps the narrower scope of each journal devoted to life sciences. It has, therefore, been decided to merge all the three sections namely, *Proceedings—Animal Sciences*, *Proceedings—Plant Sciences* and *Journal of Biosciences* into one, so that it would be possible to have a single journal with a broader scope. The journal would continue to appear as *Journal of Biosciences* after the merger. In keeping with the broader scope of the journal, there has been a necessity to reorganize the Editorial Board, which will take over from the next issue.

It is my privilege to have been the Editor of the *Journal of Biosciences* in the last years and I received excellent cooperation from the members of the Editorial Board and the Academy office at Bangalore. I would like to thank sincerely all who have contributed to the growth of the *Journal of Biosciences*. I would like to acknowledge the farsightedness of the Editorial Boards of the *Proceedings—Animal Sciences* and *Proceedings—Plant Sciences* to have agreed on this merger. On behalf of all the outgoing Editorial Boards, I would like to wish the new Editorial Board all the best. We have taken one more step towards building an international journal with high standards devoted to life sciences in the country.

G. Padmanaban

Organization and chromosomal localization of β -tubulin genes in *Leishmania donovani*

SAUMITRA DAS and SAMIT ADHYA*

Leishmania Group, Indian Institute of Chemical Biology, 4, Raja S. C. Mullick Road, Calcutta 700 032, India

MS received 19 July 1990; revised 1 October 1990

Abstract. The genomic organization and chromosomal location of the β -tubulin isogenes in *Leishmania donovani* promastigotes has been studied by nucleic acid hybridization techniques using a cloned β -tubulin gene. We have cloned a β -tubulin gene fragment, 3.3 kbp long, from genomic DNA of *Leishmania donovani* using a heterologous β -tubulin DNA as probe. Restriction maps of this clone have been prepared. It has been estimated that there are approximately 11–15 copies of the β -tubulin genes per haploid genome. The majority of these isogenes are arranged in a tandem repeat with a length of 3.5 kbp on a single chromosome. In addition a few dispersed gene copies at different chromosomal loci were detected by pulse field gradient gel electrophoresis. Part of the internal coding region of the gene has been sequenced to confirm the identity of the β -tubulin clone and is found to be nearly identical to that of *Leishmania mexicana amazonensis*.

Keywords. *Leishmania donovani*; β -tubulin; gene organization; chromosome location; DNA sequence.

Introduction

Leishmania donovani is a pathogenic protozoan parasite of the order kinetoplastida with a dimorphic life cycle including a flagellated promastigote form in sandfly vectors and a non-flagellated amastigote form in the macrophages of infected mammals. This transformation of one form to other might be a reflection of altered expression of different stage specific cellular genes.

In *Leishmania*, tubulins are developmentally regulated proteins (Fong and Chang, 1981). Biosynthesis of tubulin increases rapidly during amastigote to promastigote transformation, and decreases in the reverse direction. Thus the study of organization and expression of the tubulins at the genetic level of this organism is of particular interest. Tubulin is the major constituent of the microtubular structures in *Leishmania* comprising cytoskeletal network, mitotic spindle and motility generating flagella. There are two types of tubulin, α and β . Monomers of approximately 55,000 molecular weight form $\alpha\beta$ hetero dimers that are polymerized to form macromolecular filaments called microtubules. The nucleotide coding sequences of α - and β -tubulin genes are highly conserved across phylogenetic boundaries, but the organization and copy number vary widely. In chicken and *Drosophila* (Cleveland *et al.*, 1981) there are 4 α - and 4 β -tubulin genes. Chlamydomonas species have two α - and two β -tubulin genes (Sillflow and Rosenbaum, 1981) while the rat and human genome contain 10–20 unlinked genes for each subunit (Lemischka and Sharp, 1982; Wilde *et al.*, 1982). In *Leishmania*

*To whom all the correspondence should be addressed.

species such as *L. enrietti* (Landfear *et al.*, 1983), *L. mexicana* (Fong *et al.*, 1983), *L. tropica* (Huang *et al.*, 1984), and *L. Major* (Spithill and Samaras, 1987), multiple copies of the β -tubulin genes have been reported to be organized as tandem head-to-tail repeats. The α - and β -tubulin genes in *Trypanosoma brucei* have been found to be physically linked in tandemly repeated units of $\alpha\beta$ (Thomashow *et al.*, 1983). In addition to the tandem repeat cluster, in some cases a few dispersed loci containing β -tubulin genes have also been identified. Existence of these scattered copies raises the possibility of the existence of functionally different tubulin proteins (Fulton and Simpson, 1976; Kowit and Fulton, 1974). Heterogeneity within the sequence of tubulin genes or proteins has been observed in some organisms, *Chlamydomonas* (Witman *et al.*, 1972), sea urchin (Bibring *et al.*, 1976), etc. This structural heterogeneity reflects a functional specialization among tubulin proteins. In *Leishmania*, whether all these tubulin genes are functional and if so, whether the different genes have specialized functions, are not known. Hence it is important to correlate the tubulin gene number, chromosomal location and function to have an idea about the utilization of different tubulin proteins by the parasite.

We have studied the organization and chromosomal location of the β -tubulin genes in *L. donovani* using a homologous genomic clone of β -tubulin. By dot blot and Southern hybridization analysis the number and relative location of β -tubulin genes have been determined. Major and minor gene copies have been mapped to different chromosome-sized DNA molecules by pulsed field gradient electrophoresis. To detect micro-heterogeneity within the gene the β -tubulin clone has been partially sequenced. Results are discussed in terms of the prevailing ideas on tubulin polymorphism as determinants of cellular function.

Materials and methods

Parasite culture

L. donovani strain UR6 (WHO nomenclature—MHOM/IN/1978/UR6) promastigotes were grown at 25°C for 48–72 h in modified Ray's (1932) agar medium containing 3.7% brain-heart infusion, 1% glucose, 1.5% agar, 10,000 U/ml penicillin, 10,000 µg/ml streptomycin and 1% rabbit blood. Two other strains of *L. donovani*, AG83 and WHO reference strain DD8 were grown at 25°C in medium 199 (Gibco laboratories) supplemented with 10–20% fetal calf serum.

Isolation of parasite genomic DNA

For isolation of genomic DNA *L. donovani* promastigotes were harvested with phosphate-buffered saline (PBS), washed 3–4 times with it, and finally suspended in lysis buffer containing sodium dodecyl sulphate (SDS) and proteinase K followed by incubation at 37°C overnight. The lysate was then subjected to phenol extraction, dialysis, RNase treatment and ethanol precipitation. DNA concentration was estimated by its absorbance at 260 nm (1 A₂₆₀ unit of absorbance = 50 µg double stranded DNA) (Maniatis, *et al.*, 1982).

and *Sal*I and 3–4 kbp fragments isolated by agarose gel electrophoresis and electroelution. These fragments were cloned into pUC8 vector which had been digested with same two enzymes. Transformants were screened with pLE β 3, a β -tubulin genomic clone from *L. enrietti* (kindly provided by Dr. Scott Landfear of Harvard School of Tropical Public Health, MA, USA). Out of 200 clones screened, 3 positive, apparently identical β -tubulin clones were detected. One of these designated pLD β T1 has been used. The cloning procedure was according to Maniatis *et al.* (1982).

Copy number determination

Total *L. donovani* promastigote DNA (0.25–4 μ g) and the cloned β -tubulin gene pLD β T1 (0.125–4 ng) were denatured in 0.3 N NaOH and applied in a dot configuration on Zetaprobe (Bio-Rad) membrane using a dot blot apparatus (Bio-dot; Bio-Rad). After application the membrane was soaked in 1 \times SSC for 2 min at room temperature then baked at 80°C for 1 h. The filter was then subjected to hybridization as detailed below with nick-translated [32 P] labelled pLD β T1 (herein abbreviated as β T1) DNA probe, followed by autoradiography. Quantitation of the band intensities were performed in two ways: (i) scanning of the autoradiogram at different exposure times in an Ultrosan densitometer (LKB) followed by peak weight determination or peak area estimation from the integration trace and (ii) excision of the slots for liquid scintillation counting. A standard curve of hybridization signal versus number of molecules of plasmid was plotted and corresponding mol number for genomic DNA obtained by interpolation. Knowing the cellular DNA content of *Leishmania* (Leon *et al.*, 1978) the copy number per cell (or haploid genome) could be computed.

Southern blot analysis

Total promastigote DNA was digested with restriction enzymes as indicated, electrophoresed in 1% agarose gels and transferred to nitrocellulose or Zetaprobe membrane by the method of Southern (1975), followed by hybridization with [32 P] labelled probe. Different probes were used which were [32 P] labelled either by nick-translation (Rigby *et al.*, 1977) or oligolabelling (Feinberg and Vogelstein, 1983) method. Southern blots on Zetaprobe membrane filters were prehybridized at 42°C for 24 h in 50% deionized formamide, 5 \times SSC, 5 \times Denhardt solution, 20 mM sodium phosphate, pH 7, 0.1% SDS and 200 μ g/ml calf thymus DNA or herring sperm DNA. Hybridization was performed by adding [32 P] labelled denatured probe (3 \times 10⁵ cpm/ml) to the prehybridization solution and incubating at 42°C for 24 h. The filters were then washed twice with 2 \times SSC, 0.1% SDS, once with 0.5 \times SSC, 0.1% SDS and once with 0.1 \times SSC, 0.1% SDS, each wash being for 15 min at room temperature with vigorous shaking, and then subjected to autoradiography. For the Southern blots on nitrocellulose membrane, prehybridization performed at 65°C for 4–6 h and hybridization was carried out at the same temperature for 24 h in aqueous medium using 3 \times 10⁵ cpm/ml probe and the filters were washed once with 3 \times SSC, 0.1% SDS, thrice with 1 \times SSC, 0.1% SDS, each wash for 30 min at 65°C, followed by autoradiography (24–48 h). Specific activity of the probe was 1–2 \times 10⁷ cpm/ μ g DNA.

Pulse field gradient gel electrophoresis

Sample preparation: Promastigotes ($1.25\text{--}2.5 \times 10^7$ cells) were washed with PBS and suspended in 100 μl of SE buffer (75 mM NaCl, 25 mM EDTA, pH 8) and 100 μl of 1% low melting agarose to form agarose blocks. Cells were then lysed *situ* by incubating the blocks in 500 μl of ES buffer (0.5 M EDTA, pH 9.5; Sarkosyl) and 2.5 mg/ml proteinase K at 50°C for 48 h. The blocks were then washed thrice with $0.5 \times \text{TBE}$ and stored at 4°C until use.

Run condition: Pulse field gradient gel electrophoresis (PFGE) of chromosome-DNA of promastigotes of 3 different strains of *L. donovani* (UR6, DD8 and AG) were performed by placing these agarose blocks inside the lanes of a 1% agarose gel and applying 150 V at different pulse times (60, 80 and 100 s) for 40 h in $0.5 \times \text{TBE}$ gel running buffer at 15°C in a Pulsaphor apparatus (LKB). DNA was visualized by staining with ethidium bromide. For transfer chromosome-size DNA was depurinated by soaking the gel in 0.25 N HCl for 30 min and then blotted on Zetaprobe membranes by the method of Southern followed by hybridization with [^{32}P] labelled βT1 probe.

DNA sequencing

Part of the internal coding region and C-terminal coding portion of the cloned β -tubulin gene pLD βT1 were sequenced by enzymatic chain termination method (Hattari and Sakaki, 1986). Double stranded DNA sequencing was performed with the Klenow fragment of *Escherichia coli* DNA polymerase I in the presence of dideoxy nucleotides and [$\alpha^{32}\text{P}$] dTTP. Both universal forward and reverse primers (Promega) were used. The sequences were compared with the homologous region of the published β -tubulin gene sequence of *L. mexicana amazonensis*.

Results*Copy number determination*

To determine the copy number of the β -tubulin gene a quantitative Southern hybridization was performed by using increasing amounts of *L. donovani* promastigote genomic DNA and βT1 plasmid DNA. DNA samples were denatured and applied on a nylon membrane and hybridized with nick-translated [^{32}P] labelled βT1 DNA probe (figure 2A). By comparing the intensity of hybridization of the β -tubulin probe with the genomic DNA, to the amount which hybridizes to a known amount of the cloned β -tubulin plasmid, the copy number was determined. On the basis of densitometric analysis (see 'materials and methods') the graph of equivalence shows the amount of radiolabelled DNA in 1 μg genomic DNA corresponds to that for 1.4 ng of the βT1 plasmid standard which is equivalent to 35.3×10^{-5} pmol. The graphical equivalence obtained from liquid scintillation counting shows that the amount of radioactivity bound to 1 μg genomic DNA

genomic content 5×10^7 bp (Leon *et al.*, 1978) the copy number was estimated to be in the range of 11–15 copies per haploid genome.

Tandem arrangement of the β -tubulin genes

The organization of the multiple β -tubulin gene was studied by probing Southern blots of restriction enzyme digested genomic DNA of *L. donovani* promastigotes with [32 P] labelled β T1 DNA. The restriction map of the cloned gene (figure 1)



Figure 1. Restriction and transcription maps of the major β -tubulin locus in *L. donovani*. Locations of restriction sites on the genomic clone β T1 are shown. H, *Hind*III; P, *Pst*I; A, *Ava*I; X, *Xho*I; He, *Hae*III; B, *Bam*HI; S, *Sal*I. Square brackets flanking the restriction map represent pUC8 vector sequences. The mRNA map (Adhya *et al.*, 1990) is shown above the restriction map; thick and thin lines represent major and minor mRNA species respectively. Protein coding regions (determined by DNA sequencing) are designated by hatched bars (scale 0.8 cm = 200 bp).

showed that the gene contained single sites for *Hind*III, *Sal*I and *Xho*I enzymes, two sites for *Bam*HI and none for *Eco*RI. Digestion of genomic DNA with *Eco*RI yields a high molecular weight band (larger than 23 kbp) while with *Hind*III, *Sal*I and *Xho*I a single major band, 3.5 kbp in size was observed (figure 2B). Double digestion with *Hind*III and *Sal*I cause a reduction in the size of this band from 3.5 to 3.3 kbp. *Bam*HI digestion results in two bands of length 2.9 and 0.6 kbp (the lower band is not visible in the figure). *Hind*III and *Eco*RI double digestion yielded 3.5 kbp major band apart from a few minor bands (data not shown). From these results it was apparent that majority of the β -tubulin genes are organized as a precisely repeated structure in which the distance between adjacent sites for a given restriction enzyme is conserved, thus giving rise to a single major band. *Eco*RI enzyme has no recognition site within the gene and hence generates a single high molecular weight fragment that contains the entire repeat.

To confirm this repeated arrangement genomic DNA was partially digested with varying amounts of *Xho*I and subjected to Southern blot hybridization with [32 P] labelled β T1 probe. At intermediate concentrations of the enzyme *Xho*I a ladder of bands was observed of lengths 3.5, 7 and 10.5 kbp respectively (figure 2C). These lengths correspond to monomeric, dimeric and trimeric fragments from the cluster of tandemly repeated β -tubulin genes. Similar results were obtained using the enzymes *Hind*III and *Bam*HI (data not shown).

Recently these experiments have been repeated under conditions favouring detection of single copy fragments using probes derived from the N-terminal or C-terminal region of the gene (data not shown). Several minor bands corresponding to 5' or 3'-flanking sequences derived from the major cluster and from minor dispersed

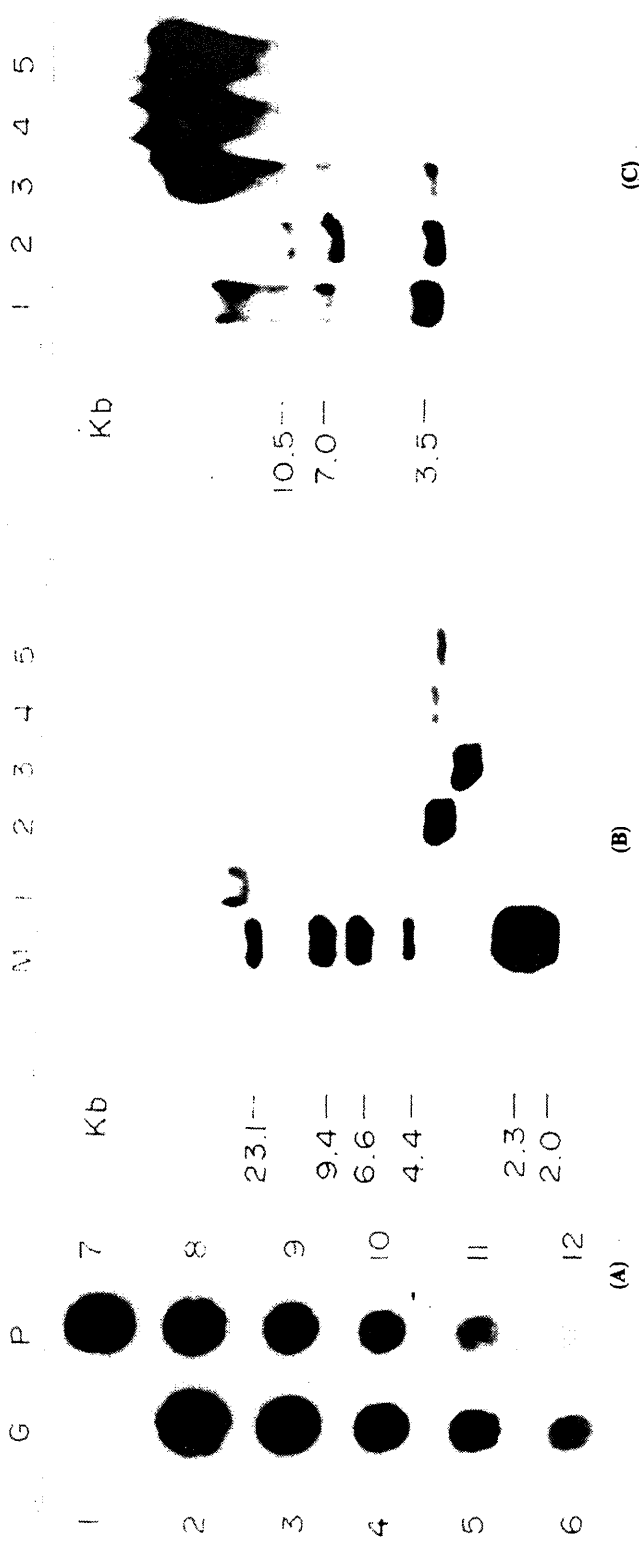


Figure 2. Hybridization analyses of β -tubulin genomic DNA with [32 P] labelled β T1 probe. (A) Copy number determination by dot blot hybridization. Lane G, dot 1, λ DNA (4 μ g); dots 2-6, *L. donovani* genomic DNA (4, 2, 1, 0.5, 0.25 μ g respectively). Lane P, dots 7-12, pLD β T1 DNA (4, 2, 1, 0.5, 0.25 and 0.125 ng respectively). The filter was hybridized with oligo-labelled [32 P] β T1 insert DNA. (B) Southern blot hybridization of genomic DNA digested with different restriction enzymes. Lane M, λ -*Hind*III markers; lanes 1-5, DNA 5-10 μ g digested with *Eco*RI, *Hind*III, *Bam*HI, *Sal*I and *Sall* + *Hind*III respectively. Numbers to the left represent sizes (in kbp) of λ -*Hind*III molecular weight markers. (C) Southern blot hybridization of genomic DNA partially digested with *Xho*I. Lanes 1-5, DNA (10 μ g) digested with 10, 2.5, 1, 0.5 and 0.25 units of *Xho*I, respectively, for 1 h at 37°. Numbers to the left show the sizes (in kbp) of the partial digest bands. In (B) and (C) filter-bound DNA was hybridized with [32 P] labelled β T1 probe, washed and autoradiographed.

to map the chromosomal location of the β -tubulin genes and to determine whether this chromosomal location is conserved among different Indian isolates of viscerotropic *Leishmania*, PFGE followed by Southern blot hybridization with β T1 probe was performed. This electrophoresis system can separate wide range of chromosome size DNA molecules (Carle and Olson, 1985; Spithill and Samaras 1985). For organisms such as *Leishmania* which do not undergo chromosome condensation during mitosis, this is the only way to perform karyotype analysis and gene mapping. Chromosomes of 3 Indian *L. donovani* strains (UR6, DD8 and AG83) were resolved into about 20 bands (figure 3A). The band profile is similar in strain UR6 and the WHO reference strain DD8, but slightly different in AG83, which emphasizes the inherent plasticity of the *Leishmania* chromosomes. Southern blot hybridization of the chromosomes with β T1 probe demonstrated 4 different loci for β -tubulin genes in *L. donovani* UR6 (figure 3B). The location of the major repeat cluster was assigned to band 20 (or even higher band, not resolved in the present gel) in all 3 isolates. The hybridization profile for the minor dispersed copies varies between the strains. Only two minor bands were detected for strain AG83 in contrast to 3 minor bands each for UR6 and DD8. As judged by its relative intensity (see below) the lower AG83 band may contain two copies on the same chromosome or one copy on each of two different unresolved chromosomes. Thus it is evident that only the chromosomal location of the major repeat is conserved, not that of the dispersed loci.

Densitometric scanning of the autoradiograms showed that the ratio of the dispersed copies to that in major repeat locus in UR6 as 1.6:1:17.7, in DD8 1.4:1:18.4 and in AG83 2.6:1:15.8.

Partial sequencing

The identity of the clone β T1 that has been used for studying organization of the β -tubulin genes, was confirmed by partial sequencing of the cloned gene from both ends using universal forward and reverse primer (Promega). The sequences were compared (figure 4A) with the published β -tubulin gene sequence of *L. mexicana* (Fong and Lee, 1988). The sequence at the internal coding region (from *Hind*III site onwards 117 bp, figure 1) shows 3 conservative base changes, one nonconservative base change (Val in *L. donovani*, Leu in *L. mexicana*) and one amino acid (histidine; position marked in the figure 4A) deletion. The C-terminal coding region (from *Sal*I site onwards 204 bp, figure 1) shows only one conservative change at the third base out of 204 nucleotides sequenced. The sequence data therefore demonstrates the high degree conservation of the β -tubulin gene sequences amongst different species of *Leishmania*.

Discussion

In this report we have shown that there are approximately 11–15 copies of β -tubulin genes per haploid genome of the pathogenic protozoan parasite *L. donovani*. The majority of these copies are arranged in a tandem repeat on a single chromosome (band 20). Additionally, a few copies are scattered on different

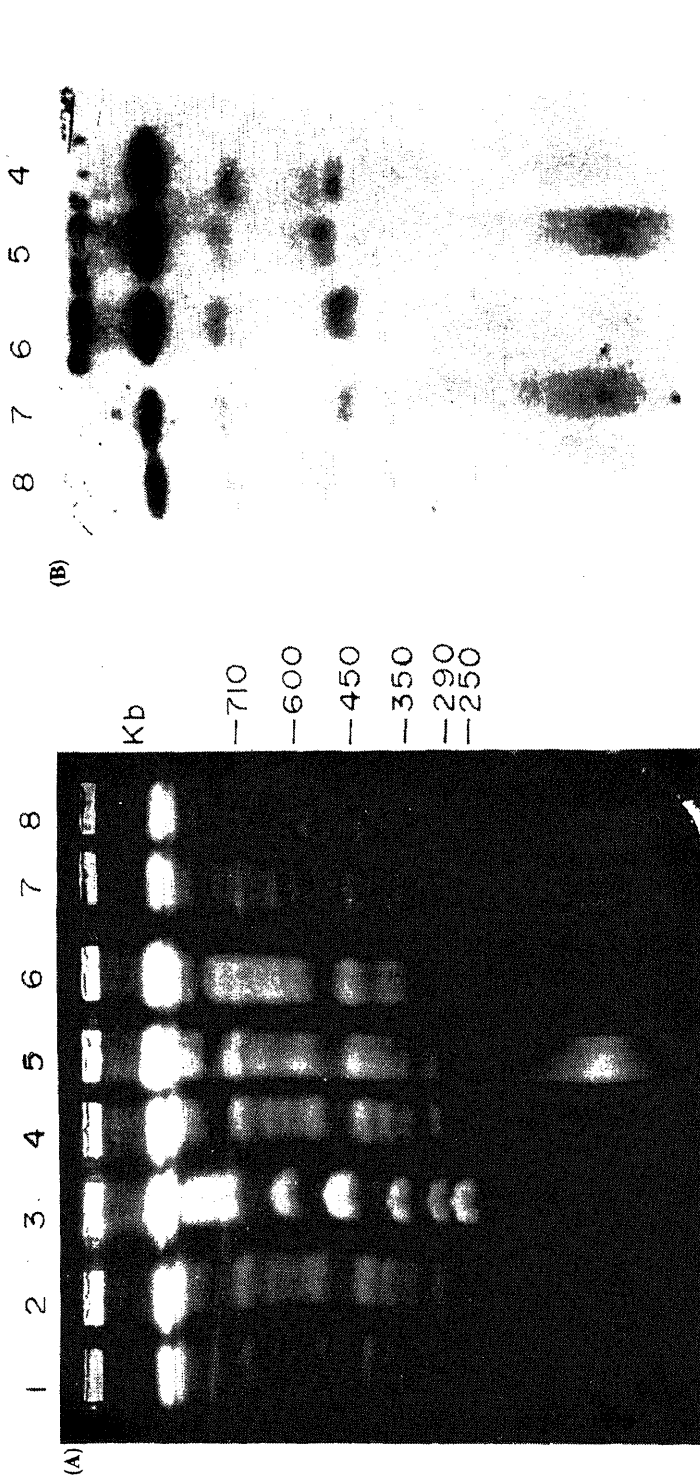


Figure 3. PFGE and Southern blot analysis of chromosomes from *L. donovani*. (A) Ethidium bromide-stained gel showing fractionation of chromosomes of *L. donovani* strains by pulse field gradient gel electrophoresis at a pulse time 80 s. Lane 1, 2 and 4, *L. donovani* strain UR6; lane 5 and 8, strain DD8; and lane 6 and 7, strain AG83. Lane 3, *S. cerevisiae* chromosomes run as molecular weight markers, whose sizes (kbp) are shown at the right. (B) Southern blot of part of the PFGE gel shown in (A) hybridized with oligo-labelled β T1 probe for chromosomal localization of β -tubulin isogenes. Lane numberings are the same as in (A).

L. L. L. L. L. L. L. L. L. L.	d. d. d. d. d. d. d. d. d. d.	me me me me me me me me me me	Phe TTC	Arg CGC	Thr ACC G	Val GTG C	Lys AAG	Leu CTG	Thr ACG	Thr ACG	Pro CCG	Thr ACG	Phe TTC						
			Gly GGT	Asp GAC	Leu CTG	Asn AAC	- CAC(His)	Leu CTC	Val GTC	Ala GCC	Ala GCT C	Val GTG	Met ATG						
			Ser TCT	Gly GGC	Val GTG	Thr ACC	Cys TGC	Cys TGC	Leu CTG	Arg CGC	Phe TTC	Pro CCT	Gly GGC						
			Gln CAG	Leu CTG	Asn AAC	Ser TCT	Asp GAC	Leu CTG	Arg CGC										
																			(A)
			Ser TCG	Thr ACC	Lys AAG	Glu GAG	Val GTG	Asp GAC	Glu GAG	Gln CAG	Met ATG	Leu CTG	Asn AAC	Val GTG	Gln CAG	Asn AAC	Lys AAG		
			Asn AAC	Ser TCC	Ser AGC	Tyr TAC	Phe TTC	Ile ATC	Glu GAG	Trp TGG	Ile ATC	Pro CCG	Asn AAC	Asn AAC	Ile ATC	Lys AAG	Ser TCC		
			Ser TCC	Ile ATC	Cys TGC	Asp GAT	Ile ATC	Pro CCG	Pro CCC	Lys AAG	Gly GGT	Leu CTC	Lys AAG	Met ATG	Ser TCC	Val GTC	Thr ACC		
			Phe TTC	Ile ATC	Gly GGC	Asn AAC	Asn AAC	Thr ACC	Cys TGC	Ile ATC	Gln CAG	Glu GAG	Met ATG	Phe TTC	Arg CGC	Arg CGC	Val GTC		
			Gly GGT	Glu GAG	Gln CAG	Phe TTC	Thr ACG	Gly GGC T	Met ATG	Phe TTC									(B)

Figure 4. Partial nucleotide sequence of the β -tubulin gene from clone pLD β T1. The sequence is compared with homologous region of the published β -tubulin gene sequence of *L. mexicana amazonensis* (Fong and Lee, 1988). Nucleotide differences between the two sequences are indicated. (A) DNA sequence of internal coding region (from *Hind*III end of the cloned gene). (B) C-terminal coding region (from *Sal*I end).

chromosomal loci. The organization of the β -tubulin repeat is very similar to that observed in other *Leishmania* species. With respect to repeat length (3.5 kbp) and restriction map, particularly, the structure most closely resembles that of *L. tropica* (Huang *et al.*, 1984). Existence of multiple copies of the tubulin genes may be a mechanism to allow high level of transcription of β -tubulin mRNA required for promastigote growth and division (Huang *et al.*, 1984).

In genomic Southern blots, apart from the major repeat band one or two dispersed copies were observed which are apparently single copy genes. The PFGE Southern blot hybridization experiment confirmed the dispersed copy genes. The ratio obtained by scanning of the autoradiogram, clearly shows the lower abundance of the dispersed tubulin genes in contrast to the major repeat. The function, if any, of these dispersed genes is unknown. They may encode functionally different variants; alternatively some or all of these genes may be non-functional pseudogenes. A transposon-interrupted β -tubulin pseudogene has been recently reported in *Trypanosoma brucei* (Affolter *et al.*, 1989). Multiple β -tubulin mRNAs have been observed in *L. donovani* (Adhya *et al.*, 1990) but only one of these is derived from the major repeat. A similar conclusion was derived in *L. major* (Spithill and Samaras, 1987). Therefore some or all of the dispersed copies are transcriptionally active. Cloning and sequencing of the dispersed genes should provide more information on their function.

The chromosomal location of the major repeat was found to be conserved in Indian isolates of *L. donovani*, but the chromosomal loci for the dispersed repeats vary somewhat between the strains. Variation in the chromosome size and location of the dispersed loci of the β -tubulin isogenes between the strains is an indication of the genomic plasticity of these organisms. It should be possible to extend the method of direct chromosomal localization to other genes of *L. donovani* for which DNA probes are available.

Acknowledgement

We are grateful to Dr. Scott Landfear and Dr. Dyann Wirth of the Harvard School of Public Health, Boston, Massachusetts, USA for providing the pLE β 3 clone. We are also indebted to Prof. A. N. Bhaduri for his help and encouragement. This work was partly supported by United Nations Development Programme project IND/87/018/A/01/99. One of the authors (S. D.) is supported by a fellowship from the Council of Scientific and Industrial Research, New Delhi.

References

- Adhya, S., Das, S. and Bhaumik, M. (1990) *J. Biosci.*, **15**, 249.
- Alfölte, M., Rindisbacher, L. and Braun, R. (1989) *Gene*, **80**, 177.
- Bibring, T., Baxandall, J., Denslow, S. and Walker, B. (1976) *J. Cell. Biol.*, **69**, 301.
- Carle, G. F. and Olson, M. V. (1985) *Proc. Natl. Acad. Sci. USA*, **82**, 3756.
- Cleveland, D. W., Hughes, S. H., Stablefield, E., Kirschner, M. W. and Varmus, H. E. (1988) *Chem.*, **256**, 3130.
- Feinberg, A. P. and Vogelstein, B. (1983) *Anal. Biochem.*, **132**, 6.
- Fong, D. and Chang, K. P. (1981) *Proc. Natl. Acad. Sci. USA*, **78**, 7624.
- Fong, D., Wallach, M., Keithly, J., Melera, P. W. and Chang, K. P. (1984) *Proc. Natl. Acad. Sci. USA*, **81**, 5782.
- Fong, D. and Lee, B. (1988) *Mol. Biochem. Parasitol.*, **31**, 97.
- Fulton, C. and Simpson, P. A. (1976) in *Cell motility* (ed. P. Goldman, T. Pollard and J. L. Rosenbaum) (New York: Cold Spring Harbor Press) p. 987.
- Hattori, M. and Sakaki, Y. (1986) *Anal. Biochem.*, **152**, 232.
- Huang, P. L., Roberts, B. E., McMahon-Pratt, D., David, J. R. and Miller, J. S. (1984) *Mol. Cell. Biol.*, **4**, 1372.
- Kowit, J. D. and Fulton, C. (1974) *Proc. Natl. Acad. Sci. USA*, **71**, 2877.
- Landfear, S. M., McMahon-Pratt, D. and Wirth, D. F. (1983) *Mol. Cell. Biol.*, **3**, 1070.
- Lemischka, I. R. and Sharp, P. A. (1982) *Nature (London)*, **300**, 330.
- Leon, W., Fouts, D. L. and Manning, J. (1978) *Nucleic Acids Res.*, **5**, 491.
- Maniatis, T., Fritsch, E. F. and Sambrook, J. (1982) *Molecular cloning, a laboratory manual* (N. B. Cold Spring Harbor Laboratory).
- Ray, J. C. (1932) *Indian J. Med. Res.*, **20**, 355.
- Rigby, P., Dieckman, M., Rhodes, C. and Berg, P. (1977) *J. Mol. Biol.*, **113**, 237.
- Silflow, C. D. and Rosenbaum, J. L. (1981) *Cell*, **24**, 81.
- Southern, E. (1975) *J. Mol. Biol.*, **98**, 503.
- Spithill, T. W. and Samaras, N. (1985) *Nucleic Acids Res.*, **13**, 4155.
- Spithill, T. W. and Samaras, N. (1987) *Mol. Biochem. Parasitol.*, **24**, 23.
- Thomashow, L. S., Milhausen, M., Rutter, W. J. and Agabian, N. (1983) *Cell*, **32**, 35.
- Wilde, C. D., Crowther, C. E. and Cowan, N. J. (1982) *Science*, **217**, 549.
- Witman, G. B., Carlson, K. and Rosenbaum, J. L. (1972) *J. Cell. Biol.*, **54**, 540.

Transcription and processing of β -tubulin messenger RNA in *Leishmania donovani* promastigotes

SAMIT ADHYA*, SAUMITRA DAS and MANTU BHAUMIK

Laboratory of Genetic Engineering (Leishmania Group), Indian Institute of Chemical Biology, 4, Raja S. C. Mullick Road, Calcutta 700 032, India

MS received 10 September 1990

Abstract. Transcription of the multicopy β -tubulin locus in *Leishmania donovani* promastigotes was examined by nucleic acid hybridization techniques. By northern analysis of promastigote RNA multiple β -tubulin mRNAs were detected. The major species of 2.2 kb RNA is derived from the tandem repeat cluster of β -tubulin genes, the other two (2.4 and 2.6 kb) are presumably derived from dispersed genomic loci. Combined S1-nuclease and primer extension mapping experiments demonstrated the presence of a single 5'-terminus with a 35 nucleotide spliced-leader sequence. The 3'-termini are heterogeneous. The development of a nuclear run-on system in *Leishmania* for studying transcription of individual genes is reported. Active but transient RNA polymerase II activity was observed in this system. Using specific DNA probes for labelled run-on RNA it was shown that β -tubulin transcription occurs asymmetrically (*i.e.*, on one strand of the DNA template) in an α -amanitin sensitive manner. The significance of these results for the life cycle of the parasite is discussed.

Keywords. *Leishmania*; β -tubulin mRNA; hybridization; nuclear transcription.

Introduction

Leishmania donovani is a kinetoplastid parasite protozoan that causes the disease known as kala-azar or visceral leishmaniasis in man. This vector-transmitted parasite has a dimorphic life cycle consisting of a free living flagellated promastigote stage within the gut of sandfly vectors, and a mammalian form, the amastigote, that resides within phagolysosomal vesicles of host macrophages (Zuckerman and Lainson, 1979).

Tubulins are major structural proteins of *Leishmania* promastigotes. During differentiation (transformation) of amastigotes to promastigotes, there is significant induction of tubulin biosynthesis in response to greater demands imposed by flagellar synthesis (Fong and Chang, 1981). The mechanism of this induction is not known. Both transcriptional (Landfear and Wirth, 1984) and post-transcriptional mechanisms (Wallach *et al.*, 1982; Fong *et al.*, 1984) have been implicated in other *Leishmania* species. Similarly, the promoter for tubulin mRNA transcription, and the biosynthesis of tubulin mRNA *via* RNA processing, are not well understood.

In this report, we characterize the β -tubulin mRNAs of *L. donovani* promastigotes in terms of number, size and 5'- and 3'-termini. We also report for the first time the development of a nuclear run-on transcription system in *Leishmania* for studying features of β -tubulin transcription.

*To whom all the correspondence should be addressed.

L. donovani strain UR6 (WHO nomenclature-MHOM/IN/1978/UR6) promastigotes were cultivated in modified Ray's (1932) agar medium containing 3.7% brain infusion (Difco), 1% glucose, 1.5% agar, 10,000 units/ml penicillin, 10,000 units/ml streptomycin and 1% whole rabbit blood. Incubation was at 25°C for 48–72 h.

Preparation of parasite DNA and RNA

Total high molecular weight promastigote DNA was prepared by lysis with sodium dodecyl sulphate (SDS) and proteinase K, followed by phenol extraction, dialysis, RNase treatment and ethanol precipitation. Total RNA was prepared by the guanidium isothiocyanate-hot phenol method and mRNA selected by oligothymine cellulose chromatography (Maniatis *et al.*, 1982).

DNA probes

Clone β T-1 contains a 3.3 kb *Hind*III-*Sall* genomic fragment of the *L. donovani* tubulin tandem repeat (figure 1; Das and Adhya, 1990). Probe C is a 1.2 kb *Hind*III-*Xho*I fragment containing coding sequences of the β -tubulin gene. Probe UT is a *Pst*I fragment derived from the 3'-untranslated region of the β -tubulin gene. Probes were labelled by the random oligonucleotide priming method (Feinberg and Vogelstein 1983) using [α - 32 P] TTP (3000 Ci/mmol, Bhabha Atomic Research Centre, Bombay). Probe A is a 240 bp *Pst*I fragment derived from the coding region of the gene (figure 1) cloned in both orientations in M13mp9 vector.

Northern blot hybridization

Total or polyadenylated RNA from *L. donovani* promastigotes was denatured as described by Thomas (1980) in 1 M deionized glyoxal, 50% dimethyl sulphoxide and 10 mM sodium phosphate, pH 7 at 50°C for 1 h. Denatured RNA was electrophoresed on a 1.2% agarose gel in 10 mM sodium phosphate, pH 7 at 100 V for 3–4 h, then transferred by capillary diffusion to Zeta probe membrane (BioLabs) using 10 \times SSC as transfer buffer. The filter was baked for 2 h at 80°C under vacuum. Glyoxal adducts were removed from the RNA by pouring 20 mM NaOH, pH 12, 1 mM EDTA at 95–100°C on the filter and allowing to cool to room temperature. The membrane was pre-hybridized at 42°C for 18 h in 50% deionized formamide, 5 \times SSC, 5 \times Denhardt's solution (Maniatis *et al.*, 1982), 20 mM sodium phosphate, pH 7, 0.1% SDS and 200 μ g/ml calf thymus or herring sperm DNA. Hybridization was performed in the same solution additionally containing the denatured, oligo-labelled DNA probe (specific activity 10⁷ cpm/ μ g, 10⁵–10⁶ cpm/ μ g) at 42°C for 48 h. The filter was then washed twice with 2 \times SSC, 0.1% SDS, then with 0.5 \times SSC, 0.1% SDS and once with 0.1 \times SSC, 0.1% SDS, each wash being for 15 min at room temperature with vigorous agitation. The filter was autoradiographed. To rehybridize the filter with a second probe, filter-bound [32 P] was stripped

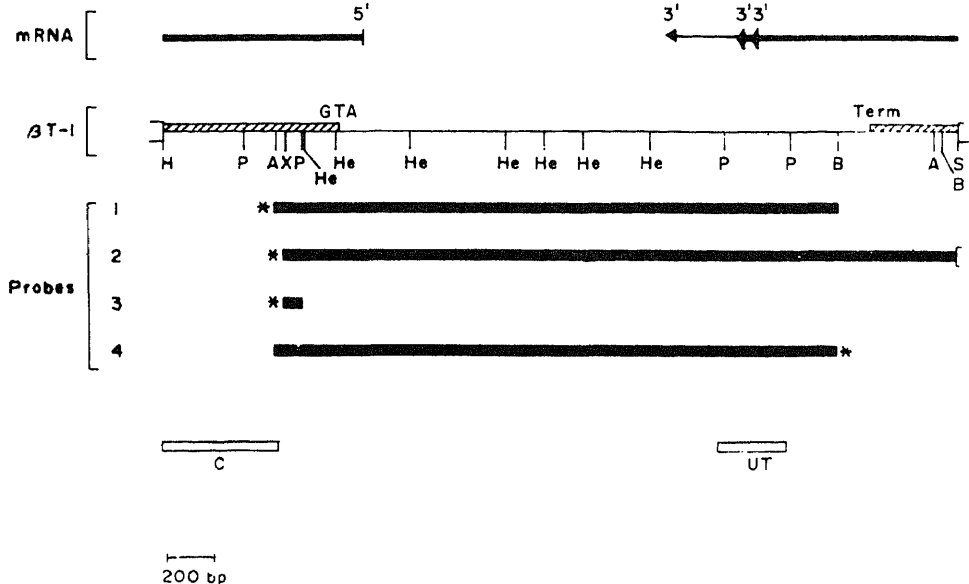


Figure 1. Restriction and transcription maps of the β -tubulin locus in *L. donovani* promastigotes. Locations of restriction sites on the genomic clone β T-1 are shown (H, *Hind*III; P, *Pst*I; A, *Ava*I; X, *Xho*I; He, *Hae*III; B, *Bam*HI; S, *Sal*I). Square brackets flanking the restriction map represent pUC8 vector sequences. The mRNA map is shown above the restriction map; thick and thin lines represent major and minor RNA species, respectively, revealed by S1 mapping. DNA probes 1-4 used for S1 mapping and primer extension are depicted as filled bars, with the labelled ends marked with asterisks. Open bars represent fragments from the coding (C) and 3'-untranslated region (UT) of the gene used as hybridization probes.

immersion in a 95°C water bath for 10 min. Pre-hybridization, hybridization and washing were then carried out as before.

S1 mapping

DNA probes used for mapping are shown in figure 1. Restriction fragments were 5'-labelled using [γ - 32 P] ATP and T4 polynucleotide kinase as described (Maniatis *et al.*, 1982). To label the 3'-terminus of the *Bam*HI end of probe 4 (figure 1), an end-filling reaction with Klenow fragment and dGTP and [α - 32 P] dATP was performed (Maniatis *et al.*, 1982). Uniquely labelled fragments were obtained by digestion with a second restriction enzyme followed by gel purification of the appropriate bands. Labelled probe (10-15,000 cpm) was hybridized with 1-2 μ g polyadenylated RNA in 10 μ l buffer containing 80% deionized formamide, 0.4 M NaCl, 40 mM PIPES, pH 6.4 and 1 mM EDTA under paraffin oil. After heating at 68°C for 10 min to denature the probe, reactions were transferred to the annealing temperature of 55°C for 6-15 h. Reactions were quenched with 0.2 ml S1 buffer (0.3 M NaCl, 30 mM sodium acetate, pH 4.5, 1 mM ZnSO₄) containing 218 units S1 nuclease (P L Biochemicals). Digestion was carried out for 30 min at 37°C, S1-

resistant products were purified by phenol-extraction and ethanol precipitation and analyzed by electrophoresis on a 5% acrylamide-8 M urea gel at 200 V for 2 h.

Primer extension

The 5'-[³²P] labelled *Xho*I/*Pst*I fragment (probe 3, figure 1) was hybridized to 1.9 µg polyadenylated RNA as described above for the S1 mapping experiment. The reaction was chilled on ice and nucleic acids were ethanol precipitated. The hybridized primer was then extended with MMLV reverse transcriptase (BRL) in a 10 µl reaction containing 50 mM Tris-HCl, pH 7.5, 75 mM KCl, 10 mM DTT, 3 mM MgCl₂, 1 mM each of the 4 deoxyribonucleoside triphosphates and 200 units of enzyme. After incubating at 37°C for 1 h, nucleic acids were ethanol precipitated and analysed by denaturing acrylamide electrophoresis as above.

Preparation of crude nuclei

All operations were carried out at 0°–4°C. *L. donovani* promastigotes were harvested from blood-agar slants and washed twice with ice-cold phosphate buffered saline (150 mM NaCl, 20 mM sodium phosphate, pH 7.2). Approximately 1 ml packed cells were suspended in 5 ml buffer A (10 mM Tris-HCl, pH 8, 10 mM NaCl, 1.5 mM MgCl₂, 1 mM EGTA, 5 mM DTT, 0.1 mM EDTA, 0.1 mM PMSF and 100 units/ml placental RNase inhibitor) containing 0.1% Triton X-100. Cells were placed on ice for 5 min, then homogenized in a Dounce homogenizer (15–20 strokes). After microscopic examination for cell lysis, the homogenate was centrifuged at 3300 *g* for 10 min in a Sorvall SS34 rotor. The crude nuclear pellet was washed once with buffer A (lacking Triton) and suspended in 4 ml nuclei storage buffer (50 mM Tris-HCl, pH 8, 1.5 mM MgCl₂, 0.1 mM EDTA, 5 mM DTT, 25% glycerol and 100 units/ml RNase inhibitor) at a concentration of 2 × 10⁹ nuclei/ml. Nuclei were stored frozen in small aliquots at –70°C.

Nuclear transcription

Reaction mixtures contained 12.5 mM Tris-HCl pH 8, 50 mM NaCl, 5 mM MgCl₂, 10 mM creatine phosphate, 1 mM each of GTP and CTP, 4 mM ATP, 10 µM UTP, 1 mCi/ml [α -³²P] UTP (Amersham, 3,000 Ci/mmol) and 10⁹ nuclei/ml. Reactions were incubated for 10 min at 25°C. To assess the effect of inhibitors, nuclei were pre-incubated with α -amanitin (20 µg/ml) or actinomycin D (200 µg/ml) for 15 min on ice before dilution with an equal volume of 2 × transcription buffer. Transcription was terminated by adding SDS (1%) and proteinase K (100 µg/ml) and incubation at 25°C for 15 min. RNA was phenol-extracted and ethanol precipitated. Contaminating DNA was removed by treatment with RNase-free DNase I (Boehringer-Mannheim). Unincorporated [³²P] triphosphates were separated by chromatography on a Sephadex G-100 column followed by ethanol precipitation of the excluded RNA peak, or by two ethanol precipitations in the presence of 2.5 M ammonium acetate. This RNA was used for hybridization. Incorporation of [³²P] nucleotide into RNA was measured by spotting aliquots of reaction mixtures on DE81 filters (Whatman), washing 5 times with 0.5 M NaH₂PO₄, twice with H₂O, once with ethanol, followed by drying and liquid scintillation counting.

[^{32}P] labelled nascent nuclear RNA was hybridized to slot of cloned plasmids (μg) on nitrocellulose or Zeta probe membranes. Filters were pre-hybridized in $5\times$ Denhardt's solution, 10 mM sodium phosphate, pH 7, 0.1% SDS and $100\mu\text{g/ml}$ tRNA for 16–18 h at 65°C . Hybridization was for 48 h at 65°C in the same buffer containing [^{32}P] nascent RNA (10^5 – 10^6 cpm/ml). After hybridization, filters were washed twice with $3\times$ SSC, 0.1% SDS for 15 min at 50°C , then twice with $0.3\times$ SSC, 0.1% SDS for 15 min at 50°C , and autoradiographed.

Results

Northern blot analysis of β -tubulin mRNA

Total or polyadenylated RNA from *Leishmania* promastigotes was electrophoresed under denaturing conditions in an agarose gel, transferred to a nylon membrane and hybridized with [^{32}P] labelled probe C (figure 1) derived from the coding region of the β -tubulin gene. As shown in figure 2, three specific β -tubulin RNA species were observed: a major species of 2.2 kb length and two minor species of 2.4

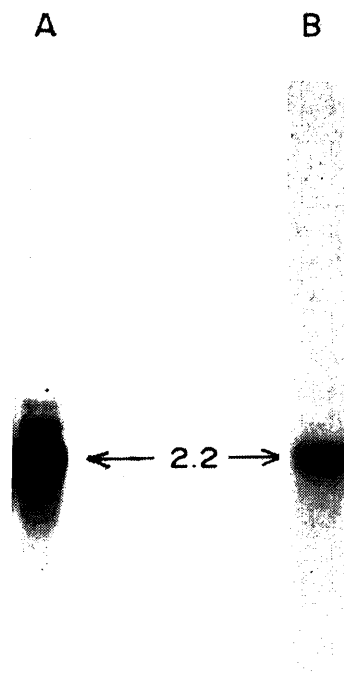


Figure 2. Northern blot hybridization of *L. donovani* promastigote RNA. Lane A, total RNA ($10\mu\text{g}$) hybridized with coding probe C (figure 1). Lane B, the same filter was stripped of probe and re-hybridized with non-coding probe UT (figure 1). The major 2.2 kb species is indicated. The minor species are of 2.4 and 2.6 kb respectively.

they are poly A⁺ RNAs (data not shown).

In a separate study (Das and Adhya, 1990) we have shown that there are at least 3 chromosomal loci for β -tubulin genes in *L. donovani*. Clone pLD β T-1 (figure 1) is derived from the major cluster of 12–15 genes. The observation of multiple β -tubulin mRNA species raises the question as to whether all are transcribed from the same chromosomal locus. To answer this question probe C was melted off the filter and filter-bound RNA re-hybridized with probe UT, which is derived from the 3'-untranslated region of the clone (figure 1). Only the major 2.2 kb species hybridized to this probe (figure 2). Since 3'-untranslated regions of the same genes at different chromosomal loci usually vary considerably in sequence, while coding regions are conserved, this result demonstrates that the 2.4 and 2.6 kb RNA species are probably transcribed from loci distinct from the major repeat cluster.

Mapping of steady state mRNA

To precisely delineate the 5' and 3' boundaries of β -tubulin mRNA on the genome, S1 nuclease mapping and primer-extension experiments with reverse transcriptase were performed on poly A⁺ promastigote RNA using end-labelled restriction fragments of β T-1 as probes or primers. When the 2.2 kb *Ava*I/*Bam*HI fragment, labelled at the *Ava*I-end (probe 1, figure 1) was hybridized to poly A⁺ RNA and the hybrid digested with S1 nuclease, a single protected labelled DNA fragment 310 nucleotides (nt) long was obtained (figure 3A, lane 2). In the absence of added mRNA, there was no protection, confirming that the observed band was due to mRNA: probe hybrid and not due to reannealing of the probe (figure 3A, lane 1). A similar result was observed when the probe fragment was 5'-labelled at the *Xho*I-end (figure 1, probe 2); in this case the protected band was 270 nt in length (figure 3B, lane 1). From these observations it is apparent that (i) the direction of the transcription is from right to left as depicted in figure 1; and that (ii) a single 5'-terminus (or discontinuity, in case of splicing) is present in the mRNA at the position shown (figure 1). The nature of the discontinuity, if any, was investigated by a primer extension experiment using a 70 bp-*Xho*I/*Pst*I fragment, 5'-labelled at the same *Xho*I site as in the S1 experiment (probe 3, figure 1), to hybridize with mRNA and subsequently extend towards the 5'-terminus of the RNA with reverse transcriptase. As shown in figure 3B, lane 2, a single primer extension product, 310 nt long was observed, which is larger than the corresponding S1-protected product by about 40 nt. It is therefore evident that an exon or leader sequence, not contiguously coded with the β -tubulin gene, is added on to the body of the mRNA by a transcriptional priming or RNA processing (splicing) event.

The 3'-termini of the steady state β -tubulin mRNA were mapped by using the 2.2 kb *Bam*HI/*Ava*I fragment, 3'-labelled at the *Bam*HI end (probe 4, figure 1), as probe for S1 nuclease mapping. As shown in figure 3C, lane 2, three protected species, 370, 440 and 740 nt long, were observed in a 3.6:9:1 ratio (as determined by densitometry of the bands). Since polyadenylated RNA was used in the experiment, these bands probably represent poly A-addition sites on the genome, mapping at the positions shown in figure 1. Thus multiple 3'-termini are present in promastigote β -tubulin mRNA.

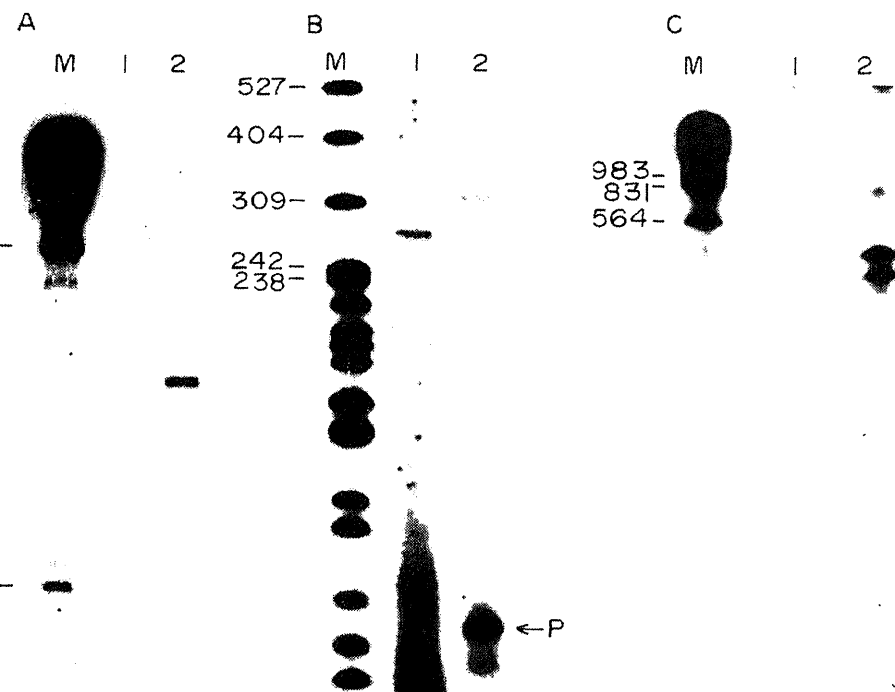


Figure 3. S1 nuclease and primer extension mapping of β -tubulin mRNA. Panel A: 5'-[32 P] labelled probe 1 (see figure 1) was hybridized to polyadenylated RNA (1.8 μ g, lane 2) or no RNA (lane 1), then digested with S1 nuclease. Panel B: Lane 1, polyadenylated RNA (1.9 μ g) was hybridized with 5'-[32 P] labelled probe 2 (see figure 1) and the hybrids were digested with S1 nuclease; lane 2, polyadenylated RNA (1.9 μ g) was hybridized with 5'-[32 P] labelled probe 3 (see figure 1) and the primer was extended with reverse transcriptase. Panel C: 3'-[32 P] labelled probe 4 (see figure 1) was hybridized with polyadenylated RNA (1.8 μ g, lane 2) or no RNA (lane 1) and the hybrids were digested with S1 nuclease. All reaction products were analyzed by 5% acrylamide-8 M urea gel electrophoresis. Lanes M, molecular weight markers, whose sizes (in nucleotides) are shown on the left of each panel.

Transcription of β -tubulin genes in isolated nuclei

The transcriptional status of specific chromosomal loci can be directly assessed by nuclear run-on assay. This method is based on the fact that in isolated nuclei chromatin, transcribing RNA polymerase remains bound to the DNA and to nascent RNA transcripts. Incubation of the nuclei or chromatin under appropriate conditions with radiolabelled ribonucleoside triphosphates results in the completion of nascent chains (run-on) with incorporation of radioactivity. Labelled RNA can then be used as a probe to hybridize with specific cloned DNA fragments.

Crude preparation of promastigote nuclei was incubated with [32 P] labelled ribonucleoside triphosphates at 25°C. Rapid incorporation of [32 P] into RNA was observed (figure 4). After 10 min the reaction rate was reduced. If incorporation was

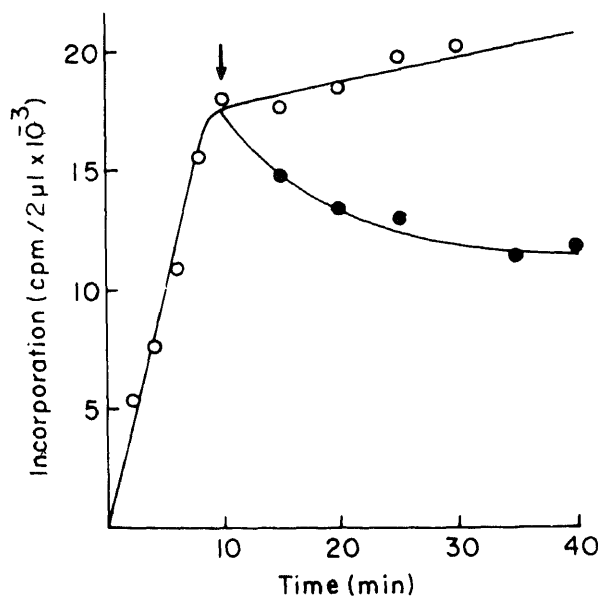


Figure 4. Kinetics of nascent RNA synthesis in isolated promastigote nuclei. A reaction mixture containing 30 μ l of isolated nuclei and 10 μ M [α - 32 P] UTP was incubated at 25°C and at times indicated 2 μ l aliquots were withdrawn for incorporation assay by DE81 filter binding (○). To assess stability of the RNA synthesized, 1 mM unlabelled UTP was added to a parallel reaction at 10 min (arrow) and incorporation assessed at intervals thereafter (●).

other experiments (not shown) we have observed more rapid degradation of nascent RNA after a peak at 10 min. It is therefore essential to block cellular nucleases with appropriate amounts of RNase inhibitor during nuclear transcription. When nuclei were pre-incubated with a low concentration (20 μ g/ml) of α -amanitin, an inhibitor of RNA polymerase II, incorporation was reduced by more than 90% (table 1). Thus the majority of nascent RNA in this system is transcribed by RNA polymerase II.

Table 1.

Reaction	Time of incubation (min)	Incorporation cpm/ μ l	Net incorporation cpm	Inhibition (%)
Complete	0	2714	—	—
	5	12878	10,154	—
	10	16831	14,112	—
Complete + 10 μ g/ml α -amanitin	0	1102	—	—
	5	2915	1813	82
	10	3073	1971	86

In the complete system, promastigote nuclei were incubated with rNTPs at 25°C in a vol of 20 μ l. To assess effect of α -amanitin, nuclei were pre-incubated with 40 μ g/ml α -amanitin for 15 min at 0°C before addition of NTPs and incubation at 25°C. Aliquots (1 μ l) were assayed for incorporation by DE81 filter binding.

Radiolabelled nuclear RNA was hybridized to specific DNA probes immobilized on nylon or nitrocellulose membranes. As shown in figure 5A, [^{32}P] nascent RNA hybridized specifically to $\beta\text{T-1}$ -DNA (slot 1), and only background binding was observed with pUC8 (slot 2). Slots 3 and 4 contained complementary single strands of the 240 bp *Pst*I fragment from the N-terminal coding region of $\beta\text{T-1}$ (figure 1) in M13. Hybridization occurred to only one strand (slot 3). Thus transcription at the β -tubulin locus is asymmetric. Specific transcription was sensitive to a low concentration (10 $\mu\text{g/ml}$) of α -amanitin (figure 5B, slot 2) and to 100 $\mu\text{g/ml}$ actinomycin D (figure 5B, slot 3). This indicates that DNA dependent RNA polymerase II mediates transcription of β -tubulin genes in this system.

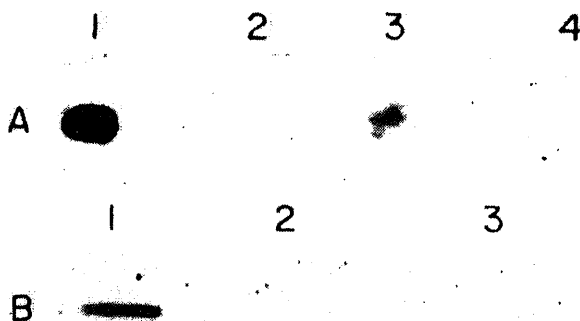


Figure 5. Hybridization analyses of nascent nuclear RNAs. [^{32}P] labelled RNA was obtained by transcription in isolated promastigote nuclei and hybridized to slots of cloned DNAs immobilized on Zeta probe (panel A) or nitrocellulose (panel B) membranes. Panel A: Specificity of β -tubulin transcription. Slot 1, $\beta\text{T-1}$ DNA (2.35 μg); Slot 2, pUC8 DNA (2.1 μg); Slot 3, M13 subclone A1 single-strand DNA (1.35 μg); Slot 4, M13 subclone A2 single-strand DNA (1.35 μg). Panel B: Effect of transcription inhibitors. Nuclear transcription was carried out in the absence of inhibitors (slot 1), or in the presence of 10 $\mu\text{g/ml}$ α -amanitin (slot 2) or 100 $\mu\text{g/ml}$ actinomycin D (slot 3). The RNAs were separately hybridized to slots of $\beta\text{T-1}$ DNA (1 μg each).

Discussion

In this report we have studied expression of β -tubulin mRNA in *Leishmania* promastigotes by nucleic acid hybridization techniques.

Recently we have cloned a genomic β -tubulin fragment from the parasite and studied chromosomal organization of β -tubulin genes using this cloned DNA as probe (Das and Adhya, 1990). These experiments showed that multiple copies of the β -tubulin gene are clustered as a tandem repeat on a single *Leishmania* chromosome. A few dispersed copies are also present. This pattern of major and minor genetic loci is reflected in the mRNA profile. Thus, one major (2.2 kb) and two minor (2.4 and 2.6 kb) species are observed. Hybridization with a gene-specific probe (figure 2) showed that major species is transcribed from the tandem repeat while the minor species may be derived from the dispersed genes. No information is yet available on the function of the minor mRNA species. They could

encode distinct β -tubulin proteins. Alternatively, one or more of these mRNAs may be developmentally regulated during transformation of one form of the parasite to another.

The major 2.2 kb β -tubulin mRNA has been mapped to the genomic DNA clone by S1 nuclease and primer extension experiments (figure 3). A unidirectional bipartite structure is evident; the two halves are separated by a spacer of approximately 1 kb (figure 1). This structure confirms the tandemly repeated arrangement of β -tubulin genes previously inferred from southern blot hybridization experiments (Das and Adhya, 1990).

S1 nuclease mapping experiments showed that a single 5'-terminus of β -tubulin mRNA is present. This includes a 35-nucleotide leader (or miniexon) sequence. Recent work with kinetoplastid protozoa (Van der Ploeg, 1986) has shown that nuclear mRNAs from these organisms have such a 5'-leader. This sequence is encoded by a separate gene cluster and spliced on to the body of cellular mRNA in a bimolecular reaction (*trans*-splicing). The function of the miniexon is not understood. Possibilities are: provision of 5'-cap structures for translation, mRNA stabilization or transport, etc. The β -tubulin system may be ideal for future investigations on RNA splicing which is undoubtedly vital for the life cycle of the parasite.

Multiple 3'-termini of β -tubulin mRNA were detected by hybridization (figure 4). These represent multiple polyadenylation sites on the same or different mRNAs. The two major S1-protected species map within a 300-bp *Pst*I fragment (figure 4). This 3'-untranslated region is not homologous to corresponding regions of the other two mRNA species of 2.4 and 2.6 kb (figure 2). Thus the two major, and probably also the minor, species are different polyadenylated versions of the 2.2 kb mRNA. There is a relatively long 3'-untranslated region of about 0.5 kb (figure 1). Such long noncoding 3'-sequences are a characteristic feature of *Leishmania* mRNAs. It remains to be seen whether such regions have any physiological function, such as mRNA stabilization and/or transport, translational regulation, etc. In summary our mapping results show that β -tubulin mRNA undergoes post-translational processing at both 5'- and 3'-termini.

Although a great deal is known about the mechanism of RNA splicing in *Leishmania* and other kinetoplastid organisms, the mechanism of transcript initiation at specific promoters remains poorly understood. There are many reasons for this: (i) the initiation sites for mRNA precursors have not been previously mapped, and (ii) *in vitro* transcription of promoter-containing DNA has not been established.

Recently, two independent reports (Bellofatto and Cross, 1989; Laban and Winkler, 1989) have described transient expression of CAT genes under control of parasite DNA. This system will be most useful for studying *Leishmania* gene expression in the future.

In order to define the transcription unit for β -tubulin we have initiated nuclear run-on experiments with *Leishmania*. Incorporation studies (table 1) show that addition of radiolabelled ribonucleoside triphosphates to nuclear-kinetoplast preparations from promastigotes leads to a rapid rise in RNA synthesis followed by a plateau. Surprisingly, about 80% of the activity is ascribable to the α -amanitin sensitive RNA polymerase II. The reason for cessation of RNA polymerase activity after about 10 min at 25°C is unknown, but may be due to inappropriate conditions of transcription. The remaining 20% of α -amanitin resistant activity

to RNA polymerases I, III and the corresponding kinetoplast enzyme. By hybridization of nascent [^{32}P] labelled nuclear RNA to specific DNA probes (4), it was demonstrated that β -tubulin genes are transcribed by RNA polymerase II in a strand-specific manner. Other polymerase II genes are also transcribed in this system (unpublished data). We are continuing such hybridization experiments to precisely define the structure of the β -tubulin pre-mRNA. This will be essential for definition of the β -tubulin promoter in *Leishmania*.

Acknowledgements

We are thankful to Prof. A. N. Bhaduri, for his continued help and encouragement. This work was partly supported by the UNDP Project No. IND/87/018/A/01/99. S. B. is a fellow of the Council of Scientific and Industrial Research, New Delhi. M. B. is supported by UNDP.

References

- Adhya, V. and Cross, G. A. M. (1989) *Science*, **244**, 1167.
Adhya, V. and Adhya, S. (1990) *J. Biosci.*, **15**, 239.
Chang, K. P. and Chang, K. P. (1981) *Proc. Natl. Acad. Sci. USA*, **78**, 7624.
Chang, K. P., Wallach, M., Keithley, J., Melera, P. W. and Chang, K. P. (1984) *Proc. Natl. Acad. Sci. USA*, **81**, 782.
Chang, K. P. and Vogelstein, B. (1983) *Anal. Biochem.*, **132**, 6.
Chang, K. P., S. M. and Wirth, D. F. (1984) *Nature (London)* **309**, 716.
Chang, K. P. and Wirth, D. F. (1989) *Proc. Natl. Acad. Sci. USA*, **86**, 9119.
Sambrook, J., Fritsch, E. F. and Sambrook, J. (1982) *Molecular cloning: a laboratory manual* (New York: Cold Spring Harbor Laboratory).
Chatterjee, C. (1932) *Indian J. Med. Res.*, **20**, 355.
Chang, K. P. S. (1980) *Proc. Natl. Acad. Sci. USA*, **77**, 5201.
Ploegh, L. H. T. (1986) *Cell*, **47**, 479.
Chang, K. P., M., Fong, D. and Chang, K. P. (1982) *Nature (London)* **299**, 650.
Fong, D., Chang, K. P. and Lainson, R. (1979) in *Parasitic protozoa* (ed. J. P. Krier) (New York: Academic Press) **1**, p. 57.

Molecular cloning and restriction enzyme analysis of a long repetitive DNA sequence in rice

V. S. GUPTA*, M. S. DHAR, B. G. PATIL, G. S. NARVEKAR,
S. R. RAWAT and P. K. RANJEKAR

Division of Biochemical Sciences, National Chemical Laboratory, Pune 411 008, India

MS received 11 November 1989; revised 8 October 1990

Abstract. Rice long repetitive DNA (9–20 kbp) reassociating at Cot 50 M.s was cloned in pBR325. Out of several recombinants (Cam^r Amp^r Tet^s), only a few were selected randomly for further characterization. The insert size in all these clones was 3–4 kbp. Restriction enzyme analysis showed the absence of *Eco*RI and *Bcl*II sites, presence of a single *Pst*I and *Pvu*II site and multiple sites for *Alu*I in 3 clones namely pRL1, pRL7 and pRL10.

The *Bam*HI-*Pst*I fragment of about 0.4 kbp in the pRL7 insert DNA (pRL7-0.4 kbp) was subcloned in M13mp18 and partially sequenced using Sanger's dideoxynucleotide chain termination method. Dot matrix comparison of this sequence with rice rDNA sequences revealed low homology with the 25S rDNA sequence of rice, however, hybridisation did not indicate any homology.

Keywords. Rice; long repetitive DNA; cloning; restriction enzyme analysis.

Introduction

In recent years, a large number of repetitive DNA sequences have been cloned and characterized from a number of plant species. Their species-specific nature has been clearly demonstrated in closely as well as distantly related plants (Jelinek, 1982; Evans *et al.*, 1983; Sorenson, 1984; Pental and Barnes, 1985; Sala *et al.*, 1985; Metzlafl *et al.*, 1986; Sonina *et al.*, 1989). Also, a specific repetitive sequence has been used as marker to study phylogenetic relationships (Hallden *et al.*, 1987). Besides cloning, a few repeat families have also been sequenced (Orgel and Crick, 1980; Deumling, 1981; Kato *et al.*, 1984), and these studies have revealed conservation/divergence of specific repeat elements.

Earlier, we have described the unique pattern of genome organization in rice wherein the repetitive DNA sequences are arranged as tandem arrays of length as high as 6.5 and 20 kbp (Gupta *et al.*, 1981; Dhar *et al.*, 1988). Furthermore, we have also shown the presence of 4 different types of repeat families in rice repetitive DNA. Out of these 4 families, the long repeats reassociating by Cot 50 M.s showed some homology to the long and short repeat sequences reassociating by Cot 0.1 M.s and to the short repeats of Cot 50 M.s itself. As a continuation of this study, we have carried out cloning and analysis of long repeats reassociating by Cot 50 M.s and these data are included in this report.

Molecular cloning and sequencing of rice repetitive DNA

The rice long repetitive DNA sequences reassociating at Cot 50 M.s (9–20) were isolated according to Dhar *et al.* (1988). These were then digested with *Bam*HI and cloned in pBR325 (Prentki *et al.*, 1981) and *Escherichia coli* DH1 as the host. Furthermore, the 0.4 kbp *Bam*HI-*Pst*I fragment was subcloned into M13mp18 and *E. coli* JM101 (Norranders *et al.*, 1983; Yannisich-Perron *et al.*, 1983) was used as the host for transformation.

The procedures followed for plasmid cloning were essentially according to Maniatis *et al.* (1982) and the steps involved in M13 cloning and sequencing according to the New England Biolab's Laboratory Manual.

Isolation of recombinant plasmid DNA

This was carried out by the rapid isolation method of Barnes (1977) and by the lysis method of Birnboim and Doly (1979) and the recombinant DNAs were used for further characterization.

Isolation and characterization of template DNA for sequencing

The recombinant (white) plaques were used for isolation of template DNA by the method of Schreier and Cortese (1979). The insert size was checked by gel electrophoresis as described by Messing (1983).

Finally, the cloned rice repetitive DNA was sequenced essentially according to Sanger *et al.* (1977).

The samples were loaded on 8% polyacrylamide gel of thickness 0.5 mm. Electrophoresis was carried out at 2000 V. After electrophoresis, the gel was transferred to a glass plate and exposed to X-ray film for about 16 h at -70°C .

Sequence analysis was carried out using SEQAID II programme of D. J. Garfield which was a kind gift by Prof. S. Muthukrishnan, Kansas State University, Manhattan, USA.

Results and discussion

Cloning of rice long repetitive DNA in pBR325

The S1 nuclease resistant long repetitive DNA sequences (9–20 kbp) reassociating at Cot 50 M.s were used for cloning in pBR325. To check the digestibility of the DNA, it was treated with a few restriction enzymes such as *Eco*RI, *Sal*I, *Pvu*II and *Bam*HI which have unique cloning sites in pBR325. Out of these enzymes *Bam*HI showed the desired digestion in the range of 2–9 kbp and hence was used during cloning. The recombinant clones were selected by their sensitivity to tetracycline and resistance towards chloramphenicol and ampicillin (Cam^r Amp^r Tet^s). The presence of rice repetitive sequences in these clones

confirmed by colony hybridisation using [$\alpha^{32}\text{P}$] labelled rice long repetitive DNA. Out of several recombinants, only a few were selected randomly for further characterisation.

Size of insert DNAs and their restriction patterns

In order to determine the insert size, the cloned DNAs were digested with *Bam*HI. As is evident from figure 1, most of the cloned DNA sequences are of size 3–4 kbp. The insert size, for example, is 3.4 kbp in pRL1, 3.6 kbp in pRL2 and pRL7, 4.0 kbp in pRL5 and 3.7 kbp in pRL8.

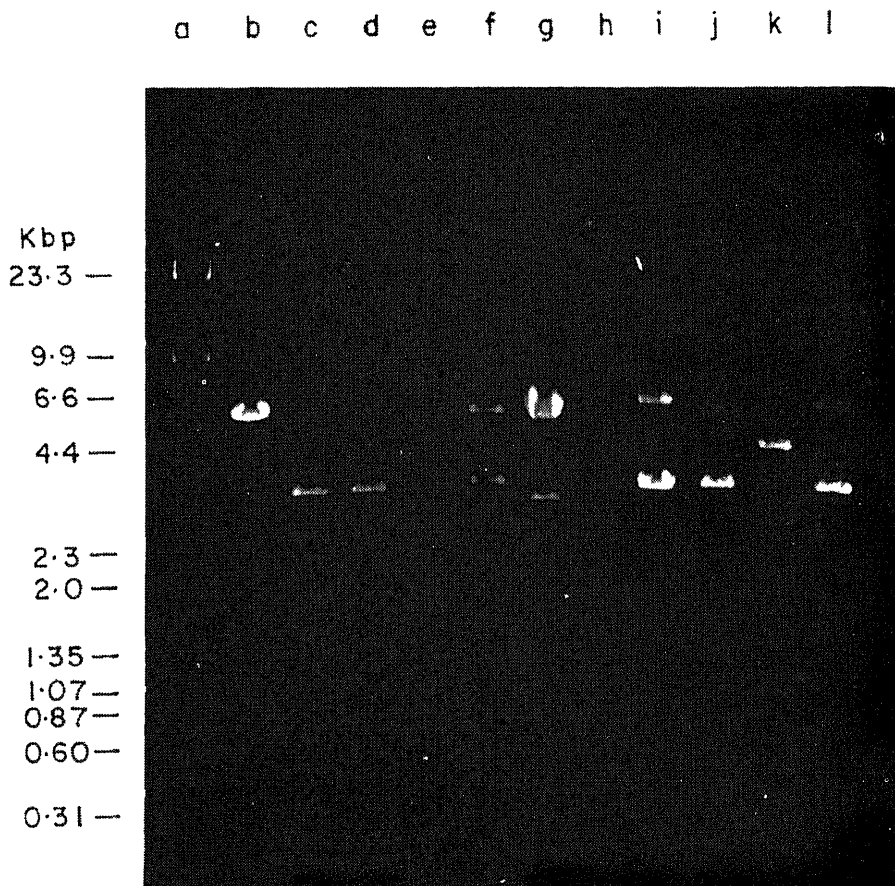


Figure 1. Digestion of pRL1-pRL10 DNAs with *Bam*HI. Lane a, lambda *Hind*III digest; lane b, pBR325 digested with *Bam*HI; lanes c-l, pRL1-pRL10 digested with *Bam*HI. The arrows indicate the molecular weights of the linearised pBR325 and the insert DNAs. Electrophoresis was carried out on 0.7% neutral agarose slab gels in TAE buffer (pH 8.1) at a constant current of 30 mA.

To assess the presence of sites for a few other restriction enzymes in the inserts, the plasmids were digested with a few enzymes like *Ava*I, *Hind*III, *Pvu*II and *Pst*I which have either single or double cutting sites in pBR325. Figure 2 shows the

l a b c d e f g h i j k l

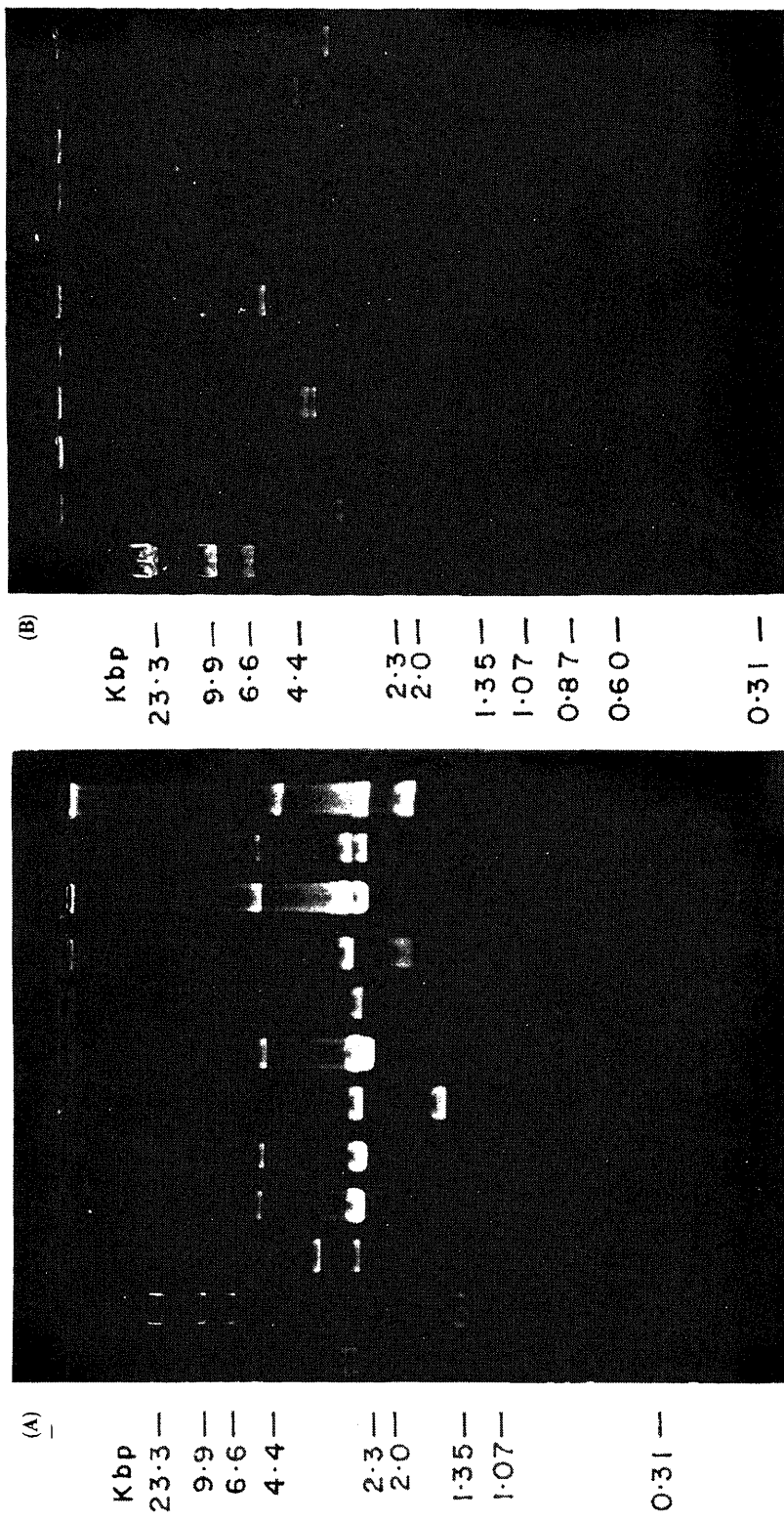


Figure 2. Digestion of pRL1-pRL10 DNAs with (A) *Pst*I and (B) *Hae*III digest and $\phi \times 174$ *Hae*III digest; lane b, pBR325; lanes c-l, pRL1-pRL10. Electrophoresis was carried out on 0.7% neutral agarose slab gels in TAE buffer (pH 8.1) at a constant current of 30 mA.

digestion patterns with *Pvu*II and *Pst*I. The differences in their digestion patterns with all these enzymes indicate the occurrence of different restriction sites in the cloned DNA sequences.

Presence of pRL7 repeat sequence in rice genome

In order to check the presence of a cloned repeat sequence in rice genome and to show that it has not undergone any change during the cloning steps, the 3.6 kbp repeat sequence (pRL7) was hybridised to rice total DNA digested with *Bam*HI (figure 3). The hybridization pattern shows a band of 3.6 kbp and 3 other bands of high molecular weight which are not the multiples of 3.6 kbp. This indicates that the 3.6 kbp repeat DNA fragment is present independently in the genome and is also a part of some sequences which are of higher molecular weights.

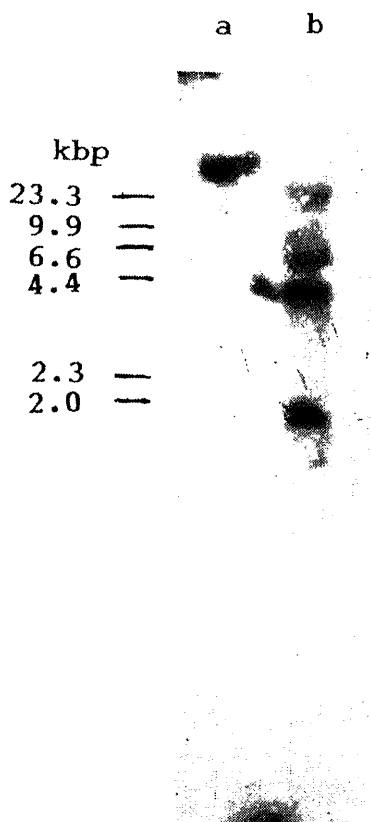


Figure 3. Autoradiogram of pRL7 insert DNA hybridized to rice shoot DNA digested with *Bam*HI. Lane a, control rice DNA; lane b, *Bam*HI digest.

Localisation of a few restriction enzyme sites in pRL1, pRL7 and pRL10

For locating a few restriction enzyme sites in the cloned sequences, 3 recombinants i.e., pRL1, pRL7 and pRL10 were selected. These plasmids were digested with

*Bam*HI and the corresponding inserts were eluted and used for further characterisation using a few enzymes like *Pvu*II, *Eco*RI, *Pst*I, *Bcl*II and *Alu*I in single and double digestions. Since the strategy followed for the analysis of various restriction enzyme digestions was the same for all the 3 plasmids, a detailed analysis of only pRL7 is described. On digestion of pRL7 plasmid DNA with *Pvu*II, 3 bands of 3.6, 3.4 and 2.6 kbp were observed which clearly revealed a *Pvu*II site in the cloned DNA cutting it into two fragments of molecular weights 1.7 and 1.9 kbp. This was confirmed when the eluted insert DNA was digested with *Pvu*II and two bands of 1.7 and 1.9 kbp were observed. In order to localise these positions, the pRL7 DNA was double digested with *Pvu*II/*Eco*RI. Since, only the 3.4 kbp band in the *Pvu*II digest of pRL7 was reduced to 3.3 kbp in *Pvu*II/*Eco*RI double digest, it fixed the position of 1.7 kbp fragment in the insert DNA towards the *Eco*RI site in pBR325 followed by 1.9 kbp *Pvu*II-*Bam*HI fragment. An appearance of 3.2 kbp band on *Pst*I digestion of pRL7 insert DNA indicated the presence of a single *Pst*I site at a distance of 0.4 kbp from the *Bam*HI site in the insert DNA. To determine at which end the *Pst*I site was present in pRL7 insert DNA, double digestion of pRL7 with *Bam*HI/*Pst*I was carried out. It showed two bands of 6.0 and 3.2 kbp and a faint band of 0.4 kbp which reflected the *Pst*I site at a distance of 3.6 kbp from position no. 1 in pBR325. Finally, enzyme digestion of pRL7 insert DNA with *Alu*I was analysed on 10% native, polyacrylamide gel. *Alu*I digest showed a number of bands in the range of 1.35 kbp to 0.068 kbp indicating a number of *Alu*I sites in the cloned DNA sequence.

Based on these studies, it can be concluded that the rice repetitive DNAs cloned in pRL1, pRL7 and pRL10 contain no sites for *Eco*RI and *Bcl*II, single sites for *Pvu*II and *Pst*I and many sites for *Alu*I (figure 4).

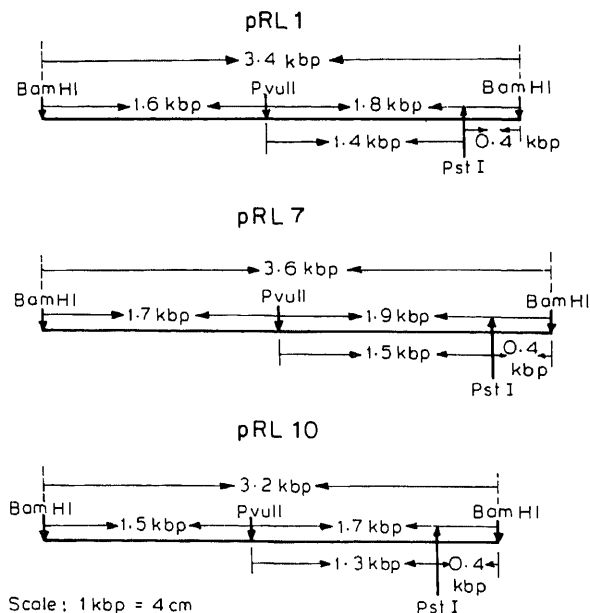


Figure 4. Line diagram showing the restriction enzyme sites in the cloned sequences in pRL1, pRL7 and pRL10 DNAs.

Cloning and sequencing of rice long repetitive DNA in M13

Introducing a few restriction enzyme sites in the pRL1, pRL7 and pRL10 insert. The next step was to determine the nucleotide sequence of these repeats. The fragment obtained after digestion of pRL7 insert DNA with *Bam*HI and *Pst*I was selected for this purpose. This fragment was also observed to be present in pRL10 insert DNAs. This fragment was then sequenced using M13 sequencing system.

Sequencing analysis of the 0.4 kbp repeat element (pRL7-0.4 kbp) using dideoxy chain termination method

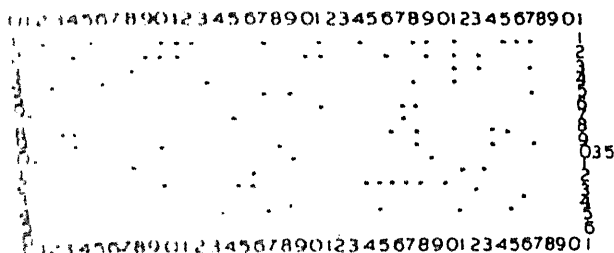
A 0.4 kbp *Bam*HI-*Pst*I fragment of pRL7 was sequenced by Sanger's dideoxy chain termination method. The partial sequence obtained from 5'→3' is given below.

```
GCAGGCTTCGCTGACGACCGAATCGACACCACAAGCGTGC
GAGGACAGCAATACCATAACCGAAGTAAGCTCGAGACTACA
AGTCGGTGCTGAGTCGCCTGTGTTACTAGCGTACACACGT
TCGCTAGTAGAGCAGAGCTAGCTACGTCTCTCATCAGTCA
CATCAGATCTATACGTACTCTGTTCAGTGTGGTGCTCAGCT
GCTTAGTCGTTAACTGACACGTACCAGGCGCGATGCGCAC
CATCAGATCTATACGTCTCTGTTCAGTGTGGTGCTCAGACT
CCTCTTACATTTCGCTCCCATCACATTACATACGATCCATG
TCTAGCTTCTTCTACCGATCTCCTCGTATCTCACTCGTCG
TAGCGCTATCCTCTTCTCTCTCTGTCTCTGTCTCTCG
AGGTACCGACTG 3'
```

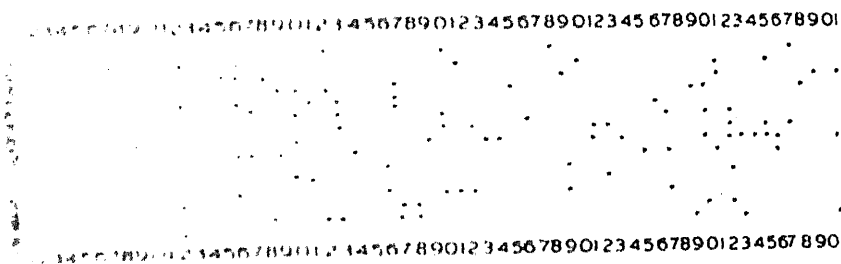
Restriction enzyme site analysis of the pRL7-0.4 kbp sequence shows the presence of single sites for some enzymes like *Fnu*DI, *Eco*RII, *Ser*FI and *Bin*I and sites for enzymes like *Alu*I, *Taq*I, *Mae*I and *Mn*II. In case of *Alu*I, it is interesting to note that most of the fragment sizes indicated by computer analysis are in good agreement with the molecular weights of a few bands observed in pRL7 insert DNA digested with *Alu*I suggesting thereby that bands of 0.068, 0.072, 0.088 and 0.102 kbp in *Alu*I digest may be a part of this *Bam*HI-*Pst*I fragment (pRL7-0.4 kbp). Further analysis shows that this sequence has a G+C content of about 45%.

To compare the pRL7-0.4 kbp sequence with the rice 25S (figure 5A), 18S (figure 5C) and the spacer fragment between 25S and 18S rDNAs (figure 5B) (Takaiwa *et al.*, 1984, 1985a,b), dot matrix was generated using the 0.4 kbp sequence on Y-axis (Y sequence) and the known sequences on X-axis (X sequence) on the principle of Novotny (1982) and Jagadeeswaran and McGuire (1982). To reduce the background noise, it was found useful not to compare small segments but 48 and 26 bases at a time. This eliminated most of the random similarity while preserving the features of true homology. In the generation of dot matrix figure (figure 5), when the segment for the above length of the sequences is equal to a minimal match of 20 or 15 bases, a dot is placed in the matrix at the coordination corresponding to the location of nucleotide

(A)



(83)



(C)

Figure 6. Dot plot comparison of the rice repetitive DNA sequence. The pRL-0.4 kbp sequence (Y-axis) is compared to the genomic DNA fragment between 25S and 17S (B) (X-axis). A dotted line indicates the spacer fragment between 25S and 17S. The number of bases at a time with 50% identity required for

continuous lines parallel to a fixed angle, from the long to the short over a long stretch of sequences, while short segments appear as shorter stretch in discrete packets of sequences. It is not clear that the sequence pRI.7-0.4 kbp shows more homology with the sequence of 25S rDNA fragment than with 17S rDNA fragment. However, there are no homologies over a long stretch in any of the 3 comparisons. It has already been reported that in the case of 8.9 kbp, there is a *Bam*HI site cutting it into two fragments of 3.8 kbp (Reddy and Padayatty, 1987). Furthermore, this 3.8 kbp fragment hybridizes with the 25S and 17S rDNA genes. However, there was no hybridization with 3.6-0.4 kbp fragments (data not presented) indicating that it is different from ribosomal DNA.

Acknowledgements

One of the authors (M.S.D.) acknowledges Council of Scientific and Industrial Research, New Delhi for the award of a fellowship. G. S. N. and S. R. R. are the recipients of the fellowship from Hindustan Lever Research Foundation, Bombay.

References

- Beatty, W. M. (1977) *Science*, **195**, 393.
- Boim, H. C. and Doly, J. (1979) *Nucleic Acids Res.*, **7**, 1513.
- Boiling B. (1981) *Proc. Natl. Acad. Sci. USA*, **78**, 338.
- Choudhary, M. S., Dabak, M. M., Gupta, V. S. and Ranjekar, P. K. (1988) *Plant Sci.*, **55**, 43.
- Choudhary, S. I. J., James, A. M. and Barnes, S. R. (1983) *J. Mol. Biol.*, **170**, 803.
- Choudhary, V. S., Gadre, S. R. and Ranjekar, P. K. (1981) *Biochim. Biophys. Acta*, **656**, 147.
- Choudhary, C., Bryngelsson, T., Sall, T. and Gustafsson, M. (1987) *J. Mol. Evol.*, **25**, 318.
- Choudhary, P. and McGuire, P. M. (1982) *Nucleic Acids Res.*, **10**, 433.
- Choudhary, W. R. (1982) *Annu. Rev. Biochem.*, **51**, 813.
- Choudhary, A., Yakura, K. and Tanifuji, S. (1984) *Nucleic Acids Res.*, **12**, 6415.
- Choudhary, T., Fritsch, E. F. and Sambrook, J. (1982) *Molecular cloning: A laboratory manual* (New York: Cold Spring Harbor University).
- Choudhary, J. (1983) *Methods Enzymol.* **101C**, 20.
- Choudhary, M., Troebner, W., Baldauf, F., Schlegel, R. and Cullum, J. (1986) *Theor. Appl. Genet.*, **72**, 207.
- Choudhary, J., Kempe, T. and Messing, J. (1983) *Gene*, **26**, 101.
- Choudhary, J. (1982) *Nucleic Acids Res.*, **10**, 127.
- Choudhary, L. E. and Crick, F. H. U. (1980) *Nature (London)*, **284**, 604.
- Choudhary, D. and Barnes, S. R. (1985) *Theor. Appl. Genet.*, **70**, 185.
- Choudhary, P., Karsch, F., Iida, S. and Meyer, J. (1981) *Gene*, **14**, 298.
- Choudhary, P. S. and Padayatty, J. D. (1987) *Indian J. Biochem. Biophys.*, **24**, 293.
- Choudhary, C., Biasini, M. G., Morandi, C., Nielson, E., Parisi, B. and Sala, F. (1985) *J. Plant Physiol.*, **118**, 409.
- Choudhary, F., Nicklen, S. and Coulson, A. R. (1977) *Proc. Natl. Acad. Sci. USA*, **74**, 5463.
- Choudhary, P. H. and Cortese, R. (1979) *J. Mol. Biol.*, **129**, 169.
- Choudhary, N. V., Lushnikova, A. A., Tihonov, A. P. and Ananiev, E. V. (1989) *Theor. Appl. Genet.*, **78**, 589.
- Choudhary, J. C. (1984) *Adv. Genet.*, **22**, 109.
- Choudhary, M., Oono, K. and Sugiura, M. (1984) *Nucleic Acids Res.*, **12**, 5441.
- Choudhary, M., Oono, K., Iida, Y. and Sugiura, M. (1985a) *Gene*, **57**, 255.
- Choudhary, M., Oono, K. and Sugiura, M. (1985b) *Plant Mol. Biol.*, **4**, 355.
- Choudhary, M., Perron, C., Vieira, J. and Messing, J. (1984) *Gene*, **33**, 103.

porphyrin metabolism in lead and mercury treated bajra (*Pennisetum typhoideum*) seedlings

D. D. K. PRASAD and A. R. K. PRASAD

Department of Biochemistry, School of Biological and Earth Sciences, Sri Venkateswara University, Tirupati 517 502, India

MS received 29 August 1990

Abstract. Lead and mercury inhibited porphyrin biosynthesis significantly in the germinating seeds of bajra (*Pennisetum typhoideum*). Both 5-aminolevulinic acid dehydratase and porphobilinogen deaminase activities were inhibited by these metals. A comparative study of the inhibition of these two enzymes under *in vivo* and *in vitro* conditions showed that 5-aminolevulinic acid dehydratase is the major site of action of heavy metals in porphyrin biosynthesis. Further, over-all production of porphyrins *viz.*, protoporphyrin-IX, Mg-protoporphyrin (ester) and protochlorophyllide was repressed by lead and mercury in both light and dark grown seedlings. Similarly, chlorophyll *a* and chlorophyll *b* and total chlorophyll contents in dark-grown seedlings were also significantly decreased, suggesting the impairment of chlorophyll biosynthesis by lead and mercury in germinating seedlings.

Keywords. Bajra (*Pennisetum typhoideum* L.); ALA dehydratase; PBG deaminase; porphyrins; heavy metals.

Introduction

Heavy metals are major environmental contaminants of air, water and soils especially in the areas of heavy automobile traffic, near metal smelters or in places where oil is burned for heating purposes (Lagerwerf, 1967). They form aerosols which disperse and precipitate with dust (Friberg *et al.*, 1971) and will then be absorbed by leaves and subsequently transported to the other plant organs (Ernst, 1989). The heavy metals induce impaired metabolism and retarded growth (Weigel and Jager, 1980a). Further, Hampp (1974) established a relationship between the number of vehicles/unit time and their speed to the lead contents in plants. Earlier reports show that cadmium, lead and mercury inhibit chlorophyll synthesis (Stobart *et al.*, 1985; Prasad and Prasad, 1987a,b) and photosynthesis in higher plants is highly sensitive to metals like cadmium and lead (Hampp *et al.*, 1976; Weigel, 1985). The first committed step of tetrapyrrole biosynthesis is the formation of 5-aminolevulinic acid (ALA). The classical ALA synthetase catalyzing the formation of ALA in bacteria, yeast and animals was not demonstrated in higher plants. However, it was shown that ALA is synthesized in plants and algae from the 4-carbon skeleton of glutamic acid (Weinstein and Beale, 1985; Kannangara *et al.*, 1988). The second rate limiting enzyme, ALA dehydratase catalyzes the conversion of porphobilinogen (PBG) from two molecules of ALA (Shemin, 1968). It is present in plants abundantly and is a sensitive enzyme to study the action of heavy metals (Nandi and Shemin, 1968).

Bogorad (1958) first reported the biosynthesis of uroporphyrinogen-III (urogen) from PBG in higher plants. Four mol of PBG were converted to one mol of urogen by the co-operative action of two enzymes, PBG deaminase and urogen co-synthetase. Urogen is the first tetrapyrrole that acts as precursor for the other porphyrins (Bogorad, 1966). In this context urogen acquires a special importance in the biosynthesis of porphyrins. Hence, it is of great significance to see the effect of heavy metals on PBG deaminase.

In the present communication we report the alteration of porphyrin biosynthesis by lead and mercury and the possible sites of action of these metals on porphyrin synthesis.

Materials and methods

Healthy seeds of Bajra (*Pennisetum typhoideum*. L. var. BK 560) were washed thoroughly with tap water and allowed to imbibe water for 6 h and spread in petri dishes lined with moist filter papers. Controls were maintained with distilled water and other lots of seeds were treated with different concentrations (50, 100 and 250 μM) of metal solutions of lead and mercury (added as lead acetate and mercuric chloride). Seedlings were maintained under natural day light for 5 days at day and night temperature of $30 \pm 2^\circ\text{C}$. Seedlings were removed at regular intervals and used for the assay of ALA dehydratase and PBG deaminase activities and for the estimation of protoporphyrin-IX (proto), Mg-protoporphyrin ester (Mp(e)) and protochlorophyllide (Pchld) contents.

Other batch of seedlings were grown in complete darkness and maintained with distilled water for 4 days. The leaves were cut into pieces, treated with different concentrations (50, 100 and 250 μM) of lead and mercury for 10 h in dark and then exposed to light (2.80 W m^{-2}) for further 7 h. All the estimations were done after final light treatment.

Assay of enzyme activities

ALA dehydratase activity was assayed by the method of Schneider (1970). Seedlings were homogenized in 50 mM Tris-HCl buffer (pH 8.2) containing 0.1 M dithiothreitol and filtered through 4 layers of muslin cloth. The filtrate was centrifuged at 12000 g for 15 min and the supernatant was used as enzyme source. One ml of the enzyme is incubated with 0.27 ml of 1 mg ml^{-1} ALA, 1.35 ml of 50 mM Tris-HCl buffer (pH 8.2) with 0.1 M dithiothreitol and 0.08 ml of 0.02 M MgCl_2 for 2.5 h at 37°C . After incubation, the reaction was arrested by the addition of 0.3 ml of 3 M TCA and centrifuged at 3000 g . The supernatant was mixed with equal volume of modified Ehrlich reagent (Mauzerall and Granick, 1956) and the absorbance was measured at 553 nm after 15 min against a zero time blank.

PBG deaminase activity was assayed by the method of Bogorad (1962) with slight modifications. Seedlings were homogenized in grinding medium (1:1 wt/vol) containing 0.2 M Tris-HCl buffer, pH 8.2 with 0.1 M cysteine, 0.1 M MgCl_2 and 0.003 M *o*-phenanthroline. The slurry was filtered through 4 layers of muslin cloth and the filtrate was directly used for enzyme assay. The assay mixture consisted of 100 μg of PBG, 0.5 μmol of 0.05 M Tris-HCl buffer (pH 8.2), 2.5 μmol of EDTA,

pH 8.2 and 0.4 ml of enzyme in a final vol. of 1 ml. The reaction was carried out at 32°C for 45 min and was stopped by using 0.1 ml of 3 M TCA. After centrifugation at 3000 g the supernatant was mixed with equal vol. of 5 M HCl. The urogen formed was measured at 406 nm after 4.5 h after which no change in absorbance was observed in light.

Protein estimations were done by the method of Lowry *et al.* (1951).

Analysis of porphyrins and chlorophylls

The 80% alkaline acetone extraction procedure and the spectroscopic method used for the quantification of proto, Mp(e), Pchld, chlorophyll *a* and chlorophyll *b* was that of Hodgins and Van Huystee (1986). Evaluation of data was performed by using BASIC computer program for the analysis of absorbance data (Hodgins and Van Huystee, 1986). Total chlorophyll content was estimated by the method of Arnon (1949).

Results

Both lead and mercury were found to inhibit PBG deaminase activity. The *in vivo* activity of the enzyme increased with age and showed more activity on 4th day as compared to 2nd day. Correspondingly, inhibition of the enzyme was also more on 4th day than 2nd day (figure 1A,B). Further, the *in vitro* incubation of the enzyme with lead and mercury showed similar type of inhibitory effect on the enzyme activity (figure 1C). Mercury was observed to be more potent inhibitor than lead.

To identify the major site of action of lead and mercury on porphyrin synthesis, an attempt has been made to compare the inhibition of ALA dehydratase and PBG deaminase activities by these metals both *in vivo* and *in vitro* (table 1). Our *in vitro* experiments show that inhibition of ALA dehydratase was greater than that of PBG deaminase. However, comparison of *in vivo* activities showed that PBG deaminase was inhibited 84% as compared to 55% inhibition of ALA dehydratase. These observations reveal that the depleted levels of PBG the substrate for PBG deaminase activity, due to inhibition of ALA. D might be the main cause for greater inhibition under *in vivo* conditions. However, under *in vitro* conditions there was no reduction of PBG availability for the deaminase activity.

Lead and mercury were found to decrease all the porphyrin levels examined in light grown seedlings. Proto levels increased with age up to 4th day of germination and decreased on day 5 in both control and metal treated seedlings (figure 2). However, the Mp(e) levels were increased with age and this increase was observed even on the 5th day of germination both in case of control and lead treated seedlings (figure 3A), where as the mercury treated seedlings responded in a different manner, in which the Mp(e) levels reached a maximum value on 3rd day of germination and there was no further increase on consequent days (figure 3B). The effect of lead and mercury on Pchld levels was observed to be similar to that of the proto (figure 4).

Similarly in dark-grown seedlings lead and mercury found to reduce proto, Mp(e) and Pchld levels in a concentration dependent manner (table 2). There was nearly 40 and 50% reduction in the levels of proto and Mp(e) respectively at 250 μ M concentration of lead and mercury. Pchld was found to be highly sensitive and

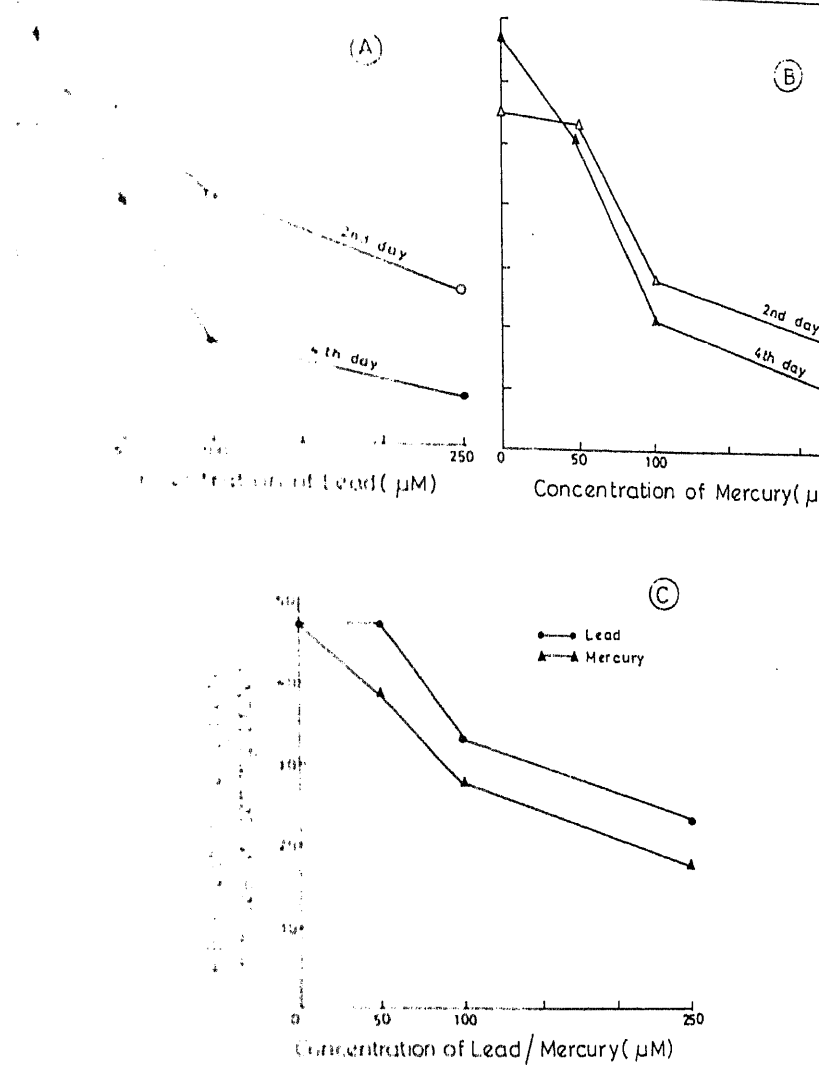


Figure 1. *In vitro* effect of lead (A) and mercury (B) on PBG deaminase activity (buffered). (C) *In vitro* effect of lead and mercury on PBG deaminase activity (buffered). The enzyme from 4-day-old seedlings of bajra were preincubated with different concentrations (0, 50, 100 and 250 μM) of lead and mercury for 15 min at 32°C. Aliquots were taken for incubation and enzyme activity was assayed as described in the text.

there was nearly 70% decrease over the control value at 250 μM concentration of the metal.

Table 4 shows the effect of lead and mercury on chlorophyll contents in 4-day-old seedlings. Both chlorophyll *a* and chlorophyll *b* levels were decreased at 250 μM concentration of lead and mercury. Similarly total chlorophyll was also reduced by 50 and 43% at 250 μM concentration of both lead and mercury treated seedlings (table 4) respectively.

Table 1. Comparison of per cent inhibition between ALA dehydratase and PBG deaminase by lead and mercury in 4-day-old bajra seedlings.

Treatment	Inhibition of enzyme activity(%)*			
	ALA dehydratase		PBG deaminase	
	<i>In vivo</i>	<i>In vitro</i>	<i>In vivo</i>	<i>In vitro</i>
Control (dist. water)	0.00	0.00	0.00	0.00
Lead (μM)				
50	16.7	23.0	41.54	0.00
100	29.5	54.0	67.0	28.0
250	55.2	65.0	84.2	48.0
Mercury (μM)				
50	15.0	50.0	26.5	20.0
100	40.0	65.0	70.6	38.0
250	52.5	73.0	85.3	59.0

Seedlings were germinated and grown in complete darkness for 4 days and the excised leaves were treated with different concn. of lead and mercury in dark for 10 h and were exposed to light for 7 h. The estimations were done after final light treatment. All manipulations in dark-grown seedlings were carried under safe dim-green light.

*Values are average of 4 separate experiments. Per cent inhibition was calculated from the activities expressed as nmol product formed mg^{-1} protein.

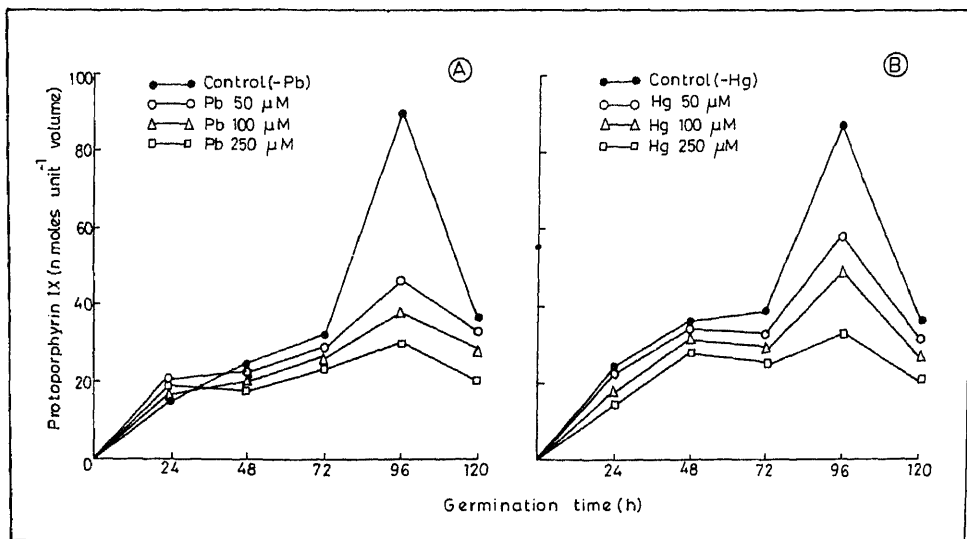


Figure 2. Effect of lead (A) and mercury (B) on proto levels in bajra seedlings.

Discussion

Our results show that porphyrin synthesis was inhibited by both lead and mercury by interacting at the level of key enzymes in the pathway. Earlier reports show that

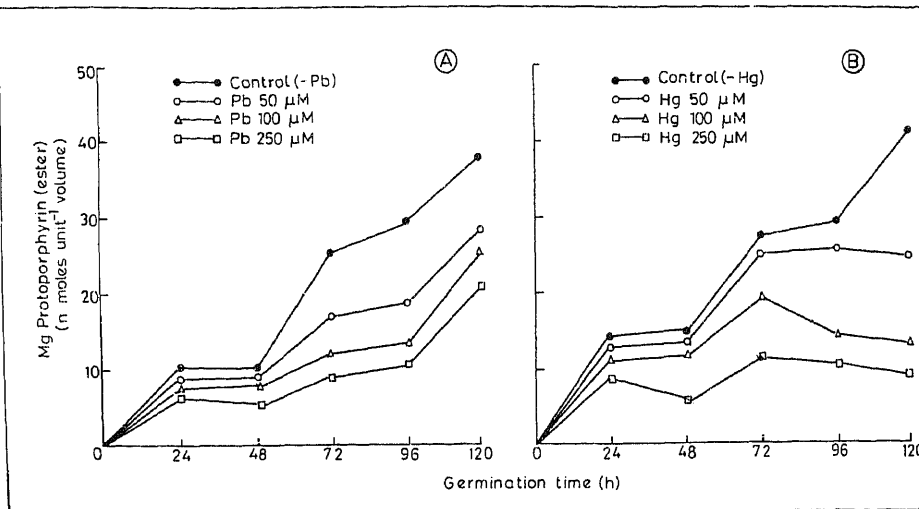


Figure 3. Effect of lead (A) and mercury (B) on Mp(e) levels in bajra seedlings.

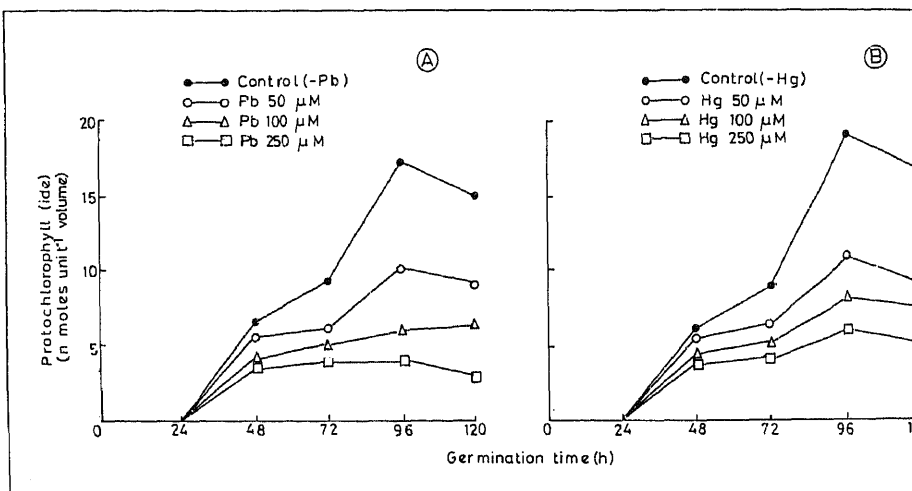


Figure 4. Effect of lead (A) and mercury (B) on Pchld levels in bajra seedlings.

the biosynthesis of tetrapyrroles proceeds through ALA dehydratase, a metal sensitive enzyme (Nandi and Shemin, 1968). Previous work from this laboratory showed that ALA dehydratase, the second enzyme in porphyrin synthesis is inhibited by lead and mercury (Prasad and Prasad, 1987a,b). There was nearly 100% inhibition of the enzyme at 250 μ M concentration of lead and mercury in *in vivo* and *in vitro*. Further, the purified bajra ALA dehydratase showed a non-competitive type of inhibition with respect to lead and mercury (Prasad *et al.*, 1987). Furthermore, the total chlorophyll content in lead and mercury treated dark-grown seedlings was also reduced to half at 250 μ M concentration of these metals.

Table 2. Effect of lead and mercury on proto, Mp(e) and Pchld contents in dark-grown bajra seedlings.

Treatment	nmol g ⁻¹ fresh weight of leaves*		
	Proto	Mp(e)	Pchld
Control (dist. water)	975 ± 50	315 ± 25	47.5 ± 2.5
Lead (μm)			
50	800 ± 30	245 ± 5	33.5 ± 2.5
100	685 ± 31	190 ± 20	20.5 ± 2.5
250	575 ± 20	140 ± 5	13.5 ± 2.0
Mercury (μm)			
50	855 ± 10	275 ± 20	36.0 ± 5
100	730 ± 20	210 ± 20	17.5 ± 5
250	565 ± 50	135 ± 15	12.6 ± 5

Same notations as in table 1.

*Values are average of 4 separate experiments ± SD.

Table 3. Effect of lead and mercury on chlorophyll *a* and *b* contents in dark-grown bajra seedlings.

Treatment	nmol g ⁻¹ fresh weight of leaves*	
	Chlorophyll <i>a</i>	Chlorophyll <i>b</i>
Control (dist. water)	740 ± 100	290 ± 20
Lead (μm)		
50	660 ± 20	250 ± 5
100	410 ± 15	165 ± 00
250	325 ± 25	130 ± 5
Mercury (μm)		
50	535 ± 30	205 ± 20
100	460 ± 20	190 ± 10
250	345 ± 15	150 ± 15

Same notations as in table 1.

*Values are average of 4 separate experiments ± SD.

observed earlier in light-grown seedlings (Hampp *et al.*, 1974; Hampp and Lendzian, 1974; Prasad and Prasad, 1987a,b).

Porphyrin synthesis was inhibited by lead and mercury by interacting with ALA dehydratase and PBG deaminase. The increase in relative levels of porphyrins *viz.*, proto, Mp(e), Pchld and PBG deaminase activity with age and inhibition of PBG deaminase activity as well decreased levels of proto, Mp(e) and Pchld by lead and mercury suggest a possible relationship between PBG deaminase activity and porphyrin synthesis. Proto, Mp(e) and Pchld contents were examined to check whether the heavy metals interact with any of the intermediate steps between ALA and chlorophyll synthesis. The decreased levels of these compounds revealed that the interaction of heavy metals was prior to proto formation, probably at the level of ALA dehydratase or PBG deaminase. However, Stobart *et al.* (1985) reported that cadmium had no effect on Pchld production but inhibited chlorophyll formation in dark-grown barley seedlings.

Table 4. Effect of lead and mercury on total chlorophyll content in dark-grown bajra seedlings.

Treatment	Inhibition (%)*
Control (dist. water)	—
Lead (μm)	
50	17
100	40
250	52
Mercury (μm)	
50	17
100	30
250	43

Same notations as in table 1.

*Values are average of 4 separate experiments. Per cent inhibition was calculated from total chlorophyll content expressed as μg chlorophyll g^{-1} fresh weight of leaves.

PBG deaminase was found to be highly specific for PBG and requires compounds for activity (Bogorad, 1958). The deaminase enzyme has reactive groups (Frydman and Frydman, 1970) and the enzyme activity was inhibited by thiol directed reagents (Frydman and Feinstein, 1974). Hence, the inhibition of PBG deaminase activity by lead and mercury can be attributed to (i) the interaction of lead and mercury with free-SH groups present at the active site of the enzyme and (ii) reduced levels of PBG, the product of ALA dehydratase catalyzed reaction which is the specific substrate for PBG deaminase. Hence, the observed sensitivity of the PBG deaminase to metals under *in vivo* conditions as compared to ALA dehydratase supports this idea.

Hemoglobin synthesis in calf-blood erythrocytes and chlorophyll synthesis in isolated spinach chloroplasts were found to be highly sensitive to lead ions (Hamp and *et al.*, 1974). Our results also show that lead and mercury reduced chlorophyll *a* and *b* levels in dark-grown seedlings and the synthesis of chlorophyll was reduced in a dose-dependent manner. Hamp and Lendzian (1974) reported in *Avina sativa* that the synthesis of chlorophyll *b* was inhibited to a greater extent than the synthesis of chlorophyll *a*. However, in bajra both chlorophyll *a* and *b* showed similar sensitivity to metals.

Present findings suggest that the entire porphyrin biosynthetic pathway is affected by lead and mercury. Further, our experiments conducted to verify whether the main site of action was at ALA dehydratase or PBG deaminase reveal that ALA dehydratase, the second rate limiting enzyme plays a major role in chlorophyll synthesis rather than PBG deaminase. The formation of PBG, the product of ALA dehydratase reaction was drastically reduced by lead and mercury. Hence, the depleted levels of PBG for PBG deaminase was observed to be a controlling factor responsible for the reduced activity of this enzyme in metal treated seedlings. In addition to the interaction of metals with free-SH groups present at the active site of the enzyme.

This study has served to clarify the site specific action of heavy metals lead and mercury on porphyrin synthesis, which results in decreased levels of chlorophyll content in greening tissues.

Acknowledgements

The authors thank Dr. R. R. Hodgins, University of Western Ontario, Canada for his kind help and one of the authors (D.D.K.P.) is thankful to the University Grants Commission, New Delhi for financial assistance.

References

- Arnon, D. I. (1949) *Plant Physiol.*, **24**, 1.
Bogorad, L. (1958) *J. Biol. Chem.*, **233**, 501.
Bogorad, L. (1962) *Methods Enzymol.*, **5**, 885.
Bogorad, L. (1966) *The chlorophylls* (London: Academic Press).
Ernst, W. H. O. (1980) in *Cadmium in environment Part-I* (ed. J. O. Nriagu) (New York, Chichester: Wiley Interscience) p. 639.
Friberg, G. L., Piscator, M. and Nordberg, G. (1971) *Cadmium in environment* (Cleveland, Ohio: Chem. Rubber Company Press).
Frydman, R. B. and Frydman, B. (1970) *Arch. Biochem. Biophys.*, **136**, 193.
Frydman, R. B. and Feinstein, G. (1974) *Biochim. Biophys. Acta*, **350**, 358.
Hampp, R. (1974) *Ber. Bayer. Bot. Ges. Erforsch. Heim. Flora*, **44**, 211.
Hampp, R., Beulich, K. and Zeigler, H. (1976) *Z. Pflanzenphysiol.*, **77**, 336.
Hampp, R., Kriebitzsch, C. and Zeigler, H. (1974) *Naturwissenschaften*, **11**, 504.
Hampp, R. and Lenzian, K. (1974) *Naturwissenschaften*, **11**, 218.
Hodgins, R. R. and Van Huystee, R. B. (1986) *J. Plant Physiol.*, **125**, 311.
Kannangara, C. G., Gough, S. P., Bruyant, P., Hooper, J. K., Kahn, A. and Wettstein, D. (1988) *Trends Biochem. Sci.*, **13**, 139.
Lagerwerf, J. V. (1967) in *Agriculture and quality of our environment* (ed. N. C. Brady) (New York: American Association of Advanced Science Publishers) p. 85.
Lowry, O. H., Rosebrough, N. J., Farr, A. L. and Randall, R. J. (1951) *J. Biol. Chem.*, **193**, 265.
Mauzerall, D. and Granick, S. (1956) *J. Biol. Chem.*, **219**, 435.
Nandi, D. L. and Shemin, D. (1968) *J. Biol. Chem.*, **243**, 1236.
Prasad, D. D. K. and Prasad, A. R. K. (1987a) *J. Plant Physiol.*, **127**, 241.
Prasad, D. D. K. and Prasad, A. R. K. (1987b) *Phytochemistry*, **26**, 881.
Prasad, D. D. K., Singh, N. K., Datta, K. and Prasad, A. R. K. (1988) *Biochem. Int.*, **17**, 87.
Schneider, H. A. W. (1970) *Z. Pflanzenphysiol.*, **62**, 133.
Shemin, D. (1968) *Porphyrins and related compounds* (New York: Academic Press).
Stobart, A. K., Griffiths, W. T., Bukhari, I. A. and Sherwood, R. P. (1985) *Physiol. Plant.*, **63**, 293.
Weigel, H. J. and Jager, J. J. (1980) *Z. Pflanzenphysiol.*, **97**, 103.
Weigel, H. J. (1985) *J. Plant Physiol.*, **119**, 179.
Weinstein, J. D. and Beale, S. I. (1985) *Arch. Biochem. Biophys.*, **237**, 454.

Magnetic resonance studies of dynamic organisation of lipids in chloroplast membranes

R. C. YASHROY*

Biology Department, Carleton University and National Research Council, Ottawa, Canada

*Present address: Electron Microscopy and Instrumentation Section, A. N. Division Buildings, Indian Veterinary Research Institute, Izatnagar 243 122, India

MS received 20 July 1990

Abstract. Spinach chloroplast membranes and aqueous dispersions of their extracted lipids have been studied by spin label (stearic acid) electron spin resonance and carbon-13 nuclear magnetic resonance techniques. Combined with electron microscope studies, first systematic evidence is found for the existence of a dynamic lipid-bilayer structure in the chloroplast membranes.

Keywords. Chloroplast; membranes; lipids; nuclear magnetic resonance; electron spin resonance.

Introduction

It is generally believed that the thylakoid membranes of the plant chloroplasts have a fluid lipid-bilayer structure interacting with membranous proteins (Curatolo, 1987). Curatolo (1987), however has credited this viewpoint to Quinn and Williams (1983), who in turn have stated that it is difficult to reconcile this view due to the fact that the predominant membrane lipid, monogalactosyl diacylglycerol (MGDG) normally takes up hexagonal-II structure when dispersed alone in water and furthermore it forms inverted lipid micellar structure when dispersed together-with the second most abundant lipid, digalactosyl diacylglycerol (DGDG), of the thylakoid membranes.

Unlike most other biological membranes which are rich in phospholipids, the chloroplast thylakoid membranes contain little phospholipid (Kates *et al.*, 1970). Despite the fact that MGDG, the major constituent lipid of chloroplast membranes, does not form an aqueous lipid-bilayer structure (Larsson and Puang-Ngern, 1979), the other lipid constituents such as DGDG, sulphaquinovosyldiacylglycerol and phospholipids may well be responsible for the formation of a lipid-bilayer structure which can serve as a suitable matrix of the thylakoid membrane in which the proteins are embedded (Murphy, 1986; Van Gurp *et al.* 1988; Anderson, 1975). Absence of studies on dynamic state of lipid molecules in membranes led Weier and Benson (1966) to propose a lipid-nonbilayer structure for thylakoid membranes. The present investigation, therefore, was undertaken to systematically study the dynamic organisation of the chloroplast photosynthetic membranes employing spin label electron spin resonance (ESR) and carbon-13 nuclear magnetic resonance (^{13}C -NMR) spectroscopy. Together-with earlier studies (YashRoy, 1980, 1990a), convincing evidence has been gathered suggesting the existence of a lipid-bilayer structure in the chloroplast membranes.

Materials and methods

The chloroplast membranes prepared (Arnon et al., 1956) from fresh spinach leaves were vortexed, under dark conditions, with a dried film of stearic acid spin label to achieve a satisfactory labelling of the membranes in about 20 min. An aliquot of lipid extract (Nichols, 1963) from the chloroplast membranes (finally dissolved in chloroform) was mixed with the spin label (dissolved in chloroform). The mixture was dried under a stream of nitrogen gas and subsequently vortexed with water for about 20 min under dark conditions for use as model membranes in the studies. The molar ratio of chlorophyll (Vernon, 1960)-to-spin label was kept constant for all ESR preparations. Vortexed lipid-water dispersions made from the extract of the chloroplast membranes were also studied by EM after negative staining (Lucy and Glauert, 1964; YashRoy, 1990a).

Spin labels (figure 1) employed for these studies contained a nitroxide (doxyl) moiety at 5, 7, 9, 12, 13, 14 and 16 carbons with respect to carboxyl

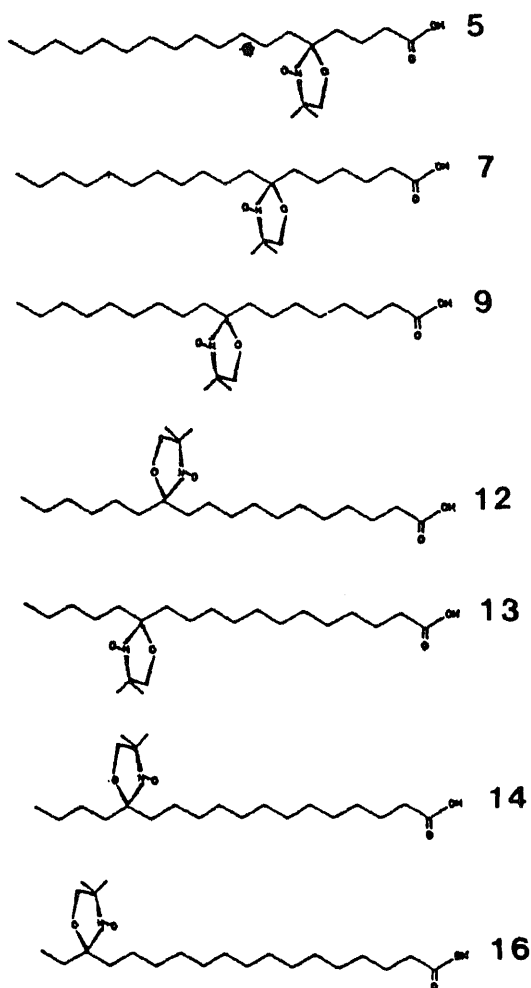


Figure 1. Diagrammatic representation of stearic acid labels showing location of nitroxyl (doxyl) moiety at 5, 7, 9, 12, 13, 14 and 16 carbons with respect to carboxyl

magnetic field used was 3232 G with scan time of 4 min, microwave power of 5 mW, scan range of 100 G, time constant of 0.3 or 1.0 s and frequency of 9 GHz. In many instances, the maxima and minima of the hyperfine splittings were resolved by increasing the receiver gain about 10-fold. The rotational correlation times and order parameters for ESR studies were also calculated (Cannon *et al.*, 1975).

Natural abundance proton-decoupled ^{13}C -NMR spectra of chloroplast membranes (YashRoy 1990b) (chlorophyll content, 5 mg/ml) suspended in deuterated water containing 0.2 M NaCl and 5 mM MgCl_2 and sonicated lipid- D_2O dispersions were obtained with Varian XL-100 or Bruker CXP-300 FT NMR spectrometer equipped with a variable temperature ($\pm 0.2^\circ\text{C}$) control unit. The spectra were collected with field frequency lock on deuterium of solvent or external fluorine; the latter was found specially useful for viscous membranes samples. An external tetramethylsilane (TMS) was used as the standard reference. The radiofrequency pulse angle of 45° and acquisition time of 0.4 s were used to obtain the Fourier transform ^{13}C -NMR spectra of chloroplast membranes and sonicated lipid microvesicles. For lipids dissolved in organic solvents such as deuterated chloroform (CDCl_3) or methanol (CD_3OD), the radiofrequency pulse angle used was 22.5° and the acquisition time was 0.8 to 1.0 s.

Results and discussion

Inspection of ESR spectra (figure 2, top-to-bottom) of the spin labelled chloroplast membranes reveals changes in line-shape, line-width and hyperfine splittings, signifying gradual increase in degree of sub-molecular motions of lipid environment from 5-doxyl to the 16-doxyl spin label positions. For example, 5-line spectra of the membrane-incorporated 5,7 and 9-doxyl labels gradually turn into 3-line spectra for 12 to 16-doxyl labels. Also, the line-widths (note the central line) become increasingly narrow in going from 7 to 16-doxyl spin labelled membranes. These variations in the spectra demonstrate existence of a fluidity of flexibility gradient in terms of increasing degree of motions in the segments of the fatty-acyl chains from near lipid headgroups to the terminal (fatty-acyl) methyl groups in the chloroplast membranes.

Model membranes prepared by aqueous dispersion of lipids extracted from the chloroplast membranes, also reveal a similar flexibility gradient. Figure 3 shows the variations in linewidth, W_0 (G) of the central spectral line of the ESR spectra of the spin-labelled chloroplast membranes and model membranes made from their lipid-extract. The observation of exceedingly shorter linewidths in the order of 9,12,14 and 16-doxyl positions of the labels incorporated in the two membrane systems signifies the existence of progressively increasing rates of segmental motions towards the terminal methyl groups of the lipid fatty-acyl chains. The similarity of this flexibility gradient between the chloroplast membranes and model membranes made from their lipid-extract indicates a similarity in the organization of the lipids in these two membrane systems. Interestingly, both in chloroplast membranes and their extracted aqueous lipid dispersions there is no significant decrease in linewidth, W_0 from 5 to 9-doxyl positions signifying persistence of a high degree of

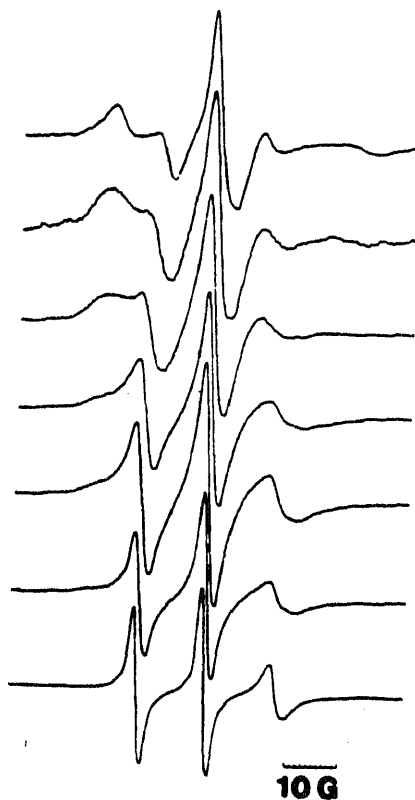


Figure 2. 9-GHz ESR spectra of the chloroplast membranes labelled with (from bottom) 5, 7, 9, 12, 13, 14 and 16-doxyl stearic acid spin labels. All the spectra were at 37°C, in dark with the chloroplast membranes suspended in 0.2 M NaCl containing MgCl_2 . The spectrometer settings were: magnetic field, 3232 G; time constant, 4 min; microwave power, 10 mw; and modulation amplitude of 1 G.

motional restriction of fatty-acyl chains in this region of the two membrane bilayers. This characteristic differentiates the flexibility gradient of a lipid bilayer from the hexagonal phase, H_{II} as inferable from the observations made by Sternin *et al.* (1988).

A flexibility gradient such as this observed here is known to exist in biological (excluding chloroplast) membranes *viz.*, mitochondrial (Vignais *et al.*, 1975), sarcoplasmic reticular (Seelig and Hasselbach, 1971) and plasma (Lippman *et al.*, 1970) membranes in addition to many model lipid bilayer membranes (McConnell and McFarland, 1972). This has been explained as due to the presence of the lipid molecules in a bilayer, with the lipid headgroups anchored at the lipid-water interface (McConnell and McFarland, 1972). Figure 4 shows the multilamellar structures formed by the aqueous lipid-extract of the chloroplast membranes. These structures correspond to the multi-bilayers (liposomes) formed by many aqueous lipid systems that constitute the basis of the lipid-bilayer model for the biological membranes (Bangham, 1968; Mühlethaler *et al.*, 1965; Yeagle *et al.*, 1990a).

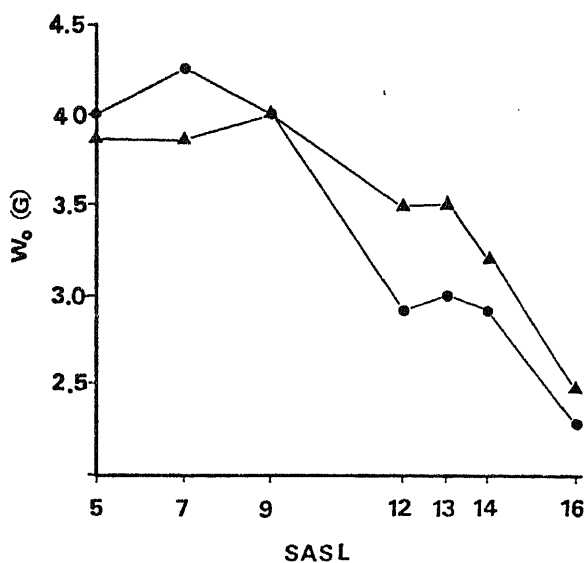


Figure 3. Variation of linewidth, W_0 in G of the central line of the ESR spectra recorded in dark from stearic acid spin labelled chloroplast membranes (▲) and their extracted aqueous lipid dispersions (●) with the position of the doxyl moiety (5, 7, 9, 12, 13, 14 and 16) on the stearic acid spin label (SASL).

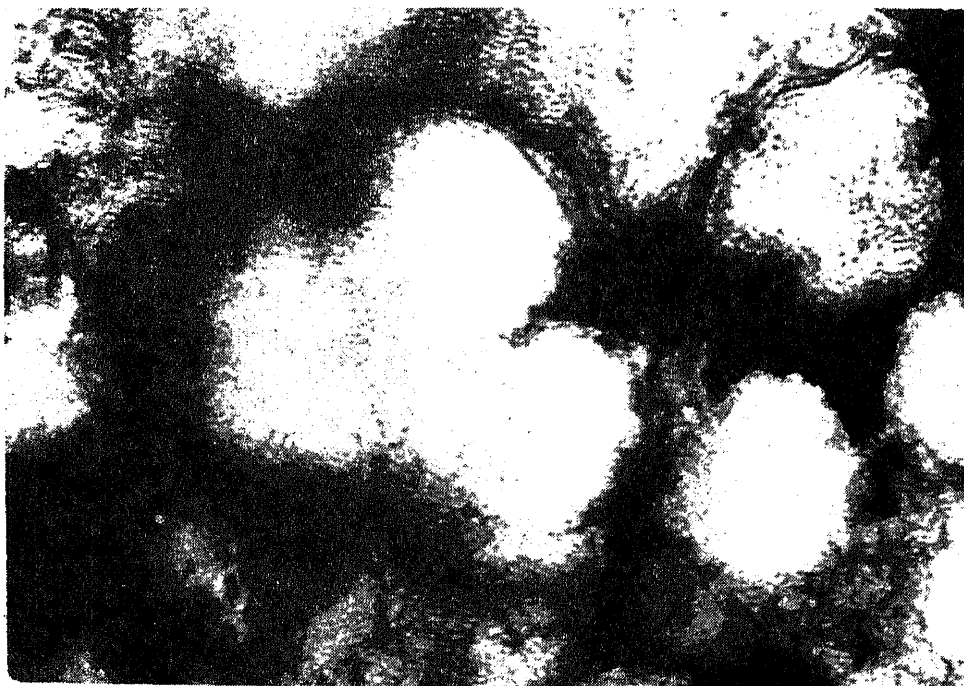


Figure 4. Electron micrograph of the aqueous dispersion of the lipids extracted from the chloroplast membranes after staining with phosphotungstic acid ($\times 190,000$).

The above observations of the flexibility gradient are also supported by NMR studies of the chloroplast membranes and their sonicated aqueous dispersions. Majority of ^{13}C -NMR resonances arising from the chloroplast membranes can be assigned to carbons of linolenic acid (YashRoy, 1981). Figure 5 summarizes the observations on the NMR line-widths of resonances

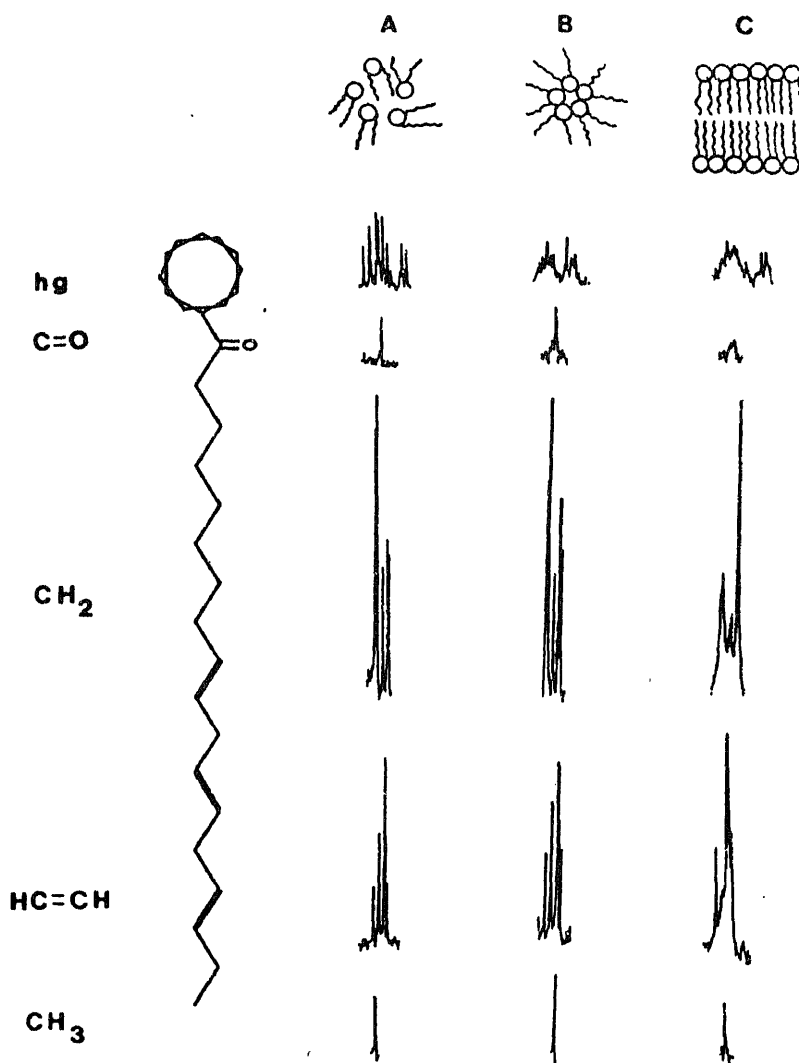


Figure 5. An overall view of the selected resonances of ^{13}C -NMR spectra extracted from chloroplast membranes. The left hand side shows a sketch of a molecule having a globular headgroup (hg) and single (for clarity) extended fatty acid chain with one carbonyl group and 3 double bonds. (A) Lipids in deuterated methanol (top-to-bottom) largely unaggregated (lipid) forms (top) and ^{13}C -NMR spectra of lipid headgroups, fatty acyl carbonyl, $-(\text{CH}_2)_n-$, $-\text{C}=\text{C}-$, and $-\text{CH}_3$.

head-side shows the model diagram of a lipid molecule with a globular headgroup and having a single (for clarity) fatty-acyl chain containing a C=O and 3 double bonds (representing linolenic fatty-acyl chain found most abundantly in chloroplast membranes). Figure 5A represents some select ^{13}C -NMR resonances arising from the extracted lipids (of chloroplast membranes) dissolved in CDCl_3 wherein these lipids, by and large, do not form any specific aggregates. This is clearly evident from sharp line-widths of all the ^{13}C -resonances whether headgroup, C=O group, fatty-acyl chain (segment) or terminal methyl group. When the same lipids are dissolved in CDCl_3 , they form aggregates with headgroups packed-in and tails fanning-but 'freely'. This is revealed by the ^{13}C -linewidths (figure 5B) which clearly show broadening of headgroup and carbonyl resonances and yet retaining narrowness of fatty-acyl chain resonances. When dispersed in D_2O as unilamellar sonicated microvesicles (Roy 1990a) (figure 5C), these lipids show variedly restricted movement consistent with a flexibility gradient, similar to that observed by ^2H -NMR and spin ESR studies of lipid-bilayer systems (Sternin *et al.*, 1988). The line-broadening is maximum on headgroups and C=O groups and somewhat less on the methylene and HC=CH segments and the least on terminal- CH_3 group of the fatty-acid chains. A similar order of restricted mobility of carbons from headgroups towards terminal methyl groups of the fatty-acyl chains is noticeable from ^{13}C -NMR spectrum of chloroplast membranes (figure 6). In essence, the fact that the electron

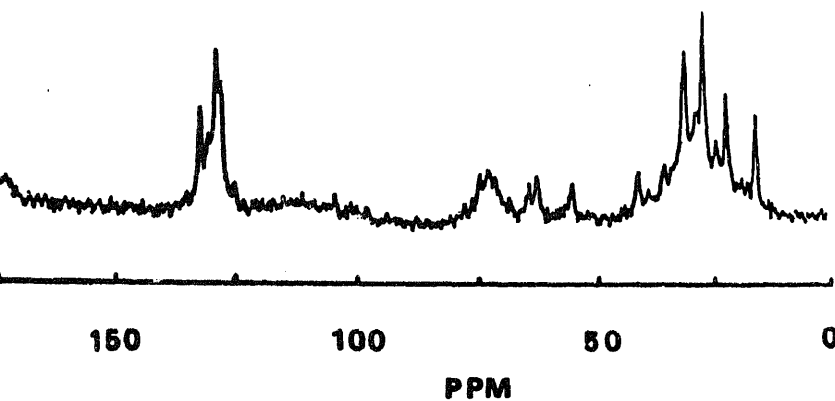


Figure 6. 75-MHz natural abundance ^{13}C -NMR spectrum of spinach chloroplast membranes at 30°C . The membranes were suspended in 0.2 M sodium chloride containing 5 mM magnesium chloride in deuterated water. Chemical shift in parts per-million (ppm) in reference to external TMS (not shown).

microscopically observable liposomal multibilayer structures (figure 4) formed by the dispersion of the lipids extracted from the chloroplast membranes depict a flexibility gradient closely paralleling the flexibility gradient revealed by the native chloroplast membranes (especially notable from ESR spectral line-widths, as in figure 3) strongly suggests that the dynamic organisation of lipids in the chloroplast membranes is largely bilayer.

Acknowledgements

The author thanks the Canadian Commonwealth Scholarship and Fellowship Committee for financial support.

References

- Anderson, J. M. (1975) *Biochim. Biophys. Acta*, **416**, 191.
- Arnon, D. I., Allen, M. B. and Whatley, F. R. (1956) *Biochim. Biophys. Acta*, **20**, 449.
- Bangham, A. D. (1968) *Prog. Biophys. Mol. Biol.*, **18**, 29.
- Cannon, B., Polnaszek, C. F., Butler, K. W., Ericksson, L. E. G. and Smith, I. C. P. (1975) *Biochem. Biophys.*, **167**, 505.
- Curatolo, W. (1987) *Biochim. Biophys. Acta*, **906**, 137.
- Kates, M., Paoletti, R. and Kritchevsky, D. (1970) *Adv. Lipid. Res.*, **8**, 225.
- Larsson, K. and Puang-Ngern, S. (1979) in *Advances lipid research* (eds L.-A. Appelquist and C. Liljenberg) (Amsterdam: Elsevier/North Holland Biomedical Press) p. 27.
- Lucy, J. A. and Glauert, A. M. (1964) *J. Mol. Biol.*, **8**, 727.
- McConnell, H. M. and McFarland, B. G. (1972) *Ann. N. Y. Acad. Sci.*, **195**, 207.
- Mühlethaler, K., Moor, H. and Szarkowski, J. W. (1965) *Planta*, **67**, 305.
- Murphy, D. J. (1986) *Biochim. Biophys. Acta*, **864**, 33.
- Nichols, B. W. (1963) *Biochim. Biophys. Acta*, **70**, 417.
- Quin, P. J. and Williams, W. P. (1983) *Biochim. Biophys. Acta*, **737**, 223.
- Rottem, S., Hubbel, W. L., Hayluk, L. and McConnell, M. M. (1970) *Biochim. Biophys. Acta*, **219**, 1.
- Seelig, J. and Hasselbach, W. (1971) *Eur. J. Biochem.*, **21**, 17.
- Sternin, E., Fine, B., Bloom, M., Tillock, C. P. S., Wong, K. F. and Cullis, P. R. (1988) *Biophys. J.*, **689**, 1.
- Van Gurp, M., Van Ginkel, G. and Levine, Y. K. (1988) *Biochim. Biophys. Acta*, **938**, 71.
- Vernon, L. P. (1960) *Anal. Chem.*, **32**, 1144.
- Vignais, P. M., Devaux, P. and Colbeau, A. (1975) in *Biomembranes-lipids, proteins and receptors* (eds R. M. Burton and L. Packer) (Missouri: BI Science Publications) p. 318.
- Weier, T. E. and Benson, A.-A. (1966) in *Biochemistry of chloroplasts* (ed. T. W. Goodwin) (New York: Academic Press) vol. 1, p. 91.
- YashRoy, R. C. (1980) *Fluidity and lipid-protein interactions in the chloroplast membranes: A magnetic resonance study*; Ph.D. thesis, Carleton University, Ottawa, Canada.
- YashRoy, R. C. (1987a) *Indian J. Biochem. Biophys.*, **24**, 177.
- YashRoy, R. C. (1987b) *J. Biochem. Biophys. Methods*, **15**, 229.
- YashRoy, R. C. (1990a) *J. Biosci.*, **15**, 93.
- YashRoy, R. C. (1990b) *J. Biochem. Biophys. Methods*, **20**, 353.

Mechanism of impaired skin collagen maturity in riboflavin or pyridoxine deficiency

R. LAKSHMI, A. V. LAKSHMI and M. S. BAMJI*

National Institute of Nutrition, Jamai Osmania, Hyderabad 500 007, India

MS received 1 June 1990; revised 24 September 1990

Abstract. To elucidate the biochemical basis of impaired skin collagen maturity in pyridoxine- or riboflavin-deficient rats the following two mechanistic possibilities were tested: (i) Reduction in the activity of skin lysyl oxidase (EC 1.4.3.13) which initiates the cross-linking of collagen and (ii) putative rise in homocysteine level leading to neutralization of allysine (α -amino adipic acid δ -semialdehyde) or hydroxyallysine (hydroxy α -amino adipic acid δ -semialdehyde) in collagen by the formation of thiazine complexes.

Skin lysyl oxidase activity was not affected in pyridoxine deficiency suggesting that pyridoxal phosphate may not be its cofactor. In riboflavin deficiency, lysyl oxidase activity was not altered in the newly regenerated rat skin but a slight reduction was observed in the skin of 18-day-old rat pups. This could be related to the body weight deficit rather than deficiency *per se*. Aldehyde content of purified salt soluble collagen of regenerated skin was significantly reduced in both the deficiencies. A 2 to 4-fold increase in the concentration of skin homocysteine was observed in both the deficiencies. The results suggest that increase in skin homocysteine level may be responsible for the impaired skin collagen maturity in riboflavin or pyridoxine deficiency.

Keywords. Impaired skin collagen maturity; riboflavin deficiency; pyridoxine deficiency.

Introduction

Collagen is the major connective tissue protein which imparts tensile strength and integrity to the skin. Earlier studies in rats show quantitative and qualitative changes in skin collagen suggestive of impaired cross-linking as well as synthesis of collagen in the skin of riboflavin- or pyridoxine-deficient rats (Prasad *et al.*, 1983, 1986a). The alteration in collagen content and maturity was severe enough to affect some of the biophysical and biomechanical properties of the skin (Prasad *et al.*, 1986b) as well as skin wound healing in these two deficiencies (Lakshmi *et al.*, 1988, 1989).

Two hypothesis have been proposed to explain the role of pyridoxine in collagen cross-linking. Lysyl oxidase which is involved in the cross-linking of collagen and elastin was considered earlier to be a pyridoxal phosphate-dependent enzyme (Bird and Levene, 1982, 1983) and a decrease in the activity of this enzyme was considered as a possible mechanism for impaired collagen cross-linking in pyridoxine- or riboflavin-deficiency. In riboflavin-deficiency secondary deficiency of pyridoxal phosphate can be expected since pyridoxamine phosphate oxidase is an FMN-dependent enzyme and the conversion of pyridoxine to pyridoxal phosphate is impaired (Lakshmi and Bamji, 1979). Recently however, pyrroloquinoline quinone was reported to be the cofactor of human placental and bovine aortic lysyl oxidase (Van der Meer and Duine, 1986; Williamson *et al.*, 1986). Levene *et al.* (1988) have suggested that, there may be species or tissue difference with regard to

*To whom all the correspondence should be addressed.

the cofactor requirement of lysyl oxidase. Based on indirect evidence, they have suggested pyridoxal or pyridoxal phosphate to be the cofactor of chick embryo lysyl oxidase.

Another possible mechanism for impaired collagen cross-linking in pyridoxine or riboflavin deficiency could be elevated level of homocysteine, which has been reported to occur in the plasma of pyridoxine-deficient rat and pig (Smolin and Benevenga, 1982; Smolin *et al.*, 1983; Myers *et al.*, 1985). Homocysteine can combine with the aldehyde products of lysyl oxidase reaction (allysine or hydroxyallysine) in collagen to form thiazine complex and prevent covalent cross-linking (Kang and Trelstad, 1973).

In the present study an attempt has been made to verify the above mentioned two hypothesis to understand the mechanism of impaired skin collagen maturity in pyridoxine- or riboflavin-deficiency.

Materials and methods

Wistar/NIN strain female rats were fed a diet containing 70% sucrose, 20% vitamin free casein, 5% peanut oil, vitamins and minerals (Lakshmi *et al.*, 1989). Pyridoxine or riboflavin deficiency was induced in the pups by maintaining the dams on low pyridoxine (2.5 mg/kg diet) or low riboflavin diet (2.5 mg/kg diet) during pregnancy and totally deficient diet during suckling. The litter size was kept similar in control and deficient groups. Deficiency was induced at preweanling stage instead of weanling, since an inhibitor of lysyl oxidase has been reported in adult mice skin (Rowe *et al.*, 1977).

Blood was drawn from the orbital plexus of 18-day-old pups which were then sacrificed by cervical dislocation. Skin was removed immediately and stored at -20°C . Lysyl oxidase activity of the skin was estimated by the method of Trackman *et al.* (1981) using 1,5-diamino pentane as the substrate. Skin homogenate in 4 M urea was used for the assay without further purification since purification resulted in considerable loss of activity. The linearity of enzyme assay in relation to the enzyme concentration was ensured. The concentrations of free sulphur amino acids, homocysteine, cystathionine and methionine were measured in the skin using Beckman 119 CL amino acid analyser.

Lysyl oxidase activity was also measured in the regenerated skin formed after infliction of incision wound in rats, since earlier studies (Lakshmi *et al.*, 1988, 1989) have shown an impairment in skin wound healing in riboflavin or pyridoxine deficiency due to reduction in collagen content and maturation. The following experimental protocol was used to obtain regenerated skin samples from control and deficient animals.

Weanling Wistar/NIN rats were divided into the following 4 groups (i) control *ad libitum* fed, (ii) riboflavin-deficient, (iii) pyridoxine-deficient and (iv) weight-matched control for the riboflavin- and pyridoxine-deficient groups. The diet composition was as described for the earlier experiment. The weight-matched control group received the same diet as the control group fed *ad libitum*, but in restricted amount so that their body weights were similar to those of the deficient groups. After 5 weeks on respective dietary regimens, the rats were subjected to

anesthesia and aseptic conditions. Closure was affected by interrupted cotton sutures, 1 cm apart. On 8th day after wounding, the animals were sacrificed by cervical dislocation and lysyl oxidase activity estimated in the regenerated skin by the method described earlier. Salt soluble collagen (1 M sodium chloride extract) purified from the regenerated skin (Piez *et al.*, 1962) and aldehyde content determined (Paz *et al.*, 1965).

Riboflavin or pyridoxine status of the animals was measured by erythrocyte xanthine oxidase activation test and erythrocyte aspartate aminotransferase activation test respectively (Bayoumi and Rosalki, 1976).

Results

Effect of enzyme concentration on the rate of reaction was tested since skin lysyl oxidase in phosphate buffer with 4 M urea was assayed without further purification. The reaction was linear for the 4 levels of protein tested and the amount of protein used in the assay (1.36 mg) was within this linear range (figure 1).

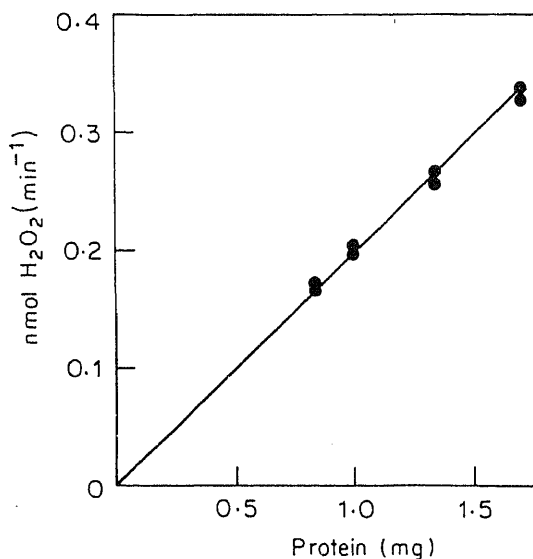


Figure 1. Effect of enzyme concentration on the rate of H₂O₂ production.

In 18-day-old rat pups, skin lysyl oxidase activity (table 1) was lower in riboflavin deficiency as compared to the control group, but it was not significantly altered in pyridoxine-deficiency. Body weights of riboflavin-deficient rats were lowest and there was a significant correlation ($r=0.7$) between the body weight of the animals and lysyl oxidase activity. When the enzyme activity was expressed per g body weight, it was similar in all the 3 groups.

Data given in table 2 show that lysyl oxidase activity of the regenerated skin was not altered either by riboflavin- or pyridoxine-deficiency. However the aldehyde content was significantly lower both in pyridoxine- and riboflavin-deficiency when compared to that of controls.

Table 1. Effect of riboflavin or pyridoxine deficiency in rat pups on skin lysyl oxidase activity.

	Adlib-fed control	Riboflavin-deficient	Pyridoxine-deficient
Body weight (g)	22.0 ± 0.16	15.0 ± 0.36	18.0 ± 1.01
Lysyl oxidase nmol H ₂ O ₂ /min/g skin	8.06 ± 0.37 ^b	5.73 ± 0.34 ^a	6.96 ± 0.28 ^{a, b}
nmol H ₂ O ₂ /min/g body weight	0.35 ± 0.05	0.37 ± 0.04	0.39 ± 0.08
Erythrocyte-glutathione reductase (activity coefficient)	1.14 ± 0.02 ^a	1.39 ± 0.04 ^b	—
Erythrocyte-aspartate aminotransferase coefficient	1.18 ± 0.02 ^a	—	1.88 ± 0.14 ^b

Values are means ± SEM/8 animals. Values in a row not sharing a common superscript are significantly different ($P < 0.05$).

Table 2. Effect of riboflavin or pyridoxine deficiency on regenerated skin lysyl oxidase activity and aldehyde content of purified salt soluble collagen.

	Adlib-fed control	Weight-matched control	Riboflavin-deficient	Pyridoxine-deficient
Body weight (g)	184.5 ± 5.83 ^b	87.8 ± 2.60 ^a	85.7 ± 4.08 ^a	90.6 ± 3.29 ^a
Lysyl oxidase nmol H ₂ O ₂ /min/g skin	11.41 ± 0.60	12.00 ± 0.91	12.00 ± 0.62	11.82 ± 0.91
Aldehyde content (μM/100 mg collagen)	1.69 ± 0.14 ^b	1.44 ± 0.08 ^b	1.02 ± 0.10 ^a	1.14 ± 0.07 ^a
Erythrocyte-glutathione reductase (activity coefficient)	1.12 ± 0.08 ^a	1.19 ± 0.06 ^a	1.49 ± 0.05 ^b	—
Erythrocyte-aspartate aminotransferase (activity coefficient)	1.18 ± 0.07 ^a	1.23 ± 0.06 ^a	—	1.67 ± 0.07 ^b

Values are means ± SEM of 9 animals. Values in a row not sharing a common superscript are significantly different ($P < 0.05$).

The concentrations of free sulphur amino acid in skin were altered both in pyridoxine and riboflavin-deficiency. Significant rise in the levels of homocysteine, cystathionine and methionine were observed in pyridoxine-deficiency, whereas in riboflavin-deficiency, only homocysteine level was raised (table 3).

Discussion

In the earlier study, Trackman *et al.* (1981) could not observe linearity in the reaction rate of lysyl oxidase when measured in the crude homogenate of aortae

Table 3. Effect of riboflavin or pyridoxine deficiency in rat pups on sulphur amino acid content of skin.

Sulphur amino acids $\mu\text{mol/g skin}$	Adlib-fed control	Riboflavin- deficient	Pyridoxine- deficient
Homocysteine	0.06 ± 0.006^a (4)	0.16 ± 0.01^b (4)	0.24 ± 0.04^c (4)
Cystathionine	0.05 ± 0.01^a (3)	0.06 ± 0.01^a (3)	0.17 ± 0.03^b (3)
Methionine	0.20 ± 0.03^a (4)	0.17 ± 0.03^a (3)	0.32 ± 0.05^b (4)

Values are means \pm SEM. Values not sharing a common superscript are significantly different ($P < 0.05$). Numbers in parentheses indicate number of samples.

ference between their observation and ours may be due to difference in species, sex as well as age of the animal. The data in figure 1 suggest that the lysyl oxidase assay used in the present study was sensitive.

The results of the present study indicate that pyridoxal phosphate is unlikely to be the cofactor of rat skin lysyl oxidase, since a decrease in the activity of this enzyme was not observed in pyridoxine-deficiency. Myers *et al.* (1985) have reported a similar finding with respect to lung lysyl oxidase in pyridoxine-deficient rats. As in the case of human placental (Van der Meer and Duine, 1986) and bovine aortic lysyl oxidase (Williamson *et al.*, 1986) the carbonyl cofactor of rat skin lysyl oxidase may also be pyrroloquinoline quinone.

The impairment in collagen maturity in these two deficiencies could be due to an increase in the homocysteine level. This may form a thiazine complex with allysine similar to D-pencillamine (Myers *et al.*, 1985; Kang and Trelstad, 1973). This could be the reason for lower aldehyde content of purified salt soluble collagen in skin generated in pyridoxine- or riboflavin-deficiency. The thiazine complex with cysteine and homocysteine has been reported to be unstable to film dialysis (Deshmukh and Nimni, 1969) or to exhaustive dialysis for 48 h (Kang and Trelstad, 1973). However, Deshmukh and Nimni (1969) have found that even after 24 h of dialysis, certain amount of cysteine remained bound to collagen, which was proportional to the aldehyde content of the collagen molecule. In the present study, salt-soluble collagen was dialysed for 24 h with only two changes of buffer. This may have been insufficient to disrupt the thiazine complex. Additionally, in a separate experiment conducted by us, the 6-membered thiazine complex between pyridoxal phosphate and homocysteine was found to be more stable to pH variations, to N-ethylmaleimide, a sulfhydryl reagent and to 50°C for 30 min than the 5-membered thiazine complex with cysteine. Decreased formation of fibrils and reducible covalent crosslinks was reported by Kang and Trelstad (1973) in an *in vivo* study using skin soluble collagen and L-homocysteine. Similar impairment in *in vitro* fibril formation by purified salt soluble skin collagen was reported earlier in riboflavin- or pyridoxine-deficiency (Prasad *et al.*, 1986b).

The plasma homocysteine and cystathionine levels are known to increase in pyridoxine-deficiency (Smolin and Benevenga, 1982; Smolin *et al.*, 1983; Myers *et al.*, 1985), since the enzymes involved in the metabolism of these two amino acids require pyridoxal phosphate as cofactor (figure 2). Higher concentration of skin homocysteine in riboflavin-deficiency is a new finding. It may be due to lower

- , R. A. and Rosalki, S. B. (1976) *Clin. Chem.*, **22**, 327.
- A. and Levene, C. I. (1982) *Biochem. Biophys. Res. Commun.*, **108**, 1172.
- A. and Levene, C. I. (1983) *Biochem. J.*, **210**, 633.
- kh, K. and Nimni, M. E. (1969) *J. Biol. Chem.*, **244**, 1787.
- H. and Trelstad, R. L. (1973) *J. Clin. Invest.*, **52**, 2571.
- A. V. and Bamji, M. S. (1979) *Biochem. Med.*, **22**, 274.
- A. V., Diwan, P. V. and Bamji, M. S. (1988) *Nutr. Res.*, **8**, 1203.
- R., Lakshmi, A. V. and Bamji, M. S. (1989) *Biochem. Med. Metab. Biol.*, **42**, 185.
- C. I., O'shea, M. P. and Carrington, M. J. (1988) *Int. J. Biochem.*, **20**, 1451.
- A., Dubick, M. A., Reynolds, R. D. and Rucker, R. B. (1985) *Biochem. J.*, **229**, 153.
- A., Blumenfeld, O. O., Rojkind, M., Henson, E., Furfine, C. and Gallop, P. M. (1965) *Arch. Chem. Biophys.*, **108**, 548.
- A., Eigner, E. A. and Lewis, M. S. (1962) *Biochemistry*, **2**, 58.
- R., Lakshmi, A. V. and Bamji, M. S. (1983) *Biochem. Med.*, **30**, 331.
- R., Lakshmi, A. V. and Bamji, M. S. (1986a) *Ann. Nutr. Metab.*, **30**, 300.
- R., Lakshmi, A. V., Bamji, M. S. and Venkatappaiah, V. (1986b) *J. Clin. Biochem. Nutr.*, **1**, 59.
- S. P. and Bailey, A. J. (1975) *Biochem. J.*, **149**, 381.
- . W., McGoodwin, E. G., Martin, G. R. and Grahm, D. (1977) *J. Biol. Chem.*, **252**, 939.
- L. A. and Benevenga, N. J. (1982) *J. Nutr.*, **112**, 264.
- L. A., Crenshaw, T. D., Kurtysz, D. and Benevenga, N. J. (1963) *J. Nutr.*, **113**, 2022.
- n, P. C., Zoski, G. C. and Kagan, H. M. (1981) *Anal. Biochem.*, **113**, 336.
- Meer, R. A. and Duine, J. A. (1986) *Biochem. J.*, **239**, 789.
- on, P. R., Moog, R. S., Dooley, D. M. and Kagan, H. M. (1986) *J. Biol. Chem.*, **261**, 16302.

hypoglycemic action of the pectin present in the juice of the inflorescence stalk of plantain (*Musa sapientum*)—Mechanism of

R. GOMATHY, N. R. VIJAYALEKSHMI and P. A. KURUP*

Department of Biochemistry, University of Kerala, Kariavattom, Trivandrum 695 581, India

MS received 11 November 1989; revised 9 July 1990

Abstract. The pectin isolated from the juice of the inflorescence stalk of plantain (*Musa sapientum*) has been found to show significant hypoglycemic effect both in normoglycemic and alloxan diabetic rats. After its administration at a dose of 20 mg/100 g body weight, there was increase in the concentration of hepatic glycogen, increased glycogenesis as evident from the increased activity of glycogen synthetase and in normoglycemic rats increased incorporation of labelled glucose into hepatic glycogen. Glycogenolysis and gluconeogenesis were lower as was evident from the decreased activity of glycogen phosphorylase and gluconeogenic enzymes.

Keywords. *Musa sapientum*; hepatic glycogen; glycogen synthetase; glycogenolysis; gluconeogenesis; glycogen phosphorylase.

Introduction

It has been shown in this laboratory that the pectin present in the juice of the stem (inflorescence stalk) of plantain (*Musa sapientum*) showed significant cholesterol and triglyceride lowering action in rats fed cholesterol free and atherogenic diet (Gomathy *et al.*, 1989). The material contained 32.4% total hexose and 52.5% uronic acid. The biochemical mechanism by which it causes reduction in the serum and liver cholesterol was also studied and the results reported (Gomathy *et al.*, 1989). It was also found in these experiments that this material also caused lowering of blood sugar in these rats. Detailed investigations have now been carried out on the hypoglycemic action of this material in normal and alloxan diabetic rats. The mechanism of its hypoglycemic action has also been studied and the results are reported in this paper.

Materials and methods

The biochemicals used in this study were purchased from Sigma Chemical Company, St. Louis, Missouri, USA. The material was isolated from fresh juice of the pith of the stem of plantain as described before (Gomathy *et al.*, 1989).

Animal experiments

Hypoglycemic rats: Male albino rats (Sprague-Dawley strain, weighing 100–120 g)

To whom all the correspondence should be addressed.

were divided into two groups with 12 rats in each group. Group 1 served as control while group 2 was given the test material (20 mg/100 g/day orally)

Alloxan diabetic rats: Diabetes was induced in another group of rats by subcutaneous administration of alloxan monohydrate (18 mg/100 g body weight) as described earlier (Malathy and Kurup, 1972).

Those rats with fasting blood glucose levels above 180 mg/100 ml, 15 days after alloxan administration were divided into two groups with 12 rats in each group.

Group 3 served as diabetic control while group 4 received the test material (20 mg/100 g/day orally).

The animals of both normal and diabetic groups were maintained on normal laboratory diet (Gold Mohur rat feed). The material dissolved in water (1 ml) was administered to animals of groups 2 and 4 orally as a single dose of 20 mg/100 g body weight. This dose was selected since in preliminary experiments with various doses (5, 10, 20 and 25 mg/100 g body weight) maximum hypoglycemic action was observed at this level. There was no further increase in the hypoglycemic action at higher levels. Duration of experiment was 45 days in the animals of group A and in the alloxan diabetic animals of group B. At the end of this period, they were deprived of food overnight, stunned by a blow at the back of the neck and killed by decapitation. The tissues were removed to ice-cold containers for various estimations.

Blood glucose was determined by the glucose oxidase method (Bergmeyer and Bernt, 1963). Glucose tolerance was determined by measuring blood glucose levels fasting and 1.5 h after an oral dose of glucose (200 mg/100 g body weight). Liver glycogen was estimated by the method of Carroll *et al.* (1956).

Estimation of enzyme activities

The following procedures were used for the estimation of various enzyme activities: Hexokinase (EC 2.7.1.1, ATP-D-hexose-6-phosphotransferase) (Crane and Sols, 1953), phosphoglucomutase (EC 2.7.5.1) (Najjar, 1955), pyruvic kinase (EC 2.7.1.40) (Theodore Bucher and Pfeleiderer, 1955), fructose-1, 6-diphosphate aldolase (EC 4.1.2.6) (Taylor *et al.*, 1948), glycogen phosphorylase (EC 2.4.1.1, α -1., 4-glucan orthophosphate glucosyl transferase) (Singh *et al.*, 1961), glycogen synthetase (EC 2.4.1.11, UDPG α -1, 4-glucosyl transferase) (Leloir and Goldemberg, 1960), glucose-6-phosphatase (EC 3.1.3.9, D-glucose-6-phosphate phosphohydrolase) (Koide and Oda, 1959), fructose 1,6-diphosphatase (EC 3.1.3.11) (Sandro Pontremoli, 1966), isocitric dehydrogenase (isocitrate: NAD oxido-reductase EC 1.1.1.41) (Kornberg and Pricer, 1951), succinic dehydrogenase (EC 1.3.99.1) (Veeger *et al.*, 1969), malate dehydrogenase (EC 1.1.1.37) (Mehler *et al.*, 1948), glucose-6-phosphate dehydrogenase (EC 1.1.1.49, glucose-6-phosphate NADP oxidoreductase) (Kornberg and Horecker, 1955).

In vivo incorporation of [^{14}C] glucose into hepatic glycogen was studied by administration of universally labelled [^{14}C] glucose (10 μCi /100 g body weight) intraperitoneally. The rats were deprived of food overnight and 2 h after administration of labelled glucose, they were killed by decapitation. The liver was quickly removed to ice-cold containers for the isolation of glycogen and

Protein was estimated in the enzyme extract after trichloroacetic acid precipitation by the method of Lowry *et al.* (1951).

Results

Concentration of blood sugar

Rats administered the material showed lower fasting blood sugar levels in both normoglycemic and alloxan diabetic groups when compared to corresponding pretreatment levels. Blood glucose level 1.5 h after glucose load was also significantly lower in the rats administered the material in both groups (table 1).

Table 1. Concentration of blood glucose and hepatic glycogen.

Groups	Blood glucose (mg/100 ml)			Hepatic glycogen (mg/g wet tissue)
	Fasting		1.5 h after glucose administration (200 mg glucose/100 g body weight)	
	Initial (pre-treatment value)	Final (post treatment value)		
Normal rats				
1. Control	92.0 ± 2.0	90.0 ± 2.16	144.69 ± 3.5	21.65 ± 0.54
2. Experimental	90.0 ± 1.9	65.65 ± 1.64 ^a	100.17 ± 2.4 ^a	35.82 ± 0.90 ^a
Alloxan diabetic rats				
3. Control	196.8 ± 4.92	212.6 ± 5.32	352.0 ± 8.0	13.14 ± 0.33
4. Experimental	208.4 ± 5.21	171.8 ± 4.30 ^a	232.0 ± 5.8 ^a	17.69 ± 0.44 ^a

The values are the mean \pm SEM for 12 rats. Group 2 has been compared with group 1 and group 4 with group 3. ^a*P* < 0.01.

There was thus significant improvement in the glucose tolerance in the rats administered the material in both normoglycemic and alloxan diabetic rats (% increase in blood glucose after oral glucose load, based on pretreatment of FBS volumes are normoglycemic—57.3 in the control and 11.3 in the experimental; alloxan diabetic—78.86 in the control and 11.52 in the experimental).

Concentration of hepatic glycogen

There was significant increase in the concentration of glycogen in the liver in the rats given the material in both normoglycemic and alloxan diabetic groups (table 1).

Activity of glycolytic enzymes in the liver

Rats administered the material showed significant increase in the activity of

hexokinase, fructose-1, 6-diphosphate aldolase, phosphoglucomutase and pyruvic kinase in the liver in both normoglycemic and alloxan diabetic groups (table 2).

Table 2. Activity of glycolytic enzymes in the liver.

Groups	Hexokinase (mg glucose Phosphorylated /min/g protein)	Fructose-1, 6-diphosphate aldolase (units/g protein)	Phosphoglucomutase (μ mol of P_i liberated/h/g protein)	Pyruvic kinase (units/g protein)**
Normal rats				
1. Control	36.5 \pm 0.80	0.49 \pm 0.01	22.81 \pm 0.57	6.95 \pm 0.174
2. Experimental	44.2 \pm 1.20 ^a	0.64 \pm 0.02 ^a	30.13 \pm 0.75 ^a	8.46 \pm 0.21 ^a
Alloxan diabetic rats				
3. Control	24.6 \pm 0.60	0.33 \pm 0.008	11.28 \pm 0.28	3.6 \pm 0.09
4. Experimental	29.1 \pm 0.72 ^a	0.41 \pm 0.01 ^a	14.10 \pm 0.35 ^a	4.9 \pm 0.13 ^a

The values are the mean \pm SEM for 12 rats. Group 2 has been compared with 1 and group 4 with group 3, ^a $P < 0.01$.

*One unit of enzyme is defined as that amount which transforms 1 mg P_i in 1/min g protein.

**One unit =
$$\frac{100}{\text{seconds for change of absorbance of } 0.1}$$

With a 1 cm light path at 366 μ m, this unit corresponds to a turnover of 1.76×10^{-5} M/min.

Activity of glycogen phosphorylase

There was significant decrease in the activity of glycogen phosphorylase in the liver in the rats administered the material in both normoglycemic and alloxan diabetic groups (table 3).

Table 3. Activity of glycogen phosphorylase, glycogen synthetase and gluconeogenic enzymes in the liver.

Groups	Glycogen phosphorylase (μ mol of P_i liberated/min/g protein)	Glycogen synthetase (μ mol of UDP formed/ min/g protein)	Glucose-6- phosphatase (μ mol of P_i liberated/h/ g protein)	Fructose-1,6- diphosphatase (μ mol of P_i liberated/h/ g protein)
Normal rats				
1. Control	5.6 \pm 0.14	27.00 \pm 0.68	128.4 \pm 4.2	64.95 \pm 1.62
2. Experimental	4.8 \pm 0.12 ^a	36.12 \pm 0.90 ^a	92.6 \pm 3.8 ^a	52.21 \pm 1.31 ^a
Alloxan diabetic rats				
3. Control	7.8 \pm 0.19	9.98 \pm 0.25	172.1 \pm 3.3	82.1 \pm 2.05
4. Experimental	6.1 \pm 0.15 ^a	14.40 \pm 0.36 ^a	107.5 \pm 2.67 ^a	69.4 \pm 1.74 ^a

The values are the mean \pm SEM for 12 rats. Group 2 has been compared with 1 and group 4 with group 3, ^a $P < 0.01$.

Activity of glycogen synthetase

There was significant increase in the activity of glycogen synthetase in the liver in

given the material in both normoglycemic and alloxan diabetic groups

f gluconeogenic enzymes

ity of glucose-6-phosphatase and fructose-1, 6-diphosphatase showed
t decrease in the rats given the material in both normoglycemic and
diabetic groups (table 3).

f citric acid cycle enzymes

of succinic dehydrogenase, isocitrate dehydrogenase and malate
enase showed significant increase in the rats given the material in both
cemic and alloxan diabetic groups (table 4).

ctivity of citric acid cycle enzymes, glucose-6-phosphate dehydrogenase in liver and the
n of [¹⁴C] glucose into hepatic glycogen.

	Succinic dehydrogenase (change in absorbance/ min/mg protein)	Isocitrate dehydrogenase (mg NAD reduced/ 30 s/mg protein)	Malate dehydrogenase (mg NADH oxidised/ mg protein/ 30 s)	Glucose-6- phosphate dehydrogenase (units/g protein)*	Incorporation of [¹⁴ C] glucose into hepatic glycogen (counts/min/g protein)
	0.09 ± 0.001	1.61 ± 0.04	12.14 ± 0.29	102.1 ± 2.6	357.2 ± 12.9
ental	0.15 ± 0.003 ^a	1.99 ± 0.05 ^a	15.79 ± 0.38 ^a	128.2 ± 3.2 ^a	656.5 ± 26.4 ^a
etic					
	0.06 ± 0.002	0.91 ± 0.03	10.90 ± 0.26	86.2 ± 2.2	NS
ental	0.08 ± 0.002 ^a	1.42 ± 0.04 ^a	15.79 ± 0.31 ^a	99.8 ± 2.5 ^a	NS

re the mean ± SEM for 12 rats. Group 2 has been compared with 1 and group 4 with group

defined as the amount of enzyme which causes an increase of 1.0 in optical density/min/g

died.

f pentose phosphate pathway enzymes

n the material showed significant increase in the activity of glucose-6-
dehydrogenase in the liver in both normoglycemic and alloxan diabetic
ble 4).

Discussion

The results indicate that the increase in the concentration of glycogen in the liver in the rats given the material may be due to increased glycogenesis as evident from the increased activity of glycogen synthetase and higher incorporation of labelled glucose into hepatic glycogen. It may also be due to decreased degradation of glycogen in normoglycemic rats as evident from the decreased activity of glycogen phosphorylase. There was decreased gluconeogenesis as evident from the lower activity of glucose-6-phosphatase and fructose-1, 6-diphosphatase. The utilization of glucose by glycolytic and citric acid cycle and also by the pentose phosphate pathway was also increased as evident from the increased activity of some of the enzymes involved in these pathways. Thus the hypoglycemic action of the material may be due to increased utilization of glucose in the liver for glycogen synthesis, decreased degradation of glycogen and also due to decreased gluconeogenesis.

In this connection, it has been found in this laboratory that rats fed isolated fiber from unripe banana by the neutral detergent procedure (Goering and Van Soest, 1970) which does not contain pectin, caused significant alterations in the activity of many enzymes of carbohydrate metabolism and this effect was found to be brought about by the higher concentration of bile acids produced in the liver as a result of feeding this fiber (Usha *et al.*, 1989). Evidence for this was obtained by studying the *in vitro* effect of cholic acid and chenodeoxycholic acid on the activity of these enzymes. It is quite possible that the effects now observed for this pectin on carbohydrate metabolism may also be due to its influence on hepatic bile acids. This material has been found to cause higher concentration of bile acids in the liver (Gomathy *et al.*, 1989).

There are reports that pectin administration decreased the absorption of glucose (Vaaler *et al.*, 1980) and decrease in glucose absorption may also contribute partly to the lower blood glucose now observed.

In this connection hypoglycemic action has been reported for many pectins (Holt *et al.*, 1976; Kanter *et al.*, 1980; Schwartz *et al.*, 1980; Vaaler *et al.*, 1980). However in these cases, the activity is observed only at high levels (500 mg and above/100 g bodyweight) while this material is active at much lower levels (20 mg/100 g body weight).

It is possible that all the observed effects of the pectin maybe mediated *via* insulin. Serum insulin levels, however have not been studied.

References

- Bergmeyer, H. U. and Bernt, Erich (1963) *Methods of enzymatic analysis*
- Carroll, N. V., Longley, R. W. and Roe, J. H. (1956) *J. Biol. Chem.*, **220**, 583.
- Crane, R. K. and Sols, A. (1953) *J. Biol. Chem.*, **203**, 273.
- Goering, H. K. and Van Soest, P. J. (1970) *Agri handbook*. No. 379 (Bethesda: Agricultural Research Service, US Dept. of Agriculture).
- Gomathy, R., Vijayalekshmi, N. R. and Kurup, P. A. (1989) *J. Biosci.*, **14**, 301.
- Holt, Stephen, Robert, C., Heading, David, Carter, Laurence. F. Prescott and Peter Tothill (1976) *Lancet*, **1**, 636.
- Kanter, Yoram, Nathan Eitan, Gerald Brook and David Barzilai (1980) *Isr. J. Med. Sci.*, **16**, 1.
- Koide, H. and Oda, T. (1959) *Clin. Chim. Acta.*, **4**, 554.
- Kornberg, A. and Pricer, W. E., Jr. (1951) *J. Biol. Chem.*, **189**, 123.
- Kornberg, A. and Horecker, B. L. (1955) *Methods Enzymol.*, **1**, 323.
- Leloir, L. F. and Goldemberg, S. H. (1960) *J. Biol. Chem.*, **235**, 919.

- Lowry, O. H., Rosebrough, N. J., Farr, A. L. and Randall, R. J. (1951) *J. Biol. Chem.*, **193**, 265.
- Malathy, K. and Kurup, P. A. (1972) *Indian J. Biochem. Biophys.*, **9**, 223.
- Mehler, A. H., Kornberg, A., Grisolia, S. and Ochoa, S. (1948) *J. Biol. Chem.*, **174**, 961.
- Molly Thomas, Leelamma, S. and Kurup, P. A. (1983) *J. Nutr.*, **113**, 1104.
- Najjar, V. A. (1955) *Methods Enzymol.*, **1**, 294.
- Sandro Pontremoli (1966) *Methods Enzymol.*, **9**, 626.
- Schwartz, S. E. and Gray, D. Levine, (1980) *Gastroenterology*, **79**, 833.
- Singh, V. N., Venkitasubramanian, T. A. and Viswanathan, R. (1961) *Biochem. J.*, **78**, 728.
- Taylor, J. F., Green, A. A. and Cori, G. T. (1948) *J. Biol. Chem.*, **173**, 591.
- Theodor Bucher and Pfeleiderer, G. (1955) *Methods Enzymol.*, **1**, 435.
- Usha, V., Vijayammal and Kurup, P. A. (1989) *Indian J. Exp. Biol.*, **27**, 445.
- Vaaler, Stein, Kristian, F., Hanseen and Oystein aagenafs (1980) *Acta Med. Scand.*, **208**, 389.
- Veeger, C., Dervartanian, D. V. and Zeylenskin, W. P. (1969) *Methods Enzymol.*, **13**, 83.

Antiatherogenic effect of a low lysine:arginine ratio of protein involves alteration in the aortic glycosaminoglycans and glycoproteins

T. RAJAMOHAN and P. A. KURUP

Department of Biochemistry, University of Kerala, Kariavattom, Trivandrum 695 581, India

MS received 17 July 1990; revised 26 November 1990

Abstract. The effect of alteration of lysine:arginine ratio of the protein on the aortic glycosaminoglycans and glycoproteins was studied in rats fed cholesterol free and atherogenic diet. The concentration of total glycosaminoglycans and of individual fractions was significantly lower in the aorta in the case of diet with lysine:arginine ratio of 1:0, than the diet with a ratio of 2:0. Rats fed globulin fraction isolated from sesame seeds, which has a lysine:arginine ratio of 0.67 also showed significantly lower concentration of total and individual glycosaminoglycan fractions in the aorta than those fed casein (lysine:arginine ratio 2:0). Concentration of total hexose and fucose in the glycoproteins was also lower in the aorta in the case of lysine:arginine ratio 1:0. These results in the light of previous reports of increase in the aortic glycosaminoglycans in the early stages of atherosclerosis and increase in the total hexose and fucose in the glycoproteins in the atherosclerotic aorta indicate that the antiatherogenic effect of a low lysine:arginine ratio in the protein involves alteration in the aortic glycosaminoglycans and glycoproteins.

Keywords. Lysine; arginine ratio; glycosaminoglycans; glycoproteins.

Introduction

It has been suggested that the hypocholesterolemic and antiatherogenic effect of many plant proteins may be related to their low lysine:arginine ratio (Kritchevsky *et al.*, 1981). Work carried out in this laboratory has shown that a Lys:Arg ratio of 1:0 significantly lowered serum and aortic cholesterol than the diet with Lys:Arg ratio of 2:0 (Rajamohan and Kurup, 1986). Lysine has been reported to be hypercholesterolemic (Hevia *et al.*, 1980). Lys:Arg antagonism has also been documented in rats and chicks (Jones *et al.*, 1966, 1967). It is known that in atherosclerosis, apart from the alterations in the aortic lipids, changes also take place in the aortic glycosaminoglycans (gg), glycoproteins (gp), collagen and elastin. Studies carried out in this laboratory (Vijayakumar *et al.*, 1975) and elsewhere (Kumar *et al.*, 1967) indicate that the concentration of sulphated gg increased in the aorta in the early stages of atherosclerosis. The aortic gp have been found by most workers to show increase in carbohydrate components—total hexose and fucose (Schonebeck *et al.*, 1962, Satakopan and Kurup, 1978). Concentration of aortic collagen has been reported to increase in the aorta (Gran *et al.*, 1967), and that of elastin to decrease in atherosclerosis (Bartelsom, 1968). In view of these, it was considered desirable to study whether the Lys:Arg ratio of the protein affects the aortic gg, gp, collagen and elastin. Lys:Arg ratio was altered by adding arginine to the diet containing casein which has a Lys:Arg ratio of 2:0. The effect of a plant protein globulin isolated from the seeds of sesame (*Sesamum indicum*) which has a

low Lys:Arg ratio when compared to casein, was also studied. This protein showed significant cholesterol lowering action in the serum and aorta in rats fed cholesterol free and atherogenic diet (Rajamohan, 1989).

Materials and methods

Lysine: arginine ratio

Rats fed cholesterol free diet: Male albino rats (Sprague-Dawley strain, body weight 80–100 g) were divided into 2 groups of 15 rats each as follows:

Group 1: Rats fed diet containing Lys:Arg ratio of 2:0.

Group 2: Rats fed diet containing Lys:Arg ratio of 1:0.

Rats fed cholesterol containing diet: In another experiment, male albino rats of similar body weight were divided into 2 groups of 15 rats each.

Group 3: Rats fed diet containing Lys:Arg ratio of 2:0.

Group 4: Rats fed diet containing Lys:Arg ratio of 1:0.

Rats of group 1 and 3 received 16% casein while those of group 2 and 4 received 16% casein + 0.656% arginine. Casein contains 4.1% arginine and 8.2% lysine and therefore its Lys:Arg ratio is 2:0. Thus the Lys:Arg ratio of group 1 and 3 was 2:0 and that of group 2 and 4 was 1:0.

The basal diet in the cholesterol free diet group contained (g/100 g): Corn starch-71, casein (vitamin and fat free)-16, groundnut oil-8, salt mixture-4 and vitamin mixture-1. The cholesterol containing diet contained (g/100 g): Corn Starch-61.5, casein-16, coconut oil-15, salt mixture-4, vitamin mixture-1, cholesterol-2, and sodium cholate-0.5. The vitamin mixture and salt mixture used had the same composition as described earlier (Menon and Kurup, 1976).

Arginine was added to the diets of group 2 and 4 at the expense of corn starch. The rats of groups 1 and 2 were given the same quantity of diet and also of groups 3 and 4, to maintain caloric intake the same. The animals were kept individually in polypropylene cages in rooms maintained at $25 \pm 1^\circ\text{C}$. Water was available *ad libitum*. The duration of the experiment was 45 days. At the end of this period, the rats in the various groups were deprived of food overnight, stunned by a blow at the back of the neck and killed by decapitation. The serum and aorta were removed to ice cold containers for various estimations.

Effect of the globulin fraction from sesame seeds on the arterial gg and gp

Isolation of globulin fraction from sesame seeds: Sesame seed cake after expelling the oil was used for this purpose. The remaining oil in the seed cake was removed by extracting with petroleum ether (40–60°C) in Soxhlet extraction apparatus. The defatted seed cake was stirred with 10% sodium chloride solution (10 l/kg of the cake) for 24 h at room temperature in large fiber glass containers using mechanical stirrers. The saline extract was collected by centrifugation at room temperature

which were covered by dialysis membrane, till the extract was chloride free. The precipitated protein was collected by centrifugation and redissolved in minimum volume of 10% saline. After centrifugation, the clear supernatant was dialysed against distilled water, the precipitated globulin fraction collected by centrifugation and dried in vacuum. The yield of the globulin fraction ranged from 90–100 g/kg defatted seed cake.

Rats fed globulin fraction from sesame: Male albino rats (Sprague-Dawley strain, body weight (100–120 g)) were divided into two groups of 15 rats each and fed cholesterol free diet as follows:

Group 5: Control rats fed casein.

Group 6: Experimental rats fed globulin fraction from sesame.

The basal diet had the same composition as described earlier, for the cholesterol free diet. The protein in the diet in the case of group 5 was 16% casein while in the case of group 6, it was 16% globulin fraction from sesame. All experimental conditions were the same as described for the Lys:Arg ratio.

Analytical procedures

Estimation of cholesterol and triglycerides in the serum and aorta was carried out as described earlier (Menon and Kurup, 1976). gg were estimated in the aorta enzymatically by the procedure described before (Jaya and Kurup, 1986). The individual gg were quantitated by estimation of uronic acid by the modified procedure of Bitter and Muir (1962). No attempt was made to estimate chondroitin-4-sulphate and chondroitin-6-sulphate separately.

For the estimation of carbohydrate components of aortic gp, the tissue was digested with papain and processed as described before (Chempakam and Kurup, 1978).

Fucose was estimated by the method of Dische and Shettles (1948), total hexose by phenol sulphuric acid method (Dische *et al.*, 1956) and sialic acid by the thiobarbituric acid method of Warren (1959).

Isolation and estimation of collagen and elastin

The procedure of Jackson and Cleary (1967) was used. The dry defatted tissue was autoclaved with water and the gelatin removed by centrifugation. The supernatant was saved. The residue was again autoclaved with water and the combined supernatant used for collagen estimation. The residue was digested with 0.1 N NaOH at 98°C for 50 min to remove other proteins. The elastin was washed with 3:1 ethanol:ether mixture and estimated by nitrogen estimation. Collagen in the supernatant was hydrolysed with 6 N HCl at 118°C for 8 h in a sealed tube and estimated by determining the hydroxy proline content by the method of Neuman and Longman (1950).

Results

Concentration of cholesterol and triglycerides in serum and aorta

The concentration of cholesterol and triglycerides in the serum and aorta was

significantly lower in the rats fed diet with Lys:Arg ratio of 1:0 than the diet with Lys:Arg ratio of 2:0. This was true in the case of rats fed cholesterol free and cholesterol containing diets. Rats fed globulin fraction also showed significantly lower levels of cholesterol and triglycerides in the serum and aorta than those fed casein (table 1).

Table 1. Concentration of cholesterol and triglycerides in the serum and aorta.

Groups	Concentration of cholesterol		Concentration of triglycerides*	
	Serum (mg/100 ml)	Aorta (mg/100 g wet tissue)	Serum (mg/100 ml)	Aorta (mg/100 g wet tissue)
Lys:Arg ratio				
Cholesterol free diet				
1. Lys:Arg ratio 2:0	76.3 ± 1.4	193.7 ± 4.3	6.2 ± 0.12	695 ± 16.7
2. Lys:Arg ratio 1:0	59.7 ± 1.2 ^a	142.8 ± 3.3 ^a	4.7 ± 0.09 ^a	545 ± 13.6 ^a
Cholesterol diet				
3. Lys:Arg ratio 2:0	168.8 ± 4.2	428 ± 12.6	12.8 ± 0.25	1415 ± 36.8
4. Lys:Arg ratio 1:0	98.2 ± 4.6 ^a	264 ± 8.6 ^a	8.8 ± 0.16 ^a	982 ± 25.5
Globulin fraction				
5. Casein	78.9 ± 2.9	205.8 ± 7.1	5.9 ± 0.12	685 ± 20.5
6. Sesame globulin	63.6 ± 2.1 ^a	147.7 ± 4.2 ^a	4.9 ± 0.1 ^a	543 ± 16.3 ^a

*Expressed as triglyceride glycerol. Average of the values from 6 experiments ± SEM. Group 2 has been compared with group 1, group 4 with group 3 and group 6 with group 5.

^aP < 0.01.

Concentration of total and individual gg fractions in the aorta

The concentration of total gg and the individual gg fractions was significantly lower in the aorta in the case of Lys:Arg diet ratio of 1:0 than ratio of 2:0, both in rats fed cholesterol free and cholesterol containing diets. Rats fed globulin fraction from sesame seeds also showed lower concentration of total gg and individual gg fractions in the aorta than those fed casein (table 2).

Concentration of carbohydrate components of aortic glycoproteins

The concentration of total hexose and fucose decreased in the aorta in the case of Lys:Arg ratio of 1:0, when compared to a ratio of 2:0 both in rats fed cholesterol free and cholesterol diet. Sialic acid decreased in the case of ratio of 1:0 in rats fed cholesterol free diet, but was not significantly altered in rats fed cholesterol diet (table 3).

Rats fed globulin fraction however showed no significant alteration in total hexose and fucose when compared to casein. Sialic acid however decreased (table 3).

Table 2. Concentration of total and individual gg fractions in the aorta.

Groups	Total gg	HA	HS	Ch-4S + Ch-6S	DS	H
(μg uronic acid/g dry defatted tissue)						
Arg ratio						
cholesterol free diet						
1. Lys:Arg ratio 2:0	5852 ± 175	592 ± 14.8	1552 ± 36	2254 ± 58	835 ± 21.7	542 ± 14
2. Lys:Arg ratio 1:0	4578 ± 137 ^a	422 ± 10 ^a	1154 ± 26 ^a	1818 ± 45 ^a	644 ± 17 ^a	448 ± 11.7 ^a
cholesterol diet						
3. Lys:Arg ratio 2:0	6158 ± 174	502 ± 21	1620 ± 32	2390 ± 61	953 ± 27.6	602 ± 14.6
4. Lys:Arg ratio 1:0	5083 ± 130 ^a	353 ± 17 ^a	1225 ± 24 ^a	2094 ± 52 ^a	831 ± 23 ^a	477 ± 11 ^a
globulin fraction						
5. Casein	5740 ± 183	637 ± 16	1574 ± 44	2042 ± 57	864 ± 24	548 ± 14
6. Sesame globulin	4206 ± 134 ^a	451 ± 11.3 ^a	1201 ± 32 ^a	1411 ± 39 ^a	630 ± 17 ^a	466 ± 13 ^a

Average of the values from 6 experiments ± SEM.

Group 2 has been compared with group 1, group 4 with group 3 and group 6 with group 5.

Hyaluronic acid; HS, heparan sulphate; Ch-4S + Ch-6S, chondroitin-4-sulphate + chondroitin-6-sulphate; DS, dermatan sulphate; H, heparin.

^aP < 0.01.

Table 3. Concentration of carbohydrate components of aortic gp.

Groups	Total hexose (mg/g protein of dry defatted tissue)	Fucose	Sialic acid
Lys:Arg ratio			
Cholesterol free diet			
1. Lys:Arg ratio 2:0	70.49 ± 1.4	11.38 ± 0.23	12.69 ± 0.37
2. Lys:Arg ratio 1:0	51.10 ± 1.1 ^a	8.14 ± 0.15 ^a	11.35 ± 0.35 ^a
Cholesterol diet			
3. Lys:Arg ratio 2:0	81.65 ± 1.6	28.5 ± 0.57	15.3 ± 0.28
4. Lys:Arg ratio 1:0	62.37 ± 1.2 ^a	21.4 ± 0.43 ^a	14.4 ± 0.29
Globulin fraction			
5. Casein	75.4 ± 1.4	12.1 ± 0.29	18.8 ± 0.39
6. Sesame globulin	74.7 ± 1.4	11.6 ± 0.27	16.7 ± 0.37 ^a

Average of the values from 6 experiments ± SEM.

Group 2 has been compared with group 1, group 4 with group 3 and group 6 with group 5.

^aP < 0.01.

When compared to a ratio of 2:0, in rats fed cholesterol diet but there was no significant alteration in the concentration of aortic elastin (table 4).

Discussion

The results now obtained indicated that the Lys:Arg ratio of 1:0 which produced significant cholesterol lowering action, has also pronounced effect on the aortic gg. The lower concentration of total and individual gg fractions in the aorta observed at this ratio is quite significant in the light of earlier reports from this laboratory

Table 4. Concentration of aortic collagen and elastin in rats fed cholesterol diet.

Groups	Collagen*	Elastin**
1. Lys:Arg ratio 2:0	56.3 ± 1.13	49.45 ± 0.94
2. Lys:Arg ratio 1:0	37.86 ± 0.76 ^a	50.78 ± 1.02

*Expressed as mg hydroxy proline per g dry defatted tissue.

**Expressed as mg nitrogen per g dry defatted tissue.

Average of the values from 6 experiments ± SEM. Group 2 was compared with group 1.

^aP < 0.01.

that the concentration of the sulphated gg increased in the aorta in the early stage of atheroma in rats (Vijayakumar *et al* 1975). Lys:Arg ratio of 1:0 thus may exert an antiatherogenic effect by keeping the concentration of these gg fractions lower, when compared to a ratio of 2:0. The globulin fraction from sesame with a low Lys:Arg ratio (0.67) which also shows pronounced cholesterol lowering action, also keeps the concentration of aortic gg lower when compared to casein with a higher Lys:Arg ratio (2:0). Thus a low Lys:Arg ratio of the protein in the diet exerts its antiatherogenic effect by altering the concentration of aortic gg, in addition to keeping the concentration of cholesterol and triglycerides low in the serum and aorta.

A Lys:Arg ratio of 1:0 compared to 2:0 also has significant effect on the carbohydrate components of aortic gp. The decrease in the total hexose and fucose in the aortic gp brought about by this ratio is again quite relevant in the light of earlier observations from this laboratory that the concentration of total hexose and fucose increased in the aorta in atheromatous rats (Satakopan and Kurup, 1978). By keeping the level of their carbohydrate components lower in the aortic gp, a ratio of Lys:Arg 1:0 may exert an antiatherogenic effect. However, the sesame protein did not affect the concentration of these carbohydrate components of the aortic gp. Probably this may due to the difference in some of the other amino acids present in this protein and casein. Sesame globulin contains more methionine, cysteine, alanine glycine and, less of tyrosine, serine, proline and aspartic acid (Rajamohan, 1989). But how these amino acids affect the carbohydrate components of gp is not known at present.

The decrease in the concentration of collagen in the aorta observed in the case of Lys:Arg ratio of 1:0, when compared to a ratio of 2:0 is also of interest. It has been reported that the concentration of aortic collagen increased in atheroma in rats while elastin decreased (Gran *et al.*, 1967; Bartelsom, 1968). Thus by keeping the concentration of aortic collagen lower and preventing the decrease in the concentration of aortic elastin, a ratio of Lys:Arg of 1:0 may exert an antiatherogenic effect.

Thus, the changes produced by Lys:Arg ratio of 1:0 when compared to ratio of 2:0 on the concentration of aortic gg, gp and collagen are opposite to those observed in atheromatous rats.

These results indicate that the antiatherogenic effect of Lys:Arg ratio of 1:0 when compared to a ratio of 2:0 is also brought about by its effect on the concentration of aortic gg, gp and collagen. The results obtained with sesame protein with a low Lys:Arg ratio (0.67) when compared to casein (ratio 2:0) also supports this finding.

References

- Bartelsom (1968) *Ann. N. Y. Acad. Sci.*, **149**, 643.
- Bitter, T. and Muir, H. M. (1962) *Anal. Biochem.*, **4**, 330.
- Chempakam, B. and Kurup, P. A. (1978) *Indian J. Biochem. Biophys.*, **15**, 122.
- Dische, Z. and Shettles, L. B. (1948) *J. Biol. Chem.*, **175**, 595.
- Dische, M., Gilles, K. A., Hamilton, J. K., Robers, P. A. and Smith, P. A., (1956) *Method Enzymol.*, **8**, 93.
- Gran, J. C., Narasimhamoorthy, D. V., Nicholas, C. W. Jr. and Charkoff, I. L. (1967) *J. Atheroscler. Res.*, **7**, 629.
- Hevia, P., Kari, F. W., Ulman, E. A. and Visek, W. J. (1980) *J. Nutr.*, **110**, 1224.
- Jackson, D. S. and Cleary, E. G. (1967) *Methods Biochem. Anal.*, **15**, 25.
- Jaya, P. and Kurup, P. A. (1986) *J. Biosci.*, **10**, 487.
- Jones, J. D., Walters, R. and Burnett, P. C. (1966) *J. Nutr.*, **89**, 171.
- Jones, J. D., Petersburg, S. J. and Burnett, P. C. (1967) *J. Nutr.*, **93**, 103.
- Kritchevsky, D., Tepper, S. A., Czarnecki, S. K., Klurfeld, D. M. and Story, J. A. (1981) *Atherosclerosis*, **39**, 169.
- Kumar, V., Berenson, G. S., Rniz, M., Dalferes, Jr. E. R. and Strong, J. P. (1967) *J. Atheroscler. Res.*, **7**, 583.
- Leelamma, S. and Kurup, P. A., (1978) *Indian J. Exp. Biol.*, **16**, 36.
- Menon, P. V. G. and Kurup, P. A. (1976) *Biomedicine*, **2**, 248.
- Neuman, R. E. and Longman, M. A. (1950) *J. Biol. Chem.*, **184**, 299.
- Rajamohan, T. and Kurup, P. A. (1986) *Indian J. Biochem. Biophys.*, **23**, 294.
- Rajamohan, T. (1989) *Dietary proteins and metabolism of lipids and connective tissue macromolecules*, Ph.D. thesis, University of Kerala, Trivandrum.
- Satakopan, V. N. and Kurup, P. A. (1978) *Indian J. Exp. Biol.*, **16**, 309.
- Schonebeck, L., Werber, U. and Voight, K. D. (1962) *J. Atheroscler. Res.*, **2**, 332.
- Scott, J. E. (1960) *Methods Biochem. Anal.*, **8**, 1954.
- Van Handel, E. and Zilver Smit, D. B. (1957) *J. Lab. Clin. Med.*, **50**, 152.
- Vijayakumar, S. T., Leelamma, S. and Kurup, P. A. (1975) *Atherosclerosis*, **21**, 1.
- Wagh, P. V., Roberts, I. B., White, H. J. and Read, R. C. (1973) *Atherosclerosis*, **18**, 83.
- Warren, L. (1959) *J. Biol. Chem.*, **234**, 1971.

Uptake of volatile *n*-alkanes by *Pseudomonas* PG-I

S. S. CAMEOTRA*† and H. D. SINGH

Biochemistry Division, Regional Research Laboratory, Jorhat 785 006, India

*Present address: Institute of Microbial Technology, Post Box 1304, Sector 39-A, Chandigarh 160 014, India.

MS received 12 May 1990

Abstract. Using a bacterial species *Pseudomonas* PG-1, evidence has been obtained which indicates that uptake of *n*-pentane to *n*-octane by microbial cells takes place primarily from the gas phase either directly or *via* the aqueous phase. Specific growth rate increased along with the increase in substrate concentration but above the alkane concentration of 0.3% by volume, specific growth rate decreased indicating substrate inhibition of growth. In the case of less volatile alkanes, *n*-nonane and *n*-decane, substrate transfer is predominantly through substrate solubilization system elaborated by the cells. EDTA, a strong inhibitor of hydrocarbon solubilization by the cells, inhibited growth on these two alkanes but had negligible effect on growth on *n*-pentane to *n*-octane.

Keywords. Uptake; volatile *n*-alkanes; *Pseudomonas* species.

Introduction

There are a few reports available on the microbial utilization of volatile liquid hydrocarbons. Cagler *et al.* (1969) and Hamer *et al.* (1980) demonstrated the possibility of using volatile liquid alkanes for the production of single cell protein. Lukins and Foster (1963) reported that mycobacterium strains which utilized *n*-propane and *n*-butane would not utilize *n*-pentane and *n*-hexane as growth substrates but in exceptional cases. Senez and Konovaltschikoff-Mazoyer (1956) reported growth of a *Pseudomonas aeruginosa* strain on *n*-heptane. Calma-Calamite *et al.* (1971) reported utilization of *n*-octane vapours by *Candida maltosa*. Merdinger and Merdinger (1970) showed that *Pullularia pullens* was capable of growing on *n*-hexane, *n*-heptane and *n*-octane. Zawdzki and Langowska (1983) reported utilization of high *n*-octane concentrations by mixed cultures. Leavitt (1969) reported that the ability of an organism to grow on volatile liquid alkanes is strongly related to the partial pressure. Uemura *et al.* (1969) showed that transfer rate of pentane increased with the increase in partial pressure of pentane. The specific growth rate also increased with the increase in the partial pressure of pentane till an optimum level, beyond which growth rate was inhibited.

In this communication, results of studies conducted to ascertain the mode of transfer of short chain liquid alkanes ranging from *n*-pentane to *n*-decane to the cells are presented. In the case of the more volatile alkanes (*n*-pentane to *n*-octane) mode of substrate transfer to the cells is primarily from the gas phase while with less volatile alkanes (*n*-nonane and *n*-decane), substrate transfer is predominantly through a substrate solubilization system elaborated by the cells.

†To whom all the correspondence should be addressed.

Abbreviations used: ESF, Emulsifying and solubilizing factor.

Guwahati (Assam). The characteristics and culture conditions of *Pseudomonas* PG-1 have been described previously (Reddy *et al.*, 1983; Cameotra *et al.*, 1983). Isolation of *n*-nonane and *n*-decane, emulsifying and solubilizing factor (ESF) from the cell-free culture broth and estimation of the alkane solubilization rate was carried out as described previously (Cameotra *et al.*, 1983). Specially designed 500 ml conical flask (figure 1) were used for the growth of organism on *n*-C₆, *n*-C₇ and *n*-C₈. These

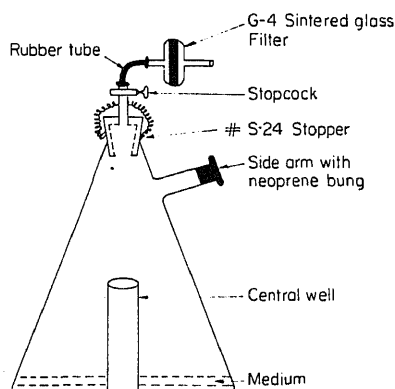


Figure 1. Fermentation flask (500 ml) used for microbial cultivation on volatile alkanes.

flasks had a central well in which the alkane was placed, a side arm closed with a rubber bung through which substrate was added and samples withdrawn with the help of a syringe, and a gas tight stop cock. At different time intervals, 1 ml of the culture broth was withdrawn and after suitable dilution, turbidity was measured in a photoelectric colorimeter at 610 nm. The turbidity value was converted to dry biomass concentration by referring to a standard calibration curve of biomass concentration against turbidity. In the case of *n*-nonane and *n*-decane direct measurement of dry biomass was made as described earlier (Singh *et al.*, 1972). The partial pressure of alkanes in the incubation flasks were estimated by referring to the calibration curves of partial pressure (P_g) against alkane concentrations using the same capacity flasks and same volume of mineral medium (figure 2).

Results and discussion

Growth of Pseudomonas PG-1 on n-pentane, n-hexane and n-heptane

Specially designed fermentation flasks (figure 1) were used for the cultivation of *Pseudomonas* PG-1 on these volatile alkanes. The effect of addition of *n*-pentane, *n*-hexane and *n*-heptane (1% v/v) directly to the culture medium and in the central well on growth of *Pseudomonas* PG-1 in gas tight flasks is illustrated in figure 3.

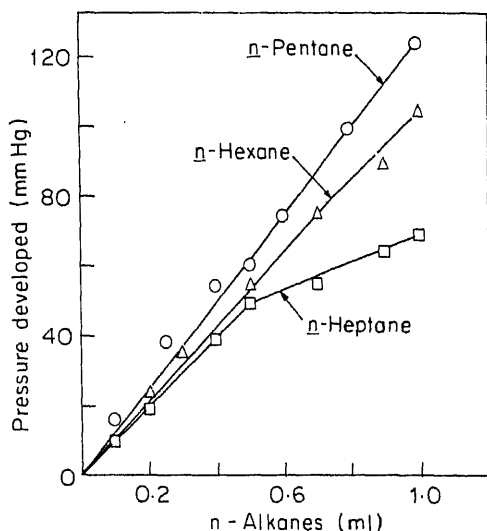


Figure 2. Calibration curve of partial pressure plotted against alkane concentration added to gas tight flask containing 50 ml mineral medium at 34°C.

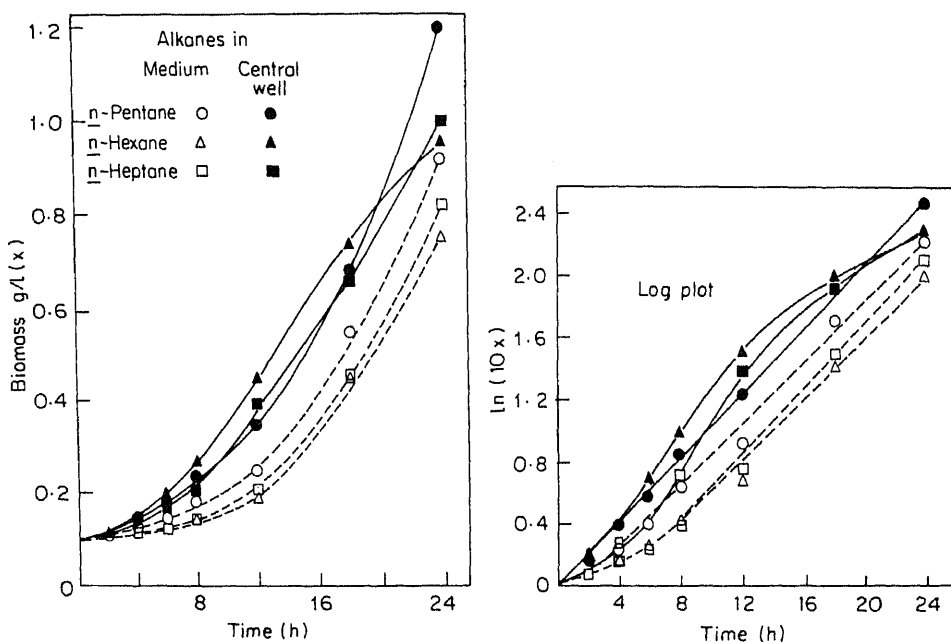


Figure 3. Effect of addition of volatile alkanes (1% v/v) to the aqueous medium and in the central well of the gas tight flasks on the growth of *Pseudomonas* PG-1.

Inhibition of growth was observed when these alkanes were added directly to the aqueous medium. The inhibition was primarily in the form of a lag phase of 2–6 h duration (figure 3, log plot). *n*-Hexane and *n*-heptane showed longer log phase (6 h) than *n*-pentane. Specific growth rates were also reduced with these two alkanes

when substrate was added to the medium. With *n*-pentane however, the specific growth rates were not much different in both modes of substrate addition. These effects could be due to higher volatility of *n*-pentane in comparison to *n*-hexane and *n*-heptane with the result that the added liquid pentane was very quickly vaporised so that practically no contact with the cells occurred. With *n*-hexane and *n*-heptane, contact time might be comparatively longer resulting in stronger inhibition.

The effect of 2.5 mM EDTA on growth characteristics of *Pseudomonas* PG-I on *n*-pentane, *n*-hexane and *n*-heptane (1% vol) added to the central well of the gas tight flasks is shown in figure 4. It is seen that EDTA caused only slight inhibition

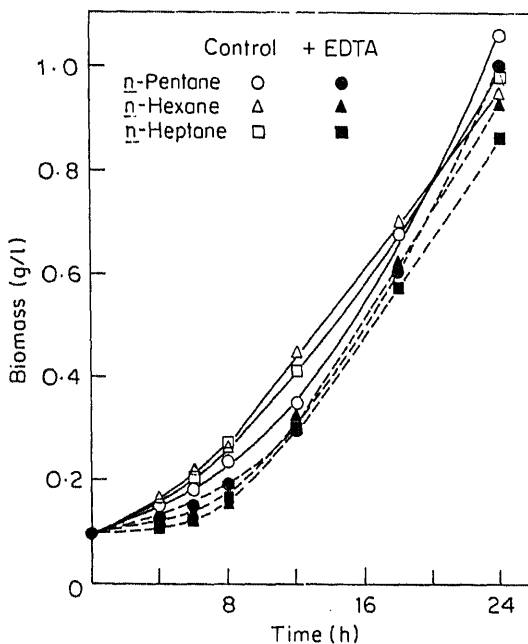


Figure 4. Effect of 2.5 μ M EDTA on the growth of *Pseudomonas* PG-1 on *n*-pentane, *n*-hexane and *n*-heptane (1% v/v) with substrates, added to the central well of the gas tight flasks.

of growth on these alkanes which is negligible in comparison to the strong inhibitory effect of EDTA observed during growth of this organism on *n*-nonane and *n*-decane. EDTA at this concentration was previously shown to be a strong inhibitor of alkane solubilizing system elaborated by this organism (Reddy *et al.*, 1982). These results suggest that substrate transfer from *n*-pentane, *n*-hexane and *n*-heptane to the cells is by diffusion from the gaseous phase.

In order to study the problem of substrate transport in depth, the effect of a wide range of *n*-hexane and *n*-heptane concentrations on the growth characteristics were studied. Hexane concentrations ranging from 0.06% to 2% by volume were added to the central well of the gas tight flasks by a syringe through the neoprene bung. The P_g of the alkane inside the flask as calculated from the calibration curve (figure 2) ranged from 3.3 to 110 mm Hg which were far below its vapour pressure of 220 mm Hg at 34°C indicating little possibility of the alkane vapour being

increased from 0.104 to 0.214 h⁻¹ along with the increase in alkane concentration from 0.396 g/l to 1.584 g/l but specific growth rate decreased along with the increase in alkane concentration above 1.98 g/l (0.3% v/v) indicating substrate inhibition of growth. A lag phase of growth was observed with alkane concentrations of 6.6 g/l (1% v/v) and 13.2 g/l (2% v/v). However, the duration of the exponential growth was longer with higher concentration of alkane. Biomass yield on alkane ranged from 0.61 to 0.73 at lower concentrations of the substrate giving an average value of 0.66. With the increase in substrate concentration biomass yield decreased and at the highest substrate concentration of 13.2 g/l (2% v/v) studied, biomass yield on alkane was a negligible value of 0.05.

Table 1. Effect of different concentrations of *n*-hexane on the growth characteristics of *Pseudomonas* PG-1 in gas-tight flasks with the substrate added to the central well.

Alkane concentration			Exponential growth				Biomass	
Vol. (%)	g/l (S)	1/S	Partial pressure (P _g) (mm Hg)	Duration (h)	Rate (μ) h ⁻¹	1/μ	Maximum biomass increase (g/l)	yield on alkane added (Y)
0.06	0.396	2.525	3.3	10 (Lag)	0.104	9.62	0.21	0.64
0.08	0.528	1.894	4.4	11	0.117	8.54	0.38	0.72
0.10	0.660	1.515	5.5	10	0.150	6.67	0.48	0.73
0.16	1.056	0.947	8.8	8	0.171	5.85	0.62	0.59
0.20	1.320	0.758	11.0	8	0.204	4.90	0.80	0.61
0.24	1.584	0.631	13.2	8	0.214	4.67	0.82	0.52
0.30	1.980	0.505	16.5	8	0.214	4.67	0.88	0.44
0.40	2.640	0.379	22.0	12	0.154	6.49	1.00	0.38
0.50	3.300	0.303	27.5	12	0.150	6.67	1.15	0.35
1.00	6.600	0.152	55.0	13 (Lag)	0.133	7.52	0.85	0.13
2.00	13.200	0.076	110.0	16 (2 h Lag)	0.117	8.55	0.67	0.04

Table 2 shows the growth characteristics of the organism on *n*-heptane concentrations ranging from 0.408 g/l (0.06% v/v) to 13.6 g/l (2% v/v) added to the central well. The partial pressure inside the flask ranged from 3 to 70 mm Hg. At 2% by volume of *n*-heptane, the flask was saturated with heptane vapour which has a vapour pressure of 70 mm Hg at 34°C. Beyond this concentration, part of the added heptane would remain in liquid phase and condensation of the vapour on liquid mineral medium would occur. As in the case of growth on *n*-hexane, specific growth rate increased with the increase in substrate concentration until an alkane concentration of 2.04 g/l was reached. Beyond this, specific growth rate decreased along with the increase of substrate concentration. An average biomass yield of 0.655 was obtained at low substrate concentrations of alkane. Unlike the growth on *n*-hexane, the duration of the exponential growth was not improved at higher substrate concentrations of heptane in comparison to that at lower alkane concentration probably due to stronger inhibition caused by *n*-heptane.

Table 2. Effect of different concentrations of *n*-heptane on the growth characteristics of *Pseudomonas* PG-1 in gas-tight flasks with the substrate added to the central well.

Alkane concentration			Exponential growth				Maximum biomass increase (g/l)	Biomass yield on alkane added (Y)
Vol. (%)	g/l (S)	l/S	Partial pressure (P_g) (mm Hg)	Duration (h)	Rate (μ) (h^{-1})	$1/\mu$		
0.06	0.408	2.451	3	9	0.088	11.36	0.25	0.61
0.08	0.544	1.838	4	9	0.117	8.55	0.38	0.70
0.10	0.680	1.471	5	9	0.142	7.04		
0.16	1.088	0.919	8	7	0.204	4.90	0.75	0.69
0.20	1.360	0.735	10	6	0.233	4.29	0.84	0.62
0.24	1.632	0.613	12	6	0.233	4.29	0.89	0.55
0.30	2.040	0.490	15	6	0.242	4.13	0.95	0.47
0.40	2.720	0.368	20	8	0.192	5.21	1.02	0.38
0.50	3.400	0.294	25	9	0.171	5.85	1.16	0.34
1.00	6.800	0.147	50	5	0.138	7.25	0.90	0.13
				(Lag)				
2.00	13,600	0.074	70	8	0.118	8.47	0.80	0.06
				(Sat. V.P.) (2 h Lag)				

The findings of the above experiments are illustrated in figure 5 which shows a plot of the specific growth rate against substrate concentration and in figure 6 which shows the double reciprocal plot of specific growth rate against substrate concentration. As shown in figure 5, the specific growth rate reached the peak at substrate concentrations of 0.24–0.3% by volume corresponding to partial pressures of 13.2–16.5 mm Hg for *n*-hexane and 12–15 mm Hg for *n*-heptane, specific growth rate sharply declined at 0.4% by volume of substrate concentration above which

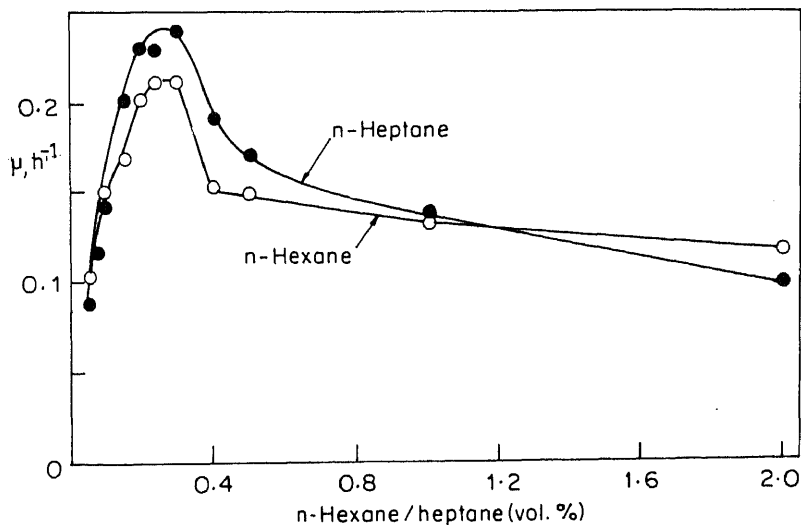


Figure 5. Effect of substrate concentration on the specific growth rate of *Pseudomonas* PG-1 growing on *n*-hexane and *n*-heptane in gas tight flasks.

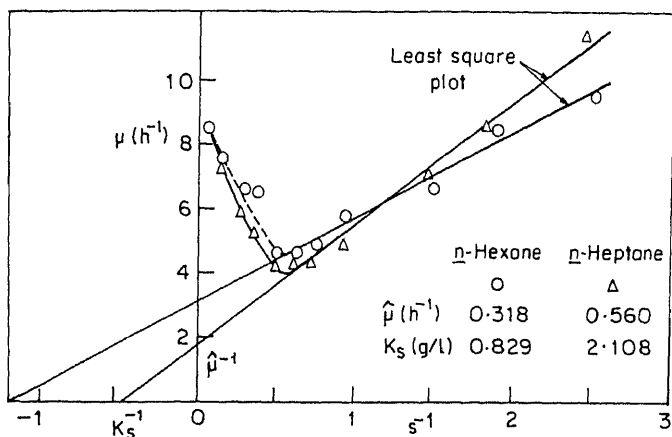


Figure 6. Growth of *Pseudomonas* PG-1 on *n*-hexane and *n*-heptane. Double reciprocal plot of specific growth rate (μ) against substrate concentration S (g/l).

the decline was gradual. It appears that substrate inhibition was maximum at substrate concentration around 0.4% by volume. An attempt was made to explain the above relationship by applying the substrate inhibition equation of Andrews (1968):

$$\mu = \frac{\hat{\mu}}{1 + K_s/S + S/K_i} \quad 1$$

where, μ = specific growth rate (h^{-1}), $\hat{\mu}$ = maximum specific growth in the absence of inhibition (h^{-1}), K_s = substrate saturation constant; lowest substrate concentration at one-half the maximum specific growth rate in the absence of inhibition (g/l), K_i = substrate inhibition constant; highest substrate concentration at which the specific growth rate is equal to one-half the maximum specific growth rate in the absence of inhibition (g/l) and S = limiting substrate concentration (g/l).

Rearranging equation 1 to the following multilinear equation:

$$\frac{1}{\mu} = \frac{1}{\hat{\mu}} + \frac{K_s}{\hat{\mu}} \cdot \frac{1}{S} + \frac{1}{K_i \hat{\mu}} \cdot S \quad 2$$

and applying it to data in tables 1 and 2, the following values of the constants were obtained through multiple regression analysis:

	<i>n</i> -hexane	<i>n</i> -heptane
$\hat{\mu} \text{ (h}^{-1}\text{)}$	0.285	0.376
$K_s \text{ (g/l)}$	0.639	1.178
$K_i \text{ (g/l)}$	8.433	9.310

Table 3 shows a comparison of the specific growth rates calculated from equation 1 using the above growth constants with the experimentally observed specific growth rates at different *n*-hexane and *n*-heptane concentrations. The data

Table 3. Calculated specific growth rates (μ) through application of Andrew's equation as compared with observed specific growth rates at different concentrations of *n*-hexane and *n*-heptane.

<i>n</i> -Hexane			<i>n</i> -Heptane		
Substrate conc. (g/l)	Observed (μ) (h^{-1})	Calculated (μ) (h^{-1})	Substrate conc. (g/l)	Observed (μ) (h^{-1})	Calculated (μ) (h^{-1})
0.396	0.104	0.107	0.408	0.088	0.096
0.528	0.117	0.125	0.544	0.117	0.117
0.660	0.150	0.139	0.680	0.142	0.134
1.056	0.171	0.158	1.088	0.204	0.171
1.320	0.204	0.174	1.360	0.233	0.187
1.584	0.214	0.179	1.632	0.233	0.198
1.980	0.214	0.183	2.040	0.242	0.209
2.640	0.154	0.183	2.720	0.192	0.218
3.300	0.150	0.180	3.400	0.171	0.220
6.600	0.133	0.152	6.800	0.138	0.197
13,200	0.117	0.109	13,600	0.118	0.147

reveal though there is a broadly similar pattern of substrate inhibition in the observed and calculated values of specific growth rates but the correlation between the two sets of data is unsatisfactory. This suggests that Andrew's equation of substrate inhibition function is not applicable in the case of volatile alkanes.

Figure 6 shows the double reciprocal plot of specific growth rate against concentrations of *n*-hexane and *n*-heptane. It was found that at low substrate concentrations, a linear relationship between $1/\mu$ and $1/S$ was obtained. This indicates that growth followed a Monod-type of relationship. Uemura *et al.* (1969) also reported Monod-type of growth at low concentrations of *n*-pentane and *n*-heptane. In the experiments described here, as the substrates were segregated in the central well of the gas tight flasks, the substrate transfer must be taking place solely from the gas phase. Correspondingly, inhibitory effect of high substrate concentration must also be solely due to high partial pressure of the gases.

Growth on n-octane

Figure 7 shows the growth pattern of *Pseudomonas* PG-1 on 0.4% by volume of *n*-octane. However, the growth was similar in both modes of substrate addition (directly to the medium or segregated in central well) indicating that substrate uptake is primarily from the gas phase. Reddy (1982) showed that even a high level of substrate concentration when added to the central well of the gas tight flask promoted a good growth of the organism. This level of alkane when added directly to the medium was strongly inhibitory to growth. This suggests that unlike *n*-pentane to *n*-heptane, inhibitory effect of *n*-octane may be mainly due to the damaging action of the liquid phase on the cells rather than the high partial pressure of the alkane.

The addition of 2.5 mM EDTA in the medium did not affect the growth of the organism on 0.4% by volume *n*-octane added directly to the medium. This suggests that alkane solubilizing mechanism which plays a predominant role in substrate transfer in case of higher chain length alkanes does not play any role in the uptake

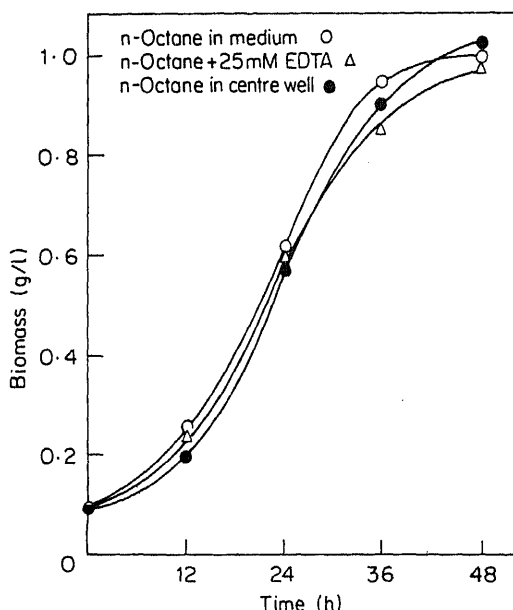


Figure 7. Growth pattern of *Pseudomonas* PG-I on 0.4% by volume of *n*-octane.

Table 4. Formation of hydrocarbon ESF from volatile and semi-volatile alkanes and the hydrocarbon solubilizing activity of the factors.

Alkanes	Yield of hydrocarbon ESF, 48 h cultivation (g/l)	Biomass 48 h cultivation (g/l)	Alkane solubilization by isolated ESF solution (100 mg %)*		
			1 min. shaking mg/l	2 min. shaking mg/l	solubilization rate mg/l h
<i>n</i> -Pentane	Not detected	1.20	—	—	—
<i>n</i> -Hexane	"	0.95	—	—	—
<i>n</i> -Heptane	"	1.00	—	—	—
<i>n</i> -Octane	"	1.00	—	—	—
<i>n</i> -Nonane**	0.360	1.00	37.6	68.0	2100
<i>n</i> -Decane**	0.382	2.00	35.6	53.6	1860

*Solubilization was done with the alkane used as growth substrate.

**Growth was done in conventional cotton-plugged conical flasks.

of *n*-octane by microbial cells. *n*-Octane uptake takes place primarily from the gas phase either directly or *via* the aqueous medium.

Growth on n-nonane and n-decane

Normal nonane and decane have higher boiling points and much lower vapour pressures than their lower homologues and therefore they are much less volatile at the temperature of cultivation. As listed in table 4, high level of these alkanes

(2% v/v) promoted formation of good biomass of the organism in the conventional cotton-plugged conical flasks. This indicates that substrate uptake from the gas phase is negligible and also that the liquid alkanes had very little toxic effect on the cells.

EDTA (2.5 mM) strongly inhibited the growth of the organism on these two alkanes. Further evidence that uptake of *n*-nonane and *n*-decane is mediated by substrate solubilization was obtained by actual isolation of the alkane solubilizing factor from the cell-free broths (table 4). As shown in the table good yields of the hydrocarbon ESFs were obtained from *n*-nonane and *n*-decane cultures while cultures grown on *n*-pentane to *n*-octane did not produce any hydrocarbon ESF. High solubilization rates of $2.1 \text{ g} \cdot \text{l}^{-1} \text{ h}^{-1}$ and $1.86 \text{ g} \cdot \text{l}^{-1} \text{ h}^{-1}$ were obtained with *n*-nonane and *n*-decane ESF respectively. These high rates of solubilization would be able to account fully the substrate uptake and growth of the organism during the growth on *n*-nonane and *n*-decane.

References

- Andrews, J. F. (1968) *Biotechnol. Bioeng.*, **10**, 707.
- Cagler, M. A., Thompson, A. R., Houston, C. W. and Rose, W. C. (1969) *Biotechnol. Bioeng.*, **11**, 417.
- Calma-Calamite, E., Arntz, P. and Bos, P. (1971) *An. Inst. Nac. Invest. Agrar. (Spain) Ser. Gen.*, **1**, 165.
- Cameotra, S. S., Singh, H. D., Hazarika, A. K. and Baruah, J. N. (1983) *Biotechnol. Bioeng.*, **25**, 2945.
- Hamer, G., Hamden, I. Y., Khamis, A. S. and Baroon, Z. H. (1980) *Biotechnol. Bioeng.*, **22**, 995.
- Leavitt, R. L. (1969) *Bacteriol. Proc.*, **118**, 166.
- Lukins, H. B. and Foster, J. W. (1963) *J. Bacteriol.*, **85**, 1074.
- Merdinger, E. and Merdinger, R. P. (1970) *Appl. Microbiol.*, **20**, 651.
- Reddy, P. G. (1982) *Studies on the utilization of aliphatic hydrocarbons by microorganisms*, Ph.D. thesis, Gauhati University, Gauhati.
- Reddy, P. G., Singh, H. D., Roy, P. K. and Baruah, J. N. (1982) *Biotechnol. Bioeng.*, **24**, 1241.
- Reddy, P. G., Singh, H. D., Pathak, M. G., Bhagat, S. D. and Baruah, J. N. (1983) *Biotechnol. Bioeng.*, **25**, 387.
- Senez, J. C. and Konoval'tshikoff-Mazoyer, M. (1956) *C. R. Acad. Sci.*, **242**, 2873.
- Singh, H. D., Barua, P. K., Pillai, K. R., Baruah, J. N. and Iyengar, M. S. (1972) *Indian J. Biochem. Biophys.*, **9**, 315.
- Uemura, N., Takahashi, J. and Veda, K. (1969) *J. Ferment. Technol.*, **47**, 220.
- Zawdzki, Z. and Langowska, I. (1983) *Acta. Microbiol. Pol.*, **32**, 191.

Lactate dehydrogenase isozyme patterns in the denervated quail (*Coturnix coturnix japonica*) muscles

ABDUL QUAIUM, T. K. VIRUPAKSHA†,
R. V. KRISHNAMOORTHY* and L. SUDHARSHANA

Department of Biochemistry and †Department of Zoology, University of Agricultural Sciences, G.K.V.K., Bangalore 560 065, India

MS received 26 April 1990; revised 9 July 1990

Abstract. Polyacrylamide gel electrophoresis of the Japanese quail (*Coturnix coturnix japonica*) muscle extracts revealed a single lactate dehydrogenase isozyme. A month after surgical unilateral brachiotomy (denervation) there was significant atrophy of the triceps, biceps and radius ulnar muscles accompanied by the appearance of an additional lactate dehydrogenase isozyme band. This extra band may be the result of the synthesis of a new lactate dehydrogenase isozyme. This new isozyme exhibited a lower affinity for lactate, less sensitivity to urea denaturation and was more thermostable than the lactate dehydrogenase of normal (innervated) quail muscles. Based on these properties, it is suggested that the newly synthesised isozyme of the denervated muscles is LDH-1 (or B₄/H₄) type. Brachiotomy also resulted in significant quantitative changes in the total lactate dehydrogenase activity of innervated muscles of the same animal.

Keywords. Japanese quail; brachiotomy; LDH isozymes in muscles; LDH activity; neurotrophic influences.

Introduction

Dystrophic conditions are now believed to be the cause of motoneuron dysfunction (Edwards and Hopkinson, 1977; Walton, 1981). Experimental or surgical denervation is known to induce muscular dystrophy in a majority of vertebrates and such atrophic muscles are considered to be models as well as tools to understand the manifestations of motoneuron functions. Recent studies indicate that different forms of muscular dystrophies in human beings and domestic animals are characterised by specific loss or synthesis of lactate dehydrogenase (LDH) subunits (Morgan *et al.*, 1980; Walton, 1981). The denervation of adult vertebrate muscles is known to alter the subunit synthesis of LDH enzymes. Denervation is commonly believed to bring forth the embryonic pattern of the LDH isozyme which might prevail under these conditions (Guth, 1968; Walton, 1981).

A fair amount of literature is available on the LDH isozyme activities and distribution in mammals and other animals but enough attention has not been bestowed on LDH isozymes of birds, in health and disease. The LDH isozyme studies in muscles of birds are important as they might be helpful in unravelling the metabolic and neurotrophic phenomena occurring in atrophic muscle disorders. This paper describes our work on LDH isozymes in the normal and denervated muscles of Japanese quail, with a view to understand the metabolic changes occurring in the atrophic muscles.

Cynogum 41 was purchased from American Cynamid Co., USA. Sodium lactate was from Boehringer, Ingelheim, Germany, and phenazine methosulphate, NAD⁺, NADH, sodium pyruvate, nitroblue tetrazolium, ammonium persulphate and bovine serum albumin (BSA) were purchased from Sigma Chemical Co., St. Louis, Missouri, USA. All other chemicals used were of reagent grade.

Birds

Disease-free Japanese quails (*Coturnix coturnix japonica*), weighing 200–250 g and white leghorn chicken (*Gallus domestica*), weighing 1–1.25 kg were obtained from the Department of Poultry Science, University of Agricultural Sciences, Bangalore. They were stocked in bird cages at the laboratory and fed *ad libitum* on cereal food until ready for surgical denervation.

Surgical denervation

Birds were ether anaesthetised and surgical denervation (brachiotectomy) was carried out under aseptic conditions in the laboratory. Skin incision of the defeathered area was made on the ventral side at the region of the upper humerus close to the shoulder joint. Ventral and dorsal branches of the brachial nerve (infra clavicular branches of brachial plexus) supplying the muscles of the forearm (wing) were denervated by sectioning about 10–15 mm length of the nerve (refer Getty, 1975, for descriptions). The operated birds were housed in individual cages and fed *ad libitum*. Streptopenicillin (5000 units/kg body weight) was injected for 3 successive days after surgery as a precautionary step.

Preparation of muscle homogenates

Excised muscle sections were minced and homogenised with 5 parts of cold phosphate buffer, 0.1 M, pH 7 in a Potter-Elvehjem glass homogeniser and centrifuged at 5000 *g* in a Remi T₄ centrifuge for 15 min. The clear supernatant was used for electrophoretic and enzymic studies.

Serum samples

Blood was collected into a test tube by puncturing the jugular vein. As soon as the clot was formed, the serum was separated, stored at 4°C and used within 5 h for the assay.

Analytical methods

Protein estimations in the serum and tissue homogenates were made according to

The modified method of Davies (1964) using anionic system was employed. The muscle homogenates were electrophoresed for 4 h and the LDH zymogram patterns were developed as described by Markert and Faulhaber (1965). Control gels were also incubated without the substrate to account for 'nothing' dehydrogenases (Shaw and Koen, 1965).

Kinetic studies

The heat inactivation, urea inactivation and lactate affinity studies were done by incubating the gels prior to staining at different temperatures or with different concentrations of urea and lactate (in 0.1 M Tris-HCl buffer, pH 8) for 15 min at 37°C and the intensity of the bands were scanned using a Biochem Densitometer (model M77) with 660 nm colour filter. The percentage loss of intensity or inhibition was estimated.

Results

The total LDH activity in the tissues of Japanese quails varies considerably (table 1). Among the skeletal muscles, the radius ulnar showed the highest and biceps the lowest activity. For comparison, the chicken tissues were also assayed for LDH activity (table 1).

Table 1. Total LDH activity of different tissues of adult Japanese quail and white leghorn chicken^a.

Tissue	Specific activity ^b	
	Japanese quail	White leghorn chicken
Triceps muscle	24.6	69.1
Biceps muscle	17.3	99.2
Radius ulnar muscle	42.5	136.5
Serum	2.7	6.5
Heart	25.4	51.4
Liver	13.9	18.6
Brain	62.7	91.8

^aAverage value of triplicate determinations.

^bActivity expressed as μmol of pyruvate reduced/min/mg protein at 37°C.

The data in table 2 show no significant differences in the LDH activity between the right wing and left wing triceps and biceps muscles of the unoperated quail. Surgical operation and subsequent denervation was accompanied by elevated LDH activity in the biceps muscle compared to its counterpart in the unoperated birds,

Table 2. LDH activity of normal and denervated Japanese quail muscles^a.

Muscle	Unoperated		Operated	
	Right wing	Left wing	Right wing ^b (innervated)	Left wing (denervated)
Triceps	24.6 ± 1.2	25.2 ± 1.8	17.8 ± 1.3*	22.2 ± 1.8*
Biceps	17.2 ± 1.4	16.9 ± 1.1	23.5 ± 4.3	24.9 ± 1.6 ^{NS}
Radius ulnar	42.2 ± 1.8	ND	33.4 ± 19.3	33.4 ± 15.9 ^{NS}

^aActivity expressed as μmol pyruvate reduced/min/mg protein (mean \pm SD of 6 experimental observations).

^bRight wing is the innervated counterpart of the surgically denervated bird in the left wing. ND, Not determined. *Significant at $P < 0.01$. ^{NS}Non significant.

while triceps and radius ulnar muscles showed lower specific LDH activity. The LDH activity of the innervated (right wing) and denervated (left wing) biceps and radius ulnar muscles did not significantly differ, while the triceps muscle showed a significant decrease in the innervated wing.

Denervation produced a 15–25% atrophy of muscle mass one month after denervation. The significant increase in the specific LDH activity corresponded with the net atrophy of triceps muscle (table 2). Radius ulnar muscle did not show significant difference in LDH activity although it atrophied to the same extent.

The innervated muscles of quail as well as of chicken showed only one LDH isozyme band in polyacrylamide gels (figure 1). Similar patterns were observed in the wing muscles of the unoperated (control) birds. The anodic mobility of LDH at pH 8.3 was much less than that of the other vertebrate muscles. One month denervated muscles of quails and chicken showed the appearance of an additional LDH band (figure 1). This isozyme might have been synthesised *de novo* in response to denervation atrophy. The additional band in all the denervated muscles was consistently reproducible. More intense and discrete bands were obtained with denervated muscles up to 3 months after denervation but the pattern got diffused as the period of denervation increased. Compared to quail, the chicken muscle isozyme was slow moving (figure 1).

The two LDH isozyme bands were further characterised on the basis of urea inhibition, thermostability and substrate (lactate) affinity studies. The muscle extracts were examined for these characters by developing LDH zymograms, and quantification of band intensities from the densitometric tracings (results not shown). The data show that the newly synthesised LDH isozyme (A_4^*) of denervated muscles is more thermostable, less urea sensitive and has higher affinity for lactate. Therefore, the additional or newly synthesised LDH isozyme band of denervated muscles is of B_4/H_4 or LDH-1 type.

Discussion

The LDH isozyme patterns of Japanese quail muscles and white leghorn chicken are similar, each showing a single slow moving band of the muscle (M_4) type, being characteristic of anaerobic tissues. Japanese quail and chicken are both ground dwellers endowed with poor flight. The wing musculature are therefore, poorly developed and are not metabolically very active as those of pigeons which possess both M_4 and H_4 types of isozymes (Wilson *et al.* 1962). Both M_4 and H_4 isozymes

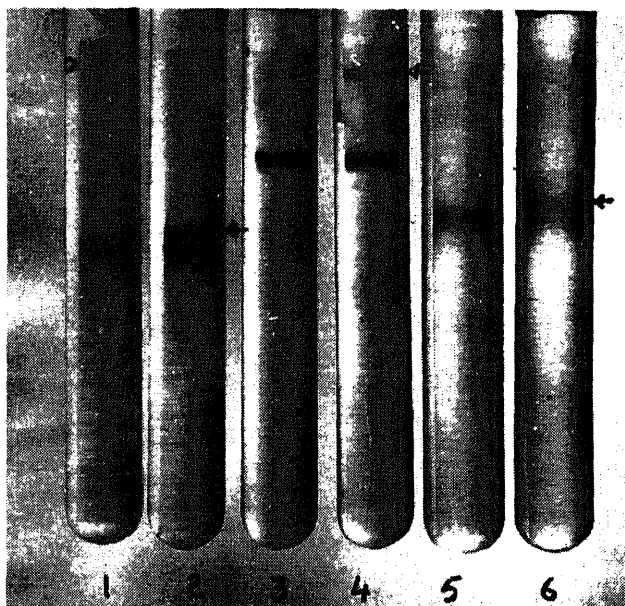


Figure 1. Zymograms of the PAGE pattern of LDH isozymes of innervated and one-month old denervated muscles of Japanese quail and white leghorn chicken. Lane 1 and 2, innervated and denervated biceps of quail; lane 3 and 4, innervated and denervated triceps of chicken; lane 5 and 6, innervated and denervated triceps of quail. Electrophoresis was done on 7.5% gels with Tris-glycine buffer pH 8.3 at 5 mA/gel for 4 h under cold conditions. Migration from top to bottom. The arrow indicates the newly synthesised band (A_4).

or their relative hybrids may be useful to fuel the oxidative reactions at a faster rate.

Denervation is known to bring forth dedifferentiation of the tissues (Gutmann 1962; Edwards and Hopkinson, 1977) resulting in a switch to the embryonic pattern of LDH isozymes. Deprivation of nerve connections to the muscles and consequent loss of 'trophic' influences may either suppress or trigger gene expression. Denervation of the quail wing muscles might have been responsible for the triggering of the gene expression accounting for the embryonic isozyme pattern reported in the present work. The results are also consistent with the finding that the new isozyme band found in denervated muscle extracts is of the H_4 or aerobic type since the embryonic muscles get less oxygen and the lactate accumulates due to anaerobic glycolysis.

It is interesting to note in the present study that the contralateral innervated biceps muscle of the operated quail shows a greater LDH activity than that of the normal biceps muscles. In excessively used muscles, hypertrophic changes may manifest (Gutmann, 1976; Walton, 1981) and in disused muscles the atrophic changes manifest. Thus the increased LDH activity of the innervated control biceps

References

- Berger, L. and Broida, D. (1974) in *Sigma Technical Bulletin* No. 500.
- Davis, B. J. (1964) *Ann. N. Y. Acad. Sci.*, **121**, 404.
- Edwards, Y. H. and Hopkinson, D. A. (1977) in *Isozymes: Current topics in biological and medical research* I. (eds M. C. Rattazzi, J. G. Scandalios and G. S. Whitt) (New York: Alan R. Liss) p. 19.
- Getty, R. (1975) in *The anatomy of the domestic animals* (eds S. Sisson and J. D. Grossmann) (Philadelphia: W. B. Saunders) p. 1815.
- Guth, L. (1968) *Physiol. Rev.*, **48**, 645.
- Gutmann, E. (1962) in *The denervated muscle* (ed. E. Gutmann) (Prague: Czechoslov Acad. Sci.) p. 479.
- Gutmann, E. (1976) *Annu. Rev. Physiol.*, **38**, 177.
- Lowry, O. H., Rosebrough, N. J., Farr, A. L. and Randall, R. J. (1951) *J. Biol. Chem.*, **193**, 265.
- Markert, C. L. and Faulhaber, I. (1965) *J. Exp. Zool.*, **159**, 319.
- Morgan, Julie, Bozyk, M. E., Bittner, S. and Cohen, L. (1980) *Res. Commun. Chem. Pathol. Pharmacol.* **30**, 555.
- Shaw, C. R. and Koen, A. L. (1965) *J. Histochem. Cytochem.*, **13**, 431.
- Walton, J. N. (1981) *Disorders of voluntary muscles* (London: Churchill Livingstone).
- Wilson, A. C., Cahn, R. D. and Kaplan, N. O. (1963) *Nature (London)*, **197**, 331.

Role of heme in mitochondrial biogenesis: Transcriptional and post-transcriptional regulation of the expression of Iso-I-cytochrome C gene during glucose repression-derepression in cells of *Saccharomyces cerevisiae*

K. S. K. BALAJI, G. GOPALAN and C. RAJAMANICKAM*

Department of Biochemistry, School of Biological Sciences, Madurai Kamaraj University, Madurai 625 021, India

MS received 9 April 1990; revised 10 September 1990

Abstract. Exogenous addition of hemin to glucose-repressed cells of *Saccharomyces cerevisiae* restores the level of Iso-I-cytochrome C messengers to that observed in derepressed cells. *In vitro* transcription in isolated nuclei has shown a 4-fold stimulation in the synthesis of Iso-I-cytochrome C messengers in repressed but hemin-treated and derepressed cells compared to the repressed cells. Studies on *in vitro* transport of RNA from isolated nuclei have revealed that there is a 50% drop in the transport of total RNA from nuclei isolated from repressed but hemin-treated and derepressed cells when compared with the nuclei from repressed cells. However, under these conditions, there is an enhanced transport of translatable RNA. Hybridization analysis of the transported RNA using Iso-I-cytochrome C gene-specific probe has shown that there is preferential transport of Iso-I-cytochrome C messengers in repressed but hemin treated and derepressed cells.

Keywords. Glucose repression-derepression; transcription; RNA transport; heme; Iso-I-cytochrome C gene.

Introduction

The phenomenon of glucose-repression of mitochondrial functions in *Saccharomyces cerevisiae* is well established (Perlman and Mahler, 1974; Polakis and Bartley, 1965; Tzagoloff, 1969) and extensively used for studying mitochondrial biogenesis (Falcone *et al.*, 1983; Szykely and Montgomery, 1984). In recent years, the regulatory mechanisms involved in the coordinated expression of nucleocytoplasmic and mitochondrial genetic systems have become the focal point of several investigations.

We have earlier shown that cAMP relieves the cells from the effect of glucose-repression by increasing the endogenous levels of heme (Gopalan and Rajamanickam, 1985). Furthermore, exogeneous addition of hemin to glucose-repressed cells alleviates glucose-repression of mitochondrial functions (Gopalan *et al.*, 1984). Our attempts to understand the molecular mechanisms responsible for the reversal of glucose repressed mitochondrial functions by exogenous addition of hemin have revealed that hemin enhances the levels of poly (A) containing RNA in the cytosol. *In vitro* translation and subsequent immunoprecipitation studies have revealed that hemin preferentially increases the messages for hemoproteins (Gopalan and Rajamanickam, 1986). Iso-I-cytochrome C (CYC1) gene and other aerobic genes have been shown to be induced by heme and the influence of heme on

the expression of these genes has been mediated by the binding of regulatory proteins (Lowry and Lieber, 1986; Pfeifer *et al.*, 1987, 1989). In an attempt to provide direct evidence and to delineate the molecular mechanism by which hemin influences the synthesis of hemoproteins, we have chosen to study the expression of CYC1 gene, a nuclear gene coding for the mitochondrial hemoprotein, cytochrome C1, during glucose repression-derepression and the role of heme in this process.

Methods

Chemicals

Most of the chemicals used in this study were of analytical grade and obtained from BDH, Bombay and all fine chemicals were purchased from Sigma Chemical Company, St. Louis, Missouri, USA. [^{32}P] phosphate (carrier free) and [^3H] UTP were purchased from Bhabha Atomic Research Centre, Bombay and [^{32}P] dCTP (3000 Ci/m mol) was purchased from Radiochemical Centre, Amersham, England.

Strain and growth conditions

A haploid strain of *S. cerevisiae* D273-10B, was used in this study. The maintenance and growth conditions were as described by Jayaraman *et al.* (1966). Cells grown overnight in YPD medium (1% glucose, 2% peptone and 1% yeast extract) were transferred into repression medium (1% glucose, 0.4% yeast extract, 0.9% KH_2PO_4 , 0.06% $(\text{NH}_4)_2\text{SO}_4$, 0.05% MgSO_4 and 0.04% CaCl_2) at a concentration of 4 mg wet weight/ml. Under these conditions, mitochondrial functions are repressed for the initial 2.5 h. Once glucose in the medium gets exhausted (at 2.5 h), the cells enter the derepression phase (Jayaraman *et al.*, 1966). A second addition of glucose to a final concentration of 1% at 2.5 h extends the repression phase (Dharmalingam and Jayaraman, 1971).

Plasmid

Plasmid pAB68 is a derivative of the shuttle vector, YEpl3 which bears CYC1 gene insert (5.2 kb *Hind*III fragment). The plasmid was a kind gift from Professor Fred Sherman, Rochester, New York. For preparing the hybridization probe, the plasmid was digested with *Sall* and *Hind*III and the 1.6 kb *Sall*-*Hind*III fragment containing the upstream sequence, the coding sequence and the 5' and 3' untranslated regions of CYC1 gene was electroeluted as described by Maniatis *et al.* (1982).

Preparation of repressed, repressed but hemin treated, derepressed and levulinic acid treated cells

Cells grown overnight in YPD medium were transferred into repression medium at

to which no addition was made were taken as derepressed cells. As a negative control, levulinic acid (1.6 mg/ml), an inhibitor of heme biosynthesis, was added to derepressed cells. The cells were grown under these conditions for 30 min.

Preparation of nuclei

For studies involving *in vitro* transcription, *in vitro* transport and for the preparation of nuclear RNA, nuclei were prepared from protoplasts and purified by density-gradient centrifugation as described by Duffus (1979). Briefly, the cells were harvested and washed twice with 1 M sorbitol and resuspended in 10 ml of 1 M sorbitol. To this 150 μ l of zymolase (10 mg/ml) was added and shaken at 30°C for about 30 min. The protoplasts were pelleted by centrifugation at 2000 *g* and washed with 1 M sorbitol. The protoplasts were lysed at 4°C by suspending 1 g of protoplasts in 10 ml of polymer solution (15–18% w/v ficoll in 0.02 M phosphate buffer, pH 6.5) and homogenised. The homogenate was centrifuged at 3000 *g* for 15 min at 4°C and the supernatant was removed and layered onto a solution of 30% ficoll in 0.02 M KH_2PO_4 (pH 6.5) and the resulting step gradient was centrifuged at 1,00,000 *g* for 45 min at 4°C. The pellet represents the purified nuclei and was suspended in appropriate buffer.

Dot blot analysis of cytosolic, polysomal and nuclear RNA

Cells grown under different conditions for 30 min were harvested, washed with saline and cell-free extracts were prepared by homogenising the cells with an equal volume of glass beads (0.45–0.5 mm) in a Braun homogeniser. The paste was extracted with a buffer containing 0.1 M Tris-HCl, pH 7.5, 0.25 M sucrose and 2 mM EDTA. The lysate was cleared by centrifugation. From the post-mitochondrial supernatant, total RNA was extracted following the method described by Shapiro *et al.* (1974).

Polysomal RNA was extracted following the method of Longacre and Rutter (1977). Briefly, the cells were homogenized in a buffer containing 10 mM Tris-HCl, pH 7.4, 10 mM NaCl, 1.5 mM MgCl_2 and cycloheximide (0.1 mg/ml). The nuclei and mitochondria were removed by centrifugation at 16000 *g* for 20 min. The supernatant was layered over 4 ml of 36% sucrose cushion in 10 mM Tris-HCl, pH 7.4, 10 mM NaCl and 1.5 mM MgCl_2 and centrifuged at 90,000 *g* for 3.5 h. The pellet was suspended gently in 5 ml of extraction medium [100 mM Tris-HCl, pH 9, 100 mM NaCl, 1 mM EDTA and 1% sodium dodecyl sulphate (SDS)] by homogenising and RNA was isolated by phenol/chloroform extraction. RNA from purified nuclei was extracted following the method described by Penman (1969).

Nick-translation of the *CYC1* gene was performed following the method of Rigby *et al.* (1977). For dot blot analysis, 20 μ g of denatured RNA (both cytosolic total as well as polysomal) was spotted onto nitrocellulose membrane and hybridized to nick-translated *CYC1* probe following the method described by Thomas (1983). Hybridization signals obtained in this study are in the linear range.

Quantitation of the hybrid

In vitro transport of CYC1 RNA from isolated nuclei

In vitro transport of RNA from cold nuclei isolated from cells subjected to different conditions (i.e., repressed, derepressed, repressed but heme treated) was performed and the transported RNA was extracted as above. Twenty μg of denatured RNA, transported under each condition was spotted onto a nitrocellulose membrane and hybridized to nick translated *CYC1* probe following the method described by Thomas (1983). In order to quantify the level of transport of *CYC1* RNA the radioactivity associated with the spots were measured in a scintillation based counter.

In vitro translation of in vitro transported RNA

In vitro translation of *in vitro* transported RNA from cold nuclei isolated from the cells grown under different conditions, was carried out in reticulocyte lysate following the method described by Pelham and Jackson (1976). A reaction mixture in a total volume of 25 μl contained 10 mM creatine phosphate, 10 μM GTP, 1 mM ATP, 300 μM spermidine, 50 μM potassium acetate, 20 mM Hepes, pH 7.4, 2 mM DTT, 25 μg creatine phosphokinase, 10 mM magnesium acetate, 10 μl of the rabbit reticulocyte lysate, 20 μg of RNA and 20 μCi of [^{35}S] methionine (800 Ci/m mol) per assay. The mixture was incubated at 37°C for 1 h. The translation products were precipitated with trichloroacetic acid and processed for counting (Beattie, 1979).

Measurement of the half-life of CYC1 mRNA in the cytosol

The cells, after growth in repression medium for 3 h (allowed the cells to derepress for 30 min), were treated with actinomycin D (15 $\mu\text{g}/\text{ml}$) and cordycepin (100 $\mu\text{g}/\text{ml}$) to block fresh transcription and transport respectively during the chase and divided into 3 portions. These were grown under repressed, repressed but heme-treated and derepressed conditions. At different time intervals, the cells were harvested and post-mitochondrial supernatant prepared. RNA was extracted and hybridized to nick-translated *CYC1* gene. The counts associated with the hybrid were checked.

Results

As a first step towards understanding the role of heme in the expression of *CYC1* gene in yeast cells undergoing glucose repression-derepression, the steady state levels of *CYC1* RNA in the cytosol was checked. For this purpose, cytosolic RNA from cells grown under repressed, repressed but heme-treated, derepressed and levulinic acid treated conditions were extracted and hybridized to a cloned *CYC1* gene. Figure 1 shows that the level of *CYC1* RNA in repressed cells is 6–8-fold

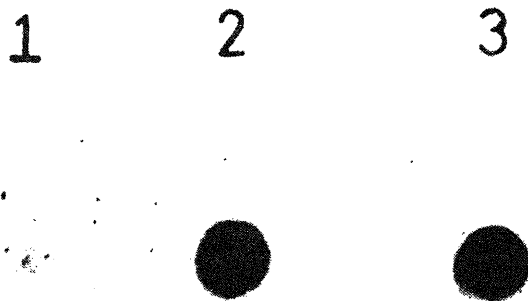


Figure 1. Dot blot analysis of CYC1 RNA in the cytosol.

The cells after growth in repression medium for 2.5 h were divided into three conditions: repressed (1), repressed but heme-treated (2), and derepressed (3). The cells were then harvested and total RNA was extracted from the mitochondrial supernatant. Total RNA (20 μ g) was heat denatured by incubation at 100°C for 5 min and hybridized to nick-translated CYC1 DNA. The counts per spot were calculated as given under 'methods'.

RNA associated with the polysomes was checked by extracting polysomes prepared from cells grown under the above conditions and hybridizing to CYC1 gene. Figure 2 shows a pattern similar to the one seen in Figure 1.

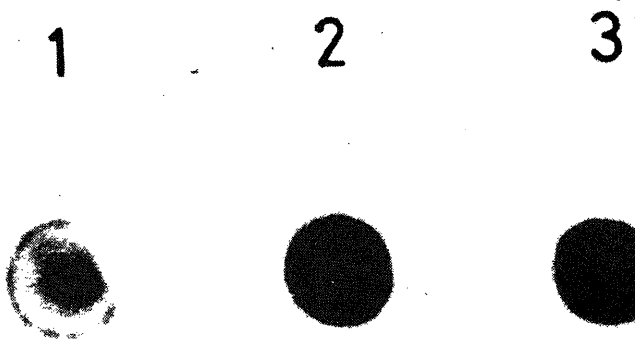


Figure 2. Relative levels of CYC1 RNA associated with the polysomes.

The cells after growth in repression medium for 2.5 h were divided into three conditions [repressed (1), repressed but heme-treated (2) and derepressed (3)]. The cells were then harvested and polysomes were prepared. Total RNA (20 μ g) was heat denatured by incubation at 100°C for 5 min and hybridized to nick-translated CYC1 DNA. The counts per spot were calculated as given under 'methods'.

In order to account for the increased levels of *CYC1* RNA in the cytosol, the possible role of heme in triggering the transcription of *CYC1* gene was investigated. Towards this, studies on *in vitro* transcription in isolated nuclei prepared from repressed, repressed but heme-treated and derepressed cells were carried out using [³H] UTP. The *in vitro* transcripts were extracted and hybridized to unlabelled *CYC1* probe immobilized on a nitrocellulose membrane. The counts associated with the hybrid was checked. Table 1 shows that there is a 4-fold stimulation in the transcription of *CYC1* gene in repressed but heme-treated and derepressed nuclei over the repressed nuclei. *In vitro* addition of hemin to repressed nuclei, however, does not restore the level to that seen in derepressed nuclei, thus excluding the possibility of direct interaction between hemin and the transcriptional machinery. In order to see whether heme plays any role in post-transcriptional regulation of *CYC1* gene expression, the transport of RNA from isolated nuclei was studied. Table 2 shows, contrary to our expectations, that the amount of RNA transported from repressed but heme-treated and derepressed nuclei is only around 50% of that observed from repressed nuclei. However, *in vitro* translation of the *in vitro* transported RNA in a heterologous cell free system revealed (table 3) a 3–4-fold stimulation in the incorporation of labelled amino acid into polypeptides with the total RNA transported from derepressed and repressed but heme-treated nuclei rather than from the repressed nuclei. These results indicate that though there is a decrease in the transport of total RNA, the amount of translatable RNA transported upon hemin treatment is greater than that observed from repressed nuclei. Hybridization of the transported RNA with *CYC1* probe has lent further evidence for the preferential transport of mRNA (figure 3).

Table 1. *In vitro* transcription of *CYC1* gene in isolated nuclei.

Source of nuclei	cpm hybridized			Stimulation (%)
	Exp. 1	Exp. 2	Exp. 3	
Repressed	30	42	33	100
Repressed + hemin (<i>in vivo</i>)	136	199	142	452.47 ± 17.77
Derepressed	126	181	140	425.07 ± 4.53
Derepressed + levulinic acid	20	27	20	63.87 ± 2.51
Repressed + hemin (<i>in vitro</i>)	35	52	37	117.83 ± 4.78

Equal numbers (4.5×10^6) of nuclei isolated from cells grown under different conditions mentioned in the table were incubated with transcription assay buffer containing [³H] UTP (50 µCi/assay). After terminating transcription following 25 min of incubation, RNA was extracted. Labelled RNA (10^5 cpm) transcribed *in vitro* was hybridized to *CYC1* DNA immobilized on (nitrocellulose) filter and the radioactivity of the hybridized RNA was measured. The results presented here represent values from 3 sets of experiments. Percentage stimulation is given as the mean ± SD of the values obtained from the 3 experiments taking repressed value as 100%.

It has been shown by Dharmalingam and Jayaraman (1971) that there is an

Table 2. *In vitro* transport of RNA from isolated nuclei.

Source of nuclei	Exp. No.	Total radio-activity in the nuclei (cpm)	Transported radioactivity (cpm)	Transport (% of total)	Decrease in transport (% of repressed)
Repressed	1	263190	21555	8.19	
	2	140148	10063	7.18	
	3	134566	9823	7.30	
Repressed + hemin	1	232090	8843	3.81	50.21 ± 6.21
	2	256310	10483	4.09	
	3	187247	6272	3.35	
Derepressed	1	324100	11408	3.52	53.23 ± 3.78
	2	183687	6172	3.36	
	3	152832	5640	3.69	

After labelling the cells with [^{32}P] phosphoric acid (20 $\mu\text{Ci/ml}$) under different conditions for 30 min, nuclei were isolated and purified. Equal numbers of nuclei ($4.5 \times 10^6/\text{ml}$) were incubated with transport assay buffer. After 30 min of incubation, nuclei were pelleted and RNA was extracted from the supernatant and checked for radioactivity. Percentage transport was calculated from the radioactivity associated with released RNA and the radioactivity associated with RNA extracted from the nuclei before incubation. The results presented here represent values from 3 sets of experiments. The mean \pm SD of the percentage decrease in transport under repressed but heme treated and derepressed conditions were calculated taking the percentage transport in repressed condition as 100%.

Table 3. *In vitro* translation of *in vitro* transported RNA.

Nuclei-source of transported RNA	Radioactivity incorporated (cpm)			Stimulation (%)
	Exp. 1	Exp. 2	Exp. 3	
Repressed	28075	32167	23522	100
Repressed + hemin	130425	146731	105734	456.74 ± 7.54
Derepressed	87750	48928	73629	311.04 ± 3.04

RNA (20 μg) transported under *in vitro* conditions from nuclei isolated from cells grown under different conditions mentioned in the table was translated in a reticulocyte lysate supplemented with 25 μCi of [^{35}S] methionine (see 'methods'). The radioactivity incorporated into the translated products were measured. The results presented here represent values from 3 sets of experiments. Percentage stimulation is given as the mean \pm SD of the values obtained from the 3 experiments taking repressed values as 100%.

Discussion

In this report we have shown that hemin increases the levels of CYC1 mRNA in the cytosol. This increase has been shown not due to the differential stability of CYC1 mRNA under different conditions employed. The fact that there is an increased association of CYC1 RNA with the polysomes upon hemin treatment, not only reflects the increased availability of CYC1 RNA in the cytosol but also the increased availability of translatable RNA. Studies on *in vitro* transcription clearly demonstrated an increased transcription of CYC1 RNA. However, the unexpected

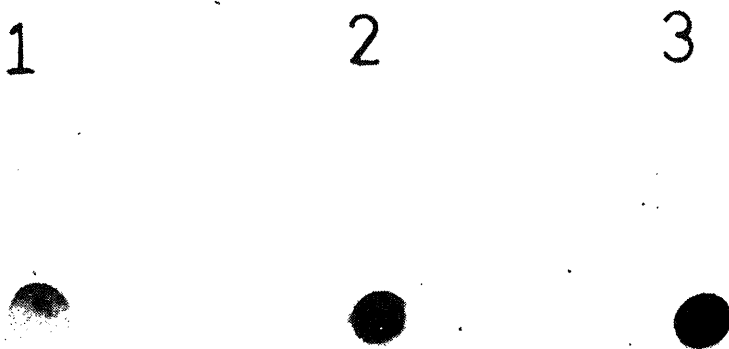


Figure 3. *In vitro* transport of *CYC1* RNA from isolated nuclei.

The cells after growth in repression medium for 2.5 h were subjected to different conditions [repressed (1), repressed but heme-treated (2) and derepressed (3)] for 30 min. The cells were then harvested and nuclei isolated. Equal numbers of nuclei ($4.5 \times 10^6/\text{ml}$) from these cells were incubated with transport assay medium at 25°C. After 30 min of incubation, the nuclei were pelleted and RNA was extracted from the supernatant. RNA (20 μg) was hybridized to nick translated *CYC1* DNA.

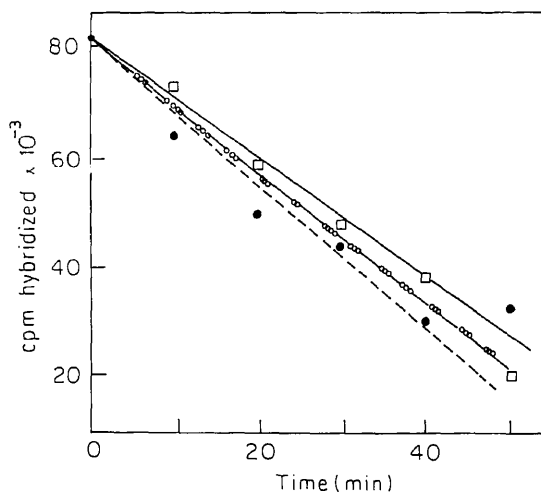


Figure 4. Half-life of *CYC1* RNA.

The cells after growth in repression medium for 3 h (the cells were allowed to derepress for 30 min) were treated with actinomycin D (15 $\mu\text{g}/\text{ml}$) and cordycepin (100 $\mu\text{g}/\text{ml}$) and divided into 3 portions. These were grown under repressed (●), repressed but heme-treated

accounted for by the transport of non-translatable RNA (mainly rRNA). This is substantiated by the findings of Kief and Warner (1981), showing that there is an increased synthesis of rRNA under repressed condition. Hence, it is possible that under derepressed and heme-treated conditions, there is an increased transport of mRNA which is substantiated by the *in vitro* translation experiments.

Studies carried out by Lowry and Lieber (1986) on the family of oxygen regulated genes have provided evidence that heme could be the intracellular regulatory signal for the induction of aerobic genes. Although transcriptional regulation of CYC1 gene by heme has already been established using heme-deficient mutants (Guarente and Mason, 1983; Zitomer *et al.*, 1979), our observation in a transient glucose repression-derepression system only implies a uniform mode of regulation by heme regardless of the manner by which heme-deficiency is created. Recently, heme in conjunction with a protein (HAP 1) has been shown to bind to the upstream activation sequences of CYC1 gene (Pfeifer *et al.*, 1987, 1989). We have also purified a protein (different from HAP 1) that specifically binds to the CYC1 gene and that the level of this protein varies depending upon the physiological status of the cell (unpublished results). Such binding has been shown to promote transcription. Similar observation has also been reported in the case of catalase T gene (Spevak *et al.*, 1986). These evidences strongly suggest that heme, in addition to being the prosthetic group of the hemoproteins, is also involved in the synthesis of the apoproteins.

In conclusion, heme has been shown to play an important role in the expression of CYC1 gene in cells undergoing glucose repression-derepression. A predominant effect has been shown to be exerted at the level of transcription and transport of CYC1 RNA. This strengthens our earlier observations that heme specifically stimulates the synthesis of hemoproteins by increasing the availability of the translatable messengers for the hemoproteins. Further work is required to demonstrate clearly whether the effect of heme observed at the level of transcription and post-transcription is specific for hemoproteins.

Acknowledgements

The authors acknowledge University Grants Commission, New Delhi for the financial assistance. One of the authors (K. S. K. B.) is grateful to the Council of Scientific and Industrial Research, New Delhi for the award of a fellowship.

References

- Beattie, D. S. (1979) *Methods Enzymol.*, **56**, 17.
- Dharmalingam, K. and Jayaraman, J. (1971) *Biochem. Biophys. Res. Commun.*, **45**, 1115.
- Duffus, J. H. (1979) *Methods Cell Biol.*, **12**, 79.
- Falcone, C., Agostinelli, M. and Frontali, L. (1983) *J. Bacteriol.*, **153**, 1125.
- Gopalan, G., Jayaraman, J. and Rajamanickam, C. (1984) *Arch. Biochem. Biophys.*, **235**, 159.
- Gopalan, G. and Rajamanickam, C. (1985) *Indian J. Biochem. Biophys.*, **22**, 214.
- Gopalan, G. and Rajamanickam, C. (1986) *Arch. Biochem. Biophys.*, **248**, 210.

- Johnson, L. F., Abelson, H. T., Green, H. and Penman, S. (1974) *Cell*, **1**, 95.
- Kafatos, F. C. and Estradiadis, A. (1979) *Nucleic Acids Res.*, **7**, 1541.
- Kiaf, D. R. and Warner, J. R. (1981) *Mol. Cell. Biol.*, **1**, 1007.
- Longacre, S. S. and Rutter, W. J. (1977) *J. Biol. Chem.*, **252**, 2742.
- Lowry, C. V. and Lieber, R. H. (1986) *Mol. Cell. Biol.*, **6**, 4145.
- Maniatis, T., Fritsch, E. F. and Sambrook, J. (1982) in *Molecular cloning: A laboratory manual* (T. Maniatis, E. F. Fritsch and J. Sambrook) (New York: Cold Spring Harbor Laboratory) p. 16.
- Meenakshi, S., Thirunavukkarasu, C. and Rajamanickam, C. (1983) *Biochem. J.*, **209**, 285.
- Pelham, H. R. B. and Jackson, R. J. (1976) *Eur. J. Biochem.*, **67**, 247.
- Penman, S. (1969) in *Fundamental techniques in virology* (eds K. Habel and N. P. Salmon) (New York: Academic Press) p. 35.
- Perlman, P. S. and Mahler, H. R. (1974) *Arch. Biochem. Biophys.*, **162**, 248.
- Pfeifer, K., Arcangioli, B. and Guarente, L. (1987) *Cell*, **49**, 9.
- Pfeifer, K., Kim, K., Kogan, S. and Guarente, L. (1989) *Cell*, **56**, 291.
- Polakis, E. S. and Bartley, W. (1965) *Biochem. J.*, **97**, 284.
- Rigby, P. W. J., Dieckman, M., Rhodes, C. and Berg, P. (1977) *J. Mol. Biol.*, **113**, 237.
- Salditt-Georgieff, M., Harpold, M., Chen-Kiang, S. and Darnell, J. E. Jr. (1980) *Cell*, **19**, 69.
- Schumm, D. E. and Webb, T. E. (1972) *Biochem. Biophys. Res. Commun.*, **48**, 1259.
- Shapiro, D. J., Taylor, J. M., Mcknight, G. S., Polakis, R., Gonzales, C., Kiley, M. L. and Schimke, R. (1974) *J. Biol. Chem.*, **249**, 3665.
- Shearer, R. W. (1974) *Biochemistry*, **13**, 1764.
- Spevak, W., Harting, A., Meindl, P. and Ruis, H. (1986) *Mol. Gen. Genet.*, **203**, 73.
- Szykely, E. and Montgomery, D. L. (1984) *Mol. Cell. Biol.*, **4**, 439.
- Thomas, P. S. (1983) *Methods Enzymol.*, **100**, 256.
- Tzagoloff, A. (1969) *J. Biol. Chem.*, **244**, 5027.
- Zitomer, R. S., Montgomery, D. L., Nichols, D. L. and Hall, B. D. (1979) *Proc. Natl. Acad. Sci. USA*, **3627**.

Characterization of antibodies to chicken riboflavin carrier protein: Antigenicity of the tryptic fragments

USHA NATRAJ*, K. S. N. IYER, VIJAYA RAGHAVAN,
SMITA MAHALE and JACINTHA PEREIRA

Institute for Research in Reproduction, Jehangir Merwanji Street, Parel, Bombay 400 012,
India

MS received 20 July 1990; revised 28 November 1990

Abstract. The antigenicity of tryptic fragments of reduced and carboxymethylated chicken riboflavin carrier protein were studied. The tryptic sites of the native riboflavin carrier protein bound to riboflavin were inaccessible. The molecular weight and the elution profile on high performance liquid chromatography (TSK 545 DEAE) were unaltered at an enzyme to substrate ratio of 1:31. However, carboxymethylated riboflavin carrier protein could be cleaved into 3 or 4 fragments at an enzyme to substrate ratio of 1:250 or 1:125. Chromatographic separation of the tryptic fragments on high pressure liquid chromatography (TSK 545 DEAE) revealed the presence of two fragments with different elution profiles but similar molecular weight 26 ± 2 kDa. Only one fragment (associated with peak 2) had the ability to displace chicken riboflavin carrier protein in an homologous chicken riboflavin carrier protein radioimmunoassay. Thus, carboxymethylated riboflavin carrier protein which does not compete with chicken riboflavin carrier protein in the radioimmunoassay, on mild trypsinization generates a fragment which interacts with chicken riboflavin carrier protein in radioimmunoassay.

Keywords. Riboflavin carrier protein; tryptic fragments; antigenicity.

Introduction

Riboflavin carrier protein (RCP) isolated from hen's egg white, is a phosphoglycoprotein of molecular weight (M_r) 34 ± 2 kDa and has been well characterized (Rhodes *et al.*, 1959; Murthy and Adiga, 1977). Its primary sequence has also been reported (Hamazume *et al.*, 1987). Interestingly, protein(s) bearing immunological homology to cRCP have been documented in rodents (Muniyappa and Adiga, 1980; Natraj *et al.*, 1987), monkeys (Visweswariah and Adiga 1987a; Natraj and Kholkute, 1989) and in human subjects (Visweswariah and Adiga, 1987b; Natraj *et al.*, 1988a). Monoclonal antibodies to cRCP have also been generated and one epitope appears to be evolutionarily conserved (Visweswariah *et al.*, 1987). Recently, we have characterized antibodies generated in rabbits against cRCP and modified cRCP to gain an insight into the relative importance of the antigenic determinants in the sequential and conformational epitopes to induce neutralizing immunity (Natraj *et al.*, 1988b). It was demonstrated that antibodies to sequential epitopes could result in neutralizing immunity.

The present study is a continuation of our earlier quest to unravel the immunodominant region of the protein. Herein, we discuss the unusual property of a large peptide fragment obtained following tryptic digestion.

*To whom all the correspondence should be addressed.

Materials and methods

Chemicals

DEAE cellulose (0.9 meq/g), CM-cellulose (0.7 meq/g), Sephadex gels, sodium dodecyl sulphate (SDS), N-tosyl-L-phenylalanine chloromethyl ketone (TPCK) trypsin were purchased from Sigma Chemical Co., St. Louis, Missouri, USA. The vectastain ABC kit from Vector Laboratories, Burlingame CA, USA. All other chemicals used were of analytical grade. High pressure liquid chromatography (HPLC) was carried out on LKB instrument using the ultropac TSK 545 DEAE (7.5 × 150 mm).

Isolation and purification of cRCP from hen's egg white

The methods for isolation and purification of RCP from hen's egg white (Murthy and Adiga, 1977) for examining its homogeneity (Natraj *et al.*, 1987) and for preparation of S-carboxymethyl RCP (Carb RCP) (Natraj *et al.*, 1988b) are as described elsewhere.

Immunological techniques

The immunization schedules for eliciting antibodies to native RCP (apoprotein) and Carb RCP (Natraj *et al.*, 1988b) in rabbits and the radioimmunoassay (RIA) procedures (Natraj *et al.*, 1987) have been described earlier.

Antigenicity of tryptic fragments

The ability of modified RCP to displace the binding of cRCP in the homologous RIA was tested, using 0.1–40 ng of cRCP and 0.1–1000 ng of the tryptic fragments.

Tryptic digestion of apo RCP, Holo RCP and Carb RCP

In a siliconized glass tube, 500 µg of the protein in 500 µl of 0.5 M ammonium bicarbonate, pH 8.5 was mixed with TPCK trypsin (1 mg/ml in 1 mM HCl) at an enzyme to substrate concentration of (1:250 to 1:31) and incubated at room temperature for 30 min to overnight. At the end of the incubation, the samples were lyophilized and subjected either to SDS-polyacrylamide gel electrophoresis (PAGE) or DEAE-HPLC for the separation of the tryptic fragments. The holoprotein was prepared by saturating the apoprotein with riboflavin followed by dialysis against water.

SDS electrophoresis

(Laemmli, 1970) as well as on 8–25% gradient gels without urea under reducing conditions (Fling and Gregerson, 1986).

Immuno blotting

The procedure employed was as described earlier (Natraj *et al.*, 1988b). The antibody dilutions used were 1:5000 for antisera (a/s) to cRCP and 1:250 for a/s to Carb RCP. The nitrocellulose paper was exposed to the biotinylated reagent for 60 min and washed once again before incubation with ABC reagent for 2 h. After washing thoroughly with PBS/tween (0.1% v/v) the paper was exposed to the substrate solution (5 mg of 3,3'-diaminobenzidine dissolved in freshly made 10 ml of PBS containing 0.01% H_2O_2) and the antigen antibody reaction photographed.

Results

Changes in the elution profile of cRCP and modified cRCP on DEAE-HPLC following trypsinization

The elution profile of cRCP bound to riboflavin did not show any change following trypsinization at any of the enzyme to substrate ratios studied. Figure 1 represents the elution profiles of cRCP bound to riboflavin and following trypsinization at an

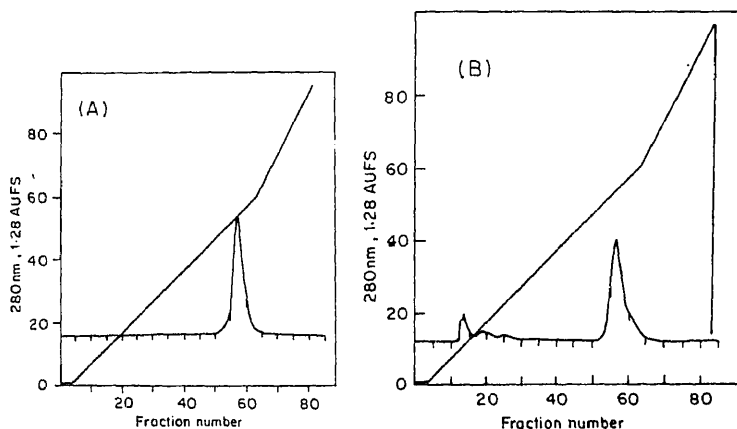


Figure 1. (A) Elution profile of cRCP bound to riboflavin on DEAE-HPLC.

100 μ g of cRCP bound to riboflavin was injected into the column (TSK 545 DEAE, 7.5 \times 150 mm). Chromatography was performed using the following solvent system

enzyme to substrate ratio of 1:31. The amount of riboflavin bound to the protein was similar to that of the native protein following trypsinization (figure 2). The trypsinization of the apoprotein on the otherhand showed minor changes in the elution profile (figure 3). Riboflavin binding was similar to that of the untreated protein.

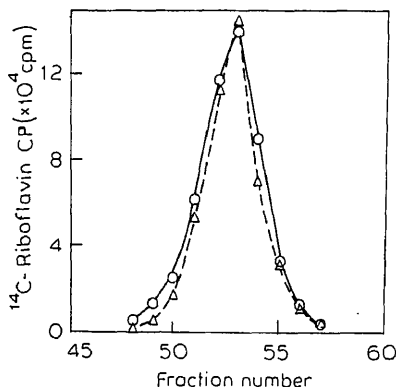


Figure 2. Unaltered riboflavin binding following trypsinization.

Apoprotein (2 mg) was incubated with saturating concentration of riboflavin containing $10 \mu\text{Ci}$ [^{14}C] riboflavin and then extensively dialysed against water. A fraction ($500 \mu\text{g}$) was subjected to trypsinization (1:31) and chromatographed on DEAE-HPLC. [^{14}C] riboflavin content of the fraction before (O) and after trypsinization (Δ) were quantitated in a Kontron Betamatic using a liquid scintillation cocktail 0.5% 2,5-diphenyloxazole in methyl cellosolve: toluene (v/v 1:1). Chromatographic conditions were same as in figure 1.

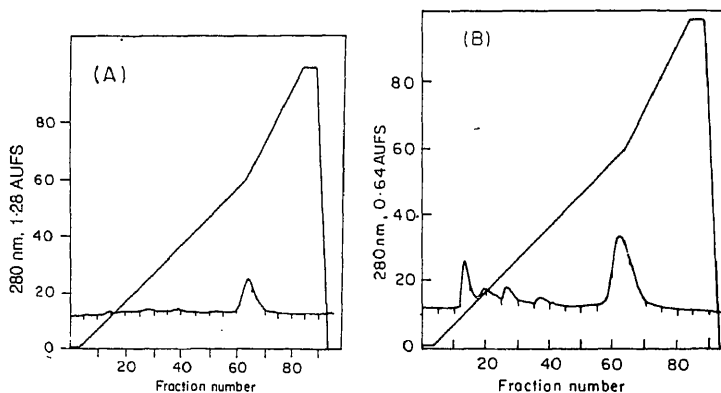


Figure 3. Elution profile of cRCP following trypsinization on DEAE-HPLC.

Trypsinization of the apoprotein was carried out as described in the text, at an enzyme to substrate ratio of 1:31. Chromatographic conditions were same as in figure 1. Protein injected was $200 \mu\text{g}$. Elution profile before (A) and after (B) trypsinization. Sensitivity was set at (A) 1.28 AUFS and (B) 0.64 AUFS.

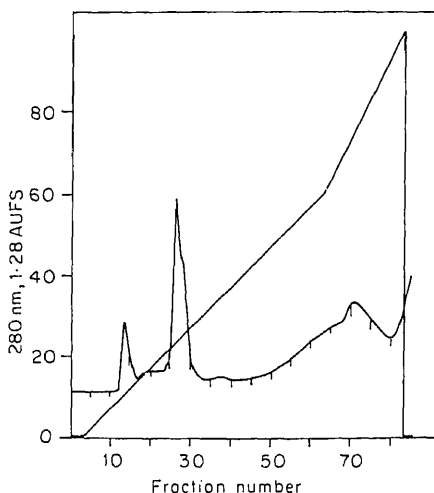


Figure 4. Elution profile of tryptic fragments on DEAE-HPLC.

Carboxymethylated RCP (1 mg) was trypsinized at an enzyme to substrate ratio of 1:25 for 90 min at room temperature as described in the text. 100 μ l (1 mg) was injected into a DEAE-HPLC and chromatographed. Chromatographic conditions were same as in figure 1.

(1:125) for 30–90 min. Two distinct peaks designated peak 1 and 2 followed by a broad peak were obtained.

These results indicate that the lysine and arginine residues of the apoprotein and the riboflavin bound protein are inaccessible to trypsin while it is easily accessible in the modified protein.

M_r determination by SDS-PAGE analysis of RCP and modified RCP treated with trypsin

The apo and holo protein were trypsinized at enzyme to substrate ratios ranging from 1:31 to 1:250 and then subjected to electrophoresis on a 12.5% SDS-gels, along with native RCP. The bands were stained with Coomassie brilliant blue. As seen in figure 5A, no differences in M_r were observed. In figure 5B, the SDS-PAGE analysis of the two peaks obtained following trypsinization of carboxymethylated RCP are seen.

The M_r of both the tryptic fragments peak 1 and 2 are similar *i.e.*, 26 ± 2 kDa (6 determinations).

Enzyme linked immunoelectro transfer blot

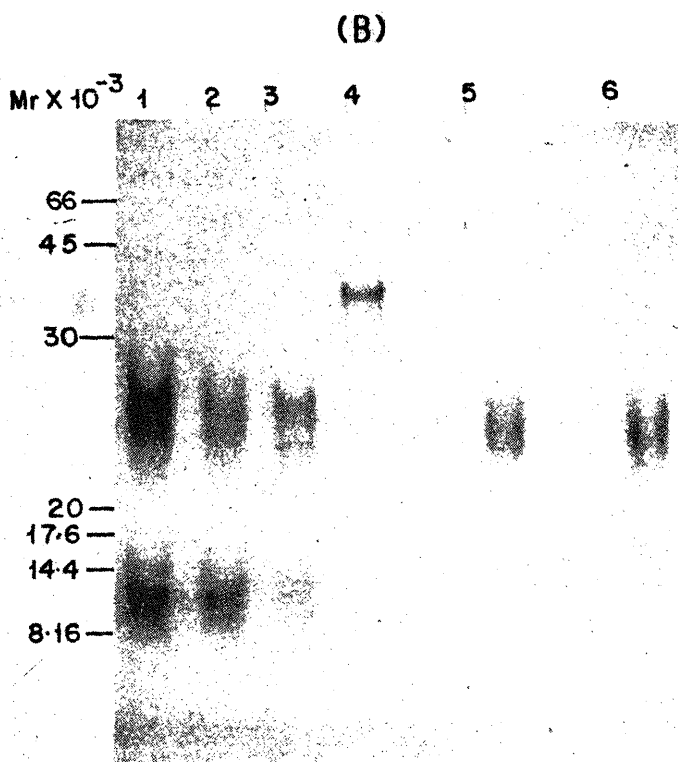
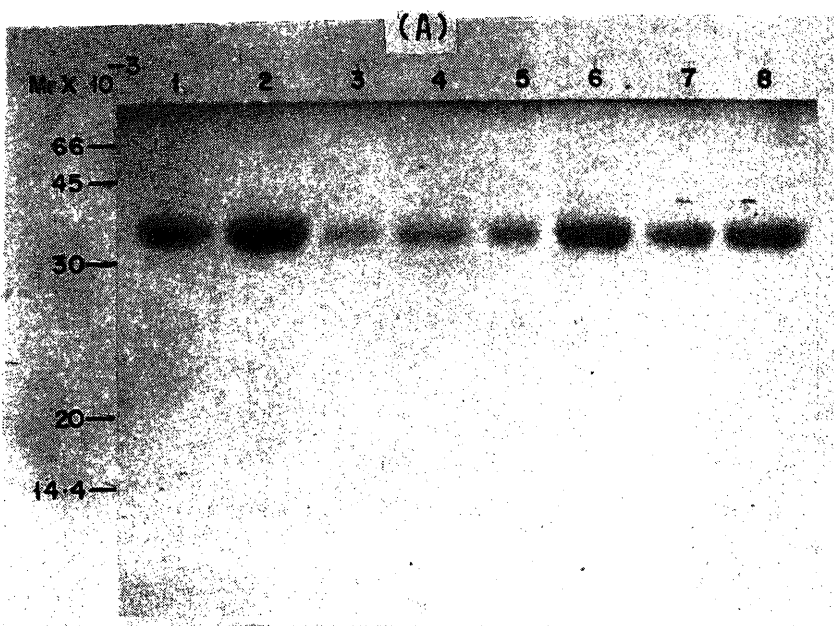


Figure 5.

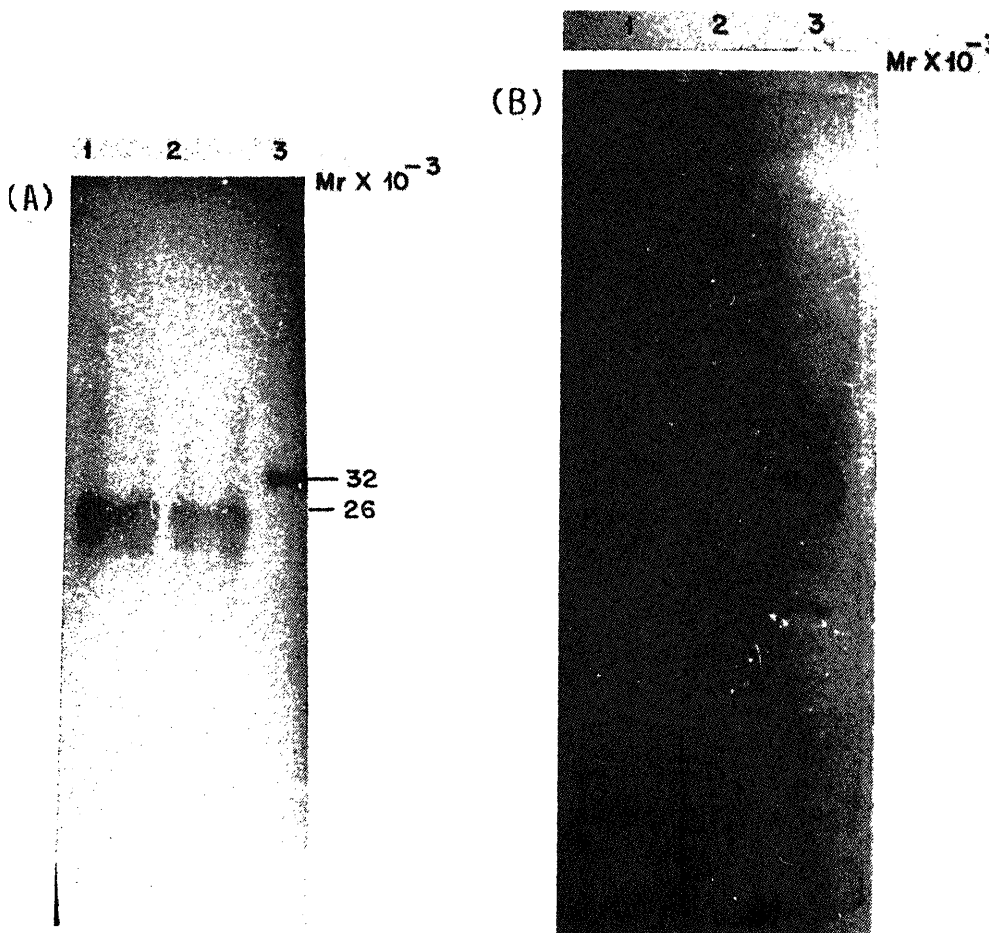


Figure 6. Antigenic activity of electrophoretic replicates.

Samples were subjected to SDS-PAGE (8–25%) followed by blotting on to nitrocellulose and then were probed with rabbit antiserum. (A) Lane 1 and 2, Carb RCP 10 μ g treated with trypsin (lane 1, *1:250; lane 2, *1:125) for 90 min; lane 3, cRCP (1 μ g). (B) Lane 1 and 2, tryptic peptide peak 1 (lane 1) and peak 2 (lane 2) (10 μ g); lane 3, Carb RCP treated with trypsin (*1:125) and stored at -70°C (25 μ g).

*Indicates the enzyme to substrate ratio used.

Figure 5. SDS-PAGE (12.5%) of cRCP, riboflavin bound RCP and Carb RCP following trypsinization.

(A) Lane 1, cRCP bound to riboflavin (10 μ g); lane 2, cRCP bound to riboflavin 25 μ g treated with trypsin (*1:125); lane 3 and 4, cRCP bound to riboflavin 10 μ g treated with trypsin (lane 3, *1:62.5; lane 4, *1:31); lane 5, cRCP (10 μ g); lane 6–8, cRCP (10 μ g) treated with trypsin (lane 6, *1:125; lane 7, *1:62.5; lane 8, *1:31). (B) Lane 1, 3, Carb RCP (10 μ g) treated with trypsin (*1:125); lane 2, 4, Carb RCP (10 μ g) treated with trypsin (*1:62.5); lane 5, 6, Carb RCP (10 μ g) treated with trypsin (*1:31).

(1:125) and stored at -70°C in the absence of a trypsin inhibitor, splits into several immunostainable peptide bands (26 kDa, 12 kDa and less). It is clear that trypsin was capable of cleaving the proteins even when stored at -70°C . Antiserum to carboxymethylated RCP (1:250) also binds strongly to the tryptic fragments (data not shown).

Antigenicity of the tryptic fragments towards the antiserum to cRCP

In an homologous cRCP RIA it was observed that of the two major tryptic fragments, only one fragment (peak 2) was able to displace native RCP (figure 7). A 50% inhibition was obtained at a concentration of 660 ng. The parent protein carboxymethylated RCP, does not displace cRCP in this assay (Natraj *et al.*, 1988b).

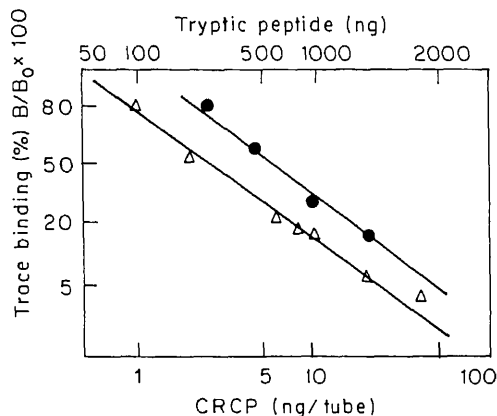


Figure 7. Antigenicity of the tryptic fragments towards the antiserum to cRCP.

The displacement of [^{125}I] labelled cRCP in an homologous RIA in the presence of cRCP (Δ) and the tryptic fragments (peak 2 on DEAE-HPLC) (\bullet) is depicted. The antibody dilution used was 1:20,000. The assay conditions are as described earlier (Natraj *et al.*, 1988b).

These results indicate that trypsinization of Carb RCP results in two major fragments (peak 1 and 2), with similar M_r (26 ± 2 kDa). However only one of these fragments (peak 2) displaces native cRCP in an homologous RIA.

Discussion

Elucidation of the antigenic structures of globular proteins require the preparation of a variety of long and overlapping peptides from various regions of the molecule, as well as a number of specifically modified and well characterized proteins and

directed against specific conformation (Benjamin *et al.*, 1984). This was found to be true for RCP which has 9 disulphide bonds (Hamazume *et al.*, 1987). It generated antibodies directed against specific conformation. However, a small percentage of the antibodies (5–25%) were directed towards sequence specific epitopes (Natraj *et al.*, 1988b). It was also demonstrated that, at least one of the sequential epitope(s) was located on the major cyanogen bromide fragment. Antiserum to Carb RCP, *i.e.*, to the sequential epitopes of the protein, induced neutralizing immunity. In the present communication, we have studied the antigenicity of the tryptic fragments. In the apoprotein and riboflavin bound RCP, the lysine and arginine residues were inaccessible for trypsin digestion as revealed both by the elution profile (figure 1) and SDS-PAGE (figure 5). However, at higher enzyme/substrate concentrations, some fragmentation of the apoprotein did occur as evidenced by the elution profile (figure 3), but SDS-PAGE analysis did not reveal the presence of smaller fragments. This could be due to either non-staining of the smaller fragments or due to fragmentation of peptides of $M_r < 2.5$ kDa. The linearized protein is easily fragmented. The trypsinized Carb RCP when chromatographed on a HPLC-DEAE or RP-18 column, separated into 3 peaks, two fragments having a M_r of 26 ± 2 kDa and a smaller fragment. Further, in the absence of proteolytic inhibitors, storage of the solution at -70°C , even at low enzyme concentrations (1:125) leads to further proteolytic cleavage where fragments of M_r 24 kDa, 12 kDa and other smaller fragments were immunostained (figure 6B, lane 3). Antiserum to cRCP and Carb RCP interacted with the 26 ± 2 kDa peptides. However, only one of the 26 ± 2 kDa peptides was able to displace cRCP in the homologous cRCP RIA. The parent protein, Carb RCP does not compete in this RIA system (Natraj *et al.*, 1988b). One of the possible explanation appears to be that the proteolytic cleavage of the linearized molecule, induces this fragment, by unknown mechanisms, to assume a conformation in solution similar to that of the native protein at the antibody combining site. The ability to displace cRCP in RIA has been examined using antibodies raised in several rabbits and similar results were obtained, indicating that this property is not unique to the antibody generated by one single rabbit.

The immunology of this large tryptic fragment needs to be evaluated to examine if it harbours the immunodominant region of the native protein.

Acknowledgements

Thanks are due to Dr. T. C. Anand Kumar for his encouragement and helpful discussion during the course of this work. This work was supported by the Science and Technology project 'Immunological Approaches to Fertility Control' of the Department of Biotechnology, New Delhi.

References

Benjamin D. C., Bergofsky J. A., Eggert J. J., Gurd F. R. N., Hannum C., Leach S. J., Margoliash E.

- Murthy, U. S. and Adiga, P. R. (1977) *Indian J. Biochem. Biophys.*, **14**, 118.
- Muniyappa, K. M. and Adiga, P. R. (1980) *Biochem. J.*, **187**, 537.
- Natraj, U., Asok Kumar, R. and Kadam, P. (1987) *Biol. Reprod.*, **36**, 677.
- Natraj, U. and Kholkute (1989) *J. Reprod. Immunol.*, **15**, 207.
- Natraj, U., George, S. and Kadam, P. (1988a) *J. Reprod. Immunol.*, **13**, 1.
- Natraj, U., George, S. and Kadam, M. S. (1988b) *Biochem. J.*, **254**, 287.
- Rhodes, M. B., Bennet, N. and Feenay, R. E. (1959) *J. Biol. Chem.*, **234**, 2054.
- Visweswariah, S. S. and Adiga, P. R. (1987a) *Biochim. Biophys. Acta*, **915**, 141.
- Visweswariah, S. S. and Adiga, P. R. (1987b) *Biosci. Rep.*, **7**, 563.
- Visweswariah, S., Karande, A. and Adiga, P. R. (1987) *J. Mol. Immunol.*, **24**, 969.

Translocation of plasminogen activator inhibitor-1 during serum stimulated growth of mouse embryo fibroblasts

S. SRINIVAS, T. NAGASHUNMUGAM and G. SHANMUGAM

Cancer Biology Division, School of Biological Sciences, Madurai Kamaraj University, Madurai 625 021, India

MS submitted 28 August 1990

Abstract. Serum-stimulated mouse embryo fibroblasts specifically secrete two proteins of molecular weights 48,000 and 26,000. The 48 kDa protein showed affinity to concanavalin A and was precipitated by antibody to plasminogen activator inhibitor. Immunoflow-cytometry using anti plasminogen activator inhibitor-1 serum indicate the presence of the 48 kDa protein in quiescent cells; this protein was virtually absent in serum-stimulated cells. The presence of the plasminogen activator inhibitor-1 related protein in quiescent cells and its absence in serum-stimulated cells in combination with the observation on the absence of this protein in the medium of quiescent cells and its presence in the medium of stimulated cells indicate that the 48 kDa protein was transferred from the cells into the medium upon serum-stimulation. The serum-mediated transfer of plasminogen activator inhibitor-1 from the cells into the medium was inhibited by actinomycin-D suggesting that the transfer process required actinomycin-D sensitive events. Treatment of pre-labelled quiescent cells with medium containing 20% fetal calf serum resulted in the gradual transfer of the labelled 48 kDa protein to the extra cellular matrix. These studies indicate that exposure of quiescent cells to fetal calf serum results in the transfer of plasminogen activator inhibitor-1 from the cells to the growth medium *via* extracellular matrix. The translocation of the protease inhibitor from the cells to the matrix and medium may enable the cellular and possibly the membrane proteases to act on growth factors or their receptors thereby initiating the mitogenic response.

Keywords. Plasminogen activator inhibitor; deposition; fibroblasts.

Introduction

The mechanisms controlling eukaryotic cell growth and the role of proteases and their inhibitors in growth control remain poorly elucidated. Its understanding requires detailed knowledge of the biochemical events that occur when a proliferative response is induced by physiological stimuli. The interaction of growth factors with specific surface receptors on resting or G_0 phase cells rapidly induces a cascade of biochemical events including the formation of phosphoinositide metabolites, phosphorylation of proteins and a transient increase of intracellular pH and free Ca^{2+} levels (Rozengurt, 1986). One or more of these biochemical events are thought to generate signals within the nucleus that activate a set of specific growth related genes resulting at the onset of DNA replication (Lau and Nathans, 1985; Denhardt *et al.*, 1986).

Secreted proteins play an important role in the regulation of cell proliferation. The secreted proteins fibronectin and collagens are extracellular matrix proteins

involved in the attachment of the cells to the substratum (Yamada *et al.*, 1985), while secreted proteases like collagenase and plasminogen activators and their inhibitors are involved in the turnover of matrix components and in tumor cell invasion (Bauer *et al.*, 1985; Hart and Rehemtulla, 1988; Moscateli and Rifkin 1988). In addition, secretion of growth inhibitors and growth factors were observed at different stages of cell growth and development (Nilsen-Hamilton and Hamilton, 1982; Harel *et al.*, 1985; Hsu and Wang 1986; Nagashunmugam and Shanmugam, 1987). Cell surface proteinases are shown to be important in growth and division of normal and transformed cells and the role of proteinases and their inhibitors in eukaryotic cell growth has been reviewed by Scott (1987). The secretion and deposition of proteases such as plasminogen activators (PA) and their inhibitors such as protease nexins and plasminogen activator inhibitors in the extracellular matrix suggest the possibility of cellular self regulation by growth related proteinases and their inhibitors (Laiho and Keski-Oja, 1989).

In the studies reported here, we have identified and characterized a serum-induced secreted protein of molecular weight (M_r) 48,000. This protein is specifically present in the growth medium of serum-stimulated cells but not in the medium of quiescent cells. Immunoprecipitation and concanavalin A (Con A) binding studies indicate that this protein is related to endothelial cell type plasminogen activator inhibitor (PAI-1). Evidence is provided for the translocation of the 48 kDa protein from the quiescent cells to the growth medium upon serum-stimulation.

Materials and methods

Cell culture

Secondary cultures of Swiss mouse embryo fibroblasts were maintained at 37°C in minimum essential medium (MEM) of Eagle (Flow Labs, UK) containing 10% bovine serum (Flow Labs, UK) and gentamycin 50 µg/ml. Cells from the fourth passage and above were used for experiments. Cells were synchronized at quiescence by maintaining sub-confluent monolayers in 0.5% serum containing medium for 72 h. Cells were released from quiescence by the addition of 20% fetal calf serum (FCS) containing medium. Serum-stimulation period was 6 h unless otherwise mentioned.

Radiolabelling of proteins

Quiescent and stimulated monolayers (120 cm²) were pulse-labelled with 50 µCi of [³⁵S] methionine (Amersham, specific activity 10.7 Ci/µmol) for 30 min in 5 ml of Hank's balanced salt solution. At the end of labelling, the medium was removed and the monolayer was washed thrice with MEM. The radioactivity was chased by

presence of 50 μ g of bovine serum albumin (BSA) and kept at 4°C for 30 min. The samples were centrifuged at 15,000 g for 20 min and the protein precipitate was air dried, dissolved in 0.1 N NaOH and then mixed with equal volume of 2 \times electrophoresis sample buffer.

Analysis of cellular fluorescence

The intracellular content of PAI-1 in quiescent, and serum-stimulated cells was quantitated using PAI-1 antiserum obtained from Dr. David Loskutoff, Scripps Clinic, San Diego, USA. FITC conjugated anti-rabbit IgG was used as second antibody and the fluorescence was quantitated in a fluorescence activated cell scanner (Becton Dickinson) as described earlier (Nagashunmugam *et al.*, 1989).

Immunoprecipitation

Immunoprecipitation of secreted and ECM proteins were carried out following the procedure of Chackalaparampil *et al.* (1985). Labelled medium (10 ml) containing secreted proteins from serum stimulated cells were concentrated to 0.5 ml by ultrafiltration and made up to 1 ml in RIPA buffer [0.1% Triton X-100, 1% sodium deoxy cholate, 0.1% sodium dodecyl sulphate (SDS), 0.15 M NaCl, 2 mM phenylmethylsulphonyl fluoride and 0.05 M Tris-HCl pH 7.2] and centrifuged at 10,000 g for 20 min. The extracellular matrix proteins were collected in RIPA buffer and centrifuged at 10,000 g for 20 min. To the 10,000 g supernatants 10 μ l of anti PAI-1 serum was added and the mixtures were incubated at 37°C for 30 min and then kept at 4°C overnight. The antigen-antibody complexes were treated with an excess of protein A sepharose (30 μ l of 50% slurry in RIPA buffer) at 4°C for 6–8 h. The absorbed complex was washed once with RIPA buffer thrice with washing buffer (50 mM Tris-HCl pH 7.4, 5% sucrose, 1% Nonidet P-40, 0.5 M NaCl and 5 mM EDTA) and finally with distilled water. The immune complexes along with protein A sepharose were subsequently suspended in 50 μ l of electrophoresis sample buffer and heated at 100°C for 3 min. The sepharose beads were pelleted and the proteins in the supernatant were electrophoresed in 5–18% SDS-polyacrylamide gradient gels.

Gel electrophoresis and autoradiography

Intracellular and secreted proteins of quiescent and serum-stimulated cells were separated on high resolution SDS polyacrylamide gradient (5–18%) gels containing 6% stacking gels (Laemmli and Favre, 1973). The protein samples were prepared in electrophoresis sample buffer and samples derived from equal amounts of cells were electrophoresed. Following electrophoresis, gels were stained with Coomassie blue and fluorographed (Bonner and Laskey, 1974). For the determination of molecular weights of the labelled polypeptides, molecular weight markers (Rajakumar and Shanmugam, 1983) were electrophoresed in parallel lanes and

Results

Secreted proteins of serum-stimulated and starved cells

Two proteins of M_r 48,000 and 26,000 were specifically secreted by quiescent cells in response to serum-stimulation (figure 1A). The 48 kDa secreted protein was absent in the conditioned medium of quiescent cells. However, high levels of this protein were present in the medium of stimulated cells. During the reverse process (serum-starvation), the level of the 48 kDa protein in the growth medium slowly declined (figure 1B). The low levels of the 48 kDa protein in the medium of serum-starved cells may be due to lack of transfer of this protein from the starved cells into the medium. This conclusion is supported by the immunofluorescence studies described below.

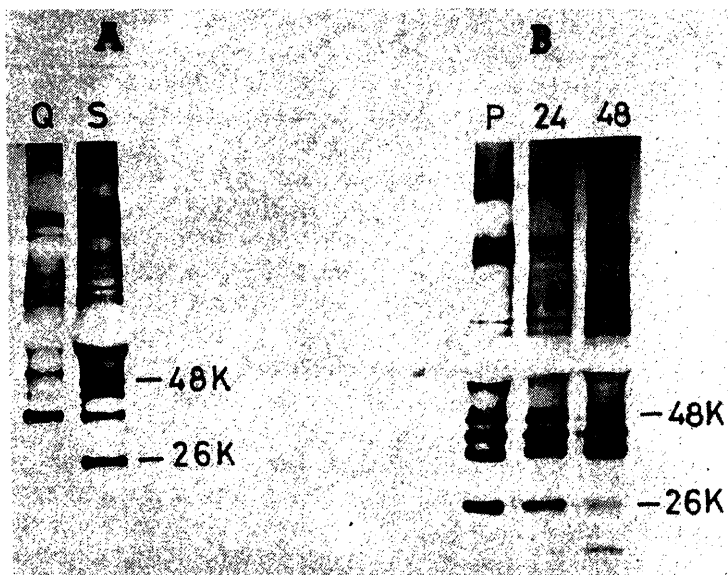


Figure 1. Effect of serum-stimulation (A) and serum-starvation (B) on the levels of secreted proteins. Q, quiescent cells; S, serum-stimulated cells; P, proliferating cells in 10% serum-containing medium. The numbers 24 and 48 indicate hours after shift of proliferating cells into serum-limiting (0.5% serum) medium. Cells were pulse labelled for 30 min with [35 S]methionine and then the radioactivity was chased for 30 min in serum-free chase medium. The proteins from the chase medium were electrophoresed in 5–18% polyacrylamide gradient gels containing SDS and fluorographed.

Another secreted protein of M_r 26,000 was also present in reduced levels in the medium of serum-starved cells in comparison to its amount in serum-stimulated cells (figure 1). Further studies on this protein are in progress. The 40 kDa secreted protein was shown to be a secreted cell-specific protein in the medium of this protein.

binding studies were done. Figure 2 lane B shows that the 48 kDa secreted protein and the 240 kDa fibronectin (Subramaniam and Shanmugam, 1985) were the predominant ConA binding proteins secreted by serum-stimulated cells. The 48 kDa protein was also found to be a major component of the ECM (lane D). Since a ConA binding ECM protein of M_r 48,000 was identified as PAI-1 (van Mourik *et al.*, 1984), it was of interest to know whether the 48 kDa protein with similar properties reported here is related to PAI-1. Immunoprecipitation assays using antiserum to endothelial cell type plasminogen activator inhibitor indicate that the 48 kDa ECM and secreted proteins are related to PAI-1 (figure 2, lanes C and E).

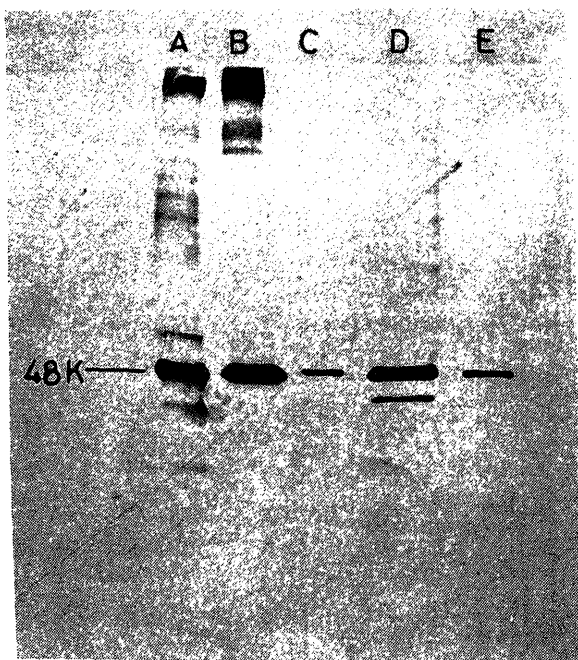


Figure 2. ConA binding and immunoprecipitation. Conditioned medium of serum-stimulated [^{35}S]methionine labelled cells were concentrated by ultrafiltration and aliquots were used for ConA binding and immunoprecipitation studies. For ConA binding, 50 μl of 50% suspension of ConA-sepharose 4B and 0.5 ml of concentrated conditioned medium were mixed and left at 4°C over night with intermittent shaking. The ConA bound proteins were isolated as described by Laiho *et al.* (1986) and electrophoresed in 5–18% polyacrylamide gradient gels. Details of immunoprecipitation are given in the 'materials and methods'. A. Secreted proteins of serum-stimulated cells. B. Proteins of serum-stimulated cells bound to ConA-sepharose. C. Immunoprecipitate obtained using anti PAI-1 serum and concentrated conditioned medium from serum-stimulated cells. D. ECM proteins of serum-stimulated cells. E. Immunoprecipitate obtained using anti PAI-1 serum and ECM proteins of serum-stimulated cells. The proteins were electrophoresed in 5–18% polyacrylamide gradient gels containing SDS and autoradiographed.

permeabilized with 0.1% Triton X-100 and reacted first with PAI-1 and then with FITC conjugated anti-rabbit IgG. The reaction was monitored by a FAC scanner (Nagashunmugam *et al.*, 1984). Cells treated with normal serum showed a single peak of low fluorescence. In contrast, quiescent cells reacted with an anti PAI-1 serum showed a second (second) peak with higher fluorescence (figure 3B). Serum-stimulated cells with PAI-1 antibody did not show the high fluorescence (second peak). However, serum-stimulated cells that were treated with actinomycin D showed the high fluorescence peak when reacted with anti PAI-1 antibody. These results indicate the presence of PAI-1 in quiescent cells, its absence in stimulated cells and its persistence in serum-stimulated cells treated with actinomycin D containing medium.

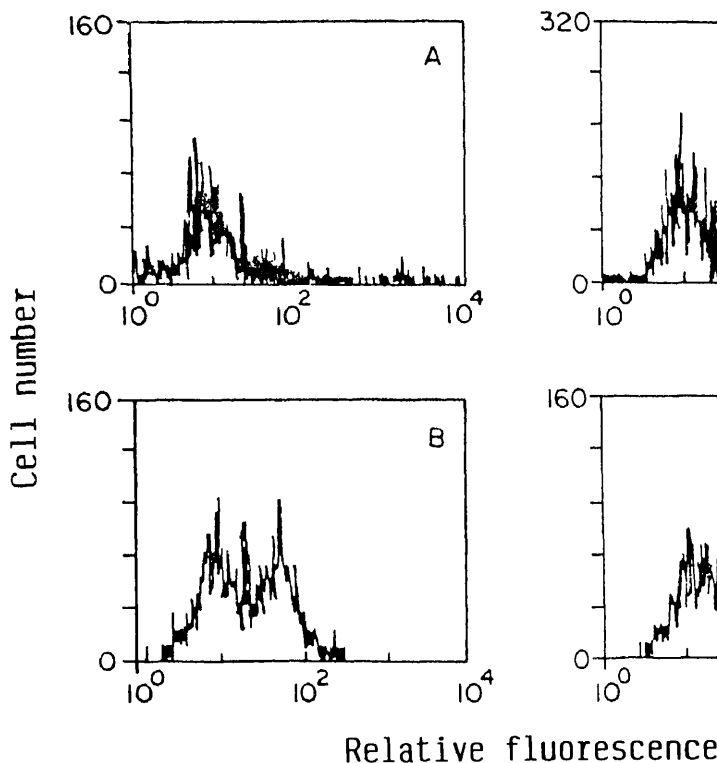


Figure 3. Quantitation of intracellular levels of PAI-1. Quiescent cells were collected, fixed with formaldehyde and permeabilized with Triton X-100. The permeabilized cells were reacted with either rabbit PAI-1 antibody or normal rabbit serum (A). After reacting with FITC conjugated anti-rabbit IgG, the fluorescence was quantitated in a FAC scanner. A, B, C, D. Serum-stimulated cells. D. Serum-stimulated cells treated with actinomycin D.

cells implies that this protein may be translocated from the quiescent cells to the matrix and growth medium upon mitogenic stimuli. Studies on the fate of pre-labelled proteins provide evidence for this hypothesis. For these studies, 4 monolayers of MEF, each with equal number of cells were made quiescent by serum-starvation for 72 h. When these quiescent cells were pre-labelled for 30 min with [35 S] methionine and then stimulated with 20% FCS in non-radioactive chase medium, substantial quantities of the labelled 48 kDa protein was found to be deposited in the extra cellular matrix of the serum-stimulated cells (figure 4). Laser

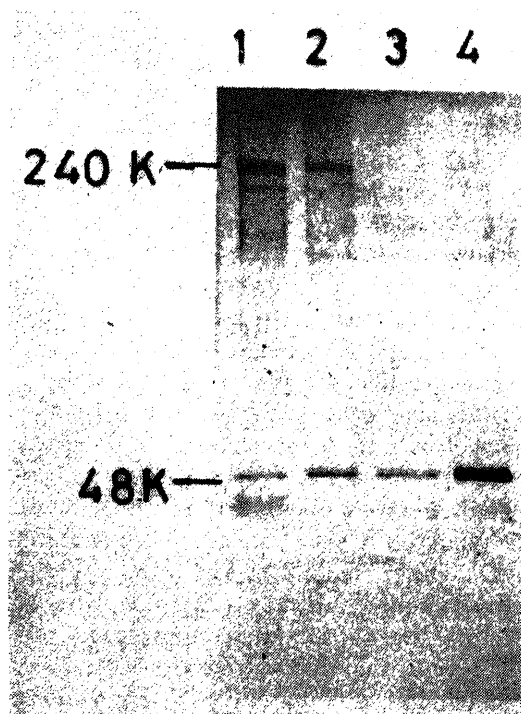


Figure 4. Fate of prelabelled 48 kDa protein. Quiescent mouse embryo fibroblasts were labelled with [35 S]methionine. After 30 min, the radioactive medium was removed, the monolayers were washed thrice with PBS and incubated for an hour in the conditioned medium obtained from quiescent cultures (Q medium). Lane 1, matrix proteins from cells that were maintained for an additional hour in Q medium. Lane 2, matrix proteins of cells that were maintained in 20% FCS containing medium for an additional hour. Lane 3, matrix proteins of cells that were maintained for an additional 2 h in Q medium. Lane 4, matrix proteins of cells that were maintained for an additional 2 h in 20% FCS containing medium. The matrix proteins were resolved by electrophoresis in 5–18% polyacrylamide gradient gels containing SDS and fluorographed.

densitometric quantitation of the radioactive 48 kDa protein bands shown in figure 4 indicates an increase of about 39% in the intensity of the band after 1 h exposure of pre-labelled cells to 20% serum-containing medium (lane 2). This increase was much higher (2.6 fold) in the matrix derived from pre-labelled cells that were treated

(Subramaniam and Shanmugam, 1985)] in the matrix declined in the first hour of exposure of quiescent cells with serum and disappeared at the end of 2 h treatment of pre-labelled cells with serum-containing medium. While FCS treatment had a spectacular effect on the time dependent transfer of the 48 kDa protein, the disappearance of the 240 kDa protein was not influenced by treatment of quiescent cells with FCS (lanes 3 and 4). These studies imply that mitogenic stimulation triggered the transfer of PAI-1 from the cells into the matrix. Previous studies indicate that PAI-1 is transferred into the medium *via* the extracellular matrix (Levin and Santell, 1987).

Discussion

In this study, we have identified a serum-induced secreted protein of M_r 48,000 as PAI-1. Based on the results of the presence of high levels of this protein in the quiescent cells and low levels in the stimulated cells, and on the absence of this protein in the quiescent cell conditioned medium and on its presence in the stimulated cell medium, we propose that the PAI-1 related 48 kDa protein is translocated from the quiescent cells to the growth medium upon mitogenic stimuli. Transfer of pre-labelled 48 kDa protein from the cell to the matrix in response to exposure of cells to 20% FCS confirms these results (figure 4).

We have used indirect immunofluorescence and its quantitation by fluorescence-activated cell analyser to get an insight on the intracellular amounts of PAI-1. The results presented in figure 3 indicate high levels of PAI-1 specific fluorescence in quiescent cells. The serum-stimulated cells did not show significant levels of PAI-1 specific fluorescence while the serum-stimulated cells treated with actinomycin D showed a PAI-1 specific fluorescence peak similar in magnitude as that observed in quiescent cells (figure 3D). The presence of PAI-1 specific peak in quiescent cells and its absence in serum-stimulated cells may indicate that the protein was lost by the stimulated cells. However, the concomitant appearance of PAI-1 in the matrix and medium upon serum-stimulation implies that the PAI-1 of the stimulated cell was transferred to the matrix and medium following serum-stimulated growth. The persistence of intracellular PAI-1 in serum-stimulated cells that were treated with actinomycin D implies that the transfer process of this protein required serum-stimulated actinomycin D sensitive proteins.

Exogenous and endogenous proteinases were shown to be involved in the release of membrane-bound mitogenic proteins (autocrine growth effectors) into the medium (Lieberman, 1983). The presence of these protease inhibitors at discrete sites may inhibit the action of proteases from triggering the mitogenic signal. Trypsin, thrombin and some serine proteinases initiate DNA synthesis in cultured cells by their action on the cell surface (Scott, 1987). Several peptide mitogens were found in association with esterolytic or proteolytic activities. Gospodarowicz and Moran (1976) have suggested that proteinases could potentiate the effect of growth factors by activation, or by conditioning the target cells, enabling them more sensitive to growth factors.

Since proteases elicit mitogenic response, removal or translocation of protease

inhibition of cleavage of pre-TGF- β (Keski-Oja and Moses, 1987). Thalacker and Nilsen-Hamilton (1987) have shown that TGF- β and TPA induced the secretion of PAI-1 in a variety of cell lines. In certain cells, TGF- β is implicated in the induction of cellular oncogenes like *c-sis*, which presumably activate *c-fos* and *c-myc* genes culminating in DNA synthesis (Leof *et al.* 1986). PAI-1 may inhibit the cleavage and subsequent activation of TGF- β and other growth factors by its presence in the quiescent cell. Translocation or removal of PAI from the quiescent cell may trigger the activation of growth related proteases in the quiescent cell enabling it to enter into the proliferating phase.

Acknowledgements

We thank Dr. D. Loskutoff for the gift of anti PAI-1 serum and Dr. S. R. Naik of Hindustan Antibiotics for gentamycin. We are grateful to Ms. Sheela and Dr. VR. Muthukkaruppan for their help in the use of FAC scanner. S. S. and T. N. S. were recipients of fellowships from the Council of Scientific and Industrial Research, New Delhi. This study was supported by a grant from the Department of Science and Technology, New Delhi.

References

- Bauer, E. A., Cooper, T. W., Huang, J. S., Altman, J. and Deuel, T. F. (1985) *Proc. Natl. Acad. Sci. USA.*, **82**, 4132.
- Bonner, W. M. and Laskey, R. A. (1974) *Eur. J. Biochem.*, **46**, 83.
- Chackalaparampil, I., Banerjee, D., Poirier and Mukherjee, B. B. (1985) *J. Virol.*, **53**, 841.
- Denhardt, D. T., Edwards, D. R. and Parfett, L. J. (1986) *Biochim. Biophys. Acta*, **805**, 83.
- Gospodarowicz, D. and Moran, J. S. (1976) *Annu. Rev. Biochem.*, **45**, 531.
- Harel, L., Blat, C. and Chatelain, G. (1985) *J. Cell. Physiol.*, **123**, 139.
- Hart, D. A. and Rehmtulla, A. (1988) *Comp. Biochem. Physiol.*, **B90**, 691.
- Hsu, Y. M. and Wang, J. L. (1986) *J. Cell Biol.*, **102**, 362.
- Keski-Oja, J. and Moses, H. L. (1987) *Med. Biol.*, **65**, 13.
- Laemmli, U. K., and Favre, M. (1973) *J. Mol. Biol.*, **80**, 575.
- Laiho, M. and Keski-Oja, J. (1989) *Cancer Res.*, **49**, 2533.
- Laiho, M., Saksela, O., Andreassen, P. A. and Keski-Oja, J. (1986) *J. Cell Biol.*, **103**, 2403.
- Lau, L. F., and Nathans, D. (1985) *EMBO J.*, **4**, 3145.
- Leof, E. B., Proper, J. A., Goustin, A. S., Shipley, G. D. and Moses, H. L. (1986) *Proc. Natl. Acad. Sci. USA*, **83**, 2453.
- Levin, E. G. and Santell, L. (1987) *J. Cell Biol.*, **105**, 2543.
- Lieberman, M. A. (1983) *J. Cell. Physiol.*, **114**, 73.
- Moscatelli, D. and Rifkin, D. B. (1988) *Biochim. Biophys. Acta*, **948**, 67.
- Nagashunmugam, T. and Shanmugam, G. (1987) *Cell Biol. Int. Rep.*, **11**, 147.
- Nagashunmugam, T., Srinivas, S. and Shanmugam, G. (1989) *Biol. Cell*, **60**, 307.
- Nilsen-Hamilton, M. and Hamilton, R. T. (1982) *Cell Biol. Int. Rep.*, **6**, 815.
- Rajakumar, A. R. A. and Shanmugam, G. (1983) *Exp. Cell Res.*, **147**, 119.
- Rozengurt, E. (1986) *Science*, **234**, 161.
- Scott, G. K. (1987) *Comp. Biochem. Physiol.*, **B87**, 1.
- Subramaniam, M. and Shanugam, G. (1985) *Cell Biol. Int. Rep.*, **9**, 51.
- Subramaniam, M. and Shanmugam, G. (1988) *Mol. Biol. Rep.*, **13**, 133.
- Thalacker, F. W. and Nilsen-Hamilton, M. (1987) *J. Biol. Chem.*, **262**, 2283.
- van Mourik, J. A., Lawrence, D. A. and Loskutoff, D. J. (1984) *J. Biol. Chem.*, **259**, 14914.

Isolation, characterization and effect of acidic pH on the unfolding-refolding mechanism of serum albumin domains

M. YAHYA KHAN† and A. SALAHUDDIN*

Department of Biochemistry, School of Life Sciences, North-Eastern Hill University, Shillong 793 014, India

*Department of Biochemistry, J. N. Medical College, Aligarh Muslim University, Aligarh 202 002, India

MS received 21 August 1990; revised 18 December 1990

Abstract. Three fragments, *viz.*, BSA-CNBr_{1–183}, BSA-CNBr_{184–582}, and BSA-T_{377–582} representing domains I, II+III and III of bovine serum albumin have been isolated and purified. The physicochemical properties have been investigated and compared with their parent albumin molecule. The values of Stokes radii (nm) and intrinsic viscosities (ml/g) have been determined to be 2.36, 3.30; 3.43, 4.36; and 2.40, 3.13 for the fragments BSA-CNBr_{1–183}, BSA-CNBr_{184–582} and BSA-T_{377–582} respectively. The acid induced unfolding-refolding transitions of intact albumin and the fragment BSA-T_{377–582} have been shown to occur in two steps while the fragments BSA-CNBr_{1–183} and BSA-CNBr_{184–582} underwent single step transitions. The formation of the acid denatured states of intact albumin, BSA-CNBr_{1–183} and BSA-CNBr_{184–582} was accompanied by an increase of about 86, 56 and 44% in the values of intrinsic viscosities respectively. Since all the transitions were reversible, the values of equilibrium constants, K_D , were calculated. The analysis of the dependence of K_D on pH indicated that the first transition ($N-X$) of albumin was caused due to the uptake of about 3 protons by the native albumin. The intermediate state, X , is converted to acid unfolded state, D , by taking up another two protons. A comparison of the results on intact albumin with that of its fragments revealed that the second transition of the fragment BSA-T_{377–582} and the two single step transitions of the fragment BSA-CNBr_{1–183} and BSA-CNBr_{184–582} were much closer to the second transition ($X-D$) of the intact albumin. The first transition of albumin has been attributed to its domain III represented by the fragment BSA-T_{377–582}.

Keywords. BSA-domains; hydration; tryptic digestion; viscosity; ultraviolet absorption; acid-induced unfolding.

Introduction

The mechanism of acquisition of 3-dimensional structure by proteins has been extensively studied over the past several years (Anfinsen and Scheraga, 1975; Baldwin, 1975, 1989; Creighton, 1978; Privalov, 1982). Among others, the idea that a globular protein might fold in independent 'structural regions' or domains before forming the crucial native structure, has emerged as one of the great achievements in the field of protein folding in recent years (Wetlaufer, 1973). This has been tested in several laboratories by studying the unfolding-refolding behaviour of small protein fragments (see Wetlaufer, 1981). However, studies with larger proteins with the possibility of having multiple nucleation centres (Wetlaufer, 1973) are still inadequate. Serum albumin is a suitable protein for this purpose because (i) it is a

large molecule with 582 amino acid residues (Brown, 1977; Reed *et al.*, 1980), (ii) it has a 3-domain structure (Brown, 1975, 1976), (iii) several albumin fragments have been isolated and characterized (Wetlauffer, 1981), and (iv) some fragmentary data on the unfolding-refolding properties of this protein are already available (Wetlauffer, 1981; Johanson *et al.*, 1986; Khan and Salahuddin, 1984; Khan, 1986; Khan *et al.*, 1987).

Keeping above points in mind, we have isolated and characterized 3 fragments of bovine serum albumin (BSA) corresponding to domains, I, II + III, and III of the intact albumin molecule. Two of the fragments have been prepared by cyanogen bromide (CNBr) cleavage of the albumin while the third fragment has been isolated from a hydrolyzate obtained by controlled tryptic digestion of the protein. The fragments have been named as BSA-CNBr₁₋₁₈₃, BSA-CNBr₁₈₄₋₅₈₂ and BSA-T₃₇₇₋₅₈₂ where 'CNBr' and 'T' indicate the mode of cleavage *i.e.*, cyanogen bromide and trypsin, and 1-183, 184-582 and 377-582 show the position of the fragments in the primary structure (Brown, 1976) of BSA respectively. The unfolding-refolding behaviour of these 3 fragments and their parent molecule under acidic conditions has been systematically investigated. We have shown that the C-terminal region of the albumin molecule is more susceptible towards acid denaturation and is important in the *N-F* transition of serum albumin (Foster, 1960; Khan, 1986). The characteristics of the acid induced transitions of the 3 albumin fragments have been reported.

Materials and methods

All the proteins including BSA (lot Nos. 10C-8080 and 100F-0249), N-acetyl-L-tyrosine ethyl ester (ATEE), N-acetyl-L-tryptophanamide (ATPA), N-acetyl-L-phenylalanine ethyl ester (APEE), dansyl chloride, dansylated amino acids, DEAE cellulose and tosyl-L-phenylalanyl-chloromethyl ketone (TPCK) were obtained from Sigma Chemical Co., USA. BSA was routinely purified by Sephadex G-100 column chromatography before use. Chymotryptic activity associated with commercial trypsin was eliminated by treating the enzyme with TPCK (Carpenter, 1967). The constant boiling HCl was prepared from the concentrated analytical grade acid using the procedure of Foulk and Hollingsworth (1923). Other chemicals were of the best commercial grade available.

Measurement of pH

Since most of the experiments described in this paper required an accurate measurement of pH, an EC digital pH meter (serial 022, pH 5651) in conjunction with EC combination electrode was exclusively used for this purpose. pHs of the solutions were measured twice (before and after the experiments) and the mean of the two readings was taken as the final reading. However, there was no significant variation in the two readings in most of the measurements.

chromatography before use. The monomeric fraction (molecular weight 68,000) of BSA thus obtained was allowed to react with L-Cys to block the lone sulfhydryl group of the protein by a method essentially due to King and Spencer (1970). The cystinylated-monomeric BSA was used for subsequent preparation of the albumin fragments. The tryptic fragment, BSA-T₃₇₇₋₅₈₂ representing domain III of the intact BSA molecule was isolated from TPCK-treated tryptic digests of the protein by the method of Habeeb and Atassi (1976). The two CNBr fragments, BSA-CNBr₁₋₁₈₃ and BSA-CNBr₁₈₄₋₅₈₂ were prepared by following procedures: 50 ml of a 2% (w/v) albumin solution in 60% (v/v) formic acid was taken in a 250 ml conical flask wrapped with black papers to make it opaque. An equal volume of 99% (v/v) formic acid containing 250 mg of CNBr was added into the flask and the content was left for 20 h at 25°C with a gentle stirring throughout the incubation period. The excess reagent was then removed by gel filtration on a Sephadex G-25 column (78.5 × 2.96 cm) equilibrated at pH 2.86 with 0.2 M ammonium formate buffer. The digestion mixture was finally concentrated and fractionated on a Sephadex G-75 column (135 × 2.95 cm) equilibrated with the above buffer. The process of gel filtration was repeated several times until symmetrical peaks giving homogeneous preparations of the respective fragments were obtained.

Protein estimations

Depending on the desired precision and sensitivity, the protein concentrations were determined by the methods of Lowry *et al.* (1951), Bradford (1976) or spectrophotometrically by using the values of $E_{1\text{ cm}}^{1\%}$ at 278 nm as 6.52, 6.76, 5.1 and 3.29 (at 276 nm) for BSA, BSA-CNBr₁₋₁₈₃, BSA-CNBr₁₈₄₋₅₈₂ and BSA-T₃₇₇₋₅₈₂ respectively.

Solvent perturbation difference spectroscopy

The degree of exposure of aromatic chromophores was measured by solvent perturbation techniques, essentially as described by Herskovits and Laskowski (1962), and Herskovits (1967). The model mixtures were made by mixing ATEE, ATPA and APEE in appropriate concentrations. Other details were the same as described earlier (Baig and Salahuddin, 1978).

Gel filtration experiments

Some hydrodynamic parameters were calculated from the data obtained by gel filtration on a Sephadex G-200 column (80 × 2.74 cm) equilibrated with 0.06 M sodium phosphate buffer, pH 7, at 25 ± 0.5°C. The elution volumes were determined gravimetrically by weighing the fractions accurately. Elution weight, W_e , thus

Determination of intrinsic viscosity

The reduced viscosity, R , and the intrinsic viscosity, $[\eta]$, were calculated with the help of the following equations (Tanford, 1955):

$$\eta_R = (t - t_o) t_o c + (1 - \bar{V}_2 \rho_o) / \rho_o \quad (1)$$

$$[\eta] = \lim_{c \rightarrow 0} (t - t_o) \text{ and } / t_o c + (1 - \bar{V}_2 \rho_o) /, \quad (2)$$

where c is protein concentration in g/ml, ρ_o is the density of the solvent in g/ml, and \bar{V}_2 is partial specific volume of the protein in ml/g. The time of flow of the solvent t_o , and that of the protein solution, t , were recorded at 25°C in a Kimax G-46 (size 25) viscometer as described earlier (Ahmad and Salahuddin, 1974).

The partial specific volumes of BSA and its fragments were calculated by the method of Haschemeyer and Haschemeyer (1973), using the following expression:

$$\bar{V}_2 = \sum_i \bar{V}_i w_i / \sum_i w_i, \quad (3)$$

where \bar{V}_i is the partial specific volume of the i th amino acid residue in the protein and w_i is the fractional molecular weight of the i th residue. Using the molecular weights of 68,000, 22,000, 44,000 and 22,000; the partial specific volumes were calculated to be 0.734, 0.728, 0.746 and 0.739 ml/g for BSA, BSA-CNBr₁₋₁₈₃, BSA-CNBr₁₈₄₋₅₈₂ and BSA-T₃₇₇₋₅₈₂ respectively.

Tryptic digestion

Tryptic digestion of BSA and its 3 fragments was performed at 25°C by a method essentially due to Paik and Kim (1972). 21.8 mg trypsin in 5 ml of 0.1 M sodium phosphate buffer, pH 7.5, was mixed with an equal volume of the same buffer containing 21.8 mg of BSA (or its fragments). After shaking the mixture properly, 1 ml aliquots were pipetted out at different time intervals and the reaction was arrested by adding 1 ml of chilled 1 M sodium acetate buffer, pH 5.1. The extent of tryptic hydrolysis in different aliquots was followed by estimating the colour yield with ninhydrin due to the newly formed amino groups by the method of Moore and Stein (1954).

Measurement of difference spectra

The difference spectra of the proteins were recorded in 0.2 M KCl in the presence and absence of acid by employing 4-cells technique. The solutions were prepared on the basis of weight in 5 ml calibrated volumetric flasks. The two cells in the reference compartment contained protein solution in KCl (pH 6.8) and a solution of KCl-HCl mixture, while the two cells in the sample compartment contained protein

Determination of the equilibrium denaturation curve

Transition studies were performed by taking stock solutions of the protein (by weight) in calibrated flasks (5 ml). To this were added 74.6 mg of KCl crystals and varying amounts of constant boiling HCl (diluted 10 times before use) and the volume was made up to 5 ml with water. The contents were thoroughly mixed and left for about 5 h for equilibration. The solutions were then filtered through millipore filter (pore size $0.5\ \mu\text{m}$) and subsequent measurements of viscosity or absorbance were made as described above. Reversibility of the transition was tested by taking proteins already exposed to acid pH for 5 h and raising their pHs to desired level by adding known volumes of 0.05 M KOH solution followed by 5 h equilibration prior to viscosity or optical measurements.

Results

Isolation and purification of the fragments

All the 3 fragments isolated in this study were found to be homogeneous on Sephadex G-100 gel chromatography and on polyacrylamide gel electrophoresis (see figure 1). Relative electrophoretic mobilities, R_m , of the 3 fragments and BSA were calculated in triplicate. The R_m of BSA and its fragments, BSA-CNBr₁₈₄₋₅₈₂ and BSA-T₃₇₇₋₅₈₂ were 80, 63 and 61% of the mobility of the fragment BSA-CNBr₁₋₁₈₃ respectively. This clearly indicated that the R_m was essentially independent of the size of the proteins and all the fragments had probably retained the globular conformation even after the separation from their parent molecule. The substantial difference in R_m of BSA and its fragments is, however, explainable in terms of the difference in the number of negative charges on the different domains of BSA at physiological pH (see Peters, 1975).

Spectral properties

Absorption spectra of BSA and its 3 fragments were recorded in 0.06 M sodium phosphate buffer, pH 7, at 25°C. The intact protein was found to absorb maximally at 278 nm. These features were retained in the spectra of the two CNBr fragments of the albumin. However, the spectrum of the fragment, BSA-T₃₇₇₋₅₈₂ was significantly different from BSA in that it had its maximum at 276 nm and trough at 256 nm with some fine structure in between those two wavelengths. This is expected because the tryptic fragment is devoid of Trp and contains 4 Tyr and 9 Phe residues in a total of 206 amino acid residues present in the fragment. Obviously the spectrum is dominated by Tyr with a minor contribution from Phe which produces the fine structure in the 256–276 nm region. For the same reason, the specific extinction coefficient, $E_{1\text{ cm}}^{1\%}$, of the tryptic fragment (3.29) is significantly lower than BSA (6.52) or its two CNBr fragments, BSA-CNBr₁₋₁₈₃ (6.76) and BSA-CNBr₁₈₄₋₅₈₂ (5.10), which contain relatively higher numbers of aromatic chromophores (Brown,

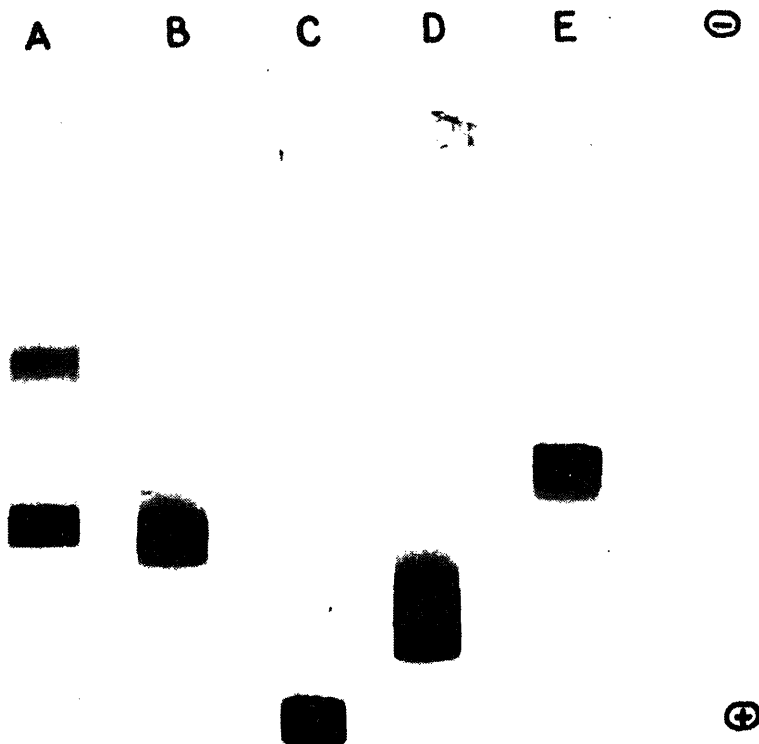


Figure 1. Polyacrylamide gel electrophoresis of (A) BSA, (B) BSA-monomer, (C) BSA-CNBr₁₋₁₈₃, (D) BSA-CNBr₁₈₄₋₅₈₂, and (E) BSA-T₃₇₇₋₅₈₂ in 7% gels. About 200 μ g of each protein was electrophoresed for about 2 h in Tris-glycine buffer, pH 8.2, ionic strength 0.02, with an anodic current of 4 mA per tube.

Solvent perturbation

Results on solvent perturbation obtained with DMSO and ethylene glycol as perturbants suggested about 35% exposure of Tyr and about 40% exposure of aromatic residues in BSA (see table 1). On the other hand, the degree of exposure of aromatic chromophores in albumin fragments was much higher as compared to the intact BSA molecule (table 1).

Like BSA, the degree of exposure of the aromatic chromophores in the 3 albumin fragments was not significantly changed on their acidification from pH 7 to pH 2 (see table 1) for small perturbants, DMSO and ethylene glycol. The polyethylene glycol-400 (PEG-400), which was successfully employed to show an increase in exposure of chromophores in BSA on its acid denaturation could, however, not be used in similar experiments with the 3 albumin fragments since they were not fully soluble in 20% (v/v) PEG-400 solution.

Higher degree of exposure of aromatic chromophores in albumin fragments was observed when the fragments were added to a solution of the chromophore

Table 1. Solvent perturbation difference spectral results on BSA and its fragments^a.

Protein in 20% (v/v) solvent	Exposure (%)			
	Tyrosine		Tryptophan	
	pH 7.0	pH 1.8	pH 7.0	pH 1.8
BSA (DMSO)	36+1	35+1	36+2	41+2
BSA (ethylene glycol)	34+1	39+2	43+2	45+3
BSA-CNBr ₁₋₁₈₃ (DMSO)	54+2	58+1	64+2	59+3
BSA-CNBr ₁₋₁₈₃ (ethylene glycol)	58+3	59+4	54+2	65+2
BSA-CNBr ₁₈₄₋₅₈₂ (DMSO)	52+2	61+3	53+2	62+1
BSA-CNBr ₁₈₄₋₅₈₂ (ethylene glycol)	57+3	59+4	50+1	57+3
BSA-T ₃₇₇₋₅₈₂ (DMSO)	59+2	56+2	—	—
BSA-T ₃₇₇₋₅₈₂ (ethylene glycol)	64+3	69+3	—	—

^aThe experiments at pH 7.0 and 1.8 were performed in 0.06 M sodium phosphate buffer and 0.15 M KCl-HCl mixture respectively. The composition of the model mixture was based on 2 Trp, 19 Tyr, 27 Phe; 1 Trp, 8 Tyr, 11 Phe; 1 Trp, 11 Tyr, 16 Phe; and 4 Tyr, 9 Phe residues per mol of BSA, BSA-CNBr₁₋₁₈₃, BSA-CNBr₁₈₄₋₅₈₂ and BSA-T₃₇₇₋₅₈₂ respectively (Reed *et al.*, 1980).

in the vicinity of the aromatic chromophores, than intact albumin molecule. This is, however, unlikely (except perhaps in the case of fragment BSA-CNBr₁₈₄₋₅₈₂) because fragments BSA-CNBr₁₋₁₈₃ and BSA-CNBr₃₇₇₋₅₈₂ exist (see below) in a compact and folded conformation. Furthermore, fragment, BSA-T₃₇₇₋₅₈₂ has been shown to have same percentage of the secondary structure as BSA (Reed *et al.*, 1975). As evident from table 1, with DMSO and ethylene glycol as the perturbants, the per cent exposures of Tyr and Trp in BSA are not significantly different from those found for the native proteins. However, with PEG-400 as the perturbant, the degree of exposure of Tyr and Trp increased from 20 and 22% to 39 and 44% respectively.

Table 2. Hydrodynamic parameters of BSA and its fragments.

Parameters	BSA	BSA-CNBr ₁₋₁₈₃	BSA-CNBr ₁₈₄₋₅₈₂	BSA-T ₃₇₇₋₅₈₂
Intrinsic viscosity (ml/g)	3.60	3.30	4.36	3.13
Axial ratio ^a (a/a_0)	2.64	2.30	3.44	2.04
Partial specific volume (ml/g) ^b	0.734	0.728	0.736	0.739
Hydration ^b (g water/g protein)	0.415	0.432	0.435	0.388
Stokes radius (nm) ^c	3.50 ^e	2.36	3.43	2.40
Frictional ratio ^d (f/f_0)	1.30 ^f	1.19	1.30	1.19
Diffusion coefficient (cm ² /sec $\times 10^7$) ^d	5.90 ^f	9.32	6.39	9.16

^aCalculated from viscosity data. ^bCalculated from amino-acid composition. ^cDetermined by gel filtration.

^dCalculated from Stokes radii. ^eTaken from Tanford *et al.* (1974). ^fTaken from Peters (1975).

conclusion is strongly supported by the intrinsic viscosity data given in the same table. The values of the intrinsic viscosities of the fragments BSA-CNBr₁₋₁₈₃ (3.30 ml/g) and BSA-T₃₇₇₋₅₈₂ (3.13 ml/g) were well within the range (3–4 ml/g) expected for native proteins having compact and globular conformation (Tanford, 1968). Thus, if these two fragments are taken to be compact and globular in shape, their Stokes radii (r) can be calculated from the measured intrinsic viscosities, $[\eta]$, with the help of following equation (Tanford, 1961):

$$[\eta] = 2.5 (N/M) (4/3) (r^3), \quad (4)$$

where M and N are the molecular weight of the proteins and Avogadro's Number (6.022×10^{23} /mol) respectively. The Stokes radii of BSA-CNBr₁₋₁₈₃ and BSA-T₃₇₇₋₅₈₂, thus calculated to be 2.26 and 2.22 nm respectively, were in agreement with those determined by gel filtration (see table 2).

Analysis of the gel filtration results on the fragment BSA-CNBr₁₈₄₋₅₈₂ (table 2) showed significant asymmetry and/or hydration of the fragment. This was also supported by viscosity data where intrinsic viscosity was found to be significantly higher than the expected range for the compact and globular proteins (table 2, Tanford, 1961).

Tryptic digestion

The rates of tryptic digestion of BSA and its 3 fragments, which would depend on the accessibility of scissile peptide bonds in the proteins (Klee, 1967), were studied at 25°C and the results are depicted in figure 2. The rates (Δ O.D./min) of hydrolysis

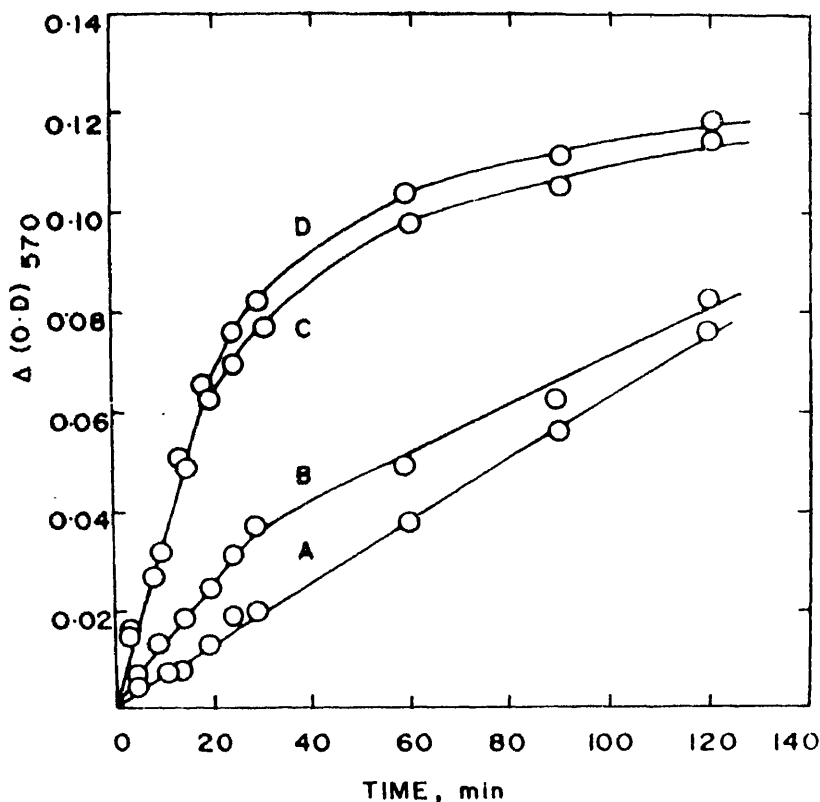


Figure 2. Rate of tryptic digestion of native fragment BSA-T₃₇₇₋₅₈₂ (A), intact BSA (B), fragment BSA-CNBr₁₈₄₋₅₈₂ (C) and fragment BSA-CNBr₁₋₁₈₃ (D).

Five ml of the enzyme solution containing 21.8 mg trypsin was added to an equal volume of the protein (21.8 mg) solution in 0.1 M sodium phosphate buffer, pH 7.5. One ml aliquots were pipetted out at different time intervals and the reaction was stopped by adding 1 ml chilled 1 M sodium acetate buffer, pH 5.1. The increase in the colour intensity with time due to newly formed amino groups was estimated at 570 nm by the method of Moore and Stein (1954).

fragment has a distorted structure as compared to its parent molecule. However, the enhanced rate of the hydrolysis of fragment BSA-CNBr₁₋₁₈₃, which has been shown above (hydrodynamic results) to exist in a compact and globular conformation, would probably indicate that among the accessible scissile peptide bonds in fragment BSA-CNBr₁₋₁₈₃ and BSA, the latter contained proportionally more peptide bonds refractory to tryptic attack. This indeed is the case is supported by the slowest hydrolytic rate observed for the fragment BSA-T₃₇₇₋₅₈₂ which constitutes domain III of the intact albumin and thus helps the latter to undergo tryptic hydrolysis at an overall slower rate as compared to the fragment BSA-CNBr₁₋₁₈₃.

Difference absorption spectra

The difference spectra of BSA and its fragments denatured at pH 1.5 were obtained

by using native protein in 0.2 M KCl at pH 6.8 as the reference. The difference between the absorbance, Δ (O.D.), of the native and acid denatured protein plotted against wavelength and a representative spectrum thus obtained for the fragment BSA-CNBr₁₋₁₈₃ is shown in figure 3. The fine structures of the difference spectrum of BSA included a pronounced trough at 287 nm, a trough at 280 nm and 'wiggles' between 250-270 nm. These features were in general shared by the spectra of the 3 albumin fragments. However, in addition to these fine structures, the spectra of BSA-CNBr₁₋₁₈₃ (see figure 3) and BSA-CNBr₁₈₄₋₅₈₂ also contained a trough at about 290 nm. Furthermore, the 'wiggles' between 250-270 nm in the spectrum of fragment BSA-T₃₇₇₋₅₈₂ were much more pronounced as compared to the two CNBr fragments and the intact albumin. These fine structures in the difference spectra of BSA and its 3 fragments were indicative of the exposure of aromatic chromophores in the acid denatured proteins. Since the characteristic absorbance was maximum at 287-288 nm, the latter were used to follow the denaturation of the proteins described below.

Viscosity results

Intrinsic viscosities, $[\eta]$, of BSA and its fragments, BSA-CNBr₁₋₁₈₃ and

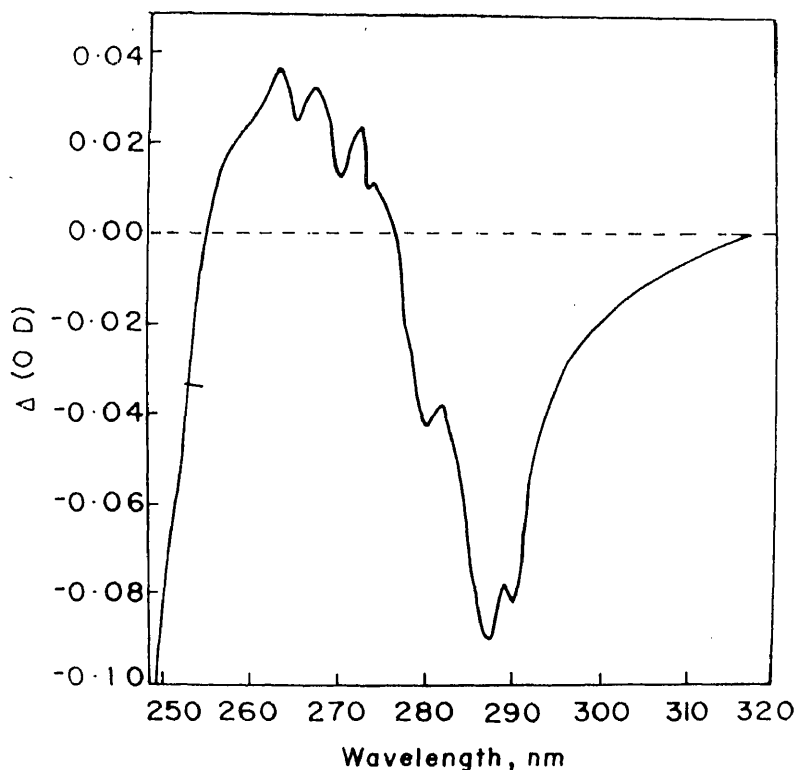


Figure 3. The acid-induced difference spectrum of the fragment BSA-CNBr₁₋₁₈₃.

CNBr₁₈₄₋₅₈₂ at pH 1.8, were found to be 6.71, 4.74 and 6.78 ml/g (see figure 4 for a representative plot for the determination of $[\eta]$) which represented an increase of 86, 56 and 44% respectively over the corresponding values of these proteins under native conditions. In view of the marked tendency of time dependent aggregation of the fragment BSA-T₃₇₇₋₅₈₂, especially at higher protein concentrations, its viscosity could not be measured with any acceptable degree of precision.

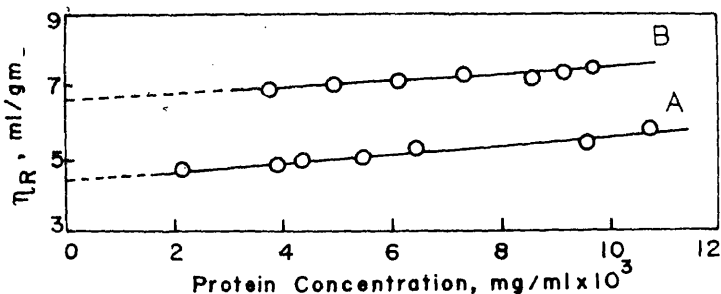


Figure 4. Reduced viscosity of BSA as a function of protein concentration in (A) 0.2 M KCl-HCl mixture, pH 3.6 and (B) 0.2 M KCl-HCl mixture, pH 1.8, at 25°C. The intercepts of the straight lines were computed by the method of least squares to be 4.50 and 6.71 respectively.

Acid induced transition of BSA and its fragments

The shift in equilibrium between native and acid denatured states of BSA and its 3 fragments was measured through the change in reduced viscosity and light absorption at 287 nm. Some of the important features of all these transitions are summarized in table 3. Superimposability of the transitions followed by viscosity and difference spectral measurements, was checked by plotting the fraction denatured (calculated as suggested by Tanford, 1968) measured by the two techniques against pH (see figure 5 for a representative curve obtained for the fragment BSA-CNBr₁₈₄₋₅₈₂).

Equilibrium data given in table 3, clearly showed that the pH induced transition of BSA and its fragment BSA-T₃₇₇₋₅₈₂, occurred in two steps involving 3 distinguishable states *N*, *X* and *D*; the transition of the fragments BSA-CNBr₁₋₁₈₃ and BSA-CNBr₁₈₄₋₅₈₂ were essentially a single step process having only native and acid denatured conformational states. All the transitions were found to be reversible since the experimental points in the denaturation as well as the renaturation experiments lied on the same curve (Tanford, 1968) as illustrated in figure 5.

Equilibrium constant

Assuming that the one step acid induced transitions of the fragments, BSA-

Table 3. Important features of the acid induced transitions in BSA and its fragments measured in 0.2 M KCl.

Protein transitions and method	pH for the onset of transition ^a	pH for the middle point of transition	pH for the completion transition	$\ln K_D/\text{pH}$ (slope)	(in
BSA					
(first transition)					
Viscosity	4.30	4.04	3.80	3.11	
Difference spectra	4.45	4.25	3.95	3.68	
BSA					
(second transition)					
Viscosity	3.40	3.15	2.75	2.56	
Difference spectra	3.60	3.14	2.45	1.42	
BSA-CNBr₁₋₁₈₃					
Viscosity	—	3.00	2.25	1.96	
Difference spectra	—	3.10	2.25	1.05	
BSA-CNBr₁₈₄₋₅₈₂					
Viscosity	—	3.20	2.50	2.21	
Difference spectra	—	3.55	2.55	1.09	
BSA-T₃₇₇₋₅₈₂					
(first transition)					
Difference spectra	5.05	4.60	4.00	1.99	
BSA-T₃₇₇₋₅₈₂					
(second transition)					
Difference spectra	3.60	3.25	2.50	3.16	

^apH for the onset of transition for the fragments BSA-CNBr₁₋₁₈₃ and BSA-CNBr₁₈₄₋₅₈₂ could not be measured with precision because the solubility of these fragments was very poor in the neighborhood of pH 5. The dependence of equilibrium constant, K_D , on pH was analysed as described by Wyman (1964). The slopes and the intercepts of the straight lines were calculated by the method of least squares.

drawn by the method of least squares were computed and the values thus obtained are given in table 3. According to the theory of linked function, described by Wyman (1964), the dependence of K_D on pH can be described by the equation

$$-\partial \ln K_D / \partial \text{pH} = \nu H_D - \nu H_N$$

where νH_D and νH_N are the number of protons bound to the acid denatured and native proteins respectively. Thus the slope of the straight line of the type shown in figure 6 (representative plot given for the fragment BSA-T₃₇₇₋₅₈₂) yields the difference between the number of protons bound by the denatured and the native states of the proteins whereas the intercept will give the value of $\log K_D$ which will be independent of pH.

Discussion

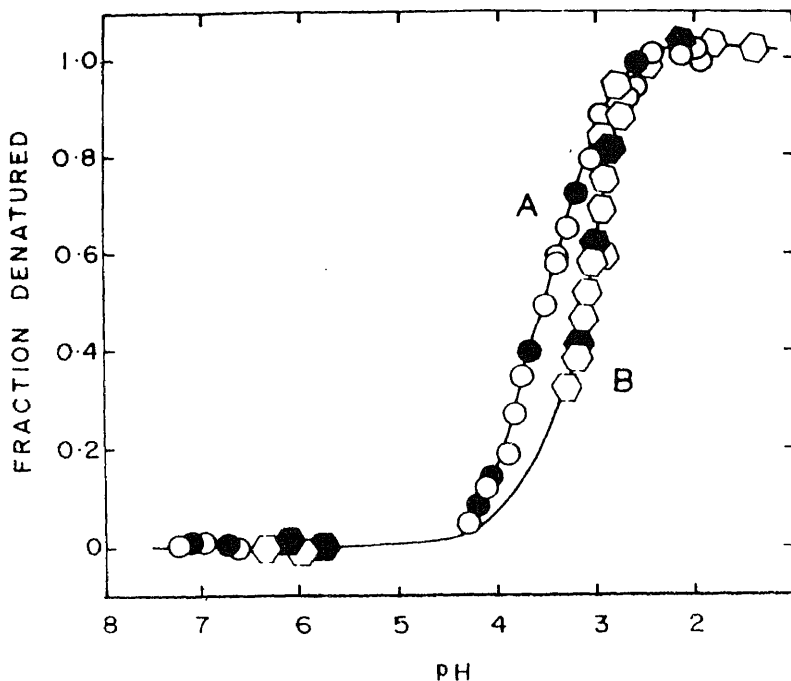


Figure 5. The acid induced transitions of fragment BSA-CNBr₁₈₄₋₅₈₂ as followed by difference spectral (○), and viscosity (◻) measurements. Filled circles and hexagons represent points taken in renaturation experiments. Protein concentrations for the spectral and viscosity measurements were 3.2–2.2 mg per ml respectively.

protein. The first transition, as measured by reduced viscosity, occurred at somewhat lower pH than the transition measured by difference spectroscopy. This would imply that the exposure of aromatic chromophores precedes the overall unfolding of BSA in the pH range 4.5–3.6. Therefore, the reduced viscosity and difference spectral results (see table 3) taken together will be consistent with the following mechanism for the first transition:



where X' and X are distinguishable only by difference spectroscopy. The transition $N \rightarrow X$ was highly cooperative and it was found that the N state must bind about 3 protons (see table 3) in order to be converted to X state which was perhaps similar to 'F' state observed by Foster (1960) during the study on $N \rightarrow F$ transition (Aoki and Foster, 1956).

Although the pH corresponding to the mid-points of the second transitions in BSA as measured by reduced viscosity and spectroscopy, were fortuitously the same, the transition measured by the two properties did not coincide with each other. The acid denatured state, D , detected by reduced viscosity was found to exist at lesser acidic pH than the corresponding state, D' , monitored by difference

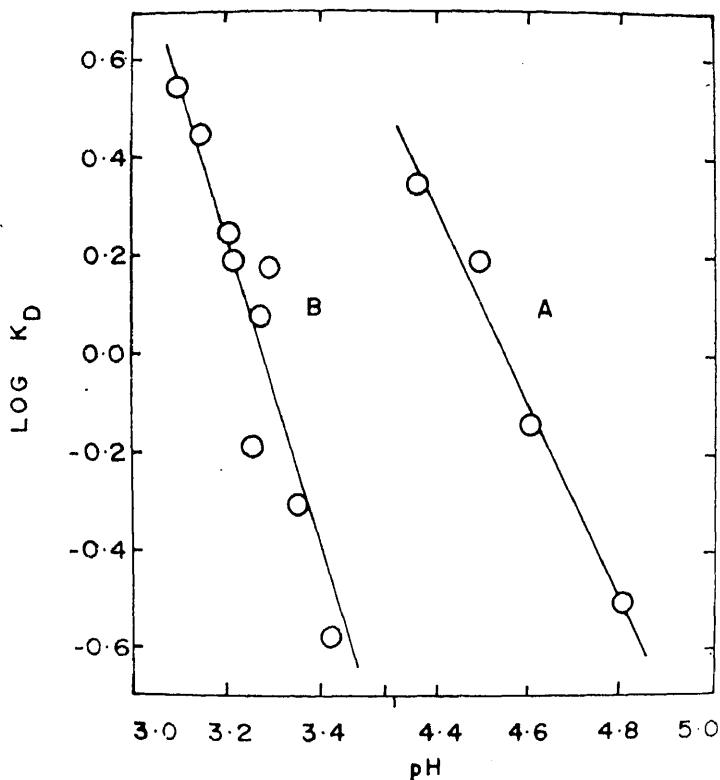


Figure 6. pH dependence of the equilibrium constant, K_D , for the acid induced unfolding of the fragment BSA-T₃₇₇₋₅₈₂ as followed by difference spectral measurements. (A), pH dependence of K_D for the N_F - X_F transition and (B), pH dependence of K_D for the X_F - D_F transition.

transitions were reversible. The two cyanogen bromide fragments underwent a single step transition involving only two major states (native and acid denatured) whereas the tryptic fragment, representing domain III of BSA, showed two step transition involving atleast one stable intermediate state, X_F . As in intact albumin, the unfolding of the fragments BSA-CNBr₁₋₁₈₃ and BSA-CNBr₁₈₄₋₅₈₂ followed by viscometry and spectroscopy, did not appear to be completely concomitant processes. However, the transitions of the fragment BSA-CNBr₁₋₁₈₃ measured by the two techniques are comparable with each other and they are closer to the second transition of intact albumin (see table 3). Likewise, the acid induced transitions (measured by both the techniques) of the fragment BSA-CNBr₁₈₄₋₅₈₂ and the second $X_F \rightarrow D_F$ transition of the fragment BSA-T₃₇₇₋₅₈₂ are closer to the second transition of intact albumin. Furthermore, the first transition ($N_F \rightleftharpoons X_F$) of BSA-T₃₇₇₋₅₈₂ although starts at slightly higher pH, is closer to $N \rightleftharpoons X'$ transition of BSA. It is therefore, possible that the second acid induced transition in BSA might represent the gross unfolding of the protein molecule during which a part of

domains of domain III from each other as well as from the rest of the albumin molecule. The second transition of BSA- $T_{377-582}$ ($X_F \rightarrow D_F$) represents its gross unfolding which is observed in the form of second transition of BSA which also represent the unfolding of domain I and II of the intact albumin. The separation of the sub-domains of domain III (Brown, 1976) from each other (which in our opinion is the cause of $N \rightarrow F$ transition in BSA and the first transition in BSA- $T_{377-582}$), may be facilitated to some extent when it (domain III) is isolated from the rest of the albumin molecule. This explains the early start of the first transition of BSA- $T_{377-582}$ as compared to the first transition of BSA. It is interesting to recall here that a fragment representing domain I+II (BSA- P_{1-385}) of BSA was unable to undergo $N \rightarrow F$ transition and exhibited a single step acid induced transition comparable to the second transition of intact albumin (Khan and Salhuddin, 1984). Furthermore, the reduced solubility of BSA (Khan *et al.*, 1985) and its increased susceptibility towards peptic digestion (Hilak *et al.*, 1974) at about pH 3.6 (known to cause $N \rightarrow F$ transition) without a major structural change, can be explained in terms of the exposure of hydrophobic amino acid residues present at the interface of domains II and III and in the connecting segments of the sub-domains of domain III. Incidentally, such residues constitute about 60% of the total amino acids present in these regions of the albumin molecule (Brown, 1976). The reason why BSA-CNBr $_{184-582}$, which also includes domain III as its constituent, shows a single-step transition is not explainable at this stage. However, one possibility could be that the structural alterations associated with the first transition of domain III had already occurred in fragment BSA-CNBr $_{184-582}$ (domain II + III) during course of its isolation making the latter unable to exhibit a two step-transition. Indeed, our results on hydrodynamic behaviour of the 3 fragments, as described earlier, have shown that fragment BSA-CNBr $_{184-582}$ is asymmetric in nature.

Acknowledgements

The financial assistance from the University Grants Commission, New Delhi, and the facilities from the Aligarh Muslim University and North-Eastern Hill University, are gratefully acknowledged.

References

- Ackers, G. K. (1967) *J. Biol. Chem.*, **242**, 3237.
- Ahmad, F. and Salahuddin, A. (1974) *Biochemistry*, **13**, 245.
- Anfinsen, C. B. and Scheraga, H. A. (1975) *Adv. Protein Chem.*, **29**, 205.
- Ansari, A. A. and Salahuddin, A. (1973) *Biochem. J.*, **135**, 705.
- Aoki, K. and Foster, J. F. (1956) *J. Am. Chem. Soc.*, **78**, 3538.
- Baig, M. A. and Salahuddin, A. (1978) *Biochem. J.*, **171**, 89.
- Baldwin, R. L. (1975) *Annu. Rev. Biochem.*, **44**, 453.
- Baldwin, R. L. (1989) *TIBS*, **14**, 291.
- Bradford, M. M. (1976) *Anal. Biochem.*, **72**, 248.
- Brown, J. R. (1976) *Fed. Proc.*, **35**, 2141.
- Brown, J. R. (1975) *Fed. Proc.*, **34**, 591.
- Brown, J. R. (1977) *Proc. 11th FEBS Meet.*, Copenhagen.
- Creighton, T. E. (1978) *Prog. Biophys. Mol. Biol.*, **33**, 237.
- Foster, J. F. (1960) in *The plasma proteins* (ed. F. W. Putnam) (New York: Academic Press) vol. 1, p. 179.

- Foulk, C. W. and Hollingsworth, M. (1923) *J. Am. Chem. Soc.*, **45**, 1220.
- Habeeb, A. F. S. A. and Atassi, M. Z. (1976) *J. Biol. Chem.*, **251**, 4616.
- Haschemeyer, R. H. and Haschemeyer, A. V. E. (1973) *Proteins: A guide to study by physical and chemical methods* (New York: Wiley).
- Herskovits, T. T. (1967) *Methods Enzymol.*, **11**, 748.
- Herskovits, T. T. and Laskowski, M., Jr. (1962) *J. Biol. Chem.*, **237**, 2481.
- Hilak, M. C., Harmsen, B. J. M., Braam, W. G. M., Joordens, J. J. M. and Vanos, G. A. J. (1974) *Int. J. Pept. Protein Res.*, **6**, 95.
- Johanson, K. O., Wetlaufer, D. B., Reed, R. G. and Peters, T., Jr. (1981) *J. Biol. Chem.*, **256**, 445.
- Khan, M. Y. (1986) *Biochem. J.*, **236**, 307.
- Khan, M. Y., Agarwal, S. K. and Hangloo, S. (1987) *J. Biochem. (Tokyo)*, **102**, 313.
- Khan, M. Y., Roy, Y. B. and Lalthantluanga, R. (1985) *Int. J. Biol. Macromol.*, **7**, 226.
- Khan, M. Y. and Salahuddin, A. (1984) *Eur. J. Biochem.*, **141**, 473.
- King, T. P. and Spencer, E. M. (1970) *J. Biol. Chem.*, **245**, 6134.
- Klee, W. A. (1967) *Biochemistry*, **93**, 514.
- Laurent, T. C. and Killander, J. (1964) *J. Chromatogr.*, **14**, 317.
- Lowry, O. H., Rosebrough, N. J., Farr, A. L. and Randall, R. J. (1951) *J. Biol. Chem.*, **193**, 265.
- Moore, S. and Stein, W. H. (1954) *J. Biol. Chem.*, **211**, 907.
- Paik, W. K. and Kim, S. (1972) *Biochemistry*, **11**, 2589.
- Peters, T., Jr. (1975) in *The plasma proteins* (ed. F. W. Putnam) (New York: Academic press) vol. 1, p. 133.
- Privalov, P. L. (1982) *Adv. Protein Chem.*, **35**, 1.
- Reed, R. G., Feldhoff, R. C., Clute, O. L. and Peters, T., Jr. (1975) *Biochemistry*, **14**, 4578.
- Reed, R. G., Putnam, F. W. and Peters, T., Jr. (1980) *Biochem. J.*, **191**, 867.
- Tanford, C. (1968) *Adv. Protein. Chem.*, **23**, 121.
- Tanford, C. (1961) *Physical chemistry of macromolecules* (New York: Wiley).
- Tanford, C. (1955) *J. Phys. Chem.*, **59**, 798.
- Tanford, C., Buzzell, J., Rands, D. and Swanson, S. (1955) *J. Am. Chem. Soc.*, **77**, 6421.
- Wetlaufer, D. B. (1981) *Adv. Protein. Chem.*, **34**, 61.
- Wetlaufer, D. B. (1973) *Proc. Natl. Acad. Sci. USA*, **70**, 687.
- Wyman, J., Jr. (1964) *Adv. Protein Chem.*, **19**, 223.

Two forms of trehalase in rabbit enterocyte: Purification and chemical modification

S. SANKER* and S. SIVAKAMI†

Department of Life Sciences, University of Bombay, Vidyanagari, Santacruz (E), Bombay 400 098, India

*Present address: Molecular Biophysics Unit, Indian Institute of Science, Bangalore 560 012, India

MS received 5 April 1990; revised 5 October 1990

Abstract. Trehalase found to be associated with the brush border membrane vesicles and the Ca^{2+} aggregated basolateral membrane vesicles were purified to homogeneity. They were found to differ in their molecular weight, subunit structure, heat stability, N-terminal residues, amino acid composition and also the active site residues. Chemical modification showed the presence of a histidine and tyrosine at the active site of brush border membrane vesicle trehalase and two histidines at the active site of basolateral membrane vesicle.

Keywords. Trehalase; brush border membrane; basolateral membrane; chemical modification; rabbit.

Introduction

Trehalase has been purified from rabbit intestinal and renal brush border previously (Galand, 1984; Nakano and Sacktor, 1985; Yokota *et al.*, 1986). These reports are conflicting especially regarding the number of molecular forms, their molecular weights and subunit structure.

While, Galand (1984) reported the presence of only one form of trehalase from the rabbit intestinal and renal brush border, exhibiting identical properties, Nakano and Sacktor (1985) purified 4 forms of trehalase from the rabbit kidney. In the purification procedure reported by Galand (1984) only 45% of total trehalase activity in the crude homogenate was recovered in the brush border membrane vesicles (BBMV). This led us to reinvestigate the behaviour of trehalase in the rabbit small intestine.

Preliminary experiments revealed the presence of two forms of trehalase, one associated with the brush border and the other with the Ca^{2+} aggregated basolateral membrane vesicles (BLMV). The enzymes purified separately differed in many functional and structural properties.

Materials and methods

Trehalose, sucrose, starch, O-dianisidine, glucose oxidase type VII, horse radish peroxidase type II, Triton X-100, Panain type VII, Tris (hydroxymethyl)

aminomethane, bovine serum albumin, phenylmethylsulfonylfluoride (PMSF), acrylamide, methylene bis acrylamide, sodium dodecyl sulphate (SDS) molecular weight markers (MW-SDS-Blue), octyl-agarose, *p*-nitrobenzene sulphonyl fluoride (NBSF), N-acetylimidazole (NAI), N-bromosuccinimide, 2-hydroxy-5-nitrobenzyl bromide, diethylpyrocarbonate, 1-ethyl-3-(3-dimethyl-aminopropyl) carbodiimide, N-ethylmaleimide, *p*-chloromercuri-benzoate, glycine methyl ester, pyridoxal phosphate, trinitrobenzene sulphonic acid, hydroxylamine, dansylchloride and dansyl amino acids were purchased from Sigma Chemical Co., St. Louis, Missouri, USA. DE-52 (DEAE cellulose) was obtained from Whatman Ltd., England. Mercaptoethanol and formic acid were from BDH, England. Folins reagent, ammonium sulphate (enzyme grade) and hydroxyapatite were obtained from Sigma Research Laboratories, Bombay. Tetranitromethane was obtained from Spectrochem Ltd., Bombay.

Assay of trehalase

Trehalase was assayed using Tris-glucose oxidase procedure of Dahlqvist (1958). Sucrose and glucoamylase were assayed in a similar manner using sucrose and starch as substrate. Protein was estimated by the procedure of Wang and Snieszko (1975), a modification of the procedure of Lowry *et al.*, (1951).

Purification of trehalase in the BBM V suspension

Brush border membranes were prepared according to the procedure of Ganapathy *et al.* (1981).

The membrane suspension (1.44 mg/ml protein) was incubated at 37°C with Triton X-100 (v/v) with 1 mM PMSF and 2.5 mM EDTA for 60 min. At the end of the time it was centrifuged at 38,000 *g* for 4 h, in a Sorvall Rc-5B refrigerated centrifuge.

The clear Triton X-100 supernatant containing about 85% trehalase activity was applied to a column of octyl-agarose (1.2 × 2.3 cm, bed volume 2.5 ml) equilibrated with 10 mM sodium phosphate buffer pH 6.8 containing 0.1% Triton X-100.

The column was sequentially washed with 10 bed volumes each, of equilibrating buffer containing 5% Triton X-100, 50% ethylene glycol and 1 M NaCl. The bound trehalase activity was then eluted with 50 mM Tris-HCl buffer pH 7 containing 0.1% Triton X-100. The fractions containing trehalase activity were dialysed against 1 mM sodium phosphate buffer pH 6.8 for 24 h with several changes.

The Tris eluate after dialysis was applied to a 1 ml column of DE-52 equilibrated with 10 mM sodium phosphate buffer pH 6.8 containing 0.1% Triton X-100. Trehalase activity which was held on the column was directly eluted with 200 mM KCl in the equilibrating buffer. The eluate was dialysed and used for further studies.

was solubilised with 1% Triton X-100 (v/v) at 10–15 mg protein concentration. The membranes were incubated with the detergent at 37°C for 60 min and centrifuged at 38,000 *g* for 4 h in Sorvall RC-5B centrifuge.

The clear supernatant was raised to 40% ammonium sulphate concentration. The precipitate was pelleted down at 13,000 *g* for 45 min. The supernatant was raised to 80% ammonium sulphate. The resultant precipitate was pelleted at 13,000 *g*, dissolved in 20 ml of 10 mM sodium phosphate buffer, pH 6.8, containing 0.1% Triton X-100 and dialysed against 1 mM sodium phosphate buffer, pH 6.8, with 4 changes.

The 40–80% precipitate containing the trehalase activity was applied to a column of DE-52 (4 × 1 cm) equilibrated with 10 mM sodium phosphate buffer, pH 6.8, containing 0.1% Triton X-100. The column was washed with 5 bed volumes of the equilibrating buffer and eluted with a linear gradient of 20–200 mM KCl in the equilibrating buffer. The fractions showing trehalase activity were pooled and dialysed against 1 mM sodium phosphate buffer pH 6.8.

The dialysate from above was applied to a column of hydroxyapatite (1.6 × 1.0 cm) equilibrated with 1 mM sodium phosphate buffer, pH 6.8, containing 0.1% Triton X-100. After washing the column with the equilibrating buffer (5 bed volumes), the column was eluted with a linear gradient from 1–50 mM sodium phosphate, pH 6.8, containing 0.1% Triton X-100. The fraction showing trehalase activity were pooled, dialysed against 1 mM sodium phosphate buffer and used for further studies.

Polyacrylamide gel electrophoresis in presence of SDS

Electrophoresis was carried out according to the method of Laemmli (1970) with 12% separating gel. The gels were run at 100 volts till the tracking dye entered the separating gel. The voltage was then increased to 150. The gels were stained with silver according to the procedure of Sammons *et al.* (1981). Prestained molecular weight (M_r) markers used were α_2 -macroglobulin (180,000), β -galactosidase (116,000), fructose-6-phosphate kinase (84,000), pyruvate kinase (58,000), fumarase (48,500), lactic dehydrogenase (38,500) and triose phosphate isomerase (26,600).

Polyacrylamide gel electrophoresis

Electrophoresis was carried out by the method of Laemmli (1970), using 9% running and 4% stacking gels at a constant voltage of 150 volts. The gels as well as electrode buffer contained 0.1% Triton X-100.

Triton X-100 extracts of crude membrane, BBMV and BLMV were applied separately and the run was continued till the tracking dye (bromophenol blue) was run out of gel. After the run, the gels were soaked in 20 mM trehalose in 100 mM sodium phosphate buffer, pH 5.6 and incubated at 37°C for 30 min. The gels were stained for trehalase activity using triphenyltetrazolium chloride in 0.5 N NaOH at 100°C for 10 min (Bhavsar *et al.*, 1983).

N-terminal analysis

Amino acid composition

Amino acid composition was determined after total hydrolysis of the protein on a Beckman automatic amino acid analyser.

Preparation of crude membrane fraction

Rabbit intestinal mucosa was scraped using a blunt knife, after washing with 1.15% KCl. A 20% homogenate was prepared using Potter-Elvehjem type homogeniser in 10 mM sodium phosphate buffer pH 6.8. The homogenate was centrifuged at 13,000 *g* for 90 min. The pellet was resuspended in the same buffer as above using a waring blender operating at maximum speed.

Extraction with n-butanol

The crude membrane suspension was diluted with buffer to give a protein concentration of 6 mg/ml. Equal volume of ice cold n-butanol was added and vortexed for 30 s and centrifuged at 38,000 *g* for 4 h. The aqueous layer was carefully removed and dialysed against 1 mM sodium phosphate buffer, pH 6.8. Trehalase and sucrose were assayed after dialysis.

Butanol extraction was carried out with Triton X-100 extract of BBMV and BLMV by a similar procedure at protein levels of 0.3 mg/ml and 2.5 mg/ml respectively.

Gel permeation chromatography

This was performed on a column of Sephacryl s-200 (0.8 × 100 cm, bed volume 200 ml) equilibrated with 10 mM sodium phosphate buffer, pH 6.8, containing 0.1% Triton X-100. The column was calibrated with the following markers: chymotrypsinogen A (25,000), albumin (egg) (43,000), albumin (bovine) (66,000), aldolase (158,000) and β -amylase (sweet potato) (200,000).

Heat inactivation

Crude membrane suspension, BBMV and BLMV suspension were kept in constant temperature water bath maintained at 55° and 60°C. Aliquots withdrawn at 20 min intervals were chilled in ice immediately and assayed for trehalase activity.

Immunological studies

Male wistar strain rats were immunised with 100 μ g of purified BLMV trehalase with equal volume of Freund's complete adjuvant. After 3 injections at weekly intervals, a booster dose of 200 μ g protein was given. Serum was collected by heart puncture 4 days after the booster dose.

polymerised in 10 mM sodium phosphate buffer pH 7, coated on a microscopic slide. Fifteen μ l of antigen (Triton X-100 extracts of BBMV and BLMV) and 15 μ l of 1:5 dilution antiserum were applied to the wells and allowed to diffuse at 37°C for 8 h.

Chemical modification using group specific reagents

Trehalase was incubated with the respective reagent at 1 mM concentration for 30 min. The reaction was stopped by addition of excess of free amino acids and chilled on ice. The residual activity was determined immediately.

Protection of modification

Trehalose, the substrate and Tris a competitive inhibitor were used for these studies. The enzyme was incubated under identical conditions as for modification with 40 mM trehalose or Tris for 5 min prior to the addition of the reagent. The incubation was continued for 30 min and then dialysed against 1 mM sodium phosphate buffer, pH 6.8, overnight. Trehalase was assayed for after dialysis.

Reversal of diethylpyrocarbonate modification with hydroxylamine

The enzyme was modified with diethylpyrocarbonate (DEPC) (1 mM) and L-histidine (20 mM) was added in equal volume to stop the reaction. Neutralised hydroxylamine (100 mM) (final concentration 50 mM) was added and the incubation continued at 22°C for 30 min. At the end of the time it was dialysed against 1 mM sodium phosphate buffer, pH 6.8 and assayed for trehalase activity.

First order reaction kinetics of DEPC and tetranitromethane modification

The enzyme (5–10 μ g protein) was incubated with varying concentration of respective reagents under conditions described earlier. Aliquots of 20 μ l were withdrawn at specific intervals were mixed with equal volume of respective amino acid, and chilled on ice. The residual activity was determined immediately. The theoretical basis for the calculation of the first and the second order rate constants are as described in Levy *et al.* (1963).

Results and discussion

The results summarised in table 1 provide evidence for the presence of two forms of trehalase in the rabbit enterocyte, one sedimenting with the brush border membrane and the other with the Ca^{2+} aggregated basolateral membrane vesicles. Of the total activity in the crude homogenate one half is present each in BBMV and

Table 1. Biochemical properties exhibited by the two forms of trehalase.

Experiment	BBMV trehalase	BLMV trehalase
Localization	Brush border membrane	Probably basolateral membrane
n-Butanol	inactivated	Solubilised in active form
(NH ₄) ₂ SO ₄ fractionation	0–40% saturation	40–80% saturation
M _r on SDS electrophoresis	165,000	97,000
M _r on Sephacryl S-200 gel filtration	165,000	97,000
Stokes radius	50 Å	39 Å
Octyl-agarose hydrophobic chromatography	Bound eluted with 100 mM Tris/HCl, pH 7	Excluded
Heat inactivation at 55°C, 60 min	90% inactivation	25% inactivation
Immunological cross reactivity	Cross reaction	Cross reaction
N-Terminal residues	Tyrosine	Arginine

Electrophoresis of the crude membrane fraction homogenised and solubilised in the presence of PMSF distinguished two well separated bands of trehalase activity.

The BBMV trehalase has been purified to homogeneity using a single chromatography step on octyl-agarose. Other purification procedures reported involve 6–8 steps with low final recoveries (Galand, 1984; Yokota *et al.*, 1986). The strong affinity showed by the BBMV trehalase for octyl-agarose appears to be a highly hydrophobic protein. The mechanism by which Tris elutes the bound enzyme is not clear, although it appears that Tris probably acts as a 'deformer' and brings about a conformational change (Shaltiel, 1984). The purified enzyme showing a specific activity of 66.66 was purified 45-fold with respect to brush border vesicles (table 2).

BLMV trehalase was purified using conventional protein purification procedures.

Table 2. Purification of trehalase from the BBMV and BLMV of the rabbit small intestine.

Fraction	Activity (μ/ml)	Total units	Protein (mg/ml)	Total protein (mg)	Specific activity	Fold purification
BBMV						
BBMV suspension	2.1	210	1.44	144	1.46	0
Triton X-100 supernatant	1.0	180	0.481	88	2.08	1.42
Octyl-agarose Tris eluate	1.2	120	0.018	1.8	66.66	45.78
BLMV						
BLMV suspension	1.96	196	24.4	2440	0.077	0
Triton X-100 supernatant	1.10	176	1.30	208	0.84	10.9

The preparation showed a specific activity of 65.36 and was 822-fold purified over the Ca^{2+} aggregated membranes (table 2). The enzyme was completely excluded from octyl-agarose, the activity emerging in the flow through.

Both the purified proteins migrated as a single band in the presence of SDS. There was a marked difference in the electrophoretic pattern of the two enzymes. Where as the BBMV trehalase appears to be a homodimer of M_r 78,000 daltons, the BLMV trehalase was found to be a monomer of M_r 97,000 daltons. The M_r and subunit structure of BBMV trehalase correlated well with already reported values (Galand, 1984; Yokota *et al.*, 1986).

Amino acid composition showed a higher amount of hydrophobic amino acids in BBMV trehalase than BLMV enzyme (table 3). This may explain the affinity

Table 3. Amino acid composition of BBMV and BLMV trehalase (residues/mol^a.)

Amino acid	BBMV trehalase	BLMV trehalase
Aspartate	155	77
Threonine	101	68
Serine	107	60
Glutamate	144	73
Proline	75	51
Glycine	170	78
Alanine	154	78
Cystine	14	8
Valine	109	92
Methionine	28	16
Isoleucine	67	41
Leucine	152	70
Tyrosine	50	34
Phenylalanine	66	35
Histidine	12	9
Lysine	92	45
Arginine	57	76
Hydrophobic amino acids ^b	548	316

^aAmino acids, residues/mol with respect to histidine.

^bPhenylalanine, leucine, isoleucine, valine and alanine are taken as hydrophobic amino acids.

exhibited by the enzyme for octyl-agarose. The two trehalases differ in sensitivity to heat (figure 1) and n-butanol. Double immunodiffusion showed a single continuous precipitin line indicating that the proteins are immunologically identical.

Chemical modification of BBMV trehalase

BBMV trehalase was inactivated by DEPC, a histidine modification reagent (Burstein *et al.*, 1974; Miles, 1977; Daron and Aull, 1982) and the 3 tyrosine modification reagents [tetranitromethene (TNM), *p*-nitrobenzene sulphonyl fluoride (NBSF) and N-acetylimidazole (NAI)] (Riordan and Vallee, 1972a, b; Glazer *et al.*, 1976; Bunning *et al.*, 1978; Liao, 1982). The other reagents had no effect on activity.

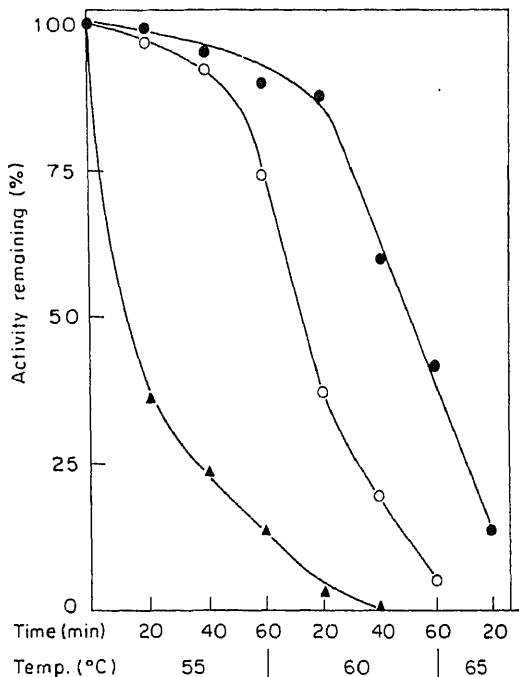


Figure 1. Heat inactivation profiles of crude membrane fraction (●), BLMV suspension (○) and BBMV suspension (▲).

Inactivation of BBMV trehalase by DEPC

A first order plot was constructed from the inactivation curves obtained at different concentrations of DEPC (300–500 μM). The plot of $\log K_{\text{app}}$ as a function of (DEPC) concentration gave a slope of 1.04, indicating that reaction with a single molecule of DEPC was probably sufficient to inactivate the enzyme (figure 2). The second order rate constant was calculated to be $0.076 \text{ min}^{-1} \cdot \text{mM}^{-1}$.

Trehalose the substrate, protected the enzyme from inactivation at 40 mM concentration. The modification by DEPC was reversed by treating the modified enzyme with hydroxylamine (Boopathy and Balasubramanian, 1985; Burstein *et al.*, 1974). A non-specific modification of tyrosine or lysine is not reversed by hydroxylamine (Burstein *et al.*, 1974; Boopathy and Balasubramanian, 1985; Baskaran and Balasubramanian, 1987). Reversal of DEPC modification of BBMV trehalase was to the extent of 79%.

Carbethoxy histidine shows a specific absorption at 242 nm. Absorption spectra of the modified enzyme could not be recorded due to the presence of Triton X-100 in the enzyme. Keeping the enzyme in 0.1% Triton X-100 was absolutely necessary as the enzyme rapidly lost activity in the absence of the detergent.

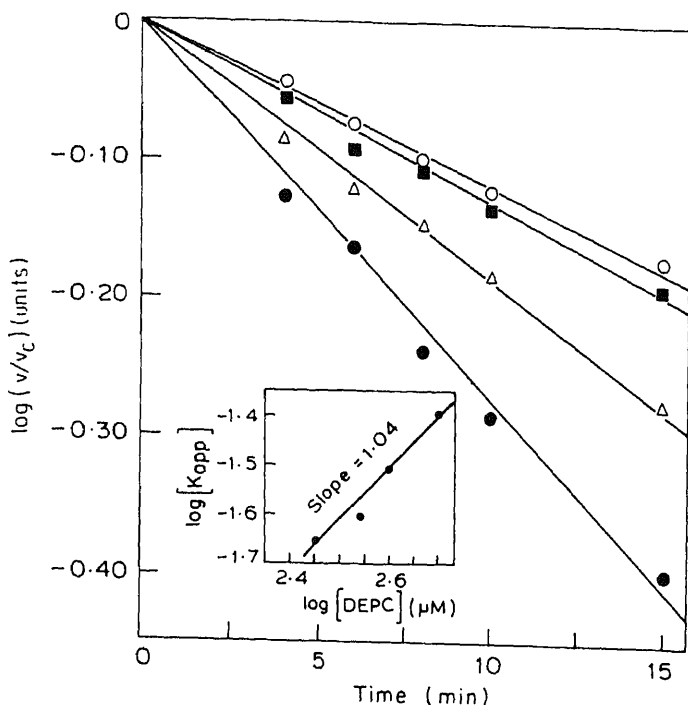


Figure 2. First order plots of inactivation of trehalase associated with BBMV by DEPC. Inactivation was carried out at different concentrations of DEPC (\circ , 300 μM ; \blacksquare , 350 μM ; \blacktriangle , 400 μM ; \bullet , 500 μM). v/v_c is the ratio of remaining activity to activity of uninhibited enzyme. Inset: Second order plot of the pseudo first order rates (K_{app}) of inactivation of different concentrations of DEPC (300–500 μM).

(10 mM)] inactivated the enzyme (Riordan and Vallee, 1972; Glazer *et al.*, 1976; Liao, 1982).

TNM was used to study the kinetics of inactivation due to its high specificity for tyrosine at pH 8 (Riordan and Vallee, 1972a, b). The rate of inactivation, at different concentrations of TNM (2–10 mM) was determined as described. The plot of $\log K_{app}$ against \log (TNM) concentration gave a straight line with a slope of 0.9, indicating that interaction with a single molecule of TNM resulted in inactivation of the enzyme (figure 3). Trehalose, the substrate and Tris a competitive inhibitor protected the enzyme from inactivation at 40 mM concentration.

Spectral studies showed a λ_{max} at 350 nm. Although nitroformate ion, a byproduct of TNM, absorbs at 350 nm, appearance of a 350 nm peak can serve as a qualitative gauge for TNM modification (Riordan and Vallee, 1972a, b). The second order rate constant for TNM modification of BBMV trehalase was $0.00526 \text{ mM}^{-1} \text{ min}^{-1}$.

The above results indicate the possible presence of one histidine and one tyrosine at the active site of BBMV trehalase.

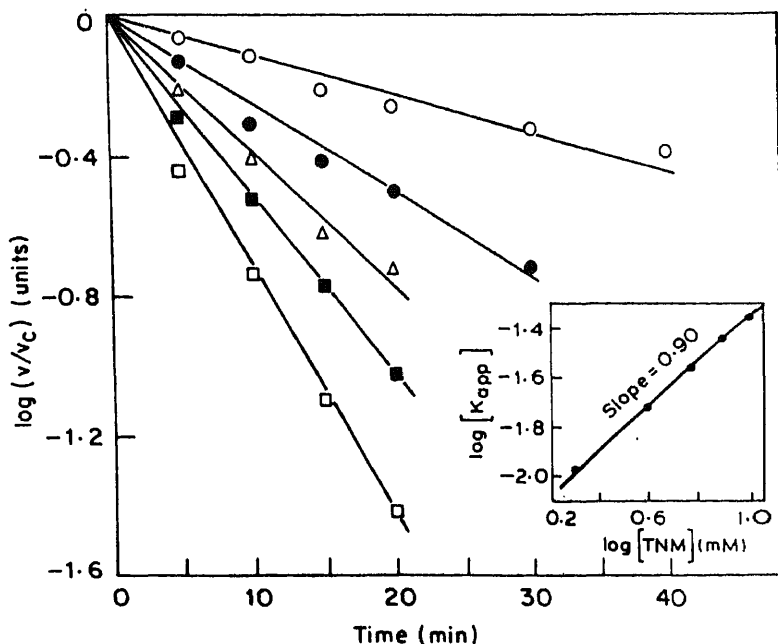


Figure 3. First order plots of inactivation of trehalase associated with BBM V. Inactivation was carried out at different concentrations of TNM (\circ , 2 mM; \bullet , 6 mM; \blacksquare , 8 mM; \square , 10 mM). v/v_c is the ratio of remaining activity to uninhibited enzyme. Inset: Second order plot of the pseudo first order rate inactivation at different concentrations of TNM (2–10 mM).

Inactivation of BLMV trehalase by DEPC

A first order plot was constructed from the inactivation curves obtained at concentrations of DEPC (600 μ M to 1 mM).

The plot of $\log K_{app}$ against \log (DEPC) concentration gave a slope indicating the possible need for two molecules of DEPC to inactivate the (figure 4). The second order rate constant was found to be 0.02190 mM^{-1} . Trehalose at 40 mM concentration protected the enzyme from modification by DEPC.

Since the modification was reversed by treating the modified enzyme with hydroxylamine at neutral pH, it is not modifying a tyrosine or lysine residue specifically (Burstein *et al.*, 1974; Boopathy and Balasubramanian, 1985; Sanker and Sivakami, 1987). The modification of the enzyme by DEPC was

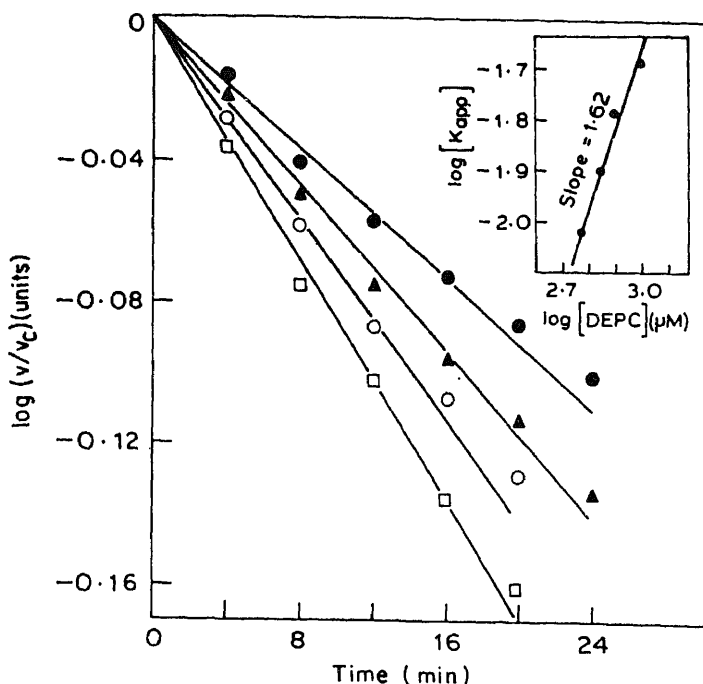


Figure 4. First order plots of inactivation of trehalase associated with BLMV by DEPC. Inactivation was carried out at different concentrations of DEPC (○, 600 μM ; ▲, 700 μM ; ●, 800 μM ; □, 1000 μM). v/v_c is the ratio of remaining activity to activity of uninhibited enzyme. Inset: Second order plot of pseudo first order rates (K_{app}) of inactivation at different concentrations of DEPC (600–1000 μM).

of little dietary significance in mammals, it is possible that, trehalase in mammalian intestine is involved in other physiological functions. The difference in the active site residues between the two forms of trehalase may possibly be serving different functions at the brush border and the basolateral membrane.

Acknowledgements

This work was supported by a grant from the University Grants Commission, New Delhi. One of the authors (S. S.) acknowledges the receipt of a fellowship from the University Grants Commission, New Delhi.

References

- Baskaran, S. and Balasubramanian, K. A. (1987) *Biochim. Biophys. Acta*, **913**, 337.
- Bhavsar, P. N., Rodrigues, V. and Siddiqi, O. (1983) *J. Biosci.*, **5**, 279.
- Boonath, P. and Balasubramanian, K. A. (1985) *Eur. J. Biochem.*, **151**, 351.

- Daron, H. H. and Aull, J. L. (1982), *Biochemistry*, **21**, 737.
- Fujita, M., Ohta, H., Kawai, K., Matsui, H. and Nakao, M. and Nakao, M. (1972) *Biochim. Biophys. Acta*, **274**, 336.
- Galand, G. (1984) *Biochim. Biophys. Acta*, **789**, 10.
- Ganapathy, V., Mendicino, F. J. and Leibach, F. (1981) *J. Biol. Chem.*, **256**, 118.
- Glazer, A. N., Delange, R. J. and Sigman, D. S. (1976) *Lab. Tech. Biochem. Mol. Biol.*, **4**, 68.
- Hartly, B. S. (1970) *Biochem. J.*, **119**, 805.
- Laemmli, U. K. (1970) *Nature (London)*, **227**, 680.
- Levy, M. H., Leber, P. D. and Ryan, E. M. (1963) *J. Biol. Chem.*, **238**, 3654.
- Liao, T. H. (1982) *J. Biol. Chem.*, **257**, 5637.
- Lowry, O. H., Roseborough, N. J., Farr, A. L. and Randall, R. J. (1951) *J. Biol. Chem.*, **193**, 265.
- Miles, E. W. (1977) *Methods Enzymol.*, **47**, 149.
- Nakano, M. and Sacktor, B. (1984) *Biochim. Biophys. Acta*, **791**, 45.
- Nakano, M. and Sacktor, B. (1985) *J. Biochem.*, **97**, 1329.
- Ouchterlony, O. (1970) *Handbook of Immunodiffusion and Immunelectrophoresis*, (Ann Arbor)
- Riordan, J. F. and Vallee, B. L. (1972a) *Methods Enzymol.*, **25**, 500.
- Riordan, J. F. and Vallee, B. L. (1972b) *Methods Enzymol.*, **25**, 515.
- Sacktor, B. (1968), *Proc. Natl. Acad. Sci. USA*, **60**, 1007.
- Sammons, W., Adams, L. D. and Nishizawa, E. E. (1981) *Electrophoresis*, **2**, 135.
- Sanker, S. and Sivakami, S. (1988), *J. Biosci.*, **13**, 153.
- Semenza, G. (1986) *Annu. Rev. Cell. Biol.*, **2**, 255.
- Shaltiel, S. (1984) *Methods. Enzymol.*, **104**, 69.
- Wang, C. S. and Smith, R. L. (1975) *Anal. Biochem.*, **63**, 414.
- Yokota, K., Nishi, Y. and Takesue, Y. (1986) *Biochim. Biophys. Acta*, **881**, 405.

Adenosine and ATP: mutually exclusive modifiers of the kinetics of ADP-induced aggregation of calf-platelets

M. JAMALUDDIN† and L. K. KRISHNAN*

Thrombosis Research Unit, Biomedical Technology Wing, Sree Chitra Tirunal Institute for Medical Sciences and Technology, Trivandrum 695 012, India

*Present address: School of Dentistry, Department of Preventive Sciences, Minneapolis, MN 55455, USA

MS received 30 July 1990; revised 9 November 1990

Abstract. Modulations of initial rate kinetics of ADP-induced aggregation of citrated calf platelet-rich plasma by adenosine and ATP were investigated employing a spectrophotometric platelet aggregation assay. The data were analysed according to the tenets of the sequential shape-change and interaction model of aggregation. Adenosine and ATP increased the slopes and intercepts of double-reciprocal plots of ADP-aggregation kinetics. Examination of their slope and intercept effects together with their effects individually and in combination, on aggregation rates, suggested that adenosine and ATP acted at multiple, nonoverlapping, sites.

Keywords. Platelet; aggregation; kinetics; ADP; adenosine; ATP (calf).

Introduction

Aggregatory reactions of blood platelets mediated by external stimuli, crucial as they are for normal haemostasis could also lead to debilitating pathological conditions (Zucker, 1980). Mechanisms are needed, therefore, to modulate or delimit their physiological response to stimuli if platelets are to meet the varying demands and exigencies of the vascular system without incapacitating it. Unravelling such mechanisms kinetically employing isolated platelets, besides being of intrinsic merit, could also help to glean insights into mechanisms operating generally to modulate intercellular interactions mediated by external stimuli. In order to facilitate this type of investigations with platelets we have recently worked out a convenient spectrophotometric method of following initial rates of calf platelet aggregation (Jamaluddin and Krishnan, 1987a; Jamaluddin *et al.*, 1987; Sreedevi *et al.*, 1987). To facilitate rational interpretation of rate data a rate equation for platelet aggregation based on a sequential shape-change and interaction model has also been worked out (Jamaluddin and Krishnan, 1987b).

We have employed these two tools to investigate the modification of the kinetics of ADP-induced aggregation of citrated platelet-rich plasma by the antagonists adenosine and ATP. The results, reported here, suggest that these antagonists might interact at mutually exclusive sites on calf platelets and point to a possible physiological significance of shape-change reactions of platelets.

Materials and methods

ADP, ATP (sodium salts) and adenosine purchased from Sigma Chemical Co., Louis, Missouri, USA were used as their freshly prepared aqueous solutions. The concentrations were determined spectrophotometrically using E_{M259} of $15.4 \text{ M}^{-1} \text{ cm}^{-1}$.

Platelet-rich plasma (PRP), platelet-poor plasma (PPP) and gel-filtered platelet (GFP) were prepared at ambient temperature (30°C) as described before (Jamaluddin and Krishnan, 1987a; Jamaluddin *et al.*, 1987).

Rates of platelet aggregation were measured as described before (Jamaluddin and Krishnan, 1987a; Jamaluddin *et al.*, 1988). Briefly, PRP diluted with PPP or GFP diluted with gel-filtration buffer, (1 ml) was taken in each of a pair of rectangular siliconized glass cuvettes (pathlength 10 mm) and placed in the reference and sample positions of a thermostated cuvette holder of a Shimadzu UV240 spectrophotometer set at 540 nm. The temperature of the cuvette holder was maintained at $32 \pm 0.1^\circ\text{C}$ by circulating water from a constant temperature bath. Aggregation reaction was initiated by stirring in the agonist to the sample cuvette using siliconized glass plunger. Turbidity changes due to activation and aggregation of platelets were recorded differentially against the turbidity of the reference cuvette as a function of time. Aggregation rates were calculated from slopes of the initial descending parts of the turbidity curve (Jamaluddin and Krishnan, 1988; Jamaluddin *et al.*, 1988).

Other experimental details are as given in the figure legends.

Rate data were analysed using double-reciprocal plots or Edie type of plots or fitting them to the equation (Jamaluddin and Krishnan, 1987b):

$$\gamma_0 = \frac{RA}{S_{0.5} + A}$$

according to the method of Wilkinson (1961). In equation (1) R is the maximal rate, A the agonist concentration and $S_{0.5}$ the half-maximal saturation concentration of the agonist, that is, agonist concentration at which $\gamma_0 = 0.5 R$.

Results

The alteration of aggregation rates (γ_0) of calf PRP as a function of ADP concentrations was hyperbolic as reported previously (Jamaluddin and Krishnan, 1987a) giving linear double-reciprocal plots both in the absence and in the presence of adenosine or ATP (figures 1 and 3). Adenosine at lower concentrations increased the slopes and at higher concentrations the intercepts as well of double-reciprocal plots (figure 1). Edie type graphical presentation of data, considered to be statistically superior to double-reciprocal plots for detecting deviations from linearity (Wong, 1975), brought out the effect of adenosine on R values (abscissa intercepts) more clearly (figure 2) and plots of the data according to Corni-Bowden (1974) yielded converging lines (not shown). Moreover fitting the data to

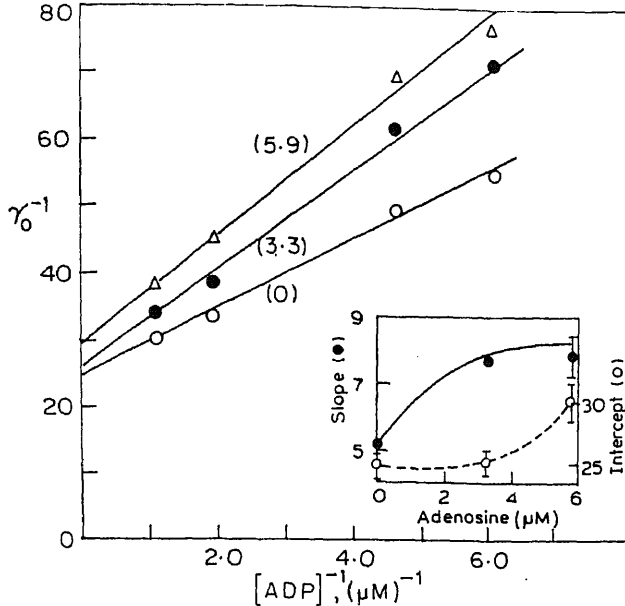


Figure 1. Effect of adenosine on the initial rates of aggregation of calf PRP by ADP, reported as double-reciprocal plots. The numbers below the lines indicate the concentrations (μM) of adenosine the PRP ($A_{540}=0.46$) was preincubated with, for 1 min, before initiating aggregation by adding ADP. *Inset:* Replots of intercepts (\circ) and slopes (\bullet) (in arbitrary units) against adenosine concentration. Intercepts and slopes and their standard errors were obtained by linear regression analysis. Standard errors larger than the symbols are shown. Aggregation rates were variable with donors and platelet preparations but the effects reported were reproducible. Results of one experiment representative of 5 similar others reported.

rate measurements in the presence of adenosine preceded those in its absence showing that the change in the R values was not because of a desensitization of platelets to ADP with time.

In order to delineate whether inhibition by adenosine could be by a modifier type of function as indicated by its intercept effect on double-reciprocal plots γ_0 was measured at fixed (nonsaturating) concentrations of ADP as a function of increasing adenosine concentrations and $(\gamma_0)^{-1}$ were plotted against adenosine concentration. These plots reached plateaus (not shown) suggesting that the inhibition was by a modifier type of function so that total inhibition could not be attained.

Since adenosine and ATP affected both intercepts and slopes of double-reciprocal plots it was of interest to know whether they acted at mutually exclusive sites or not. If they act at totally independent specific sites the fractional inhibition, y , obtainable when both are simultaneously present at individually saturating concentrations, is given by (Webb, 1963):

$$y = x_1 + x_2 - x_1x_2 \quad (2)$$

where x_1 is the fractional inhibition at saturating adenosine and x_2 that at saturating ATP. If they act at the same site, however, mutual antagonism will make y to be bounded by x_1 and x_2 . The results of an experiment of this type are presented in table 1. Adenosine produced a fractional inhibition (x_1) of 0.25 and ATP a

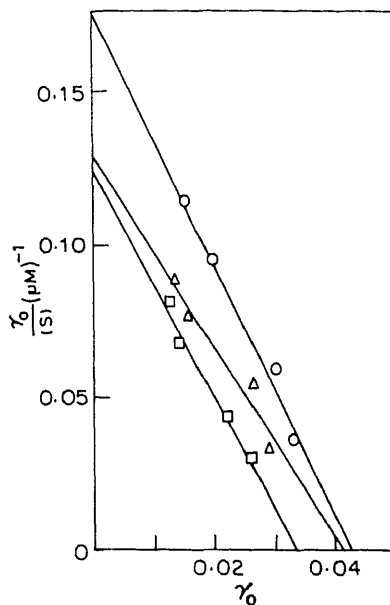


Figure 2. Edie plot of the data presented in figure 1. (O), Data in the absence of adenosine; (Δ), in the presence of 3.3 μM -adenosine; (□), in the presence of 5.9 μM -adenosine.

fractional inhibition (x_2) of 0.45. ATP and adenosine together should give, according to equation (1), a fractional inhibition of 0.59 if they were to act at independent sites, and the fractional inhibition should fall between 0.25 and 0.45, if they were to act at the same site(s). The observed inhibition of 0.60 showed that the two modifiers acted at totally independent sites.

Discussion

Adenosine and ATP are seen to increase both the slopes and intercepts of double-reciprocal plots of ADP-induced aggregation kinetics of calf PRP as followed by the spectrophotometric method. As anticipated, they were also found to inhibit by a modifier type of function and γ_0 values remained finite at infinite modifier concentrations. Essentially the same type of results was obtained with GFP, which suggest that plasma factors are not responsible for the kinetic results (data not shown). Although keeping platelet preparations for longer than 2 h led to a desensitization to ADP the intercept effects could not be attributed to this desensitization because interchanging rate assays in the absence and in the presence of modifiers had no effect on the results.

Skoza *et al.* (1967) found adenosine to increase only the slopes of double-reciprocal plots of ADP-induced aggregation of human citrated PRP but Macfarlane and Mills (1975) found that adenosine inhibition was not completely

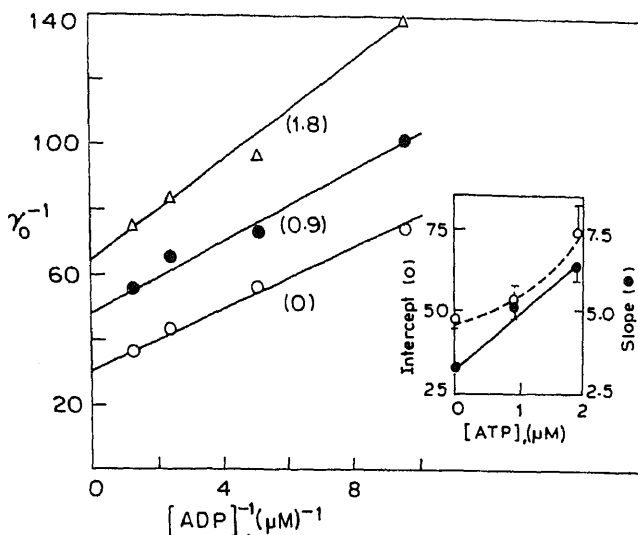


Figure 3. Effect of ATP on the initial rates of platelet aggregation by ADP reported as double-reciprocal plots. The numbers below the lines indicate the concentrations (μM) of ATP the PRP ($A_{540}=0.4$) was preincubated with, for 1 min, before initiating aggregation by adding ADP. Replots of intercepts (○) and slopes (●), in arbitrary units, are shown in the inset. Intercepts and slopes and their standard errors were obtained by linear regression analysis. Standard errors larger than the symbols are shown. Aggregation rates varied with donors and platelet preparations but the effects reported were reproducible. Results of one experiment out of three with similar results reported.

et al., 1983; Huettemann *et al.*, 1984) with different affinities (Huettemann *et al.*, 1984). Therefore noncompetitive inhibition observed by Macfarlane and Mills (1975) and Salzman *et al.* (1969) with human platelets is in agreement with its mode of action. The results of the present paper appear to suggest that Edie and Cornish-Bowden graphical presentations may be better for discriminating between inhibitory mechanisms in aggregation kinetics.

The intercept effects of ATP on double-reciprocal plots of ADP-induced aggregation of calf PRP was clearly more marked (figure 3) than was the case with adenosine. Macfarlane and Mills (1975) found that inhibition of ADP-induced aggregation of human PRP was almost completely overcome by ADP but they also state that the conventional photometric aggregation assay employed by them was insensitive to small changes in aggregation rates. The spectrophotometric method employed by us has good sensitivity and precision (Jamaluddin and Krishnan, 1987a). The data in figure 3 clearly show that ATP inhibition of ADP-induced aggregation of calf platelets was not of a competitive type. The intercept and slope effects of adenosine and ATP exhibited in figures 1 and 3 may be rationalized in terms of the sequential shape-change and interaction model (Jamaluddin and Krishnan, 1987b) as follows:

$$A + P \xrightleftharpoons[k_{-1}]{k_1} AP \xrightleftharpoons[k_{-2}]{k_2} AP^* \xrightarrow{k_3} \text{Aggregated state} \quad (2)$$

Table 1. Inhibition of ADP-induced aggregation of calf platelets by ATP and adenosine separately and in combination.

Addition	γ_0	Fractional inhibition
None	0.020	—
Adenosine (6 μ M)	0.015	0.25
ATP (1.6 μ M)	0.011	0.45
Adenosine (6 μ M) + ATP (1.6 μ M)	0.008	0.60

The PRP ($A_{540}=0.587$) was preincubated with the inhibitor, at the indicated concentrations, for 1 min before initiating aggregation reaction by the addition of ADP (0.16 μ M). At this concentration of ADP, the concentrations of adenosine and ATP employed were found to be saturating, in separate experiments. In the experiment in which both inhibitors were present, ATP was added immediately after adenosine, and preincubated for 1 min. The average of duplicate initial rate measurements, the values of which agreed within 2%, is given. Aggregation rates as well as fractional inhibitions were variable with donors and platelet preparations but the effects reported were reproducible.

In this model P represents nonaggregable discoid platelets which interact specifically with an agonist A to form a platelet-agonist complex, PA , which upon being converted sequentially to shape-changed platelet forms, P^* and P^{**} , leads to their aggregatory reaction with a rate constant k . An antagonist A^* may interact reversibly and specifically with P to form a platelet antagonist complex PA^* as shown. K_i is an equilibrium constant of the reaction represented.

This model leads to a rate equation which in double-reciprocal form, is given by:

$$(\gamma_0)^{-1} = \frac{K_1^\gamma K_2^\gamma K_3^\gamma \left[1 + \frac{(A^*)}{K_4^\gamma} \right]}{k(P_\gamma)} (A)^{-1} + \frac{1 + K_3^\gamma + K_2^\gamma K_3^\gamma}{k(P_\gamma)} \quad (3)$$

where P_γ stands for the total platelet concentration and K_1^γ for the inverse of K_1 . Equation (3) shows that A^* increases slopes of double-reciprocal plots in a concentration-dependent manner, without affecting their intercepts (competitive inhibition).

If A^* interacts with a platelet form different from that which interacts with A , for example PA in the model depicted above, the rate equation in double-reciprocal form becomes:

$$K_1^\gamma K_2^\gamma K_3^\gamma \left\{ 1 + K_4^\gamma + K_2^\gamma K_3^\gamma (1 + (A^*)/K_4^\gamma) \right\}$$

between PA and A^* . A^* is seen to increase the intercepts of double-reciprocal plots without affecting their slopes. This is true if A^* reacts with P^* or P^{**} instead of PA (uncompetitive inhibition).

Since adenosine and ATP increased both slopes and intercepts of double-reciprocal plots they may be said to interact with a platelet form that interacts with ADP as well as with other forms. The occurrence of intercept effects accounts for the inability of ADP to completely overcome the inhibitory effects of the antagonists.

ATP is widely regarded as a competitive inhibitor of ADP-induced aggregation and is used to ascertain the role of released ADP in platelet aggregation mediated by other agonists (Burch and Lamb 1983). In the light of the results of this paper it appeared that species-dependent variation in the mechanism of inhibition of ATP could exist.

The inability of platelet preparations to keep for sufficiently long periods made ascertaining the patterns of change of slopes and intercepts over wide ranges of adenosine and ATP concentrations, impracticable. Therefore the patterns of change shown in the insets of figures 1 and 3 with only two concentrations of the modifiers can, at best, be treated as being qualitative but the data did, however, show that both modifiers interacted at more than one site at the platelet surface. Interestingly the sites of one modifier seemed, according to the present method of analysis, to exclude those of the other (table 1).

Some speculation as to the physiological significance of the kinetic results seems to be warranted. Modulations of responsiveness of platelets when cooperativity is absent as in the case of ADP-induced aggregation, by realistic changes in the levels of an individual modifier acting at a single site cannot be large. Having the modifier act at more than one site will improve the situation which will be better still if it can act in concert with others acting similarly at exclusive sites. This, seen in the light of the kinetic models (equation 2) leading to equations 3 and 4, may well be the evolutionary advantage of setting shape-change reactions in multiple, reversibly-connected, steps each involving a chain of interacting biochemical and biophysical events, between agonist interaction and aggregation. Shape-change reactions then appear purposive and physiologically relevant.

Acknowledgements

We thank Jose Jacob for technical assistance. This work was supported by a grant from the Department of Science and Technology, New Delhi.

References

- Burch, J. W. and Lamb, R. J. (1983) *Thromb. Res.*, **31**, 747.
- Cornish-Bowden, A. (1974) *Biochem. J.*, **137**, 143.

- Salzman, E. W., Ashford, T. P., Chambers, D. A., Neri, L. L. and Dempster, A. P. (1969) *Am. J. Physiol.*, **217**, 1330.
- Skoza, L., Zucker, M. B., Jerushalmy, Zucker and Grant, R. (1967) *Thromb. Diath. Haemorrh.*, **18**, 713.
- Sreedevi, C., Thomas, A. and Jamaluddin, M. (1987) *Curr. Sci.*, **56**, 483.
- Webb, J. L. (1963) *Enzymes and metabolic inhibitors*, Volume 1 (New York: Academic Press).
- Wilkinson, G. N. (1961) *Biochem. J.*, **80**, 324.
- Wong, J. T-F. (1975) *Kinetics of enzyme mechanisms* (London: Academic Press).
- Zucker, M. B. (1980) *Sci. Am.*, **242**, 86.

Purification and characterization of cathepsin B from goat brain

RAMESH C. KAMBOJ, SURESH PAL and HARI SINGH*

Biochemistry Laboratory, Department of Chemistry, Kurukshetra University, Kurukshetra 132 119, India

MS received 22 June 1990; revised 15 November 1990

Abstract. Cathepsin B was purified to an apparent homogeneity from goat brain utilizing the techniques of homogenization, autolysis at pH 4, 30-70% $(\text{NH}_4)_2\text{SO}_4$ fractionation, Sephadex G-100 column chromatography, organomercurial affinity chromatography and ion-exchange chromatography on CM-Sephadex C-50. The enzyme had a pH optima of 6 with α -N-benzoyl-D, L-arginine- β -naphthylamide, benzyloxycarbonyl-arginine-arginine-4-methoxy- β -naphthylamide and azocasein as substrates. The K_m values for the hydrolysis of α -N-benzoyl-D, L-arginine- β -naphthylamide and benzyloxycarbonyl-arginine-arginine-4-methoxy- β -naphthylamide were 2.36 and 0.29 mM respectively in 2.5% dimethylsulphoxide. However, the corresponding K_m values for these substrates in 1% dimethylsulphoxide were 0.51 and 0.09 mM. The enzyme was strongly inhibited by thiol inhibitors and tetrapeptidyl chloromethylketones. Leupeptin inhibited the enzyme competitively with K_i value of 12.5×10^{-9} M. Dithioerythritol was found to be the most potent activator of this sulfhydryl protease. Molecular weight estimations on sodium dodecyl sulphate-polyacrylamide gel electrophoresis and on analytical Sephadex G-75 column were around 27,000 and 29,000 daltons respectively. Cathepsin B was found to reside in the lysosomes of goat brain. The highest percentage of cathepsin B was in cerebrum. However, the specific activity of the enzyme was maximum in pituitary gland.

Keywords. Cathepsin B; brain; thiol protease.

Introduction

Lysosomal proteinases are primarily responsible for the turnover of intracellular proteins (Dean, 1975; Segal, 1975; Ward *et al.*, 1977). These may also serve more specialized functions such as enzyme activation (Neurath and Walsh, 1976; Uy and Wold, 1977) or conversion of precursor proteins to their active forms. Among the lysosomal enzymes, cathepsin B (EC 3.4.22.1) has been implicated in the formation of insulin from proinsulin in pancreas (Smith and Van Frank, 1975) and albumin from proalbumin in the liver (Quinn and Judah, 1978). This enzyme has also been found to be involved in various diseased conditions like invasion and metastasis of tumors (Sylvén, 1974; Poole *et al.*, 1978; Sloane *et al.*, 1986), muscular dystrophy (Sher *et al.*, 1981; Noda *et al.*, 1981), emphysema (Burnett *et al.*, 1983), rheumatoid inflammation (Ostensen, 1983) and pancreatitis (Shikimi *et al.*, 1987).

In the central nervous system, small bioactive peptides act as neurotransmitters and regulators of various metabolic activities. The generation/inactivation of these bioactive peptides in brain is possibly governed by proteolytic enzyme system (Marks, 1977) composed of mainly cysteine proteinases like cathepsin B. The aim of

*To whom all the correspondence should be addressed.

Abbreviations used: BANA, α -N-benzoyl-D, L-arginine- β -naphthylamide; Z-Arg-Arg-4mBNA, benzyloxycarbonyl-arginine-arginine-4-methoxy- β -naphthylamide; DTE, dithioerythritol; SDS-PAGE, sodium dodecyl sulphate-polyacrylamide gel electrophoresis; E 64, L-trans-epoxysuccinyl-leucylamide (4-

present study is to purify and characterize cathepsin B from goat brain. It also includes the regional and subcellular distribution of cathepsin B in goat brain.

Materials and methods

Chemicals

All the chemicals (analytical grade) and biochemicals used were either purchased from Sigma Chemical Co., USA or from Bachem Feinchemikalien AG, Switzerland. Sephadex G-100, CM-Sephadex C-50 and Sepharose-4B were obtained from Pharmacia Fine Chemicals, Uppsala, Sweden. All the solutions used were prepared fresh in glass-distilled conductivity water. The source of enzyme was fresh goat brain obtained from local slaughter house.

Purification of goat brain cathepsin B

All the purification steps were carried out at 4°C unless otherwise stated. Purification of the enzyme was carried out according to the method of Singh and Kalnitsky (1978) using the following steps:

Homogenisation: Goat brain acetone powder (120 g) was added to 3000 ml of cold 0.1 M sodium acetate buffer pH 5.5 containing 0.2 M NaCl and 1 mM EDTA with stirring and was allowed to reconstitute for 1 h. It was then homogenised in a mixer-cum-grinder 3 times for a period of 15 s each time. After further stirring for 1 h, it was centrifuged at 13000 *g* for 30 min in a refrigerated centrifuge. The supernatant S₁ was decanted and the pellet was rejected.

Acid-autolysis: The pH of the supernatant S₁ prepared above was lowered from 5.5 to 4.0 by gradual addition of cold 1 N HCl with stirring and was autolysed at room temperature overnight. This sample was then centrifuged at 13000 *g* for 30 min and supernatant S₂ was collected.

Fractionation with ammonium sulphate: The supernatant S₂ obtained above was saturated to 30% by gradual addition of solid (NH₄)₂SO₄ with constant and gentle stirring. After stirring for 30 min more, the suspension was centrifuged at 25000 *g* for 15 min. The resulting supernatant S₃ was then saturated to 70% by further addition of solid (NH₄)₂SO₄. It was then centrifuged at 25000 *g* for 15 min and the supernatant was discarded. The resultant pellet designated as P₄ was suspended in 0.1 M sodium acetate buffer pH 4.6 having 0.2 M NaCl and 1 mM EDTA and dialysed against the same buffer overnight with several changes. Then, this fraction was concentrated through Amicon Diaflo using YM10 membrane.

Sephadex G-100 column chromatography: The above dialysed and concentrated sample was fractionated by gel permeation chromatography on Sephadex G-100 column using 0.1 M sodium acetate buffer pH 4.6 containing 0.2 M NaCl, 1 mM EDTA and 2 mM β -mercaptoethanol. The fractions active against α -N-benzoyl-D, L-arginine- β -naphthylamide (BANA) and benzyloxycarbonyl-arginine-arginine-4-methoxy- β -naphthylamide (Z-Arg-Arg-4m β NA) were pooled and concentrated.

Organomercurial affinity chromatography: The concentrated pool obtained from Sephadex G-100 column was reduced with 5 mM dithioerythritol (DTE) for 30 min,

dialysed to remove DTE and immediately applied on the organomercurial affinity column equilibrated with 50 mM sodium acetate buffer, pH 4.6, containing 0.2 M NaCl and 1 mM EDTA. The bound enzyme was eluted with 10 mM cysteine. These fractions containing cathepsin B were then pooled, concentrated and dialysed immediately against 50 mM sodium acetate buffer pH 5.3 containing 1 mM EDTA and 2 mM β -mercaptoethanol.

Ion-exchange chromatography on CM-Sephadex C-50: The above obtained cathepsin B sample was then applied on CM-Sephadex C-50 column. After washing the column free of any unbound protein, the enzyme bound on the column was eluted with a linear NaCl gradient (0–0.7 M). The active fractions were pooled, concentrated through YM-10 membrane and stored at 0°C. The purity of the purified enzyme cathepsin B was established through Davis gel electrophoresis at pH 8.4 (Davis, 1964), Reisfeld gel electrophoresis at pH 4.5 (Reisfeld *et al.*, 1962) and sodium dodecyl sulphate-polyacrylamide gel electrophoresis (SDS-PAGE) at pH 7.2 (Weber and Osborn, 1969). The molecular weight estimations were made by SDS-PAGE and analytical Sephadex G-75 column.

Enzyme assay

Cathepsin B activity was determined by the colorimetric method of Barrett (1977) using either BANA or Z-Arg-Arg-4m β NA as substrates. The assay mixtures (2 ml) containing 75 mM phosphate buffer pH 6, 1 mM DTE, 1 mM EDTA, 50 μ l substrate stock solution and 0.5 ml of enzyme solution were incubated at 37°C for 10 min. The released β -naphthylamine or 4-methoxy- β -naphthylamine was coupled with Fast Garnet GBC (*o*-aminoazotoluene diazonium sulphate). After 10 min, the coupled product was extracted in 4 ml *n*-butanol and the colour was estimated at 520 nm. One unit of enzyme activity was defined as the amount of enzyme which released 1 μ mol of β -naphthylamine or 4-methoxy- β -naphthylamine per min at 37°C from the substrates BANA and Z-Arg-Arg-4m β NA respectively. The molar extinction coefficients of β -naphthylamine and 4-methoxy- β -naphthylamine determined under the assay conditions were 25,000 and 36,000 respectively.

Kinetic studies

K_m for cathepsin B in respect of BANA and Z-Arg-Arg-4m β NA was determined by taking different concentrations of each substrate separately, keeping one at its saturating level at pH 6, to minimize the cooperative effect and thereby obtaining a Michaelis pattern. K_i value was determined by using Dixon (1953) plot after measuring the activity at pH 6 with substrate Z-Arg-Arg-4m β NA at 0.1 and 1 mM final concentrations in the presence of different concentrations of leupeptin.

Regional and subcellular distribution

The subcellular localization of cathepsin B was established through fractionation of goat brain by differential centrifugation method (Koenig, 1974). The nuclear,

brain was divided into its constituent parts whereby the total activity as well as specific activity of each brain part were determined separately.

Results and discussion

Figure 1 shows the elution profile of different enzymes on Sephadex G-100 gel

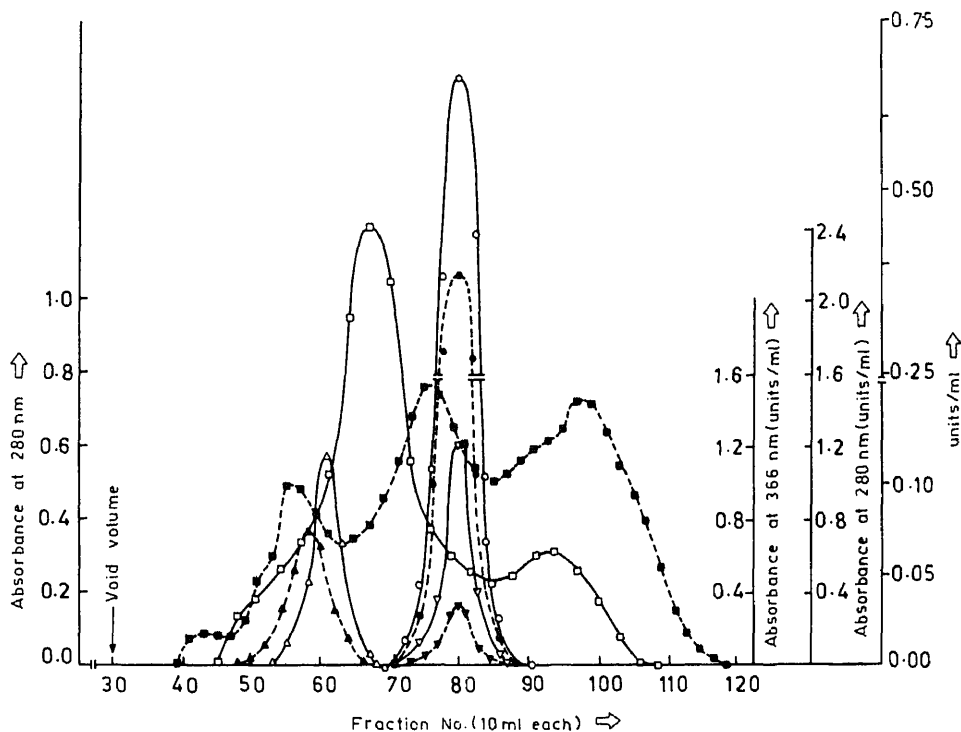


Figure 1. Gel filtration chromatography on Sephadex G-100 column. Ammonium sulphate (30–70%) fraction of goat brain homogenate was applied on the column protein (---■---), BANA-hydrolysing activity (---▼---), Z-Arg-Arg-4m β NA-hydrolysing activity (---●---), Z-Phe-Arg-4m β NA-hydrolysing activity (○), azocasein-hydrolysing activity (▽), haemoglobin-hydrolysing activity (□), DPPI (---▲---) and DPPII (△) activities.

permeation chromatography along with cathepsin B. Figure 2 shows the further fractionation of active G-100 fraction on organomercurial sepharose-4B and figure 3 indicates the elution profile of cathepsin B on CM-sephadex C-50 column using linear gradient of NaCl. The results of the purification (table 1) illustrate ~2000-fold purification with ~43% yield of activity. In the purification procedures of cathepsin B (Barrett, 1973; McGregor *et al.*, 1979; Suhar and Marks, 1979; Takio *et al.*, 1980; Bradley and Whitaker, 1986), the chromatography on an ion-exchange

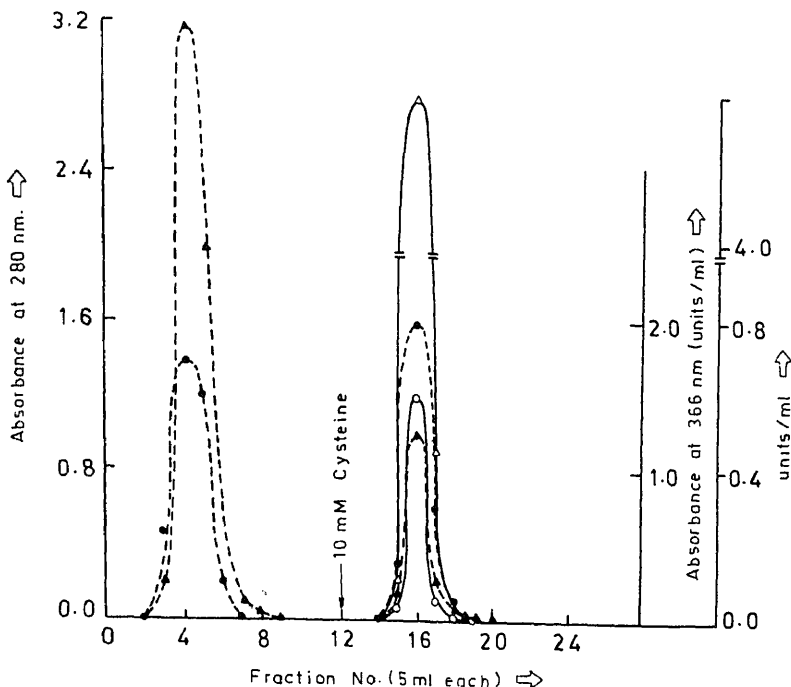


Figure 2. Affinity chromatography on organomercurial-Sepharose 4B. Protein (---▲---) BANA- (○), Z-Arg-Arg-4mβNA- (Δ) and azocasein- (---●---) hydrolysing activities.

ammonium sulphate (30–70%) precipitate was fractionated on Sephadex G-100 column as shown in figure 1. This method becomes very economical particularly when several proteases like DPPI, DPPII, cathepsin D and cathepsin B are to be simultaneously isolated. As is evident from their elution profiles in figure 1, the proteases separate from each other because of the differences in their molecular sizes.

The next step of purification of cathepsin B on affinity column (figure 2) was so designed as to separate all the non-thiol proteases/proteins from the thiol protease, cathepsin B. The affinity column was prepared by immobilizing *p*-aminophenylmercuric acetate on CNBr-activated Sepharose 4B. The chosen priority of utilizing a mercury-derived affinity chromatography at this early stage of purification stems from the fact that the two well-known thiol proteases DPPI (EC 3.4.14.1) and cathepsin B₂ (EC 3.4.18.1) had been separated from cathepsin B on molecular sieve Sephadex G-100 column chromatography and thus no interference from them in terms of binding to organomercurial column. Secondly, a large amount of non-thiol proteins could be removed from cathepsin B as unbound proteins. Finally, the sample eluted by cysteine from organomercurial column was dialysed and applied to ion-exchange chromatography on CM-Sephadex C-50 at pH 5.3 (figure 3). This pH determined by several trial experiments proved very effective in removing the proteins other than cathepsin B as unadsorbed on the column. The bound protein was eluted with

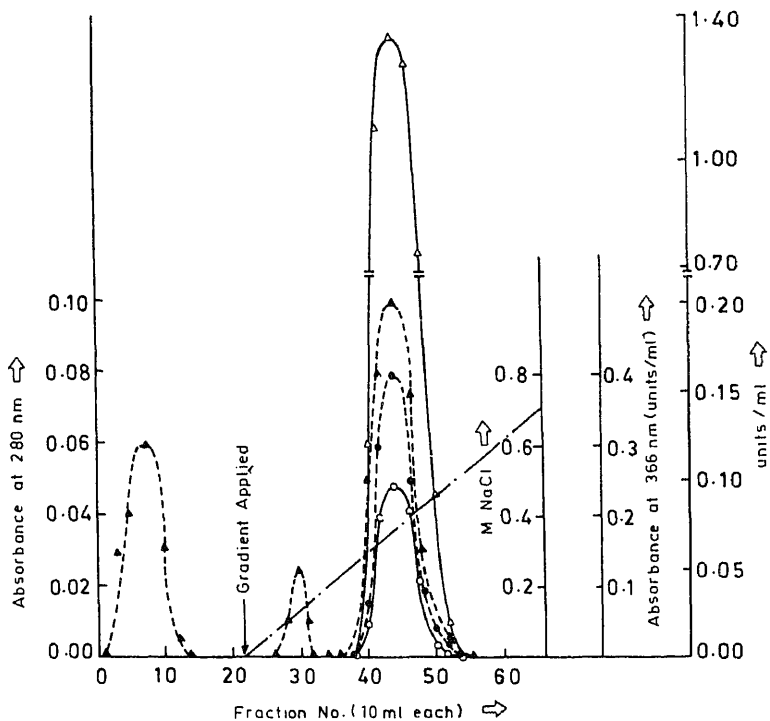


Figure 3. Elution profile of cathepsin B on ion-exchange chromatography with CM-Sephadex C-50. Protein (---▲---), BANA- (○), Z-Arg-Arg-4mβNA- (△) and azocasein- (---●---) hydrolysing activities.

Table 1. Purification of cathepsin B.

Purification step	Total activity units	Total protein (mg)	Specific activity (units/mg)	Purification factor	Yield (%)
Crude extract supernatant, S ₁	167.24	30,178.00	0.0055	1.00	100.00
Acid fractionation supernatant, S ₂	165.09	9,545.00	0.0172	3.12	98.71
30–70% (NH ₄) ₂ SO ₄ pellet, P ₄	155.77	735.00	0.2119	38.52	93.14
Sephadex G-100 pool	115.54	240.00	0.4814	87.53	69.09
Organomercurial-Sepharose 4B pool	100.43	17.05	5.8903	1070.96	60.05
CM-Sephadex C-50 pool	73.15	6.65	11.0000	2000.00	43.74

Z-Arg-Arg-4mβNA was used as substrate to measure the activity of cathepsin B. The activity units are expressed as μmol of 4-methoxy-β-naphthylamine liberated per min at 37°C.

at pH 7.2. In all these 3 types of electrophoresis, cathepsin B afforded a single protein band (figure 4). At pH 4.5 where the enzyme retained its activity, the protein band corresponded well with the activity stain band with substrate Z-Arg-Arg-4mβNA (figure 4, shown by '↑'). The molecular weight calculated from SDS-PAGE

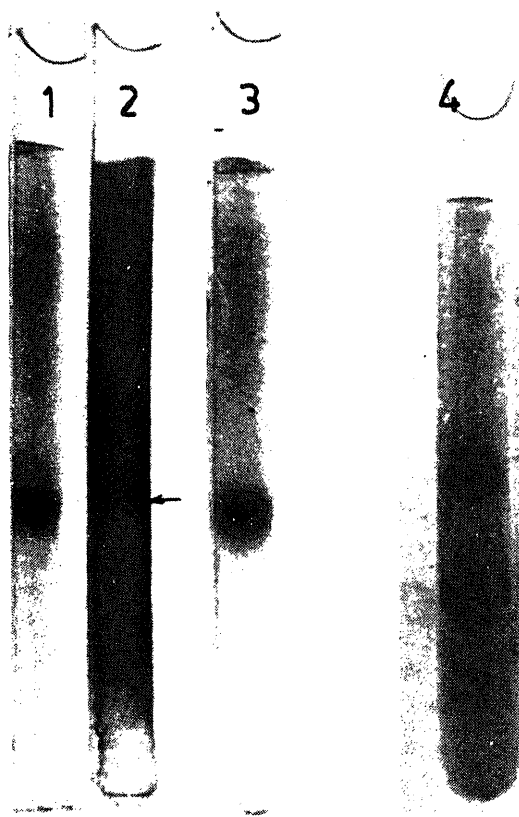


Figure 4. Gel 1 and 2, Reisfeld gel electrophoresis at pH 4.5, protein stain and activity stain with Z-Arg-Arg-4m β NA respectively, Gel 3, Davis gel electrophoresis at pH 8.4. Gel 4, SDS-PAGE in the presence of β -mercaptoethanol at pH 7.2.

reported that cathepsin B consists of two polypeptide chains of molecular weights 25,000 and 5,000 daltons (Takio *et al.*, 1980; Bradley and Whitaker, 1986). In our hands, even drastic conditions such as heating the enzyme protein in the presence of SDS and β -mercaptoethanol for prolonged duration failed to dissociate the enzyme protein.

Substrate specificity

Of the various substrates tested, the order of susceptibility for the hydrolysis of synthetic substrates is Z-Val-Lys-Lys-Arg-4m β NA, Z-Ala-Arg-Arg-4m β NA, Z-Arg-Arg-4m β NA, Z-Phe-Arg-4m β NA, Bz-L-Arg- β NA, Bz-D, L-Arg- β NA and Bz-L-Arg-4m β NA (table 2). No dipetidyl peptidase substrate was hydrolysed at all. When p-

Table 2. Substrate specificity of cathepsin B from goat brain.

Substrate	Cathepsin B activity units/mg enzyme protein
Z-Arg-Arg-4m β NA	36.1 (100.0)
Z-Phe-Arg-4m β NA	35.4 (98.1)
Z-Val-Lys-Lys-Arg-4m β NA	45.2 (125.2)
Z-Ala-Arg-Arg-4m β NA	42.4 (117.5)
Bz-L-Arg- β NA	4.7 (10.2)
Bz-D, L-Arg- β NA	2.6 (7.2)
Bz-L-Arg-4m β NA	2.3 (6.4)
Gly-Arg-4m β NA	—
Lys-Ala-4m β NA	—
Arg- β NA	—
Ala- β NA	—
Leu- β NA	—
Met- β NA	—
Z-Arg-Arg-pNA	7.58 (20.9)
Z-Phe-Arg-pNA	6.85 (19.0)
Bz-L-Arg-pNA	2.34 (6.5)
Bz-D, L-Arg-pNA	1.20 (3.3)
Z-L-Arg-pNA	1.43 (4.0)
L-Lys-pNA	—

The final concentration of each substrate in the assay mixture was 2.5 mM. The activity of cathepsin B with Z-Arg-Arg-4m β NA was taken as 100 and the per cent activities with other substrates were calculated relative to this substrate. The activity units are μ mol of β -naphthylamine or 4-methoxy- β -naphthylamine released per min per mg enzyme protein at 37°C. The figures in brackets represent the per cent relative activity. '—', Indicates no action.

Invariably, cathepsin B has less affinity for *p*-nitroanilide substrates as compared to the corresponding β -naphthylamide and 4-methoxy- β -naphthylamide derivatives. The K_m and V_{max} values of 2.36 mM and 10 μ mol of β -naphthylamine released per min per mg enzyme protein respectively were obtained for goat brain cathepsin B with BANA as substrate in 2.5% DMSO concentration. This value is lower compared to K_m value of 3.6 mM for lung cathepsin B (Singh and Kalnitsky, 1980), 4.3 mM for human liver enzyme (Knight, 1980) and 5.1 mM for bovine brain cathepsin B (Bradley and Whitaker, 1986). The K_m and V_{max} data obtained for this enzyme with respect to Z-Arg-Arg-4m β NA as substrate in 2.5% DMSO were 0.29 mM and 40 μ mol of 4-methoxy- β -naphthylamine released per min per mg enzyme protein at 37°C respectively. The K_m value, 0.29 mM compares favourably with the value (0.23 mM) reported for human liver enzyme (Knight, 1980). However, when the final concentration of DMSO in the assay mixtures was reduced to 1%, the K_m values in respect of BANA (0.5 mM) and Z-Arg-Arg-4m β NA (0.09 mM) were found to be significantly lower. This difference results from the inhibitory

Activation and inhibition studies

Among the various thiol activators tested, dithioerythritol in conjunction with EDTA was found to be the best activator of goat brain cathepsin B followed by dithiothreitol, glutathione, cysteine, β -mercaptoethanol and thioglycolic acid (table 3). As is evident from the table, the metal chelating agent EDTA alone had no

Table 3. Effect of thiol activators and EDTA on cathepsin B from goat brain.

Thiol activator	Final concentration (mM)	EDTA	Cathepsin B activity (%)
None	—	—	100
None	—	+	100
Dithioerythritol	1.0	—	179
Dithioerythritol	1.0	+	225
Dithiothreitol	1.0	—	159
Dithiothreitol	1.0	+	214
Glutathione	2.0	—	130
Glutathione	2.0	+	199
Cysteine	2.0	—	124
Cysteine	2.0	+	181
β -Mercaptoethanol	2.0	—	114
β -Mercaptoethanol	2.0	+	144
Thioglycolic acid	2.0	—	108
Thioglycolic acid	2.0	+	135

'+' and '—' indicate the inclusion and absence of 1 mM EDTA respectively in assay mixture.

effect whatsoever, on goat brain cathepsin B. Similar results were also reported by Singh and Kalnitsky (1978) for lung cathepsin B. Cathepsin B, being a cysteine proteinase was inhibited by thiol blocking and alkylating reagents like *p*-chloromercuribenzoic acid, 2,2'-dipyridyl disulphide, 5,5'-dithiobis (2-nitrobenzoic acid), iodoacetate, iodoacetamide and L-trans-epoxy succinyl-leucylamido (L-guanidino)-butane (E-64). The Trypsin inhibitors α -N-tosyl-lysine chloromethyl ketone (TLCK) and α -N-tosyl-phenylalanine chloromethyl ketone (TPCK) were also inhibitory to this enzyme, while leucine chloromethyl ketone, an inhibitor for aminopeptidase and cathepsin H (EC 3.4.22.16), showed no inhibition at all. The metal ions like Zn^{2+} , Mn^{2+} , Hg^{2+} also inhibited the activity of cathepsin B. The inhibition by Zn^{2+} and Mn^{2+} was reversed by EDTA whereas the inhibition by Hg^{2+} was not reversed. The elastase inhibitors $\text{Ac}(\text{Ala})_4\text{-CH}_2\text{Cl}$, $\text{Ac}(\text{Ala})_2\text{-Pro-Ala-CH}_2\text{Cl}$ and $\text{Ac}(\text{Ala})_2\text{-Pro-Val-CH}_2\text{Cl}$ were very potent inhibitors. Among the microbial peptide inhibitors antipain [(s)-1-carboxy-2-phenylethyl]-carbamoyl-L-arginyl-L-valyl-L-argininal) and leupeptin (acetyl-L-leucyl-L-leucyl-L-argininal) strongly inhibited the goat brain cathepsin B activity. Leupeptin was a competitive inhibitor with an inhibition constant K_i of 12.50×10^{-9} M. In contrast, K_i value for human liver cathepsin B (Knight, 1980) was reported to be 7.0×10^{-9} M.

decreases gradually losing 50% activity at 58°C and the enzyme is completely denatured up to 70°C. Towatari *et al.* (1979) have reported similar results for cathepsin B from rat liver. As regards the pH stability, the enzyme cathepsin B was less stable below pH 4 and above pH 6. In alkaline pH, the enzyme is least stable giving only 18% of activity after exposure of 10 min at pH 8. The enzyme has a

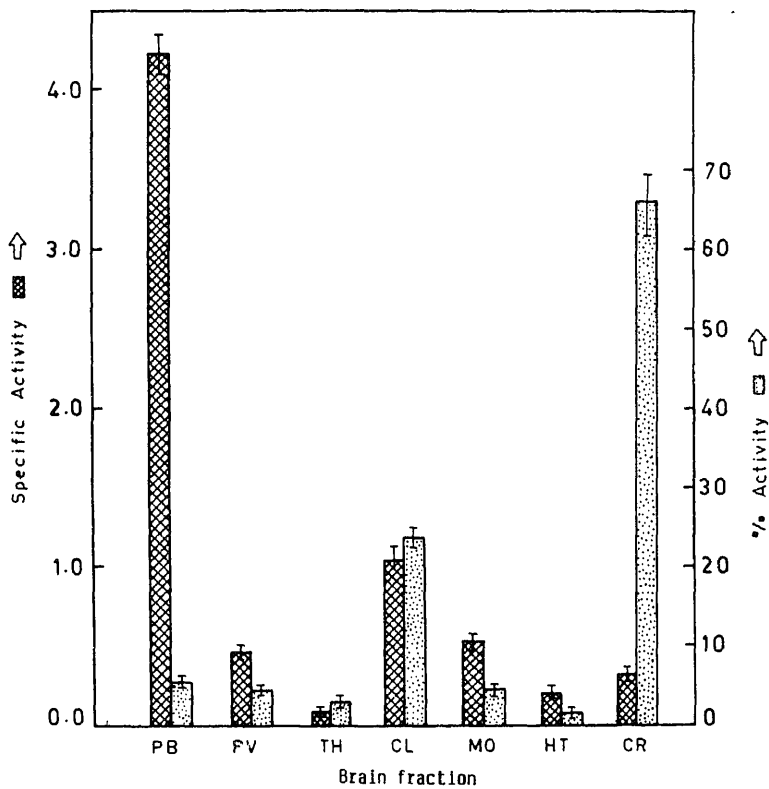


Figure 5. Determination of regional distribution of cathepsin B in different parts of goat brain. (PB, Pituitary body; PV, pons-varolli; TH, thalamus; CL, cerebellum; MO, medulla-oblongata; HT, hypothalamus; CR, cerebrum).

Table 4. Subcellular localization of cathepsin B.

Cathepsin B activity	Acid phosphatase	Cathepsin D
----------------------	------------------	-------------

temperature optima of 50°C with an activation energy of 16 kcal/mol. The regional distribution of cathepsin B is shown in figure 5. It was found that maximum total activity of cathepsin B was in cerebrum followed by cerebellum, pituitary body, medulla-oblongata, pons-varolli, thalamus and hypothalamus in that order. However, the specific activity of cathepsin B i.e., activity per mg enzyme protein was maximum in pituitary body followed by cerebellum, medulla-oblongata, pons-varolli, cerebrum, hypothalamus and thalamus. When the nuclear, mitochondrial-lysosomal fraction and soluble fractions obtained by differential centrifugation of brain homogenate were estimated for their cathepsin B content (table 4), it was found that cathepsin B resided mainly in the mitochondrial-lysosomal fraction (71.3%). The purity of mitochondrial-lysosomal fraction was checked with the known lysosomal marker enzymes, acid-phosphatase (deDuve *et al.*, 1962) and cathepsin D (Ferren *et al.*, 1978). This lysosomal nature of cathepsin B in brain is reported for the first time here. The lysosomal nature of cathepsin B has been reported by other workers in other tissues (Otto, 1971; Davidson and Poole, 1975; Ferren *et al.*, 1978).

References

- Barrett, A. J. (1973) *Biochem J.*, **131**, 809.
- Barrett, A. J. (1977) in *Proteinases in mammalian cells and tissues* (ed. A. J. Barrett) (Amsterdam: North-Holland) p. 181.
- Bradley, J. D. and Whitaker, J. N. (1986) *Neurochem. Res.*, **11**, 851.
- Burnett, D., Crocker, J. and Stockley, A. A. (1983) *Am. Rev. Respir. Dis.*, **128**, 915.
- Davidson, E. and Poole, B. (1975) *Biochim. Biophys. Acta*, **397**, 437.
- Davis, B. J. (1964) *Ann. N. Y. Acad. Sci.*, **121**, 404.
- Dean, R. T. (1975) *Eur. J. Biochem.*, **58**, 9.
- deDuve, C., Wittiaux, R. and Baudhuin, P. (1962) *Adv. Enzymol.*, **24**, 291.
- Dixon, M. (1953) *Biochem. J.*, **55**, 170.
- Ferren, L. G., Stauber, W. R. and Kalnitsky, G. (1978) *Proc. Soc. Exp. Biol. Med.*, **159**, 239.
- Knight, C. G. (1980) *Biochem. J.*, **189**, 447.
- Koenig, H. (1974) *Methods Enzymol.*, **31**, 457.
- Marks, N. (1977) in *Peptides in neurobiology*, (ed. H. Gainer) (New York: Plenum Press) p. 221.
- McGregor, R. R., Hamilton, J. W., Shofstall, R. E. and Cohn, D. V. (1979) *J. Biol. Chem.*, **254**, 4423.
- Neurath, H. and Walsh, K. A. (1976) *Proc. Natl. Acad. Sci. USA*, **73**, 3825.
- Noda, T., Isogai, K., Katunuma, N., Torumoto, Y. and Ohzeki, M. (1981) *J. Biochem. (Tokyo)*, **90**, 893.
- Ostensen, M., Morland, B., Husbr, G. and Rekvig, O. P. (1983) *Clin. Exp. Immunol.*, **54**, 397.
- Otto, K. (1971) in *Tissue proteinases* (eds A. J. Barrett and J. T. Dingle) (Amsterdam: North-Holland) p. 1.
- Poole, A. R., Tiltman, K. J., Recklies, A. D. and Stoker, T. A. M. (1978) *Nature (London)*, **273**, 545.
- Quinn, P. S. and Judah, J. D. (1978) *Biochem. J.*, **172**, 301.
- Reisfeld, R. A., Lewis, U. J. and Williams, D. E. (1962) *Nature (London)*, **195**, 281.
- Segal, H. L. (1975) in *Lysosomes in biology and pathology* (eds J. T. Dingle and R. T. Dean) (Amsterdam: North-Holland) p. 295.
- Sher, J. H., Stracher, A., Shafiq, S. A. and Hardy-Stashin, J. (1981) *Proc. Natl. Acad. Sci. USA*, **79**, 7742.
- Shikimi, T., Yamamoto, D. and Handa, M. (1987) *J. Pharmacobio-Dynamics (Jpn.)*, **10**, 750.
- Singh, H. and Kalnitsky, G. (1978) *J. Biol. Chem.*, **253**, 4319.
- Singh, H. and Kalnitsky, G. (1980) *J. Biol. Chem.*, **255**, 369.

- Takio, K., Towatari, T., Katunuma, N. and Titani, K. (1980) *Biochem. Biophys. Res. Commun.*, **97**, 3.
- Towatari, T., Kawabata, Y. and Katunuma, N. (1979) *Eur. J. Biochem.*, **102**, 279.
- Uy, R. and Wold, F. (1977) *Science*, **198**, 890.
- Ward, W. F., Cox, J. R. and Mortimore, G. E. (1977) *J. Biol. Chem.*, **252**, 6955.
- Weber, K. and Osborn, M. (1969) *J. Biol. Chem.*, **244**, 4406.

Role of Ca^{2+} in induction and secretion of dengue virus-induced cytokines

RITU DHAWAN, MADHU KHANNA, U. C. CHATURVEDI* and ASHA MATHUR

Postgraduate Department of Microbiology, K. G. Medical College, Lucknow 226 003, India

MS received 24 April 1990; revised 6 July 1990

Abstract. The present study was undertaken to investigate the role of calcium ions (Ca^{2+}) in the induction and secretion of the dengue type 2 virus induced cytotoxic factor and the cytotoxin. This was done by using calcium channel blocking drugs such as verapamil, nifedipine or diltiazem hydrochloride. The production of cytotoxic factor was significantly reduced by treatment of dengue type 2 virus infected mice with verapamil. Similarly, a dose-dependent inhibition of the secretion of cytotoxic factor was observed, when spleen cells of the virus-primed mice were treated *in vitro* with the 3 calcium channel blockers. The production of cytotoxin by macrophages was abrogated by pretreatment with calcium channel blockers but had little effect on its secretion as shown by treatment of macrophages with verapamil at 1 h after the induction to later periods up to 18 h. The findings thus show that in the induction of both the cytokines Ca^{2+} plays a critical role; on the other hand it is required for the secretion of the cytotoxic factor but not for that of the cytotoxin.

Keywords. Ca^{2+} ; cytokines; dengue virus; cytotoxic factor; calcium channel blockers.

Introduction

Calcium plays an important role in the regulation of a large number of vital cellular activities and mediates cellular responses to a wide range of stimuli. When calcium ion (Ca^{2+}) is bound to calmodulin, it modulates the activities of a number of intracellular enzymes, including those involved in protein phosphorylation, secretory functions and calcium flux etc. Ca^{2+} also plays a critical role in a number of pathological and toxicological processes (Orrenius *et al.*, 1989). Activation of T lymphocytes (Lichtman *et al.*, 1983), natural killer cells (Hiserodt *et al.*, 1982) and macrophages (Wright *et al.*, 1985) have been shown to be Ca^{2+} -dependent. Further, target cell killing by various activated cells may be mediated by cytotoxic molecules, secretion of which may be Ca^{2+} -dependent or independent (Kelly, 1985; reviewed by Young and Liu, 1988).

Dengue type 2 virus (DV) induces a subpopulation of T lymphocytes of mice to produce a cytotoxic protein, the cytotoxic factor (CF). CF kills I-A negative macrophages and helper T cells (Chaturvedi *et al.*, 1987; Khanna *et al.*, 1988), but induces I-A positive macrophages to produce another cytotoxin (CF_2). Both CF and CF_2 are biologically active protein molecules which kill different types of cells and produce various immunological and pathological effects including increased capillary

permeability (Dhawan *et al.*, 1990; Khanna *et al.*, 1989, 1990; reviewed by Chaturvedi, 1986, 1989). The present study demonstrates the importance of Ca^{2+} in the production and secretion of CF and CF_2 by the primed cells.

Materials and methods

Animals

The study was carried out on inbred Swiss albino mice aged 2–4 months which were obtained from the colony maintained in this Department.

Virus

The brain of adult mouse, infected with DV, strain P23085, was used as a source of the virus (Chaturvedi *et al.*, 1977).

Reagents

Verapamil and nifedipine were purchased from the Sigma Chemical Co., St. Louis, Missouri, USA and were dissolved in 30% ethyl alcohol as stock solution. Diltiazem hydrochloride was from the Anglofrench Drug Co. Eastern Ltd., Bangalore and was dissolved in the medium used. The stock solutions of the drugs were prepared and used on the same day. The drugs had no cytotoxicity in the concentrations used in the tests.

Preparation of CF

CF was prepared from the spleen cells of DV-infected mice by the technique described elsewhere (Chaturvedi *et al.*, 1980a,b; Khanna *et al.*, 1989). Briefly, mice were given DV intracerebrally in doses of 10^3LD_{50} and the spleens were harvested aseptically from the sick moribund mice on 9–11 postinfection day. The spleens were teased out in chilled phosphate-buffered saline (PBS), pH 7 with the help of forceps, and a single cell suspension was obtained. The cells were cultured for 24 h at 37°C in the presence of 5% CO_2 and then centrifuged at $2000g$ for 10 min at 4°C . The supernatant was assayed for cytotoxic activity and stored at -70°C for further use as CF.

Preparation of CF_2

CF_2 was prepared by the technique described elsewhere (Gulati *et al.*, 1983a,b). Briefly, 5 ml of heparinized minimum essential medium (MEM) was inoculated intraperitoneally into the mouse and the peritoneal lavage was aspirated under

glass-adherent cell sheet and incubated for 1 h at 4°C. The cell sheet was then washed thoroughly with MEM and cultured in normal saline for 24 h. The supernatant fluid was collected and the cells were scraped off with a rubber policeman and clear supernatant obtained after sonication. Both the preparations were cleared by centrifugation at 2000 *g* for 10 min and were stored at -70°C and used as CF₂.

Assay of cytotoxic activity

Cytotoxic activity of the preparations was assayed using a single cell suspension of normal mouse spleen cells as target. The technique for the assay of cytotoxic activity of CF and CF₂ has been described elsewhere (Chaturvedi *et al.*, 1980a, 1983; Gulati *et al.*, 1983a; Khanna *et al.*, 1989). Briefly, equal volumes (100 µl) of the test solution and the target cells (2×10^6 /ml) were mixed in microtitre U-well persplex plate and incubated at 4°C for 1 h. Viable target cells were counted using trypan blue dye exclusion method and the percentage of non-viable cells was calculated after counting 200–300 cells. The tests were set up in triplicate and were repeated at least thrice. The results have been presented after subtracting the background non-viable cells. The data have been analysed using Students *t* test. A *P* value of more than 0.05 was considered insignificant.

Results

Effect on secretion of CF

Mouse spleen cells obtained 9–11 days after intracerebral infection with DV, secrete CF in culture fluid (Chaturvedi *et al.*, 1980a; Khanna *et al.*, 1989). Effects of calcium channel blockers on the secretion of CF by such DV-primed spleen cells was investigated. The drugs used were verapamil, nifedipine or diltiazem hydrochloride at concentrations of 10^{-3} , 10^{-5} or 10^{-7} M. A single cell suspension of DV-infected mice spleen cells (2×10^7 cells) was mixed with various calcium channel blocking drugs and the mixture was cultured for 24 h at 37°C in the presence of 5% CO₂. After centrifugation at 2000 *g* for 10 min at 4°C the supernatant was collected and assayed for cytotoxic activity. Untreated cells mixed with the diluent or the drug alone were used as controls.

Effect of various drugs on secretion of CF by spleen cells is shown in figure 1. It was observed that the culture fluid obtained from untreated cells killed $36 \pm 2\%$ target cells. In contrast, the culture fluid from cells treated with 10^{-3} , 10^{-5} or 10^{-7} M concentration of verapamil killed 7 ± 2 , 19 ± 4 , $31 \pm 1\%$ target cells respectively. The effect of the drug was thus, found to be dose dependent. Similar results were obtained by treating target cells with nifedipine or diltiazem (figure 1). The drugs as such had no adverse effect on the target cells with the concentrations used in the test (data not presented).

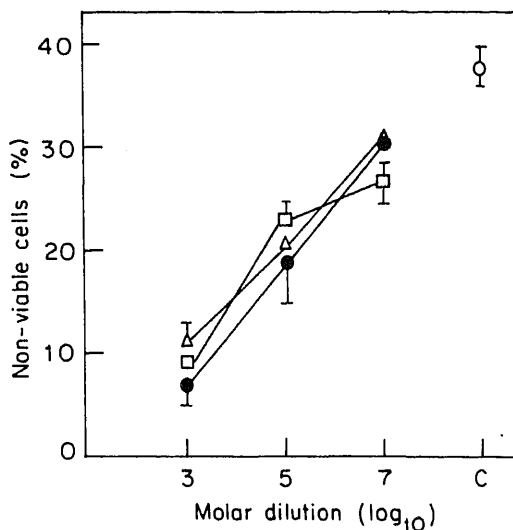
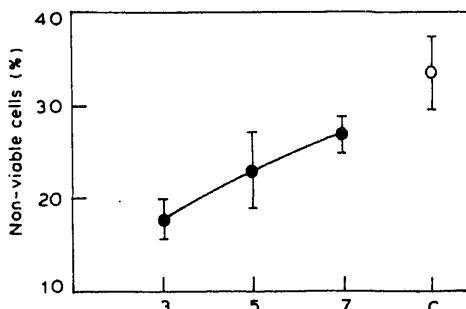


Figure 1. Effect of calcium channel blocking drugs on the secretion of CF by the spleen cells obtained from DV-primed mice. (●), Verapamil; (Δ), nifedipine; (□), diltiazem. (C) Untreated control.

treatment of DV-primed cells with various calcium channel blocking drugs. In another series of experiments, an effort was made to investigate the effect of such drugs on the production of CF. Mice were inoculated at 0 h with 0.1 ml of various dilutions of verapamil intraperitoneally and DV intracerebrally. Mice were sacrificed on the 10th day and the spleen cells were either sonicated or cultured for 24 h. The sonicate and the culture fluid were cleared at 2000 *g* and assayed for the cytotoxic activity. It was observed that the cytotoxic activity of the culture supernatants from mice not treated with verapamil was $33 \pm 4\%$. The supernatant from mice treated with 10^{-3} M verapamil had an activity of $18 \pm 3\%$ ($P < 0.001$) while that obtained from mice treated with 10^{-7} M dilution of the drug was $27 \pm 2\%$. This showed that the drug significantly inhibited the production of CF in a dose dependent manner (figure 2). Among the sonicates, the cytotoxic activity of

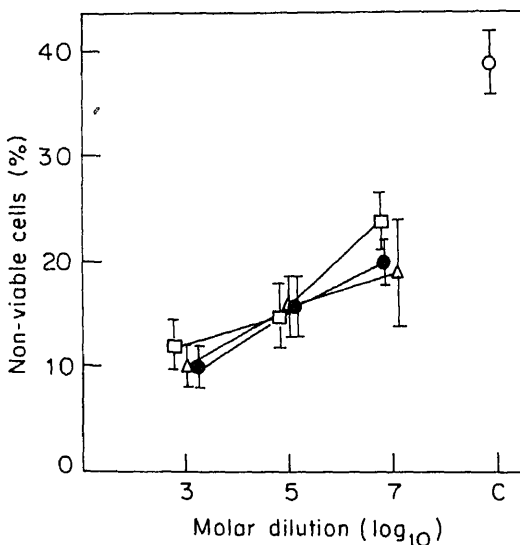


control, drug untreated mice was $40 \pm 6\%$. The sonicates obtained from mice treated with verapamil had a cytotoxic activity of 18 ± 3 , 26 ± 2 and $33 \pm 3\%$ respectively at 10^{-3} , 10^{-5} and 10^{-7} M dilutions of the drug. In another set of experiments the mice were given two doses of the various dilutions of the drug, one at 0 h and the second on the 4th day. It was observed that with the dose of 10^{-3} M the cytotoxic activity was $13 \pm 3\%$. A similar effect was observed by giving two doses of 10^{-5} or 10^{-7} M dilution of the drug.

Effect on secretion of CF₂

CF induces mouse macrophages to produce CF₂ which is secreted out of the cells (Gulati *et al.*, 1983a,b; Chaturvedi *et al.*, 1987). The effect of calcium channel blocking drugs on the secretion of CF₂ by MØ was investigated in the present experiment. Mouse peritoneal MØ monolayers were prepared. The MØ monolayers were pretreated with calcium channel blockers, at 37°C for 1 h (verapamil, nifedipine or diltiazem) at 10^{-3} , 10^{-5} or 10^{-7} M concentration. The fluid was then decanted and the MØ monolayers were inoculated with CF (1:30 dilution). After a further incubation at 4°C for 1 h the MØ monolayers were washed thrice and cultured for 24 h at 37°C in the presence of 5% CO₂. The culture fluid was then collected and clear supernatant obtained after centrifugation at 2000 *g* for 10 min was assayed for cytotoxic activity. MØ-monolayers were similarly inoculated with CF but were not treated with the drugs, and were used as controls. In another control the cells were treated with the drugs only.

The data presented in figure 3 show that the culture fluid obtained from untreated MØ-monolayers killed $39 \pm 3\%$ target cells, thus showing secretion of CF₂ in the fluid. On the other hand culture fluid from cells treated with 10^{-3} , 10^{-5} or 10^{-7} M verapamil killed 10 ± 2 , 16 ± 3 and $20 \pm 2\%$ target cells respectively. Thus



a dose dependent inhibition of the secretion of CF_2 was observed. A similar significant reduction in the secretion of CF_2 was observed with nifedipine and diltiazem. The 3 drugs bind to 3 distinct sites on the calcium channel receptors of the cells and may synergise the effect when used in combination. In the next set of experiments, therefore, the 3 drugs were used in doses of 10^{-5} M in various combinations as shown in table 1, using above protocol. No summation of the effect was seen by using different combinations of the 2 drugs but by using all the 3 drugs simultaneously a higher reduction in cytotoxic activity was noted (table 1).

Table 1. Effect on the production of CF_2 by treatment of MØ with various combinations of the calcium channel blocking drugs.

Groups	Drug treatment (10^{-5} M)	Cytotoxicity (%)	Reduction in cytotoxicity (%)
1	Ver + Nif*	13 ± 3	63
2	Ver + Dil	16 ± 2	54
3	Nif + Dil	13 ± 2	63
4	Ver + Nif + Dil	9 ± 5	74
5	None (control)	35 ± 4	0

*Ver, Verapamil; Nif, nifedipine; Dil, diltiazem hydrochloride.

From the above experiments it could not be concluded whether the reduced cytotoxic activity in the culture fluid was due to blockade of secretion or due to blockade of production of CF_2 . Therefore, in another series of experiments MØ sheets were treated with CF for 1 h at $4^\circ C$ and then after thorough washing were cultured in normal saline. After 1, 3, 5 or 18 h the cultures were washed thoroughly and then recultured with normal saline containing 10^{-3} M verapamil. The fluid of the control cultures to which the drug was not added were similarly processed. At 24 h the culture fluid was collected and assayed for cytotoxicity. Further, the MØ cells were scraped off, sonicated and centrifuged at $2000 g$ for 10 min. The clear supernatants thus obtained were also assayed for cytotoxicity. The findings presented in figure 4 show that the cytotoxic activity of culture supernatants of the MØ treated with verapamil at 1–18 h was 19 ± 2 – $27 \pm 4\%$. The cytotoxic activity in the control cultures, not treated with the drugs, was similar in the various groups and the mean value obtained was $29 \pm 2\%$. Similar findings were observed when the cell sonicates were tested. Thus verapamil appears to block production of CF_2 .

Discussion

The role of Ca^{2+} in production/secretion of two DV-induced cytokines, the CF and CF_2 , has been demonstrated in the present study. This has been shown by the inhibition of their production/secretion by treatment with various calcium channel blocking drugs, namely verapamil, nifedipine or diltiazem. It was observed that the production of CF was significantly reduced by treatment of DV-infected mice with verapamil. Similarly, when spleen cells obtained from DV-primed mice were treated *in vitro* with either of the above drugs a dose dependent inhibition of the secretion

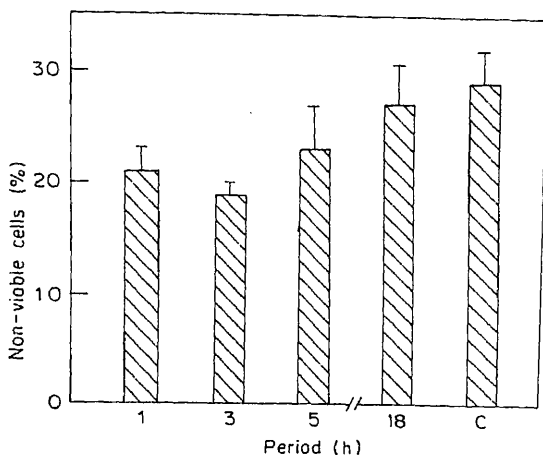


Figure 4. Effect of pretreatment of primed macrophages with verapamil on the secretion of CF_2 .

pretreatment of MØ by any of the 3 drugs. A higher degree of inhibition was seen when all the 3 drugs were used simultaneously but no summation was noted by using combination of any of the 2 drugs. On the other hand, the calcium channel blockers had almost no effect on its secretion. It has been shown earlier that following induction with CF the MØ start producing CF_2 which continues to be secreted up to 24 h (Chaturvedi *et al.*, 1983a). The findings of the present study show that treatment of such MØ with verapamil after 1 h of induction or at later periods up to 18 h had no effect on the secretion of CF_2 .

In several studies the calcium channel blocking drugs have been used to elucidate the role of Ca^{2+} . For example suppression of mitogen-induced activation of lymphocytes by such drugs suggests a pivotal role of calcium in initial activation of T cells (Birx *et al.*, 1984). Activation of macrophages to a tumoricidal state is inhibited by the pharmacological agents that inhibit calcium influx or inhibit calmodulin function (Wright *et al.*, 1985). We have recently demonstrated that the presence of Ca^{2+} is obligatory for the cytotoxic activity of CF and CF_2 and the target cell killing is associated with an influx of Ca^{2+} in the susceptible target cells (Khanna *et al.*, 1990; Dhawan *et al.*, 1991).

Secretion of the cytotoxic molecules can be *via* calcium-dependent or independent pathways. When such molecules are in the form of secretory granules, their exocytosis requires Ca^{2+} as a second messenger, while in certain systems the release is constitutive which does not require calcium (Kelly, 1985). The release of tumour necrosis factor is Ca^{2+} independent (Liu *et al.*, 1987); CF_2 resembles it in this aspect. On the other hand, perforin/cytolysin secreted by cytotoxic T lymphocyte are absolutely dependent on Ca^{2+} for assembly, secretion and function (Henkart *et al.*, 1984; Podack *et al.*, 1984, 1985). Similarly secretion of serine esterase is Ca^{2+} dependent (Ostergaard *et al.*, 1987). Ca^{2+} is an important mediator in MØ activation also as shown by enhanced secretion of cytolytic factor from MØ by

important role in the transmission of the signal in T lymphocytes to produce CF and in MØ to produce CF₂.

The findings of the present study thus show that besides playing an important role in mediation of the cytotoxic activity of CF/CF₂, as described elsewhere, Ca²⁺ is also necessary for their production/secretion from the primed cells.

Acknowledgement

The study was carried out with the financial assistance of the Council of Scientific and Industrial Research, New Delhi.

References

- Birx, D., Berger, M. and Fleisher, T. A. (1984) *J. Immunol.*, **133**, 2904.
- Chaturvedi, U. C. (1986) *Immunol. Today*, **7**, 159.
- Chaturvedi, U. C. (1989) in *Hand-book on viral immuno-suppression* (eds S. Specter, M. Bendinelli and H. Friedman) (New York: Plenum Press) p. 253.
- Chaturvedi, U. C., Tandon, P. and Mathur, A. (1977) *J. Gen. Virol.*, **36**, 449.
- Chaturvedi, U. C., Bhargava, A. and Mathur, A. (1980a) *Immunology*, **40**, 665.
- Chaturvedi, U. C., Dalakoti, H. and Mathur, A. (1980b) *Immunology*, **41**, 387.
- Chaturvedi, U. C., Shukla, M. I. and Mathur, A. (1982) *Ann. Immunol. (Inst. Pasteur)* **133**, 83.
- Chaturvedi, U. C., Gulati, L. and Mathur, A. (1983) *Indian J. Exp. Biol.*, **21**, 275.
- Chaturvedi, U. C., Nagar, R., Gulati, L. and Mathur, A. (1987) *Immunology*, **61**, 247.
- Dhawan, R., Khanna, M., Chaturvedi, U. C. and Mathur, A. (1990) *Br. J. Exp. Pathol.*, **71**, 83.
- Dhawan, R., Khanna, M., Chaturvedi, U. C. and Mathur, A. (1991) *Int. J. Exp. Pathol.*, (in press).
- Drysdale, B. E., Zacharchuk, C. M. and Shin, H. S. (1983) *J. Immunol.*, **131**, 2362.
- Gulati, L., Chaturvedi, U. C. and Mathur, A. (1983a) *Immunology*, **49**, 121.
- Gulati, L., Chaturvedi, U. C. and Mathur, A. (1983b) *Br. J. Exp. Pathol.*, **64**, 185.
- Hiserodt, J. C., Britvan, L. J. and Targan, S. C. (1982) *J. Immunol.*, **129**, 2266.
- Henkart, P. A., Millard, P. J., Regnolds, C. W. and Henkart, M. P. (1984) *J. Exp. Med.*, **160**, 75.
- Kelly, R. (1985) *Science*, **230**, 25.
- Khanna, M., Chaturvedi, U. C. and Mathur, A. (1988) *Curr. Sci.*, **57**, 411.
- Khanna, M., Chaturvedi, U. C., Srinivasa, B. R., Swaminathan, K. R. and Mathur, A. (1989) *Immunology*, **67**, 32.
- Khanna, M., Chaturvedi, U. C., Sharma, M., Pandey, V. C. and Mathur, A. (1990) *Immunology*, **69**, 449.
- Lichtman, A. H., Segel, G. B. and Lichtman, M. A. (1983) *Blood*, **61**, 413.
- Liu, C. C., Steffen, M., King, F. and Young, J. D. E. (1987) *Cell*, **51**, 393.
- Ostergaard, H., Kane, K., Mescher, M. and Clark, W. (1987) *Nature (London)*, **330**, 71.
- Orrenius, S., McConkey, J. D., Bellomo, G. and Nicotera, P. (1989) *TIPS*, **10**, 281.
- Podack, E., Konigsberg, P., Acha, H., Pirchner, H. and Hengartner, H. (1984) *Adv. Exp. Med. Biol.*, **184**, 99.
- Podack, E., Young, J. and Cohn, Z. (1985) *Proc. Natl. Acad. Sci. USA*, **82**, 8629.
- Wright, B., Ziemann, I., Greig, R. and Poste, G. (1985) *Cell. Immunol.*, **95**, 46.
- Young, J. D. E. and Liu, C. C. (1988) *Immunol. Today*, **9**, 140.

Biological activity of an antibiotic puromycin—A theoretical study

R. P. OJHA and N. K. SANYAL

Biophysics Unit, Department of Physics, University of Gorakhpur, Gorakhpur 273 009, India

MS received 1 March 1990; revised 20 July 1990

Abstract. Puromycin is known to be an anti-tumor agent. Evaluation of interaction energy of this molecule with nucleic acid bases and base pairs has been performed using quantum-mechanical perturbation technique. Both in-plane and stacking energies have been evaluated. These energy values along with their sites of association have been compared with the standard values during transcription process. The results have been examined in the light of their biological significance.

Keywords. Antibiotics; interaction energy; puromycin.

Introduction

The amino acid sequence of a protein is encoded in the nucleotide sequence of mRNA. A sequence of 3 nucleotides, the codon, directs the incorporation of the specific amino acid into the protein to be synthesized. The association of proper amino acids with mRNA codons is accomplished at the ribosome with the mediation of tRNA. Each tRNA carries an amino acid and contains a nucleotide triplet, the anticodon, which is complementary to the codon specifying that amino acid.

The recognition of the codon by the anticodon involves the formation of 3 hydrogen-bonded base pairs. Two of the base pairs, those in the 5' and middle position, must be of the Watson and Crick (1953) type. However, the third, according to the 'Wobble' theory (Crick, 1966), may be of a different type. The importance of a given proton donor or acceptor group in the formation of codon-anticodon base pairs can be investigated by incorporating chemically modified nucleobases into the codon.

Puromycin is a broad-spectrum antibiotic with anti tumor activity that inhibits protein synthesis *in vivo* and *in vitro* (Suhadolnik, 1970; Nathans, 1967). Puromycin has been used to study (i) the mode of action of elongation (Pestka, 1972), (ii) the inhibition of protein synthesis (Nair and Emmanuel, 1977; Sugiyama *et al.*, 1985; Vara *et al.*, 1988) and (iii) the movement of protein synthesis initiator (Benne and Voorma, 1972). Puromycin has an inhibitory effect that could be related to similar substrate recognition mechanism by rRNA in the ribosome and by M1 RNA in RNase P (Viogue, 1989). Photo incorporation reaction shows that it may covalently incorporate into protein and to a much lesser extent into RNA (Gilley and Pellegrini, 1985). It binds to RNA at positions involved in tRNA interaction (Moazed and Noller, 1987a, b). Complete inhibition of binding of the aminoacyl-

codon, AUG is used. Lacalle *et al.* (1989) have shown that transcription starts at or next to a C residue 35 bp upstream from the putative ATG start codon in *pac* gene encoding a puromycin N acetyl transferase. The amino nucleoside component of puromycin [(N⁶-dimethyl-9-(3'-amino-3'-deoxy- β -D)-ribofuranosyl)adenine(PAN)] (figure 1) is 3–4 times more active against trypanosoma *Equiperdum* than puromycin. Amino-purine nucleoside of puromycin inhibited rRNA and the RNA content of the cells, but did not affect the rate of cell division for several generations (Studzinski *et al.*, 1968; Taylor and Stanners, 1968). Vince *et al.* (1976) reported that 5'-deoxy-PAN and the demethylated derivative show no nephrotoxicity. Puromycin significantly inhibits collagen synthesis (Barile *et al.*, 1989) and affects hormone binding (Farese, 1984). The effect of dietary protein and converting enzyme inhibition on chronic puromycin amino nucleoside nephropathy have been studied (Marinides *et al.*, 1990).

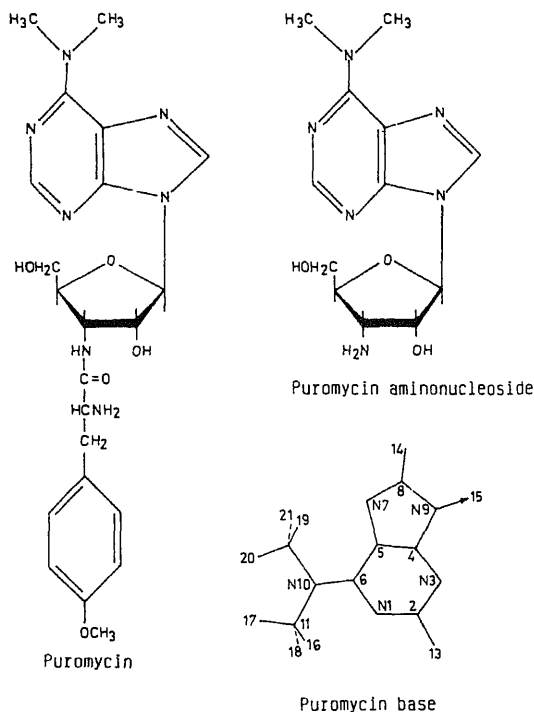


Figure 1. Chemical structure of puromycin.

The crystal structure of puromycin has been solved by several workers (Sunderlingam and Arora, 1969; Morr and Ernst, 1979; Sheldrick and Morr, 1980). Puromycin adopt an *anti* conformation about the glycosylic C(1')–N(9) bond. The position of the C(5')–O(5') bond relative to the ribose ring is *gg* or *gt* conformation.

A number of nucleoside analogue have been studied such as pyrazolopyrimidine

consequence (Sanyal *et al.*, 1986a, b) has been employed here to study the biological activity of puromycin.

Procedure

The procedure, described in our earlier studies (Sanyal *et al.*, 1984, 1986a, 1987a, b; Ojha *et al.*, 1987, 1988; Ojha and Sanyal, 1989) has been applied successfully to the study of the complexing selectivity of puromycin. The binding energy has been computed as a sum of terms, electrostatic interaction (E_{el}), polarization (E_{pol}), dispersion (E_{disp}) and repulsion (E_{rep}). These parameters have been chosen to reproduce results based on accurate *ab-initio* calculations on small systems. The crystallographic coordinates of puromycin base have been taken from Sunderlingam and Arora (1969). The molecular charge distribution on the interacting molecule has been computed by CNDO/2 method. These mono poles and dipoles at the atomic centers of puromycin base and nucleic acid bases and base pairs have been used to calculate the interaction energies between interacting systems. The binding site of the interacting molecule has been obtained by the minimization process (Sanyal *et al.*, 1986a, b, 1987a, b) for the optimization of energies. The energy values and site of association of puromycin have been compared with the recommended energy values and site of association of nucleic acid bases for the process transcription.

The computations were carried out on CDC cyber-170 computer at Tata Institute of Fundamental Research, Bombay.

Results and discussion

The molecular charge distributions on the atomic centers of puromycin are presented in table 1, corresponding to the atomic indices at the atomic centers of analogue base in figure 1. The table 1 also shows the net charges at the atomic centers of adenine computed by the same method. It is clear from the table that the charges at the atomic centers of the two molecules are similar, except at the positions affected by the substitution and in its neighborhood. The charge distribution on puromycin indicates that the capacity to accept proton is increased at position 1, and decreases at atom N(3) and N(6). The variations in the atomic charges and the presence of methyl group change the capability of internal hydrogen bonding in the nucleoside analogue.

Interaction energy

The in-plane interaction energy (base pairing) between normal bases and analogue bases is helpful in understanding the basic biological functions such as replication and transcription. Earlier, such calculations have been carried out (Sanyal *et al.*,

Table 1. Molecular charge distribution (monopole and dipoles) on puromycin and net charges at the atomic centers of adenine.

			Atomic dipoles (Debyes)			Net charges on adenine	
Atom No.	Atom	Charge	X	Y	Z	Atom	Charge
1	N1	-0.301	0.790	1.589	0.000	N1	-0.285
2	C2	0.233	-0.024	0.152	0.000	C2	0.232
3	N3	-0.253	-1.898	0.097	0.000	N3	-0.261
4	C4	0.212	0.166	0.290	0.000	C4	0.219
5	C5	-0.058	0.135	0.049	0.000	C5	-0.060
6	C6	0.255	-0.214	-0.100	0.000	C6	0.265
7	N7	-0.212	1.805	-0.716	0.000	H7	-0.204
8	C8	0.178	0.183	-0.324	0.000	C8	0.174
9	N9	-0.155	-0.080	0.025	0.000	N9	-0.145
10	N(6)	-0.125	0.001	0.004	0.000	N(6)	-0.227
11	C(6)	0.092	0.146	0.310	0.000	H(9)	-0.014
12	C'(6)	0.088	0.188	-0.288	0.000	H(8)	-0.017
13	H(2)	-0.045	0.000	0.000	0.000	H'(6)	0.122
14	H(8)	-0.022	0.000	0.000	0.000	H''(6)	0.119
15	H(9)	0.120	0.000	0.000	0.000	H(2)	-0.045
16	H(Me)	-0.001	0.000	0.000	0.000		
17	H'(Me)	-0.004	0.000	0.000	0.000		
18	H''(Me)	-0.001	0.000	0.000	0.000		
19	H(Me')	0.000	0.000	0.000	0.000		
20	H'(Me')	-0.002	0.000	0.000	0.000		
21	H''(Me')	0.000	0.000	0.000	0.000		

Pairing energy of puromycin base (PUR) has been calculated with the normal bases (pyrimidine). The minimum energy values for these configurations are very small and are not stable in comparison to the normal base pairs in the Watson-Crick positions (table 2), therefore, these configurations are not shown. Due to the presence of methyl group at N(6) position, only one hydrogen bond formation is possible at N1 atom by a proton donator of the complimentary base (pyrimidine). The incorporation of puromycin is not possible during replication process.

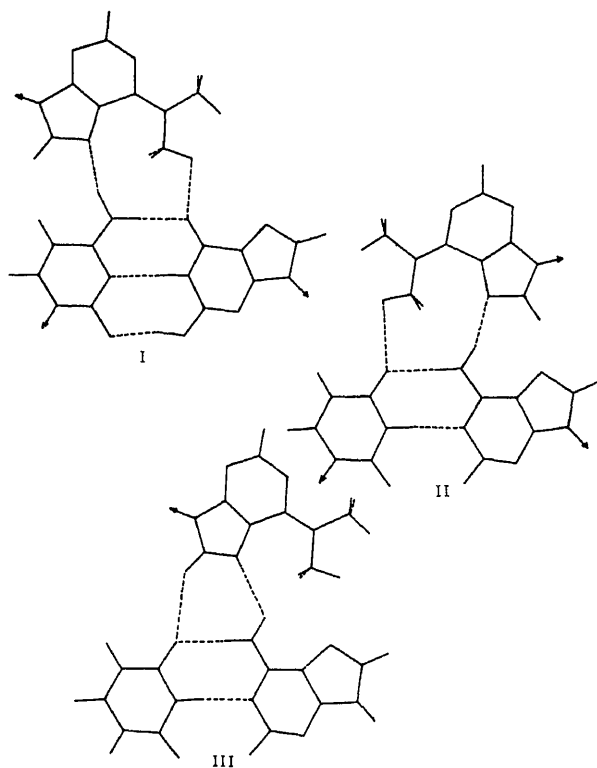
Table 2. Recommended energy values of nucleic acid bases during transcription (kcal/mol).

Pairing energy		Trimer energy	
Complex	Energy	Complex	Energy
G-C	-20.55	(G-C)-G	-20.91
		(G-C)-C	-14.75
A-U	-8.52	(A-U)-A	-5.01
		(A-U)-U	-8.55
A-T	-8.49	(A-T)-A	-4.42
		(A-T)-T	-8.10

Table 3. Trimer energy: Hydrogen bonding energy (in kcal/mol) of puromycin with nucleic acid base pairs.

Base pair	Complex	E_{qq}	$E_{q\mu}$	$E_{\mu\mu}$	E_{el}	E_{pol}	E_{disp}	E_{rep}	E_{tot}
GC	I	-1.4608	-2.3156	0.9276	-2.8488	-2.3051	-7.2255	5.7435	-6.6358
AU	II	-0.9279	-1.8694	0.8122	-1.9851	-1.2558	-7.0525	5.1499	-5.1435
	III	-0.3591	-0.9757	0.9987	-0.3360	-0.8202	-5.3210	2.8796	-3.5976

Total energy (E_{tot}) = $E_{el} + E_{pol} + E_{disp} + E_{rep}$; $E_{el} = E_{qq} + E_{q\mu} + E_{\mu\mu}$.

**Figure 2.** Minimum energy configurations of puromycin base with nucleic acid base pairs (G-C and A-U) from the deep groove side.

spatial positions of these interaction sites are illustrated by the arrow diagram (figure 3), where the arrows represent the glycosidic bond. The head of the arrow pointing towards the sugar and tail is at the N9 atom of puromycin base. The comparative study of the spatial positions are shown in figure 3, where the arrows with asterisk represent the site of interaction of the normal nucleic acid bases. From table 3, it is clear that the dispersion term is dominant for all the complexes but the

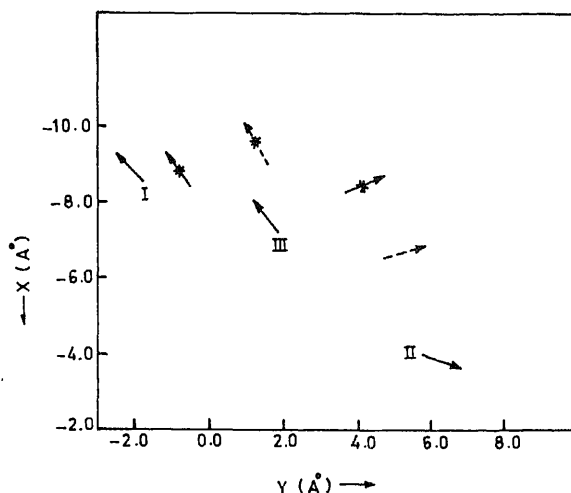


Figure 3. Arrow diagram corresponding to sugar ends of the entrant analogue base puromycin in the minimum energy configurations of base pair interaction. The arrow with asterisk represents the recommended site of interaction. The origin is constructed at the N1 atom of purine in the base pair and the X-axis is along the N1-C2 bond of purine. The Y-axis is perpendicular to X-axis in the molecular plane. The Z-axis is considered perpendicular to the plane of the molecule.

The interaction energy value (-6.6358 kcal/mol) of complex I (anti) for (G-C)-PUR is small as compared to the standard complexes for (G-C)-G and (G-C)-C (table 2) and the site of association is displaced from the standard site as indicated in figure 3. Therefore incorporation is not possible.

The interaction energy complexes of (A-U)-PUR corresponding to complexes II (*syn*) and III (anti) have energy values -5.1435 and -3.5976 kcal/mol respectively. From figure 3, it is clear that complex II is widely deviated from the standard site of association; however, its energy value is comparable to the recommended energy values (table 2). Therefore, the incorporation of puromycin is not probable through complex II but the binding of the puromycin through complex II (*syn*) cannot be ignored. The binding of puromycin through complex II will result in the loss of dyad symmetry by growing RNA chain. This will stop the growth of the RNA chain and in agreement with experimental observations (Taylor and Stanners, 1968; Studzinski and Ellen, 1968; Viogue, 1989). Complex III (anti) is displaced from the standard site and bears energy values less than the recommended energy value (table 2). From figure 3, it is clear that complex III may reach the standard site, resulting in reduction in energy values for the corresponding complex (III) or in other words it requires some additional energy to reach the recommended site of association, suggesting that incorporation is possible only in some drastic conditions, when the source of energy is available in the system (Sanyal *et al.*, 1981, 1984, 1986a, b, 1987a, b; Saenger, 1984; Ojha *et al.*, 1987, 1988; Ojha and Sanyal,

puromycin and source of energy in the biological system play an important role in the incorporation process. It is clear from the above discussion that puromycin may be incorporated in the RNA chain in place of adenosine. These RNAs grow like normal RNA but show abnormal properties. Incorporation of puromycin in place of adenosine in the RNA chain changes the codons and would affect the translation process (protein synthesis). Miscoding leads to inhibition of protein synthesis (Nair and Emmanuel, 1977; Gilley and Pellegrini 1985; Sugiyama *et al.*, 1985; Moazed and Noller, 1987a; Vara *et al.*, 1988; Lacalle *et al.*, 1989; Marinides *et al.*, 1990; etc.).

Stacking energy

The stacking energy of puromycin base with the nucleic acid bases has been given in table 4, while the corresponding minimum energy configurations are shown in figure 4. Table 4, also contains the separation between two interacting molecules at

Table 4. Stacking energy (in kcal/mol) of puromycin with nucleic acid bases.

Inter-acting base	Seperation (Å)	E_{qq}	E_{qm}	E_{mm}	E_{el}	E_{pol}	E_{disp}	E_{rep}	E_{tot}
G	3.12	-0.4345	-4.1076	-2.1711	-6.7132	-1.7855	-10.6099	6.0830	-13.0256
A	3.06	-0.2439	-2.5156	-2.0463	-4.8057	-0.6667	-10.2505	6.4818	-9.2411
C	3.24	-0.0764	-4.4230	-2.2491	-6.7485	-1.4242	-8.8601	5.1918	-11.8410
U	3.30	-0.5960	-2.0721	-1.0873	-3.7554	-1.0243	-8.4771	4.4213	-8.8355
T	3.34	-0.6657	-2.0566	-0.8447	-3.5670	-1.0075	-8.4628	4.0528	-8.9845

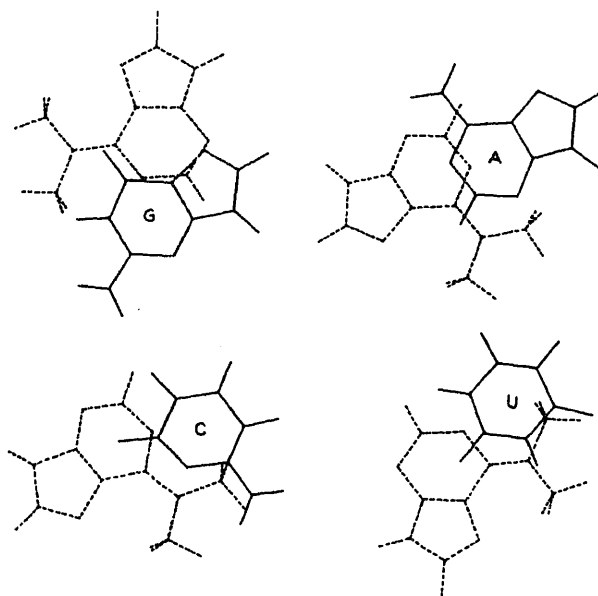
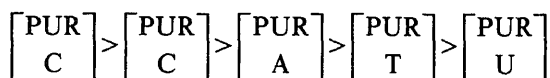


Fig. 4. Minimum energy configurations of stacked complexes of puromycin with

equilibrium position. The dispersion energy values are dominant for all complexes with significant values for repulsion forces which reduces the resultant effect on Kitaigorodaskii term. The electrostatic terms are appreciable and play a decisive role in binding of these complexes; however, polarization energy is weak and has been used to stabilize these complexes. The stability of the stacked complexes formed by puromycin with nucleic acid bases is in the following order:



This indicates that the complexes formed by puromycin with polar bases are more stable. The comparative energy values of these complexes show the particular specificity of puromycin and the base for binding during the transcription process under similar conditions. It prefers to bind near guanine (G) or cytosine (C) in the chain. The preference of purine or pyrimidine base to stack with puromycin base during elongation process depends on the selection of the template for recognition in the biological system. Therefore, puromycin may incorporate in place of adenosine, in the RNA chain, near guanosine or cytidine and the corresponding nucleotide will produce some faulty protein or it may work as a inhibitor of protein synthesis. These findings based on theoretical calculations, are in agreement with the experimental observations (Bretscher and Marker, 1966; Nathans, 1967; Suhadolnik, 1970; Pestka, 1970, 1972; Benne and Voorma, 1972; Nair and Emmanuel, 1977; Guerrier-Takada *et al.*, 1984; McClain *et al.*, 1987; Moazed and Noller, 1987a, b; Lacalle *et al.*, 1989, etc.).

Conclusion

Based on our incorporation model, the above discussion indicates that puromycin may be incorporated in place of adenosine in RNA chain during the process of transcription. The preferred site of association of puromycin in the RNA chain is in the neighborhood of guanosine or cytosine. The incorporation of puromycin results in the inhibition of protein synthesis. Its binding through complex II may result in inhibition of protein synthesis, but puromycin may not be an inhibitor of the replication process. These results are in agreement with experimental observations.

Acknowledgements

The authors are thankful to Prof. G. Govil and Prof. A. Saran, Tata Institute of Fundamental Research, Bombay for the computational facilities and helpful discussion. This work was supported by DST grant MO5/87 and UGC grant 52-SC-1/88 to RPO.

References

- Crick, F. H. C. (1966) *J. Mol. Biol.*, **19**, 548.
- Farese, R. V., Sabir, M. A. and Davis, T. S. (1984) *Biochim. Biophys. Acta*, **793**, 317.
- Gilley, M. and Pellegrini, M. (1985) *Biochemistry*, **24**, 5781.
- Guerrier-Takada, C., McClain, W. H. and Altman, S. (1984) *Cell*, **38**, 219.
- Lacalle, R. A., Pulid, D., Vara, J., Zalacain, M. and Jimenez, A. (1989) *Gene*, **79**, 375.
- Marinides, G. M., Groggel, G. C., Cohen, A. H. and Border, W. A. (1990) *Kidney Int.*, **37**, 749.
- McClain, W. H., Guerrier-Takada, C. and Altman, S. (1987) *Science*, **238**, 527.
- Moazed, D. and Noller, N. F. (1987a) *Nature (London)*, **327**, 389.
- Moazed, D. and Noller, N. F. (1987b) *Biochimie*, **69**, 879.
- Morr, M. and Ernst, L. (1979) *Chem. Br.*, **112**, 2815.
- Nair, V. and Emmanuel, D. J. (1977) *J. Am. Chem. Soc.*, **99**, 1571.
- Nash, H. A. and Bradley, D. F. (1966) *J. Chem. Phys.*, **45**, 1380.
- Nathans, D. (1967) in *Antibiotic* (eds D. Goltleib and P. D. Shaw) (Berlin: Springer-Verlag) vol. 1, p. 259.
- Ojha, R. P., Roychoudhury, M. and Sanyal, N. K. (1987) *J. Biosci.*, **12**, 311.
- Ojha, R. P., Roychoudhury, M. and Sanyal, N. K. (1988) *Indian J. Biochem. Biophys.*, **19**, 237.
- Ojha, R. P. and Sanyal, N. K. (1989) *J. Biosci.*, **14**, 319.
- Pestka, S. (1970) *Arch. Biochem. Biophys.*, **136**, 89.
- Pestka, S. (1972) *Proc. Natl. Acad. Sci. USA*, **69**, 624.
- Saenger, W. (1984) *Principles of nucleic acid structure* (New York: Springer-Verlag).
- Sanyal, N. K., Ojha, R. P. and Roychoudhury, M. (1986a) *Int. J. Biol. Macromol.*, **8**, 183.
- Sanyal, N. K., Ojha, R. P. and Roychoudhury, M. (1986b) *J. Comp. Chem.*, **7**, 13, 20, 30.
- Sanyal, N. K., Ojha, R. P. and Roychoudhury, M. (1987a) *Int. J. Biol. Macromol.*, **9**, 19.
- Sanyal, N. K., Ojha, R. P. and Roychoudhury, M. (1987b) *J. Comp. Chem.*, **8**, 272.
- Sanyal, N. K., Roychoudhury, M. and Ojha, R. P. (1981) *Int. J. Quant. Chem.*, **20**, 159.
- Sanyal, N. K., Roychoudhury, M. and Ojha, R. P. (1984) *J. Theor. Biol.*, **110**, 505.
- Sheldrick, W. S. and Morr, M. (1980) *Acta. Crystallogr.*, **B36**, 2328.
- Studzinski, G. P. and Ellen, K. O. L. (1968) *Cancer Res.*, **28**, 1773.
- Sugiyama, M., Paik, S. Y. and Nomi, R. (1985) *J. Gen. Microbiol.*, **131**, 1999.
- Suhadolnik, R. J. (1970) *Nucleoside antibiotics* (New York: Wiley).
- Sunderlingam, M. and Arora, S. K. (1969) *Proc. Natl. Acad. Sci. USA*, **64**, 1021.
- Taylor, J. M. and Stanners, C. P. (1968) *Biochim. Biophys. Acta*, **155**, 424.
- Vara, J. A., Pulido, D., Lacalle, R. A., Jimenez, A. (1988) *Gene*, **69**, 135.
- Vince, R., Almquist, R. G., Ritter, C. L., Shiota, F. N. and Nagasawa, H. T. (1976) *Life Sci.*, **18**, 345.
- Viogues, A. (1989) *FEBS Lett.*, **246**, 137.
- Watson, J. D. and Crick, F. H. C. (1953) *Nature (London)*, **171**, 737.

Human placental calcium activated neutral proteinase: Separation and functional characterization of subunits

RADHIKA SHASTRI, G. JAGADEESH and M. P. J. S. ANANDARAJ*

Molecular Genetics Unit, Institute of Genetics and Hospital for Genetic Diseases, Begumpet, Hyderabad 500 016, India

MS submitted 3 August 1990

Abstract. The subunits of human placental milli calcium activated neutral proteinase and micro calcium activated neutral proteinase have been separated by partial denaturation with urea followed by molecular sieving, with a recovery of 82-91% of activity. The separated subunits were homogeneous, as judged by sodium dodecyl sulphate-polyacrylamide gel electrophoresis. Their molecular sizes, catalytic activities and sulphhydryl contents suggest that both the subunits of these two calcium activated neutral proteinases are distinct. The subunits were highly specific and could not be interchanged. Both the subunits of micro calcium activated neutral proteinase were catalytically active whereas only the 80 k subunit of milli calcium activated neutral proteinase was active. 30 k subunit of milli calcium activated neutral proteinase has a regulatory role since maximum activity of the 80 k subunit was elicited only in its presence. Activity of the re-associated subunits indicated that interaction is essential for the expression of optimum activity. Interaction of subunits rendered the enzymes less susceptible to inhibition by endogenous calcium activated neutral proteinase inhibitor.

Keywords. Proteinase; Ca^{2+} activated; subunits; separation procedure; thiol content; human placenta.

Introduction

Calcium activated neutral proteinase (CANP), a non lysosomal endopeptidase (EC 3.4.22.17) is active at neutral pH, only in the presence of calcium ions. Two forms of this enzyme (mCANP and μ CANP) requiring different calcium concentrations for their activities have been identified in several tissues. While mCANP is maximally active only in the presence of mM calcium, μ CANP is active at μ M levels of calcium. The two forms of this enzyme (mCANP and μ CANP) coexist with an endogenous CANP inhibitor (ECI) in various tissues. This endogenous inhibitor is implicated in the regulation of CANP in several tissues (Murachi 1983; Ishiura, 1981). It has been established that both the CANPs are heterodimers with a large (80 k) and a small (30 k) subunit. Their actual molecular weight (M_r) range is 72-90 kDa (80 k) and 25-30 kDa (30 k) (Suzuki *et al.*, 1984). The large subunits of both mCANP and μ CANP have been found to have catalytic activity, but the function of the small subunits is not clearly defined (Tsuji and Imahori, 1981a). The subunits of rabbit skeletal muscle mCANP (Tsuji and Imahori, 1981), human erythrocyte μ CANP, porcine erythrocyte μ CANP and porcine kidney mCANP

Various relationships between the two CANPs have been postulated. Suzuki *et al.* (1981) consider μ CANP to be derived by the autolysis of mCANP and Dayton *et al.* (1981) consider that phosphorylation of μ CANP converts it to mCANP. We had observed that the two CANPs are distinct species (Shastri and Anandaraj, 1986). A comparative study of the individual subunits of the two enzymes from a single tissue would clearly indicate their relationship.

A procedure for the effective separation of the subunits of both mCANP and μ CANP is reported in this paper. Some properties of the individual subunits have been studied in an attempt to elucidate the role of each subunit in the overall catalytic reaction.

Materials and methods

Materials

Soluble casein (A.R.) was a product of B.D.H., Poole, UK. Ultrogel AcA 54 was purchased from LKB, Bromma, Sweden. Acrylamide, dithiobisnitrobenzoic acid (DTNB), iodoacetic acid (IAA), Tris and M_r markers were obtained from Sigma Chemical Co., St. Louis, Missouri, USA. Other reagents used were of the highest grade of purity available.

Methods

Purification of CANPs and ECI: μ CANP and mCANP were purified to homogeneity from human placenta, as described earlier (Shastri and Anandaraj, 1986; Rabbani *et al.*, 1986). The procedure included chromatography on DEAE cellulose, Ultrogel AcA 34 or AcA 22 and DEAE Sephadex A50, in succession. ECI was partially purified as described earlier (Shastri and Anandaraj, 1986).

Assay of CANP and ECI: Activity of the enzymes and inhibitor was monitored using alkali-denatured casein as substrate, as described earlier (Shastri and Anandaraj, 1986; Rabbani *et al.*, 1986). The assay mixture consisted of 1–5 μ g of the enzyme or subunit in a total volume of 0.5 ml containing 0.25% alkali-denatured casein in 20 mM Tris-HCl buffer, pH 7.5, 10 mM 2-mercaptoethanol and CaCl_2 (5 mM for mCANP and 100 μ M for μ CANP). Controls had 5 mM EDTA instead of CaCl_2 . Reaction was terminated after 90 min at 30°C with cold 10% TCA and A_{280} of the TCA soluble supernatant was monitored with control as blank. A unit of activity is defined as the amount that catalyses an increase of one A_{280} unit under the standard assay conditions.

Four μ g of mCANP when preincubated at 30°C for 15 min with the inhibitor in the range of 5–15 μ g, it was observed that 5 μ g of inhibitor gave a 50% inhibition. When subunits were assayed for enzyme activity 1 μ g of purified subunit (μ or m 80 k), activity was in the linear range. Therefore with 1 μ g of subunit in the presence

Initial experiments on reassociation of subunits were ascertained by 7.5% non denaturing polyacrylamide gel electrophoresis (PAGE) in the presence of 0.375 M Tris HCl buffer pH 7.5 (Williams and Reisfeld, 1964). However the restoration of activity presented in table 1 was based on a stoichiometric mixing of the subunits (stoichiometry having been arrived at on the basis of A_{280} ratios of the subunits eluted from AcA 54 column).

Sulphydryl titration: Sulphydryl groups in the subunits and native enzymes were titrated with DTNB according to the method of Ellman (1959). The subunits or native enzymes were dialysed extensively against 20 mM Tris-HCl, pH 7.5, containing 5 mM EDTA. Protein (40–80 μ g) was added to 6 ml of 50 mM phosphate buffer pH 8 with or without 1 mM CaCl_2 or 6 M urea. The samples were divided between reference and sample cuvettes. Reaction was initiated by the addition of 0.02 ml of 10 mM DTNB reagent. The initial absorbance at 412 nm was noted immediately. The absorbance steadily increased and stabilised by about an hour. The increase in absorbance which is proportional to the number of sulphydryl groups titrated was calculated using a molar extinction co-efficient of $13,600 \text{ cm}^{-1} \text{ M}^{-1}$ for the thionitrobenzoate ions liberated.

Results

Separation of subunits

The subunits of both mCANP and μ CANP were separated by limited denaturation with urea. Separation was carried out at 4°C. The purified enzyme (mCANP or μ CANP) was incubated with 6 M urea for 30 min and chromatographed on an Ultrogel AcA 54 column (1.25 \times 20 cm), previously equilibrated with buffer A (20 mM Tris-HCl, pH 7.5, 10 mM 2-mercaptoethanol, 5 mM EDTA). The subunits were eluted with buffer A and absorbance at 280 nm of each fraction was monitored (figure 1). Both the enzymes were heterodimers and eluted as two peaks, constituting the 80 k and 30 k subunits, respectively. The peak fractions were pooled and used as individual subunits for further study. They were found to be homogeneous as judged by sodium dodecyl sulphate (SDS)-PAGE (figure 2). M_r of the mCANP subunits were 70 and 32 kDa; and those of μ CANP were 74 and 32 kDa. This difference in the molecular size of the 80 k subunits of mCANP and μ CANP was observed on gelfiltration chromatography also, where the μ 80 k was eluted earlier than m80 k. The yield of the subunits of mCANP was in a molar ratio of 1:2.5 (80 k:30 k), whereas that of μ CANP was in a molar ratio of 1:1.4 (80 k:30 k). Both the subunits of μ CANP were catalytically active whereas only the 80 k subunit of mCANP showed activity.

Reassociation of subunits

The subunits of mCANP and μ CANP were mixed at molar ratios of 1:2.5 (80 k:30 k) and 1:1.4, respectively, and their activity was monitored. The molar ratios of the subunits, as observed from their yields after separation, were chosen for reassociation studies since this would reflect their ratios in the native enzymes.

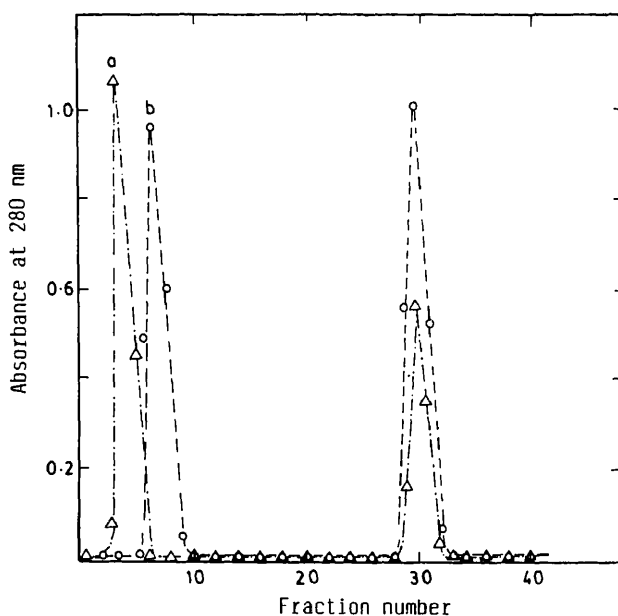


Figure 1. Separation of subunits. 1.1 mg of μ CANP (a) or 1.4 mg of mCANP (b) were fractionated on separate Ultrogel AcA 54 columns. The purified enzymes were incubated with urea (6 M) for 30 min at 4°C and chromatographed on Ultrogel AcA 54 column (1.25 \times 20 cm), previously equilibrated with buffer A. The subunits were eluted with buffer A. 1 ml fractions were collected at a flow rate of 30 ml/h and the absorbance of each fraction was monitored at 280 nm. The elution profiles are plotted on the same graph to facilitate comparison of the subunits.

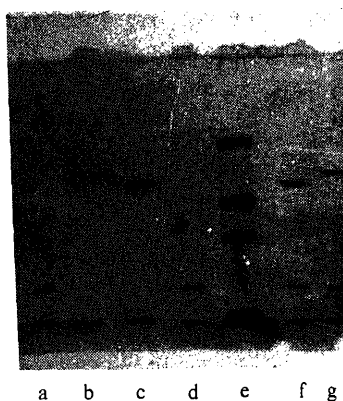


Figure 2. SDS-PAGE of subunits. 2 μ g of each subunit was electrophoresed on 10% SDS-polyacrylamide gel by the method of Laemmli (1970). The gels were stained with AgNO_3 . (a) μ 30 k; (b) μ 80 k; (c) m80 k; (d) m30 k; (e) standard proteins; (f) native mCANP; (g) native μ CANP. The standard proteins used were phosphorylase b (97.4 kDa), BSA (66 kDa), ovalbumin (45 kDa) and lysozyme (14.3 kDa).

Table 1. Reassociation of subunits.

	Specific activity (units/mg)	Activity (% of original activity)
μ CANP	410	100
μ 80 k	256.3	62.5
μ 30 k	294.8	71.9
μ 80 k + μ 30 k ^a	336.2	82.0
μ 80 k + m30 k ^a	176.3	43.0
mCANP	445	100
m80 k	263.9	59.3
m30 k	0	0
m80 k + m30 k ^b	406.7	91.4
m80 k + μ 30 k ^b	178.0	40.0

^aMolar ratio of 80 k:30 k was 1:1.4^bMolar ratio of 80 k:30 k was 1:2.5

the activity of native mCANP was recovered. The maximum activity recovered on interchanging the subunits was 43% (μ 80 k + m30 k) or 40% (m80 k + μ 30 k).

Effect of endogenous inhibitor

Native μ CANP was not inhibited by ECI. However, its 80 k subunit was partially inhibited (14.3% inhibition) and μ 30 k subunit was not inhibited by ECI. The activity (78%) of m80 k was inhibited by ECI which could inhibit only 50% of native mCANP activity.

Thiol content of the subunits

Sulphydryl groups of CANP have been classified based on their reaction with DTNB as class I: exposed, class II: buried but exposed in the presence of Ca^{2+} and class III: buried and titrated only on denaturation (Tsuji *et al.*, 1981). The sulphydryl content of native enzymes and their subunits, based on this classification is given in table 2.

Table 2. Titration of sulphydryl groups.

	Sulphydryl Groups (mol/mol protein)					
	mCANP			μ CANP		
	80 k	30 k	Native enzyme	80 k	30 k	Native enzyme
Native state	1.82	1.90	4.10	2.20	1.41	3.62
+ CaCl_2	3.10	2.01	4.99	3.10	1.80	4.79
+ Urea	3.20	3.00	6.30	3.24	1.91	5.03

The native enzymes and their subunits were inhibited by potent thiol inhibitors such as IAA and Ep 475 (epoxy succinate derivative of butane), indicating the involvement of thiol groups in catalytic activity (results not shown).

Discussion

The subunits of both mCANP and μ CANP have been separated by partial denaturation with urea followed by molecular sieving on Ultrogel AcA 54. Incubation of the purified enzymes was limited to 30 min, since prolonged incubation (1 h or more) with urea resulted in nonspecific degradation of the subunits. Recovery of activity after reassociation of the subunits was 82% for μ CANP and 91% for mCANP. Tsuji and Imahori (1981) could recover 92% of the original activity (at molar ratio of 1:1) after renaturation of the subunits of rabbit skeletal muscle mCANP. However, their procedure of separation, described for mCANP alone, involved prolonged exposure to urea and several steps for renaturation of the subunits. Kikuchi *et al.* (1984) could recover a maximum of 62% of the original activity of μ CANP (at a molar ratio of 80 k:30 k of 1:1.25) and 69% of mCANP activity (at a molar ratio of 1:1.4) in the porcine tissues. The procedure reported here, for the separation of the subunits of both the CANPs, is thus, more efficient than those reported so far and has the added advantage of denaturation for a short period. Moreover, there is no necessity of renaturation of the separated subunits as urea is not used in the eluting buffer. One hundred per cent recovery of activity was not possible indicating that separation of subunits results in the loss of some activity although the subunits were intact, as seen from their SDS-PAGE profiles.

Only 40–43% of enzyme activity was recovered on interchanging the subunits, suggesting that subunit interaction of the placental CANPs is highly specific. Kikuchi *et al.* (1984) observed that the subunits of porcine mCANP and μ CANP and human erythrocyte μ CANP are interchangeable. This discrepancy may be due to the difference in the separation procedure. Their procedure (using NaSCN) resulted in the loss of activity and Ca^{2+} sensitivity of the subunits (Kikuchi *et al.*, 1984). Probably, the specificity of the subunits was also affected by their procedure.

Catalytic activity was observed in both the subunits of μ CANP, whereas only the 80 k subunit of mCANP was active. Although m30 k was not catalytically active, it was essential for the recovery of activity. Thus, m30 k has a regulatory function whereas μ 30 k has catalytic activity as well. The regulatory role of μ 30 k is seen from the following observations. When the subunits of μ CANP were mixed, the resulting activity was much lower than the sum of the activities of the two subunits. This suggests that interaction of subunits creates some conformation essential for the expression of optimum activity, which may not necessarily be the maximum attainable. This view is supported by the observation that 14% of μ 80 k was inhibited whereas the native μ CANP and its 30 k subunit were not inhibited by ECI. The inhibition of native mCANP by ECI was much lower (50%) than that of its 80 k subunit (78%). These results clearly indicate an interaction of the subunits which promotes catalysis and reduces inhibition by ECI in both μ and mCANP. The 30 k subunits of bovine heart mCANP (DeMartino *et al.*, 1986) and rabbit skeletal muscle mCANP (Imajoh *et al.*, 1986) have been postulated to activate and regulate proteolytic activity.

Based on the classification of sulphydryl groups of CANP by Tsuji *et al.* (1981), the class II sulphydryl groups appear to be essential for catalysis, since the enzyme requires a thiol reagent and calcium for activity. Sulphydryl titration of the placental CANPs showed that only the 80 k subunit of mCANP had a class II sulphydryl group, whereas both the subunits of μ CANP had one class II sulphydryl group each. This probably is the reason for the activity of both the subunits of μ CANP and the absence of activity in the 30 k subunit of mCANP. A class II sulphydryl group appears, to have been exposed for titration on the separation of the subunits of μ CANP. This indicates that the subunits interact in such a way so as to expose a class II sulphydryl group, *i.e.*, convert it to the class I type in the native enzyme. This could also be the reason for the higher activities of the individual subunits as compared to native μ CANP. Rabbit skeletal muscle mCANP also has only one class II sulphydryl group located in the 80 k subunit which is catalytically active (Tsuji and Imahori, 1981). Sequencing of CANP genes has indicated Ca^{2+} binding sites in the 80 k subunits of chicken skeletal muscle mCANP (Ohno *et al.*, 1984; Emori *et al.*, 1986) and also in the 30 k subunit of porcine μ CANP (Sakihama *et al.*, 1985), suggesting that these subunits may have catalytic activity. However, Kikuchi *et al.* (1984) did not detect any activity in the 30 k subunits of porcine and human erythrocyte μ CANP. This may be attributed to their separation procedure which resulted in a loss of Ca^{2+} sensitivity and catalytic activity of the subunits (Kikuchi *et al.*, 1984).

Both the subunits of placental mCANP and μ CANP are distinct. They are highly specific and not interchangeable. The μ 80 k is larger than the m80 k. Although m30 k and μ 30 k have identical M_r , they are functionally distinct. Whereas μ 30 k had catalytic activity and a class II sulphydryl group, m30 k was catalytically inert and lacked the class II sulphydryl group. Structural similarity of the 30 k subunits and dissimilarity of the 80 k subunits of mCANP and μ CANP from various tissues have been reported. The 30 k subunits of mCANP and μ CANP have been found to have identical peptide maps and immunological cross reactions (Sasaki *et al.*, 1983; Kitahara *et al.*, 1984; Wheelock, 1982). The two forms of CANP have been found to be distinct species based on differences in M_r of their 80 k subunits, Ca^{2+} sensitivities of μ CANP and autolysed mCANP and the lack of immunological cross reaction of the autolysed mCANP with anti- μ CANP serum (Shastri and Anandaraj, 1986). The present study shows that the subunits are functionally distinct and thus supports our earlier report on the status of the two enzymes.

Acknowledgements

This work was supported by the Indian Council of Medical Research and the Department of Science and technology, New Delhi.

References

- Dayton, W. R., Schollmeyer, J. V., Lepley, R. A. and Cortes, L. R. (1981) *Biochim. Biophys. Acta*, **659**, 48.
- DeMartino, G. N., Huff, D. A. and Croall, D. E. (1986) *J. Biol. Chem.*, **261**, 12047.
- Ellman, G. L. (1959) *Arch. Biochem. Biophys.*, **82**, 70.
- Emori, Y., Ohno, S., Tobito, M. and Suzuki, K. (1986) *FEBS Lett.*, **194**, 249.
- Imajoh, S., Kawasaki, H. and Suzuki, K. (1986) *J. Biochem.*, **99**, 1281.

- Ishiura, S. (1981) *Life Sci.*, **29**, 1079.
- Kikuchi, T., Yumoto, N., Sasaki, T. and Murachi, T. (1984) *Arch. Biochem. Biophys.*, **234**, 639.
- Kitahara, A., Sasaki, T., Kikuchi, T., Yumoto, N., Yoshimura, N., Hatanaka, M. and Murachi, T. (1984) *J. Biochem.*, **95**, 1759.
- Laemmli, U. K. (1970) *Nature (London)*, **227**, 680.
- Murachi, T. (1983) *Trends Biochem. Sci.*, **8**, 167.
- Ohno, S., Emori, Y., Imajoh, S., Kawasaki, H., Kisaragi, M. and Suzuki, K. (1984) *Nature (London)*, **312**, 566.
- Rabbani, N., Shastri, R. and Anandaraj, M. P. J. S. (1986) *Placenta*, **7**, 73.
- Sakihama T., Kakidani, H., Zenita, K., Yumoto, N., Kikuchi, T., Sasaki, T., Kannagi, R., Nakanishi, S., Ohmori, M., Takio, K., Titani, K. and Murachi, T. (1985) *Proc. Natl. Acad. Sci. USA*, **82**, 6075.
- Sasaki, T., Yoshimura, N., Kikuchi, T., Hatanaka, M., Kitahara, A., Sakihama, T. and Murachi, T. (1983) *J. Biochem.*, **94**, 2055.
- Shastri, R. and Anandaraj, M. P. J. S. (1986) *Biochim. Biophys. Acta*, **873**, 260.
- Suzuki, K., Tsuji, S., Ishiura, S., Kimura, Y., Kubota, S. and Imahori, K. (1981) *J. Biochem.*, **90**, 1787.
- Suzuki, K., Kawashima, S. and Imahori, K. (1984) in *Calcium regulation in biological systems* (ed. S. Ebashi) (Japan: Takeda Science Foundation) p. 213.
- Tsuji, S. and Imahori, K. (1981) *J. Biochem.*, **90**, 233.
- Tsuji, S., Ishiura, S., Nakamura, T. M., Katamoto, T., Suzuki, K. and Imahori, K. (1981) *J. Biochem.*, **90**, 1405.
- Wheelock, M. J. (1982) *J. Biol. Chem.*, **257**, 12471.
- Williams, D. E. and Reisfeld, R. A. (1964) *Ann. N. Y. Acad. Sci.*, **121**, 373.

Endogenous inhibitor of calcium activated neutral proteinase from human placenta: Purification and possible mechanism of proteinase regulation

RADHIKA SHASTRI, B. SHAILAJA and M. P. J. S. ANANDARAJ*

Molecular Genetics Unit, Institute of Genetics and Hospital for Genetic Diseases, Begumpet, Hyderabad 500 016, India

MS submitted 3 August 1990

Abstract. An endogenous inhibitor of calcium activated neutral proteinase has been purified from human placenta. The procedure included chromatography on DEAE cellulose, Ultrogel AcA 22 and milli calcium activated neutral proteinase-sepharose in succession. Endogenous calcium activated neutral proteinase inhibitor was a tetramer with identical subunits of molecular weight 68 kDa. It was specific for milli calcium activated neutral proteinase (Calpain II) which is inhibited by the formation of an inactive enzyme-inhibitor complex and not by sequestering Ca^{2+} from the medium. Although micro calcium activated neutral proteinase (Calpain I) was not inhibited by endogenous calcium activated neutral proteinase inhibitor, it was protected from autolysis in the presence of the inhibitor. The placental endogenous calcium activated neutral proteinase inhibitor thus regulates Ca^{2+} activated proteolysis by ensuring micro calcium activated neutral proteinase activity, while inhibiting milli calcium activated neutral proteinase.

Keywords. Proteinase; human placenta; proteinase regulation; endogenous inhibitor.

Introduction

Calcium activated neutral proteinase (CANP), a nonlysosomal endopeptidase, is involved in a variety of physiological processes such as activation of enzymes (Huston and Krebs 1968; Ishiura 1981; Suzuki *et al.*, 1984), cleavage of cytoskeletal proteins of erythrocytes, platelets and nerve tissues (Ishiura *et al.*, 1982; Murachi 1983; Suzuki *et al.*, 1984), turnover of myofibrillar proteins (Reddy *et al.*, 1975; Dayton *et al.*, 1976, 1981) and regulation of hormone receptors (puca *et al.*, 1977; Baudry and Lynch, 1980; Vedekis *et al.*, 1980). Two forms of CANP (mCANP and μ CANP) coexist in several tissues (Ishiura, 1982). The precise physiological role of these two forms of CANP has not been defined. An endogenous CANP inhibitor (ECI) has been found to regulate Ca^{2+} activated proteolysis in several tissues (Murachi 1983; Imajoh *et al.*, 1984; Suzuki *et al.*, 1984). However, the mechanism of this regulation is not clearly understood except that the inhibitor enzyme complex is reversibly formed (Pontremoli and Melloni, 1986). It is also suggested that formation of CANP-ECI complex prevents the association and activation of the proteinase at the cell membrane (Suzuki, 1987). The characterization of ECI has been hampered due to discrepancy in the reported molecular sizes of the inhibitor from different tissues. The values range from 24 kDa

*To whom all the correspondence should be addressed.

(Nakamura *et al.*, 1984) to 450 kDa (Imajoh *et al.*, 1984) which include those for monomers, oligomers and their aggregates. The values for monomers are as diverse as 68 kDa (Ishiura *et al.*, 1982), 70 kDa (Takano and Murachi, 1982), 107 kDa (Takano *et al.*, 1984), 145 kDa (Mellgren and Carr, 1983) and 172 kDa (Lepley *et al.*, 1985). Such molecular diversity has been observed in ECI from a single species also (Takano *et al.*, 1984, 1986b). Imajoh and Suzuki (1985) observed fragmentation of the 107 kDa inhibitor on storage without loss of activity. The 107 kDa inhibitor from pig heart cross reacted with antiserum against 68 kDa ECI from pig erythrocytes (Takano *et al.*, 1986a), suggestive of a precursor-product relationship between the two species. The discrepancy in the reported values of molecular size of ECI may, thus, be attributed to fragmentation of ECI due to rather drastic procedures (heat, acid and/or urea treatments) used for its purification. These results suggest the necessity for milder purification procedures to obtain intact inhibitor molecules to enable their characterization. ECI had been partially purified from human placenta and some of its basic properties had been reported earlier (Rabbani *et al.*, 1986; Shastri and Anandaraj, 1986).

In this paper, a milder procedure (without heat, acid or urea treatments) is reported for the purification of ECI from human placenta. Some properties of the inhibitor have been studied in order to understand the mechanism of regulation of Ca^{2+} activated proteolytic activity.

Materials and methods

Soluble casein (AR) was a product of B.D.H., UK. DEAE cellulose, acrylamide and Tris were purchased from Sigma Chemical Co., St. Louis, Missouri, USA. Ultrogel AcA 22 was from LKB, Sweden. Activated CNBr-Sepharose 4B was from Pharmacia Fine Chemicals, Sweden. Other chemicals used were of the highest grade of purity available.

Assay of ECI

Inhibitor activity was monitored using mCANP as substrate. Residual activity of mCANP was monitored with alkali denatured casein as its substrate, as described earlier (Rabbani *et al.*, 1986). A unit of inhibitor is defined as the amount that inhibits one unit of mCANP. The concentration of ECI bringing about 50% inhibition of mCANP was used in all assays, unless mentioned otherwise.

Preparation of mCANP-sepharose column

mCANP was purified from human placenta, as described earlier (Rabbani *et al.*, 1986). The purified enzyme was coupled to CNBr-activated sepharose 4B according to the manufacturer's instructions. 0.5 g of CNBr-activated sepharose 4B was suspended in 1 mM HCl. After swelling, the gel was washed for 15 min with 100 ml

away with coupling buffer and any remaining active groups were blocked with 0.1 M Tris-HCl buffer, pH 8 for 16 h at 4°C. The resulting product was then washed with 3 cycles of alternating pH. Each cycle consisted of a wash with 0.1 M acetate buffer, pH 4 containing 0.5 M NaCl, followed by a wash with 0.1 M Tris buffer, pH 8 containing 0.5 M NaCl. The product was stored in 0.1 M Tris buffer, pH 8 containing 0.5 M NaCl, at 4°C till further use.

Polyacrylamide gel electrophoresis

Sodium dodecyl sulphate (SDS)-polyacrylamide gel electrophoresis (PAGE) was carried out by the method of Laemmli (1970).

Autolysis of CANP

mCANP and μ CANP were purified from human placenta as described earlier (Rabbani *et al.*, 1986; Shastri and Anandaraj, 1986). The purified enzyme (mCANP or μ CANP) was incubated at 30°C with CaCl_2 (1 mM). Aliquots were withdrawn at 5 min intervals and residual proteolytic activity was monitored as described earlier (Shastri and Anandaraj, 1986).

Results

Purification of ECI

All procedures were carried out at 4°C. Purification of ECI from human placenta involved the following steps:

Preparation of tissue homogenate: Human placenta was collected on ice and processed immediately. The tissue was freed of membranes, sliced and washed extensively with ice-cold saline. This was then homogenized in 5 volumes of 20 mM NaHCO_3 , 5 mM EDTA in a sorvall omnimixer for 10 s at top speed and centrifuged at 10,000 *g* for 10 min. The pH of the supernatant was reduced to 4.5 with 1 N acetic acid and was centrifuged at 20,000 *g* for 15 min.

Chromatography on DEAE cellulose and Ultrogel AcA 22: The 20,000 *g* precipitate (iso electric precipitate) was extracted in buffer A (20 mM Tris-HCl, pH 7.5, 5 mM EDTA, 10 mM 2-mercaptoethanol). The pH of this extract was raised to 7.5 with 1 M NaOH and it was then centrifuged at 20,000 *g* for 15 min. The supernatant was loaded onto a DEAE cellulose column (30 \times 3 cm), previously equilibrated with buffer A. The column was washed with 250 ml buffer A and developed with 700 ml of a linear gradient (0–0.6 M) of NaCl. Fractions (10 ml) were collected at a flow rate of 30 ml/h. All the fractions were assayed for μ CANP, ECI and mCANP. ECI and

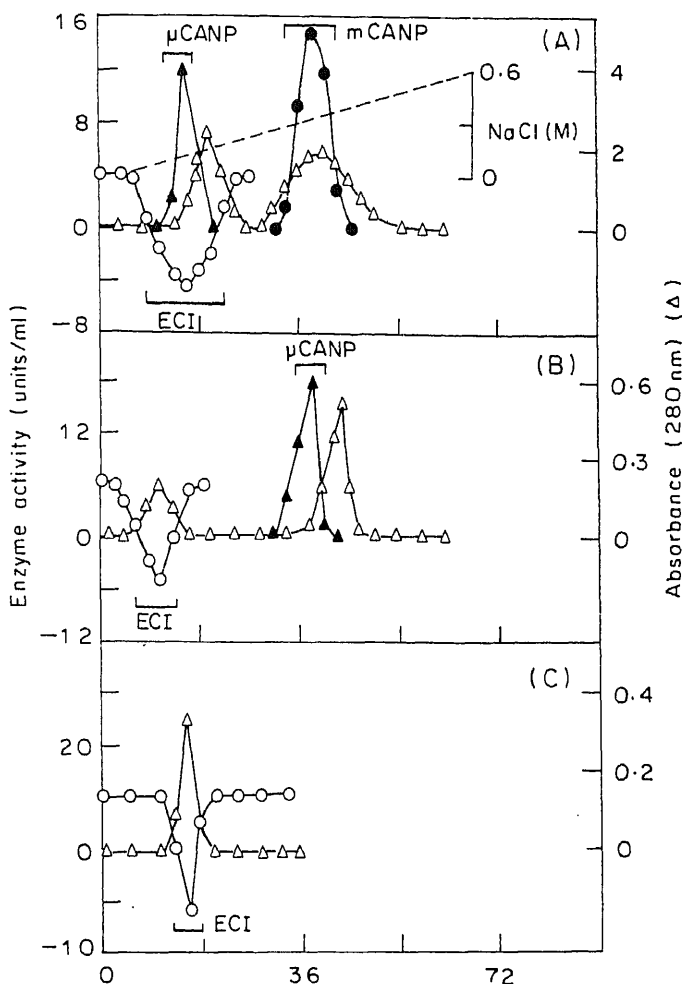


Figure 1. Purification of ECI.

ECI was purified from the iso-electric precipitate by chromatography on (A) DEAE cellulose, (B) Ultrogel Aca 22 and (C) mCANP-sepharose columns, in succession. Active fractions were pooled as indicated.

corresponding to about 250 kDa and μ CANP at about 110 kDa and were thus separated.

Affinity chromatography on mCANP-sepharose: ECI fractions from the Ultrogel Aca 22 column were pooled and dialysed against phosphate buffer saline (PBS) (0.01 M phosphate buffer, pH 7.5, 0.5 M NaCl) overnight at 4°C and loaded onto mCANP-sepharose 4B column (5 × 0.5 cm), previously equilibrated with PBS. The column was washed with PBS till A_{280} of the eluant retained to the baseline. Bound

5383-fold over the homogenate with a recovery of 48%. The purified inhibitor had a specific activity of 2692 (table 1), and was homogenous as judged by SDS-PAGE. The M_r of ECI was 68 kDa based on its mobility on SDS-PAGE.

Table 1. Purification of ECI.

Step	Total protein (mg)	Specific activity (units/mg)	Total activity (units)	Purification (fold)	Recovery (%)
1. Homogenate	6,318	0.5	3159	1.0	100
2. Isoelectric precipitate	1,702	2.0	2825	3.0	89
3. DEAE cellulose chromatography	45	58	2641	117	84
4. Ammonium sulphate precipitate	9	261	2323	522	74
5. Ultrogel AcA 22 chromatography	1	1496	1676	2992	53
6. mCANP-sepharose chromatography	0.6	2692	1434	5,383	49

ECI was purified from human placenta (295 g wet weight).

Specificity of ECI

The effect of ECI on proteases such as mCANP, μ CANP, trypsin and chymotrypsin was monitored in order to determine its specificity. mCANP alone was inhibited by ECI. The other proteases tested were not inhibited even at a ratio of ECI:protease of 15:1 (w/w). Inhibition (50%) of mCANP was at a ratio of 1.2:1 (w/w) or molar ratio of 1:2 (ECI:mCANP), with a k_m of 0.02 nmol. The specificity of ECI and the extent of inhibition of mCANP were not affected when Ca^{2+} was introduced.

Mechanism of inhibition of mCANP

The effect of ECI on mCANP activity was monitored at different levels of enzyme and inhibitor (figure 2a). In the absence of the inhibitor, proteolytic activity increased in proportion to the level of the enzyme. When the inhibitor was introduced, enzyme activity could be observed only above a certain ratio of the enzyme: inhibitor. This ratio showed that one mol of ECI inactivated two mol of mCANP. The rate of increase of enzyme activity was not affected by the presence or level of the inhibitor although the maximum activity decreased in proportion to the amount of the inhibitor.

Ca^{2+} sensitivity of mCANP was monitored in the presence of ECI, in order to

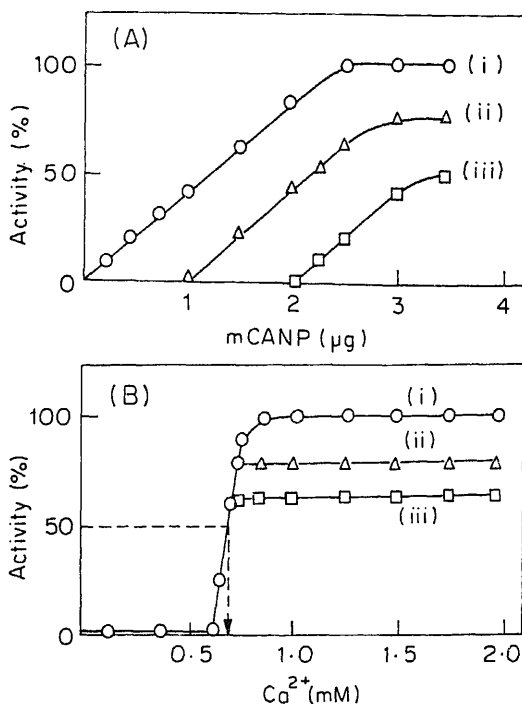


Figure 2. Mechanism of inhibition of mCANP.

A. Proteolytic activity of mCANP was monitored in the absence (i) or in presence of 1.2 μg (ii) and 2.4 μg (iii) of ECI. **B.** Ca^{2+} sensitivity of mCANP was monitored in the absence (i) or presence of 1 μg (ii) and 2 μg (iii) of ECI. Other assay conditions are described in materials and methods.

Effect of ECI on autolysis of CANP

mCANP and μCANP undergo autolysis in the presence of appropriate amount of calcium ions and specifically in the absence of substrate. In order to understand the possible role of ECI in the regulation of this process mCANP and μCANP were autolysed in the presence of ECI. The rate of autolysis of mCANP (measured by the amount of residual activity, since autolysis results in loss of activity) was not altered by the presence of ECI. However the rate of autolysis of μCANP was prevented by the presence of ECI. Apparently the interacting sites of μCANP to inhibitor is necessary for the autolysis.

Discussion

ECI was purified to homogeneity from human placenta by chromatography on DEAE cellulose, Ultrogel AcA 22 and mCANP-sepharose 4B, in succession. This

This step enables the elimination of drastic steps, such as acid, heat and/or urea treatments, employed for the purification of the inhibitor from several tissues (Imajoh *et al.*, 1984; Lepley *et al.*, 1985), which could have been one of the reasons for the reported variations in size of ECI. Chromatography on mCANP-sepharose may also be used to purify ECI from cruder preparations of the inhibitor. The placental inhibitor is a tetramer with identical subunits of 68 kDa each, since it was eluted from the Ultrogel AcA 22 column at a position corresponding to about 250 kDa and had a M_r of 68 kDa on SDS-PAGE.

Of the proteases tested, the inhibitor was found to inhibit mCANP specifically. It did not inhibit μ CANP even at a molar ratio of 6.4:1 (ECI: μ CANP). ECI from various tissues has been reported to inhibit both mCANP and μ CANP (Takano and Murachi, 1982; Murachi, 1983; Imajoh *et al.*, 1984; Suzuki *et al.*, 1984). It is not known if this difference is due to variations in the tissues, due to different roles of CANP and/or ECI in various tissues or due to the differences in the purification procedures.

Activity of ECI was found to be independent of the presence of Ca^{2+} . Neither the specificity of ECI nor the extent of inhibition of mCANP was affected by the presence of Ca^{2+} . It is logical to expect the activity of the inhibitor to be independent of Ca^{2+} , since simultaneous activation of CANP and its inhibitor by Ca^{2+} would be self negating. Takano and Murachi (1982) observed that the activity of human erythrocyte ECI was independent of Ca^{2+} . However, Melloni *et al.* (1982) observed that human erythrocyte ECI was active only in the presence of Ca^{2+} . Similarly, ECI from rabbit skeletal muscle (Nakamura *et al.*, 1981), human liver (Imajoh and Suzuki, 1985) and platelets (Shiba *et al.*, 1983) were found to be active only in the presence of Ca^{2+} . The reason for this discrepancy is not understood.

In the presence of ECI, the rate of increase of enzyme activity remained unaltered although the maximal level of activity decreased in proportion to the amount of inhibitor (figure 2a). This suggests that inhibition is by the formation of inactive enzyme-inhibitor complex. One mol of ECI inactivated two mol of the enzyme. Formation of CANP-ECI complexes have been observed in several tissues (Ishiura *et al.*, 1982; Imajoh *et al.*, 1984). However, various ratios of ECI: CANP in these complexes have been reported. This discrepancy may be attributed to the different molecular sizes of not only ECI but also CANP from various sources. The Ca^{2+} sensitivity of mCANP was not affected by ECI, suggesting that inhibition is not due to depletion of Ca^{2+} available to the enzyme. ECI from some tissues has been found to be independent of Ca^{2+} (Nishiura *et al.*, 1978; Ishiura *et al.*, 1982; Takano and Murachi, 1982).

μ CANP alone has detectable activity at an intracellular Ca^{2+} concentrations (10 μM), whereas mCANP is active beyond 0.6 mM Ca^{2+} (Shastri and Anandaraj, 1986). However, autolysis reduces the Ca^{2+} requirement of both mCANP and μ CANP (Suzuki *et al.*, 1981a,b, 1987; Dayton, 1982) enabling their activity to be manifested at intracellular Ca^{2+} concentrations (0.01–10 μM) (Nelson and Traub, 1982). Autolysis of both the CANPs was monitored in the presence of ECI to determine if their coexistence in tissues could have any physiological significance.

(by protecting it from autolysis) while inhibiting mCANP activity. Such discriminatory effect of ECI on mCANP and μ CANP may have implications in the turnover of proteins under physiological conditions.

Acknowledgements

This work was supported by the Indian Council of Medical Research, Departments of Science and Technology and Atomic Energy, New Delhi.

References

- Baudry, M. and Lynch, G. (1980) *Proc. Natl. Acad. Sci. USA*, **77**, 2298.
- Dayton, W. R., Goll, D. E., Zeece, M. G., Robson, R. M. and Reville, W. J. (1976) *Biochemistry*, **15**, 2150.
- Dayton, W. R., Schollmeyer, J. V., Lepley, R. A. and Cortes, L. R. (1981) *Biochim. Biophys. Acta*, **659**, 48.
- Dayton, W. R. (1982) *Biochim. Biophys. Acta*, **709**, 166.
- Huston, R. B. and Krebs, E. G. (1968) *Biochemistry*, **7**, 2116.
- Imajoh, S., Kawasaki, H., Kisaragi, M., Mukai, M., Sugita, H. and Suzuki, K. (1984) *Biomed. Res.*, **5**, 481.
- Imajoh, S. and Suzuki, K. (1985) *FEBS Lett.*, **187**, 47.
- Ishiura, S. (1981) *Life Sci.*, **29**, 1079.
- Ishiura, S., Tsuji, S., Murofushi, H. and Suzuki, K. (1982) *Biochim. Biophys. Acta*, **701**, 216.
- Laemmli, U. K. (1970) *Nature (London)*, **227**, 680.
- Lepley, R. A., Pampusch, M. and Dayton, W. R. (1985) *Biochim. Biophys. Acta*, **828**, 95.
- Mellgren, R. L. and Carr, T. C. (1983) *Arch. Biochem. Biophys.*, **225**, 779.
- Melloni, E., Sparatore, B., Salamino, R., Michetti, M. and Pontremoli, S. (1982) *Biochem. Biophys. Res. Commun.*, **106**, 731.
- Murachi, T. (1983) *Trends Biochem. Sci.*, **8**, 167.
- Nakamura, M., Tsuji, S., Suzuki, K. and Imahori, K. (1981) *J. Biochem.*, **90**, 1583.
- Nakamura, M., Inomata, M., Hayashi, M., Imahori, K. and Kawashima, S. (1984) *J. Biochem.*, **96**, 1399.
- Nelson, W. J. and Traub, P. (1982) *J. Biol. Chem.*, **257**, 5544.
- Nishiura, I., Tanaka, A., Yamoti, S. and Murachi, T. (1978) *J. Biochem.*, **84**, 1657.
- Pontremoli, S. and Melloni, E. (1986) *Annu. Rev. Biochem.*, **55**, 455.
- Puca, G. A., Nola, E., Sica, V. and Bresciani, F. (1977) *J. Biol. Chem.*, **252**, 1358.
- Rabbani, N., Shastri, R. and Anandaraj, M. P. J. S. (1986) *Placenta*, **7**, 73.
- Reddy, M. K., Etlinger, J. D., Rabinowitz, M., Fischman, D. A. (1975) *J. Biol. Chem.*, **250**, 4278.
- Shastri, R. and Anandaraj, M. P. J. S. (1986) *Biochim. Biophys. Acta*, **873**, 260.
- Shiba, E., Tsujinaka, T., Kambayashi, J. and Kosaki, G. (1983) *Thromb. Res.*, **32**, 207.
- Suzuki, K., Tsuji, S., Kubota, S., Kimura, Y. and Imahori, K. (1981a) *J. Biochem.*, **90**, 275.
- Suzuki, K., Tsuji, S., Ishiura, S., Kimura, Y., Kubota, S. and Imahori, K. (1981b) *J. Biochem.*, **90**, 1787.
- Suzuki, K., Kawashim, S. and Imahori, K. (1984) in *Calcium Regulation in biological systems* (ed.) S. Ebashi (Japan: Takeda Science Foundation) p. 213.
- Suzuki, K. (1987) *Trends Biochem. Sci.*, **12**, 103.
- Takano, E. and Murachi, T. (1982) *J. Biochem.*, **92**, 2021.
- Takano, E., Yumoto, N., Kanagi, R. and Murachi, T. (1984) *Biochem. Biophys. Res. Commun.*, **122**, 912.
- Takano, E., Kitahara, A., Sasaki, T., Kannagi, R. and Murachi, T. (1986a) *Biochem. J.*, **235**, 97.
- Takano, E., Maki, M., Hatanaka, M., Mori, H., Zenita, K., Sakihama, T., Kanagi, R., Marti, T., Titani, K. and Murachi, T. (1986b) *FEBS Lett.*, **208**, 199.
- Vedekis, W. V., Freeman, M. R., Schrader, W. T. and O'Malley, B. W. (1980) *Biochemistry*, **19**, 335.

Journal of Biosciences

Vol. 15, March–December 1990

SUBJECT INDEX

- ADP
Adenosine and ATP: mutually exclusive modifiers of the kinetics of ADP-induced aggregation of calf- platelets 389
- α -Adrenergic receptor
Polyvanadate acts at the level of plasma membranes through α -adrenergic receptor and affects cellular calcium distribution and some oxidation activities 205
- ALA dehydratase
Porphyrin metabolism in lead and mercury treated bajra (*Pennisetum typhoideum*) seedlings 271
- 5-Amino levulinic acid
Expression of 5-amino levulinic acid induced photodynamic damage to the thylakoid membranes in dark sensitized by brief pre-illumination 199
- ATPases
Effect of doxorubicin on the intestinal membranes in rats—Influence of α -tocopherol administration 31
- ATP (calf)
Adenosine and ATP: mutually exclusive modifiers of the kinetics of ADP-induced aggregation of calf-platelets 389
- Acid-induced unfolding
Isolation, characterization and effect of acidic pH on the unfolding-refolding mechanism of serum albumin domains 361
- Adenine methylation
5-Methylcytosine content and methylation status in six millet DNAs 47
- Adenosine
Adenosine and ATP: mutually exclusive modifiers of the kinetics of ADP-induced aggregation of calf-platelets 389
- Affinity chromatography
Affinity chromatography of estrogen- and progesterone-binding proteins of human uterus 1
- Aggregation
Adenosine and ATP: mutually exclusive modifiers of ovarian follicle cells of *Drosophila nausta* 99
- Amyloplasts
Enzyme activities associated with developing wheat (*Triticum aestivum* L.) grain amyloplasts 77
- Anion transporter
Inhibition of anion transport in the red blood cell membrane by anionic and non-anionic arginine-specific reagents 179
- Annexins
Functional and pathological significance of phospholipid asymmetry in erythrocyte membranes 187
- Antibiotics
Biological activity of an antibiotic puromycin—A theoretical study 417
- Antigenicity
Characterization of antibodies to chicken riboflavin carrier protein: Antigenicity of the tryptic fragments 341
- Antikeratin antibodies
Desmosome and intermediate filament assembly during differentiation and stratification of epithelial cells 227
- Antioxidant
Effect of doxorubicin on the intestinal membranes in rats—Influence of α -tocopherol administration 31
- Antizyme
Control of ornithine decarboxylase activity in jute seeds by antizyme 83
- Arginine ratio
Antitherogenic effect of a low lysine: arginine ratio of protein involves alteration in the aortic glycosaminoglycans and glycoproteins 305
- Arginine-specific reagents
Inhibition of anion transport in the red blood cell membrane by anionic and non-anionic arginine-specific reagents 179
- BSA-domains

treated bajra (<i>Pennisetum typhoideum</i>) seedlings	271	Chloroplast	
Basolateral membrane		Lamellar dispersion and phase separation of chloroplast membrane lipids by negative staining electron microscopy	93
Effect of doxorubicin on the intestinal membranes in rats—Influence of α -tocopherol administration	31	Magnetic resonance studies of dynamic organization of lipids in chloroplast membranes	281
Two forms of trehalase in rabbit enterocyte: Purification and chemical modification	377	Cholecystokinin-antagonist	
Biophysical changes		Cholecystokinin antagonist, proglumide, stimulates growth hormone release in the rat	17
Non-enzymatic glycosylation induced changes <i>in vitro</i> in some molecular parameters of collagen	23	Cholecystokinin-receptors	
Brachiectectomy		Cholecystokinin antagonist, proglumide, stimulates growth hormone release in the rat	17
Lactate dehydrogenase isozyme patterns in the denervated quail (<i>Coturnix coturnix japonica</i>) muscles	323	Chorion genes	
Brain		<i>In situ</i> study of chorion gene amplification in ovarian follicle cells of <i>Drosophila nausta</i>	99
Purification and characterization of cathepsin B from goat brain	397	Chou-Fasman analysis	
Brush border membrane		Predicted secondary structure of maltodextrin phosphorylase from <i>Escherichia coli</i> as deduced using Chou-Fasman model	53
Effect of doxorubicin on the intestinal membranes in rats—Influence of α -tocopherol administration	31	Chromosome location	
Two forms of trehalase in rabbit enterocyte: Purification and chemical modification	377	Organization and chromosomal localization of β -tubulin genes in <i>Leishmania donovani</i>	239
Ca^{2+}		Chronic myelogenous leukemia	
Role of Ca^{2+} in induction and secretion of dengue virus-induced cytokines	409	Functional and pathological significance of phospholipid asymmetry in erythrocyte membranes	187
Ca^{2+} activated		Circulating filarial antigen	
Human placental calcium activated neutral proteinase: Separation and functional characterization of subunits	427	Analysis, characterization and diagnostic use of circulating filarial antigen in bancroftian filariasis	37
Calcium		Cloning	
Polyvanadate acts at the level of plasma membranes through α -adrenergic receptor and affects cellular calcium distribution and some oxidation activities	205	Molecular cloning and restriction enzyme analysis of a long repetitive DNA sequence in rice	261
Calcium channel blockers		Cold shock	
Role of Ca^{2+} in induction and secretion of dengue virus-induced cytokines	409	Magnetic resonance methods for studying intact spermatozoa	125
Carbohydrate metabolism		Collagen	
Enzyme activities associated with developing wheat (<i>Triticum aestivum</i> L.) grain amyloplasts	77	Non-enzymatic glycosylation induced changes <i>in vitro</i> in some molecular parameters of collagen	23
Cathepsin B		Cytochrome P-450	
Purification and characterization of cathepsin B from goat brain	397	Developmental regulation of cytochrome P-450 (b+e) and glutathione transferase (Ya+Yc) gene expression in rat liver	107
Cell-surface		Cytokines	
Dephosphorylation of cell-surface phosphoproteins of goat spermatozoa	217	Role of Ca^{2+} in induction and secretion of dengue virus-induced cytokines	409
Cellular interactions		Cytosine methylation	
Functional and pathological significance of phospholipid asymmetry in erythrocyte membranes	187	5-Methylcytosine content and methylation status in six millet DNAs	47
Chemical modification		Cytotoxic factor	
Two forms of trehalase in rabbit enterocyte: Purification and chemical modification	377	Role of Ca^{2+} in induction and secretion of dengue virus-induced cytokines	409
		DNA sequence	
		Organization and chromosomal localization of β -tubulin genes in <i>Leishmania donovani</i>	239

- Delayed type hypersensitivity**
Coupling of proteins to liposomes and their role in understanding delayed type of hypersensitivity in human and mice 235
- Dengue virus**
Role of Ca^{2+} in induction and secretion of dengue virus-induced cytokines 409
- Deposition**
Translocation of plasminogen activator inhibitor-1 during serum stimulated growth of mouse embryo fibroblasts 351
- Desmosome**
Desmosome and intermediate filament assembly during differentiation and stratification of epithelial cells 227
- Detergents**
Erythrocyte stability under imposed fields 135
- Diabetes**
Optimization of sodium orthovanadate to treat streptozotocin-induced diabetic rats 67
- Differential scanning calorimetry**
Nuclear magnetic resonance and thermal studies of drug doped dipalmitoyl phosphatidyl choline- H_2O systems 117
- Differentiation**
Desmosome and intermediate filament assembly during differentiation and stratification of epithelial cells 227
- Dipalmitoyl phosphatidyl choline**
Nuclear magnetic resonance and thermal studies of drug doped dipalmitoyl phosphatidyl choline- H_2O systems 117
- Diphenylhexatriene**
Fluidity of detergent micelles plays an important role in muscarinic receptor solubilization 149
- Diphtheria toxin**
pH-Dependent membrane interactions of diphtheria toxin: A genetic approach 169
- Doxorubicin**
Effect of doxorubicin on the intestinal membranes in rats—Influence of α -tocopherol administration 31
- Drosophila***
In situ study of chorion gene amplification in ovarian follicle cells of *Drosophila nausta* 99
- Drug-membrane interaction**
Nuclear magnetic resonance and thermal studies of drug doped dipalmitoyl phosphatidyl choline- H_2O systems 117
- Ecto-protein**
Dephosphorylation of cell-surface phospho-
- Peptide induced polymorphism in model membranes 153
- Electron spin resonance**
Magnetic resonance studies of dynamic organisation of lipids in chloroplast membranes 281
- Electron transport chain**
Magnetic resonance methods for studying intact spermatozoa 125
- Endogenous inhibitor**
Endogenous inhibitor of calcium activated neutral proteinase from human placenta: purification and possible mechanism of proteinase regulation 435
- Endoreplication**
In situ study of chorion gene amplification in ovarian follicle cells of *Drosophila nausta* 99
- Enzyme linked immunosorbent assay**
Analysis, characterization and diagnostic use of circulating filarial antigen in bancroftian filariasis 37
- Enzymes**
Enzyme activities associated with developing wheat (*Triticum aestivum* L.) grain amyloplasts 77
- Enzymic A**
pH-Dependent membrane interactions of diphtheria toxin: A genetic approach 169
- Erythrocyte membrane**
Functional and pathological significance of phospholipid asymmetry in erythrocyte membranes 187
- Erythrocytes**
Erythrocyte stability under imposed fields 135
- ESR spin labelling**
Magnetic resonance methods for studying intact spermatozoa 125
- Estrogen-binding protein**
Affinity chromatography of estrogen- and progesterone-binding proteins of human uterus 1
- Fetal liver**
Developmental regulation of cytochrome P-450(b+e) and glutathione transferase (Ya+Yc) gene expression in rat liver 107
- Fibroblasts**
Translocation of plasminogen activator inhibitor-1 during serum stimulated growth of mouse embryo fibroblasts 351
- Filarial serum immunoglobulin G**
Analysis, characterization and diagnostic use of circulating filarial antigen in bancroftian filariasis 37
- Fluidity**

Fluorescence polarization

Calcium and magnesium induced changes in the relative fluidity of phosphatidylcholine liposomes 193

Fluidity of detergent micelles plays an important role in muscarinic receptor solubilization 149

Fluorescence quenching

Depth profiling in membranes by fluorescence quenching 143

Gene expression

Developmental regulation of cytochrome P-450 (b + e) and glutathione transferase (Ya + Yc) gene expression in rat liver 107

Gene organization

Organization and chromosomal localization of β -tubulin genes in *Leishmania donovani* 239

Gluconeogenesis

Hypoglycemic action of the pectin present in the juice of the inflorescence stalk of plantain (*Musa sapientum*)—Mechanism of action 297

Glucose repression-derepression

Role of heme in mitochondrial biogenesis: Transcriptional and post-transcriptional regulation of the expression of Iso-I-cytochrome C gene during glucose repression-derepression in cells of *Saccharomyces cerevisiae* 329

Glutathione transferase

Developmental regulation of cytochrome P-450 (b + e) and glutathione transferase (Ya + Yc) gene expression in rat liver 107

Glycogenolysis

Hypoglycemic action of the pectin present in the juice of the inflorescence stalk of plantain (*Musa sapientum*)—Mechanism of action 297

Glycogen phosphorylase

Hypoglycemic action of the pectin present in the juice of the inflorescence stalk of plantain (*Musa sapientum*)—Mechanism of action 297

Glycogen synthetase

Hypoglycemic action of the pectin present in the juice of the inflorescence stalk of plantain (*Musa sapientum*)—Mechanism of action 297

Glycoproteins

Antiatherogenic effect of a low lysine: arginine ratio of protein involves alteration in the aortic glycosaminoglycans and glycoproteins 305

Glycosaminoglycans

Antiatherogenic effect of a low lysine: arginine ratio of protein involves alteration in the aortic glycosaminoglycans and glycoproteins 305

Glycosylation

Non-enzymatic glycosylation induced changes *in vitro* in some molecular parameters of collagen 23

Goat reproductive organ

Magnetic resonance methods for studying intact spermatozoa 125

Heavy metals

Porphyrin metabolism in lead and mercury treated bajra (*Pennisetum typhoideum*) seedlings 271

α -Helix

Predicted secondary structure of maltodextrin phosphorylase from *Escherichia coli* as deduced using Chou-Fasman model 53

Heme

Role of heme in mitochondrial biogenesis: Transcriptional and post-transcriptional regulation of the expression of Iso-I-cytochrome C gene during glucose repression-derepression in cells of *Saccharomyces cerevisiae* 329

Hepatic glycogen

Hypoglycemic action of the pectin present in the juice of the inflorescence stalk of plantain (*Musa sapientum*)—Mechanism of action 297

^1H NMR

Nuclear magnetic resonance and thermal studies of drug doped dipalmitoyl phosphatidyl choline- H_2O systems 117

Human placenta

Endogenous inhibitor of calcium activated neutral proteinase from human placenta: Purification and possible mechanism of proteinase regulation 435

Human placental calcium activated neutral proteinase: Separation and functional characterization of subunits 427

Human semen

Magnetic resonance methods for studying intact spermatozoa 125

Human uterus

Affinity chromatography of estrogen- and progesterone-binding proteins of human uterus 1

Hybridization

Transcription and processing of β -tubulin messenger RNA in *Leishmania donovani* promastigotes 249

Hydration

Isolation, characterization and effect of acidic pH on the unfolding-refolding mechanism of serum albumin domains 361

Hypothalamus

Cholecystokinin antagonist, proglumide, stimulates growth hormone release in the rat 17

Immuno-electron microscopy

Desmosome and intermediate filament assembly during differentiation and stratification of epithelial cells 227

Impaired skin collagen maturity

Mechanism of impaired skin collagen maturity in riboflavin or pyridoxine deficiency 289

In situ hybridization

In situ study of chorion gene amplification in ovarian follicle cells of *Drosophila nausta* 99

Interaction energy		enger RNA in <i>Leishmania donovani</i> promastigotes	249
Biological activity of an antibiotic puromycin—A theoretical study	417	<i>Leishmania donovani</i>	
Intermediate filaments		Organization and chromosomal localization of β -tubulin genes in <i>Leishmania donovani</i>	239
Desmosome and intermediate filament assembly during differentiation and stratification of epithelial cells	227	Lipid packing	
Intestine		Functional and pathological significance of phospholipid asymmetry in erythrocyte membranes	187
Effect of doxorubicin on the intestinal membranes in rats—Influence of α -tocopherol administration	31	Lipid peroxidation	
Ionic strength		Optimization of sodium orthovanadate to treat streptozotocin-induced diabetic rats	67
Erythrocyte stability under imposed fields	135	Lipids	
Ionophores		Lamellar dispersion and phase separation of chloroplast membrane lipids by negative staining electron microscopy	93
Erythrocyte stability under imposed fields	135	Magnetic resonance studies of dynamic organization of lipids in chloroplast membranes	281
Iron-regulated membrane proteins		Liposome	
Iron-regulated membrane proteins and bacterial virulence	173	Identification and isolation of ATP transport protein in mycobacillin sensitive <i>Aspergillus niger</i>	163
Iso-l-cytochrome C gene		Liposome-coupled lepromin	
Role of heme in mitochondrial biogenesis: Transcriptional and post-transcriptional regulation of the expression of Iso-l-cytochrome C gene during glucose repression-derepression in cells of <i>Saccharomyces cerevisiae</i>	329	Coupling of proteins to liposomes and their role in understanding delayed type of hypersensitivity in human and mice	235
Isolation of ATP transport protein		Liposomes	
Identification and isolation of ATP transport protein in mycobacillin sensitive <i>Aspergillus niger</i>	163	Peptide induced polymorphism in model membranes	153
Japanese quail		Functional and pathological significance of phospholipid asymmetry in erythrocyte membranes	187
Lactate dehydrogenase isozyme patterns in the denervated quail (<i>Coturnix coturnix japonica</i>) muscles	323	Calcium and magnesium induced changes in the relative fluidity of phosphatidylcholine liposomes	193
Keratin		Long repetitive DNA	
Desmosome and intermediate filament assembly during differentiation and stratification of epithelial cells	227	Molecular cloning and restriction enzyme analysis of a long repetitive DNA sequence in rice	261
Kinetics		Lysine	
Kinetic mechanisms of mitochondrial carriers catalysing exchange reactions	159	Antiatherogenic effect of a low lysine: arginine ratio of protein involves alteration in the aortic glycosaminoglycans and glycoproteins	305
Adenosine and ATP: mutually exclusive modifiers of the kinetics of ADP-induced aggregation of calf-platelets	389	Maltodextrin phosphorylase	
King cobra venom		Predicted secondary structure of maltodextrin phosphorylase from <i>Escherichia coli</i> as deduced using Chou-Fasman model	53
Effect of king cobra venom on α_2 -macroglobulin and proteases in human blood plasma	59	Membrane penetration depth	
LDH activity		Depth profiling in membranes by fluorescence quenching	143
Lactate dehydrogenase isozyme patterns in the denervated quail (<i>Coturnix coturnix japonica</i>) muscles	323	Membrane vesicles	
LDH isozymes in muscles		Identification and isolation of ATP transport protein in mycobacillin sensitive <i>Aspergillus niger</i>	163
Lactate dehydrogenase isozyme patterns in the denervated quail (<i>Coturnix coturnix japonica</i>) muscles	323	Membranes	
<i>Leishmania</i>		Magnetic resonance studies of dynamic organization of lipids in chloroplast membranes	281
Transcription and processing of β -tubulin messenger RNA in <i>Leishmania donovani</i> promastigotes	249	Lamellar dispersion and phase separation of	

- chloroplast membrane lipids by negative staining electron microscopy 93
- 5-Methylcytosine content
- 5-Methylcytosine content and methylation status in six millet DNAs 47
- Micelle fluidity
- Fluidity of detergent micelles plays an important role in muscarinic receptor solubilization 149
- Millet
- 5-Methylcytosine content and methylation status in six millet DNAs 47
- Mitochondrial carriers
- Kinetic mechanisms of mitochondrial carriers catalysing exchange reactions 159
- Musa sapientum*
- Hypoglycemic action of the pectin present in the juice of the inflorescence stalk of plantain (*Musa sapientum*)—Mechanism of action 297
- Muscarinic receptor
- Fluidity of detergent micelles plays an important role in muscarinic receptor solubilization 149
- Myelin
- Activities of myelin bound cytidine 5'-diphosphate-choline 1,2 diacylglycerol choline phosphotransferase and uridine 5'-diphosphate-galactose-ceramide galactosyltransferase under restricted food intake 223
- Neurotrophic influences
- Lactate dehydrogenase isozyme patterns in the denervated quail (*Coturnix coturnix japonica*) muscles 323
- Nicotinic acid
- Role of nicotinic acid as modulator of liposomal microviscosity 145
- Nuclear magnetic resonance
- Magnetic resonance studies of dynamic organisation of lipids in chloroplast membranes 281
- Nuclear transcription
- Transcription and processing of β -tubulin messenger RNA in *Leishmania donovani* promastigotes 249
- Nutritional stress
- Activities of myelin bound cytidine 5'-diphosphate-choline 1,2 diacylglycerol choline phosphotransferase and uridine 5'-diphosphate-galactose-ceramide galactosyltransferase under restricted food intake 223
- Ornithine decarboxylase
- Control of ornithine decarboxylase activity in jute seeds by antizyme 83
- affects cellular calcium distribution and some oxidation activities 205
- PBG deaminase
- Porphyrin metabolism in lead and mercury treated bajra (*Pennisetum typhoideum*) seedlings 271
- Peptides
- Peptide induced polymorphism in model membranes 153
- Phase transition
- Role of nicotinic acid as modulator of liposomal microviscosity 145
- pH-dependent lethality
- pH-Dependent membrane interactions of diphtheria toxin: A genetic approach 169
- Phosphatidylcholine
- Calcium and magnesium induced changes in the relative fluidity of phosphatidylcholine liposomes 193
- Phosphatidylserine
- Functional and pathological significance of phospholipid asymmetry in erythrocyte membranes 187
- Phospholipid
- Role of nicotinic acid as modulator of liposomal microviscosity 145
- Phospholipid asymmetry
- Functional and pathological significance of phospholipid asymmetry in erythrocyte membranes 187
- Phosphoproteins
- Dephosphorylation of cell-surface phosphoproteins of goat spermatozoa 217
- Phosphorous NMR
- Peptide induced polymorphism in model membranes 153
- Photosystem
- Expression of 5-amino levulinic acid induced photodynamic damage to the thylakoid membranes in dark sensitized by brief preillumination 199
- Ping-pong mechanism
- Kinetic mechanisms of mitochondrial carriers catalysing exchange reactions 159
- Plasma α_2 -macroglobulin
- Effect of king cobra venom on α_2 -macroglobulin and proteases in human blood plasma 59
- Plasma growth hormone
- Cholecystokinin antagonist, proglumide, stimulates growth hormone release in the rat 17
- Plasminogen activator inhibitor
- Translocation of plasminogen activator inhibitor-1 during serum stimulated growth of

β -Pleated sheet

- Predicted secondary structure of maltodextrin phosphorylase from *Escherichia coli* as deduced using Chou-Fasman model 53

³¹P NMR

- Nuclear magnetic resonance and thermal studies of drug doped dipalmitoyl phosphatidyl choline- H₂O systems 117
- Magnetic resonance methods for studying intact spermatozoa 125

Polyacrylamide gel electrophoresis

- Analysis, characterization and diagnostic use of circulating filarial antigen in bancroftian filariasis 37

Polyamines

- Control of ornithine decarboxylase activity in jute seeds by antizyme 83

Polymorphism

- Peptide induced polymorphism in model membranes 153

Polyols

- Erythrocyte stability under imposed fields 135

Polyvanadate

- Polyvanadate acts at the level of plasma membranes through α -adrenergic receptor and affects cellular calcium distribution and some oxidation activities 205

Pores

- Erythrocyte stability under imposed fields 135

Porphyrins

- Porphyrin metabolism in lead and mercury treated bajra (*Pennisetum typhoideum*) seedlings 271

Progesterone-binding protein

- Affinity chromatography of estrogen- and progesterone-binding proteins of human uterus 1

Protein dephosphorylation

- Dephosphorylation of cell-surface phosphoproteins of goat spermatozoa 217

Proteinase

- Human placental calcium activated neutral proteinase; Separation and functional characterization of subunits 427
- Endogenous inhibitor of calcium activated neutral proteinase from human placenta: Purification and possible mechanism of proteinase regulation 435

Proteinase regulation

- Endogenous inhibitor of calcium activated neutral proteinase from human placenta: Purification and possible mechanism of proteinase regulation 435

Proteinphosphatase**Puromycin**

- Biological activity of an antibiotic puromycin—A theoretical study 417

Putrescine

- Control of ornithine decarboxylase activity in jute seeds by antizyme 83

Pyridoxine deficiency

- Mechanism of impaired skin collagen maturity in riboflavin or pyridoxine deficiency 289

RNA transport

- Role of heme in mitochondrial biogenesis: Transcriptional and post-transcriptional regulation of the expression of Iso-1-cytochrome C gene during glucose repression-derepression in cells of *Saccharomyces cerevisiae* 329

Rabbit

- Two forms of trehalase in rabbit enterocyte: Purification and chemical modification 377

Receptor solubilization

- Fluidity of detergent micelles plays an important role in muscarinic receptor solubilization 149

Reconstituted liposome

- Identification and isolation of ATP transport protein in mycobaccillin sensitive *Aspergillus niger* 163

Red blood cell

- Inhibition of anion transport in the red blood cell membrane by anionic and non-anionic arginine-specific reagents 179

Restriction enzyme analysis

- Molecular cloning and restriction enzyme analysis of a long repetitive DNA sequence in rice 261

Reticuloendothelial system

- Functional and pathological significance of phospholipid asymmetry in erythrocyte membranes 187

Reverse β -turn

- Predicted secondary structure of maltodextrin phosphorylase from *Escherichia coli* as deduced using Chou-Fasman model 53

Riboflavin carrier protein

- Characterization of antibodies to chicken riboflavin carrier protein: Antigenicity of the tryptic fragments 341

Riboflavin deficiency

- Mechanism of impaired skin collagen maturity in riboflavin or pyridoxine deficiency 289

Rice

- Molecular cloning and restriction enzyme analysis of a long repetitive DNA sequence in rice 261

Rossmann-fold super secondary structure

- Predicted secondary structure of maltodextrin

- proteinase: Separation and functional characterization of subunits 427
- Sodium dodecyl sulphate
Analysis, characterization and diagnostic use of circulating filarial antigen in bancroftian filariasis 37
- Spermatozoa
Dephosphorylation of cell-surface phosphoproteins of goat spermatozoa 217
- Spermidine
Control of ornithine decarboxylase activity in jute seeds by antizyme 83
- Sperms
Magnetic resonance methods for studying intact spermatozoa 125
- Spin labelled phospholipids
Depth profiling in membranes by fluorescence quenching 143
- Stratification
Desmosome and intermediate filament assembly during differentiation and stratification of epithelial cells 227
- Subunits
Human Placental calcium activated neutral proteinase: Separation and functional characterization of subunits 427
- Sulphydryl groups
Effect of doxorubicin on the intestinal membranes in rats—Influence of α -tocopherol administration 31
- Thiol content
Human placental calcium activated neutral proteinase: Separation and functional characterization of subunits 427
- Thiol protease
Purification and characterization of cathepsin B from goat brain 397
- Third ventricle cannulae
Cholecystokinin antagonist, proglumide, stimulates growth hormone release in the rat 17
- Thylakoid membrane
Expression of 5-amino levulinic acid induced photodynamic damage to the thylakoid membranes in dark sensitized by brief pre-illumination 199
- α -Tocopherol
Effect of doxorubicin on the intestinal membranes in rats—Influence of α -tocopherol administration 31
- Transcription
Role of heme in mitochondrial biogenesis: Transcriptional and post-transcriptional regulation of the expression of *Iscl* proto-oncogene C
- Trehalase
Two forms of trehalase in rabbit enterocyte: Purification and chemical modification 377
- Triticum aestivum*
Enzyme activities associated with developing wheat (*Triticum aestivum* L.) grain amyloplasts 77
- Tryptic digestion
Isolation, characterization and effect of acidic pH on the unfolding-refolding mechanism of serum albumin domains 361
- Tryptic fragments
Characterization of antibodies to chicken riboflavin carrier protein: Antigenicity of the tryptic fragments 341
- β -Tubulin
Organization and chromosomal localization of β -tubulin genes in *Leishmania donovani* 239
- β -Tubulin mRNA
Transcription and processing of β -tubulin messenger RNA in *Leishmania donovani* promastigotes 249
- UDP-galactose-ceramide galactosyltransferase
Activities of myelin bound cytidine 5'-diphosphate-choline 1,2 diacylglycerol choline phosphotransferase and uridine 5'-diphosphate-galactose-ceramide galactosyltransferase under restricted food intake 223
- Ultraviolet absorption
Isolation, characterization and effect of acidic pH on the unfolding-refolding mechanism of serum albumin domains 361
- Uptake
Uptake of volatile *n*-alkanes by *Pseudomonas* PG-I 313
- Uptake and release of ATP
Identification and isolation of ATP transport protein in mycobacillin sensitive *Aspergillus niger* 163
- Vanadate optimization
Optimization of sodium orthovanadate to treat streptozotocin-induced diabetic rats 67
- Venom and plasma proteases
Effect of king cobra venom on α_2 -macroglobulin and proteases in human blood plasma 59
- Viscosity
Isolation, characterization and effect of acidic pH on the unfolding-refolding mechanism of serum albumin domains 361
- Volatile *n*-alkanes
Uptake of volatile *n*-alkanes by *Pseudomonas* PG-I 313

AUTHOR INDEX

- Adhya, Samit
 see Saumitra Das 239
 Transcription and processing of β -tubulin messenger RNA in *Leishmania donovani* promastigotes 249
- Agarwal, S.
 see Jana, A. K. 211
- Anandaraj, M. P. J. S.
 see Radhika Shastri 427, 435
- Asha Mathur,
 see Ritu Dhawan 409
- Asima Lahiri Majumder
 Desmosome and intermediate filament assembly during differentiation and stratification of epithelial cells 227
- Balaji, K. S. K.
 Role of heme in mitochondrial biogenesis; Transcriptional and post-transcriptional regulation of the expression of Iso-1-cytochrome C gene during glucose repression-derepression in cells of *Saccharomyces cerevisiae* 329
- Balasubramaniam, N.
 see Sekar, N. 67
- Bamji, M. S.
 see Lakshmi, R. 289
- Barua, M.
 Dephosphorylation of cell-surface phosphoproteins of goat spermatozoa 217
- Basu, R.
 see Chatterjee, M. 145
- Bharati Ghosh,
 see Malabika Pandit 83
- Bhaumik, Mantu
 see Adhya, Samit 249
- Bose, S. K.
 see Chowdhury, Bhabadeb 163
- Cameotra, S. S.
 Uptake of volatile *n*-alkanes by *Pseudomonas* PG-I 313
- Chakraborty, N
 Expression of 5-amino levulinic acid induced photodynamic damage to the thylakoid membranes in dark sensitized by brief pre-illumination 199
- Charidrakasan, G.
 see Rathi, A. N. 23
- Chatterjee, M.
 Role of nicotinic acid as modulator of liposomal microviscosity 145
- Chaturvedi, V.
 see Sengupta, U. 235
- Chaturvedi, U. C.
 see Ritu Dhawan 409
- Cheirmaraj, K.
 see Parkhe, K. A. 37
- Chowdhury, Bhabadeb
 Identification and isolation of ATP transport protein in mycobacillin sensitive *Aspergillus niger* 163
- Collier, R. John
 pH-Dependent membrane interactions of diphtheria toxin: A genetic approach 169
- Dhar, M. S.
 see Gupta, V. S. 261
- Duyckaerts, C.
 see Sluse, F. E. 159
- Dwarki, V. J.
 Developmental regulation of cytochrome P-450 (b + e) and glutathione transferase (Ya + Yc) gene expression in rat liver 107
- Evens, A.
 see Sluse, F. E. 159
- Francis, V. S. N. K.
 see Dwarki, V. J. 107
- Gauri S. Singhal,
 see Mishra, R. K. 193
- Geeta Datta
 see Usha Deniz, K. 117
- Geetha, A.
 Effect of doxorubicin on the intestinal membranes in rats—Influence of α -tocopherol administration 31
- Goffart-Sluse, C. M.
 see Sluse, F. E. 159
- Gomathy, R.
 Hypoglycemic action of the pectin present in the juice of the inflorescence stalk of plantain (*Musa sapientum*)—Mechanism of action 297
- Gopalan, G.
 see Balaji, K. S. K. 329
- Govil, Girjesh
 see Ratna S. Phadke 125, 153
- Govindasamy, S.
 see Sekar, N. 67
- Griffiths, E.

- Gupta, C. M.
 see Sengupta, U. 235
- Harinath, B. C.
 see Parkhe, K. A. 37
- Hendre, R. R.
 see Lalitha S. Kumar 47
- Iyer, K. S. N.
 see Usha Natraj 341
- Jacintha Pereira
 see Usha Natraj 341
- Jagadeesh, G.
 see Radhika Shastri 427
- Jamaluddin, M.
 Adenosine and ATP: mutually exclusive modifiers
 of the kinetics of ADP-induced aggregation of
 calf-platelets 389
- Järv, Jaak
 see Kõiv, Anu 149
- Kamarajan, P.
 see Sekar, N. 67
- Kamboj, Ramesh, C.
 Purification and characterization of cathepsin B
 from goat brain 397
- Kemper, Susan
 see Schlegel, Robert A. 187
- Khan, M. Yahiya
 Isolation, characterization and effect of acidic
 pH on the unfolding-refolding mechanism of
 serum albumin domains 361
- Khetrapal, C. L.
 see Usha Deniz, K. 117
- Kõiv, Anu
 Fluidity of detergent micelles plays an important
 role in muscarinic receptor solubilization 149
- Krishnamoorthy, R. V.
 see Quaium, Abdul 323
- Krishnan, L. K.
 see Jamaluddin, M. 389
- Kumar, Anil
 Predicted secondary structure of maltodextrin
 phosphorylase from *Escherichia coli* as deduced
 using Chou-Fasman model 53
- Kumari, G. L.
 see Thapar, M. 1
- Kurup, P. A.
 see Gomathy, R. 297
 see Rajamohan, T. 305
- Kurup, C. K. Ramakrishna
 see Ramasarma, T. 205
- Lakshmi, A. V.
 see Lakshmi, R. 289
- Lalitha S. Kumar,
 5-Methylcytosine content and methylation status
 in six millet DNAs 47
- Madhu Khanna,
 see Ritu Dhawan 409
- Mahajan, R.
 Enzyme activities associated with developing
 wheat (*Triticum aestivum* L.) grain amyloplasts 77
- Majumder, G. C.
 see Barua, M. 217
- Malabika Pandit,
 Control of ornithine decarboxylase activity in
 jute seeds by antizyme 83
- Maya Roche
 Effect of king cobra venom on α_2 -macroglobulin
 and proteases in human blood plasma 59
- McCann, S. M.
 see Vijayan, E. 17
- Mishra, R. K.
 Calcium and magnesium induced changes in the
 relative fluidity of phosphatidylcholine lipo-
 somes 193
- Nagashunmugam, T.
 see Srinivas, S. 351
- Nandy, P.
 see Chatterjee, M. 145
- Narayanan, R. B.
 see Sengupta, U. 235
- Narvekar, G. S.
 see Gupta, V. S. 261
- Ohja, R. P.
 Biological activity of an antibiotic puromycin—A
 theoretical study 417
- Padmanaban, G.
 see Dwarki, V. J. 107
- Padmini, S.
 Activities of myelin bound cytidine 5'-diphos-
 phate-choline 1, 2 diacylglycerol choline phos-
 photransferase and uridine 5'-diphosphate-
 galactose-ceramide galactosyltransferase under
 restricted food intake 223
- Pal, Suresh
 see Kamboj, Ramesh, C. 397
- Parkhe, K. A.
 Analysis, characterization and diagnostic use of
 circulating filarial antigen in bancroftian

- Pattabiraman, T. N.
 see Maya Roche 59
- Prasad, D. D. K.
 Porphyrin metabolism in lead and mercury
 treated bajra (*Pennisetum typhoideum*) seedlings 271
- Prasad, A. R. K.
 see Prasad, D. D. K. 271
- Quaium, Abdul
 Lactate dehydrogenase isozyme patterns in the
 denervated quail (*Coturnix coturnix japonica*)
 muscles 323
- Radhika Shastri
 Human placental calcium activated neutral
 proteinase: Separation and functional cha-
 racterization of subunits 427
 Endogenous inhibitor of calcium activated
 neutral proteinase from human placenta: Puri-
 fication and possible mechanism of proteinase
 regulation 435
- Raghotama, S.
 see Ramanathan, K. V. 117
- Rajamanickam, C.
 see Balaji, K. S. K. 329
- Rajamohan, T.
 Antiatherogenic effect of a low lysine: arginine
 ratio of protein involves alteration in the aortic
 glycosaminoglycans and glycoproteins 305
- Ramanathan, K. V.
 see Usha Deniz, K. 117
- Ramaprasad, P.
 see Parkhe, K. A. 37
- Ramasarma, T.
 Polyvanadate acts at the level of plasma
 membranes through-adrenergic receptor and
 affects cellular calcium distribution and some
 oxidation activities 205
- Ranjekar, P. K.
 see Lalitha S. Kumar 47
 see Gupta, V. S. 261
- Rathi, A. N.
 Non-enzymatic glycosylation induced changes
 in vitro in some molecular parameters of
 collagen 23
- Ratna S. Phadke
 Magnetic resonance methods for studying intact
 spermatozoa 125
 Peptide induced polymorphism in model
 membranes 153
- Rawat, S. R.
 Ritu Dhawan,
 Role of Ca^{2+} in induction and secretion of
 dengue virus-induced cytokines 409
- Sachdeva, S. K.
 see Thapar, M. 1
- Salahuddin, A.
 see Khan, Yahya, M. 361
- Sankar, R.
 see Geetha, A. 31
- Sanker, S.
 Two forms of trehalase in rabbit enterocyte:
 Purification and chemical modification 377
- Sanyal, N. K.
 see Ojha, R. P. 417
- Saumitra Das
 Organization and chromosomal localization of
 β -tubulin genes in *Leishmania donovani* 239
 see Adhya, Samit 249
- Schlegel, Robert A.
 Functional and pathological significance of
 phospholipid asymmetry in erythrocyte mem-
 branes 187
- Sekar, N.
 Optimization of sodium orthovanadate to treat
 streptozotocin induced diabetic rats 67
- Sengupta, U.
 Coupling of proteins to liposomes and their role
 in understanding delayed type of hypersensiti-
 vity in human and mice 235
- Shailaja, B.
 see Radhika Shastri 435
- Shanmugam, G.
 see Srinivas, S. 351
- Sharada Gullapalli,
 see Ramasarma, T. 205
- Shrivastava, T. G.
 see Thapar, M. 1
- Shuler, Charles F.
 see Asima Lahiri Majumder 227
- Shyamala Devi, C. S.
 see Geetha, A. 31
- Singh, H. D.
 see Cameotra, S. S. 313
- Singh, Hari
 see Kamboj, Ramesh C. 397
- Singh, Randhir
 see Mahajan, R. 77
- Sinha, Sudhir
 see Sengupta, U. 235
- Sitaramam, V.
 Erythrocyte stability under imposed fields 135

- Smita Mahale
 see Usha Natraj 341
- Sreevatsa
 see Sengupta, U. 235
- Srinivas, S.
 Translocation of plasminogen activator inhibitor-1 during serum stimulated growth of mouse embryo fibroblasts 351
- Srinivasarao, P.
 see Padmini, S. 223
- Sudha Srivastava
 see Ratna S. Phadke 125, 153
- Sudharshana, L.
 see Quaium, Abdul 323
- Sujata, P.
 see Thapar, M. 1
- Suryaprakash, N.
 see Usha Deniz, K. 117
- Thankamani Marar
 see Geetha, A. 31
- Thapar, M.
 Affinity chromatography of estrogen- and progesterone-binding proteins of human uterus 1
- Tiwari, P. K.
 In situ study of chorion gene amplification in ovarian follicle cells of *Drosophila nausta* 99
- Tripathy, B. C.
 see Chakraborty, N. 199
- Usha Deniz, K.
 Nuclear magnetic resonance and thermal studies of drug doped dipalmitoyl phosphatidyl choline-H₂O systems 117
- Usha Natraj
 Characterization of antibodies to chicken ribo-flavin carrier protein: Antigenicity of the tryptic fragments 341
- Vidya Shivaswamy
 see Ramasarma, T. 205
- Vijaya Raghavan
 see Usha Natraj 341
- Vijayalekshmi, N. R.
 see Gomathy, R. 297
- Vijayan, E.
 Cholecystokinin antagonist, proglumide, stimulates growth hormone release in the rat 17
- Virupaksha, T. K.
 see Quaium, Abdul 323
- William, S.
 see Sekar, N. 67
- Williamson, Patrick
 see Schlegel, Robert A. 187
- YashRoy, R. C.
 Lamellar dispersion and phase separation of chloroplast membrane lipids by negative staining electron microscopy 93
 Magnetic resonance studies of dynamic organization of lipids in chloroplast membranes 281
- Zaki, Laila
 Inhibition of anion transport in the red blood cell membrane by anionic and non-anionic arginine-specific reagents 179

Journal of Biosciences

ACKNOWLEDGEMENTS

The editorial board wishes to place on record the valuable assistance rendered by the following scientists in reviewing manuscripts received for publication in the *Journal of Biosciences*.

Dr. Y. P. Abrol, New Delhi
Dr. P. R. Adiga, Bangalore
Dr. T. C. Anand Kumar, Bombay
Dr. N. Appaji Rao, Bangalore
Dr. Ashok Banerjee, Calcutta
Dr. Ashok Khar, Hyderabad
Dr. Ashwini Kumar, Lucknow
Dr. Asis Datta, New Delhi
Dr. A. S. Balasubramanian, Vellore
Dr. Balraj Mittal, Lucknow
Dr. M. S. Bamji, Hyderabad
Dr. A. Banerjee, Calcutta
Dr. A. B. Banerjee, Calcutta
Dr. M. K. Basu, Calcutta
Dr. A. N. Bhaduri, Calcutta
Dr. Alok Bhattacharya, New Delhi
Dr. A. K. Bhattacharya, Calcutta
Dr. B. B. Bhowmik, Calcutta
Dr. B. B. Biswas, Calcutta
Dr. S. K. Brahmachari, Bangalore
Dr. S. L. Chakrabarti, Calcutta
Dr. P. Chakrabarty, Calcutta
Dr. G. Chandrakasan, Madras
Dr. B. P. Chatterjee, Calcutta
Dr. S. N. Chatterjee, Calcutta
Dr. M. R. Das, Hyderabad
Dr. P. R. Dasgupta, Calcutta
Dr. S. Duraiswamy, Delhi
Dr. S. V. Gangal, Delhi
Dr. J. J. Ghosh, Calcutta
Dr. S. Ghosh, Calcutta
Dr. Gopal Pande, Hyderabad
Dr. K. P. Gopinathan, Bangalore

Dr. Indira Nath, New Delhi
Dr. A. Jagannadha Rao, Bangalore
Dr. J. Jayaraman, Madurai
Dr. Joseph Thomas, Madras
Dr. M. S. Karla, Ludhiana
Dr. Kasturi Datta, New Delhi
Dr. S. S. Katyare, Baroda
Dr. G. Lakshmi Kumari, New Delhi
Dr. A. K. Lala, Bombay
Dr. P. R. Mahadevan, Bombay
Dr. G. C. Majumdar, Calcutta
Dr. Malathi Lakshmikumaran, New Delhi
Dr. R. K. Mandal, Calcutta
Dr. Manju Sarkar, Calcutta
Dr. R. Manjunath, Bangalore
Dr. Maruthi Mohan, Hyderabad
Dr. A. F. Mascarenhas, Pune
Dr. N. G. Mehta, Bombay
Dr. S. L. Mehta, New Delhi
Dr. Monisha Bose, Calcutta
Dr. A. S. Mukherjee, Calcutta
Dr. V. H. Mulimani, Gulbarga
Dr. P. S. Murthy, New Delhi
Dr. R. Nagabhushanam, Aurangabad
Dr. V. Nagaraja, Bangalore
Dr. R. Nagarajan, Madras
Dr. P. Nandy, Calcutta
Dr. M. V. Narurkar, Bombay
Dr. R. Nath, Chandigarh
Dr. R. Nayak, Bangalore
Dr. G. Padmanaban, Bangalore
Dr. M. W. Pandit, Hyderabad
Dr. T. N. Pattabiraman, Manipal
Dr. H. P. Pathak, Mysore

Dr. H. G. Raj, Delhi
Dr. D. Rajagopala Rao, Mysore
Dr. V. S. Rama Das, Hyderabad
Dr. A. Ramaiah, New Delhi
Dr. C. Ramakrishnan, Bangalore
Dr. T. Ramasarma, Bangalore
Dr. P. K. Ranjekar, Pune
Dr. P. K. Ray, Lucknow
Dr. C. Renuka Prasad, Bangalore
Dr. K. K. Rohatgi Mukherjee, Calcutta
Dr. T. B. Samanta, Calcutta
Dr. A. Saran, Bombay
Dr. P. K. Sarkar, Calcutta
Dr. G. R. Sarma, Madras
Dr. H. S. Savithri, Bangalore
Dr. R. Selvam, Madras
Dr. A. R. Sheth, Bombay

Dr. Shobana Sharma, Bombay
Dr. O. P. Shukla, Lucknow
Dr. C. S. Shyamala Devi, Madras
Dr. T. P. Singh, New Delhi
Dr. V. Sitaramam, Pune
Dr. K. Subba Rao, Hyderabad
Dr. Sudhir Sopory, New Delhi
Dr. T. N. Tandon, New Delhi
Dr. Usha Natraj, Bombay
Dr. M. S. Valiathan, Trivandrum
Dr. Veena Parnaik, Hyderabad
Dr. P. S. Veerabhadrapa, Bangalore
Dr. K. Vijaya Raghavan, Bombay
Dr. S. Vijaya, Bangalore
Dr. Vijayalakshmi Ravindranath,
Bangalore
Dr. E. Vijayan, Pondicherry